

# 2007 Atomic, Molecular, Optical Sciences **Research Meeting**



Airlie Conference Center  
Warrenton, Virginia  
September 9-12, 2007



Sponsored by:  
U.S. Department of Energy  
Office of Basic Energy Sciences  
Chemical Sciences, Geosciences & Biosciences Division

**Cover Art Courtesy of Diane Marceau  
Chemical Sciences, Geosciences and Biosciences  
Division, Basic Energy Sciences, DOE**

**This document was produced under contract number DE-AC05-06OR23100  
between the U.S. Department of Energy and Oak Ridge Associated Universities.**

## **Foreword**

This volume summarizes the 2007 Research Meeting of the Atomic, Molecular and Optical Sciences (AMOS) Program sponsored by the U. S. Department of Energy (DOE), Office of Basic Energy Sciences (BES), and comprises descriptions of all of the current research sponsored by the AMOS program. The research meeting is held annually for the DOE laboratory and university principal investigators within the BES AMOS Program in order to facilitate scientific interchange among the PIs and to promote a sense of program identity.

The BES/AMOS program is vigorous and forward-looking, and enjoys strong support within the Department of Energy. This is entirely due to our scientists, the outstanding research they perform, and its relevance to DOE missions. While the FY2007 appropriation for DOE increased overall funding for science, hoped-for new initiatives related to AMOS were not funded. We were challenged to meet our established commitments to researchers. Nevertheless, because of the relevance of AMOS research, BES continued to increase its strategic investments in the national laboratory ultrafast x-ray efforts. We were pleased also to initiate two new grants under the auspices of the DOE EPSCoR program.

We are deeply indebted to all of the members of the scientific community who have contributed valuable time toward the review of proposals and programs, either by mail review of grant applications or on-site reviews of our multi-PI programs. These thorough and thoughtful reviews have been central to the continued vitality the AMOS Program.

We owe special thanks to Elliot Kanter for his invaluable help in managing the AMOS program this year. We anticipate having a new AMOS program manager in place soon – possibly by the time of this meeting! Michael looks forward to continued association with the AMOS program as leader for the Fundamental Interactions team. Eric is now our Division Director with responsibility for BES Chemical Sciences, including the AMOS program.

Thanks also to the staff of the Oak Ridge Institute for Science and Education, in particular Sophia Kitts, and Angie Lester, and to the Airlie Conference Center for assisting with the meeting. We thank our colleagues in the Chemical Sciences, Biosciences, and Geosciences Division - Diane Marceau, Robin Felder, and Michaelena Kyler-King - for indispensable behind-the-scenes efforts in support of the BES/AMOS program.

Michael P. Casassa  
Richard Hilderbrandt  
Eric A. Rohlfing  
Chemical Sciences, Geosciences and Biosciences Division  
Office of Basic Energy Sciences  
Department of Energy



# *Agenda*



**2007 Meeting of the Atomic, Molecular and Optical Sciences Program**  
**Office of Basic Energy Sciences**  
**U. S. Department of Energy**

**Arlie Center, Warrenton, Virginia, September 9-12, 2007**

**Sunday, September 9**

3:00-6:00 pm	**** Registration ****
6:00 pm	**** Reception (No Host) ****
7:00 pm	**** Dinner ****

**Monday, September 10**

7:30 am	**** Breakfast ****
8:45 am	<i>Welcome and Introductory Remarks</i> <b>Michael Casassa</b> , BES/DOE

**Session I** Chair: **Margaret Murnane**

9:00 am	<i>Ultrafast X-Ray Coherent Control</i> <b>David Reis</b> , University of Michigan
9:30 am	<i>Resonant X-Ray Absorption by Laser-Aligned Molecules</i> <b>Steve Southworth</b> , Argonne National Laboratory
10:00 am	<i>Structural Dynamics in Chemical Systems</i> <b>Kelly Gaffney</b> , Stanford Linear Accelerator Center
10:30 am	**** Break ****
11:00 am	<i>Strong-Field Control of X-Ray Absorption</i> <b>Robin Santra</b> , Argonne National Laboratory
11:30 am	<i>X-Ray Spectroscopy of Optical-Field-Ionized Atoms</i> <b>Bob Dunford</b> , Argonne National Laboratory
12:00 noon	<i>Laser-Produced X-Ray Sources</i> <b>Don Umstadter</b> , University of Nebraska
12:30 pm	**** Lunch ****

<b>Session II</b>	Chair: <b>Lou DiMauro</b>
4:00 pm	<i>Dynamics of Few-Body Atomic Processes</i> <b>Anthony F. Starace</b> , University of Nebraska
4:30 pm	<i>Molecular Dynamics with Ion and Laser Beams</i> <b>Itzik Ben-Itzhak</b> , Kansas State University
5:00 pm	<i>Attosecond Atomic and Molecular Dynamics</i> <b>Chii-Dong Lin</b> , Kansas State University
5:30 pm	<i>PULSE (Photon Ultrafast Laser Science and Engineering) Center</i> <b>Philip Bucksbaum</b> , Stanford Linear Accelerator Center
5:45 pm	<i>Ultrafast X-Ray Science Laboratory (UXSL)</i> <b>Bill McCurdy</b> , Lawrence Berkeley National Laboratory
6:00 pm	**** Reception (No Host) ****
6:30 pm	**** Dinner ****
<b>Session III</b>	Chair: <b>Ron Phaneuf</b>
7:30 pm	<i>Probing Complexity Using the Advanced Light Source</i> <b>Nora Berrah</b> , Western Michigan University
8:00 pm	<i>Breakup of Atoms and Molecules by Multiple Photoionization or Electron Attachment</i> <b>Bill McCurdy</b> , Lawrence Berkeley National Laboratory
8:30 pm	<i>Low-Energy Charge Exchange Using Ion-Atom Merged-Beams</i> <b>Charlie Havener</b> , Oak Ridge National Laboratory
<b>Tuesday, September 11</b>	
7:30 am	**** Breakfast ****
<b>Session IV</b>	Chair: <b>Allen Landers</b>
8:30 am	<i>Photoabsorption by Free and Confined Atoms and Ions</i> <b>Steve Manson</b> , Georgia State University
9:00 am	<i>Resonant and Nonresonant Vibrational Effects in the Photoionization Dynamics of Asymmetric Systems</i> <b>Erwin Poliakoff</b> , Louisiana State University
9:30 am	<i>Electron/Photon Interactions with Atoms/Ions</i> <b>Alfred Msezane</b> , Clark Atlanta University
10:00 am	<i>Low-Energy Electron Interactions with Interfaces and Biological Targets</i> <b>Thom Orlando</b> , Georgia Tech
10:30 am	**** Break ****

11:00 am	<i>Electron-Driven Excitation and Dissociation of Molecules</i> <b>Ann Orel</b> , University of California, Davis
11:30 am	<i>Studies of Autoionizing States Relevant to Dielectronic Recombination</i> <b>Tom Gallagher</b> , University of Virginia
12:00 noon	<i>Recent Work Using the LTDSE Method for Atomic Collisions and New Opportunities in Molecular Physics at the ORNL MIRF</i> <b>Dave Schultz</b> , Oak Ridge National Laboratory
12:30 pm	**** Lunch ****
<b>Session V</b>	<b>Chair: Uwe Thumm</b>
4:00 pm	<i>Single Molecule Fluorescence in Nanoscale Environments</i> <b>Lukas Novotny</b> , University of Rochester
4:30 pm	<i>Optical Two-Dimensional Fourier Transform Spectroscopy of Disordered Semiconductor Quantum Wells and Quantum Dots</i> <b>Steve Cundiff</b> , JILA/University of Colorado
5:00 pm	<i>Femtosecond and Attosecond Laser-Pulse Energy Transformation and Concentration in Nanostructured Systems</i> <b>Mark Stockman</b> , Georgia State University
5:30:pm	<i>Single-Exciton Optical Gain in Semiconductor Nanocrystals Using Engineered Exciton-Exciton Interactions</i> <b>Victor Klimov</b> , Los Alamos National Laboratory
6:00 pm	**** Reception (No Host) ****
6:30 pm	**** Dinner ****

## Wednesday, September 12

7:30 am	**** Breakfast ****
<b>Session VI</b>	<b>Chair: Neil Shafer-Ray</b>
8:30 am	<i>Ultracold Molecules: Physics in the Quantum Regime</i> <b>John Doyle</b> , Harvard University
9:00 am	<i>Strongly-Interacting Quantum Gases</i> <b>Murray Holland</b> , University of Colorado
9:30 am	<i>Theoretical Investigations of Atomic Collision Physics</i> <b>Alex Dalgarno</b> , Harvard University
10:00 am	**** Break ****

10:30 am      *Interactions of Ultracold Molecules: Collisions, Reactions, and Dipolar Effects*  
                **Dave DeMille**, Yale University

11:00 am      *Population Dynamics in Coherent Excitation of Cold Atoms*  
                **Brett DePaola**, Kansas State University

11:30 am      *Closing Remarks*  
                **Michael Casassa**, BES/DOE

11:40 am      \*\*\*\* Lunch \*\*\*\*

# *Table of Contents*



## Laboratory Research Summaries (by institution)

<b>AMO Physics at Argonne National Laboratory .....</b>	<b>1</b>
<i>Resonant X-Ray Absorption by Laser-Aligned Molecules</i>	
<b>S. H. Southworth .....</b>	<b>1</b>
<i>X-Ray Absorption by Laser-Dressed Atoms</i>	
<b>R. Santra .....</b>	<b>3</b>
<i>X-Ray Spectroscopy of Optical-Field-Ionized Atoms</i>	
<b>R. W. Dunford .....</b>	<b>5</b>
<i>Nonlinear X-Ray Processes Using a Self-Amplified Spontaneous Emission Free-Electron Laser</i>	
<b>R. Santra .....</b>	<b>7</b>
<i>Dynamics in Laser-Generated Plasmas</i>	
<b>E. P. Kanter .....</b>	<b>8</b>
<i>Picosecond X-Rays at Argonne's Advanced Photon Source</i>	
<b>B. Krässig.....</b>	<b>9</b>
<i>Theory of X-Ray Diffraction from Single Molecules at X-Ray FELs</i>	
<b>R. Santra .....</b>	<b>10</b>
<b>Overview of J. R. Macdonald Laboratory Program for Atomic, Molecular, and Optical Physics .....</b>	<b>13</b>
<i>Structure and Dynamics of Atoms, Ions, Molecules, and Surfaces: Molecular Dynamics with Ion and Laser Beams</i>	
<b>Itzik Ben-Itzhak .....</b>	<b>14</b>
<i>Controlling Attosecond Pulse Spectra with Carrier-Envelope Phase</i>	
<b>Zenghu Chang .....</b>	<b>18</b>
<i>Structure and Dynamics of Atoms, Ions, Molecules and Surfaces: Atomic Physics with Ion Beams, Lasers and Synchrotron Radiation</i>	
<b>C.L. Cocke .....</b>	<b>22</b>
<i>Photo-Association and Coherent Excitation of Cold Atoms</i>	
<b>B. D. DePaola.....</b>	<b>26</b>

<i>Time-Dependent Treatment of Three-Body Systems in Intense Laser Fields</i>	
<b>B. D. Esry</b> .....	<b>30</b>
<i>Theoretical Studies of Atoms and Molecules with Intense Laser Pulses</i>	
<b>C. D. Lin</b> .....	<b>34</b>
<i>Structure and Dynamics of Atoms, Ions, Molecules and Surfaces: Atomic Physics with Ion Beams, Lasers and Synchrotron Radiation</i>	
<b>I. V. Litvinyuk</b> .....	<b>38</b>
<i>Electronic Excitations and Dynamics in Carbon Nanotubes Induced by Femtosecond Pump-Probe Laser Pulses</i>	
<b>Pat Richard</b> .....	<b>42</b>
<i>Structure and Dynamics of Atoms, Ions, Molecules and Surfaces: Atomic Physics with Ion Beams, Lasers and Synchrotron Radiation</i>	
<b>Uwe Thumm</b> .....	<b>45</b>
<b>Atomic, Molecular and Optical Science at Los Alamos National Laboratory</b> .....	<b>49</b>
<i>Multiparticle Processes and Interfacial Interactions in Nanoscale Systems Built from Nanocrystal Quantum Dots</i>	
<b>Victor Klimov</b> .....	<b>49</b>
<b>Atomic, Molecular and Optical Sciences at LBNL</b> .....	<b>53</b>
<i>Inner-Shell Photoionization and Dissociative Electron Attachment of Small Molecules</i>	
<b>Ali Belkacem</b> .....	<b>54</b>
<i>Electron-Atom and Electron-Molecule Collision Processes</i>	
<b>T. N. Rescigno and C. W. McCurdy</b> .....	<b>58</b>
<i>Ultrafast X-Ray Science Laboratory</i>	
<b>Ali Belkacem</b> .....	<b>62</b>
<b>Atomic and Molecular Physics Research at Oak Ridge National Laboratory</b> .....	<b>66</b>
<i>Phase IV of the MIRF Upgrade Project</i>	
<b>C. R. Vane</b> .....	<b>66</b>

<i>Low-Energy Ion-Surface Interactions</i>	
<b>F. W. Meyer .....</b>	<b>67</b>
<i>Low-Energy Charge Exchange Using the Upgraded Ion-Atom Merged-Beams Apparatus</i>	
<b>C. C. Havener .....</b>	<b>69</b>
<i>Production of molecular hydrogen anions H<sub>2</sub><sup>-</sup> and D<sub>2</sub><sup>-</sup> on a KBr surface</i>	
<b>C. C. Havener .....</b>	<b>71</b>
<i>Electron-Molecular Ion Interactions</i>	
<b>M. E. Bannister .....</b>	<b>72</b>
<i>Grazing Surface Studies at Intermediate Energy</i>	
<b>H. F. Krause.....</b>	<b>74</b>
<i>Atomic Ion-Atom and Molecular Ion-Atom Electron Transfer</i>	
<b>C.R.Vane.....</b>	<b>75</b>
<i>Molecular Dynamics Simulations of Chemical Sputtering</i>	
<b>C. O. Reinhold.....</b>	<b>77</b>
<i>Manipulation and Decoherence of Rydberg Wavepackets</i>	
<b>C. O. Reinhold.....</b>	<b>78</b>
<i>Development of the LTDSE Method for Atomic Collisions</i>	
<b>D. R. Schultz .....</b>	<b>79</b>
<i>Electron Detachment in Ion-Atom Collisions</i>	
<b>J. H. Macek .....</b>	<b>80</b>
<b>PULSE: The Stanford Photon Ultrafast Laser Science and Engineering Center .....</b>	<b>87</b>
<i>High Harmonic Generation in Molecules</i>	
<b>Philip H. Bucksbaum .....</b>	<b>91</b>
<i>Laser Control of Molecular Alignment and Bond Strength</i>	
<b>Philip H. Bucksbaum .....</b>	<b>95</b>
<i>Ultra-Fast Coherent Imaging of Non-Periodic Structure</i>	
<b>Janos Hajdu.....</b>	<b>98</b>
<i>Structural Dynamics in Chemical Systems</i>	

<b>Kelly J. Gaffney.....</b>	<b>102</b>
------------------------------	------------

## **University Research Summaries (by PI)**

*Probing Complexity Using the Advanced Light Source*

<b>Nora Berrah.....</b>	<b>105</b>
-------------------------	------------

*Bose and Fermi Gases with Strong Anisotropic Interactions*

<b>John Bohn .....</b>	<b>109</b>
------------------------	------------

*Exploiting Universality in Atoms with Large Scattering Lengths*

<b>Eric Braaten .....</b>	<b>113</b>
---------------------------	------------

*Atomic and Molecular Physics in Strong Fields*

<b>Shih-I Chu .....</b>	<b>117</b>
-------------------------	------------

*Formation of Ultracold Molecules*

<b>Robin Côté .....</b>	<b>121</b>
-------------------------	------------

*Optical Two-Dimensional Fourier-Transform Spectroscopy of Semiconductors*

<b>Steven T. Cundiff .....</b>	<b>125</b>
--------------------------------	------------

*Theoretical Investigations of Atomic Collision Physics*

<b>A. Dalgarno.....</b>	<b>129</b>
-------------------------	------------

*Coherent Control of Multiphoton Transitions in the Gas and Condensed*

*Phases with Ultrashort Shaped Pulses*

<b>Marcos Dantus .....</b>	<b>133</b>
----------------------------	------------

*Interactions of Ultracold Molecules: Collisions, Reactions, and Dipolar Effects*

<b>D. DeMille .....</b>	<b>137</b>
-------------------------	------------

*Attosecond Science: Generation, Metrology, and Application*

<b>Louis F. DiMauro.....</b>	<b>140</b>
------------------------------	------------

*Imaging of Electronic Wave Functions During Chemical Reactions*

<b>Louis F. DiMauro.....</b>	<b>144</b>
------------------------------	------------

*High Intensity Femtosecond XUV Pulse Interactions with Atomic Clusters*

<b>Todd Ditmire .....</b>	<b>147</b>
---------------------------	------------

*Ultracold Molecules: Physics in the Quantum Regime*

<b>John Doyle .....</b>	<b>151</b>
-------------------------	------------

*Atomic Electrons in Strong Radiation Fields*

<b>J. H. Eberly</b> .....	<b>155</b>
<i>Few-Body Fragmentation Interferometry</i>	
<b>James M Feagin</b> .....	<b>159</b>
<i>Studies of Autoionizing States Relevant to Dielectronic Recombination</i>	
<b>T.F. Gallagher</b> .....	<b>163</b>
<i>Experiments in Ultracold Collisions and Ultracold Molecules</i>	
<b>Phillip L. Gould</b> .....	<b>167</b>
<i>Physics of Correlated Systems</i>	
<b>Chris H. Greene</b> .....	<b>170</b>
<i>Strongly-Interacting Quantum Gases</i>	
<b>Murray Holland</b> .....	<b>173</b>
<i>Using Intense Short Laser Pulses to Manipulate and View Molecular Dynamics</i>	
<b>Robert R. Jones</b> .....	<b>177</b>
<i>Ultrafast Atomic and Molecular Optics at Short Wavelengths</i>	
<b>Henry C. Kapteyn and Margaret M. Murnane</b> .....	<b>181</b>
<i>Detailed Investigations of Interactions between Ionizing Radiation and Neutral Gases</i>	
<b>Allen Landers</b> .....	<b>184</b>
<i>Properties of Actinide Ions from Measurements of Rydberg Ion Fine Structure</i>	
<b>Stephen R. Lundeen</b> .....	<b>188</b>
<i>Photoabsorption by Free and Confined Atoms and Ions</i>	
<b>Steven T. Manson</b> .....	<b>191</b>
<i>Electron-Driven Processes in Polyatomic Molecules</i>	
<b>Vincent McKoy</b> .....	<b>195</b>
<i>Electron/Photon Interactions with Atoms/Ions</i>	
<b>Alfred Z. Msezane</b> .....	<b>199</b>
<i>Theory and Simulations of Nonlinear X-Ray Spectroscopy of Molecules</i>	
<b>Shaul Mukamel</b> .....	<b>203</b>
<i>Nonlinear Photoacoustic Spectroscopies Probed by Ultrafast EUV Light</i>	
<b>Keith A. Nelson</b> .....	<b>207</b>
<i>Nonlinear Frequency Mixing with Coupled Gold Nanoparticles</i>	

<b>Lukas Novotny .....</b>	<b>211</b>
<i>Electron-Driven Excitation and Dissociation of Molecules</i>	
<b>A. E. Orel .....</b>	<b>215</b>
<i>Low-Energy Electron Interactions with Interfaces and Biological Targets</i>	
<b>Thomas M. Orlando.....</b>	<b>219</b>
<i>Energetic Photon and Electron Interactions with Positive Ions</i>	
<b>Ronald A. Phaneuf .....</b>	<b>223</b>
<i>Resonant and Nonresonant Photoelectron-Vibrational Coupling</i>	
<b>Erwin Poliakoff and Robert Lucchese .....</b>	<b>227</b>
<i>Control of Molecular Dynamics: Algorithms for Design and Implementation</i>	
<b>Herschel Rabitz .....</b>	<b>231</b>
<i>Interactions of Cold Rydberg Atoms in a High-Magnetic-Field Atom Trap</i>	
<b>G. Raithel .....</b>	<b>235</b>
<i>Dual Quantum Gases of Bosons: From Atomic Mixtures to Heteronuclear Molecules</i>	
<b>Chandra Raman.....</b>	<b>239</b>
<i>Coherent and Incoherent Evolution of Rydberg Atoms</i>	
<b>F. Robicheaux.....</b>	<b>242</b>
<i>High Harmonic Generation in Discharge-Ionized Plasma Channels</i>	
<b>Jorge J. Rocca.....</b>	<b>246</b>
<i>Development and Characterization of Replicable Tabletop Ultrashort Pulse X-Ray Sources</i>	
<b>Christoph G. Rose-Petrucci .....</b>	<b>250</b>
<i>New Directions in Intense-Laser Alignment</i>	
<b>Tamar Seideman .....</b>	<b>254</b>
<i>Ro-Vibrational Relaxation Dynamics of PbF Molecules</i>	
<b>Neil Shafer-Ray .....</b>	<b>258</b>
<i>Dynamics of Few-Body Atomic Processes</i>	
<b>Anthony F. Starace .....</b>	<b>262</b>

<i>Femtosecond and Attosecond Laser-Pulse Energy Transformation and Concentration in Nanostructured Systems</i>	
<b>Mark I. Stockman .....</b>	<b>266</b>
<i>Molecular Structure and Electron-Driven Dissociation and Ionization</i>	
<b>Vladimir Tarnovsky.....</b>	<b>270</b>
<i>Inner-Shell Electron Spectroscopy and Chemical Properties of Atoms and Small Molecules</i>	
<b>T. Darrah Thomas .....</b>	<b>274</b>
<i>Quantum Dynamics of Optically-Trapped Fermi Gases</i>	
<b>John E. Thomas.....</b>	<b>278</b>
<i>Laser-Produced Coherent X-Ray Sources</i>	
<b>Donald Umstadter .....</b>	<b>282</b>



# *Laboratory Research Summaries*

*(by institution)*



## **AMO Physics at Argonne National Laboratory**

R. W. Dunford, E. P. Kanter, B. Krässig, R. Santra, S. H. Southworth, L. Young  
*Argonne National Laboratory, Argonne, IL 60439*

dunford@anl.gov, kanter@anl.gov, kraessig@anl.gov, rsantra@anl.gov,  
southworth@anl.gov, young@anl.gov

Our central goal is to establish a quantitative understanding of x-ray interactions with free atoms and molecules. During the past year we have found that qualitatively new phenomena are accessible using strong optical fields derived from ultrafast lasers to control x-ray processes in isolated atoms and molecules. We have explored the intensity regime between  $10^{12}$ - $10^{15}$  W/cm<sup>2</sup> where the atomic and molecular response to a non-resonant laser field evolves from perturbation of atomic energy levels to strong-field ionization. At an intensity of  $10^{12}$  W/cm<sup>2</sup> we have demonstrated control of x-ray absorption by laser alignment of molecules. X-ray methods to detect aligned molecules are very general – unlike the optical dissociation/ionization methods which are confined to gas phase samples. At an intensity of  $10^{13}$  W/cm<sup>2</sup>, we have investigated the response of two prototypical atoms, krypton and neon. In neon we have theoretically predicted the phenomena of electromagnetically induced transparency (EIT) for x-rays. EIT provides an economical route to create and shape x-ray pulses using ultrafast laser pulses and thus may have considerable impact in ultrafast x-ray science. In both the aforementioned situations, the effect of the laser is completely reversible. However, at an intensity of  $10^{15}$  W/cm<sup>2</sup>, irreversible strong-field ionization of valence electrons occurs – enabling measurements of x-ray absorption spectra of ions. Beyond simple spectroscopy, we have this year used x-ray dichroism to deduce quantum state distributions of the residual ion and thus gain insight into the strong-field ionization process. We have also used the x-ray microprobe methodology to monitor collective response in the laser-produced plasma as a function of density and electron temperature. Our research represents a merging of two scientific areas - optical strong-field and x-ray physics. The advent of the world's first x-ray free electron laser, the Linac Coherent Light Source (LCLS) at Stanford in 2008/9 pushes this merger to an extreme as the exploration of nonlinear and strong-field phenomena in the hard x-ray regime becomes accessible for the first time. In preparation, we are investigating phenomena such as multiphoton hollow atom production and assisting in the design of first experiments. Finally, we are strongly engaged in the Short Pulse X-ray Project to produce tunable, polarized 1-ps hard x-ray pulses at Argonne's Advanced Photon Source. Recent progress and future plans are described below.

### **Resonant x-ray absorption by laser-aligned molecules**

S.H. Southworth, E.R. Peterson, C. Buth, D.A. Arms<sup>1</sup>, R.W. Dunford, C. Höhr,  
E. P. Kanter, B. Krässig, E.C. Landahl<sup>1</sup>, S.T. Pratt, R. Santra, L. Young

In the presence of a strong nonresonant linearly polarized laser field, molecules align due to interaction of the laser electric field vector with the molecular anisotropic polarizability. The alignment process is of intrinsic interest and of interest in applications to spectroscopy and photophysics, quantum control, high-harmonic generation, chemical

reactivity, liquids and solvation, and x-ray structural determination. Molecular alignment is normally probed by additional laser pulses that dissociatively ionize the molecule within an ion spectrometer that projects the fragments onto a position-sensitive detector and displays asymmetric fragmentation patterns. Our approach is different; we employ an x-ray spectroscopic probe of molecular alignment.

This year, we used tunable, polarized, microfocused x-ray pulses at Argonne's Advanced Photon Source to probe laser-aligned  $\text{CF}_3\text{Br}$ . The alignment was observed using the  $\text{Br } 1s \rightarrow \sigma^*$  x-ray absorption resonance at 13.476 keV. Since the absorption dipole moment is parallel to the C—Br axis, the absorption probability is sensitive to the angle between the molecular figure axis and the linear polarization vector of the x rays.  $\text{CF}_3\text{Br}$  was chosen because the x-ray beamline works well at the Br *K* edge, the pre-edge resonance is strong, and a rotationally-cooled molecular beam could be produced by expansion of a 5%- $\text{CF}_3\text{Br}$ /95%-He mixture through a pinhole nozzle. The molecules were aligned by 2 mJ, 95 ps, 1 kHz pulses from a 800-nm Ti:sapphire laser. A lens focused the laser pulses to 40  $\mu\text{m}$  FWHM within the molecular beam at a spatially-averaged peak intensity of  $\sim 9 \times 10^{11} \text{ W/cm}^2$ . A half-wave plate controlled the angle between the linear polarization vectors of the laser and x rays. Narrow band ( $\sim 0.7 \text{ eV}$  FWHM), 150 ps, 272 kHz x-ray pulses tuned to the  $\sigma^*$  resonance were focused to  $\sim 10 \mu\text{m}$  FWHM within the laser focal volume. Relative x-ray absorption rates were measured by recording 11.9-keV Br  $K\alpha$  x-rays with Si drift detectors positioned perpendicular to the beams. For timing control, the laser oscillator and Pockels' cell trigger are referenced to the storage ring's RF system. The fluorescent x rays were tagged "laser on" or "laser off" with timing gates.

An essential component of this project is the concurrent theoretical prediction of the laser alignment and x-ray probe observables for specific pulse parameters and molecular rotational temperature. A quantitative theoretical description of laser-controlled molecular x-ray absorption experiments was developed and applied to these experiments. Theory and experiment were compared for the cross correlation between laser and x-ray pulses, dependence of the x-ray absorption probability on the angle between the laser and x-ray polarization vectors, and dependence of the alignment on laser intensity. These comparisons led us to conclude that the rotational temperature of our molecules was  $\sim 20 \text{ K}$ . Consequently, the observable effects were modest ( $\sim 20\%$  variations) and the calculated  $\langle \cos^2 \theta \rangle \approx 0.40\text{--}0.45$ . However, the calculations also predict that much more dramatic effects would be observed for rotational temperatures  $\sim 5 \text{ K}$  and below. The calculations further show that, for our temperature regime, the alignment process can be described as essentially adiabatic, even though the 95 ps pulse duration is smaller than the 235 ps ground state rotational period.

A computer program was written (Buth and Santra) to calculate the rotational wave-packet dynamics of linear and symmetric-top molecules in a pulsed laser field. Input parameters such as the components of the polarizability tensor were calculated using the coupled-cluster method (CCSD) as implemented in the *ab initio* quantum chemistry package DALTON. Right below the bromine *K*-edge, the x-ray absorption spectrum of the  $\text{CF}_3\text{Br}$  molecule displays a strong absorption feature associated with a transition from  $\text{Br } 1s$  to a molecular  $\sigma^*$  orbital ( $A_1$  symmetry in  $C_{3v}$ ). Because the excitation of a bromine *K*-shell electron probes only the immediate vicinity of the Br nucleus, it is primarily the  $\text{Br } 4p_z$  AO component of the  $\sigma^*$  orbital that contributes to the

absorption cross section. (Here, the C-Br axis has been referred to as the z axis of the molecule-fixed frame.) Hence, for symmetry reasons, in the molecular frame two of the three components of the transition dipole vector vanish. In order to determine how the x-ray absorption anisotropy that is measured in the experiment is related to the degree of alignment of the molecular figure axis, we transformed the x-ray polarization vector from the laboratory frame to the instantaneous molecular frame. Currently, a central application of our theory is the extraction of the initial rotational temperature of the molecules from the laser-dependent x-ray absorption data. Our focus so far has been on relatively long laser and x-ray pulses. The upcoming 1-ps source at the APS will make it possible to study molecular alignment in the impulsive case, where the molecular frame does not adiabatically follow the temporal evolution of the aligning laser pulse. Using the code we have developed, it is planned to theoretically investigate x-ray absorption of impulsively aligned molecules using 1-ps x-ray pulses. A natural extension of this work will be the description of x-ray diffraction from laser-aligned molecules, another class of experiments that may be carried out at the APS. Here, one can use standard angular momentum algebra to transform the diffraction pattern from the molecular frame to the laboratory frame. The treatment of the rotational dynamics remains unchanged, of course.

In related experiments, the Ti:sapphire laser alone was used both to align and probe  $\text{CF}_3\text{Br}$ . A fraction of the pulse energy was compressed to 50 fs to strong-field ionize and dissociate the aligned molecules. The ion fragments were projected onto a position-sensitive detector, and the alignment was observed from the angular patterns of energetic  $\text{Br}^+$  fragments. Since the strong-field laser ionization and fragmentation process is not well known in this case, the data analysis is more complicated than for the relatively simple x-ray probe experiments.

A near-term goal of future work is to attain lower rotational temperatures of the target molecules in order to observe stronger alignment and probe signatures. A major effort is underway at the APS to produce x-ray pulse durations of one or a few ps using RF deflection cavities on the stored electron bunches. Short x-ray pulses will enable use of more flexible laser-alignment parameters and, more generally, of coherent control techniques. We are also planning to develop x-ray diffraction probes of aligned molecules for direct determination of molecular geometries.

### X-ray absorption by laser-dressed atoms

R. Santra, C. Butth, A. Belkacem<sup>3</sup>, R.W. Dunford, D.L. Ederer<sup>2</sup>, T.E. Glover<sup>3</sup>,  
P. Heimann<sup>3</sup>, E.P. Kanter, B. Krässig, R.W. Schoenlein<sup>3</sup>, S. H. Southworth, L. Young

A longstanding interest of our group has been the modification and control of x-ray processes using strong optical fields. The laser-induced modification of the x-ray photoabsorption cross section is the most basic of processes. In pursuit of this, we have developed an *ab initio* theory for the x-ray photoabsorption cross section of atoms in the field of an intense optical laser (up to  $10^{13} \text{ W/cm}^2$ ) [4]. The laser dresses the core-excited atomic states, which introduces a dependence of the cross section on the angle between the polarization vectors of the two linearly polarized radiation sources. We use the Hartree-Fock-Slater approximation to describe the atomic many-body problem in

conjunction with a non-relativistic quantum-electrodynamic approach to treat the photon-electron interaction. The continuum wave functions of ejected electrons are treated with a complex absorbing potential that is derived from smooth exterior complex scaling. The interaction with the laser is treated non-perturbatively by numerical diagonalization of the complex symmetric matrix representation of the x-ray-free part of the Hamiltonian. The coupling to the x-rays is treated perturbatively. We have used the theory to study the x-ray photoabsorption cross section of krypton atoms near the  $K$  edge [4]. A noticeable modification of the cross section is found in the presence of the optical laser. It may be possible to study this effect at the APS.

When we applied our theory of x-ray absorption by laser-dressed atoms to neon [1], we discovered that the dressing effect on the near- $K$ -edge spectrum is much more pronounced than in the case of Kr. A reason for this is that the lifetime of a  $K$ -shell hole in Ne is longer by a factor of ten in comparison to Kr. The amazing result of our *ab initio* studies is that we see a strong signature of electromagnetically induced transparency (EIT) in laser-dressed neon gas. This is the first example of EIT in the x-ray domain. We would like to mention that the EIT effect enabled researchers to slow light down to the speed of a bicycle. In the optical domain, where the decay widths are relatively small, one can use relatively weak lasers to induce EIT. Here, however, the minimum laser intensity required to observe EIT is of the order of  $10^{12} \text{ W/cm}^2$ , requiring short-pulse lasers. Since the binding energy of the Rydberg states populated via x-ray absorption is only of the order of 1 eV, the laser-electron interaction is highly nonperturbative. Our theory is suitable for describing this challenging situation, shown in Fig. 1. As discussed in Ref. [1], this work will open new opportunities for research with ultrafast x-ray sources. In particular, EIT can be used to produce ultrashort x-ray pulses using existing synchrotron radiation facilities. The disadvantage is that such pulses are not easily tunable. The research published in Ref. [1] is the subject of media coverage by AIP Physics News Update, PhysOrg.Com, and Argonne News. By exploiting EIT in Ne, tailored x-ray pulses near 870 eV can be produced, as shown in Fig. 2. We plan to use our code to study EIT near the  $K$  edge of argon. We hope to demonstrate that efficient x-ray pulse shaping near 3.2 keV is possible.

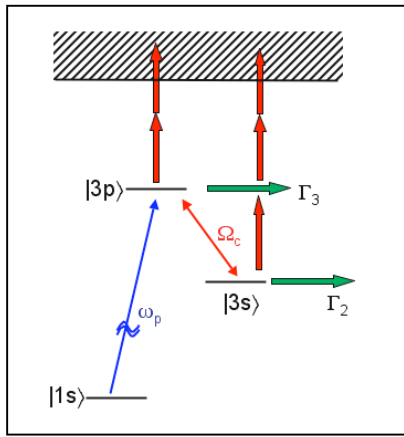


Fig. 1. X-ray EIT in neon. Transparency is induced on the  $1s \rightarrow 3p$  transition (blue arrow) via a 800 nm laser (red arrow) at an intensity  $\sim 10^{13} \text{ W/cm}^2$ . Competing processes – laser ionization, Auger decay are shown.

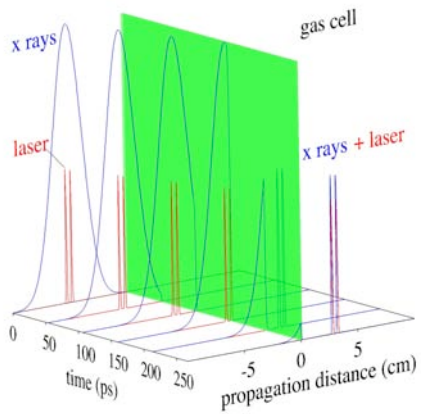


Fig. 2. Formation of two short x-ray pulses with laser-induced EIT in Ne. See Ref [1] for details.

We plan to experimentally demonstrate EIT for x rays at Berkeley's Advanced Light Source using the femtosecond laser slicing beamline to produce 200 fs soft x-ray pulses resonant with the  $1s \rightarrow 3p$  transition in neon. Overlap with an 800 nm dressing beam at an intensity of  $10^{13}$  W/cm<sup>2</sup> is predicted to produce a dramatic change in the  $1s \rightarrow 3p$  absorption cross section. An apparatus to detect the near  $K$ -edge absorption spectrum of laser-dressed neon, via both absorption and fluorescence signatures, was commissioned during a run in February 2007. Another beamtime is scheduled for October 2007.

### X-ray spectroscopy of optical-field-ionized atoms

R.W. Dunford, C. Buth, E. P. Kanter, B. Krässig, R. Santra,  
S. H. Southworth, L. Young

The strong electric fields produced by focused pulses of ultrafast optical lasers interact with atoms nonperturbatively and remove an outer-shell electron by multi-photon or tunnel ionization. Strong-field laser-atom interactions underlie current efforts to push high-harmonic generation into the soft x-ray regime and to generate and utilize attosecond light pulses. Theoretical models of laser ionization and high-harmonic generation are usually tested by comparison with measurements of ion charge-state yields, photoelectron spectra, or high-harmonic radiation. We have developed a spectroscopic probe of atoms and molecules in intense laser fields that uses tunable, polarized, microfocused x-ray pulses to record the associated x-ray absorption spectra [16]. Going beyond our initial observation that spin-orbit coupling was required to explain the ion alignment, this year we have developed methods to deduce the full quantum state distribution resulting from the strong-field ionization process using resonant polarized spectroscopic probes [2, 8]

Reference [16] by Argonne's AMOP group inspired Prof. Leone in Berkeley to perform a similar experiment [2]. Drs. Buth and Santra performed the theoretical analysis of the data. In the Berkeley experiment, it was demonstrated that high-order harmonic absorption spectroscopy allows one to resolve the complete  $|j,m\rangle$  quantum state distribution of  $\text{Xe}^+$  generated via optical strong-field ionization of Xe atoms. The laser-produced extreme ultraviolet (EUV) radiation probes the transition from the 4d core level to the 5p valence level of the  $\text{Xe}^+$  photoion. The extracted population distribution  $\rho_{j,|m|}$  is  $\rho_{3/2,1/2} : \rho_{1/2,1/2} : \rho_{3/2,3/2} = 75 \pm 6 : 13 \pm 6 : 12 \pm 3 \%$ , where the quantization axis is parallel to the polarization vector of the pump beam. A tunnel ionization calculation with the inclusion of spin-orbit coupling yields 83 : 14 : 3 % for the above ratio. Good agreement between experiment and theory for the  $\rho_{3/2,1/2} : \rho_{1/2,1/2}$  ratio highlights the importance of including spin-orbit coupling in tunnel ionization calculations. On the other hand, the measured  $\rho_{3/2,3/2} : \rho_{3/2,1/2}$  ratio is  $\sim 4$  times larger than the theoretical value and suggests the onset of nonadiabatic behavior in the strong-field ionization.

In our previous work on x-ray absorption spectroscopy of krypton ions produced in a strong optical field [16], we observed that when x-ray and laser polarizations are parallel, the resonant absorption associated with the  $1s \rightarrow 4p$  transition is stronger by a factor of two than in the case when the two polarization vectors are perpendicular. We were able to explain [19] that the primary reason why the ratio between the two cases is not nearly as large as expected in conventional strong-field ionization theories is the

impact of spin-orbit interaction in the cation. However, it was originally not attempted to use the experimental data to determine the  $\rho_{j,\lvert m \rvert}$  quantum-state distribution of the Kr ions. Inspired by the successful extraction of the  $\rho_{j,\lvert m \rvert}$  populations of laser-generated Xe ions (see above), it was realized that a similar procedure could be applied to the krypton data. The situation is more challenging because of the large decay width of the K-shell excited states observed in the Kr experiment carried out at the Advanced Photon Source. Therefore, more care is needed to separate the individual fine-structure components of the  $1s \rightarrow 4p$  transition. New experimental data with a higher resolution x-ray monochromator ( $\Delta E/E \sim 0.5 \times 10^{-5}$ ) were combined with newly formulated theoretical tools to extract the  $\rho_{j,\lvert m \rvert}$  populations [8]. Using the accurate reduced matrix elements calculated previously by Don Beck's group, we determined the experimental  $\rho_{j,\lvert m \rvert}$  quantum-state distribution and compared them with theory [8]. Theory and experiment agree that the majority of  $\text{Kr}^+$  ions produced are in the  $j = 3/2$  state. Theory predicts a noticeable degree of alignment in this state:  $\rho_{3/2;3/2}/\rho_{3/2;1/2} = 0.056$ . As in the Berkeley experiment, the observed ratio  $\rho_{3/2;3/2}/\rho_{3/2;1/2}$  is larger than the theoretical ratio. This may be an indication of a partial failure of the adiabatic picture. It turns out that in the Kr experiment at the APS, the sensitivity to the spatial anisotropy of the laser-produced ion is higher by an order of magnitude than in the Berkeley experiment on Xe.

Our adiabatic strong-field ionization theory reproduces the observed  $\rho_{j,\lvert m \rvert}$  with reasonable, though definitely not perfect accuracy [2,8]. In order to identify the origin of the remaining discrepancies, we plan to incorporate spin-orbit effects in Floquet theory. Within the tunneling picture, it is assumed that the atomic electrons follow the time evolution of the laser electric field instantaneously; an equivalent assumption is that the laser field oscillates extremely slowly. This assumption of adiabaticity works best in the infrared. But at optical wavelengths, it may not be sufficiently accurate. Nonadiabatic effects, caused by the fact that a photon carries a finite amount of energy, are most efficiently taken into account using Floquet theory, which may be derived from quantum electrodynamics in the strong-field limit [4]. The Floquet code we have written [1, 4] is based on nonrelativistic quantum mechanics. We anticipate that combining Floquet theory with spin-orbit coupling theory, quantitative agreement of our strong-field ionization calculations with the experiments mentioned above can be obtained.

In Refs. [2, 19], we have demonstrated that, at least in the case of Kr and Xe, the laser electric field, even at saturation, is not sufficiently strong to break spin-orbit coupling. However, our treatment was unsuitable to predict coherences in the density matrix of the residual cation that may be caused by the finite photon energy or the finite duration of the laser pulse. This makes a full time-dependent quantum treatment necessary. All shortcomings of the adiabatic approximation can be avoided in this way. (The Floquet theory mentioned in the previous paragraph will not allow us to identify effects that are due to finite pulse duration.) Therefore, we plan to extend the d-SAE method developed in Refs. [15, 23] by including spin-orbit interaction. We will derive the equations of motion and implement them in a computer program. This code will be used to investigate whether in the process of optical strong-field ionization, coherences remain in the ion density matrix. We expect that this will be the case for the light noble gases, but probably not for the heavier ones. If this turns out to be correct, then strong-field-ionized Ne (and maybe Ar) would be an excellent system for studying ultrafast electronic wave-packet dynamics in a time-resolved manner. This work provides

theoretical support for a planned experiment of our group in collaboration with Lou DiMauro and Pierre Agostini from Ohio State University.

There we plan to study strong-field ionization in an ion with lower Z,  $\text{Ne}^+$ , where the spin-orbit period (43 fs) is longer than in  $\text{Kr}^+$  and the field strength necessary for ionization is higher. Such a measurement will require shorter pump and probe pulses. We intend to use few-cycle infrared pump pulses and attosecond high-harmonic probe pulses produced in the Attosecond Laboratory at Ohio State University. We will measure the  $2s \rightarrow 2p$  cycling transition in  $\text{Ne}^+$  as a function of the pump probe delay for both parallel and perpendicular polarization directions to search for the characteristic oscillations of coherently excited quantum states.

### **Nonlinear x-ray processes using a self-amplified spontaneous emission free-electron laser**

R. Santra and N. Rohringer

Radiation pulses from free-electron lasers based on the principle of self-amplified spontaneous emission are chaotic. In general, this renders studies of multiphoton physics challenging. This project originally focused mainly on the question of pulse characterization. However, as we made progress, we realized that we have interesting things to say about the specific nature of x-ray nonlinear optics [7]. We applied a perturbative quantum electrodynamics approach to study nonlinear optical processes in the x-ray regime and their dependence on the generalized coherence properties of the radiation field. We focused on the parameter regime that is relevant for upcoming atomic physics experiments at short-wavelength free-electron lasers such as the LCLS. In contrast to the long-wavelength regime, x-ray nonlinear optical processes are characterized in general by sequential single-photon single-electron interactions. In principle, despite this fact, probabilities for these multiphoton processes involve higher-order correlation functions of the radiation field. We demonstrated that double-core-hole formation via x-ray two-photon absorption is enhanced by chaotic photon statistics. Numerical calculations using rate equations illustrated the impact of field chaoticity on x-ray nonlinear ionization of helium and neon for photon energies near 1 keV. In the case of neon, processes were discussed that involve up to seven photons. Assuming an x-ray coherence time of 2.6 fs, double-core-hole formation in neon was found to be statistically enhanced by about 30% at an x-ray intensity of  $10^{16} \text{ W/cm}^2$ . It also became clear during the course of this investigation that for processes that did not require photon absorption to take place within the lifetime of an inner-shell vacancy, the detailed x-ray pulse properties are irrelevant, as long as one averages over a number of shots. This means that for most experiments using LCLS, there is no need for a detailed shot-by-shot characterization of the x-ray pulses. So far we concentrated on the  $p \cdot A$  interaction operator. This is the only one that matters in the optical domain. However, at short wavelengths, this is only approximately true. The  $A^2$  operator must be expected to contribute to above-threshold ionization in the x-ray regime. We plan to look into this in the near future.

## Dynamics in laser-generated plasmas

E. P. Kanter, R. W. Dunford, D. L. Ederer<sup>2</sup>, C. Höhr, B. Krässig, E. C. Landahl<sup>1</sup>,  
E. R. Peterson, J. Rudati<sup>1</sup>, R. Santra, S. H. Southworth, L. Young

When strong optical lasers are focused on gas-phase atoms and molecules, one necessarily produces a transient plasma when the target atoms are ionized by the laser. The densities are fairly high ( $\sim 10^{14}/\text{cm}^3$ ), while the laser-ionized electrons are fairly hot ( $\sim U_p = 12 \text{ eV}$ ). The Debye length is large ( $\sim 2\mu\text{m}$ ) compared to the interparticle spacing ( $\sim 0.1\mu\text{m}$ ) and the plasmas are weakly coupled ( $\Gamma \sim 0.6$ ). As a result of these considerations, a fraction of the hot electrons leave the volume explored by our x-ray microprobe comparatively rapidly (typically 10-20 ns) leaving behind the colder positive ions which then expand due to their mutual Coulomb repulsion.

In the past year, we have completed a comprehensive set of measurements investigating the spatial- and time-dependence of the ion distributions for various densities. This work was carried out with both circular and linearly polarized light. This allows us to explore the dependence of the expansion on the electron velocity distribution resulting from the initial strong-field ionization (see Fig. 3). The figure shows spatial

distributions of the  $\text{Kr}^+$  ions for different delays of the x-ray probe from the ionizing laser pulse. With the hotter electron distribution created by the circularly-polarized laser, one observes a faster rate of expansion of the ion cloud. We also performed a measurement of the laser-produced alignment in the presence of an external magnetic field that corroborated our previous finding of a substantially slower depolarization time with magnetic field than without. A more extensive study of the magnetic field effect will be carried out later this year. We plan to use these new data, together with ongoing simulations, to elucidate the role of electron-ion collisions in the depolarization of the tunnel-ionized ions.

In order to understand the data obtained by probing this complex environment, we developed a computer code to simulate the electron and ion dynamics in this plasma and during the past year have made a number of improvements to

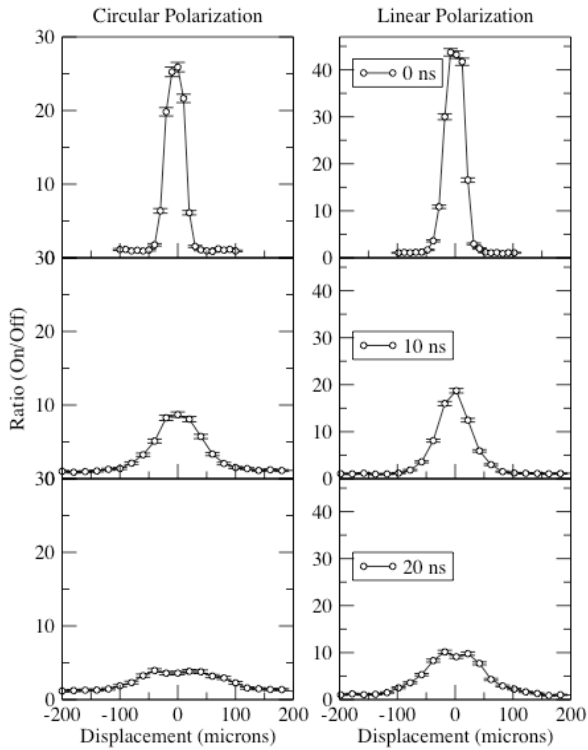


*Fig. 3. Expansion of a laser-produced plasma for different electron temperatures derived from linearly- and circularly polarized strong-field ionization.*

that code to improve the accuracy and permit the application of external fields. Simulations have previously been carried out with a highly specialized computer code that follows the trajectories of 10,000 particles ( $\text{Kr}^+$ ,  $\text{Kr}^{++}$ , and  $e^-$ ) using 4th-order Runge-Kutta numerical integration of the equations of motion with adaptive step control based on conservation of energy. The initial conditions were given by a Stark-ionization calculation using Herman-Skillman wavefunctions, a complex absorbing potential and numerical integration of rate equations. Using effective masses and charges scaled to give the Coulomb energy and particle accelerations corresponding to the actual experimental Kr density, we were able to deduce final kinetic energies as well as the time-dependent spatial densities of both charge states from the simulated results. While highly successful at computing those quantities, those computations provided only a crude approximation and cannot be used for simulating collisional processes at higher densities. We have now developed a new method that overcomes those shortcomings. It is based on computing the motion in the transverse plane assuming each of the source points to be represented by a finite line of charge. This method allows us to work at the proper density in a thin slab and thus will permit generalizations such as external fields and ion-electron collisions. By parallelizing the force computation, the most cpu-intensive part of the calculation, we plan on porting this work to Argonne's 350-node Jazz computing cluster. Such a development would allow the generalizations discussed above.

### **Picosecond x rays at Argonne's Advanced Photon Source**

B. Krässig, R.W. Dunford, E.P. Kanter, S.H. Southworth, L. Young,  
Photosynthesis Group, FOCUS, APS staff

Development of a broadly tunable, polarized 1-ps x-ray source at the Sector 7 undulator beamline has been undertaken by the Advanced Photon Source and many collaborators. This complex project has been named the Short Pulse X ray Project (SPX). The APS storage ring has a nominal bunchlength of 100 ps, but rf deflection methods proposed by Zholents *et al.* to tilt the electron bunch can produce much shorter x-ray pulses when viewed through a slit. The projected output is 1-ps x-ray pulses, tunable between 6-20 keV, with  $10^6$  photons/pulse in a 1% bandwidth operating at 1 kHz. While the projected pulse length is longer than the LCLS and the photon number smaller, the easy tunability makes this source complementary and useful for tracking many processes with picosecond and picometer resolution. The SPX project has three main tasks: 1) additions to the storage ring structure, 2) optimization of the x-ray optics beamline and 3) development of experimental capabilities. The AMO group has been participating actively in the latter two tasks. The APS accelerator group has modeled extensively the electron trajectories in the storage ring and devised designs for the rf deflection cavities. It is anticipated that installation of the rf cavities will be completed in September 2008. The AMOP group is spearheading an effort to improve flux 100 $\times$ , using pink beam, to permit studies of non-periodic samples, i.e. isolated molecules in gas or solution phase.

## Theory of x-ray diffraction from single molecules at x-ray FELs

R. Santra

Creating an x-ray diffraction pattern from a *single* molecule using a *single* x-ray pulse implies that more than one photon must be scattered during the collision of the x-ray pulse with the molecule. This means that the usual description of x-ray diffraction in terms of one-photon scattering, which is valid for experiments with existing x-ray sources, is insufficient for the proposed single-(bio)molecule imaging experiments planned at x-ray FELs. Standard x-ray scattering theory, which among other things assumes a static electron distribution during the elastic collision of the molecule with the x-ray photon, is not suited to describing this new situation. Our plan is to extend the theory developed in Ref. [7] in connection with pure x-ray absorption to the problem of combined x-ray absorption and scattering. This should be relatively straightforward, because at photon energies high above all inner-shell thresholds, x-ray scattering is mediated exclusively by individual single-point vertices with respect to the  $A^2$  operator. Finally, using density-matrix techniques [7], we plan to explore the impact of the longitudinal incoherence (chaoticity) of LCLS on nonlinear x-ray diffraction. The information obtained will be important for future x-ray diffraction experiments using free-electron lasers.

<sup>1</sup>Advanced Photon Source, Argonne National Laboratory, Argonne, IL 60439

<sup>2</sup>Tulane University

<sup>3</sup>Lawrence Berkeley National Laboratory, Berkeley, CA 94720

### Publications 2005 - 2007

- [1] Electromagnetically induced transparency for x rays  
Christian Buth, Robin Santra, Linda Young, Phys. Rev. Lett. **98**, 253001 (2007).
- [2] Quantum state-resolved probing of strong-field-ionized xenon atoms  
Z-H. Loh, M. Khalil, R. E. Correa, R. Santra, C. Buth, S. Leone, Phys. Rev. Lett. **98**, 143601 (2007).
- [3] Measurement of the x-ray mass attenuation coefficient and determination of the imaginary component of the atomic form factor of tin of the energy range of 29-60 keV.  
M. de Jonge, C. Tran, C.T. Chantler, Z. Barnea, B.B. Dhal, D. Paterson, E.P. Kanter, S.H. Southworth, L. Young, M.A. Beno, J. A. Linton and G. Jennings, Phys. Rev. A **75**, 032702 (2007).
- [4] Theory of x-ray absorption by laser-dressed atoms  
C. Buth and R. Santra, Phys. Rev. A **75**, 033412 (2007).
- [5] A simple short-range point-focusing spatial filter for time-resolved x-ray fluorescence  
C. Höhr, E.R. Peterson, E.C. Landahl, D. A. Walko, R.W. Dunford, E.P. Kanter, and L. Young, SYNCHROTRON RADIATION INSTRUMENTATION: Ninth International Conference on Synchrotron Radiation Instrumentation, AIP Conference Proceedings 879, 1226-1229 (2007).

- [6] Alignment dynamics in a laser-produced plasma  
C. Höhr, E.R. Peterson, J. Rudati, D.A. Arms, E.M. Dufresne, R.W. Dunford, D.L. Ederer, E.P. Kanter, B. Krässig, E.C. Landahl, R. Santra, S.H. Southworth, and L. Young Phys. Rev. A 75, 011403R (2007).
- [7] X-ray nonlinear optical processes using a self-amplified spontaneous emission free-electron laser  
N. Rohringer and R. Santra, Phys. Rev. A submitted (2007).
- [8] K-edge absorption spectra of laser-generated  $\text{Kr}^+$  and  $\text{Kr}^{2+}$   
S.H. Southworth, D.A. Arms, E.M. Dufresne, R.W. Dunford, D.L. Ederer, C. Höhr, E.P. Kanter, B. Krässig, E.C. Landahl, E.R. Peterson, J. Rudati, R. Santra, D. A. Walko, and L. Young, Phys. Rev. A submitted (2007).
- [9] Strong-field control of x-ray absorption  
R. Santra, C. Butth, E. Peterson, R.W. Dunford, E.P. Kanter, B. Krässig, S.H. Southworth, L. Young, submitted (2007).
- [10] X-ray absorption by laser-aligned molecules  
E.R. Peterson et al., submitted (2007).
- [11] Double  $K$ -shell photoionization of silver  
E. P. Kanter, I. Ahmad, R. W. Dunford, D. S. Gemmell, B. Krässig, S. H. Southworth and L. Young, Phys. Rev. A 73, 022708, 1-11 (2006).
- [12] Photo double detachment of  $\text{CN}^-$ : electronic decay of an inner-valence hole in molecular anions  
R. C. Bilodeau, C. W. Walter, I. Dumitriu, N. D. Gibson, G. D. Ackerman, J. D. Bozek, B. S. Rude, R. Santra, L. S. Cederbaum and N. Berrah, Chem. Phys. Lett. 426, 237-241 (2006).
- [13] Two-photon decay in gold atoms,  
R. W. Dunford, E. P. Kanter, B. Krässig, S. H. Southworth, L. Young, P. H. Mokler, T. Stöhlker and S. Cheng, Phys. Rev. A 74, 012504, 1-11 (2006).
- [14] Three-step model for high harmonic generation in many-electron systems  
R. Santra and A. Gordon, Phys. Rev. Lett. 96, 073906 (2006).
- [15] Role of many-electron dynamics in high harmonic generation,  
A. Gordon, F. X. Kärtnner, N. Rohringer and R. Santra, Phys. Rev. Lett. 96, 223902 (2006).
- [16] X-ray microprobe of orbital alignment in strong-field ionized atoms,  
L. Young, D. A. Arms, E. M. Dufresne, R. W. Dunford, D. L. Ederer, C. Höhr, E. P. Kanter, B. Krässig, E. C. Landahl, E. R. Peterson, J. Rudati, R. Santra and S. H. Southworth, Phys. Rev. Lett. 97, 083601 (2006).
- [17] Low-energy nondipole effects in molecular nitrogen valence-shell photoionization,  
O. Hemmers, R. Guillemin, D. Rolles, A. Wolska, D. W. Lindle, E. P. Kanter, B. Krässig, S. H. Southworth, R. Wehlitz, B. Zimmermann, V. McKoy and P. W. Langhoff, Phys. Rev. Lett. 97, 103006 (2006).
- [18] Why complex absorbing potentials work : a DVR perspective,  
R. Santra, Phys. Rev. A 74, 034701 (2006).
- [19] Spin-orbit effect on strong-field ionization of krypton,  
R. Santra, R. W. Dunford and L. Young, Phys. Rev A 74, 043403 (2006).

- [20] X-ray microprobe of optical strong-field processes,  
 L. Young, R. W. Dunford, C. Höhr, E. P. Kanter, B. Krässig, E. R. Peterson, S. H. Southworth, D. L. Ederer, J. Rudati, D. A. Arms, E. R. Dufresne and E. C. Landahl, Radiat. Phys. Chem. **75**, 1799 (2006).
- [21] Double  $K$ -photoionization of heavy atoms,  
 E. P. Kanter, R. W. Dunford, B. Krässig, S. H. Southworth and L. Young, Radiat. Phys. Chem. **75**, 1529 (2006).
- [22] Nondipole asymmetries of  $K$ -shell photoelectrons of Kr, Br<sub>2</sub>, and BrCF<sub>3</sub>,  
 S. H. Southworth, R. W. Dunford, E. P. Kanter, B. Krässig, L. Young, L. A. LaJohn and R. H. Pratt, Radiat. Phys. Chem. **75**, 1574 (2006).
- [23] Configuration-interaction-based time-dependent orbital approach for ab initio treatment of electronic dynamics in a strong optical laser field  
 N. Rohringer, A. Gordon, and R. Santra, Phys. Rev. A **74** (2006) 043420
- [24] Higher-order processes in x-ray photoionization of atoms,  
 E. P. Kanter, R. W. Dunford, B. Krässig, S. H. Southworth and L. Young, Radiat. Phys. Chem. **75**, 2174 (2006).
- [25] Coster-Kronig transition probability  $f_{23}$  in gold atoms,  
 R. W. Dunford, E. P. Kanter, B. Krässig, S. H. Southworth, L. Young, P. H. Mokler, T. Stöhlker, S. Cheng, A. G. Kochur and I. D. Petrov, Phys. Rev. A **74**, 062502 (2006).
- [26] Imaging molecular orbitals using photoionization,  
 R. Santra, Chem. Phys. **329**, 357 (2006).
- [27] Interaction of intense vuv radiation with large xenon clusters,  
 Z. B. Walters, R. Santra and C. H. Greene, Phys. Rev. A **74**, 043204 (2006).
- [28] Nondipole effects in molecular nitrogen valence shell photoionization,  
 O. Hemmers, R. Guillemin, D. Rolles, A. Wolska, D. W. Lindle, E. P. Kanter, B. Krässig, S. H. Southworth, R. Wehlitz, B. Zimmermann, V. McKoy and P. W. Langhoff, J. Elec. Spec. **144-147**, 155-156 (2005).
- [29] Photo double ionization of helium 100 eV and 450 eV above threshold : C. gerade and ungerade amplitudes and their relative phase,  
 A. Knapp, B. Krässig, A. Kheifets, I. Bray, T. Weber, A. L. Landers, S. Schössler, T. Jahnke, J. Nickles, S. Kammer, O. Jagutzki, L. P. H. Schmidt, M. Schöffler, T. Osipov, M. H. Prior, H. Schmidt-Böcking, C. L. Cocke and R. Doerner, J. Phys. B **38**, 645-657 (2005).
- [30] Extreme-ultraviolet wavelength and lifetime measurements in highly ionized krypton, K. W. Kukla, A. E. Livingston, C. M. V. Vogt, H. G. Berry, R. W. Dunford, L. J. Curtis and S. Cheng, Can. J. Phys. **83**, 1127-1139 (2005).
- [31] Time-resolved activities at the Advanced Photon Source requiring the pulsed structure of the x-ray beam,  
 J. Wang, E. Landahl, T. Gruber, R. Pahl, L. Young, L. X. Chen and E. E. Alp, Synch. Rad. News **18**, 24 (2005).

## OVERVIEW 2007

The J.R.Macdonald Laboratory focuses on the interaction of intense-laser pulses with matter. The targets include neutral single atoms and molecules in the gas phase, single ions in our accelerator beams, trapped atoms in our MOTRIMS systems and nanostructures. In addition we pursue several outside collaborations at other facilities and with other groups (ALS, ALLS, University of Colorado, Columbia University, Weizmann Institute). Most of the work is associated with one or more of the following themes:

**1) Attosecond physics** (*Chang, Cocke, Lin, Ben-Itzhak, Litvinyuk*): The ultimate goal of this work is to follow, in real time, electronic motion in atoms and molecules. We have developed a double optical gating method (polarization gating combined with second harmonics) which greatly increases the efficiency with which single attosecond pulses can be generated. EUV/infrared pump-probe experiments are being carried out for diagnosis of the attosecond pulses. Theoretical analyses of EUV/EUV pump-probe experiments have shown that highly correlated electron motion in atoms can be probed with attosecond pulse pairs. The general role of electron extraction and rescattering, including harmonic generation and elastic scattering, has been investigated both theoretically and experimentally.

**2) Time-resolved dynamics of heavy-particle motion in neutral molecules** (*Cocke, Esry, Litvinyuk, Lin, Thumm*): We continue to develop methods for following the evolution of heavy particle motion in simple molecules in real time, following excitation by short laser pulses. We have identified rotational wave packet revivals in molecular H<sub>2</sub> and D<sub>2</sub> and have investigated the time dependent isomerization of acetylene to vinylidene. We have identified a new resonant mechanism for dissociative ionization of H<sub>2</sub>(<sup>+</sup>) and D<sub>2</sub>(<sup>+</sup>) over a range of photon wavelengths. We have explored a number of new theoretical approaches to the analysis of the dynamics of these few-body systems.

**3) Control** (*Chang, Cocke, DePaola, Esry, Lin, Litvinyuk, Thumm*): Methods for controlling the motion of heavy particle motion in small molecules continue to be developed. Theoretically, the ability to control the dissociation of molecules (H<sub>2</sub><sup>+</sup>, D<sub>2</sub><sup>+</sup>) into different final channels has been investigated by the application of pulse pairs and CEP control has been explored. The extraction of potential surfaces from experimental measurements of kinetic energy release versus pump-probe time delay has been demonstrated. The use of MOTRIMS to analyze in real time the evolution of population distributions in laser pumped targets has been extended to associative ionization. Short shaped (chirped) pulses from the KLS, which present a broad range of frequencies whose relative phases are known, are being used to explore mechanisms for the latter process.

**4) Studies involving simultaneous use of laser and accelerators** (*Ben-Itzhak, Carnes, Chang, Cocke, DePaola, Esry*): Ionization and dissociation of H<sub>2</sub><sup>+</sup>, D<sub>2</sub><sup>+</sup>, N<sub>2</sub><sup>+</sup> and O<sub>2</sub><sup>+</sup> has been investigated using the ion beams from our ECR source. New mechanisms for these processes have been identified using the momentum distributions from the products. Development of short ion pulses from our Tandem accelerator continues.

**5) Photons from the KLS interacting with solids and clusters** (*Richard, Thumm*):

Electron dynamics in photo-ionization and excitation of nanotubes continues. An external collaboration in this area with Columbia University has been established. Theoretical investigation of neutralization of negative ions near surfaces has been carried out.

Details of the above projects are provided in the individual contributions of the above-named PIs.

## Structure and Dynamics of Atoms, Ions, Molecules, and Surfaces: Molecular Dynamics with Ion and Laser Beams

*Itzik Ben-Itzhak, J. R. Macdonald Laboratory, Kansas State University  
Manhattan, Ks 66506; ibi@phys.ksu.edu*

*The goal of this part of the JRML program is to study the different mechanisms for molecular dissociation initiated by ultrashort intense laser pulses or following fast or slow collisions. To that end we typically use molecular ion beams as the subject of our studies.*

Below we give a couple of examples of our recent work<sup>1</sup>.

**Enhanced high-order above-threshold dissociation of a H<sub>2</sub><sup>+</sup> beam in 7 fs laser pulses,** *J. McKenna, A.M. Sayler, F. Anis, B. Gaire, Nora G. Johnson, E. Parke, H. Mashiko, C.M. Nakamura, E. Moon, Z. Chang, K.D. Carnes, B.D. Esry, I. Ben-Itzhak*

*This work is the direct result of close collaboration between theory and experiment. The control of transitions in crossings between dressed states was investigated experimentally and theoretically. As a consequence, a new mechanism of molecular dissociation was uncovered, above threshold dissociation of the n=2 manifold, and high-order ATD was enhanced.*

Extensive laser-molecule interrogation of the hydrogen molecular ion [1] continues to unveil new surprises, helping to generate a more complete view of molecular dynamics. Most recently this has been evidenced by new structure in the kinetic energy release (KER) spectra of this molecule following intense-field ionization [2, Pub. #10].

Our recent molecular-ion beam work, using coincidence 3D momentum imaging [Pub #5,11], was focused on the fragmentation of H<sub>2</sub><sup>+</sup>, HD<sup>+</sup>, and D<sub>2</sub><sup>+</sup> induced by intense few-cycle (7 fs) 790 nm laser pulses. Pulses of this duration open the exciting prospect of dynamically studying sub-vibrational period (< 14 fs) processes. In particular, we set our goal to enhance high-order ( $\geq$  3-photon) above-threshold dissociation (ATD) by closing the routes to lower photon-number channels. This is conceptually demonstrated in Fig. 1(left), where the 3-photon ATD leads to either a higher KER if the dissociating wave packet stays on the 2pσ<sub>u</sub>-3ω curve or a lower KER if a transition to the 1sσ<sub>g</sub>-2ω dressed state occurs at the next crossing. If the laser intensity falls fast enough between the moment ATD was initiated and the time the wave packet passes through the next crossing, then the transition probability to the 1sσ<sub>g</sub>-2ω state will be significantly reduced, i.e. this channel will be closed. The successful control of the latter transition will manifest itself as an enhancement of high-KER dissociation. It is important to note that in most measurements only net 2-photon ATD (i.e. 1sσ<sub>g</sub>-2ω final state) is observed, thus indicating how impressive the first observation of ATD [3] was.

Numerical solution of the full-dimensional Schrödinger equation (including vibration, rotation, and electronic excitation – see Esry's abstract for details) shows that high-order ATD from the lowest H(n=1) manifold yields high-KER dissociation as expected from the simple argument above. In addition, however, the calculations show that ATD from the excited H(n=2) manifold can be equally important. These exciting findings are indeed evidenced in our experimental results, shown in Fig. 1(right). Note that the slower dissociating D<sub>2</sub><sup>+</sup> yields higher KER than H<sub>2</sub><sup>+</sup> indicating a more efficient channel closing. This assertion is supported by our calculations that predict less excitation to the n=2 manifold for the more massive D<sub>2</sub><sup>+</sup>. In contrast, most of the high KER observed for H<sub>2</sub><sup>+</sup> is due to ATD from the n=2 excited states.

---

<sup>1</sup>Some of our studies are done in collaboration with Z. Chang's group, C.W. Fehrenbach, and others.

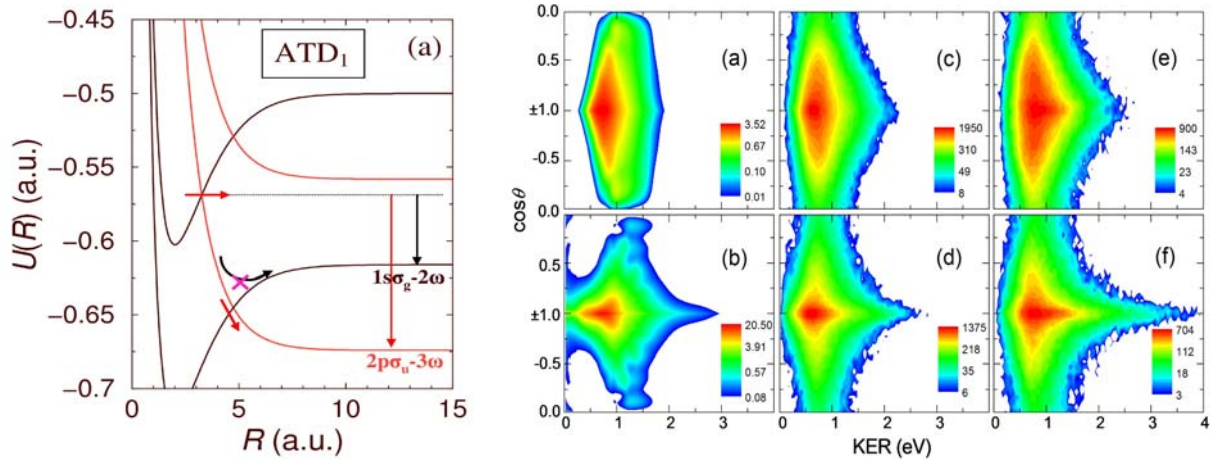


**Figure 1.** *Left:* The diabatic Floquet potentials for  $H_2^+$ . Besides the molecular quantum numbers, each curve carries a photon number label. *Right:* (a) and (b) computed KER-cos $\theta$  distributions for  $2 \times 10^{13}$  and  $1 \times 10^{14}$  W/cm $^2$ , respectively. (c) and (d) measured KER-cos $\theta$  distributions for  $H_2^+$  at  $2 \times 10^{13}$  and  $2.5 \times 10^{15}$  W/cm $^2$ , respectively. (e) and (f) measured KER-cos $\theta$  distributions for  $D_2^+$  at the same intensities.

**Intense short pulse laser-induced ionization and dissociation of  $O_2^+$  and  $N_2^+$  beams – A.M. Sayler, P.Q. Wang, B. Gaire, Nora G. Johnson, E. Parke, K.D. Carnes, B.D. Esry, I. Ben-Itzhak**

*The goal for this project was to expand the knowledge we have gained from  $H_2^+$  studies to more complex molecules and identify their dissociation pathways and mechanisms.*

The laser induced dissociation and ionization of multi-electron molecular ions yields a structure-rich KER and angular spectrum [1, Pub. #16], as shown in Fig. 2(left). However, the interpretation of these spectra is much more complex than for  $H_2^+$  due to the plethora of potential energy curves available (i.e. possible electronic states). Recently, we have presented a method to identify the dissociation pathways of  $O_2^+$  in 45 fs laser pulses [Pub. #13]. The method takes advantage of the shape of the measured KER distribution of each feature in the KER-cos $\theta$  spectra (e.g. channels  $\alpha$  and  $\beta$  in Fig. 2), the angular distribution – separating parallel and perpendicular transitions, the intensity slices – helping identify the number of photons involved, as well as all the knowledge we have gained from our  $H_2^+$  studies. For example, channel  $\beta$  that dominates the lower intensities measured has an angular distribution matching well the decay of the metastable  $a^4\Pi_u$  state [4] through the pathway  $a^4\Pi_u \rightarrow f^4\Pi_g - 1\omega \rightarrow ^4\Sigma_u^+ - 2\omega$ , as shown in Fig. 2(right). The two consequent parallel and perpendicular transitions (i.e.  $\Delta\Lambda=0,1$ ) can be viewed as a “double bond softening” dissociation mechanism.

At present we are studying the dissociation and ionization of  $N_2^+$  and  $O_2^+$  by 7 fs intense laser pulses (up to  $\sim 10^{15}$  W/cm $^2$ ). The  $N_2^+$  molecular-ion beam, produced in an electron impact ion source, is a unique system to study as its initial state is mostly in the lowest vibrational levels (mostly  $v=0$  and 1). Thus, in contrast to other molecular-ion beams, contributions from a broad range of vibrational states are eliminated. Furthermore, since the  $v=0$  state of  $N_2^+$  is deeply bound by an energy of more than 5 photons, all breakup channels are in the many-photon regime, and dissociation and ionization rates are comparable. We observed several intriguing features, including low ( $\sim 1$  eV) and unusually high ( $\sim 8$  eV) kinetic energy release (KER) many-photon dissociation of  $N_2^+$ . This is in contrast to our  $O_2^+$  data, which displays significantly different dynamics as it is initially in a wide vibrational distribution of both the doublet ground state and lowest-lying quartet state [4]. Similarly, the ionization of  $N_2^+$  shows a high-KER distribution

about 7 eV above the more common distribution centered around 8 eV. The latter is the only peak in our  $O_2^+$  data.

We have also measured the angular distributions of  $O_2^+$  and  $N_2^+$  ionization. The angular distributions for the respective neutral molecules are significantly different from each other, reflecting the difference between the “electron clouds” [5]. Our data is consistent with previous findings indicating that the assumptions about electron rescattering in the previous study, which are not needed in our case, were valid. Furthermore, our data indicates that post-ionization rotation is important as suggested by Tong *et al.* [6].

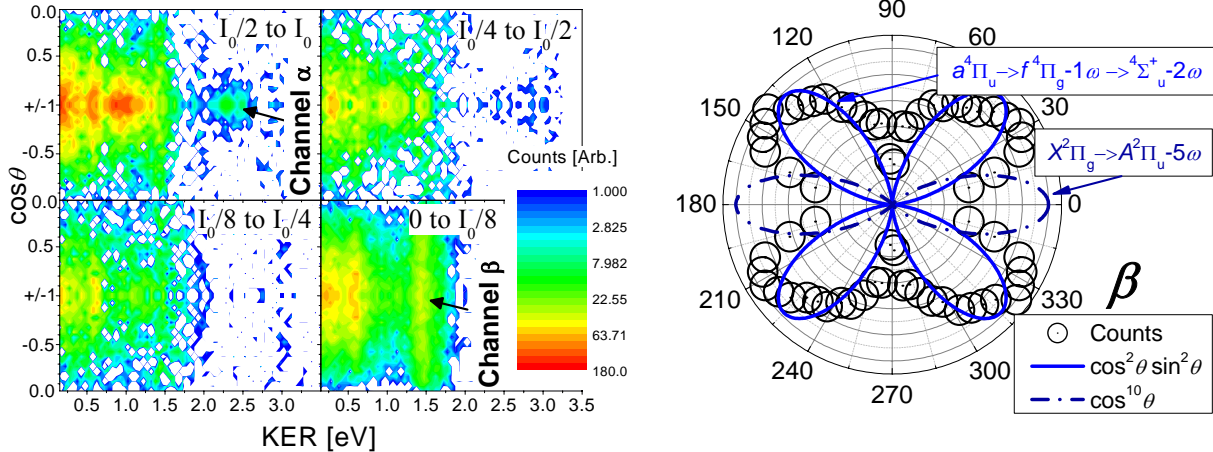


**Figure 2.** *Left:* KER- $\cos\theta$  distributions for  $O_2^+$ , where  $\theta$  is the angle between the molecular axis and the laser polarization. The four panels represent the distributions for different intensity slices obtained using the intensity difference spectrum method [Pub. #3], where  $I_0 \approx 1.3 \times 10^{15} \text{ W/cm}^2$ . *Right:*  $\cos\theta$  distributions for the channel labeled  $\beta$  in the KER- $\cos\theta$  distribution. This is a particularly interesting dissociation channel as the angular distribution is not aligned along the laser polarization.

In addition to the projects described in some detail above, we have studied a few other molecular-ion beams with our short-pulse laser and extended our studies to include few-cycle pulses. Furthermore, we have conducted a few ion-molecule collision experiments [see, for example, Pub. #9,14]. In parallel, we are upgrading our molecular dissociation imaging setup for upcoming studies of collisions of a few keV molecular ion beams with atomic targets.

**Future plans:** We are in the process of analyzing recent measurements of molecular-ion beams interrogated by intense few cycle pulses. We will continue interrogating  $H_2^+$  beams with shorter pulses, and attempt to measure the predicted effects of the carrier envelop phase (CEP) on  $HD^+$  laser induced dissociation [7]. Further improvements are required to bring this project to completion. Progress has been made on the understanding of the dissociation and ionization of more complex diatomic molecules, such as  $O_2^+$  and  $N_2^+$ , and we will continue our efforts in this direction. Finally, we hope to finish the upgrade of our new experimental setup, which will enable kinematically complete studies of dissociative capture at keV energies.

1. J.H. Posthumus, Rep. Prog. Phys. **67**, 623 (2004); and references therein.
2. A. Staudte *et al.*, Phys. Rev. Lett. **98**, 073003 (2007).
3. P.H. Bucksbaum, A. Zavriyev, H.G. Muller, and D.W. Schumacher, Phys. Rev. Lett. **64**, 1883 (1990); A. Zavriyev, P.H. Bucksbaum, H.G. Muller, and D.W. Schumacher, Phys. Rev. A **42**, 5500 (1990).
4. A. Tabche-Fouhaille, *et al.*, Chem. Phys. **17**, 81 (1976).
5. A.S. Alnaser, Phys. Rev. Lett. **93**, 113003 (2004).
6. X. M. Tong *et al.*, J. Phys. B **38**, 333 (2005).
7. V. Roudnev, B.D. Esry, and I. Ben-Itzhak, Phys. Rev. Lett. **93**, 163601 (2004).

## Publications of DOE sponsored research in the last 3 years:

16. "Molecular ion beams interrogated with ultrashort intense laser pulses", I. Ben-Itzhak, *Progress in Ultrafast Intense Laser Science*, edited by Kaoru Yamanouchi and Andreas Becker (Springer Book Series Chemical Physics 2007) (**accepted**) (2007).
15. "Picosecond Ion pulses from an EN tandem created by a femtosecond Ti:sapphire laser", K.D. Carnes, C.L. Cocke, Z. Chang, I. Ben-Itzhak, H.V. Needham, and A. Rankin, *Nucl. Instrum. Methods B* **261**, 106 (2007).
14. "Systematic study of charge state and energy dependence of TI to SC ratios for F<sup>q+</sup> ions incident on He", R. Ünal, P. Richard, I. Ben-Itzhak, C.L. Cocke, M.J. Singh, H. Tawara, and N. Woody, *Phys. Rev. A* **76**, 012710 (2007).
13. "Determining laser-induced dissociation pathways of multi-electron diatomic molecules: application to the dissociation of O<sub>2</sub><sup>+</sup> by high intensity ultrashort pulses", A.M. Sayler, P.Q. Wang, K.D. Carnes, B.D. Esry, and I. Ben-Itzhak, *Phys. Rev. A* **75**, 063420 (2007).
12. "Determining the absolute efficiency of a delay line microchannel-plate detector using molecular dissociation", B. Gaire, A.M. Sayler, P.Q. Wang, Nora G. Johnson, M. Leonard, E. Parke, K.D. Carnes, and I. Ben-Itzhak, *Rev. Sci. Instrum.* **78**, 024503 (2007).
11. "Dissociation of H<sub>2</sub><sup>+</sup> in intense femtosecond laser fields studied by coincidence three-dimensional momentum imaging", P.Q. Wang, A.M. Sayler, K.D. Carnes, J.F. Xia, M.A. Smith, B.D. Esry, and I. Ben-Itzhak, *Phys. Rev. A* **74**, 043411 (2006).
10. "Above threshold Coulomb explosion of molecules in intense laser pulses", B.D. Esry, A.M. Sayler, P.Q. Wang, K.D. Carnes, and I. Ben-Itzhak, *Phys. Rev. Lett.* **97**, 013003 (2006).
9. "Preference for breaking the O-H bond over the O-D bond following HDO ionization by fast ions", A.M. Sayler, M. Leonard, K.D. Carnes, R. Cabrera-Trujillo, B.D. Esry, and I. Ben-Itzhak, *J. Phys. B* **39**, 1701 (2006).
8. "Measurement of alignment dependence in single ionization of hydrogen molecules by fast protons", Nora G. Johnson, R.N. Mello, Michael E. Lundy, J. Kapplinger, Eli Parke, K.D. Carnes, I. Ben-Itzhak, and E. Wells, *Phys. Rev. A* **72**, 052711 (2005).
7. "One- and two-electron processes in collisions between hydrogen molecules and slow highly charged ions", E. Wells, K.D. Carnes, H. Tawara R. Ali, E.Y. Sidky, C. Illescas, and I. Ben-Itzhak, *Nucl. Instrum. and Methods B* **241**, 101 (2005).
6. "Proton-carbon monoxide collisions from 10 keV to 14 MeV", I. Ben-Itzhak, E. Wells, Vidhya Krishnamurthi, K.D. Carnes, N.G. Johnson, H.D. Baxter, D. Moore, K.M. Bloom, B.M. Barnes, and H. Tawara, *Phys. Rev. A* **72**, 022726 (2005).
5. "Dissociation and ionization of H<sub>2</sub><sup>+</sup> by ultrashort intense laser pulses probed by coincidence 3D momentum imaging", I. Ben-Itzhak, P.Q. Wang, J.F. Xia, A.M. Sayler, M.A. Smith, K.D. Carnes, and B.D. Esry, *Phys. Rev. Lett.* **95**, 073002 (2005).
4. "Highlighting the angular dependence of bond softening and bond hardening of H<sub>2</sub><sup>+</sup> in an ultrashort intense laser pulse", P.Q. Wang, A.M. Sayler, K.D. Carnes, J.F. Xia, M.A. Smith, B.D. Esry and I. Ben-Itzhak, *J. Phys. B* **38**, L251 (2005). *Chosen to appear in the J. Phys. B. Highlights of 2005* <http://herald.iop.org/jphysb-highlights2005/m51/crk/164563/link/211>.
3. "Intensity-selective differential spectrum: Application to laser-induced dissociation of H<sub>2</sub><sup>+</sup>", P.Q. Wang, A.M. Sayler, K.D. Carnes, B.D. Esry, and I. Ben-Itzhak, *Opt. Lett.* **30**, 664 (2005).
2. "Dissociation and ionization of molecular ions by ultra-short intense laser pulses probed by coincidence 3D momentum imaging", I. Ben-Itzhak, P.Q. Wang, J.F. Xia, A.M. Sayler, M.A. Smith, K.D. Carnes, and B.D. Esry, *Nucl. Instrum. and Methods B* **233**, 56 (2005).
1. "Bond rearrangement caused by sudden single and multiple ionization of water molecules", I. Ben-Itzhak, A.M. Sayler, M. Leonard, J.W. Maseberg, D. Hathiramani, E. Wells, M.A. Smith, J.F. Xia, P.Q. Wang, K.D. Carnes, and B.D. Esry, *Nucl. Instrum. and Methods B* **233**, 284 (2005).

# Controlling attosecond pulse spectra with carrier-envelope phase

Zenghu Chang

J. R. Macdonald Laboratory, Department of Physics,  
Kansas State University, Manhattan, KS 66506, chang@phys.ksu.edu

The goals of this aspect of the JRML program are (1) to study new gating methods for generating attosecond pulses with higher photon flux, (2) to develop carrier-envelope phase stabilization and control technologies for few-cycle, high power lasers and (3) to apply ultrafast x-ray streak camera in x-ray laser and picoseconds ion beam studies.

**1. Double optical gating: a new attosecond switch.** *H. Mashiko, S. Gilbertson, C. Li, E. Moon, S. Khan, M. Shakya, and Zenghu Chang.* Previously we generated XUV supercontinua by polarization gating of high harmonic generation (HHG) process. Recently we proposed and demonstrated a new gating method called double optical gating for generating single isolated attosecond pulses. The polarization gating pulse can be considered to be a combination of two orthogonally polarized fields, where one serves as a driving field while the other acts as a gating field. When a linearly polarized second harmonic field is added to the driving field, the time interval between adjacent attosecond pulses becomes one full optical cycle of the fundamental wave. To allow one attosecond pulse emission, the width of the polarization gating should be close to one full cycle of the driving field, which is two times what is required by the conventional polarization gating. Consequently, the delay between the two circular pulses can be reduced by a factor of two. Since the ratio between the field strengths inside and outside of the polarization gate depends strongly on the delay, adding the second harmonic field allows the effective polarization gating to occur with lower field amplitude in the leading edge, which reduces the ground state population depletion. Hence the higher laser intensity or longer lasers pulses can be used. Our simulation shows that for lasers between 5 fs and 10 fs, the single attosecond pulses generated by the double optical gating is always stronger than that from the conventional polarization gating, due to the reduced depletion of the ground state population, weak plasma induced beam defocusing and less phase mismatch. Techniquely, 10fs laser pulses are much easier to generate, propagate and manipulate than the 5 fs pulses used in the past for polarization gating. The double optical gating can be applied to gases with larger ionization potential to generate isolated attosecond pulses with durations approaching one atomic unit.

## 2. Development of Carrier-envelope phase control technology on Kansas Light Source

**2.1 Carrier-envelope phase stabilized 5.6 fs, 1.2 mJ pulses,** *H. Mashiko, C. M. Nakamura, C. Li, E. Moon, H. Wang, J. Tackett, and Zenghu Chang.* To obtain attosecond pulses from high harmonic generation (HHG), a driving laser with duration close to one laser cycle is desirable. To reduce the pulses to few-cycle duration, additional spectral broadening is achieved via self-phase modulation using a hollow waveguide filled with a noble gas. The field strengths of few-cycle pulses depend strongly on the carrier-envelope (CE) phase. Therefore, the CE phase is a critical parameter for strong-field interactions with atoms and molecules such as HHG, and therefore for attosecond pulse generation as well. For increasing attosecond pulse photon flux and reducing the attosecond pulse duration, the energy of the CE phase stabilized few-cycle pulse should be as high as possible. Previously, the energy of CE phase stabilized few-cycle pulses was limited to ~0.5 mJ. The major limitation is posed by the energy of the seeding pulses

to the hollow-core fiber, which were produced from a CPA system that uses a glass block and prism pairs to stretch and compress pulses in a single stage multi-pass amplifier. We generated 1.2 mJ pulses with duration of 5.6 fs from a neon filled hollow-core fiber seeded with carrier-envelope phase stabilized 2.2 mJ, 25 fs pulses. The high energy seed pulse was generated by a grating-based CPA system (Kansas Light Sourec) whose CE phase was stabilized by stabilizing the carrier-envelope frequency and by controlling the separation of the gratings in the stretcher [1-5]. The pulse shape and phase are shown in Fig. 1, which were measured by a Frequency Resolved Optical Gating apparatus. The carrier-envelope phase after the fiber was measured by a second, out-loop  $f$ -to- $2f$  interferometer. With seed pulse power locked, the carrier-envelope phase of the two-cycle pulses is controlled to a standard deviation of 370 mrad, as shown in Fig. 2. The peak power of the carrier-envelope phase stabilized pulses, 0.2 TW, is twice that previously generated. The grating based CPA system should be able to produce CE phase locked pulses with much higher energy than demonstrated here (2.2 mJ), thus it is anticipated that the energy of the CE phase stabilized few-cycle pulses be scaled to even higher values.

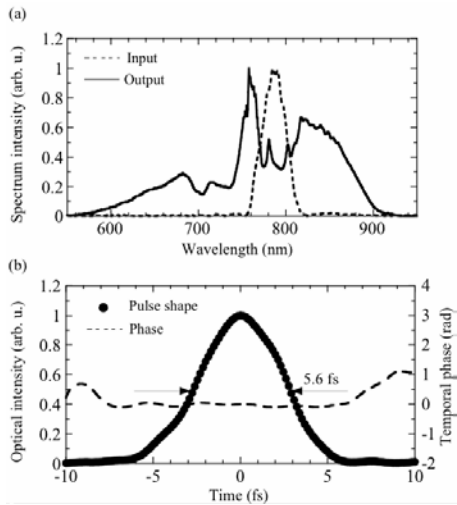


Fig. 1. (a) The spectra of the input (dashed line) and output (solid line) of the fiber. (b) The pulse shape (filled circle) and temporal phase (dashed line) as reconstructed by FROG.

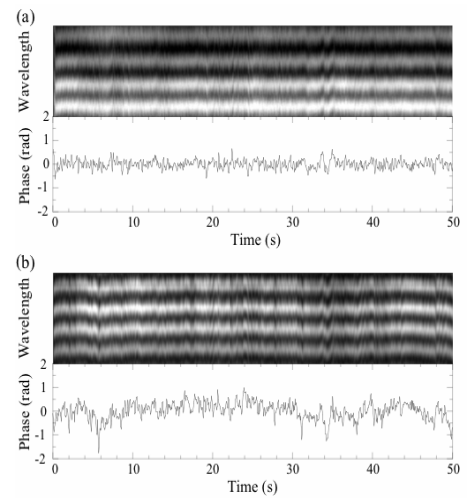


Fig. 2. (a) The CE phase fringes and phase drift of the seeding pulses. (b) The CE Phase fringes and phase drift of the 5.6 fs pulses at Ne gas pressure of 3 bar. The seed power was locked to 0.6%.

**2.2 Determining phase-energy coupling coefficient in carrier-envelope phase measurements,** C. Li, E. Moon, H. Wang, H. Mashiko, C. M. Nakamura, J. Tackett, and Zenghu Chang. For  $f$ -to- $2f$  interferometers based on white-light generation in sapphire plates, the accuracy of the carrier-envelope phase measurement and stabilization is affected by the laser energy fluctuation. We demonstrated a new method to determine the value of the coupling coefficient between the carrier-envelope phase and the laser energy. In our experiments, the coefficient is determined by modulating the pulse energy in the in-loop  $f$ -to- $2f$  interferometer while measuring the carrier-envelope phase variation with an out-loop interferometer. When the

total spectral phase measured by the in-loop interferometer is locked, a 1% laser energy changes causes a 160 mrad shift in carrier-envelope phase of the output pulses [7].

Our measured value  $C_{PE} = 160 \text{ mrad}/1\%$  of energy change is two times of that previous value measured using linear interferometers. This new value should be more accurate because the measurements took into account the effects of more factors. This result is important for the measurement and stabilization of the carrier envelope phases of high power laser pulses. It was discovered that group delay between the  $f$  pulse and the  $2f$  pulses changes significantly with laser energy but its effects on CE phase measurement is canceled out by other energy dependent phase terms. This finding is useful for understanding filament formation in solid materials.

**2.3. Power locking for improving carrier-envelope phase stability,** *H. Wang, C. Li, J. Tackett, H. Mashiko, C. M. Nakamura, E. Moon and Zenghu Chang*. Recently the rapid development of the ultrafast laser has drawn a lot of attention in various areas because of its ultrashort pulse duration, high peak intensity, and broad spectrum properties. One important parameter to evaluate the laser performance is the average power stability between pulses, which is important not only in the nonlinear laser-atom interaction, but also in femtosecond laser micro/nano machining. We have shown that the effect of power fluctuation on carrier-envelope (CE) phase stability is the major error in CE phase control and measurement.

Typical diode pumped kilohertz femtosecond laser systems is 1.5% RMS. The long term energy drift is also close to this value. Previously, a stabilization scheme making use of a photoconductive switch to drive Pockels cell discharge was introduced. Although the energy fluctuation was suppressed from 7% to 0.64%, 50% of the total energy was lost during the stabilization process. Moreover, since the added Pockels cell is located after the amplifier, the high power pulses may cause nonlinear effects or even damage the device. We demonstrated a method to improve the laser power stability of multi-pass amplifiers by using the Pockels cell located before the amplification. It is easier to produce shorter pulses from multipass amplifiers because the dispersion and gain narrowing effect is much less as compared to that of the regenerative amplifiers.

We developed a feedback scheme that minimizes the energy fluctuation of the high power femtosecond pulses from a 1 kHz laser amplifier. The pulse energy variation in the frequency bandwidth 0-500 Hz is obtained by a photodiode and a low pass filter. The measured signal is fed to a proportional-integral-derivative controller that changes the amplitude of the high voltage pulses applied on a Pockels cell. The variation of average power was reduced from 1.33% RMS to 0.28% RMS, which improved the carrier-envelop phase stability from 500 mrad to 200 mrad measured by two  $f$ -to- $2f$  interferometers. This new power locking scheme has been demonstrated in many strong field atomic physics experiments using the Kansas Light Source.

**3. Femtosecond x-ray streak camera application.** We will continue the collaboration with Prof. J. Rocca at Colorado State University. The x-ray streak camera is an idea too for studying the dynamics of the x-ray laser [8]. Progress is also made on applying the camera to the pico-pulse project, i.e., accelerating the ultrashort ion pulses producing by intense laser pulses in a tandem accelerator [9]. We will work closely with other JRM groups on dynamic studies using the Kansas Light Source laser facility [10, 11].

## **PUBLICATIONS (2006-2007):**

1. Bing Shan, Chun Wang and Zenghu Chang, "High peak-power kilohertz laser systems employing single-stage multi-pass amplification", U. S. Patent No. 7,050,474, issued on May 23, 2006.
2. E. Moon, Chengquan Li, Zuoliang Duan, J. Tackett, K. L. Corwin, B. R. Washburn, and Zenghu Chang, "Reduction of fast carrier-envelope phase jitter in femtosecond laser amplifiers," *Optics Express* **14**(21), pp. 9758-9763 (2006).
3. Chengquan Li, Eric Moon, and Zenghu Chang, "Carrier-envelope phase shift caused by variation of grating separation," *Optics Letters* **31**, pp. 3113-3115 (2006).
4. Zenghu Chang, "Carrier envelope phase shift caused by grating-based stretchers and compressors," *Applied Optics* **45**, 8350(2006).
5. Chengquan Li E. Moon, Hiroki Mashiko, C. Nakamura, P. Ranitovic, C. L. Cocke, and Zenghu Chang, G. G. Paulus, "Precision control of carrier-envelope phase in grating based chirped pulse amplifiers," *Optics Express* **14**, 11468-11476 (2006).
6. Hiroki Mashiko, Christopher M. Nakamura, Chengquan Li, Eric Moon, He Wang, Jason Tackett, and Zenghu Chang, "Carrier-envelope phase stabilized 5.6 fs, 1.2 mJ pulses," *Applied Physics Letters*, **90**, 161114 (2007).
7. Chengquan Li, Eric Moon, He Wang, Hiroki Mashiko, Christopher M. Nakamura, Jason Tackett, and Zenghu Chang, "Determining the Phase-Energy Coupling Coefficient in Carrier-envelope Phase Measurements," *Optics Letters* **32**, 796 (2007).
8. M. A. Larotonda, Y. Wang, M. Berrill, B. M. Luther and J. J. Rocca, Mahendra Man Shakya, S. Gilbertson and Zenghu Chang, "Pulse duration measurements of grazing incidence pumped table-top Ni-like Ag and Cd transient soft x-ray lasers," *Optics Letters* **31**, 3043-3045 (2006).
9. K.D. Carnes, C.L. Cocke, Z. Chang, I. Ben-Itzhak, H.V. Needham, A. Rankin, "Picosecond ion pulses from an EN tandem created by a femtosecond Ti:sapphire laser," *Nuclear Instruments and Methods in Physics Research B* **261**, 106 (2007).
10. M. Zamkov, A. S. Alnaser, N. Woody, B. Shan, Z. Chang, and P. Richard , "Probing the intrinsic conductivity of multiwalled carbon nanotubes," *Applied Physics Letters* **89**, 093111 (2006).
11. M. Zamkov, A. S. Alnaser, B. Shan, Z. Chang, and P. Richard, "Exciton dynamics in bundles of single walled carbon nanotubes," *Chemical Physics Letters* **437**, 104 (2007).

## Structure and Dynamics of Atoms, Ions, Molecules and Surfaces: Atomic Physics with Ion Beams, Lasers and Synchrotron Radiation

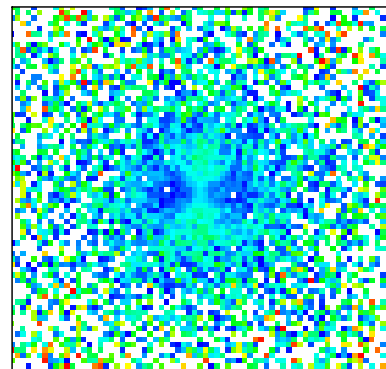
C.L.Cocke, Physics Department, J.R. Macdonald Laboratory, Kansas State University,  
Manhattan, KS 66506, [cocke@phys.ksu.edu](mailto:cocke@phys.ksu.edu)

*We continue to explore the ionization of atoms, ions and small molecules by intense laser pulses. During the past year we have concentrated on electron emission from aligned molecules, on developing X-ray-pump/IR probe experiments, on developing short reliable CEP stabilized pulses for use in COLTRIMS experiments and on exploring to what extent laser induced electron scattering can be analyzed in terms of free- electron-ion scattering. We have also pursued collaborative experiments on related topics at the ALS and the Univ. of Colorado.*

### Recent progress:

**1) Electron emission from aligned molecules,** *C. M. Maharjan, D. Ray, P. Ranitovic, B. Gramkow, I. Bocharova, M. Magrakevildze, B. Ulrich, I. V. Litvinyuk, and C. L. Cocke.* The emission of electrons from a neutral molecule by short intense laser pulses is known to have angular structure which is influenced by the laser polarization and resonant structure of high lying states of the molecule. During the past year we have been investigating to what extent the angular distribution can also influenced by the structure of the outermost orbital of the molecule from which the electron is being removed. We have previously reported evidence that the structure of this orbital is revealed in multistep processes involving rescattering excitation of the molecule followed by dissociation. The latter process provided *a posteriori* alignment of the molecule. The more direct approach we use here requires that the molecule be aligned prior to ionization. We have done this for oxygen using rotational revivals. A weak linearly polarized pump pulse is used to launch a rotational wave packet of the molecule without ionizing it. The molecule is then ionized by a strong probe pulse at a chosen later time during the rotational revival structure. We use momentum imaging techniques to record the full energy and angular structure of the electrons emitted by the probe as a function of the delay time between pump and probe. The images display the following features: a) The influence of the alignment of the molecule on the raw images is very small. (b) However, when the images are normalized to those obtained from unaligned molecules, a clear alignment influence on the emissions patterns is observed; (c) This alignment structure in the case of oxygen can be associated with the  $\pi_g$  structure of the most loosely bound orbital of this molecule. A sample spectrum is shown in figure 1.

Figure 1.: Electron momentum spectrum from aligned oxygen. The graph shows the ratio between aligned and non-aligned oxygen, where the alignment is in the vertical direction and the ionizing pulse is directed out of the page. The momentum scale is 4 a.u. across on each side of the figure. The “cloverlike” shape is evidence of the  $\pi_g$  structure of the outermost orbital of the neutral oxygen molecule.



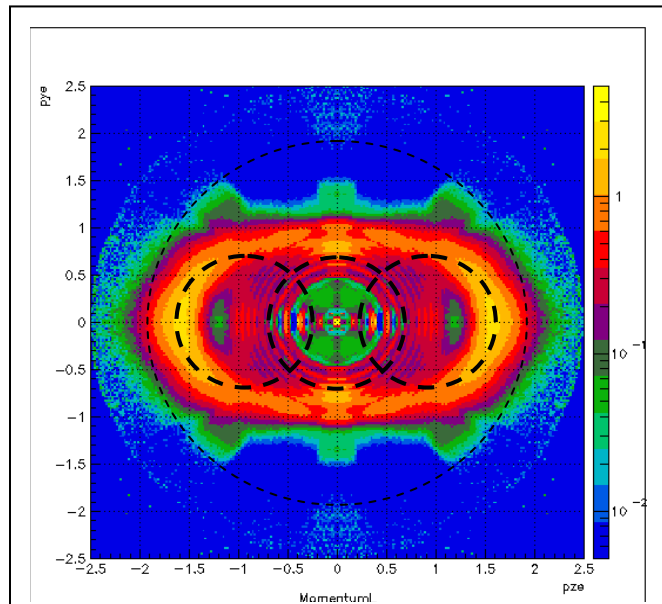
**2) Pump-probe experiments using EUV-IR:** *P. Ranitovic, B. Gramkow, I. Bocharova, M. Magrakevildze, I. V. Litvinyuk, and C. L. Cocke.* A long-range goal of ultrafast science, and attoscience, is to be able to pump and probe atomic and molecular systems on an electronic time scale. Such a process requires a time resolution in at least the tens-of-attoseconds region and a corresponding band width of at least tens of eV. As a beginning in this direction, we have been developing a system to allow us to pump atomic and molecular targets with attosecond pulse trains and pulses, generated using the 800 nm IR beam from the JRML KLS, and to probe them using the IR beam itself. A time resolution of approximately 6-8 fs is achieved from the length of the pulse trains and the IR pulse. Shorter time scales can be addressed using single attosecond pulses and the phase relationship between this pulse and the IR. Our original attempts to construct a COLTRIMS apparatus suitable for these experiments was successful two years ago in producing photoelectron spectra with EUV pulses up to 40 eV, but further development showed that this apparatus was situated too far from the KLS to be sufficiently stable for the pump-probe experiments. During the past year we have rebuilt and considerably improved this apparatus, and expect to be doing experiments with it by the time this abstract appears in the proceedings of this workshop. In the meantime we have pursued collaborative experiments with the group of M. Murnane and H. Kapteyn at the University of Colorado, and the first results on EUV/IR pump probe experiments on N<sub>2</sub> have been submitted for publication. See their abstract, and publication 5, for further details. A similar study of oxygen is underway.

**3) Development of reliable short CEP stabilized pulses for COLTRIMS experiments.** *D. Ray, P. Ranitovic, C. M. Maharjan, B. Gramkow, I. Bocharova, M. Magrakevildze, I. V. Litvinyuk, G. Paulus (Texas A&M Univ.) and C. L. Cocke.* During the past year we have worked to deliver to our COLTRIMS apparatus short (6 fs or less) CEP stabilized pulses suitable for pump/probe experiments with CEP control. During the past two years we have reported a number of experimental results on pump/probe manipulations of molecular breakup in molecular hydrogen (deuterium), oxygen and nitrogen. The goal of the present work is to allow us better control over the shape of both the pump and probe pulses in these experiments and in particular to be able to remove the right-left asymmetry of the pulses using CEP stabilized pulses. Although CEP stabilized pulses from the KLS are available, we have not yet been able to achieve sufficiently stable phase locking and sufficiently short pulses to see left-right asymmetry in COLTRIMS experiments. As part of this program, we have entered a collaboration with Prof. G. Paulus of Texas A&M University, and have now in the laboratory a “Paulus Phasemeter” which we use to analyze the length and phase of the pulse just prior to its entering our COLTRIMS arrangement. We have been able to demonstrate phase locked pulses in the phasemeter, but the pulse length has not yet been sufficiently short to allow strong CEP effects in the COLRTIMS system to be observed. We are continuing this collaboration in several directions to both improve the pulse characteristics and to extend the work to polarization-gated pulses.

**4) To what extent can electron rescattering processes in short laser pulses be described as free-electron-ion scattering?** *D. Ray, B. Ulrich, C. M. Maharjan, P. Ranitovic, B. Gramkow, I. Bocharova, M. Magrakevildze, I. V. Litvinyuk, G. Paulus(Texas A&M Univ.), C.D.Lin and*

*C. L. Cocke.* The removal of an electron from an atom or molecule by a short laser pulse is quickly followed by the re-visitation of the parent ion by that electron. Many processes, including harmonic generation and non-sequential multiple ionization, take place through this rescattering. Over the years many treatments of rescattering have been based on treating this rescattering as a free-electron-ion scattering. C.D.Lin and collaborators have recently shown that the angular distribution of the elastically back-scattered electrons in a short laser pulse are expected to quite accurately reflect the differential scattering cross sections for free electron ion scattering (See contribution of C.D.Lin, section 1 and publication B1). They predict a well defined backscattering “ring” in momentum space corresponding to electrons returning to the target with a maximum return energy and then being re-boosted by the vector potential at the time of the rescattering. This ring is predicted to be a quite visible feature in the momentum images of the continuum electrons in the plateau region and to have an angular structure which is quite target-dependent, as would be predicted from backscattering of electrons from ions. We have sought experimental evidence for this feature. We have recorded momentum-space images of electrons rescattered from argon targets with both COLTRIMS and phasemeter (see section 3 above) apparatuses. We observe clear ring structures. The structures are centered on displaced centers as would be expected from the vector potential boost which they gain from the field subsequent to the rescattering. However, the structures we observe appear to be attributable not to the highest energy electron returns but to electrons emitted at other phases of the cycle. A preliminary image is shown in figure 2. Analysis of this data is still under way.

Figure 2. Momentum space image of electrons from argon ionized by a  $2.2 \times 10^{14} \text{ w/cm}^2$  30 fs 800 nm pulse. The polarization vector is horizontal and lies in the plane of the page. Electrons with energies below 6.5 eV are suppressed by a retarding grid. Electrons with momentum above 1 a.u. are due to rescattering. The data have been normalized so as to emphasize higher energy electrons.



**5) Synchrotron radiation experiments,** *T. Osipov, P.Ranitovic, C.Marhajan, B.Ulrich, C.L. Cocke (KSU), A. Landers (Auburn Univ.), R. Dörner, Th. Weber, L. Schmidt,A. Staudte, H. Schmidt-Böcking, et al. (U. Frankfurt), M.H. Prior (LBNL) and others.* We continue to participate in a multi-laboratory collaboration involving the University of Frankfurt, LLBL, Auburn Univ. and KSU at the ALS. Recent projects include the measurement of the Auger/photoionization dynamics when neon is ionized near the K shell threshold, on the identification of localized K holes from K shell ionization of nitrogen using the continuum photoelectron angular distributions to adjust the parities of the hole states, on symmetry

breaking in photodouble ionization of hydrogen molecules and on control of two slit patterns in single photon double photoionization of molecular hydrogen, using the momenta of the two electrons to dissect the entangled final two-electron wave.

**Future plans:**

Projects 2-4 listed above are all in progress, and work will proceed on all three of these. We will continue the collaboration in 5.

**Publications 2006-2007:**

- 1."Attosecond Strobing of Two-Surface Population dynamics in dissociating H<sub>2</sub><sup>+</sup>, A.Staudte, D.Pavicic, S.Chelkowski, D.Zeidler, M.Meckel, H.Niikura, M.Schöffler, S.Schhossler, B.Ulrich, P.P.Rajeev, Th.Weber, T.Jahnke, D.M.Villeneuve, A.D.Bandrauk, C.L.Cocke, P.B.Corkum and R.Dörner, Phys.Rev. Lett 98, 07003(2007).
2. "Single Photon-Induced Symmetry Breaking of H<sub>2</sub> Dissociation", F.Martin, J.Fernandez, T.Havemeier, L.Foucar, Th. Weber, K.Kreidi, M.Schöffler, L.Schmidt, T.Jahnke, O.Jagutzki, A.Czasch, E.P.Benis, T.Osipov, A.L.Landers, A.Belkacem, H.H.Prior, H.Schmidt-Böcking and C.L.Cocke and R.Dörner, Science 315, 629 (2007).
3. "Wavelength dependence of momentum-space images of low-energy electrons generated by short intense laser pulses at high intensities," C. M. Maharjan, A. S. Alnaser, I. Litvinyuk, P. Ranitovic, and C. L. Cocke, J. Phys. B: At. Mol. Opt. Phys. 39 1955 (2006).
4. "Momentum-imaging investigations of the dissociation of D<sub>2</sub><sup>+</sup> and the isomerization of acetylene to vinylidene by intense short laser pulses," A.S.Alnaser, I.Litvinyuk, T.Osipov, B.Ulrich,A. Landers, E.Wells, C.M.Maharjan, P.Ranitovic, I.Bocharova, D.Ray and C.L.Cocke, J. Phys. B: At. Mol. Opt. Phys. 39, S485(2006).
5. "Soft x-ray driven femtosecond molecular dynamics", Etienne Gagnon, Predrag Ranitovic, Xiao-Min Tong, C.L.Cocke, Margaret M. Murnane, Henry C. Kapteyn and Arvinder S. Sandhu, Science (submitted, 2007).

# Photo-Association and Coherent Excitation of Cold Atoms

B. D. DePaola

J. R. Macdonald Laboratory Department of Physics  
Kansas State University  
Manhattan, KS 66056  
depaola@phys.ksu.edu

## Program Scope

MOTRIMS, or magneto optical trap recoil ion momentum spectroscopy, combines the technology of cold atom trapping with that of ultra-high resolution time of flight (TOF) spectroscopy. Originally developed for the study of ion-atom or photon-atom collisions, MOTRIMS has more recently been used as a probe of population dynamics in cold, trapped atomic samples. For example, we have recently published results in which the population dynamics in a system undergoing the coherent excitation scheme referred to as STIRAP are measured on the nanosecond time scale. Another example of population dynamics is in a recent publication in which we use MOTRIMS to measure the excited fraction in a MOT under a range of trapping parameter values.

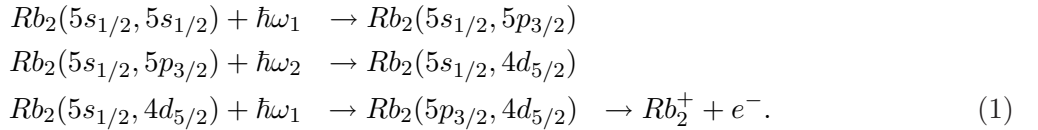
In a more recent application, we use MOTRIMS as a diagnostic of cold collisions in the present of optical radiation. In the following sections, we describe experiments which focus on the process of photo-association followed by excitation, followed by autoionization. In these experiments, we use light from quasi-cw and/or ultra-fast lasers to control the association and excitation.

## Recent Progress 1: Photo-Association with Quasi-CW Lasers

Photo-association (PA) occurs when very slow atoms collide in the presence of an optical field that is resonant with a transition to an excited molecular state. True PA then occurs if, after this free-bound transition, the excited molecule decays to a bound electronic ground state. In nearly all experimental and theoretical studies, efforts are focussed on enhancing decay to a bound state of the molecule. In some cases, these studies attempt to improve decay rates to a low-lying vibrational state in the electronic ground state of the molecule. In contrast, our work follows a complementary track in which the first step in PA is followed by two color, two photon excitation to an autoionizing state of the molecule. We then detect the molecular ions. This line of experiments has some potential advantages over the usual studies that focus on the simpler PA process. First, it gives us the opportunity to do high resolution spectroscopy on multiply excited molecular states at internuclear separations that are otherwise inaccessible. More importantly, it adds to the number of states through which we can coherently move populations in an effort to obtain a large Franck-Condon overlap with a vibrationally cold electronic ground state. Thus, in principle one may be able to “stall for time” through the use of longer lived excited molecular states, allowing the internuclear separation to become small enough for efficient transfer of population to the desired final state. We can track our progress in moving populations by using the autoionizing molecular state as a sort of probe of the efficiency with which we move the populations.

Using tunable CW lasers to study the process of photo-association and excitation has the advantage that one has complete control over the frequencies, and therefore the levels through which the population moves. This has been used with great advantage in photo-association spectroscopy [1] on the manifold of molecular levels associated with the Rb(5s)-Rb(5p) system. In our experiments, two external cavity diode lasers are used in the association, excitation, and ionization of the cold Rb in our MOT. These lasers, as well as the optical radiation coming from them are referred to as L1 and L2, and have wavelengths of about 780 nm and 1529 nm, respectively. L1 was detuned 53 MHz to the red of the  $5s_{1/2}, (F=2) \rightarrow 5p_{3/2}, (F'=3)$  atomic transition while L2 was locked 53 MHz to the blue of the  $5p_{3/2}, (F=3) \rightarrow 4d_{5/2}$  atomic transition, with unresolved hyperfine structure in the 4d state. Using acousto-optic modulators (AOMs), 50 ns pulses are extracted from both L1 and L2; these are superimposed both spatially and temporally on a cloud of cold ( $\sim 150\mu\text{K}$ )  $^{87}\text{Rb}$  atoms in the MOT.

In the process we are studying, before any spectroscopic studies can be meaningful, we must first determine the excitation path. Thus, the major question is, by what mechanism(s) are the  $\text{Rb}_2^+$  ions produced. We have proposed the excitation/ionization paths expressed by:



Here,  $\hbar\omega_1$  and  $\hbar\omega_2$  refer to photons from L1 and L2, respectively.

A photon from L1 first excites a state in the  $\text{Rb}_2(5s_{1/2}, 5p_{3/2})$  manifold of molecular states, the same starting point seen in other PAI experiments [2]. A photon is then absorbed from L2, exciting the molecule to a level in the  $\text{Rb}_2(5s_{1/2}, 4d_{5/2})$  manifold. A second photon from L1 is then absorbed, bringing the system to a level in the  $\text{Rb}_2(5p_{3/2}, 4d_{5/2})$  molecular manifold. The atoms move together along this bound potential curve until autoionization can occur at a curve crossing with a  $\text{Rb}_2^+$  potential curve, leading to the final product.

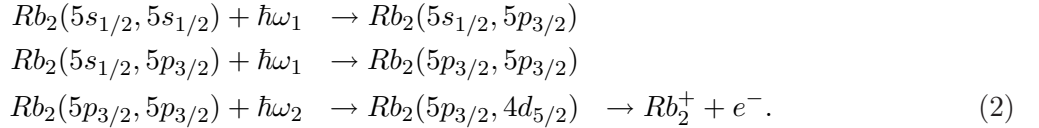
From published molecular curve data [3], an L1 detuning of 53 MHz implies excitation of  $\text{Rb}_2(5s_{1/2}, 5p_{3/2})$  at an internuclear separation of about 1000 atomic units. Note the order of photon absorption is L1-L2-L1, rather than L1-L1-L2. We know that the latter route is not followed because after a resonant (due to the  $1/R^3$  curvature of the 5s-5p levels) absorption of L1, another L1 would be  $\sim 106$  MHz red of resonance with the 5p-5p manifold, while an L2 would be on resonance with the 5s-4d manifold. Experimentally, we have seen that with the L2 pulse delayed with respect to the L1 pulse, the ionization rate is significantly reduced. If, however, L1 and L2 are pulsed simultaneously, and some time later L1 is pulsed again, we see significant ionization from the second L1 pulse.

## Recent Progress 2: Photo-Association with an Ultra-Fast Laser

The major disadvantage of CW lasers is that one must have a different laser for every manifold of transitions one wishes to explore. Furthermore, if one wishes to maximally exploit coherent excitation, one should phase lock each of the lasers. By using an ultra-fast laser, one has available in a single pulse, a very large range of frequencies, all of which have a well-defined phase relationship to each other. Furthermore, using readily available technologies, the spectral amplitude and phase (including higher order phases) can be controlled. Thus, the prospects for coherent control of the processes leading up to  $\text{Rb}_2^+$  production are very encouraging.

In the ultra-fast experiments carried out at K-State, we have first focussed on determining the association, excitation, and ionization pathways; there is no guarantee that these are the same as

in the CW laser case. In fact, we find that for the ultra-fast case, the excitation pathway can be expressed as:



Here  $\omega_1$  refers to optical radiation from the Kansas Light Source (KLS) while, as before,  $\omega_2$  refers to light from a 1529 nm external cavity CW diode laser. We can think of the last line in (2), that is, the excitation by L2 to an autoionizing state, as a probe of the association/excitation process carried out by the KLS laser light. Note that, in contrast with the L1-L2-L1 path followed by the all-CW laser association/excitation pathway, the ultra-fast laser scheme follows the L1-L1-L2 path. However, both processes end up on the same autoionizing state.

So, now that we know the excitation pathway, can we exploit the coherent nature of the KLS light to enhance  $Rb_2^+$  production? The answer is yes. In a simple experiment, we measure  $Rb_2^+$  production as a function of  $d^2\phi/d\omega^2$  or spectral chirp. We measured a very strong dependence on the spectral chirp, with negative chirp giving a large enhancement of  $Rb_2^+$  production and positive chirp actually reducing  $Rb_2^+$  production. We believe that this dependence on spectral chirp is due to interference of the excitation amplitudes along the many paths from the “initial”  $Rb(5s)$ - $Rb(5s)$  state to the “final”  $Rb(5p)$ - $Rb(4d)$  state. This belief is qualitatively supported by theory.

## Future Plans

The emphasis of the recent results presented here has been on measuring the production of  $Rb_2^+$  from the photo-association, coherent excitation, and autoionization of Rb atoms that have been cooled and trapped in a MOT. In one series of experiments, all CW lasers were used for the process, opening the door for precision spectroscopy on the multiply excited molecular states. The next step is to make spectroscopic studies on the excited molecular levels through which the population passes. In particular, these are the states corresponding to  $Rb(5s)$ - $Rb(4d)$  manifold.

In a second series of experiments described here, light from the K-State ultra-fast laser facility was used to study coherent excitation of the associated cold molecule. The dependence of the association/excitation process on spectral chirp was measured; future work will include measurements of the polarization dependence. In addition, we will attempt a full-blown optimization of  $Rb_2^+$  production using a genetic algorithm to modify the spectral amplitude and several orders of spectral phase.

## References

- [1] Kevin M. Jones, Eite Tiesinga, Paul D. Lett, and Paul S. Julienne. Ultracold photoassociation spectroscopy: Long-range molecules and atomic scattering. *Rev. Mod. Phys.*, 78:483–535, 2006.
- [2] D. Leonhardt and J. Weiner. Direct two-color photoassociative ionization in a rubidium magneto-optic trap. *Phys. Rev. A*, 52:R4332–R4335, 1995.
- [3] M. Kemmann, I. Mistrik, S. Nussmann, H. Helm, C. J. Williams, and P. S. Julienne. Near-threshold photoassociation of  $^{87}Rb_2$ . *Phys. Rev. A*, 69:022715, 2004.

## Recent Publications

- “Numerical Exploration of Coherent Excitation in Three-Level Systems”, H. A. Camp, M. H. Shah, M. L. Trachy, O. L. Weaver, and B. D. DePaola, Phys. Rev. A **71** 053401 (2005).
- “Entropy Lowering in Ion-Atom Collisions”, H. Nguyen, R. Brédy, T. G. Lee, H. A. Camp, H. Awata, and B. D. DePaola, Phys. Rev. A **71** 062714 (2005).
- “Relative Charge Transfer Cross Section from Rb(4d)”, M. H. Shah, H. A. Camp, M. L. Trachy, X. Fléchard, M. A. Gearba, H. Nguyen, R. Brédy, S. R. Lundeen, and B. D. DePaola, Phys. Rev. A **72** 024701 (2005).
- “A Novel Method for Laser Beam Size Measurement”, G. Veshapidze, M. L. Trachy, M. H. Shah, and B. D. DePaola, Appl. Opt. **45**, 6197 (2006).
- “Model-Independent Measurement of the Excited Fraction in a Magneto-Optical Trap”, M. H. Shah, H. A. Camp, M. L. Trachy, G. Veshapidze, M. A. Gearba, and B. D. DePaola, Phys. Rev. A **75**, 053418 (2007).
- “MOTRIMS: Magneto-Optical Trap Recoil Ion Momentum Spectroscopy”, B. D. DePaola, R. Morgenstern, and N. Andersen, in *Advances in Atomic, Molecular, and Optical Processes*, Elsevier Press, 2007.
- “Measurement of Population Dynamics in Stimulated Raman Adiabatic Passage”, M. A. Gearba, H. A. Camp, M. L. Trachy, G. Veshapidze, M. H. Shah, H. U. Jang, and B. D. DePaola, Phys. Rev. A **76**, 013406 (2007).
- “Photoassociation in Cold Atoms via Ladder Excitation”, M. L. Trachy, G. Veshapidze, M. H. Shah, H. U. Jang, and B. D. DePaola, Phys. Rev. Lett. 2007 (accepted).

# TIME-DEPENDENT TREATMENT OF THREE-BODY SYSTEMS IN INTENSE LASER FIELDS

**B.D. Esry**

*J. R. Macdonald Laboratory, Kansas State University, Manhattan, KS 66506*

[esry@phys.ksu.edu](mailto:esry@phys.ksu.edu)

<http://www.phys.ksu.edu/personal/esry>

## 1 Program Scope

The primary goal of my program is to quantitatively understand the behavior of  $H_2^+$  in an ultrashort, intense laser field. As we gain this understanding, we will work to transfer it to other more complicated molecules. In this effort, my group works closely with the experimental groups in the J.R. Macdonald Laboratory, including I. Ben-Itzhak's, C.L. Cocke's, and I. Litvinyuk's.

Because even  $H_2^+$  has more degrees of freedom than can be directly treated computationally when an intense field is present, past theoretical descriptions have artificially reduced the dimensionality of the problem or excluded one or more of the important physical processes: electronic excitation, ionization, vibration, and rotation. Such simplifications were justified with intuitive arguments, but have been little tested. One component of this work is thus to systematically include these processes in three dimensions and gauge their importance based on actual calculations. Further, as laser pulses get shorter and more intense, approaches that have proven useful in the past may become less so. The application of kinematically complete measurement techniques is also revealing effects that are likely not captured correctly in these simplified models. A second component of my program is thus to develop novel analytical and numerical tools to describe molecules,  $H_2^+$  in particular. The ultimate goal is to understand the dynamics of these strongly coupled systems in quantum mechanical terms.

## 2 Recent progress

The last year has seen significant development in both components of my program mentioned above. Computationally, my graduate student, Fatima Anis, has finished a computer code to solve  $H_2^+$  in an intense laser including all physical processes save ionization. Analytically, my former postdoc, Vladimir Roudnev, devised a novel representation of carrier-envelope phase (CEP) effects in a very general way.

### 2.1 Computational development

We can now solve the problem of  $H_2^+$  in an intense laser including nuclear vibration and rotation as well as electronic excitation. The only physical process excluded is ionization. We can thus reliably perform calculations up to an intensity of roughly  $10^{14}$  W/cm<sup>2</sup>. For higher intensities, ionization plays a non-negligible role.

To solve the time-dependent Schrödinger equation, we expand the electronic degrees of freedom on Born-Oppenheimer states and the nuclear rotational degrees of freedom on Wigner  $D$ -functions. The Schrödinger equation is then reduced to coupled, time-dependent equations for the nuclear radial wave functions. These functions are labeled by the electronic state and total angular momentum. This remaining radial dependence is discretized using finite differences, and the time evolution is accomplished through a combination of split operator techniques and Crank-Nicolson propagation. Unlike most finite difference implementations, ours allows the use of nonuniform grids to economize the calculation. Further economy is achieved by allowing the number of angular momenta included to be determined adaptively by the code. A similar procedure will be implemented for the radial grid size. We calculate the Born-Oppenheimer states and all of their dipole couplings, including as many excited states as desired.

More than ten years ago, people were already exploring the role of nuclear rotation in intense field dissociation of  $H_2^+$  (see Ref. [1] and references therein). For the longer, less intense laser pulses available at the time, it was concluded that the “semiquantitative features predicted by the 1D models are close to reality” [1]. The 1D models referred to assume that the molecular axis is aligned with the external linearly polarized field and does not rotate during or after the pulse. These models further assume that

the contribution of molecules not perfectly aligned with the field is negligible. The validity of such 1D models has not really been reconsidered even as the pulse lengths have gotten shorter and their intensities higher. In fact, they continue to be one of the mainstays for interpreting  $\text{H}_2^+$  experimental results and likely do correctly yield the gross features. Figure 1, for instance, shows our calculations of the dissociation probability with rotation included, Fig. 1(a), and with the molecule fixed along the laser polarization, Fig. 1(b). The figure shows that the main features *are* similar in the two: the low vibrational states

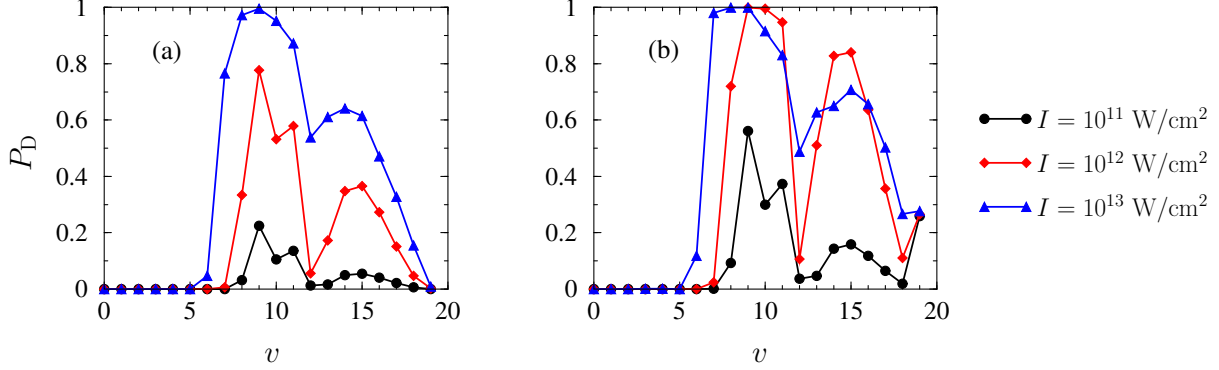


Figure 1: The probability for dissociation  $P_D$  of  $\text{H}_2^+$  in a 45 fs, 800 nm laser pulse as a function of the initial vibrational state  $v$ : (a) including rotation, (b) no rotation.

dissociate very little, the maximum dissociation is around  $v=9$ , and the high vibrational states dissociate less. The aligned model in (b) is clearly only “semiquantitative”, though, since the magnitude of  $P_D$  is very different than in (a). Even the qualitative behavior with intensity is not correctly reproduced, however, for the higher vibrational states: with rotation included,  $P_D$  increases monotonically with intensity where it actually decreases with increasing intensity in some cases for the aligned model. This decrease is what has led to the idea of vibrational trapping (or stabilization). These plots show that such strong stabilization is really a consequence of the reduced dimensionality. This result has been seen in past calculations including rotation for much longer pulses (again, see Ref. [1]). Since the mechanism of vibrational trapping should be more effective for short pulses, though, it might be expected that trapping would be seen in our calculations including rotation but there is no strong evidence for it.

### Future plans

This discussion gives an example of the comparisons that we are starting to make. We are working to use this code to check other commonly held ideas of intense field  $\text{H}_2^+$  dissociation as well. For instance, we want to check the validity of the axial recoil approximation quantum mechanically. In the process, we can also check the classical estimate of post-pulse rotation made in Ref. [2]. We want to try to quantify, if possible, the contributions of the mechanisms of “dynamical alignment” and “geometrical alignment” as well. We are working to investigate the ro-vibrational revivals of  $\text{H}_2^+$  using pump-probe schemes much like those used in Refs. [3,4]. In addition to these research directions, we can now pursue quantitative comparisons with the two-dimensional momentum distributions obtained experimentally since we can now calculate the angular distribution theoretically.

## 2.2 Analytical developments

We have made significant progress in the analytic description of CEP effects over the past year as well. In brief, we have rigorously derived a representation in terms of Floquet amplitudes — even for short pulses — that allows CEP effects to be interpreted as interference between different  $n$ -photon amplitudes. Moreover, this interpretation applies, in principle, to all systems. The representation we obtain shows how to write the wave function as a Fourier series in the CEP itself. Consequently, the full CEP dependence of any physical observable can be obtained from the  $n$ -photon components at a single value of the CEP.

An additional benefit of the picture that emerges from this analysis is the ability to make estimates of the magnitude of CEP effects in a given system. Figure 2, for instance, shows the pulse length dependence of the

CEP effect in excitation of a two-level system. For the figure, we characterize this magnitude by the standard deviation of the CEP-dependent excitation probability at each pulse length. Besides the numerical results, this figure shows a simple analytical estimate based on the parameters of the system. The agreement between the two is quite good given the simplicity of the estimate. Both show that the magnitude of the CEP effect decreases exponentially with pulse length, the first such characterization and explanation of the pulse length dependence. We can similarly understand the dependence on the pulse intensity and other system parameters.

### Future plans

We can explain the CEP dependence of  $\text{H}_2^+$  dissociation rather naturally within this representation, and we have already used it to reduce the computational requirements for the CEP dependence of atomic excitation and ionization. We will continue to take advantage of it in our other, ongoing CEP calculations.

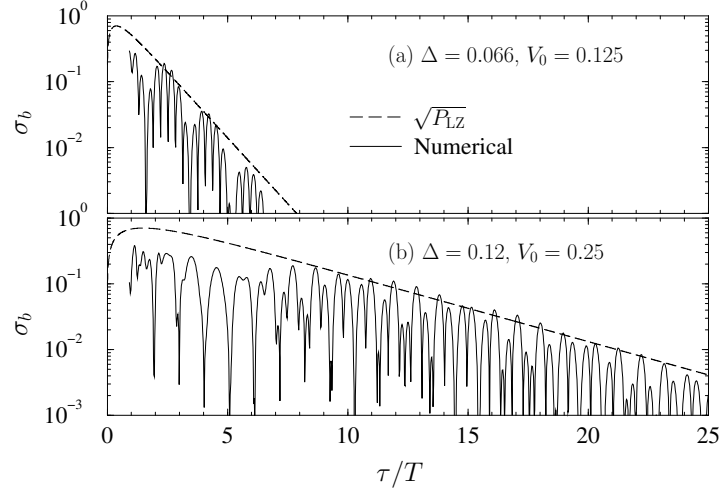


Figure 2: Magnitude  $\sigma_b$  of the CEP effect in excitation of a two-level system by a Gaussian pulse of FWHM  $\tau$  that gives a peak interaction energy  $V_0$ . The laser period is  $T$  and the energy gap is  $\Delta$ . The solid line is obtained by integrating the time-dependent Schrödinger equation, and the dashed line is an estimate based on the Landau-Zener approximation applied within the representation described in the text.

## 3 References

1. A. Giusti-Suzor, F.H. Mies, L.F. DiMauro, E. Charron, and B. Yang, J. Phys. B **28**, 309 (1995).
2. X.M. Tong, Z.X. Zhao, A.S. Alnaser, S. Voss, C.L. Cocke, and C.D. Lin, J. Phys. B **38**, 333 (2005).
3. A.S. Alnaser, B. Ulrich, X.M. Tong, I.V. Litvinyuk, C.M. Maharjan, P. Ranitovic, T. Osipov, R. Ali, S. Ghimire, Z. Chang, C.D. Lin, and C.L. Cocke, Phys. Rev. A **72**, 030702(R) (2005).
4. Th. Ergler, A. Rudenko, B. Feuerstein, K. Zrost, C.D. Schröter, R. Moshammer, and J. Ullrich, Phys. Rev. Lett. **97**, 193001 (2006).

## 4 DOE-supported publications from the last three years

- P13. “HD<sup>+</sup> in a short, strong laser pulse: practical consideration of the observability of carrier-envelope phase effects,” V. Roudnev and B.D. Esry, Phys. Rev. A (accepted), (2007).
- P12. “Determining laser-induced dissociation pathways of multi-electron diatomic molecules: application to the dissociation of O<sub>2</sub><sup>+</sup> by high intensity ultrashort pulses,” A.M. Sayler, P.Q. Wang, K.D. Carnes, B.D. Esry, and I. Ben-Itzhak, Phys. Rev. A **75**, 063420 (2007).
- P11. “Dissociation of H<sub>2</sub><sup>+</sup> in intense femtosecond laser field studied by coincidence 3D momentum imaging,” P.Q. Wang, A.M. Sayler, K.D. Carnes, J.F. Xia, M.A. Smith, B.D. Esry, and I. Ben-Itzhak, Phys. Rev. A **74**, 043411 (2006).
- P10. “Above threshold Coulomb explosion of molecules in intense laser pulses,” B.D. Esry, A.M. Sayler, P.Q. Wang, K.D. Carnes, and I. Ben-Itzhak, Phys. Rev. Lett. **97**, 013003 (2006).

- P9. "Laser-assisted charge transfer in  $\text{He}^{2+} + \text{H}$  collisions," F. Anis, V. Roudnev, R. Cabrera-Trujillo, and B.D. Esry, Phys. Rev. A **73**, 043414 (2006).
- P8. "Preference for breaking the O-H bond over the O-D bond following HDO ionization by fast ions," A.M. Sayler, M. Leonard, K.D. Carnes, R. Cabrera-Trujillo, B.D. Esry, and I. Ben-Itzhak, J. Phys. B **39**, 1701 (2006).
- P7. "Lattice approach for  $\text{H}_2^+$  collisions," S.C. Cheng and B.D. Esry, Phys. Rev. A **72**, 022704 (2005).
- P6. "Dissociation and ionization of  $\text{H}_2^+$  by ultra-short intense laser pulses probed by coincidence 3D momentum imaging," I. Ben-Itzhak, P.Q. Wang, J.F. Xia, A.M. Sayler, M.A. Smith, K.D. Carnes, and B.D. Esry, Phys. Rev. Lett. **95**, 073002 (2005).
- P5. "Highlighting the angular dependence of bond softening and bond hardening of  $\text{H}_2^+$  in an ultrashort intense laser pulse," P.Q. Wang, A.M. Sayler, K.D. Carnes, J.F. Xia, M.A. Smith, B.D. Esry, and I. Ben-Itzhak, J. Phys. B **38**, L251 (2005). *Selected as a "J. Phys. B Highlight of 2005".*
- P4. "Bond rearrangement caused by sudden single and multiple ionization of water molecules," I. Ben-Itzhak, A.M. Sayler, M. Leonard, J.W. Maseberg, D. Hathiramani, E. Wells, M.A. Smith, J. Xia, P. Wang, K.D. Carnes, and B.D. Esry, Nucl. Instrum. Meth. B **233**, 284 (2005).
- P3. "Dissociation and ionization of molecular ions by ultra-short intense laser pulses probed by coincidence 3D momentum imaging," I. Ben-Itzhak, P. Wang, J. Xia, A.M. Sayler, M.A. Smith, K.D. Carnes, and B.D. Esry, Nucl. Instrum. and Meth. B **233**, 56 (2005).
- P2. "Intensity-selective differential spectrum: Application to laser-induced dissociation of  $\text{H}_2^+$ ," P.Q. Wang, A.M. Sayler, K.D. Carnes, B.D. Esry, and I. Ben-Itzhak, Opt. Lett. **30**, 664 (2005).
- P1. "HD<sup>+</sup> photodissociation in the scaled coordinate approach," V. Roudnev and B.D. Esry, Phys. Rev. A **71**, 013411 (2005).

## Theoretical Studies of Atoms and Molecules with intense laser pulses

C. D. Lin

J. R. Macdonald Laboratory  
Kansas State University  
Manhattan, KS 66506  
e-mail: cdlin@phys.ksu.edu

### Program Scope:

We investigate the interaction of intense lasers and attosecond light pulses with atoms and molecules, including high-order harmonic generation, energy and momentum spectra of the electrons or ions, with the goal of interpreting and/or guiding experimental observations.

### 1. Potential for rescattering based ultrafast imaging of molecules with infrared lasers

#### *Recent progress*

When an atom or molecule is exposed to an intense infrared laser pulse, an electron which was released earlier may be driven back to recollide with the parent ion. The resulting **rescattering** phenomena carry information on the structure of the target. Using "exact" results from the solution of the time-dependent Schrödinger equation (TDSE), we established the general conclusion that accurate elastic and photo-recombination cross sections of the target ion with free electrons can be accurately extracted from laser-generated high-energy photoelectron momentum spectra and high-order harmonic spectra, respectively. Both electron scattering and photoionization (the inverse of photo-recombination) are the conventional means for studying the structure of atoms and molecules. Combing with the temporal resolution of a few femtoseconds for infrared laser pulses, these results point out the potential of using existing infrared lasers for ultrafast imaging of transient molecules which are undergoing chemical or biological transformations.

The interaction of atoms and molecules with intense laser pulses is a nonlinear process. In this work, we have found that elastic scattering cross sections and recombination cross sections can be extracted from laser-generated phenomena. This is possible since the returning electrons after the initial ionization can be regarded as a self-generated electron wave packet. This electron wave packet can be elastically backscattered by the ion core, or recombined with it to generate harmonics. By focusing on the momentum spectra of the backscattered electrons, we showed that elastic scattering cross sections, as well as the electron wave packet, can be extracted. Similarly, from the high-order harmonic spectra, we concluded that photo-recombination cross sections and the electron wave packet can be identified. Furthermore we were able to conclude that the derived electron wave packet is nearly independent of the target, and furthermore, the wave packets derived form solving the TDSE and from the strong-field approximation are the same. Two reports based on this work have been submitted for publication [**B1,B2**].

### *Future plan*

The results obtained for atoms described above have many possible applications for molecular targets. For molecules, accurate calculations based on solving the TDSE equation is not possible. Based on the general results obtained for atoms, we intend to develop a quantitative laser-molecule interaction theory in the following manner. We will develop (or adopt) codes for calculating elastic scattering cross sections and photoionization cross sections of molecules over a broad range of energies. Combining with the electron wave packet for a given laser pulse which can be extracted from atomic targets or calculated from the strong-field approximation, we will be able to obtain high-energy electron momentum spectra and high-order harmonic spectra for molecules accurately, making a quantitative laser-molecule interaction theory possible.

## **2. Attosecond pulses probing two-electron dynamics**

### *Recent progress*

In the last year, we have witnessed continuing progress in the development of uv and xuv light sources with pulse duration down to about 130 attoseconds. Such pulses are comparable to the time-scale of the electronic motion in atoms and molecules, thus they open up the possibility for the time-resolved study of electron dynamics, in analogy to femtosecond lasers for probing the atomic motion in a molecule. Ideally one would like to use these pulses to study the many-body nature of electrons, or the so-called electron correlation effect, in the time domain. How to extract meaningful information from future pump-probe experiments with attosecond pulses turns out to be not as straightforward as one would like.

In describing the motion of atoms in a molecule, the atoms can be adequately described using classical concept. This is not the case for electrons, which are described by quantum mechanics. A precise determination of the time inevitably loses accurate information on the energy and the momentum of the electron. Experimentally the best one can do is to be able to measure the momentum vector of all the electrons that are ionized. Information on the time evolution of the electron wave packet has to be extracted from the measured electron momentum spectra. Clearly, each measurement can only reveal partial information and it is important to understand what probe pulses be used for probing specific aspects of the electronic wave packet.

In a recent paper [A2] we studied the dynamics of a two-electron wave packet which was formed by a pump pulse. The time-resolved correlated motion of the two electrons are probed by measuring their six-dimensional momentum distributions. In this paper, as an example, we showed how the multi-dimensional momentum distributions be analyzed, i.e., by choosing appropriate coordinates, in order to reveal the time-dependence of the stretching, the rotational and the bending vibrational modes of their joint motion in momentum space.

### *Future plan*

We will continue exploring the time-dependent behavior of the joint motion of two electrons. In the next year, we will test parameters of attosecond pulses that would reveal

the dynamics of the double ionization of helium atoms by an attosecond pulse. Depending on the photon energy, double ionization proceeds with two mechanisms: shake off vs the so-called TS2. In shakeoff, the first electron leaves quickly and the second electron is ionized via the relaxation process. In TS2, the second electron is ionized via electron-electron interaction as the first electron emerges from the atom. We will examine parameters of the attosecond pulses where these two different mechanisms can be distinguished in their time dependence using a second attosecond pulse.

### **3. Low-energy 2D electron momentum spectra of atoms by intense laser pulses**

#### *Recent progress*

This project was initiated by the interesting experimental observations by Dr. Lew Cocke's group at Kansas State, and by the Heidelberg group. Using lasers of different wavelengths and intensities, these experiments found that the two-dimensional electron momentum spectra at low-energies exhibit ubiquitous fan-like structures. We obtained the 2D momentum spectra by solving the time-dependent Schrodinger equation and observed that these fan-structures do appear in the calculated spectra. The "fans" are related to the fact that there is one dominant angular momentum for the low energy electrons generated by lasers, and we have been able to derive a general rule which would predict the value of this angular momentum quantum number [A6]. This value depends only on the minimum number of photons needed to ionize the atom, and independent of the target, nor of the wavelength or intensity. We also concluded that the fan-like structure exists only when the Coulomb interaction between the electron and the ion-core is included. We further show that the effect of the laser focus volume and the depletion of the atom during the laser pulse should be included in order to achieve good agreement with experiments [A4].

#### *Future plan*

Having identified the ubiquitous features of 2D momentum spectra from atoms, we will examine what features would appear in negative ions.

### **4. Other projects**

#### *Recent progress*

We also have examined the dissociative ionization and double ionization of H<sub>2</sub> and D<sub>2</sub> molecules by few-cycle pulses [A1,A3]. For atomic ions emerging with energies of the order of 4 eV or higher, the dissociation or the second ionization is initiated by the rescattering process. The dissociation products, with protons emerging on the right or on the left, depend on the carrier-envelope phase (cep) of the few-cycle pulse. Based on the rescattering theory, and taking into account of the laser coupling between the two lowest states of D<sub>2</sub><sup>+</sup>, we were able to interpret the experimental observation of Kling et al [Science 312, 246 (2006)]. We also calculated the ratio of double vs. single ionization by few-cycle pulses and their dependence on the cep, but no such experimental results are available so far.

Other activities not discussed here can be found from the publication list below.

## **Publications**

### **A. Published papers**

- A1. X. M. Tong and C. D. Lin, "Dynamics of light-field control of molecular dissociation at the single-cycle limit", Phys. Rev. Lett. 98, 123002 (2007).
- A2.. Toru Morishita, S. Watanabe and C. D. Lin, "Attosecond light pulses to reveal the time-dependent rovibrational motion of the correlated electron pairs in helium", Phys. Rev. Lett. 98, 083003 (2007)
- A3. X. M. Tong and C. D. Lin, "Carrier-envelope phase dependence of nonsequential double ionization of H<sub>2</sub> by few-cycle laser pulses", J. Phys. B40, 641 (2007).
- A4. Toru Morishita, Z. Chen, S. Watanabe and C. D. Lin, " Two-dimensional electron momentum spectra of argon ionized by short intense lasers: Comparison of theory with experiment", Phys. Rev. A. 75, 023407 (2007)
- A5. A. T. Le, X. M. Tong and C. D. Lin, "Alignment dependence of high-order harmonic generation from CO<sub>2</sub>", J. Mod. Optics , 54, 967 (2007). [\[CrossRef\]](#)
- A6. Z. Chen, Toru Morishita, A. T. Le, M. Wickenhauser, X. M. Tong and C. D. Lin, " Analysis of two-dimensional photoelectron momentum spectra and the effect of long-range Coulomb potential in single ionization of atoms by intense lasers", Phys. Rev. A74, 053405 (2006).
- A7. M. Wickenhauser, X. M. Tong, D. G. Arbo, J. Burgdorfer and C. D. Lin, "Signature of multiphoton and tunneling ionization in the electron momentum distributions of atoms by intense few-cycle laser pulses", Phys. Rev. A74, 041402(R), (2006).
- A8. C. D. Lin and X. M. Tong, "Dependence of tunneling ionization and harmonic generation on the structure of molecules by short intense laser pulses", J. photochemistry and photobiology, 182, 213 (2006)
- A9. Patricia Barragan, Anh-Thu Le, and C.D. Lin, " Hyperspherical close-coupling calculations for electron-capture cross sections in low-energy Ne(10+) + H(1s) collisions, Phys. Rev. A 74, 012720 (2006)
- A10. X. M. Tong, Z. X. Zhao and C. D. Lin, Comment on "Correlation quantum dynamics between an electron and D2+ molecules with attosecond resolution", Phys. Rev. Lett. 97, 049301 (2006)

### **B. Papers submitted for publications**

- B1. Toru Morishita, Z. Chen, A. T. Le and C. D. Lin, "Theory of rescattering based ultrafast imaging of molecules with infrared laser pulses", submitted to Science.
- B2. A. T. Le, Toru Morishita and C. D. Lin, "Improved three-step model for high-harmonic generation of atoms and molecules with scattering wavefunctions ", submitted to Phys. Rev. Lett.

## Structure and Dynamics of Atoms, Ions, Molecules and Surfaces: Atomic Physics with Ion Beams, Lasers and Synchrotron Radiation

I.V. Litvinyuk, Physics Department, J.R. Macdonald Laboratory, Kansas State University,  
Manhattan, KS 66506, [ivl@phys.ksu.edu](mailto:ivl@phys.ksu.edu)

### **1. Time-resolved dynamics of heavy-particle motion in neutral molecules and molecular ions**

*Our goal is to study and understand the physics of ultrafast processes involving the motion of nuclei associated with the rotation, vibration, rearrangement and dissociation of molecules and molecular ions. We apply pump-probe techniques in combination with COLTRIMS detection to study the dynamics of nuclear motion as it takes place in real time with the ultimate goal of recovering the time-dependent molecular structure and orientation — making a “molecular movie”.*

#### **Recent progress:**

**1.1 Pump-probe studies of vibrational and rotational dynamics in light and heavy hydrogen using few-cycle pulses and Coulomb explosion as a probe,** *I. Bocharova, M. Magrakvelidze, D. Ray, C. Maharjan, P. Ranitovic, C.L. Cocke and I.V. Litvinyuk.* We studied nuclear dynamics in H<sub>2</sub> and D<sub>2</sub> induced by intense few-cycle 800 nm pulses, building on our previous studies [1, 2]. While in those works we were restricted by our pump-probe setup to at most 200 fs of delay, we now removed that limitation by using Mach-Zehnder interferometer for generating time-delayed pump and probe pulses. We can now measure dynamics at any delay with additional advantage of independently controlling pump and probe polarization. With this new setup we studied vibrational and rotational dynamics in H<sub>2</sub> and D<sub>2</sub> in much wider time range (up to 3000 fs). For molecules ionized by the pump pulse we observe both dissociation, occurring on the electronically excited σ<sub>u</sub> potential energy surface, and vibrational dynamics, taking place on the bound ground-state σ<sub>g</sub> surface. Bound vibrational dynamics is characterized by fast decoherence and later revivals of vibrational wavepackets. Molecules that survive the pump pulse without being ionized are also affected by it. Due to their anisotropic polarizability, coherent rotational wavepackets are generated, which persist without any decoherence for very long time. We measured dynamics of rotational wavepackets for both H<sub>2</sub> and D<sub>2</sub>. In D<sub>2</sub>, which is heavier with smaller separation between rotational energy levels, rotations of up to J = 9 are excited by the pump, resulting in well localized wavepackets with clear revivals. However in H<sub>2</sub>, we could only excite rotations up to J = 3 due to large separation between the levels. Therefore, rotational wavepackets for each nuclear spin form of light hydrogen (ortho or para) consisted of at most two rotational states (1 and 3 for ortho and 0 and 2 for para) and instead of clear revivals we observed periodic beating between the two states. That was the first direct time-resolved measurement of coherent rotational dynamics in light hydrogen – the fastest rotating molecule in nature (T<sub>r</sub> ≈ 270 fs).

**1.2 Pump-probe studies of ultrafast intra-molecular proton transfer in acetylene,** *M. Smolarski, T. Osipov, I. Bocharova, M. Magrakvelidze, D. Ray, C. Maharjan, P. Ranitovic, C.L. Cocke and I.V. Litvinyuk.* Acetylene dication (C<sub>2</sub>H<sub>2</sub><sup>2+</sup>) produced by double ionization of neutral molecule is known to undergo fast intramolecular proton transfer to vyniledene form (C-CH<sub>2</sub>) followed by asymmetric breakup [2]. The transfer time was estimated to be less than 60 fs [3].

In collaboration with U. Frankfurt (Smolarski) and LBLN (Osipov) we conducted an experiment at JRML aimed at observing this ultrafast process in real time using pump-probe approach with few-cycle IR pulses. By measuring time dependence of relative angles between momenta of various Coulomb explosion fragments dynamics of chemical transformation could be revealed. The results of this experiment are being analyzed.

**Future plans:** We are planning to continue pump-probe studies of fast molecular dynamics, extending it to tri-atomic molecules ( $\text{CO}_2$ , preliminary experiment has already been conducted). We are also planning to study dynamics of molecules *during* the pulse, using long ( $>30$  fs) pump and few-cycle probe pulses. Our other plan is to conduct pump-probe experiment on hydrogen with coincident ion and electron detection.

## 2. Mechanisms of strong-field double ionization of atoms and molecules studied by ion recoil momentum spectroscopy at Advanced Laser Light Source (ALLS)

*This international collaboration is directed towards understanding dynamics and mechanisms of multiple ionization of atoms and molecules by intense laser pulses. To achieve that, we measure momentum spectra of resulting ion fragments for a series of different laser intensities and wavelength using high power OPA beamline at ALLS.*

**Recent progress:**

**2.1 Non-sequential double ionization of Ne and Ar: wavelength scaling similarity**, A. Alnaser, D. Comtois, A. Hasan, D. Villenueve and I.V. Litvinyuk. Strong-field double ionization of atoms in non-sequential regime produces longitudinal ion momentum distributions with a characteristic double-peak structure. At 800 nm laser wavelength in  $\text{Ne}^{2+}$  the structure is very pronounced with a well resolved dip at zero momentum, while for  $\text{Ar}^{2+}$  the dip is very shallow, possibly indicating different mechanisms in the two atoms [3]. We investigated the source of this difference by measuring longitudinal momentum distributions of  $\text{Ne}^{2+}$  and  $\text{Ar}^{2+}$  ions at different laser wavelengths (485, 800, 1313 and 2000 nm) and intensities (Figure 1).

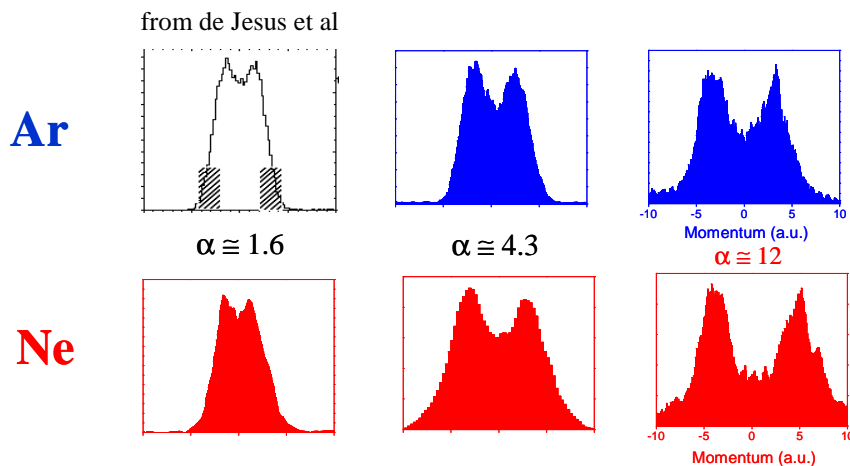


**Figure 1.** Longitudinal momentum distributions for  $\text{Ne}^{2+}$  and  $\text{Ar}^{2+}$  can be made to look similar with appropriate scaling of laser wavelength. Scaling parameter:  
 $\alpha = \frac{\text{Up}(I_{\text{sat}})/\text{IP}(I_+)}{\text{Up}} - \text{ratio of largest possible re-collision electron energy}$   
 $(3.17 \text{ Up}_{\text{p}} \text{ at saturation intensity for first ionization}) \text{ to the second ionization potential.}$

The shapes of experimental momentum distributions for the two atoms exhibit a simple wavelength scaling relationship: they are similar for the same value of a scaling parameter given by the ratio of maximum electron recollision energy ( $3.17 U_p$  at saturation intensity for single ionization) to ionization potential of a singly charged ion. This similarity indicates that the difference between Ne and Ar observed at 800 nm should not be attributed to differences in relative electron impact ionization and excitation cross-sections of the two atoms, stemming from their electronic structure, as was thought previously. It is rather due to interplay between values of maximum energy of recollision electrons at any given wavelength and ionization potential of a singly charged ion.

**2.2 Double ionization of H<sub>2</sub> and D<sub>2</sub>: evidence of a three-photon resonant pathway,** A. Alnaser, D. Comtois, A. Hasan, D. Villeneuve and I.V. Litvinyuk. A new and unexpected observation of structured KER spectra of D<sup>+</sup>/H<sup>+</sup> Coulomb explosion fragments at 800 nm [4] motivated this study. The suggested explanation involves interference of two possible paths taken by nuclear wavepackets on ground state and excited electronic surfaces of molecular ion [5]. To clarify this issue, we studied double-ionization of H<sub>2</sub> and D<sub>2</sub> by intense femtosecond laser pulses of different wavelengths (500, 600, 800, 1300, 2000 nm) and peak intensities. The kinetic energy release (KER) spectra measured in the Coulomb explosion of the molecules were used to identify the various mechanisms responsible for the dissociation and ionization of H<sub>2</sub>/D<sub>2</sub> in the laser fields. In addition to fragments from well known bond softening and enhanced ionization channels, high energy protons/deuterons of KER (around 10.5 eV for 500 nm) were for the first time observed when using short wavelengths (500 and 600 nm) at high-peak intensities (Figure 2). This channel exhibited wavelength dependence, with KER decreasing for longer wavelengths. Our observations are consistent with presence of two co-existing pathways: one- and three-photon excitation followed by enhanced ionization. For the three-photon pathway nuclei gain extra kinetic energy before reaching the critical distance for enhanced ionization. This explanation is also consistent with the explanation offered in [4]: at longer wavelength the wavepackets propagating along the two pathways strongly overlap in energy leading to observed interference structures in KER spectra. We are working with theorists on preparing these findings for publication.

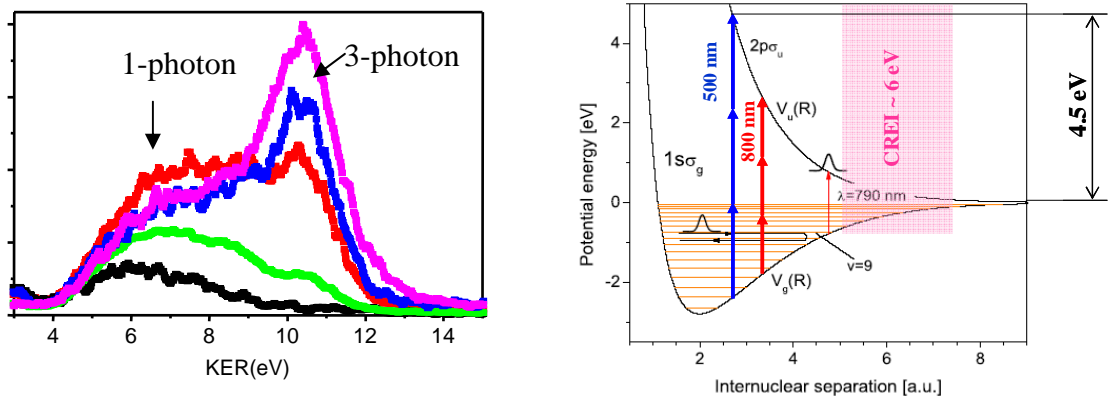


**Figure 2.** KER spectra of D<sup>+</sup> fragments produced by 500 nm pulses of 100 fs duration with intensities of 1, 2, 3, 4 and  $7 \times 10^{13}$  W/cm<sup>2</sup>. Right panel shows potential energy diagrams for D<sub>2</sub><sup>+</sup>.

**Future plans:** We are planning to continue this collaboration, extending wavelength-dependent studies of multiple ionization mechanisms to larger molecules ( $N_2$ ,  $O_2$ ,  $CO_2$ ). Next beamtime at ALLS is planned for August 2007.

### References:

1. Alnaser *et al*, Phys. Rev. A **72**, 030702(R) (2005)
2. Alnaser *et al*, J. Phys. B: At. Mol. Opt. Phys. **39**, S489 (2006)
3. de Jesus *et al*, J. Phys. B: At. Mol. Opt. Phys. **37**, L161 (2004)
4. Staudte *et al*, Phys. Rev. Lett. **98**, 073003 (2007)
5. Chelkowsky *et al*, Phys. Rev. A **76**, 013405 (2007)

### Publications in 2006-07:

1. *Wavelength dependence of momentum-space images of low-energy electrons generated by short intense laser pulses at high intensities*, C.M. Maharjan, A.S. Alnaser, I. Litvinyuk, P. Ranitovic and C.L. Cocke, **J. Phys. B: At. Mol. Opt. Phys. 39, 1955 (2006)**
2. *Momentum-imaging investigations of the dissociation of D<sub>2</sub><sup>+</sup> and the isomerization of acetylene to vinylidene by intense short laser pulses*, A.S. Alnaser, I. Litvinyuk, T. Osipov, B. Ulrich, A. Landers, E. Wells, C.M. Maharjan, P. Ranitovic, I. Bocharova, D. Ray and C.L. Cocke, **J. Phys. B: At. Mol. Opt. Phys. 39, S489 (2006)**
3. *Multi-photon resonant effects in strong-field ionization: origin of the dip in experimental longitudinal momentum distributions*, A.S. Alnaser, C.M. Maharjan, P. Wang and I.V. Litvinyuk **J. Phys. B: At. Mol. Opt. Phys. 39, L323 (2006)**

**Electronic Excitations and Dynamics in Carbon Nanotubes Induced by Femtosecond  
Pump-Probe LASER Pulses**

Pat Richard

JR Macdonald Laboratory, Physics Department, Kansas State University  
Manhattan, Kansas 66506  
[richard@phys.ksu.edu](mailto:richard@phys.ksu.edu)

We have continued our efforts in the J. R. Macdonald Laboratory, JRML, directed toward the study of electronic excitations and dynamics in carbon nanotubes excited by femtosecond pump-probe laser pulses generated by the ultra-fast Ti:Sapphire Kansas Light Source, KLS. We use time-of-flight of electrons emitted from carbon nanotubes to deduce the energy and time behavior of the electronic states of the nanotubes. Experiments have been performed on multiwalled carbon nanotubes, MWNT, and more recently on both double walled carbon nanotubes, DWNT, and single walled carbon nanotubes, SWNTs. We have also completed earlier studies of transfer-ionization and single-electron capture in heavy ion gas target collisions. This year we are beginning a new effort to study the properties of single walled carbon nanotubes by observing the time-resolved anti-Stokes Raman scattering from selected diameter SWNTs in collaboration with Prof. Tony Heinz at Columbia University. We plan to measure the room temperature lifetime of the G-mode phonons for SWNTs in different environments. This work will be performed at Columbia.

---

During the coming year we will be studying both electron emission and optical emission (anti-Stokes scattering) from SWNTs. The electron emission studies will continue at the JRM KLS lab and the optical studies will be performed at the Columbia University in New York. We will be using the target production technology developed at Columbia to study SWNTs with a narrow range of selected diameters. The energy of the Raman scattering peaks will be used to isolate on (6,5) chiral index SWNTs. The studies will be performed at room temperature. One KSU graduate student, Ioannis Chatzakis, will spend the academic year 2007-08 at Columbia performing the experiments. I will be at Columbia for two weeks during the experiments. The collaboration brings two important new aspects to our research efforts at KSU. One is the use of the optical system consisting of a femtosecond Ti:Sapphire laser, two OPAs, and an efficient high resolution optical spectrometer system. The second is the technology of SWNT target fabrication. Targets fabricated at Columbia and used in the optical experiments will be used at KSU in subsequent experiments.

A summary of our recent efforts is best described in the abstracts which are given below of two papers published since last year's DOE workshop. These are diverse projects. The first subject presents the fifth in a series of papers on the study of electron emission from carbon nanotubes using ultra-fast pump-probe laser beams from the JRML KLS facility. The second subject presents the results of momentum imaging of high velocity, highly-charged ion beam collisions on a supersonic He gas jet target to uniquely separate transfer-ionization from pure single-electron capture using the JRML Van de Graaff accelerator.

# Excitons in bundles of single walled carbon nanotubes

M. Zamkov <sup>a</sup>, A. Alnaser , Z. Chang , P. Richard

Chemical Physics Letters **437** 104–107 (2007)

*J.R. Macdonald Laboratory, Department of Physics, Kansas State University,  
Manhattan, Kansas 66506, USA*

a. present address: School of Chemical Sciences, University of Illinois at Urbana-Champaign, Box 71-6 CLSL, 600 South Mathews Avenue, Urbana, IL 61801, USA

Time-resolved photoemission was used to differentiate between excitons and free carriers in non-fluorescing bundles of single walled carbon nanotubes (SWNT). Present findings show that direct interband excitations in semiconductive SWNTs lead to the formation of strongly bound excitons, indicating that proximity effects in SWNTs bundles do not destroy a one-dimensional character of optical excitations.

## Systematic study of charge-state and energy dependences of transfer-ionization to single- electron capture ratios for $F^{q+}$ ions incident on He

R. Ünal,<sup>\*</sup> P. Richard, I. Ben-Itzhak, C. L. Cocke, M. J. Singh,<sup>‡</sup> H. Tawara,<sup>§</sup> and N. Woody

PHYSICAL REVIEW A **76**, 012710 (2007)

*J.R. Macdonald Laboratory, Department of Physics, Kansas State University,  
Manhattan, Kansas 66506, USA*

<sup>\*</sup>Present address: Afyon Kocatepe University, Afyon, Turkey.

<sup>‡</sup>Present address: The Institute for Plasma Research, Bhat Gandhinagar, India.

<sup>§</sup>Present address: Max Planck Institute for Nuclear Physics, Heidelberg, Germany

This paper presents an investigation of the charge-state and energy dependences of transfer-ionization, TI, and single-electron capture, SC, processes for fluorine ions ( $q = 4+$  to  $9+$ ) incident on a supersonic He jet target. The measurements were made for beam energies between 0.5 and 2.5 MeV/u. A recoil ion momentum spectrometer was used to separate TI and SC based on the longitudinal momentum transfer and time of flight of the recoil ions. The cross-section ratios for TI to SC, ( $R = TI /SC$ ), were determined and observed to decrease monotonically with velocity. The values of  $R$  were combined with measured total transfer cross sections to deduce the cross sections for both SC and TI. Coupled-channel calculations of the energy dependence of TI and SC for  $F^{9+} + He$  were compared to the experimental cross sections as well as the values of  $R$ . The calculated cross sections were found to be slightly lower and the  $R$  values slightly higher than the measured values, but with approximately the same energy dependences. A  $q^2$  scaling of

the  $\text{He}^{2+} + \text{He}$  data was also compared to the present data and was found to give unexpected good agreement.

---

**Publication # 1: Excitons in bundles of single walled carbon nanotubes** M. Zamkov, Ali S. Alnaser, Bing Shan, Zenghu Chang, and P. Richard, Chemical Physics Letters **437** 104–107 (2007).

**Publication # 2: Systematic study of charge-state and energy dependences of transfer-ionization to single-electron-capture ratios for  $\text{F}^{q+}$  ions incident on He** R. Ünal, P. Richard, I. Ben-Itzhak, C. L. Cocke, M. J. Singh, H. Tawara, and N. Woody, Phys. Rev. A **76**, 012710 (2007).

**Publication # 3: Probing the intrinsic conductivity of multiwalled carbon nanotubes** M. Zamkov, Ali S. Alnaser, Bing Shan, Zenghu Chang, and P. Richard, Applied Physics Lett. **89**, 093111 (2006).

**Publication # 4: Lifetime of Charge Carriers in Multi-walled Nanotubes** M. Zamkov, N. Woody, B. Shan, Z. Chang and P. Richard, Phys. Rev. Lett. **94**, 056803 (2005).

**Publication # 5: Investigation of triply excited states of Li-like ions in fast ion-atom collisions by zero-degree Auger projectile electron spectroscopy** T.J.M. Zouros, E.P. Benis, M. Zamkov, C.D. Lin , T.G. Lee , P. Richard , T.W. Gorczyca, T. Morishita, Nucl. Instr. and Meth. in Phys. Res. B **233**, 161–171(2005)

# Structure and Dynamics of Atoms, Ions, Molecules and Surfaces: Atomic Physics with Ion Beams, Lasers and Synchrotron Radiation

Uwe Thumm, J.R. Macdonald Laboratory, Kansas State University  
Manhattan, KS 66506 [thumm@phys.ksu.edu](mailto:thumm@phys.ksu.edu)

## 1. Laser-molecule interactions (with T. Niederhausen and B. Feuerstein)

**Project scope:** We seek to develop numerical and analytical tools to i) efficiently predict the effects of a strong laser field on the bound and free electronic and nuclear dynamics in small molecules and ii) to fully image the laser-controlled molecular dynamics.

**Recent progress:** We continued our investigation of the dissociation and ionization of  $D_2$  and  $D_2^+$  in short intense laser pulses by applying wave-packet propagation methods. In particular, we investigated the possibility of manipulating the vibrational-state decomposition of bound vibrational wave packets with a sequence of short control laser pulses at minimal dissociative loss. In a proof-of-principles effort, we introduced an internuclear-distance-dependent harmonic imaging technique that allows vibrational beat frequencies, molecular potential curves, and the nodal structure of nuclear wave functions to be derived from measured kinetic-energy-release (KER) spectra.

### **Example 1:** Controlled vibrational quenching of nuclear wave packets in $D_2^+$ .

Ionization of neutral  $D_2$  molecules by a short and intense pump laser pulse may create a vibrational wave packet on the lowest ( $1s\sigma_g^+$ ) adiabatic potential curve of the  $D_2^+$  molecular ion [1]. We showed numerically that a single ultra-short intense near-infrared (800 nm) control pulse with an appropriate time delay can strongly quench the vibrational-state distribution of the nuclear wave packet by increasing the contribution of selected stationary vibrational states of  $D_2^+$  to more than 50% [2]. We found that a second identical control pulse with a carefully adjusted delay can further squeeze the vibrational state distribution, likely without dissociating the molecular ion, thereby suggesting a multi-pulse control protocol for generating (almost) stationary excited nuclear wave functions (Fig. 1). The quality of this Raman-control mechanism can be tested experimentally by Coulomb-explosion imaging, i.e., by fragmenting the molecular ion with a probe pulse and by identifying the nodal structure of the surviving vibrational state in the KER spectrum of the molecular fragments [1,2].

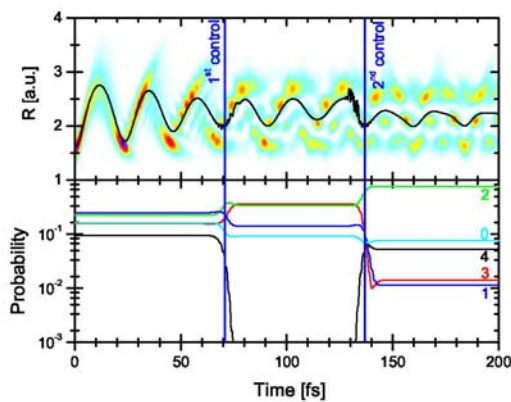


**Fig. 1. Top:** Time evolution of the nuclear wave function probability density as a function of the internuclear distance  $R$  for two 6 fs,  $10^{14}$  W/cm $^2$  control pulses with delay times of  $\tau_1=70.7$  fs and  $\tau_2=136.8$  fs relative to the launch time ( $t=0$ ). The superimposed curve shows the expectation value  $\langle R \rangle$ .

**Bottom:** Time evolution of a few stationary-vibrational-state contributions to the wave packet.

**Future plans:** Coherent control schemes for quenching moving vibrational wave packets into stationary states using one or several standardized control pulses will be further examined. The quality of such schemes can be conveniently assessed by Coulomb-explosion mapping of the stationary state's nodal structure.

**Example 2:** Towards the complete imaging of molecular dynamics with ultra-short laser pulses. Time-resolved Coulomb explosion mapping of vibrating and dissociating  $D_2^+$  molecules allowed us to perform an internuclear distance- ( $R$ -) dependent Fourier analysis of the corresponding wave packets [3]. Our calculations demonstrate that the obtained two-dimensional  $R$ -dependent frequency spectra enable the complete characterization of the wave-packet dynamics and directly visualize the field-modified molecular potential curves in intense, ultra-short laser pulses, including 'bond softening' and 'bond hardening' processes. Figure 2 shows examples of this imaging scheme for the complete mapping of molecular potential curves for the fundamental deuterium molecular ion, for laser-free propagation of  $D_2^+$  nuclear wave packets (Fig. 2a) and including the interaction with a laser electric field (Fig. 2b). These examples show how the molecular potential and its bound vibrational wave function are modified by the added laser field.

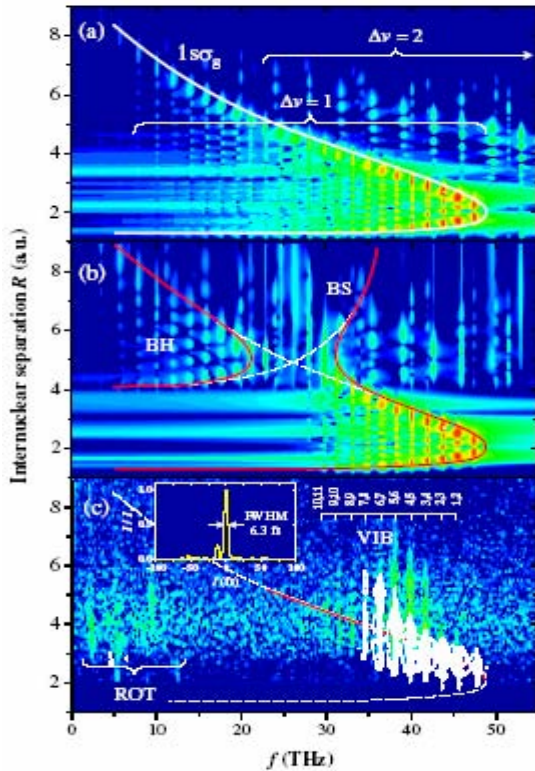


**Fig. 2.** Power spectrum  $|w(R,f)|^2$  as function of the frequency  $f$  and  $R$  for  $T=3$  ps. (a): numerical field-free wave packet propagation of an initial Franck-Condon distribution. (b): as (a) but with a 50 fs pedestal of  $0.01$  PW/cm $^2$  preceding the probe pulse causing 'bond softening' (BS) and 'bond hardening' (BH). (c): Experimental distribution extracted from coincident  $D^+$  pairs with vibrational (VIB) and rotational (ROT) contributions. White contours: numerical results using the actual laser pulse profile (see inset).

Our method relies on the Fourier transformation,  $w(R,f)$ , over a sampling time  $T$  of the time- and  $R$ -dependent probability density  $w(R,t)$  of the  $D_2^+$  nuclear wave packet. Applied to numerically propagated  $D_2^+$  vibrational wavepackets, it allows us to simulate the outcome of novel experiments. The simulated experiments are assumed to be based on the Coulomb-explosion mapping of pump-probe-delay ( $\tau$ )-dependent KER spectra and subsequent  $R$ -dependent harmonic analysis for finite  $T$  ( $0 < \tau < T$ ). Preliminary experimental results [3] shown in Figure 2c reproduce the known vibrational beat

frequencies  $f$  and retrace the outer part of the potential well. So far, the inner part of the potential well could not be observed due to highly suppressed ionization rates at small  $R$ .

**Future plans:** Extending this technique to more complicated polyatomic molecular systems or reacting complexes will enable the investigation of molecular dynamics across the (field-modified) potential barrier along a particular reaction coordinate, and, thus, provide a basis for novel schemes of multidimensional optical control of reactions. Other extensions of this method can be applied to quantify the progression of decoherence in the nuclear motion, based on a time series of KER spectra.

## **2. Neutralization of negative hydrogen ions near vicinal metal surfaces (with Boyan Obreshkov)**

**Project scope:** We attempt to understand the transfer of a single electron, initially bound to the projectile, during the reflection of a slow ion or atom at an arbitrarily shaped, nanostructured metal surface as a function of the collision parameters, the surface electronic structure, and crystal orientation of the surface.

**Recent progress:** We continued to develop a new set of computer programs to calculate the ground-state electronic structure of arbitrarily shaped metallic surfaces and tested our codes in applications to flat and vicinal metal and semi-conductor surfaces [4,5]. We improved our density functional model of the ground-state electronic structure of the surface by including linear and quadratic electronic response terms and heuristic core potentials centered at the lattice points in order to provide realistic, self-consistent surface potentials (Fig. 3). We employed these potentials to model the charge-transfer dynamics during the ion-surface collisions, based on a Newns-Anderson approach and including image-charge interactions and electron translation factors [6].

**Example:** We calculated *ab-initio* the yield of outgoing negative hydrogen ions that are normally incident on a Si(100) surface with kinetic energies between 50 and 150 eV [6]. We find that the outgoing  $H^-$  fraction is mainly determined by electron capture from dangling-bond surface-state resonances at relatively large distances from the surface (Fig. 4). We find good qualitative agreement with the experimental results of Maazouz *et al.* (Surf. Sci. 398, 49 (1998)) and with recent independent calculations by Garcia *et al.* (Surf. Sci. 600, 2195 (2006)).

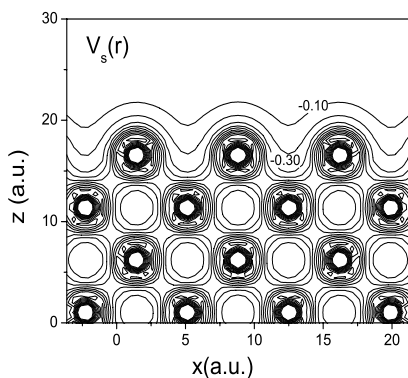


**Fig. 3.** Contour map of the potential energy of an electron near the Si(100) surface. The contour-line spacing is 0.1 a.u. The labels give potential energies relative to the vacuum energy level.

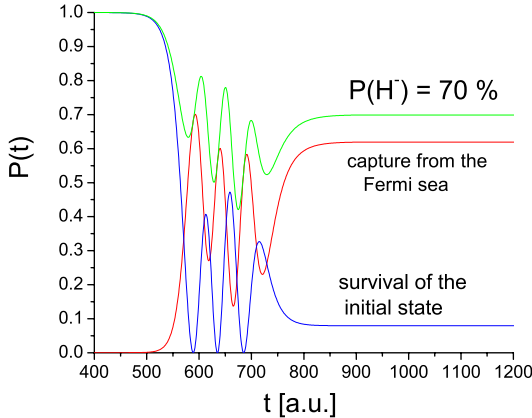


**Fig. 4.** Survival probability for normally incident 150 eV  $H^-$  ions as a function of time.

**Future plans:** We plan to investigate resonance formation and charge exchange near vicinal and other structured surfaces. In particular, we will investigate the importance of lateral confinement effects (evidence for which was found in photo-emission experiments).

- [1] B. Feuerstein and U. Thumm, Phys. Rev. A **67**, 063408 (2003); Phys. Rev. A **67**, 043405 (2003); J. Phys. B **36**, 707-716(2003).
- [2] T. Niederhausen and U. Thumm, submitted to Phys. Rev. A.
- [3] B. Feuerstein, Th. Ergler, A. Rudenko, K. Zrost, C. D. Schröter, R. Moshammer, and J. Ullrich, T. Niederhausen and U. Thumm, submitted to Phys. Rev. Lett.
- [4] B. Obreshkov and U. Thumm, Phys. Rev. A **74**, 012901 (2006)
- [5] B. Obreshkov and U. Thumm, Surf. Sci. **601**, 622 (2007).
- [6] B. Obreshkov and U. Thumm, submitted to Phys. Rev. A.

#### Other DoE-sponsored publications (2004-2007):

- M. Zamkov, H.S. Chakraborty, A. Habib, N. Woody, U. Thumm, and P. Richard, Phys. Rev. B**70**, 115419 (2004).
- M. Zamkov, N. Woody, S. Bing, H.S. Chakraborty, U. Thumm, and P. Richard, Phys. Rev. Lett. **93** 156803 (2004).
- T. Niederhausen, B. Feuerstein, and U. Thumm, Phys. Rev. A **70**, 023408 (2004).
- H.S. Chakraborty, T. Niederhausen, and U. Thumm, Phys. Rev. A **69**, 052901 (2004).
- H.S. Chakraborty, T. Niederhausen, and U. Thumm, Phys. Rev. A **70**, 052903 (2004).
- H.S. Chakraborty, T. Niederhausen, and U. Thumm, Nucl. Instrum. Methods B **241**, 43 (2005).
- T. Niederhausen and U. Thumm, Phys. Rev. A **73**, 041404(R) (2006).

# Multiparticle Processes and Interfacial Interactions in Nanoscale Systems Built from Nanocrystal Quantum Dots

Victor Klimov

*Chemistry Division, C-PCS, MS-J567, Los Alamos National Laboratory  
Los Alamos, New Mexico 87545, klimov@lanl.gov, http://quantumdot.lanl.gov*

## 1. Program Scope

By exploiting the effects of quantum confinement, one can control electronic and optical properties of matter at the most fundamental, electronic-wavefunction level. The approach explored most extensively involves the use of nanoscale semiconductor structures such as size/shape-controlled semiconductor nanocrystals. While being a powerful tool for engineering spectral responses, size control at the nanoscale has limited applicability for engineering the dynamical and nonlinear responses of nanostructures or for introducing new functionality to a material. In this project, we explore novel approaches for controlling carrier-carrier nonlinear interactions and carrier dynamical behavior using multicomponent nanocrystals. Specifically, we study multishell, multicomponent nanocrystals based on both semiconductor and metal materials that allow us to independently control spectral characteristics (by engineering confinement energies), dynamical responses (by engineering electron-hole wavefunction overlap and the exciton spin structure), and nonlinear, multiexciton interactions (by engineering Coulomb coupling). Our studies in this project address such important and interesting problems as the realization of low-threshold nanocrystal lasing in the single-exciton regime via the use of repulsive exciton-exciton interactions, highly efficient exciton multiplication for a new generation of solar cells, and novel, multifunctional behaviors from hybrid, semiconductor/metal nanoscale materials.

## 2. Recent Progress: Single-exciton optical gain in semiconductor nanocrystals

**2.1 Background.** Nanocrystal quantum dots show high photoluminescence quantum yields and size-dependent emission colours that are tunable through the quantum-confinement effect. Despite these favorable light-emitting properties, nanocrystals (NCs) are difficult to use in optical amplification and lasing. Because of almost exact balance between absorption and stimulated emission in nanoparticles excited with single electron-hole pairs (excitons), optical gain can only occur due to NCs that contain at least two excitons. A complication associated with this multiexcitonic nature of light amplification is fast optical-gain decay induced by nonradiative Auger recombination, a process in which one exciton recombines by transferring its energy to another. During the past year, we demonstrated a practical approach for obtaining optical gain in the single-exciton regime, which completely eliminates the problem of Auger decay. Specifically, we have developed core/shell hetero-NCs engineered in such a way as to spatially separate electrons and holes between the core and the shell (type-II hetero-structures). The resulting imbalance between negative and positive charges produces a strong local electric field, which induces a giant ( $\sim 100$  meV or greater) transient Stark shift of the absorption spectrum with respect to the luminescence line of singly excited nanocrystals. This effect breaks the exact balance between absorption and stimulated emission and allows us to demonstrate optical amplification due to single excitons.

**2.2 The concept of single-exciton gain.** Optical gain corresponds to a light-matter interaction regime for which generation of photons by stimulated emission dominates over photon absorption. As in other lasing media, optical gain in NCs requires population inversion, i.e., the situation in which the number of electrons in the excited state is greater than that in the ground state. The lowest-energy emitting transition in NCs of II-VI semiconductors studied here can be described in terms of a two-level system that has two electrons in its ground state. Excitation of a single electron (single exciton) across the energy gap ( $E_g$ ) in this system does not produce optical gain but rather results in optical transparency, for which stimulated

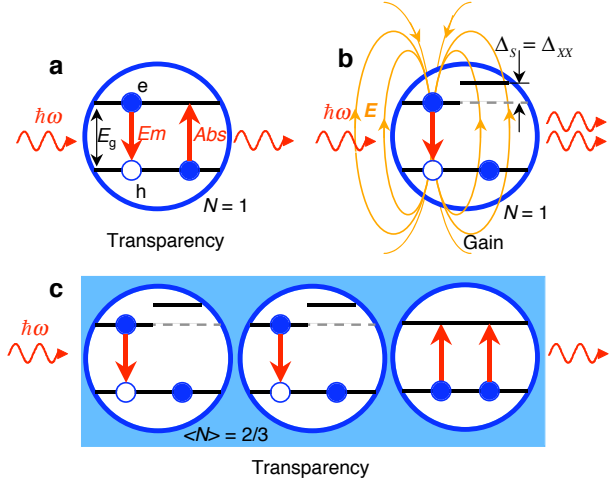


**Figure 1.** The single-exciton gain concept (see text for details)

absorption energy of the electron remaining in the valence band by the carrier-induced Stark effect (Fig. 1b). If the magnitude of the Stark shift ( $\Delta_s$ ) is comparable to or greater than the transition line width ( $\Gamma$ ), it can completely eliminate absorption losses at the emission wavelength in excited NCs, which should allow optical gain using single-exciton states. Specifically, the threshold for population inversion in the presence of the transient transition shift is determined by the condition  $\langle N \rangle = 2 / (3 - \exp(-\Delta_s^2 / \Gamma^2))$ .

If  $\Delta_s \ll \Gamma$ , it reduces to  $\langle N \rangle = 1$ , which corresponds to the usual case of multiexciton optical gain. However, if  $\Delta_s \gg \Gamma$ ,  $\langle N \rangle = 2/3$  (Fig. 1c), which implies that optical gain does *not* require multiexcitons.

**2.3 Engineered exciton-exciton interactions in type-II NCs.** The carrier-induced Stark effect can be described in terms of the Coulomb interaction of the initially generated exciton with the exciton created in the second excitation act. In this description, the transient Stark shift is determined by the exciton-exciton

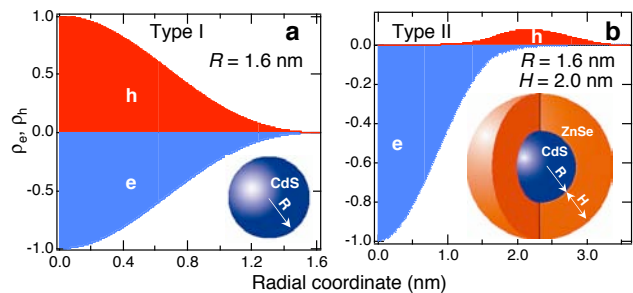


**Figure 2.** Spatial distribution of positive and negative charges in type I (a) and type II (b) NCs.

( $\psi_e$ ) and hole ( $\psi_h$ ) wavefunctions,  $\rho_x(\mathbf{r})$  is [ $\rho_x(\mathbf{r}) = e(|\psi_h(\mathbf{r})|^2 - |\psi_e(\mathbf{r})|^2) \approx 0$ ,  $e$  is the electron charge] (Fig. 2a), which leads to relatively small X-X interaction energies of  $\sim 10$  to  $\sim 30$  meV. These values are smaller than typical transition line widths in existing NC samples (ensemble broadening of  $\sim 100$  meV or greater) and, therefore, do not allow significant suppression of absorption at the emission wavelength.

The separation of electrons and holes between the core and the shell in type-II NCs (Fig. 2b) can lead to sizable local charge densities and, hence, large Coulomb interaction energies. To analyze the effect of charge separation on X-X interactions and its influence on optical gain properties of NCs, we

emission by a conduction-band electron is exactly compensated by absorption due to the electron remaining in the valence band (Fig. 1a). Stimulated emission dominates over absorption only if the second electron is also excited across the energy gap indicating that optical gain requires doubly excited NCs, i.e., biexcitons. These considerations imply that population inversion in an NC ensemble can only be achieved if the average number of excitons per NC,  $\langle N \rangle$ , is greater than 1.

The condition for optical gain, however, changes if one accounts for a local electric field associated with an excited electron-hole pair. This field can alter the

(X-X) Coulomb interaction energy ( $\Delta_{xx} = \Delta_s$ ) defined as  $\Delta_{xx} = E_{xx} - 2E_x$ , where  $E_x$  and  $E_{xx}$  are single- and biexciton energies, respectively. The energy  $\Delta_{xx}$  depends on the local electrical charge density  $\rho_x(\mathbf{r})$  associated with a single-exciton state and, hence, on the sum of the hole ( $\rho_h$ ) and the electron ( $\rho_e$ ) charge densities:  $\rho_x(\mathbf{r}) = \rho_h(\mathbf{r}) + \rho_e(\mathbf{r})$  ( $\mathbf{r}$  is the spatial coordinate). Because of almost identical spatial distributions of electron

nearly zero in homogeneous NCs

study hetero-nanostructures composed of a CdS core overcoated with a ZnSe shell (Fig. 2b, inset). Upon photoexcitations, these NCs produce a charge-separated state with an electron residing in the core and the hole in the shell.

**2.4 Optical amplification in the single-exciton regime.** To analyze light amplification in type-II CdS/ZnSe NCs, we compare their optical-gain properties with those of traditional type-I CdSe NCs with matching emission wavelengths (Fig. 3). For the biexcitonic gain mechanism operating in type-I NCs, a sharp peak of amplified spontaneous emission (ASE) is red-shifted with respect to the single-exciton band (Fig. 3a, upper spectrum) because of X-X attraction, which decreases the emission energy of biexcitons compared to that of single excitons. For type-II samples, we observe that as we increase the pump level a new, sharp emission feature develops near the position of the single-exciton band (2.01 eV) (Fig. 3b, and the lower spectrum in Fig. 3a). This new peak shows a clear excitation threshold of  $\sim 2 \text{ mJ cm}^{-2}$  and a fast, super-linear growth with

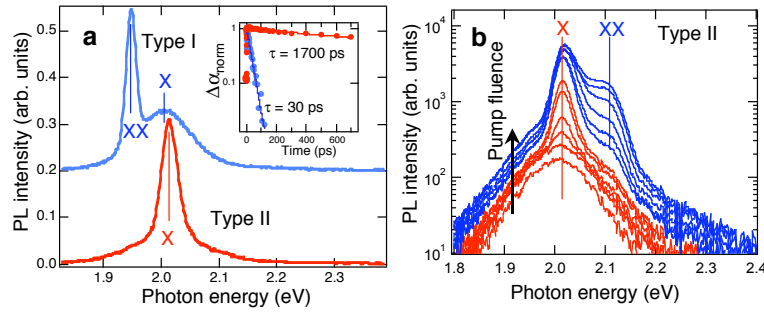


**Figure 3.** (a) ASE spectra of type-I and type-II NCs (PL stands for photoluminescence). (b) The development of ASE due to single-excitons and biexcitons in type-II NCs.

increasing pump fluence (Fig. 3b). The development of a similar sharp feature is also detected using a fixed pump fluence and increasing the size of the excitation spot (variable-stripe-length configuration). These behaviors are consistent with the ASE regime. An important observation is that the ASE peak develops near the center of the single-exciton band (X feature in Fig. 3a) indicating that it is due to stimulated emission of single excitons. This assignment is further confirmed by the observation of a second ASE feature at higher fluences (excitation threshold of  $\sim 6 \text{ mJ cm}^{-2}$ ), which develops near the position of the high-energy biexciton band (XX feature in Fig. 3b) and is due to the traditional biexcitonic gain mechanism.

**2.5 Impact.** The single-exciton-gain regime demonstrated here should significantly simplify real-life applications of chemically synthesized NCs in lasing technologies and specifically should allow realization of NC lasing under continuous-wave (cw) excitation. The pump intensity threshold for producing cw lasing is determined by the ratio of the threshold fluence measured using ultrafast excitation and the gain lifetime. Because of Auger recombination, this lifetime is in the sub-100 ps range for the multiexcitonic gain mechanism, which leads to very high cw lasing thresholds that are well above the NC-photostability limit. For single-exciton gain, the intrinsic gain dynamics is determined by the radiative single-exciton lifetime, which is typically orders of magnitude longer than the Auger-decay time constants. The difference in relaxation behaviors for single- and biexciton gain mechanisms is illustrated in the inset of Fig. 3a, which shows that in type-I NCs the gain decay time is 30 ps while it is more than 50 times longer (1700 ps) for the type-II NCs. Significant lengthening of the optical gain lifetime allowed by the single-exciton gain regime could greatly enhance the technological potential of colloidal NCs as “soft,” chemically processible optical-gain media.

### 3. Future Plans

One focus of our future work will be the implementation of single-exciton gain strategies in the infrared using type-II NCs based on, e.g., PbSe and PbTe. For the latter class of materials, the benefit of the single-exciton gain regime can be particularly large. Rock-salt NCs are characterized by a high, eight-fold degeneracy of the emitting electron and hole states. In this case, the gain threshold requires

excitation of four excitons per NC on average. This high exciton multiplicity results in very short gain lifetimes because of rapid shortening of the Auger time constants with the number of excitons. Using single-exciton gain regime one can reduce the gain threshold to below unity and simultaneously greatly increase optical gain lifetimes.

Another focus of our work will be the realization of optical amplification in NCs using electrical injection. Specifically, we will explore energy-transfer from a proximal quantum well as a means for rapid pumping of excitons into the NCs. The feasibility of this injection mechanism has been demonstrated by our recent experiments on CdSe NCs combined with InGaN/GaN quantum wells. In our optical-gain work we will use analogous structures, in which CdSe NCs will be replaced with type-II NCs made of, e.g., CdS (core) and ZnSe (shell).

#### 4. Publications (2006 - 2007)

1. V. I. Klimov, S. A. Ivanov, J. Nanda, M. Achermann, I. Bezel, J. A. McGuire, and A. Piryatinski, Single-exciton optical gain in semiconductor nanocrystals, *Nature* **447**, 441 (2007).
2. A. Piryatinski, S. A. Ivanov, S. Tretiak, and V. I. Klimov, Effect of quantum and dielectric confinement on the exciton-exciton interaction energy in type II core/shell semiconductor nanocrystals, *Nano Lett.* **7**, 108 (2007)
3. V. I. Klimov, Spectral and dynamical properties of multiexcitons in semiconductor nanocrystals, *Annu. Rev. Phys. Chem.* **58**, 635 (2007).
4. J. Nanda, S. A. Ivanov, J. Nanda, M. Achermann, I. Bezel, A. Piryatinski, V. I. Klimov Light Amplification in the single-exciton regime using exciton-exciton repulsion in type-II nanocrystal quantum dots, *J. Phys. Chem. B* (2007).
5. S. A. Ivanov, A. Piryatinski, J. Nanda, S. Tretiak, D. Werder, V. I. Klimov, Type-II core/shell CdS/ZnSe nanocrystals: Synthesis, electronic structures, and spectroscopic Properties, *J. Am. Chem. Soc.* (2007).
6. N. G. Liu, B. S. Prall, and V. I. Klimov, Hybrid gold/silica/nanocrystal quantum-dot superstructures: Synthesis and analysis of semiconductor-metal interactions, *J. Am. Chem Soc.* **128**, 15362-15363 (2006).
7. V. I. Klimov, Mechanisms for photogeneration and recombination of multiexcitons in semiconductor nanocrystals: Implications for lasing and solar energy conversion, *J. Phys. Chem. B, Feature Article* **110**, 16827 (2006).
8. R. D. Schaller, M. Sykora, S. Jeong, and V. I. Klimov, High-efficiency carrier multiplication and ultrafast charge separation in semiconductor nanocrystals studied via time-resolved photoluminescence, *J. Phys. Chem. B* **110**, 25332 (2006).
9. V. I. Klimov, Detailed-balance power-conversion limits of nanocrystal-quantum-dot solar cells in the presence of carrier multiplication, *Appl. Phys. Lett.* **89**, 123118 (2006).
10. M. Sykora, M. A. Petruska, J. Alstrum-Acevedo, I. Bezel, T. J. Meyer, and V. I. Klimov, Photoinduced charge transfer between CdSe nanocrystalline quantum dots and Ru-polypyridine complexes, *J. Am. Chem. Soc.* **128**, 9984 (2006).
11. M. Achermann, A. P. Bartko, J. A. Hollingsworth, and V. I. Klimov, The effect of Auger heating on intraband relaxation in semiconductor quantum rods **2**, 557 *Nature Physics* (2006).
12. M. Achermann, M. A. Petruska, D. D. Koleske, M. H. Crawford, and V. I. Klimov, Nanocrystal-based light emitting diodes utilizing high-efficiency nonradiative energy transfer for color conversion, *Nano Lett.* **6**, 1396 (2006).
13. R. D. Schaller and V. I. Klimov, Non-Poissonian exciton populations in semiconductor nanocrystals via carrier multiplication, *Phys. Rev. Lett.* **96**, 097402 (2006).
14. J. Nanda, S. A. Ivanov, H. Htoon, I. Bezel, A. Piryatinski, S. Tretiak, and V. I. Klimov, Absorption cross sections and Auger recombination lifetimes in inverted core/shell nanocrystals: Implications for lasing performance, *J. Appl. Phys.* **99**, 034309 (2006).
15. R. D. Schaller, M. Sykora, J. M. Pietryga, and V. I. Klimov, Seven excitons at a cost of one: Redefining the limits for conversion efficiency of photons into charge carriers, *Nano Lett.* **6**, 424 (2006).
16. G. R. Maskaly, M. A. Petruska, J. Nanda, I. V. Bezel, R. D. Schaller, H. Htoon, J. M. Pietryga, and V. I. Klimov, Enhancements to the stimulated light emission of semiconductor nanocrystals due to a photonic crystal pseudogap, *Advanced Materials* **18**, 343 (2006).
17. M. Furis, H. Htoon, M. A. Petruska, V. I. Klimov, T. Barrick, and S. A. Crooker, Bright-exciton fine structure and anisotropic exchange in CdSe nanocrystal quantum dots, *Phys. Rev. B* **73**, 241313 (R) (2006).

# **Atomic, Molecular and Optical Sciences at LBNL**

**A. Belkacem, M. Hertlein, C.W. McCurdy, T. Osipov, T. Rescigno and T. Weber**

Chemical Sciences Division, Lawrence Berkeley National Laboratory, Berkeley, CA 94720

Email: abelkacem@lbl.gov, mphertlein@lbl.gov, cwmccurdy@lbl.gov, [tosipov@lbl.gov](mailto:tosipov@lbl.gov),  
[tnrescigno@lbl.gov](mailto:tnrescigno@lbl.gov), tweber@lbl.gov

## **Objective and Scope**

The AMOS program at LBNL is aimed at understanding the structure and dynamics of atoms and molecules using photons and electrons as probes. The experimental and theoretical efforts are strongly linked and are designed to work together to break new ground and provide basic knowledge that is central to the programmatic goals of the Department of Energy. The current emphasis of the program is in three major areas with important connections and overlap: inner-shell photo-ionization and multiple-ionization of atoms and small molecules; low-energy electron impact and dissociative electron attachment of molecules; and time-resolved studies of atomic processes using a combination of femtosecond X-rays and femtosecond laser pulses. This latter part of the program is folded in the overall research program in the Ultrafast X-ray Science Laboratory (UXSL).

The experimental component at the Advanced Light Source makes use of the Cold Target Recoil Ion Momentum Spectrometer (COLTRIMS) to advance the description of the final states and mechanisms of the production of these final states in collisions among photons, electrons and molecules. Parallel to this experimental effort, the theory component of the program focuses on the development of new methods for solving multiple photo-ionization of atoms and molecules. This dual approach is key to break new ground and solve the problem of photo double-ionization of small molecules and unravel unambiguously electron correlation effects.

The relativistic collisions part of the program has been phased out in favor of branching into dissociative electron attachment measurements using COLTRIMS in support of the theoretical effort in the area of electron driven chemistry. These studies make use of the group's expertise at performing "complete" experiments using COLTRIMS. The theoretical project seeks to develop theoretical and computational methods for treating electron driven processes that are important in electron-driven chemistry and that are beyond the grasp of first principles methods.

# Inner-Shell Photoionization and Dissociative Electron Attachment of Small Molecules

**A. Belkacem, M. P. Hertlein, T. Osipov and T. Weber**

Chemical Sciences Division, Lawrence Berkeley National Laboratory, Berkeley, CA 94720

Email: abelkacem@lbl.gov, [mphertlein@lbl.gov](mailto:mphertlein@lbl.gov), [tosipov@lbl.gov](mailto:tosipov@lbl.gov), tweber@lbl.gov

## Objective and Scope

The goal of this part of the LBNL AMOS program is to understand the structure and dynamics of atoms and molecules using photons as probes. The current research carried at the Advanced Light Source is focused on studies of inner-shell photoionization and photo-excitation of atoms and molecules, as well as breaking new ground in the interaction of x-rays with atoms and molecules dressed with femto-second laser fields. The low-field photoionization work seeks new insight into atomic and molecular processes and tests advanced theoretical treatments by achieving new levels of completeness in the description of the distribution of momenta and/or internal states of the products and their correlations. The intense-field two-color research is designed to provide new knowledge of the evolution on a femto-second time scale (ultimately attosecond) of atomic and molecular processes as well as the relaxation of atomic systems in intense transient fields. This latter part of the program is folded in the overall research program in the new LBNL's Ultrafast X-ray Science Laboratory (UXSL).

## Single photon induced symmetry breaking of D<sub>2</sub> dissociation

Symmetries are essential building blocks of our physical, chemical and biological models. For macroscopic objects symmetries are always only approximate. By reducing the complexity in the microcosm these symmetries often become strict. In H<sub>2</sub> and H<sub>2</sub><sup>+</sup> respectively D<sub>2</sub> and D<sub>2</sub><sup>+</sup>, the smallest and most abundant molecules in the universe, this complexity is reduced to the minimum. They have perfectly symmetric ground states. What does it take to break this symmetry ?

In our study we show how and why the inversion symmetry of the hydrogen (respectively deuterium) molecule can be broken by absorption of a linearly polarized photon, which itself has inversion symmetry. The emission of an electron with subsequent dissociation of the remaining D<sub>2</sub><sup>+</sup> shows that under some circumstances no symmetry to the ionic and neutral fragment. This is the smallest and most fundamental molecular system for which such symmetry breaking is possible. The mechanisms identified behind this symmetry breaking are general for all molecules. Fully differential angular cross sections for fixed in space molecules as function of the kinetic energy release of the nuclear fragments, which have been experimentally obtained with the COLTRIMS technique are compared with a state-of-the art quantum mechanical approach implementing B-spline basis sets.

## **Interference and decoherence in the photo-double ionization of molecular hydrogen**

We have studied experimentally the influence of the molecular alignment and spacing on the electron emission from a two body Coulomb potential induced by single photon absorption with 130, 160, 200 and 240 eV circular polarized light at the Advanced Light Source. Applying successfully the technique of COLTRIMS, it was possible to measure fully differential cross sections (FDCS) for the photo double photo ionization of hydrogen for fixed in space molecular orientations by detecting three particles in coincidence. The measurements covered 4p solid angle.

In the angular distributions of the electrons we studied the influence of diffraction, symmetry effects, selection rules and molecular orientations in body fixed frames. Thus for the first time a T. Young double slit experiment of a correlated electron pair inside a hydrogen molecule can be presented [1]. We can illustrate the evolution from knock-off to shake-off processes and the interference of single particles as well as correlated pairs, while changing the deposited photon energy as well as the energy sharing of the two electrons. In addition the angular distributions show a distinct dependency on the Kinetic Energy Release (KER) of the recoiling ions, e.g. the size of the molecular double slit. The experimental results are also compared with quantum mechanical calculations.

## **K-shell photoionization of acetylene and isomerization to vinylidene**

In this study we investigate the K-shell photoionization of acetylene and the dynamics of the following breakup pathways by measuring the momenta of the positively charged ions in coincidence with Auger electrons. The photoionization and the subsequent Auger process lead to the formation of the doubly charged  $C_2H_2^{++}$  ion that dissociates into two or more fragments. We observe two clearly separated Auger electron peaks correlated with different kinetic energies taken by the fragments. The result of this analysis in the 2-D plot (Auger energy – kinetic energy of ions) shows that the isomerization to vinylidene is associated with a very sharp peak around 255 eV Auger energy and 4.5 eV ion kinetic energy. This gives a clear insight on the isomerization process. Following the emission of the 255 eV Auger electron  $\{C_2H_2^+ \rightarrow C_2H_2^{2+} + e_A(255 \text{ eV})\}$  the di-cation ends up in the lower laying states  $^1\Sigma_g^+$ ,  $^1\Delta_g$  and  $^3\Sigma_g^-$ . The di-cation is trapped behind a high (3-4 eV) and wide barrier preventing it from directly dissociating along the C-C bond or C-H bond. The dissociation appears to be achieved after an isomerization to vinylidene first followed by dissociation along the C-C bond forming  $C^+ + CH_2^+$  fragments.

## **Double-photoionization of CO few eV above threshold.**

We measured double photoionization of CO molecules at 48 eV photon energy. The double ionization of CO produces mostly  $C^+ + O^+$  fragments with non-measurable amounts of  $CO^{2+}$ . The formation of  $C^+ + O^+$  can proceed through two possible channels: a) Direct ionization of two electron into the continuum – similar to the  $H_2$  double ionization – direct channel. b) Ionization of one electron into the continuum followed by autoionization of a second electron – Indirect channel. The electron distribution measured with a COLTRIMS shows a very clear distinction of the direct and indirect channels. The kinetic energy release spectrum shows a series of peaks corresponding to the transient vibrational states of the various electronic states of  $(CO^{2+})^*$ . These states are similar to previous measurements at higher energies (K-shell photoionization).

$(CO^{2+})^*$  is found to predissociate through a  $^3\Sigma^-$  and  $^1\Delta$  dissociative states leading to considerably faster dissociation times than natural lifetimes of the electronic bound states. We plan to improve our current measurement by detecting both electrons in coincidence. We will be able to estimate the dissociation time of these states by using an analysis technique similar to that used to estimate the time of the isomerization of acetylene to vinylidene.

### Dissociative electron attachment of small molecules.

A Coltrims method is developed for measuring the angular distribution of fragment negative ions arising from dissociative electron attachment of molecules. A low energy pulsed electron gun us used in combination with pulsing the extraction plates of the Coltrims spectrometer. The angular distribution measurements are particularly important for dissociative electron attachment, due to the selection rules, which connects the states of the neutral molecule to the negative ion resonant states and the orientation of the neutral molecule with respect to the momentum vector of the incoming electron. Thus the angular distribution contains information on the symmetry of the negative ion state and the angular momentum of the captured electron. The formation of the resonant dissociative negative molecular states typically peak at electron energies below 10 eV. Thus a major technical problem is the production of a controlled, defined low electron beam that can strike the molecular jet within the uniform electric field field of the COLTRIMS spectrometer. Our approach uses the uniform field and an orthogonal uniform magnetic field. This ExB field steers the electrons along the directions of the gas jet without (or minimally) affecting the electron energy. The low magnetic field ( $\sim 10$  G) used has a minimal effect on the motion of the slow heavy negative ion. This COLTRIMS configuration allowed us the injection of a usable low electron beam into the interaction region of the spectrometer. Earlier studies of DEA found in the literature measured angular distributions of negative ion products, however the COLTRIMS approach will result in higher sensitivity and simultaneous coverage of a wide range of negative ion final momenta. We applied this modified Coltrims technique to the measurement of dissociative electron attachment of  $O_2$ . The formation of  $O^-$  from  $O_2$  is known to appear as a broad peak centered at 6.5 eV. These negative ions are formed with considerable kinetic energy making  $O_2$  a very good test of the apparatus. The 3D angular distribution of  $O^-$  changes as the energy of the electrons is swept across the broad resonance. At the maximum of cross section (6.5 eV) the angular distribution shows clear minima both when the  $O_2$  molecule is aligned parallel or perpendicular to the electron beam direction. The maximum yield is observed at  $45^\circ$  degree angles which is interpreted as a strong signature of a  $\Pi$  contribution.

### Future Plans

We plan to continue application of the COLTRIMS approach to achieve complete descriptions of the single photon double ionization of CO and its analogs. New measurements will be made close to the double ionization threshold and approaching the regime where the outgoing electrons and the ions have nearly the same velocities. Our earlier observations of the isomerization of acetylene to the vinylidene configuration forms a basis for possible further studies of this phenomena perhaps using deuterated acetylene to alter the relative time scales of molecular rotation and the dissociation dynamics.

## Recent Publications

"A two-electron double slit experiment – interference and entanglement in photo double ionization"

D. Akoury, K. Kreidi, T. Jahnke, T. Weber, A. Staudte, M. Schöffler, N. Neumann, J. Titze, L. Ph. Schmidt, A. Czasch, O. Jagutzki, R. Costa Fraga, R. Grisenti, R. Diez Muino, N. Cherepkov, S. Semenov, P. Ranitovic, C.L. Cocke, T. Osipov, H. Adaniya, J. Thompson, M. Prior, A. Belkacem, A. Landers, H. Schmidt-Böcking, R. Dörner  
Resubmitted to Science (2007).

"Single photon induced symmetry breaking of H<sub>2</sub> dissociation"

F. Martin, J. Fernandez, T. Havermeier, L. Foucar, T. Weber, K. Kreidi, M. Schöffler, L. Schmidt, T. Jahnke, A. Landers, O. Jagutzki, A. Czasch, E. Benis, T. Osipov, A. Belkacem, M. Prior, H. Schmidt-Böcking, C.L. Cocke, R. Dörner  
Science 315, (2007), 629

"Inner-shell ionization of potassium atoms ionized by femtosecond laser", M.P. Hertlein, H. Adaniya, J. Amini, C. Bressler, B. Feinberg, M. Kaiser, N. Neumann, M.H. Prior and A. Belkacem, Phys. Rev. A 73, 062715 (2006)

"The pair-production channel in atomic processes", A. Belkacem and A. Sorensen, Radiation Physics and Chemistry 75, 656-695 (2006).

"Electron correlation during photoionization and relaxation of potassium and argon after K-shell photoexcitation", M. Hertlein, H. Adaniya, K. Cole, B. Feinberg, J. Maddi, M. Prior, R. Schriel and A. Belkacem, Phys. Rev. A 71, 022702 (2005)

A. Knapp, B. Krassig, A. Kheifets, I. Bray, Th. Weber, A. Landers, S. Schossler, T. Jahnke, J. Nickles, S. Kammer, O. Jagutzki, L. Ph. H. Schmidt, M. Schöffler, T. Osipov, M. Prior, H. Schmidt-Böcking, C.L. Cocke and R. Dörner, J. Phys. B: At. Mol. Opt. Phys. **38**, 615 (2005)

A. Knapp, B. Krassig, A. Kheifets, I. Bray, Th. Weber, A. Landers, S. Schossler, T. Jahnke, J. Nickles, S. Kammer, O. Jagutzki, L. Ph. H. Schmidt, M. Schöffler, T. Osipov, M. Prior, H. Schmidt-Böcking, C.L. Cocke and R. Dörner, J. Phys. B: At. Mol. Opt. Phys. **38**, 635 (2005)

A. Knapp, B. Krassig, A. Kheifets, I. Bray, Th. Weber, A. Landers, S. Schossler, T. Jahnke, J. Nickles, S. Kammer, O. Jagutzki, L. Ph. H. Schmidt, M. Schöffler, T. Osipov, M. Prior, H. Schmidt-Böcking, C.L. Cocke and R. Dörner, J. Phys. B: At. Mol. Opt. Phys. **38**, 645 (2005)

"Vibrationally resolved K-shell photoionization of CO with circularly polarized light", T. Jahnke, L. Foucar, J. Titze, R. Wallauer, T. Osipov, E. P. Benis, A. Alnaser, O. Jagutzki, W. Arnold, S. K. Semenov, N. A. Cherepkov, L. Ph. H. Schmidt, A. Czasch, A. Staudte, M. Schöffler, C. L. Cocke, M. H. Prior, H. Schmidt-Böcking, and R. Dörner, Phys. Rev. Lett. **93**, 083002 (2004)

"Complete photo-fragmentation of the deuterium molecule" T. Weber, A. O. Czasch, O. Jagutzki, A. K. Mueller, V. Mergel, A. Kheifets, E. Rotenberg, G. Meigs, M. H. Prior, S. Daveau, A. Landers, C. L. Cocke, T. Osipov, R. Diez Muño, H. Schmidt-Böcking and R. Dörner, Nature, **431**, 437 (2004)

"Fully Differential Cross Sections for Photo-Double-Ionization of D<sub>2</sub>", Th. Weber, A. Czasch, O. Jagutzki, A. Müller, V. Mergel, A. Kheifets, J. Feagin, E. Rotenberg, G. Meigs, M.H. Prior, S. Daveau, A.L. Landers, C.L. Cocke, T. Osipov, H. Schmidt-Böcking and R. Dörner, Phys. Rev. Lett, **92**, 163001 (2004).

## Electron-Atom and Electron-Molecule Collision Processes

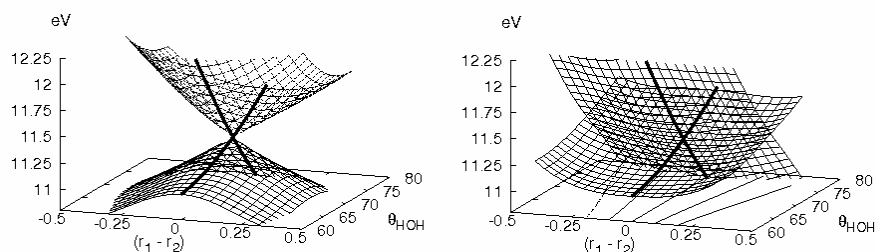
T. N. Rescigno and C. W. McCurdy

Chemical Sciences, Lawrence Berkeley National Laboratory, Berkeley, CA 94720  
[tnrescigno@lbl.gov](mailto:tnrescigno@lbl.gov), [cwmccurdy@lbl.gov](mailto:cwmccurdy@lbl.gov)

**Program Scope:** This project seeks to develop theoretical and computational methods for treating electron collision processes that are important in electron-driven chemistry and physics and that are currently beyond the grasp of first principles methods, either because of the complexity of the targets or the intrinsic complexity of the processes themselves. New methods are being developed and applied for treating low-energy electron collisions with polyatomic molecules. A second focus is the development of new approaches for solving multiple photoionization and electron-impact ionization of atoms and molecules. Finally, novel time-dependent methods to treat multiple ionization of atoms and molecules by intense fields are being developed and tested.

**Recent Progress and Future Plans:** We report progress in two areas covered under this project, namely electron-polyatomic molecule collisions and double photoionization.

### 1. Electron-Molecule Collisions



Conical intersection between  $^2A_1$  and  $^2B_2$  states of the water anion plotted in asymmetric stretch and bending. Left: adiabatic, Right: diabatic representation

We have completed a four-year study of dissociative electron attachment (DEA) to water, which is governed by complex nuclear and electronic resonance dynamics. DEA proceeds via formation of negative ion, Feshbach resonances of  $^2B_1$ ,  $^2A_1$  and  $^2B_2$  symmetry, which are coupled through conical intersections and Renner-Teller interactions. The complicated topology of the water anion surfaces was detailed in a paper that has appeared in *Phys. Rev. A* (ref. 5). The complex-valued resonance surfaces were obtained from fixed-nuclei scattering and large-scale electronic structure calculations and the final-state-specific cross sections and branching ratios into all two-body dissociative channels were obtained from time-dependent wavepacket calculations. This benchmark study of DEA, which has now been published in two long papers in *Phys. Rev. A* (refs. 19 and 20), is the first to treat, from first principles, all aspects of an electron polyatomic collision, including not only the determination of the fixed-nuclei electronic cross sections, but also a treatment of the nuclear dynamics in full dimensionality.

We have continued to examine the underpinnings of various complex potential models, which have formed the basis of much of the work on resonant electron-molecule scattering, by studying a model 2-dimensional problem which can be solved without

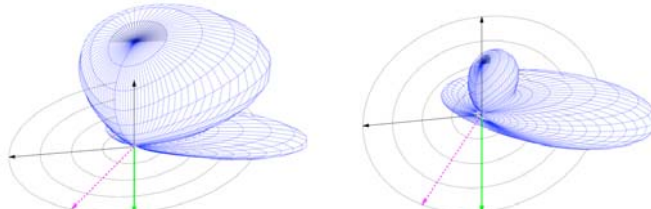
making the Born-Oppenheimer approximation. The first phase of our study, which examined the limitations of the local complex potential model and was published in *Physical Review A* (ref. 11), has now been extended to include the non-local complex potential model for resonance collisions of electrons with diatomic molecules. We have examined all the underlying assumptions used in formulating the non-local approximation to our model, have derived explicit expressions for the resonant and non-resonant (background) components of the scattering amplitude and have gained new insights into the meaning and relative importance of “non-local” and “non-adiabatic” effects in resonance scattering. We are now preparing this work for publication.

## 2. Double Photoionization

We have completed a theoretical study of double photoionization (DPI) of molecular hydrogen. Our initial study of the triply differential cross sections for aligned H<sub>2</sub>, which was published in *Science* (ref. 9), was subsequently followed with an independent check using finite elements and the discrete variable representation (DVR) that produced fully converged results. This benchmark study, which has been published in *Physical Review A* (ref. 15), has shown that theory and experiment are now in excellent agreement. We have also studied the dependence of DPI on internuclear distance (R) and explained the origin of recently observed variations with R of the fully differential cross sections. The results have been published in *Physical Review Letters*.

We have made substantial progress on implementing exterior complex scaling with a hybrid method that combines a grid-based discrete variable representation (DVR) with Gaussian functions. This method will form the basis of our approach to studying double photoionization of more complex molecules. We have completed most of the coding required to study photoionization of Li<sub>2</sub><sup>+</sup>, which is very difficult to study using purely grid-based single-center expansions, and have obtained preliminary results which are very encouraging.

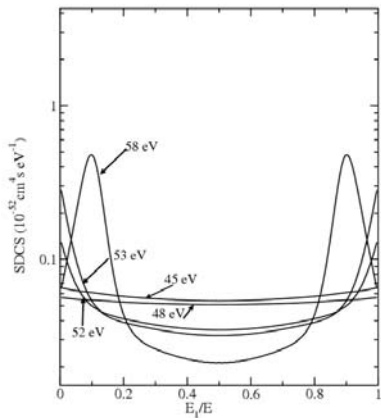
We have completed a theoretical study of double photoionization of H<sup>-</sup>, obtaining the first fully differential cross sections for this system. DPI is exquisitely sensitive to electron correlation, so we wished to see whether initial state correlation, which is very important in H<sup>-</sup>, would leave a strong signature in the triply differential cross sections (TDCS). We found significant differences between the TDCS for H<sup>-</sup> and helium which were most striking in cases of extreme unequal energy sharing, where the effects of final-state electron correlation are suppressed.



Comparison of H<sup>-</sup> (left) and He (right) TDCS. The fixed electron is at 30° from the photon polarization direction and has 15% of the available energy in both cases.

Finally, we extended our earlier studies of DPI in helium to the more difficult case of two-photon double ionization, which has been the focus of much recent theoretical work. Since our calculations treat electron correlation in the initial, virtual intermediate, and final states essentially exactly, they show that the large degree by which previous

theoretical calculations disagree is not necessarily due to the various levels at which correlation was treated, but rather that numerical approximations made using either time-independent or time-dependent descriptions of this process are to blame. Our calculations were carried out for photon energies both below and above the threshold for sequential ionization (54.4 eV). Remarkably, even below 54.4 eV, sequential ionization leaves a clear signature in the magnitude and shape of both the total and energy sharing cross sections - even though at these energies it is only a virtual process. We have submitted a paper describing this work to *Physical Review Letters* (ref. 24).



Singly differential cross sections for two-photon, double ionization of helium at various photon energies.

### 3. Time-Dependent Processes

We are developing non-perturbative methods for studying the interaction of time-varying, short-wavelength radiation with atoms and molecules, starting with the time-dependent Schrödinger equation. Although a variety of methods are available for propagating a wavepacket in a time-varying field, there are still some fundamental difficulties concerned with the extraction of physical scattering information from such a wavepacket, particularly in cases involving more than one ionized electron in the final state. The typical approach has been to project the wavepacket onto an approximate final state. We have developed an alternative method that extracts amplitudes for single and double ionization from a quantum wave packet after a short radiation pulse, but while the electrons are still interacting. The procedure involves the use of exterior complex scaling to effectively propagate the solution at the end of the radiation pulse to infinite times, thereby allowing the use of existing integral formulas for single and double ionization amplitudes for two electron atoms and molecules. The method has been fully described in a manuscript that has been accepted in *Physical Review A* (ref. 23). We are currently carrying out calculations on He in the perturbative regime, where the new method gives results that compare favorably with cross section results obtained using time-independent methods, and will subsequently extend these studies to stronger intensities.

#### Publications (2005-2007):

1. D. A. Horner, C. W. McCurdy and T. N. Rescigno, "Electron-Helium Scattering in the S-wave Model Using Exterior Complex Scaling", *Phys. Rev. A* **71**, 012701 (2005).
2. W. Vanroose, F. Martin, T. N. Rescigno and C. W. McCurdy, "Nonperturbative Theory of Double Photoionization of the Hydrogen Molecule", *Phys. Rev. A* **70**, 050703 (R) (2004).
3. D. A. Horner, C. W. McCurdy and T. N. Rescigno, "Electron Impact Excitation-Ionization of Helium in the S-Wave Limit", *Phys. Rev. A* **71**, 010701 (2005).

4. C. S. Trevisan, K. Houfek, Zh. Zhang, A. E. Orel , C. W. McCurdy and T. N. Rescigno, “A Nonlocal, Ab Initio Model of Dissociative Electron Attachment and Vibrational Excitation of NO”, *Phys. Rev. A* **71**, 052714 (2005).
5. D.J. Haxton, T. N. Rescigno and C. W. McCurdy, “Topology of the Adiabatic Potential Energy Surfaces for the Resonance States of the Water Anion”, *Phys. Rev. A* **72**, 022705 (2005).
6. F. Martín, D. A. Horner, W. Vanroose, T. N. Rescigno and C. W. McCurdy, “First Principles Calculations of the Double Photoionization of Atoms and Molecules using B-splines and Exterior Complex Scaling”, Proceedings of the Thirteenth International Symposium on Polarization and Correlation in Electronic and Atomic Collisions and the International Symposium on (e,2e), Double Photoionization and Related Topics, Buenos Aires, 2005 (American Institute of Physics, 2006).
7. T. N. Rescigno, D. A. Horner, F. L. Yip and C. W. McCurdy, “A Hybrid Approach to Molecular Continuum Processes Combining Gaussian Basis Functions and the Discrete Variable Representation ”, *Phys. Rev. A* **72**, 052709 (2005).
8. C. S. Trevisan, A. E. Orel and T. N. Rescigno, “Resonant Electron-CF Collision Processes” , *Phys. Rev. A* **72**, 062720 (2005).
9. Wim Vanroose, F. Martín, T. N. Rescigno and C. W. McCurdy, “Complete Photofragmentation of the H<sub>2</sub> Molecule as a Probe of Molecular Electron Correlation”, *Science* **310**, 1787 (2005).
10. T. N. Rescigno and C. W. McCurdy (with B. C. Garrett *et al.*), “Role of Water in Electron-Initiated Processes and Radical Chemistry: Issues and Scientific Advances” *Chemical Reviews* **105**, 355-389 (2005).
11. K. Houfek, T. N. Rescigno and C. W. McCurdy, “A Numerically Solvable Model for Resonant Collisions of Electrons with Diatomic Molecules ”, *Phys. Rev. A* **73**, 032721 (2006).
12. T. N. Rescigno, C. S. Trevisan and A. E. Orel, “Dynamics of Low-Energy Electron Attachment to Formic Acid”, *Phys. Rev. Lett.* **96**, 213201 (2006).
13. D. J. Haxton , C. W. McCurdy and T. N. Rescigno, “Angular Dependence of Dissociative Electron Attachment to Polyatomic Molecules: Application to the <sup>2</sup>B<sub>1</sub> Metastable State of the H<sub>2</sub>O and H<sub>2</sub>S Anions”, *Phys. Rev. A* **73**, 062724 (2006).
14. C. S. Trevisan, A. E. Orel and T. N. Rescigno, “Elastic scattering of low-energy electrons by tetrahydrofuran”, *J. Phys. B* **39**, L255 (2006).
15. Wim Vanroose, D. A. Horner, F. Martín, T. N. Rescigno and C. W. McCurdy, “Double Photoionization of Aligned Molecular Hydrogen”, *Phys. Rev. A* **74**, 052702 (2006).
16. T. N. Rescigno, Wim Vanroose, D. A. Horner, F. Martín and C. W. McCurdy , “First Principles Study of Double Photoionization of H<sub>2</sub> Using Exterior Complex Scaling”, *J. Elec. Spectros., Rel. Phenom.* **XX**, xxxx (2007).
17. C.S. Trevisan, A.E. Orel and T. N. Rescigno), Low-energy Electron Scattering by Formic Acid, *Phys. Rev. A* **74**, 042716 (2006).
18. D. A. Horner, W. Vanroose, T. N. Rescigno, F. Martin and C. W. McCurdy, Role of Nuclear Motion in Double Ionization of Molecular Hydrogen by a Single Photon, *Phys. Rev. Lett.* **98**, 073001 (2007).
19. D. J. Haxton , C. W. McCurdy and T. N. Rescigno Dissociative Electron Attachment to the H<sub>2</sub>O molecule I: Complex-valued Potential Energy Surfaces for the <sup>2</sup>B<sub>1</sub>, <sup>2</sup>A<sub>1</sub> and <sup>2</sup>B<sub>2</sub> Metastable States of the Water Anion, *Phys. Rev. A* **75**, 012710.
20. D. J. Haxton, T. N. Rescigno and C. W. McCurdy, Dissociative Electron Attachment to the H<sub>2</sub>O molecule II: Nuclear Dynamics on Coupled Electronic Surfaces Within the Local Complex Potential Model, *Phys. Rev. A* **75**, 012711.
21. F. L. Yip, D. A. Horner, C. W. McCurdy and T. N. Rescigno, Single and Triple Differential Cross Sections for Double Photoionization of H<sup>-</sup>, *Phys. Rev. A* **75**, 042715 (2007).
22. D. J. Haxton, C. W. McCurdy and T. N. Rescigno, Comment on “A Wave Packet Method for Treating Nuclear Dynamics on Complex Potentials” , *J. Phys. B* **40**, 1461 (2007).
23. A. Palacios, T. N. Rescigno and C. W. McCurdy, Extracting Amplitudes for Single and Double Ionization from a Time-Dependent Wavepacket, *Phys. Rev. A* (accepted for publication).
24. D. A. Horner, F. Morales, T. N. Rescigno, F. Martin and C. W. McCurdy, Two-Photon Double Ionization of Helium Above and Below the Threshold for Sequential Ionization, *Phys. Rev. Lett.* (submitted for publication).

## Ultrafast X-ray Science Laboratory

Ali Belkacem, Roger Falcone, Oliver Gessner, Thornton E. Glover, Martin Head-Gordon,  
Stephen Leone, C. William McCurdy, Daniel Neumark, Robert W. Schoenlein, Thorsten Weber

*Chemical Sciences, Lawrence Berkeley National Laboratory, Berkeley, CA 94720*

[ABelkacem@lbl.gov](mailto:ABelkacem@lbl.gov), [rwf@berkeley.edu](mailto:rwf@berkeley.edu), [OGessner@lbl.gov](mailto:OGessner@lbl.gov), [TEGlover@lbl.gov](mailto:TEGlover@lbl.gov), [MHeadGordon@lbl.gov](mailto:MHeadGordon@lbl.gov), [SRLeone@lbl.gov](mailto:SRLeone@lbl.gov), [CWMcCurdy@lbl.gov](mailto:CWMcCurdy@lbl.gov), [DMNeumark@lbl.gov](mailto:DMNeumark@lbl.gov),  
[RWSchoenlein@lbl.gov](mailto:RWSchoenlein@lbl.gov), [TWeber@lbl.gov](mailto:TWeber@lbl.gov)

**Program Scope:** This program seeks to bridge the gap between the development of ultrafast X-ray sources and their application to understand processes in chemistry and atomic and molecular physics that occur on both the femtosecond and attosecond time scales. Current projects include: (1) The construction and application of high harmonic generation sources in chemical physics, (2) Applications of a new ultrafast X-ray science facility at the Advanced Light Source at LBNL to solution-phase molecular dynamics, (3) Time-resolved studies and non-linear interaction of femtosecond x-rays with atoms and molecules (4) Theory and computation treating the dynamics of two electrons in intense short pulses, and the development of tractable theoretical methods for treating molecular excited states of large molecules to elucidate their ultrafast dynamics.

### **Recent Progress and Future Plans:**

#### **1. Soft X-ray high harmonic generation and applications in chemical physics**

This part of the laboratory is centered around a unique high repetition rate femtosecond VUV pulse source. It will provide light pulses in the VUV- and soft X-ray regime with pulse durations on the sub-100 fs timescale and repetition rates up to 3 kHz. The source will be complemented by state-of-the-art photoelectron and photoion detection schemes to create a platform for next generation ultrafast chemical dynamics studies. It is based on high harmonic generation of an IR fundamental in gaseous media. The driving IR laser provides pulses of 25 fs duration at 3 kHz repetition rate with pulse energies up to 5 mJ. After separation from the fundamental, a narrow band of high harmonic photon energies is selected by means of filters, multilayer mirrors, and gratings. The driving Ti:Sapphire IR laser is now operational. The first beamline providing ultrashort pulses at 23.7 eV photon energy is expected to be operational by the end of fiscal year 2007.

The first experiments will focus on the ionization dynamics of pure and doped Helium droplets. An existing experimental setup consisting of a Helium cluster source and a velocity-map-imaging photoelectron spectrometer, is currently being modified in order to record femtosecond time-resolved photoelectron energy- and angular-distributions. Synchrotron based studies have revealed the emission of extremely slow (<1 meV) electrons by Helium droplets that are excited ~1 eV below the atomic Helium ionization threshold. Furthermore, the photoelectron spectra of doped Helium droplets show a rich structure that depends on the photon energy and cluster size. Most of these observations in the energy domain are only poorly understood as of now. We will use a (femtosecond VUV pump) - (femtosecond IR probe) scheme in order to directly probe the decay dynamics of the VUV-excited Helium droplets in the time domain. This will

shed new light on the ionization dynamics and energy transfer mechanisms inside the superfluid clusters which constitute a unique form of matter.

Ultimately, the high-repetition high harmonics source will be equipped with 3 beam lines in order to make optimum use of the femtosecond driving laser. Photoelectron-photoion coincidence imaging experiments will be installed at the additional beam lines. By providing kinematically complete information on photoelectron emission- and molecular breakup-momentum vectors, these experiments enable highly differential measurements like molecular frame photoelectron angular distributions and correlated photoelecton-photoion kinetic energy distributions. We will use these measurements to study the electronic entanglement between molecular fragments, intramolecular energy redistribution processes, and structural dynamics during a molecular dissociation in real-time. Finally, 4th generation light sources like the LCLS at Stanford CA will benefit from the experience gained in laboratory-based ultrafast VUV and soft X-ray studies.

## **2. Applications of the new femtosecond undulator beamline at the Advanced Light Source to solution-phase molecular dynamics**

The objective of this research program is to advance our understanding of solution-phase molecular dynamics using ultrafast x-rays as time-resolved probes of the evolving electronic and atomic structure of solvated molecules. Two new beamlines have been constructed at the Advanced Light Source, with the capability for generating ~200 fs x-ray pulses from 200 eV to 10 keV. During the past year, the soft x-ray beamline has been commissioned, and is now operational. Construction of the hard x-ray beamline is completed, and commissioning is now underway.

Present research is focused on charge-transfer processes in solvated transition-metal complexes, which are of fundamental interest due to the strong interaction between electronic and molecular structure. In particular, Fe<sup>II</sup> molecular complexes exhibit strong coupling between structural dynamics, charge-transfer, and spin-state interconversions. We have recently reported the first time-resolved EXAFS measurement of the atomic structural dynamics associated with the Fe<sup>II</sup> spin-crossover transition using ALS bend-magnet beamline 5.3.1. This study clearly showed the dilation of the Fe-N bond distance by ~0.2 Å within 70 ps of photoexcitation into the MLCT<sup>1</sup> state. An important objective will be to extend these measurements to the femtosecond time scale with the pending availability of ALS undulator beamline 6.0.1, providing high-brightness femtosecond hard x-rays.

A new technical capability for transmission XAS measurements of thin liquid samples in the soft x-ray range is now being developed. We are also developing wire-guided jets for creating liquid films of a few microns thickness. This approach will be implemented in a new endstation for BL6.0.1.2, operating in He at atmospheric pressure, and isolated from the beamline via a thin Si<sub>3</sub>N<sub>4</sub> window at the exit slit of the monochromator. Using these techniques for soft x-ray measurements of thin liquid samples, a new understanding of the evolution of the valence electronic structure, and the influence of the ligand field dynamics of the Fe 3d electrons, will be obtained by time-resolved XANES measurements at the Fe L-edge. This is an essential complement to studies of the Fe-ligand structural dynamics using time-resolved EXAFS.

An important future goal is to apply time-resolved X-ray techniques to understand the structural dynamics of more complicated reactions in a solvent environment. Of current interest is the photochemical reaction dynamics of aqueous chlorine dioxide (O-Cl-O) which exists in stratospheric polar clouds and plays a significant role in sunlight-induced atmospheric chemistry due to its ability to produce atomic Cl. We will apply time-resolved EXAFS and XANES techniques to follow the changing oxidation state of the Cl, thereby distinguishing between various competing reaction pathways that cannot be unambiguously identified through visible spectroscopy but may be solvent dependent.

### **3. Time-resolved studies and non-linear interaction of femtosecond x-rays with atoms and molecules:**

*Development of a high intensity high harmonic source:* While the strong interaction regime has typically been inaccessible to (low peak power) synchrotron sources, it can be accessed with recently developed and with foreseeable sources. X-ray Free Electron Lasers will offer high flux ( $\sim 10^{12}$  photons/pulse) while high harmonics sources have recently been demonstrated to achieve focal intensities up to  $\sim 10^{14}$  W/cm<sup>2</sup>. We plan to study fundamental high field and nonlinear interactions with simple atomic and molecular systems using a high harmonic source optimized for high peak power. We have finished the construction of a high harmonic source based on a 40 mJ, 10 Hz, 800 nm laser systems (10 Hz, 800 nm). We have measured an initial flux of  $\sim 5 \times 10^9$  photon/shot for the 25<sup>th</sup> harmonic using argon as a gas converter. We use a 5-cm focal length multilayer coated mirror to focus the 25<sup>th</sup> harmonic to micron size resulting in initial intensities of order of 10<sup>13</sup> W/cm<sup>2</sup>. As a test case of the intensities achieved we observed a first two-photon sequential double ionization of argon using the 25<sup>th</sup> harmonic. Our initial experiments will focus on studying two-photon triple ionization of xenon to investigate the quadrupole contribution to the excitation of the giant 4d resonance in xenon. We will extend these non-linear studies to two-photon double ionization of He and nuclear dynamics and isomerization of acetylene and ethylene.

In addition we are developing an electron imaging apparatus, which is capable to measure the 3d final momentum vectors of at least two electrons and two nuclei. This apparatus will be used in two-photon double ionization experiments of He, small molecules and some solids. In pump and probe experiments solid states can be excited or ionized with a femtosecond laser pulse and probed with a soft x-ray photon ionizing a doped atom. The ionization process and the speed of information transfer can be investigated as a function of lateral pump-probe-distance as well as the time delay of the pulses and the temperature of the target.

### **4. Theory and computation**

An initial focus of our work is the development of computational methods that will allow the accurate treatment of multiple ionization of atoms and molecules by short pulses in the VUV and soft X-ray regimes. We have extended our numerical methods based on the finite-element discrete variable representation to the essentially exact time-dependent treatment of two electron atoms in a radiation field. A central challenge for the theory of time-dependent multiple ionization processes, that we have recently solved, is the rigorous extraction of the amplitudes for ionization from these wave packets, and the separation of single and double ionization probabilities. The exterior complex scaling

approach that successfully surmounted this difficulty in our time-independent calculations now forms the basis of a new time-dependent approach that avoids the ambiguities concerning the correct characterization of the final state that have characterized essentially all time-dependent descriptions of multiple ionization.

These developments put the investigation of attosecond pump and probe processes in atoms, including multiphoton absorption, within reach. For molecules the challenge remains to include nuclear motion in calculations that accurately treat correlated electronic motion so that processes occurring over 10s of femtoseconds can be treated accurately.

We are working on the development of tractable theories for molecular excited states that can yield a proper description of both bright and dark excited states, and in due course, also their non-adiabatic couplings as needed to describe radiationless transitions. As a first step, we have demonstrated the ability of a scaled second order perturbation theory to yield molecular excitation energies in organic molecules to within 0.2 eV, while being self-interaction-free, and efficient enough to apply to systems in the 100 atom regime. Work in progress is aimed at obtaining a proper description of bielectronic excited states, and formulating next-generation density functionals that are asymptotically self-interaction free. The former development will be crucial for describing radiationless chemistry, while the latter will permit description of key UV/vis spectral features in large molecules where existing density functional theories fail due to self-interaction errors.

### Publications:

1. "Inner-shell ionization of potassium atoms ionized by femtosecond laser", M.P. Hertlein, H. Adaniya, J. Amini, C. Bressler, B. Feinberg, M. Kaiser, N. Neumann, M.H. Prior and A. Belkacem, *Phys. Rev. A* **73**, 062715 (2006).
2. M. Khalil, M.A. Marcus, A.L. Smeigh, J.K. McCusker, H.H.W. Chong, and R.W. Schoenlein, "Picosecond x-ray absorption spectroscopy of a photoinduced iron(II) spin crossover reaction in solution," *J. Phys. Chem. A*, **110**, pp. 38-44 (2006).
3. A.Cavalleri, M.Rini, R.W. Schoenlein, "Ultra-broadband femtosecond measurements of the photo-induced phase transition in VO<sub>2</sub>: From the mid-IR to the hard x-rays" *J. Phys. Soc. Jap.*, **75**, p. 011004, (2006).
4. J.M. Byrd, Z. Hao, M.C. Martin, D.S. Robin, F. Sannibale, R.W. Schoenlein, A.A. Zholents, and M.S. Zolotorev, "Tailored Terahertz Pulses from a Laser-Modulated Electron Beam," *Phys. Rev. Lett.*, **96**, 164801, (2006).
5. A. Cavalleri, S. Wall, C. Simpson, E. Statz, D.W. Ward, K.A. Nelson, M.Rini, and R.W. Schoenlein, "Tracking the motion of charges in a terahertz light field by femtosecond X-ray diffraction," *Nature*, **442**, 664 (2006).
6. J. M. Byrd, Z. Hao, M. C. Martin, D.S. Robin, F. Sannibale, R.W. Schoenlein, A. A. Zholents, M.S. Zolotorev, "Laser seeding of the storage ring microbunching instability for high-power coherent terahertz radiation," *Phys. Rev. Lett.*, **97**, 074802, (2006).
7. M. Khalil, M.A. Marcus, A.L. Smeigh, J.K. McCusker, H.H.W. Chong, and R.W. Schoenlein, "Picosecond x-ray absorption spectroscopy of photochemical transient species in solution," in **Ultrafast Phenomena XV**, Springer Series in Chemical Physics , **88**, P. Corkum, D. Jonas, D. Miller, A.M. Weiner, Eds., Springer-Verlag, (2007).
8. "Scaled second order perturbation corrections to configuration interaction singles: efficient and reliable excitation energy methods", Y.M. Rhee and M. Head-Gordon, *J. Phys. Chem. A* **111**, 5314 (2007).

**ATOMIC AND MOLECULAR PHYSICS RESEARCH  
AT  
OAK RIDGE NATIONAL LABORATORY**

David R. Schultz, Group Leader, Atomic Physics  
[schultzd@ornl.gov]  
ORNL, Physics Division, P.O. Box 2008  
Oak Ridge, TN 37831-6372

**Principal Investigators**

H. Aliabadi,<sup>\*</sup> E. Bahati,<sup>\*</sup> M. E. Bannister, M. R. Fogle, Jr.<sup>\*</sup> C. C. Havener,  
H. F. Krause, J. H. Macek, F. W. Meyer, C. Reinhold, D. R. Schultz,  
C. R. Vane, L. I. Vergara,<sup>\*</sup> and H. Zhang<sup>\*</sup>

<sup>\*</sup>Postdoctoral Fellow

The OBES atomic physics program at ORNL has as its overarching goal the understanding of states and interactions of atomic-scale matter. These atomic-scale systems are composed of multiply charged ions, charged and neutral molecules, atoms, atomic ions, electrons, solids, and surfaces. Particular species and interactions are chosen for study based on their relevance to gaseous or plasma environments of basic energy science interest such as those in fusion energy, atmospheric chemistry, and plasma processing. Towards this end, the program has developed and operates the Multicharged Ion Research Facility (MIRF) which has recently undergone a broad, multi-year upgrade. Work is also performed as needed at other facilities such as ORNL's Holifield Radioactive Ion Beam Facility (HRIBF) and the CRYRING heavy-ion storage ring in Stockholm. Closely coordinated theoretical activities support this work as well as provide leadership in complementary or synergistic research.

**Phase IV of the MIRF Upgrade Project – C. R. Vane, M. E. Bannister, M. R. Fogle, J. W. Hale, C. C. Havener, H. F. Krause, and F. W. Meyer**

The major components of the MIRF upgrade are now completed. The facility is now an extended phase of development designed to substantially advance our molecular ion research program toward electron- and atomic-collision dissociation measurements with state-specific capability. The facility is being enhanced by addition of a supersonic expansion, cold molecular ion source (CMIS) to provide a variety of molecular cations with initially well-defined internal states, and an ion trap endstation for further cooling and characterization. The CMIS, a design similar to that used recently for cold  $H_3^+$  dissociative recombination studies at CRYRING,<sup>1</sup> is being mounted on the new high voltage platform in front of the existing permanent magnet ECR ion source. The ion trap is being constructed on an extension of the zero-degree port of the new high-energy beamline and consists of partially cryogenic ‘Zajfman’-like electrostatic mirror trap.<sup>2,3</sup>

The complete ion trapping endstation consists of a new ultra-high vacuum beamline with computer controlled, fast-reaction electrostatic deflection and focusing elements, the electrostatic trap with a low-energy (5-100 eV) crossed electron beam located between mirrors, and a number of beam diagnostic and product characterization components, including an imaging detector system for neutral and charged fragments arising from dissociation of the cooled molecular ions. Ultimately, this apparatus will be combined with the COLTRIMS endstation and used in developing more sophisticated preparation and characterization techniques in which atomic and molecular ions can be held for several seconds, radiatively cooled to their ground states, and then used directly, or selectively re-excited to chosen excited states, for controlled studies of state-

specific collisional interactions with photons, electrons, and other atomic and molecular systems. Establishment of this apparatus is in direct support of our mission goal of developing the experimental capabilities for state-selectively producing and manipulating atomic and molecular ions to implement studies of a broad range of plasma relevant ion-interactions in as controlled a manner as possible.

- 
1. B. J. McCall *et al.*, *J. Phys.: Conf. Ser.* **4**, 92-97 (2005).
  2. H. F. Krause *et al.*, pp. 126-129, *AIP Conf. Proc.* **576**, New York, NY (1994).
  3. O. Heber *et al.*, *Rev. Sci. Instrum.* **76**, 013104 (2005).

### **Low-Energy Ion-Surface Interactions – F. W. Meyer, H. F. Krause, and H. Zhang**

A critical problem in the development of commercially viable fusion technology is identification of materials for use in plasma facing components (PFC's). Because of their high-thermal conductivities, excellent shock resistance, absence of melting, low activation, and low atomic number, carbon-based materials are very attractive candidates for such environments. Different types of graphite or carbon fiber composites (CFC's) are already used in present tokamaks, and CFC tiles (together with some tungsten) are being considered for use in the ITER divertor.

The use of carbon-based materials has its drawbacks, however. Oxygen etches carbon very efficiently, forming CO and CO<sub>2</sub> loosely bound to the carbon surface. At the low-plasma temperatures characterizing the divertor environment, chemical erosion of the carbon surface by low-energy hydrogen-ion impact, leading to the ejection of light hydrocarbon molecules, is significant, and determines in large part the carbon-based-material lifetime. Considering the additional planned use of Be and W in PFC's outside the ITER divertor,<sup>1</sup> the potential exists for a complex mixture of materials at the divertor strike points (due to CFC erosion and CFC/W/Be redeposition) that may significantly alter chemical sputtering yields (and thus core impurities, tritium retention, and target plate lifetimes). The issue of how these material mixtures affect the chemical sputtering yield from graphite surfaces that have been exposed to high-power tokamak operating conditions has remained largely unexplored. Such effects are difficult to explore in tokamak environments. Laboratory experiments providing fundamental chemical sputtering data in conjunction with theoretical simulations of re- and co-deposition may provide an alternative approach to understanding and assessing the importance of such effects.

With this motivation, we initiated a joint experimental and theoretical research program a few years ago to study the interactions of slow ions with surfaces underlying chemical sputtering of fusion-relevant graphite surfaces, and provide needed data for plasma modeling. Our interests include very low kinetic energy behavior, the dependence on the nature of the incident beams (e.g., atomic vs molecular hydrogen, and incident hydrogen isotope), and their influence on the chemical sputtering species distribution. In the theoretical part of this activity, described in greater detail in another section, the focus is on the development and application of theoretical tools describing the dynamics of the electronic degrees of freedom and molecular dynamics simulations incorporating the many-body dynamics of the heavy particles involved in the interaction.

In past years, our measurements concentrated on the region of very low-impact energies (i.e., below 10 eV/D), where there is currently no available experimental data, and which is the anticipated regime of operation of the ITER divertor. We measured chemical sputtering yields for virgin ATJ graphite<sup>2</sup> and highly ordered pyrolytic graphite (HOPG).<sup>3</sup> Due to the high D<sup>+</sup> currents obtainable with our ECR ion source, and the highly efficient beam deceleration optics employed at the entrance to our floating scattering chamber, comparison between same velocity atomic and molecular ion impact was possible with our apparatus at energies as low as 10 eV/D. These measurements permitted a test of the commonly made assumption that isovelocity atomic and

molecular species lead to identical sputtering yields when normalized to the D constituent number of the incident projectiles. We found projectile dependent yields below  $\sim$ 60 eV/D, with the atomic projectile, i.e.,  $D^+$ , having the smallest yields and  $D_3^+$  projectiles the biggest.<sup>4</sup> A similar dependence was found in the simulations carried out in parallel with our measurements.<sup>5,6</sup> At higher energies, where immediate dissociation of incident molecular projectiles is highly probable, the observed yields for equivelocity incident atomic and molecular ions are the same, as has been noted in previous work.<sup>7</sup> It is speculated that at the lower energies, the higher mass, or increased energy deposition density of the undissociated, or just dissociated molecules may enhance the kinetically assisted desorption of sputter products, thereby increasing the observed yields.

During the past year we expanded our measurements to include low energy  $H^+$ ,  $H_2^+$ , and  $H_3^+$  ions incident on ATJ graphite, in order to determine the presence of a possible isotope effect on the methane production yield. Even though this effect would have major implications on tile erosion and T retention in ITER once D-T operation is started, there is currently significant disagreement about the magnitude of this effect in the literature. Disagreements range from less than a factor of two in the yield going from D to T ions by researchers using a quadrupole mass spectrometer approach similar to ours, to almost an order of magnitude estimated by other researchers using weight loss measurements. Our own measurements for methane production by H and D ion impact agreed within our experimental error of  $\sim$ 30% at energies below about 60 eV/amu, thus tending to support the former estimate.

Also this year, we completed a study of chemical sputtering of HOPG that has a well-defined crystalline structure prior to irradiation; HOPG was thought to be more amenable to simulation in the parallel theoretical effort. This turned out not to be the case, because of the longer range AIREBO potential<sup>8</sup> required to reproduce the large basal plane separations in the simulation, and because the simulated irradiations would have to start from zero hydrogen concentration in the HOPG simulation cell, instead of the 30–40% hydrogen concentration that could be incorporated into the amorphous carbon simulation cells by other means. Both factors together made the computation time prohibitively large. The simulation of HOPG was therefore deferred until increasing computing resources and speeds become better matched to the simulation requirements.

The first focus of our HOPG measurements was on comparison of chemical sputtering yields obtained for two different HOPG samples mounted side-by-side in our scattering chamber: one with basal plane orientation parallel to the sample surface and the other perpendicular. The expectation was that, after sufficient beam irradiation to reach steady state sputtering yields, the samples should completely amorphize, and thus give identical yields. This expectation could not be confirmed, with the perpendicular surface always giving bigger methane yields at higher energies than the parallel surface even for accumulated fluences in excess of  $10^{18}/\text{cm}^2$ . This result suggests that methane molecules produced at end of range more easily diffuse back to the surface between the widely spaced basal planes in the case of the “perpendicular” sample than through them for the “parallel” sample.<sup>3</sup> This finding will guide the simulation effort when theoretical work on HOPG resumes.

An additional aim of our HOPG measurements was investigation of the molecular size and isotope effects studied earlier in ATJ graphite. Using  $H^+$ ,  $H_2^+$ ,  $H_3^+$ ,  $D^+$ ,  $D_2^+$ , and  $D_3^+$  incident ions in the energy range 10–250 eV/amu, we were able to confirm the same trends with molecular size and isotope as observed with ATJ graphite.

In parallel with the sputtering measurements, during the past year, we have initiated collaborations with ORNL Materials Science and Technology personnel to characterize the surface modifications induced by the hydrogen and deuterium irradiation in the course of the chemical sputtering measurements. Preliminary SEM studies showed changes of surface morphology very similar to those seen on plasma exposed graphite tiles removed from the DIII-D tokomak at General Atomics. In addition, the feasibility of using Raman spectroscopy was

demonstrated to monitor nanostructural changes of the graphite resulting from beam irradiation. This approach will be used in the near future to do a comparative study of isovelocity atomic and molecular D ion irradiations at high and low energies in an attempt to understand the atomic vs. molecular yield differences observed at low energy.

Also planned in the near term are chemical sputtering measurements of deuterated amorphous thin films provided by W. Jacob of the Institut für Plasma Physik at Max-Planck Institute - Garching. Such films are expected to approximate more closely the deuterated amorphous carbon cells used in the simulations, and as such should serve as more meaningful benchmarks of the theoretical results.

1. R. Aymar and ITER International Team, *J. Nucl. Mater.* **307-311**, 1 (2002).
2. L. I. Vergara, F. W. Meyer, and H. F. Krause, *J. Nucl. Mater.* **347**, 118 (2005).
3. F. W. Meyer, H. Zhang, L. I. Vergara, and H. F. Krause, *Nucl. Instrum. Methods Phys. Res. B* **258**, 264 (2007).
4. L. I. Vergara, F. W. Meyer, H. F. Krause, P. Traskelin, K. Nordlund, and E. Salonen, *J. Nucl. Mater.* **357**, 9 (2006).
5. P. S. Krstic, C. O. Reinhold, and S. J. Stuart, *New J. Phys.* **9**, 219 (2007).
6. F. W. Meyer, P. S. Krstic, L. I. Vergara, H. F. Krause, C. O. Reinhold, and S. J. Stuart, *Phys. Scr. T128*, 50 (2007).
7. M. Balden and J. Roth, *J. Nucl. Mater.* **280**, 39 (2000).
8. S. J. Stuart, A. B. Tutein, and J. A. Harrison, *J. Chem. Phys.* **112**, 6472 (2000).

#### **Low-Energy Charge Exchange Using the Upgraded Ion-Atom Merged-Beams Apparatus – C. C. Havener, H. Aliabadi, D. G. Seely, and C. R. Vane**

Our current ability to reliably predict low energy (meV/u – keV/u) collision processes relies on our understanding of the dynamics and our ability to model the quasi-molecular states formed during collisions. The ion-atom merged-beams apparatus together with the intense ion beams made available from ECR ion sources provides a unique opportunity to provide benchmark measurements to test theory. The higher velocity, more intense, and less divergent beams from the new MIRF High-Voltage (HV) platform enable a new class of measurements.<sup>1,2</sup>

The ion-atom merged-beams experiment demands the highest quality (intense with minimum divergence) beams from the platform. An extensive shakedown of the HV platform, beamline, and ion-atom apparatus resulted in several improvements needed in order to perform merged-beam measurements. They include additional beam diagnostics, finer gas control on the platform, and improvements in vacuum. Critical to operation is the implementation of a NEC dual wire-scanner with LabView software<sup>3</sup> that enables real-time determination of the divergence and overlap of the beams. Our first successful ion-atom merged-beams experiment<sup>4</sup> was for Ne<sup>2+</sup> + D and is shown in Fig. 1. Our previous measurements, due to a limited acceleration available at the CAPRICE source, could not be extended below 150 eV/u, and thus could not establish the low-energy behavior of the charge-exchange cross section. The 60-eV/u data point is also an example of the new sensitivity of the apparatus, measuring cross sections below 10<sup>-17</sup> cm<sup>2</sup>. The structure in the decreasing cross section has been linked to the role of rotational coupling in a exponentially decreasing cross section. No signal was detected at energies as low as 15 eV/u.

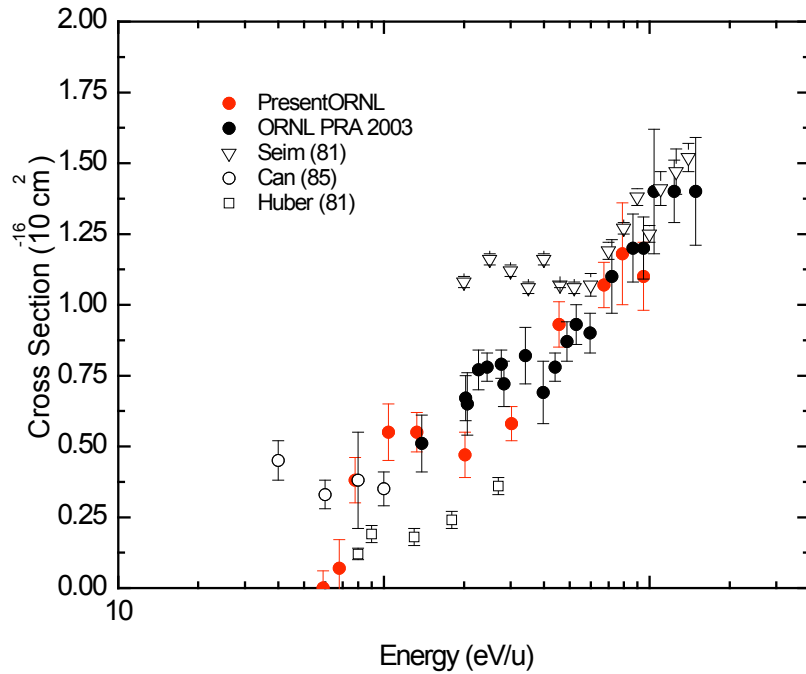


**Fig. 1.** The first ion-atom merged-beams measurement using beams from the HV platform are shown in red and are for  $\text{Ne}^{2+} + \text{D}$ . The measurements extend our previous work to lower energy and resolve the inconsistency of previous data.

The higher velocity ion beams now available from the platform permit charge-exchange measurements with heavier ions and measurements with both H and D at eV/u energies and below to directly observe isotope effects.<sup>1</sup> Isotopic differences in the charge-exchange cross section are the result of trajectory effects caused by the ion-induced dipole potential. Our experimental and theoretical investigations<sup>5</sup> of the  $\text{He}^{2+} + \text{H}$  system has been extended by Stolterfoht *et al.*<sup>6</sup> to predict unusually large isotope effects for this fundamental system. In this case, large differences in the cross section are due to mass-dependent effects in the rotational coupling mechanism. We are currently exploring the isotope effect for several different systems. Measurements for the  $\text{N}^{2+} + \text{H}$  (D) and  $\text{Si}^{4+} + \text{H}$ (D) systems are underway. While the  $\text{N}^{2+}$  system is predicted to show little or no dependence (or variation), the  $\text{Si}^{4+}$  cross section for H is predicted to be a factor of two higher than the cross section for D at 10 meV/u.

The intense beams from the HV platform will be used to perform a benchmark study of low-energy charge exchange for fully stripped and H-like ions on atomic hydrogen. While there have been numerous studies at keV/u energies, there is a real lack of total and state-selective data and appropriate quantal theory at eV/u energies and below. X-ray emission measurements are planned for a variety of bare and H-like ions (e.g., C, N, O) + H. For charge transfer at low energies, capture to non-statistical angular momentum states leads to observable signatures in the subsequent X-ray emission. Such measurements are possible using a high efficiency detector mounted directly above the merge path. The sounding rocket X-ray calorimeter at the University of Wisconsin<sup>7</sup> is being considered for these measurements. The X-ray detector is characterized by a high-energy resolution (5 – 12 eV FWHM) along with high throughput (1000 times greater than dispersive X-ray detectors).

1. C. C. Havener and R. Rejoub, p. 522, *Proceedings, XXIV International Conference on Photonic, Electronic, and Atomic Collisions, Rosario, Argentina, July 20-26, 2005* (World Scientific, 2006).
2. C. C. Havener, E. Galutschek, R. Rejoub, and D. G. Seely, Nucl. Instrum. Methods Phys. Res. B **261**, 129 (2007).
3. D. G. Seely, H. Bruhns, D. W. Savin, T. J. Kvale, E. Galutschek, H. Aliabadi and C. C. Havener, submitted to Nucl. Instrum. Methods Phys. Res. A (2007).
4. B. Serendyuk, H. Bruhns, D. W. Savin, D. Seely, H. Aliabadi, E. Galutschek, and C. C. Havener, Phys. Rev. A **75**, 054701 (2007).
5. C. C. Havener, R. Rejoub, P. S. Krstic, and A.C.H. Smith, Phys. Rev. A **71**, 042707 (2005).
6. N. Stolterfoht *et al.*, to be published in Phys. Rev. Lett. (2007).
7. D. McCammon *et al.*, Astrophys. J **576**, 188 (2002).

**Production of molecular hydrogen anions  $\text{H}_2^-$  and  $\text{D}_2^-$  on a KBr surface – C. C. Havener, F. W. Meyer, and D. G. Seely**

$\text{H}_2^-$  is one of the most fundamental metastable molecular ions and is an important intermediate state to various collision processes like dissociative attachment ( $e^- + \text{H}_2 \rightarrow \text{H} + \text{H}^-$ ), associative attachment ( $\text{H} + \text{H}^- \rightarrow \text{H}_2 + e^-$ ), and collisional attachment ( $\text{H} + \text{H}^- \rightarrow \text{H} + \text{H} + e^-$ ). While the predicted short-lived molecular ion was suspected to exist for many years, only until recently was there direct evidence for the anion's production in a sputter ion source.<sup>1</sup> These ions are predicted to be created in high angular momentum states with short lifetimes. Investigations of the lifetimes in an electrostatic ion-beam trap<sup>2</sup> lead to observation of much longer lifetimes than predicted.<sup>3</sup> However, flight times to the trap were on the order of  $16\ \mu\text{sec}$  which precluded the study of short lifetimes. A complication in generating the molecular ions in an ion source is the possibility of isotopic contamination.

In order to produce  $\text{H}_2^-$  and  $\text{D}_2^-$ , we used 8 – 19 keV  $\text{H}_3^+$ ,  $\text{D}_2\text{H}^+$ , and  $\text{D}_3^+$  ions from the CAPRICE ECR ion source at MIRF and directed them at grazing incidence onto a large-area KBr single-crystal surface where the ions underwent dissociative and electron capture interactions without significant change in energy. The different scattered mass and charge states are dispersed in a large acceptance two-stage electrostatic analysis system and detected by a two-dimensional position-sensitive detector. The different fragments were easily resolved. This apparatus was designed for single-atom detection of  $^{14}\text{C}$ .<sup>4</sup> The change of mass and charge at the surface eliminates the possibility of isotopic contamination for incident  $\text{D}_2\text{H}^+$  and  $\text{D}_3^+$ . Preliminary results are promising, up to  $10^6$   $\text{H}_2^-$  and  $\text{D}_2^-$  are produced by incident  $\mu\text{A}$  beams of  $\text{H}_3^+$  and  $\text{D}_3^+$  ions. Higher conversions are expected with improvements in the quality of the KBr surface. The production of a  $\text{D}_2^-$  beam by grazing interactions with a surface by a fast beam allows the possibility of studying shorter lifetimes ( $\sim 1\ \mu\text{sec}$ ) than previously possible when the molecular anions were created in an ion source. Plans are underway to explore the creation of the molecular anions for meV/u collisions of  $\text{H}^- + \text{H}$  using the ion-atom merged-beams apparatus in a self-merged beams mode.

- 
1. R. Golser *et al.*, Phys. Rev. Lett. **94**, 223003 (2005).
  2. O. Heber *et al.*, Phys. Rev. A **73**, 060501 (2006).
  3. M. Cizek, J. Horacek, and W. Domcke, J. Phys. B **31**, 2571 (1998).
  4. F. W. Meyer, *Book of Abstracts, XXIII ICPEAC, Stockholm, Sweden, July 23-29, 2003*.

**Electron-Molecular Ion Interactions – M. E. Bannister, C. R. Vane, E. Bahati, M. Fogle, and H. Aliabadi**

Electron-molecular ion recombination, dissociation, and excitation and ionization processes are important from a fundamental point of view, especially in that they provide a testable platform for investigating and fully developing our understanding of the mechanisms involved in electronic energy redistribution in fragmenting many-body quantum mechanical systems. These processes are also important practically in that electron-ion collisions are in general ubiquitous in plasmas and molecular ions can represent significant populations in low to moderate temperature plasmas. Neutral and charged radicals formed in dissociation of molecules in these plasmas represent some of the most highly reactive components in initiating and driving further chemical reaction pathways. Thus electron-molecular ion collisions are important in determining populations of some of the most reactive species in a wide variety of environments, such as the divertor and edge regions in fusion reactors, plasma enhanced chemical vapor deposition reactors, environments where chemistries are driven by secondary electron cascades, for example in mixed radioactive waste, the upper atmospheres of planets, and cooler regions of the solar or other stellar atmospheres. To correctly model these environments it is absolutely essential to know the strengths (cross sections and rates), branching fractions, and other kinematical parameters of the various possible relevant collision processes.

**Dissociative Excitation and Ionization:** Measurements of cross sections for electron-impact dissociative excitation (DE) and dissociative ionization (DI) of molecular ions have continued using the MIRF crossed-beams apparatus.<sup>1</sup> In coordination with our dissociative recombination (DR) investigations of di-hydride ions, we have commenced a systematic study of the DE and DI channels for these ions. Experiments, during this period, included measurements on heavy-fragment ion channels of  $\text{OD}_2^+$  and  $\text{ND}_2^+$ . Below the DI threshold, the cross sections for dissociation of  $\text{OD}_2^+$  ions forming  $\text{OD}^+$  and  $\text{O}^+$  fragments are in near-perfect agreement with the DE measurements of  $\text{OH}_2^+$  performed at ASTRID.<sup>2</sup> This leads to two conclusions for this system: (1) the isotope effect is negligible for the DE channel and (2) the cross sections are not dependent on the vibrational distribution of the  $\text{OD}_2^+$  ions, since the ASTRID experiments used cold ( $v=0$ ) ions, while our target ions had a “hot” vibrational distribution typical of an ECR ion source. In addition, DE/DI cross sections were measured for the  $\text{ND}^+$  and  $\text{N}^+$  ion fragment channels for  $\text{ND}_2^+$ . The  $\text{ND}^+$  channel exhibited a resonance-like feature near 15 eV, similar to the structure observed in the cross section for dissociation of  $\text{DCO}^+$  ions producing  $\text{CO}^+$  ions<sup>3</sup> and for the production of  $\text{CH}^+$  from the dissociation of  $\text{CH}_2^+$ .<sup>4</sup> For the  $\text{XH}^+/\text{XD}_2^+$  fragment channel in DE/DI of di-hydrides  $\text{XH}_2^+/\text{XD}_2^+$  ( $\text{X}=\text{C},\text{N},\text{O}$ ), it was found that for energies above four times the dissociation threshold  $E_{\text{th}}$  the cross sections follow the scaling given by  $\sigma(E/E_{\text{th}}) \propto (1/E_{\text{th}}) f(E/E_{\text{th}})$  for a smooth function  $f(x)$ . This scaling does not hold as well for the  $\text{X}^+$  fragment channel.

The dissociation experiments discussed above used molecular ions produced by the ORNL MIRF Caprice ECR ion source,<sup>5</sup> but other cooler sources will also be used in order to understand the role of electronic and ro-vibrational excited states. A second ion source, a hot-filament Colutron ion source, is presently online and expected to produce fewer excited molecular ions. An even colder pulsed ion source, very similar to the one used for measurements<sup>6</sup> on the dissociative recombination of rotationally cold  $\text{H}_3^+$  ions at CRYRING, is under development for use at the ORNL MIRF. Additionally, work continues on a similar supersonic source that uses a piezoelectric mechanism for more reliable pulsed valve operation. With this range of ion sources, one can study dissociation with both well-characterized cold sources and with hotter sources that better approximate the excited state populations in plasma environments found in applications such as fusion, plasma processing, and aeronomy.

1. M. E. Bannister, H. F. Krause, C. R. Vane *et al.*, Phys. Rev. A **68**, 042714 (2003).
2. M. J. Jensen *et al.*, Phys. Rev. A **60**, 2970 (1999).
3. E. M. Bahati, R. D. Thomas, C. R. Vane, and M. E. Bannister, J. Phys. B **38**, 1645 (2005).
4. C. R. Vane, E. M. Bahati, M. E. Bannister, and R. D. Thomas, Phys. Rev. A **75**, 052715 (2007).
5. F. W. Meyer, p. 117, in *Trapping Highly Charged Ions: Fundamentals and Applications*, edited by J. Gillaspy (Nova Science, Huntington, NY, 1997).
6. B. J. McCall *et al.*, Nature **422**, 500 (2003).

**Dissociative Recombination:** The process of dissociative recombination (DR) of relatively simple three-body molecular ions is being studied in our ongoing collaboration with Prof. Mats Larsson and colleagues at the Manne Siegbahn Laboratory (MSL), Stockholm University. Absolute cross sections, branching fractions, and measurements of the dissociation kinematics, especially of the three-body breakup channel, are being investigated at zero relative energy for a variety of light and heavy vibrationally cold triatomic di-hydrides and other molecular ions with three-body channels. This research is carried out using the MSL CRYRING heavy-ion storage ring facility, which is still expected to continue to be available for our electron-molecular ion measurements at least through calendar year 2007.

In the last year, we have performed studies of the di-hydride system  $\text{BH}_2^+$ . These experiments are a continuation of previous measurements concerning the DR of similar molecules, such as  $\text{H}_2\text{O}^+$ ,  $\text{NH}_2^+$ ,  $\text{CH}_2^+$ ,  $\text{SD}_2^+$ , and  $\text{O}_3^+$  that have all revealed three-body breakup as the dominant reaction channel.<sup>1-6</sup> In order to study the three-body breakup dynamics in detail, a high-resolution imaging technique is used to measure the displacement of the fragments from the center of mass of the molecule.<sup>7</sup> The displacement is related to the kinetic energy of the fragments and therefore information about the dynamics involved in the process can be obtained, i.e., the internal state distribution of the fragments. These event-by-event measurements yield information about how the kinetic energy is distributed between the two light fragments and the angular distribution of the dissociating molecules. In all of the triatomic di-hydride systems previously studied, the branching fractions showed very roughly (7:2:1) ratios for ( $\text{X} + \text{H} + \text{H}$ ;  $\text{XH} + \text{H}$ ;  $\text{X} + \text{H}_2$ ), while the observed energy sharing and angular distributions of the three-body breakup product channel could depend heavily on the structure, bonding and charge centre of the parent molecular ion. Experiments during this review period concentrated on measurements of cross sections, branching fractions, and three-body breakup dynamics of  $\text{BH}_2^+$  undergoing dissociative recombination (DR) with zero-eV electrons. Interestingly, it was found that this ion dissociates preferentially (56%) into  $\text{BH} + \text{H}$ . Surprisingly, about a third (35%) proceeds through three-body decay to  $\text{B} + \text{H} + \text{H}$ , which for almost all other tri-atomic di-hydrides is the dominant channel. The two-body  $\text{B} + \text{H}_2$  channel contributes less than 9%. Despite the relatively small fraction of fragmentation leading to three-body breakup, this channel was investigated with the imaging technique described above. The dynamics were observed to be very similar to the other di-hydride ions, with the kinetic energy almost randomly distributed between the H atoms while the dissociation occurs predominantly from open- and closed-geometry states, that is, with the angle between the bonds near 180 or 0 degrees, respectively.

Preliminary investigations of DR of molecular ions using the fragment imaging technique have commenced on the merged electron-ion beams energy-loss apparatus<sup>8</sup> at ORNL. These measurements on the DR of  $\text{H}_2^+$  indicate that the vibrational distribution for these ions peaks at about  $v=4$  or 5. The dissociation of  $\text{H}_2^+$  near zero energy was also investigated using a discrete-dynode detector to count the neutrals produced. Because of the non-negligible contribution of DE at low energies for  $\text{H}_2^+$  ions with a “hot” vibrational distribution, the measured rates were a sum of the DR and DE channels. Future experiments will also include measurements using energy-sensitive solid-state detectors to separate the DE (one H atom) and DR (two H atoms)

contributions. These studies are made possible by the recent construction of a 250-kV high-voltage platform with an all-permanent magnet ECR ion source at the ORNL MIRF. The cold molecular ion sources discussed above are also being adapted for use on the HV platform.

1. R. Thomas *et al.*, Phys. Rev. A **71**, 032711 (2005).
2. M. Larsson and R. Thomas, Phys. Chem. Chem. Phys. **3**, 4471 (2001).
3. Å. Larson *et al.*, Astrophys. J. **505**, 459 (1998).
4. S. Rosén *et al.*, Faraday Discuss. **115**, 295 (2000).
5. F. Hellberg *et al.*, J. Chem. Phys. **122**, 224314 (2005).
6. V. Zhaunerchyk *et al.*, Phys. Rev. Lett. **98**, 223201 (2007).
7. R. Thomas *et al.*, Phys. Rev. A **66**, 032715 (2002).
8. E. W. Bell *et al.*, Phys. Rev. A **49**, 4585 (1994).

### Grazing Surface Studies at Intermediate Energy – H. F. Krause, C. R. Vane, and F. W. Meyer

This work is part of the larger beam-surface effort at the ORNL MIRF that seeks to develop a fundamental understanding of charge exchange, neutralization, energy dissipation and sputtering processes that occur when singly and multiply charged atomic and molecular ions interact with metal, semiconductor and insulator surfaces.

A new high-voltage platform installed at the ORNL Multicharged Ion Research Facility (MIRF) has extended the energy range of ions available for experimental investigations of their interactions with electrons, atoms, molecules and solid surfaces.<sup>1</sup> This year we installed a new beamline and end station that enables multiple-parameter coincidence grazing surface studies to be performed at energies up to 250 keV/q, where q is the charge state of the ion of interest. It will be possible to uniquely identify scattered charge states, emitted electrons, states involved in Auger processes, photons, and products sputtered from the surface that arise in the same collision event.

In the past, we performed experimental investigations of the transport, angular scattering, charge exchange and energy loss of low-energy (5–20 keV/q), multicharged ions in anodic nanocapillary arrays.<sup>2,3</sup> Using the new beamline, we studied 80 keV/q D<sub>2</sub><sup>+</sup>, O<sub>2</sub><sup>+</sup>, and O<sup>5+</sup> ions transmitted through aligned nanopores in an Al<sub>2</sub>O<sub>3</sub> insulator substrate coated with 8-nm gold films. At these higher energies, transmission properties are similar to those observed at lower energies except that the transmitted ions are not significantly steered and the angular distribution widths are controlled primarily by the incident beam collimation. In q-state resolved experiments, the incident projectile ion is the predominant transmitted species (>95%) and the fraction in all lower charge states of O<sup>5+</sup> and the neutralized fraction is always below 1% of the initial q state. The molecular breakup fraction for D<sub>2</sub><sup>+</sup> and O<sub>2</sub><sup>+</sup>, which is independent of the nanopore's alignment with the beam direction, is below 1%; no exiting negative ions are observed. The arrays can be used to attenuate and control (switch transmitted ions on/off using incident low-energy electrons) the transmission of highly charged or molecular ion beams.<sup>3</sup>

Some future studies will focus on the interaction of ions near crystalline insulator surfaces where less detailed information is available. We plan to probe “hollow atom” states formed in the proximity of a LiF surface using fast multiply charged projectiles (e.g., He<sup>2+</sup> and Li<sup>3+</sup>) in the 25–100-keV/u range. Using time-coincidence techniques, the ultra-grazing experiments will also provide state-selected information about coherent and incoherent processes such as projectile excitation, de-excitation, and electron emission induced by projectile motion in the periodic electric fields<sup>4</sup> near the crystal surface (e.g., resonant coherent excitation resonances by a repetitive pulse train in the femtosecond to attosecond regime). This technique should allow a small portion of the full ion-surface grazing path length to be selectively probed. Singly and doubly excited states of ions formed above the surface will be investigated.

The beamline will be used also to extend our previous studies of Al<sub>2</sub>O<sub>3</sub> nanoscale capillaries and to investigate arrays of aligned carbon nanotubes using multiply charged atomic ions in a broad range of incident energies up to 250 keV/q, when the aligned arrays become available at ORNL. These coincidence studies are expected to yield fundamental information on electron or photon production processes in addition to the ion scattering, energy transfer, and charge changing processes studied in our recent nanocapillary research.

- 
1. F. W. Meyer *et al.*, Nucl. Instrum. Methods Phys. Res B **242**, 71 (2006).
  2. H. F. Krause, C. R. Vane, and F. W. Meyer, Phys. Rev. A **75**, 042901 (2007).
  3. H. F. Krause, C.R. Vane, F.W. Meyer, and H. M. Christen, *Proceedings of the 13th International Conference on the Physics of Highly Charged Ions, Belfast, Northern Ireland, UK*, J. Phys.: Conf. Ser. **58**, 323-326 (2007).
  4. Herbert F. Krause and Sheldon Datz, *Advances in Atomic, Molecular, and Optical Physics*, Academic Press, Inc. (1996), pp. 139-180.

**Atomic Ion-Atom and Molecular Ion-Atom Electron Transfer – C. R. Vane, M. E. Bannister, C. C. Havener, H. F. Krause, and H. Aliabadi**

The ORNL COLTRIMS apparatus, originally developed for use in high-energy atomic collisions research at the EN tandem facility,<sup>1</sup> has been modified and implemented as part of a relatively mobile, multi-purpose endstation for studies employing both the high- and low-energy ion beam sources at the upgraded MIRF facility. It is being used in a variety of experiments, including studies of state-selective electron capture by atomic ions, as well as measurements of dissociative electron transfer by molecular ions interacting with atomic targets. The former is complimentary to merged ion-atom electron capture measurements at lower relative energies, while the latter compliments our ongoing research involving interactions of free electrons with molecular ions.

In low- to moderate-energy ion-atom collisions electron transfer from target to projectile bound states dominates over ionization. Access to accurate, reliable data for such processes is central to understanding and accurate modeling of many important plasma environments. Formation of excited final states produced in electron capture from the neutral beams injected into fusion plasma devices leads to radiative cascades and the photon emission is routinely used to diagnose impurity ion concentrations and velocity profiles in fusion plasmas.<sup>2-4</sup> Similarly, X-ray diagnostics of upper terrestrial atmospheric, as well as astrophysical and cometary, photoionized plasmas depend on reliable cross sections.<sup>5</sup> Essential to all of these applications and many others is the accurate information on state-selective electron capture cross sections involving highly charged ions.

Cold-target recoil ion momentum spectroscopy (COLTRIMS) has developed into a mature technology within the last decade, becoming the method of choice for many investigations of electron capture and ionization processes.<sup>6-9</sup> COLTRIMS enables simultaneous *Q*-value and projectile scattering angle measurements, both obtained with  $4\pi$  solid angle efficiency, through momentum spectroscopy of the target recoils. Since the resolution depends only to second order on the momentum spread of the incoming projectile, COLTRIMS permits relatively simple high-resolution *Q*-value measurements, especially at low collision energies. With sufficient resolution, events involving projectiles carrying excess energy (metastable excited-state ions) can be separated, enabling independent studies of electron capture with ground-state versus metastable ions, as well as providing a means for examination of the incident metastable fractions. Another important and unique feature of the COLTRIMS technique is its intrinsic capability to measure prompt characteristics of the collision. The recoil ion final vector momentum is determined by the collision dynamics from the very beginning of the interaction, relatively unaffected by various post collision effects occurring in separated components, such as radiative decay or auto-ionizing

evolution of the projectile or target after the collision. All these features make COLTRIMS a very powerful tool, which we are exploiting for high-resolution measurements of differential cross sections in state-selective electron capture.

**State-Selective Electron Capture by Multiply-Charged Atomic Ions:** Multiply-charged low-energy ions from the Caprice ECR source and floating beamline, or higher energy ions from the 250 kV high-voltage platform ECR are crossed at 90° with cold supersonic He, Ne, and Ar targets, (or in the future with highly-collimated H, Na, or Cs atomic target beams) in the COLTRIMS apparatus. Charge-changed projectiles are electrostatically separated and counted downstream, in a fast, high-count rate (MHz), discrete dynode electron multiplier detector. X-rays emitted from charge-changed projectile ions formed by electron capture to excited states ( $n,l$ ) are measured in a windowless x-ray detector. Recoil ions formed by electron capture to the projectiles are analyzed using the COLTRIMS apparatus and counted in a MCP position-sensitive recoil detector. Extra electrons ejected into the continuum in target multiply ionizing processes can also be measured. By analyzing the COLTRIMS data and identifying particular  $Q$ -value collision events, the cross sections for electron transfer to specific states of the projectiles are measured as a function of collision energy. Similarly, studies of metastable fractions in the incident ECR-produced ion beams will be implemented as a diagnostic technique using high-resolution  $Q$ -value measurements for identification of electron-capture fractions proceeding via these states. Knowledge of the inherent metastable ion fractions present in the incident ions is also important in a number of other MIRF studies.

**Dissociative Electron Capture of Molecular Ions:** This research involves measurements of electron capture from target atoms by projectile molecular ions, leading to molecular dissociation yielding neutral and/or ionic fragments. The process, labeled Dissociative Electron Capture (DEC) of molecular ions, has a long history, and has been investigated using a number of experimental techniques.<sup>10-15</sup>

Cool, dense sub-regions of plasmas, far from equilibrium, present complex environments in which there may be significant populations of all the available components; i.e., of the constituent neutral atoms, molecules, and their ions, as well as a variety of their neutral and ionic fragments. Such environments naturally arise in a number of plasma-to-gas or plasma-to-surface transition regions, such as in plasma processing reactors and at the diverter edges of fusion plasma containment devices. The neutral components can present significant target densities for collisions with electrons and both atomic and molecular ions. Fragmentation of molecular ions through DEC processes provides a channel for production of highly reactive neutral and ionic species.

The ORNL COLTRIMS endstation has been fitted with fragment analysis detectors including a special, energy sensitive detector for determination of chemical branching fractions, and an imaging detector system permitting multi-hit detection and position sensitive capability for studies of DEC. Measurements are being performed for DEC by diatomic and simple triatomic molecular ions, and the results compared with branching fractions and kinematics observed for dissociative recombination, dissociative excitation and dissociative ionization measured at CRYRING and at the MIRF electron-ion crossed beams apparatus for similar ion species. Atomic beams sources will also be added to this endstation to permit studies of DEC from molecular ions interacting with highly collimated atomic beams of H, H<sub>2</sub>, Li, Na, and Cs.

We have measured fragmentation fractions for electron capture dissociation of H<sub>2</sub><sup>+</sup>, HD<sup>+</sup>, H<sub>3</sub><sup>+</sup>, and H<sub>2</sub>D<sup>+</sup> from the HV platform ECR ion source interacting with an argon gas target using a new, ultra-thin window, energy sensitive silicon detector. The silicon detector has 100% detection efficiency and permits unique identification of the various charged or neutral fragments by the mass-dependent energy carried by each mass, leading to precise determination of branching in a few moments of beam time. For example, 80-keV H<sub>3</sub><sup>+</sup> passing through a thin argon target yield

completely separated (8 keV FWHM) 1-H, 2-H, and 3-H peaks at 26.7, 53.3, and 80 keV arising from collisional dissociation (CD) and from dissociative electron capture (DEC). Measurements with and without a partial transmission grid permit unique evaluation of the associated branching fractions. These measurements were made with internally ‘hot’ molecular ions from the ECR, and without detection of the recoiling target ions. Future studies will be carried out with internally cold ions from the new CMIS and employing the COLTRIMS technique in coincidence with fragment measurements to permit identification of the specific channels of electron capture leading to dissociation.

These measurements are made possible by the higher available energies per unit mass afforded by the new high voltage platform and beamlines. Higher energy facilitates complete collection of a much broader range of kinetic energy of release systems, using the advantage of greater kinematic compression onto the beam axis in the lab frame. It also permits highly efficient, mass selective detection of molecular fragments (e.g., H ions and atoms) in the ultra-thin window Si detector. We are presently concentrating on the molecular projectile ions  $\text{H}_2^+$ ,  $\text{HD}^+$ ,  $\text{H}_3^+$ , and  $\text{CH}_2^+$  with He, Ne, and Ar targets. We plan to follow with studies of the same molecular ions on H,  $\text{H}_2$ , and Cs targets.

- 
1. M. A. Abdallah *et al.*, Phys. Rev. Lett. **85**, 278 (2000).
  2. R. C. Isler, Plasma Phys. Controlled Fusion **36**, 171 (1994).
  3. E. Wolfrum *et al.*, Rev. Sci. Instrum. **64**, 2285 (1993).
  4. M. Von Hellermann *et al.*, Plasma Phys. Controlled Fusion **33**, 1805 (1991).
  5. T. R. Kallman, *Atomic Processes in Plasmas*, AIP Conf. Proc. 322 (AIP, New York, 1995), pp. 36–52.
  6. M. Barat *et al.*, J. Phys. B **25**, 2205 (1992).
  7. H. Cederquist *et al.*, Phys. Rev. A **51**, 2169 (1995).
  8. P. Jardin *et al.*, *Recoil Ion Kinetics* AIP Conf. Proc. **274** (AIP, New York, 1993), pp. 291–293.
  9. J. Ullrich *et al.*, Comments At. Mol. Phys. **30**, 285 (1994).
  10. C. L. Cocke *et al.*, Phys. Rep. **205**, 153 (1991).
  11. V. Mergel *et al.*, Phys. Rev. Lett. **74**, 2200 (1995).
  12. G. W. McClure, Phys. Rev. **140**, A769 (1965).
  13. B. Meierjohann and M. Volger, J. Phys. B: At. Mol. Phys. **9**, 1801 (1976).
  14. D. P. de Brujin *et al.*, Chem. Phys. **85**, 215 (1984).
  15. C. M. Laperle *et al.*, Phys. Rev. Lett. **93**, 153202 (2004).

### Molecular Dynamics Simulations of Chemical Sputtering – C. O. Reinhold and P. S. Krstic

Bombardment of carbon-based deuterated surfaces by low-energy ( $E < 50\text{ eV}$ ) H, D, T atoms and molecules (and ions) induces chemical reactions that ultimately lead to emission of stable hydrocarbons. Since these processes are an important source of erosion of plasma-facing materials causing degradation of fusion reactor and energy-conversion processes, there is a strong need for quantitative predictions of the corresponding yields. Motivated by these needs and by recent beam-surface experiments at ORNL, we have undertaken a series of large-scale classical molecular dynamics (MD) simulations of D and  $\text{D}_2$  impinging on deuterated amorphous carbon surfaces in the energy range of 7.5–30 eV/D.<sup>1,2</sup> By mimicking experimental conditions, we have shown that proper attention has to be given to the self-consistent preparation of the deuterated carbon surfaces as a function of impact fluence, energy and type of projectile species, and to the internal (rovibrational) state of the projectile. Only under these conditions the correct distributions of saturated hydrocarbons are produced, reflected in a good quantitative agreement of the sputtering yields between simulation and experiment.<sup>3</sup> After validating our absolute yields we have started to use our simulations to predict heretofore unknown quantities such as the mass,

kinetic energy and momentum spectra of the sputtered species,<sup>1</sup> as well as their dependence on the rovibrational state of the impinging molecule.<sup>2</sup> In the short term, we plan to study the dependence of chemical sputtering yields as a function of the mass of the impinging H, D, or T atoms or molecules (i.e., isotope effects) and of the sample temperature. The main idea would be that these parameters should affect, for example, the thresholds for breaking the C-C bonds that ultimately result in the emission of hydrocarbons. Another important influence of temperature is the hydrogenation content, which may critically influence the chemical sputtering mechanism. Such studies will allow us to gain more insight into how the energy and momentum transfer delivered by the impinging particle along its collisional cascade (the latter increasing with mass) can be translated into the production of the various hydrocarbons. We are also studying the rovibrational spectra of ejected molecules and, of particular importance for fusion applications, mimicking plasma-surface rather than beam-surface interactions. In the longer term, we plan to spend considerable effort in developing improvements of the potentials used in our MD simulations. These are needed for extending our simulations to higher impact energies and addressing the interest within the Fusion community to study materials different from pure carbon.

- 
1. P. S. Krstic, C. O. Reinhold, and S. J. Stuart, *New J. Phys.* **9**, 219 (2007).
  2. P. S. Krstic, C. O. Reinhold, and S. J. Stuart, *Europhys. Lett.* **77**, 33002 (2007).
  3. F. W. Meyer, P. S. Krstic, L. I. Vergara, H. F. Krause, C. O. Reinhold, and S. J. Stuart, *Phys. Scr.* **T128**, 50 (2007).

### **Manipulation and Decoherence of Rydberg Wavepackets – C. O. Reinhold**

Rydberg states with large values of principal quantum number  $n$  provide a valuable laboratory in which to explore control of the quantum states of mesoscopic systems. Recent advances have stimulated the investigation of possible protocols to manipulate and probe the dynamics of Rydberg atoms using tailored pulsed unidirectional electric fields, termed half-cycle pulses (HCPs). We have recently demonstrated that starting with very-high- $n$  quasi-one-dimensional (quasi-1D) Rydberg atoms it is possible to create localized wavepackets and place them in selected regions of phase space.<sup>1</sup> This is a critical first step for further steering the electron in phase space using HCP trains. A train with a given frequency and strength can trap the electron in a stable island creating a non-dispersive wavepacket. The new and exciting issue to be explored is whether these trapped wavepackets can be stirred at will into different regions of phase space using a chirped train of pulses by adiabatically modifying the amplitude and/or frequency of the HCP train. The challenge to theory is to develop control protocols for chirped pulses matching the experimental profiles. Of interest is the transition from adiabatic to diabatic behavior as the chirp rate is increased. Calculations show that an adiabatic rather than a sudden change in the train of pulses should permit the initial localized wavepacket to be driven to selected locations in phase.

The ubiquitous coupling of any wavepacket to its environment destroys the coherent superposition by randomly dephasing the wavepacket. This *decoherence* provides a fundamental limitation to coherent quantum manipulation. Decoherent dephasing converts a coherent superposition into an incoherent statistical mixture and is often invoked in understanding the quantum-to-classical transition. We are currently investigating noise induced dephasing and damping of quantum beats in Stark wavepackets. Experimentally, it is possible to electronically synthesize colored noise with a spectral distribution that matches characteristic frequencies of the system. In order to isolate the effect of noise, it is important to separate the result of reversible dephasing from that of irreversible dephasing, i.e., decoherence. We have shown that this can be accomplished through the analysis of Stark quantum beat echoes produced by reversing the electric field that governs the Stark precession of the atomic dipole.<sup>2</sup> We are currently

investigating noise-induced decoherence using Stark echoes and improvements based on multiple field reversals. In the long term, we also plan to use as “noise” a gas of polar molecules (whose density can be varied) and to utilize the rate of decoherent dephasing as a tool to measure cross sections for quasi-elastic electron-atom (or molecule) collisions at energies extending down to micro electron volts.

- 
1. W. Zhao, J. J. Mestayer, J. C. Lancaster, F. B. Dunning, C. O. Reinhold, S. Yoshida, and J. Burgdörfer, Phys. Rev. Lett. **97**, 253003 (2006).
  2. S. Yoshida, C. O. Reinhold, J. Burgdörfer, W. Zhao, J. J. Mestayer, J. C. Lancaster, and F. B. Dunning, Phys. Rev. Lett. **98**, 203004 (2007).

**Development of the LTDSE Method for Atomic Collisions – D. R. Schultz, T. Minami, T.-G. Lee, M. S. Pindzola, J. H. Macek, and S. Yu. Ovchinnikov**

Plasma science applications, such as fusion energy, material processing, and the chemistry of the upper atmosphere, continue to drive the study of atomic collisions. In turn, this research demands reaching new levels of accuracy and completeness in calculations which has motivated development of new computational approaches, such as the lattice, time-dependent Schrödinger equation (LTDSE) method. At the same time, development of these computational approaches synergistically enables exploration of very fundamental aspects of atomic collisions that remain challenging.

Working towards these ends, efforts over the past year have both built on previous development of the LTDSE approach and undertaken significant new adaptations of it. For example, it has been a longstanding problem to treat ionization, and in particular the ejected electron spectrum, in ion-atom collisions owing to the multiple length scales involved in propagation of the electronic probability density from the region encompassing the near collision to the distant, two-center field of the residual ions. We first tackled this problem using the LTDSE approach several years ago<sup>1</sup> as did others such as Sidky and Lin using complementary techniques, and a number of features seen in pioneering experiments were qualitatively explained. However, owing to the finite size of the space spanned by the grid possible in the calculations, and the numerical problems posed in accurately propagating the rapidly spreading outgoing electronic flux, we could not extend the calculation in time far enough to reach asymptotic distances. We explored several methods of continuation of the calculation, as did our collaborators<sup>2</sup>, but a robust solution was not obtained. As described in the report in this Section by Macek and Ovchinnikov, we have now solved this problem by using the LTDSE approach in a transformed space<sup>3</sup>. This approach holds promise for treating a variety of problems that involve multiple length scales and therefore present difficulties for grid-based methods.

We have also considered several atomic collisions of interest in modeling high temperature plasmas in the past year, namely two ion-ion systems<sup>4</sup>,  $H^+ + He^+$  and  $He^{2+} + Li^{2+}$ , and in a separate work<sup>5</sup>,  $He^{2+} + H$ . While providing needed data, these studies were carried out particularly to test the accuracy of LTDSE, other theoretical methods, and experiments. For example, the ion-ion studies allowed a stringent test of two principal variants of the LTDSE approach in comparison with other advanced theories and some new measurements. The alpha particle work complements our previous calculations for  $Be^{4+}$  impact<sup>6</sup>, and utilized the recently developed LTDSE-AOCC hybrid approach<sup>7</sup>, in order to produce a range of benchmark, state-selective charge transfer data of use in plasma modeling and diagnostics.

An oral presentation will seek to place these recent studies in context with the energy research applications that motivate them, provide an overview of the computational and few-body physics advances that they constitute, and give an outlook on future directions of study.

1. D. R. Schultz, C. O. Reinhold, P. S . Krstic, and M. R. Strayer, Phys. Rev. A **65**, 052722 (2002).
2. J. H. Macek and S. Yu. Ovchinnikov, Phys. Rev. A **70**, 052702 (2004).
3. T.-G. Lee, S. Yu. Ovchinnikov, J. Sternberg, V. Chupryna, D. R. Schultz, and J. H. Macek, submitted to Phys. Rev. Lett. (2007).
4. T. Minami, M. S. Pindzola, T.-G. Lee, and D. R. Schultz, accepted in J. Phys. B (2007).
5. T. Minami, M. S. Pindzola, T.-G. Lee, and D. R. Schultz, submitted to J. Phys. B (2007).
6. T. Minami, M. S. Pindzola, T.-G. Lee, and D. R. Schultz, J. Phys. B **39**, 2877 (2006).
7. T. Minami, C. O. Reinhold, D. R. Schultz, and M. S. Pindzola, J. Phys. B **37**, 4025 (2004).

### Electron Detachment in Ion-Atom Collisions – *J. H. Macek and S. Yu. Ovchinnikov*

Electron detachment in ion-atom collisions is a process that has long been studied owing to its importance for the fundamental understanding of ion-atom interactions. Recent experiments involving electron detachment in collisions of  $H^-$  ions with He targets in the 2 keV – 10 keV impact energy range highlight some of the major gaps in our understanding of this process, especially when the relative ion velocity is below the mean velocity of the active electrons.<sup>1</sup>

The data of Ref. 1 indicate that two-electron processes are needed to account for high-velocity electrons ejected by  $H^-$  impact but even one-electron processes are not completely understood at low-impact velocities. For example, benchmark computations of ionization in proton-hydrogen atom collisions applicable to plasma diagnostics are needed but, at low energies and at the cross section maxima near 25 keV, only essentially exact methods such as the Lattice Time Dependent Schrödinger Equation (LTDSE) are reliable. Even here discrepancies with experiment are of the order of 20%. More troublesome is the 20% discrepancy between Sturmian calculations<sup>2</sup> and LTDSE cross sections.

To more closely compare the LTDSE theory with the  $H_2^+$  Sturmian theory, we have derived a regularized Schrödinger equation by implementing a transformation used in the former theory. This regularized equation has much better mathematical properties and allows for a more accurate computation of the ionization component of atomic wave functions using the LTDSE algorithms. The new method employs the regularized lattice time-dependent Schrödinger equation (RLTDSE) and is found to be remarkably stable and allows integration to macroscopically large target-projectile separations.

Using this method, we have been able to integrate to truly asymptotic distances, of the order of  $10^4$  a.u., without approximations needed in the LTDSE approach.<sup>3</sup> We have verified, for the first time, the recapture from continuum mechanism. A movie showing this effect has been made and excerpts (Fig. 2) from that movie have been submitted for publication.

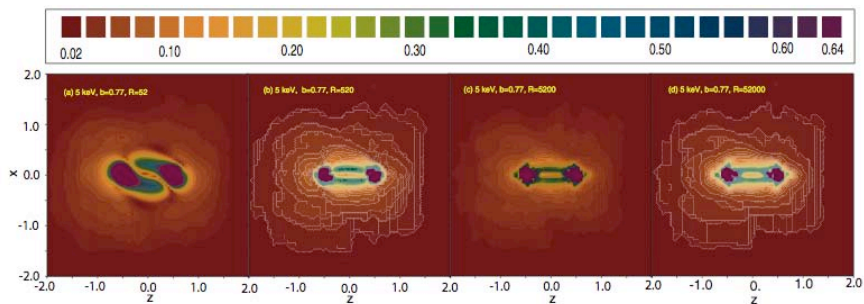


**Fig. 2.** The magnitude of the time-dependent wave function for proton impact on atomic hydrogen computed using the RLTDSE method shown as a contour plot for varying internuclear distances. The electron coordinates are scaled by the internuclear distance  $R$ , with  $z$  parallel to the relative velocity,  $x$  parallel to the impact parameter, and the third coordinate is zero.

We will compute total ionization cross sections using the RLTDSE method. Our goal is to obtain benchmark ionization cross sections in the 1 keV – 1 Mev impact energy region. As an additional test, we will compare cross sections for excitation and capture of high Rydberg states with those computed using standard methods. Finally, we will develop adapt the RLTDSE method to two-electron processes.

- 
1. G. N. Ogurtsov, V. M. Mikoushkin, S. Yu. Ovchinnikov, and J. H. Macek, Phys. Rev. A **74**, 042720 (2006).
  2. S. Yu Ovchinnikov, G. N. Ogurtsov, J. H. Macek, and Yu. S. Gordeev, Phys. Rep. **389**, 119 (2004).
  3. J. H. Macek and S. Yu. Ovchinnikov, Phys. Rev. A **70**, 052702 (2004).

#### **References to Publications of DOE Sponsored Research from 2005-2007 (descending order)**

“Experiments on Interactions of Electrons with Molecular Ions in Fusion and Astrophysical Plasmas,” M. E. Bannister, H. Aliabadi, E. Bahati Musafiri, M. R. Fogle, P. S. Krstic, C. R. Vane, A. Ehlerding, W. Geppert, F. Hellberg, V. Zhaunerchyk, M. Larsson, and R. D. Thomas, *Proceedings, 15<sup>th</sup> International Conference on Atomic Processes in Plasmas*, Gaithersburg, MD, March 19-22, 2007.

“Low Energy Electron Capture by Ne<sup>2+</sup> Ions from H(D),” B. Seredyuk, H. Bruhns, D. W. Savin, D. G. Seely, H. Aliabadi, E. Galutschek, and C. C. Havener, Phys. Rev. A (2007), in press.

“Quantum and Classical Transport of Excited States of Ions,” C. O. Reinhold, M. Seliger, T. Minami, D. R. Schultz, J. Burgdörfer, E. Lamour, J.-P. Rozet, and D. Vernhet, Nucl. Instrum. Methods Phys. Res. B (2007), in press.

“Angular Distribution of Ions Transmitted by an Anodic Nanocapillary Array,” H. F. Krause, C. R. Vane, F. W. Meyer, and H. M. Christen, *Proceedings of the 13th International Conference on the Physics of Highly Charged Ions, Belfast, Northern Ireland, UK*, J. of Physics: Conf. Ser. **58**, 323-326 (2007).

“Electron-impact Dissociation of CH<sub>2</sub><sup>+</sup> Ions: Measurement of CH<sup>+</sup> and C<sup>+</sup> Fragment Ions,” C. R. Vane, E. Bahati Musafiri, M. E. Bannister, and R. D. Thomas, Phys. Rev. A **75**, 052715 (2007).

“Atomic Collisions at Ultrarelativistic Energies,” C. R. Vane and H. F. Krause, Nucl. Instrum. Methods Phys. Res. B **261**, 244 (2007).

“Three-Body Breakup in Dissociative Recombination of the Covalent Triatomic Molecular Ion O<sub>3</sub><sup>+</sup>,” V. Zhaunerchyk, W. D. Geppert, M. Larsson, R. D. Thomas, E. Bahati, M. E. Bannister, M. R. Fogle, C. R. Vane, and F. Österdahl, Phys. Rev. Lett. **98**, 223201 (2007).

“Ions Transmitted through an Anodic Nanocapillary Array,” H. F. Krause, C. R. Vane, and F. W. Meyer, Phys. Rev. A **75**, 042901 (2007).

“The New ORNL Multicharged Ion Research Facility Floating Beamline,” F. W. Meyer, M. R. Fogle, and J. W. Hale, *Proceedings, 22<sup>nd</sup> Particle Accelerator Conference (PAC'07), Albuquerque, NM, June 25-29, 2007*.

“Merged-Beams Measurements of Absolute Cross Sections for Electron-Impact Excitation of S<sup>4+</sup> ( $3s^2 \ ^1S \rightarrow 3s3p \ ^1P$ ) and S<sup>5+</sup> ( $3s \ ^2S \rightarrow 3p \ ^2P$ ),” B. Wallbank, M. E. Bannister, H. F. Krause, Y.-S. Chung, A.C.H. Smith, N. Djuric, and G. H. Dunn, Phys. Rev. A **75**, 052703 (2007).

“Low Energy Chemical Sputtering of ATJ Graphite by Atomic and Molecular Deuterium Ions,” F. W. Meyer, P. S. Krstic, L. I. Vergara, H. F. Krause, C. O. Reinhold, and S. J. Stuart, Phys. Scr. **T128**, 50 (2007).

“Chemical Sputtering of Room Temperature ATJ Graphite and HOPG by Slow Atomic and Molecular Ions,” F. W. Meyer, H. Zhang, L. I. Vergara, and H. F. Krause, Nucl. Instrum. Methods Phys. Res. B **258**, 264 (2007).

“Chemical Sputtering from Amorphous Carbon under Bombardment by Deuterium Atoms and Molecules,” P. S. Krstic, C. O. Reinhold, and S. J. Stuart, New J. Phys. **9**, 219 (2007).

“Regge Oscillations in Electron-Atom Elastic Cross Sections,” D. Sokolovski, Z. Felfli, S. Yu. Ovchinnikov, J. H. Macek, and A. Z. Msezane, Phys. Rev. A **76**, 1 (2007).

“Electric Dipole Echoes in Rydberg Atoms,” S. Yoshida, C. O. Reinhold, J. Burgdörfer, W. Zhao, J. J. Mestayer, J. C. Lancaster, and F. B. Dunning, Phys. Rev. Lett. **98**, 203004 (2007).

“Low Energy Chemical Sputtering of ATJ Graphite by Atomic and Molecular D Ions,” F. W. Meyer, P. S. Krstic, L. I. Vergara, H. F. Krause, C. O. Reinhold, and S. J. Stuart, Phys. Scr. **T128**, 50 (2007).

“Time Scales of Chemical Sputtering of Carbon,” C. O. Reinhold, P. S. Krstic, and S. J. Stuart, Nucl. Instrum. Methods Phys. Res. B **258**, 274 (2007).

“Chemical Sputtering by Impact of Excited Molecules,” P. S. Krstic, C. O. Reinhold, and S. J. Stuart, Europhys. Lett. **77**, 33002 (2007).

“Capture and Transport of Electronic States of Fast Ions Penetrating Solids: An Open Quantum System Approach with Sinks and Sources,” M. Seliger, C. O. Reinhold, T. Minami, D. R. Schultz, M. S. Pindzola, S. Yoshida, J. Burgdörfer, E. Lamour, J.-P. Rozet, and D. Vernhet, Phys. Rev. A **75**, 032714 (2007).

“Dephasing of Stark Wavepackets Induced by Colored Noise,” S. Yoshida, C. O. Reinhold, J. Burgdörfer, W. Zhao, J. J. Mestayer, J. C. Lancaster, and F. B. Dunning, Phys. Rev. A **75**, 013414 (2007).

“Methane Production by Deuterium Impact at Carbon Surfaces,” S. J. Stuart, P. S. Krstic, T. A. Embry, and C.O. Reinhold, Nucl. Instrum. Methods Phys. Res. B **255**, 202 (2007).

## Year 2006 publications

“Methane Production from ATJ Graphite by Slow Atomic and Molecular D Ions: Evidence for Projectile Molecule-Size-Dependent Yields at Low Energies,” L. I. Vergara, F. W. Meyer, H. F. Krause, P. Träskelin, K. Nordlund, and E. Salonen, J. Nucl. Mater. **357**, 9 (2006).

“Recent ORNL Measurements of Chemical Sputtering of ATJ Graphite by Slow Atomic and Molecular D Ions,” F. W. Meyer, L. I. Vergara, and H. F. Krause, *Workshop on New Directions*

*for Advanced Computer Simulations and Experiments in Plasma Surface Interactions, March 21-23, 2005, Phys. Scr. **T124**, 44 (2006).*

“Dipole Polarization Effects on Highly-Charged Ion-Atom Electron Capture,” C. C. Havener and R. Rejoub, p. 522, *Proceedings, International Conference on Photonic, Electronic, and Atomic Collisions, Rosario, Argentina, July 20-26, 2005* (World Scientific, 2006).

“Laser Ion Source Tests at the HRIBF on Stable Sn, Ge, and Ni Isotopes,” Y. Liu, C. Baktash, J. R. Beene, H. Z. Bilheux, C. C. Havener, H. F. Krause, D. R. Schultz, D. W. Stracener, C. R. Vane, K. Breuck, Ch. Geppert, T. Kessler, K. Wendt, Nucl. Instrum. Methods Phys. Res. B **243**, 442-452 (2006).

“The ORNL Multicharged Ion Research Facility Upgrade Project,” F. W. Meyer, M. E. Bannister, D. Dowling, J. W. Hale, C. C. Havener, J. W. Johnson, R. C. Jurus, H. F. Krause, A. J. Mendez, J. Sinclair, A. Tatum, C. R. Vane, E. Bahati Musafiri, M. Fogle, R. Rejoub, L. Vergara, D. Hitz, M. Delaunay, A. Girard, L. Guillemet, and J. Chartier, *Proceedings, 14th International Conference on Ion Beam Modification of Materials, Asilomar, CA, Sept. 5-10, 2004*, Nucl. Instrum. Methods Phys. Res. B **242**, 71 (2006).

“Realization of the Kicked Atom at High Scaled Frequencies,” C. O. Reinhold, S. Yoshida, J. Burgdörfer, W. Zhao, J. J. Mestayer, J. C. Lancaster, and F. B. Dunning, Phys. Rev. A **73**, 033420 (2006).

“Influence of a DC Offset Field on Kicked Quasi-One-Dimensional Rydberg Atoms: Stabilization and Frustrated Field Ionization,” S. Yoshida, C. O. Reinhold, J. Burgdörfer, W. Zhao, J. J. Mestayer, J. C. Lancaster, and F. B. Dunning, Phys. Rev. A **73**, 033411 (2006).

“Correlated Electron Detachment in H<sup>-</sup> - He Collisions,” G. N. Ogurtsov, V. M. Mikoushkin, S. Yu. Ovchinnikov, and J. H. Macek, Phys. Rev. A **74**, 042720 (2006).

“Bidirectionally Kicked Rydberg Atoms: Population Trapping near the Continuum,” W. Zhao, J. J. Mestayer, J. C. Lancaster, F. B. Dunning, C. O. Reinhold, S. Yoshida, and J. Burgdörfer, Phys. Rev. A **73**, 015401 (2006).

“The Kicked Rydberg Atom,” F. B. Dunning, J. C., Lancaster, C. O. Reinhold, S. Yoshida, and J. Burgdörfer, Adv. At. Mol. Phys. **52**, 49 (2006).

“Lattice, Time-dependent Schrödinger Equation Approach for Charge Transfer in Collisions of Be<sup>4+</sup> with Atomic Hydrogen,” T. Minami, M. S. Pindzola, T.-G. Lee,, and D. R. Schultz, J. Phys. B **39**, 2877 (2006).

“Collisions of Slow Highly Charged Ions with Surfaces,” J. Burgdörfer, C. Lemell, C. O. Reinhold, K. Schiessl, B. Solleeder, K. Tokesi, and L. Wirtz, p. 30, *Proceedings, International Conference on Photonic, Electronic, and Atomic Collisions, Rosario, Argentina, July 20-26, 2005* (World Scientific, 2006).

“Navigating Localized Wavepackets in Phase Space,” W. Zhao, J. J. Mestayer, J. C. Lancaster, F. B. Dunning, C. O. Reinhold, S. Yoshida, and J. Burgdörfer, Phys. Rev. Lett. **97**, 253003 (2006).

“Chemical Sputtering of Fusion Plasma-Facing Carbon Surfaces,” P. S. Krstic, S. J. Stuart, and C. O. Reinhold, pp. 201-208, *Proceedings, 23<sup>rd</sup> Summer School and International Symposium on the Physics of Ionized Gases, Aug.28 – Sept. 1, 2006, Kopaonik, Serbia*, AIP Conf. Proc. **876**, 201 (2006).

“Charge Transfer and Ionization by Intermediate-Energy Heavy Ions,” L. H. Toburen, S. L. McLawhorn, R. A. McLawhorn, N. Evans, E.L.B. Justiniano, J. L. Shinpaugh, D. R. Schultz, and C. O. Reinhold, Rad. Prot. Dosim. **122**, 26 (2006).

“State-to-State Rotational Transitions in H<sub>2</sub>+H<sub>2</sub> Collision at Low Temperatures,” T.-G. Lee,, N. Balakrishnan, R. C. Forrey, P. C. Stancil, D. R. Schultz, and G. J. Ferland, J. Chem. Phys. **125**, 114302 (2006).

### Year 2005 publications

“Path Dependence of the Charge-State Distributions of Low-Energy F<sup>q+</sup> Ions Back-scattered from RbI(100),” L. I. Vergara, F. W. Meyer, and H. F. Krause, Nucl. Instrum. Methods Phys. Res. B **230**, 379 (2005).

“New Directions for Computer Simulations and Experiments in Plasma-Surface Interactions for Fusion: Report on the Workshop (Oak Ridge National Laboratory, Oak Ridge TN, USA, 21–23 March 2005),” J. T. Hogan, P. S. Krstic, and F. W. Meyer, Nucl. Fusion **45**, 1202 (2005).

“Charge Transfer in Low-Energy Collisions of He<sup>2+</sup> with Atomic Hydrogen,” C. C. Havener, R. Rejoub, P. S. Krstic, and A. C. H. Smith, Phys. Rev. A **71**, 042707 (2005).

“Electron Capture by Ne<sup>4+</sup> Ions from Atomic Hydrogen,” C. C. Havener, R. Rejoub, C. R. Vane, H. F. Krause, D. W. Savin, M. Schnell, J. G. Wang, and P. C. Stancil, Phys. Rev. A **71**, 034702 (2005).

“Electron-Impact Dissociation of D<sup>13</sup>CO<sup>+</sup> Molecular Ions to <sup>13</sup>CO<sup>+</sup> Ions,” E. M. Bahati, R. D. Thomas, C. R. Vane, and M. E. Bannister, J. Phys. B **38**, 1645 (2005).

“Engineering Very-High-n Polarized Rydberg States Using Tailored HCP Sequences,” W. Zhao, J. J. Mestayer, J. C. Lancaster, F. B. Dunning, C. O. Reinhold, S. Yoshida, and J. Burgdörfer, Phys. Rev. Lett. **95**, 163007 (2005).

“Collisional Decoherence in Very-High-n Rydberg Atoms,” C. O. Reinhold, J. Burgdörfer, and F. B. Dunning, Nucl. Instrum. Methods Phys. Res. B **233**, 48 (2005).

“The Periodically Kicked Atom: Effect of the Average DC Field,” W. Zhao, J. C. Lancaster, F. B. Dunning, C. O. Reinhold, and J. Burgdörfer, J. Phys. B **38**, S191 (2005).

“Three-Body Fragmentation Dynamics of Amidogen and Methylene Radicals via Dissociative Recombination,” R. Thomas, F. Hellberg, A. Neau, S. Rosen, M. Larsson, C. R. Vane, M. E. Bannister *et al.*, Phys. Rev. A **71**, 032711 (2005).

“Investigating the Breakup Dynamics of Dihydrogen Sulfide Ions Recombining with Electrons,” F. Hellberg, V. Zhaunerchyk, A. Ehlerding, W. D. Geppert, M. Larsson, R. D. Thomas, M. E. Bannister, E. Bahati, C. R. Vane, F. Österdahl, P. Hlavenka, and M. af Ugglas, J. Chem. Phys. **122**, 224314 (2005).

“The Effect of Bonding on the Fragmentation of Small Systems,” R. Thomas, A. Ehlerding, W. Geppert, F. Hellberg, M. Larsson, V. Zhunerchyk, E. Bahati, M. E. Bannister, C. R. Vane, A. Petigrani, W. J. van der Zande, P. Andersson, and J.B.C. Pettersson, *J. Phys.: Conf. Ser.* **4**, 187 (2005).

“Target Orientation Dependence of the Charge Fractions Observed for Low-Energy Multicharged Ions  $\text{Ne}^{q+}$  And  $\text{F}^{q+}$  Backscattered from  $\text{RbI}(100)$ ,” L. I. Vergara, F. W. Meyer, and H. F. Krause, *Surf. Coat. Technol.* **196**, 19 (2005).

“An All-Permanent Magnet ECR Ion Source for the ORNL MIRF Upgrade Project,” D. Hitz, M. Delaunay, A. Girard, L. Guillemet, J. M. Mathonnet, J. Chartier, and F. W. Meyer, *Proceedings, 16th International Workshop on ECR Ion Sources (ECRIS '04), Sept. 26-30, 2004*, AIP Conf. Proc. **749**, 123 (2005).

“Traveling Wave Vs. Cavity RF Injection for the ORNL HRIBF ‘Volume-Type’ ECR Ion Source,” Y. Liu, F. M. Meyer, and J. M. Cole, *Proceedings, 16th International Workshop on ECR Ion Sources (ECRIS '04), Sept. 26-30, 2004*, AIP Conf. Proc. **749**, 187 (2005).

“Non-Unitary Master Equation for the Internal State of Ions Transversing Solids,” M. Seliger, C. O. Reinhold, T. Minami, and J. Burgdörfer, *Nucl. Instrum. Methods Phys. Res. B* **230**, 7 (2005).

“Non-Unitary Quantum Trajectory Monte Carlo Method for Open Quantum Systems,” M. Seliger, C. O. Reinhold, T. Minami, and J. Burgdörfer, *Phys. Rev. A* **71**, 062901 (2005).

“Steering Rydberg Wave Packets Using a Chirped Train of Half-Cycle Pulses,” S. Yoshida, C. O. Reinhold, E. Persson, J. Burgdörfer, and F. B. Dunning, *J. Phys. B* **38**, S209 (2005).

“Performances of “Volume” vs “Surface” ECR Ion Sources,” Y. Liu, F. M. Meyer, H. Bilheux, J. M. Cole, and G. D. Alton, *Proceedings, 16th International Workshop on ECR Ion Sources (ECRIS '04), Sept. 26-30, 2004*; AIP Conf. Proc. **749**, 191 (2005).

“Measurements of Chemical Erosion of ATJ Graphite by Low Energy  $\text{D}_2^+$  Impact,” F. W. Meyer, H. F. Krause, and L. I. Vergara, *Proceedings, International Conference on Plasma Surface Interactions, Portland, ME, May 24-28, 2004*, *J. Nucl. Mater.* **337-339**, 922 (2005).

“The ORNL Multicharged Ion Research Facility (MIRF) High Voltage Platform Project,” F. W. Meyer, M. E. Bannister, J. W. Hale, J. W. Johnson, and D. Hitz, pp. 1853-1855, *Proceedings, Particle Accelerator Conference (PAC'05)*, Knoxville, TN, May 16-20, 2005, published on CD, IEEE Cat. No. 05CH37623C, IEEE, Piscataway, NJ, 2005.

“Control System for the ORNL Multicharged Ion Research Facility High-Voltage Platform,” M. E. Bannister, F. W. Meyer, J. Sinclair, pp. 3591-3593, *Proceedings, Particle Accelerator Conference (PAC'05)*, Knoxville, TN, May 16-20, 2005, published on CD, IEEE Cat. No. 05CH37623C, IEEE, Piscataway, NJ, 2005.

“Isobar Suppression by Photodetachment in a Gas-filled RF Quadrupole Ion Guide,” Y. Liu, J. R. Beene, C. C. Havener, and J. F. Lang, *Appl. Phys. Lett.* **87**, 113504 (2005).

“Isobar Suppression by Photodetachment in a Gas-Filled RF Quadrupole Ion Guide,” Y. Liu, J. R. Beene, C. C. Havener, J. F. Liang, A. C. Havener, pp. 3250-3252, *Proceedings, Particle*

*Accelerator Conference (PAC'05)*, Knoxville, TN, May 16-20, 2005, published on CD, IEEE Cat. No. 05CH37623C, IEEE, Piscataway, NJ, 2005.

“Chemical Sputtering of ATJ Graphite Induced by Low-Energy D<sub>2</sub><sup>+</sup> Bombardment,” L. I. Vergara, F. W. Meyer, and H. F. Krause, *J. Nucl. Mat.* **347**, 118 (2005).

“Chemical Sputtering of ATJ Graphite Induced by Low-Energy D<sub>2</sub><sup>+</sup> Bombardment,” L. I. Vergara, F. W. Meyer, and H. F. Krause, *J. Nucl. Mater.* **337-339**, 922 (2005).

“Experiments on Electron-Impact Ionization of Atomic and Molecular Ions,” M. E. Bannister, pp. 172-179, *Proceedings of the 4<sup>th</sup> ICAMDATA Conference, Oct. 5-8, 2004, Toki, Japan*, AIP Conf. Proc. **730**, Woodbury, NY (2005).

“Excitation and Charge Transfer in p+H(2s) Collisions,” M. S. Pindzola, T.-G. Lee, T. Minami, and D. R. Schultz, *Phys. Rev. A* **72**, 062703 (2005).

“Close-Coupling Calculations of Low-Energy Inelastic and Elastic Processes in <sup>4</sup>He Collisions with H<sub>2</sub>: A Comparative Study of Two Potential Energy Surfaces,” T.-G. Lee, C. Rochow, R. Martin, T. K. Clark, R. C. Forrey, N. Balakrishnan, P. C. Stancil, D. R. Schultz, A. Dalgarno, and G. J. Ferland, *J. Chem. Phys.* **122**, 024307 (2005).

“Nonadiabatic Processes near Barriers,” J. Burgdörfer, N. Rohringer, P. S. Krstic, and C. O. Reinhold, Book Chapter, *Nonadiabatic Transition in Quantum Systems*, edited by V. I. Osherov, L. I. Ponomarev, Chernogolovka, Russia (2004), Institute of Chemical Physics RAS ISBN 5-901675-48-7, p. 205

“In-situ Electron Cyclotron Resonance (ECR) Plasma Potential Determination Using an Emissive Probe,” H. J. You, Y. Liu, and F. W. Meyer, pp. 2035-2037, *Proceedings, Particle Accelerator Conference (PAC'05), Knoxville, TN, May 16-20, 2005*, published on CD, IEEE Cat. No. 05CH37623C, IEEE, Piscataway, NJ, 2005.

“Laser Ion Source Development for ISOL Systems at RIA,” Y. Liu, C. Baktash, J. R. Beene, H. Z. Bilheux, C. C. Havener, H. F. Krause, D. R. Schultz, D. W. Stracener, C. R. Vane, K. Brück, Ch. Geppert, T. Kessler, and K. Wendt, pp. 1640-1642, *Proceedings, Particle Accelerator Conference (PAC'05), Knoxville, TN, May 16-20, 2005*, published on CD, IEEE Cat. No. 05CH37623C, IEEE, Piscataway, NJ, 2005.

## **PULSE: The Stanford Photon Ultrafast Laser Science and Engineering Center**

PULSE Primary Investigators: Y. Acremann, P.H. Bucksbaum, M. Fayer, D. Fritz, J. Hajdu, B. Hedman, K. Hodgson, K. Gaffney, A. Lindenberg, H. Siegmann, J. Stohr

**PULSE mission:** The Stanford PULSE Center conducts research in areas of ultrafast science at SLAC that support the research program of the LCLS. PULSE has initiated research in ultrafast materials science, condensed matter physics, molecular physics, physical chemistry, atomic physics, structural biology, electron beams and x-ray laser physics. PULSE also maintains close links to areas of ultrafast science that are critically served by LCLS, but which lie outside the scope of mission activities in BES. These include plasma physics and high energy density physics.

The PULSE Center participated in the recently completed SPPS project at SLAC, which produced and used the world's brightest beams of sub-100 fs x-rays during its two-year run. PULSE scientists also are involved in several projects at FLASH, the soft-x-ray FEL at DESY. We are also building laboratories at SLAC in the areas of ultrafast materials science, ultrafast chemistry, ultrafast AMO Physics, and coherent x-ray imaging of biology. Current PULSE instrumentation includes a CEP stabilized laser, a high harmonics source of ultrafast vuv, and laboratories for ultrafast chemistry and atomic physics. PULSE occupies temporary space at SSRL, and also has research in laboratories in the Varian Physics Building on the Stanford main campus.

PULSE activities have divided funding. Four tasks are funded by Chemical Sciences: Attosecond and femtosecond vuv spectroscopy; strong-field molecular wave packet dynamics and quantum control; ultrafast x-ray studies of chemical processes; and coherent x-ray imaging. Other PULSE programs are funded by the Materials Science Division, in the areas of ultrafast magnetic materials and THz-induced materials science. High energy density science and ultrafast source science are pursued with funding outside of these two research divisions of BES. This abstract book will only summarize the AMOS-funded activities. Kelly Gaffney is the coordinator for those activities.

**PULSE organizational activities for research in FY07:** PULSE was originally to have been housed in the LCLS Central Laboratory and Office Complex, but plans for this building were removed from the LCLS project in 2006. An alternative location was found in the SLAC Central Laboratory. Funds for renovation will not be available until FY08, but some office and lab space was created in FY07 in advance of this. Funding for preliminary work in ultrafast materials science (referred to as pre-PULSE) made it possible to initiate limited research in AMO, UMD, and Source Science, and a separate DOE grant was obtained for chemistry. Meanwhile, the PULSE proposal for baseline funding from BES was submitted in FY06, but the decision to fund was delayed through most of FY07 because of problems stemming from the Congressional Continuing Resolution, together with the simultaneous reorganization of SLAC to become a BES laboratory. The current status is that PULSE has no DOE funding for central administration until FY08, and several of the research projects funded under pre-PULSE and described in last year's abstract for the AMOS Contractor's Meeting were eliminated from the funding profile by BES guidance, again largely because of problems stemming from the lack of Congressional approval of an FY07 budget. The

initial funding of four programs in Chemical Sciences will be described in abstracts following this general summary. This is summarized in the organization chart (Fig. 1).

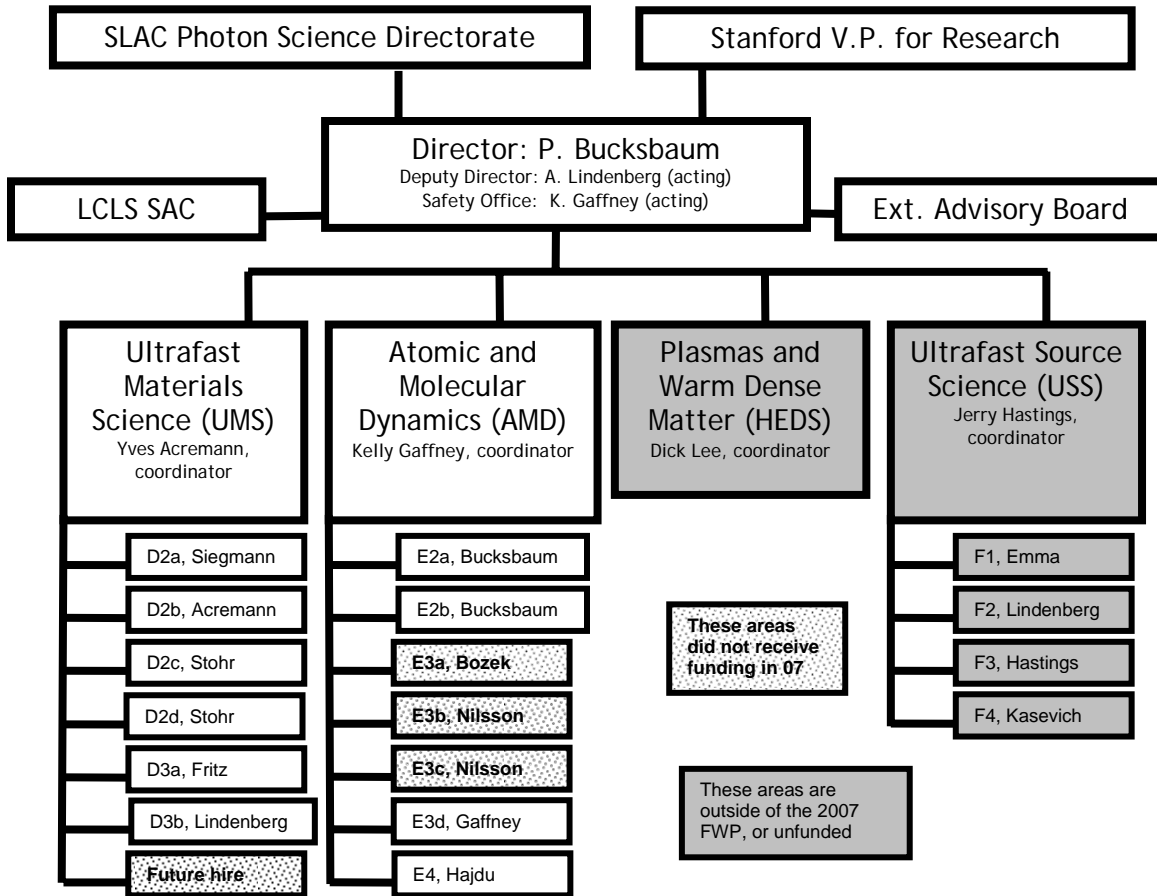


Fig. 1: PULSE organization chart

The PULSE Center will seek other avenues to pay for research in the unfunded parts of the PULSE proposal, most of which received very positive support from the reviewers of the proposal.

*Ultrafast source science:* BES provided guidance that ultrafast source research should be funded in many cases out of the LCLS operating budget. That budget line will not commence until FY09, but we will pursue it with LCLS management at that time. Meanwhile, the areas of research in the Ultrafast Source Science column on our organization chart have either been suspended, or are continuing to seek other funding. For example, PULSE has contributed along with LCLS and the Accelerator Group at SLAC to the BES call for advanced accelerator research. This may fund advanced work on beam conditioning for LCLS. The Kasevich project continues outside of the PULSE Center, with some funding from DARPA. The Hastings project on ultrafast electron diffraction was rejected by BES for budget reasons after there were earlier indications that it might be funded, but there is still strong interest in pursuing it in future years.

*High Energy Density Science:* This is still seeking funding through an MOU with the University of California (SUCCEEDS). The funding source will not be BES, but we are hopeful that this can be funded because this research is a critical science driver for LCLS and other XFEL's. Preliminary work has been carried out at FLASH in Hamburg, and there may be interest in pursuing significant HEDS in the European XFEL. We believe that it would be a great loss in an important area of U.S. Science if there were no significant program here.

*Catalysis and surface chemistry:* This program headed by Anders Nilsson reviewed well, but was not funded for budgetary reasons. We will continue to attempt to start funding in this important area of energy-related chemistry.

*Ultrafast Materials Science:* PULSE has six tasks in this area, all funded by the BES Division of Materials Science. These are described in abstracts in the DOE x-ray and neutron scattering contractor's meeting. The tasks cover investigations of ultrafast magnetic and dielectric properties of materials.



Fig. 2: 2007 PULSE Ultrafast X-ray Summer School poster

**PULSE Central Activities** Although there will be no funding for central management of the PULSE Center until the FY08 budget, we have nonetheless been able to begin to organize our central management, using resources donated from the SSRL Director's Office, from the SLAC Director, and most especially, from the Stanford Dean of Research. PULSE is eligible to receive some direct support from the Dean of Research because it has been chartered as an Independent Laboratory of Stanford University.

*Summer School:* The Stanford Dean of Research helped us to sponsor and organize an extremely successful Ultrafast X-ray Summer School at the Kavli Institute on the SLAC campus in June. Professor Nora Berrah of Western Michigan University was the Summer School Chair. The school was attended by more than 100 students and postdocs. Information is on the following website:  
<http://photonscience.slac.stanford.edu/pulse/uxss2007/index.php>. This summer school will be repeated annually as we seek to build a community of researchers for XFEL science.

*Visitors Program:* PULSE maintains a visitors program to enable researchers from around the world to work in our center. Our present sabbatical visitor is Dr. Hamed Merdji from Saclay. Dr. Merdji has contributed to PULSE research in attosecond physics, strong field AMO physics, and ultrafast x-ray source science.

# High harmonic generation in molecules

Philip H. Bucksbaum and Markus Gühr

Stanford PULSE Center, Stanford Linear Accelerator Center, Menlo Park, CA 94025  
and

Physics Department, Stanford University, Stanford, CA 94305

## Scope

The project aims at understanding the influence of the molecular orbital symmetry on the amplitude and phase of strong field high harmonics. It explores the applications of high harmonic generation for the dynamical imaging of electrons during chemical processes. Furthermore it aims at the shaping of high harmonic spectra leading to amplitude and phase shaped attosecond pulses.

## Recent Progress

M. Gühr, B. K. McFarland, J. P. Farrell and P. H. Bucksbaum

### a) Simulations on HHG on N<sub>2</sub> and CO<sub>2</sub>

The three step model of High Harmonic Generation (HHG) [1,2] divides the process into ionization of an atom, subsequent acceleration of the free electron in the laser field and recombination of the electron with the original ion. The returning electron can be imagined as a wave, containing different kinetic energies. In a quantum model, it is superposed with the HOMO from which it was initially ionized and creates a time varying dipole that radiates the High Harmonics (HH). The HOMO itself has nodes with positive and negative phases on either side, so that the superposition gives rise to constructive and destructive interferences in the emitted HH. We calculated the dynamic interference pattern of the recolliding free electron wave with the HOMO of N<sub>2</sub> and CO<sub>2</sub> and the resulting dipole [3]. The HOMOs were obtained from an *ab initio* program (Gaussian) [4] and the free electron wave was calculated by Newton's propagation in the laser electric field, neglecting the molecular Coulomb potential. For N<sub>2</sub>, we varied the internuclear distance in the calculation of the HOMO. The HH spectrum clearly shows a minimum, which moves to larger photon energies as the internuclear separation is diminished. We compared the energetic position of the minima in the spectrum to the predictions of a two point scattering model [5] and found a good agreement for large internuclear distances bigger than 2.5 a<sub>0</sub> and major shifts at the equilibrium position (2 a<sub>0</sub>) and smaller internuclear separations. The two point scattering model is artificially restricting the HOMO to the nuclei, thereby neglecting the effects of orbital overlap from the participating atoms. This overlap of the atomic p-orbitals constituting the molecular σ<sub>g</sub> HOMO shifts the average size of the HOMO to larger distances if the nuclei are close together, as a Fourier transformation of the HOMO shows [3]. This leads to the redshift of our calculations with respect to the two point model.

For CO<sub>2</sub>, we divide our analysis into two geometries. In the first geometry, the lobes of the π<sub>g</sub> HOMO lie out of the plane spanned by the internuclear axis and the returning electron wave packet k-vector  $\mathbf{k}_e$ . The predictions of our simulations for this geometry agree with the two point model. However, in most experimental situations, the HH radiation generated in this geometry cannot be phase matched and remains invisible. For the second geometry, the lobes of the π<sub>g</sub> HOMO lie out of the  $\mathbf{k}_e$  – internuclear axis plane. The radiation can be phase matched but it does not agree with the two point model for the antibonding symmetry of the CO<sub>2</sub> HOMO. Instead it

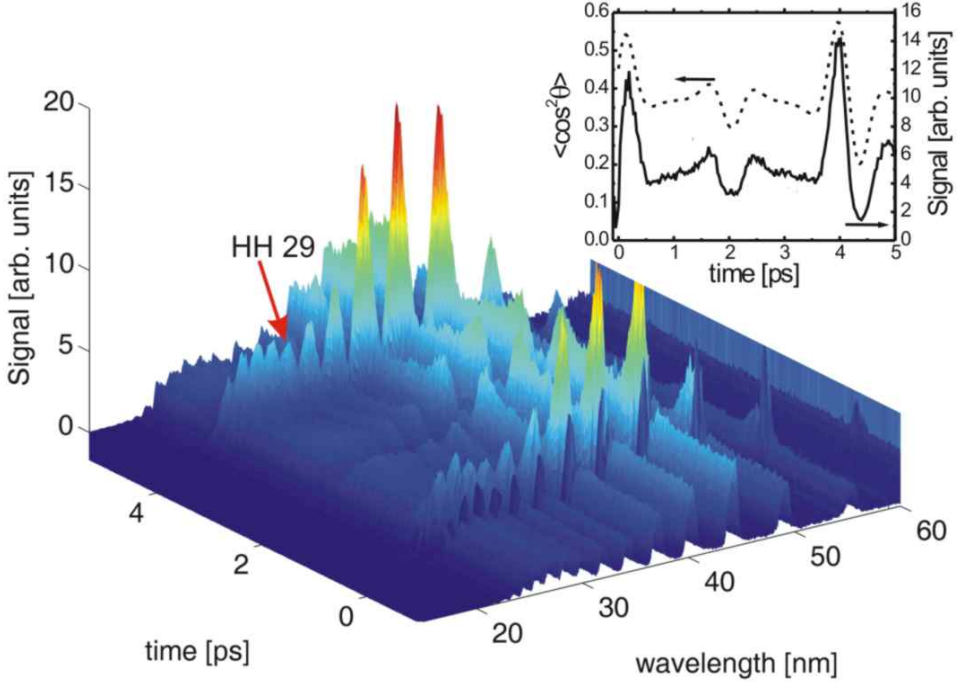


**Figure 1:** High harmonic spectra for  $\text{N}_2$  as a function of the delay between alignment pulse and high harmonic generating pulse. A minimum at the 29<sup>th</sup> harmonic is seen at the half revival at 4 ps and the immediate alignment after the pump pulse. Inset: HH 23 as a function of the pump-probe delay (solid line) compared to a simulation of the alignment parameter  $\langle \cos^2 \theta \rangle$  for  $\text{N}_2$  at 30 K.

agrees well with a corresponding bonding symmetry. The results are in agreement with experiments on  $\text{CO}_2$  and provide new insight in the HHG process in molecules [6].

### b) Measuring amplitude and phase of High Harmonics

In our simulations, the amplitude of the HH emission is greatly diminished, if the free electron wave packet has a wavelength such that a destructive interference occurs in the superposition with the HOMO. Since the free electron wave packet is chirped from long to short de Broglie wavelengths, a minimum in the HH spectrum appears. We also theoretically observe a phase shift of about  $\pi$  in the HH spectral phase at this point, as predicted by [5].

Full amplitude and phase information about the HH will eventually lead to a HOMO reconstruction (see [7], where only the amplitude was experimentally available and the phase was taken from calculations).

Experimentally, we are focusing on the  $\text{N}_2$  molecule. In all our measurements, we aligned the molecules by a nonresonant laser pulse, shorter than the characteristic rotational time constant of the molecule. Thereby, we induced a coherent superposition of rotational eigenstates, leading to a rotational wave packet and field free revivals as can be seen in our simulations in Fig.1. The alignment is needed, because the interference pattern of the free electron wave function with the HOMO depends on the recollision angle, which is the angle between internuclear axis and the high harmonic generating polarization. We set up a fully working HHG experiment with a 25 fs laser (also capable of producing carrier envelope stabilized 6 fs pulses by spectral broadening in a hollow core fiber filled with neon). A first laser pulse (pump pulse) aligns the molecules that are supersonically expanding through a small nozzle into a high vacuum. A stronger second laser pulse (probe pulse) generates harmonics that are dispersed in a spectrometer and imaged onto a MCP-phosphor screen detector.

Figure 1 shows the emitted intensity for different harmonics as a function of the pump-probe delay. Looking at the intensity as a function of the high harmonic order at the highest alignment exhibits a minimum in around the 29<sup>th</sup> harmonic. A comparison with the simulated wave packet revivals (calculated following a procedure in Ref. [8]) in the inset of Fig.1 shows an enhancement of the harmonics at high alignment and a decrease at the anti alignment. This is in agreement with the previous publications on HHG in N<sub>2</sub> [9,10]. The energetic position of the minimum is actually intensity dependent and shifts to higher energies with rising intensity.

We are currently working on determining the  $\pi$  phase jump at this minimum. Our experimental technique makes use of interference of the nitrogen harmonics with those of an argon reference radiator. Measuring the Ar and N<sub>2</sub> HH spectra separately and afterwards determining the high harmonic intensity from a mixture of the two allows deducing the relative phase between the Ar and N<sub>2</sub> harmonics. Since our calculations show, that the Ar phase is smooth over the range where we expect the  $\pi$  jump in N<sub>2</sub>, the relative phase gives the energetic position of the absolute  $\pi$  phase jump in N<sub>2</sub>. We observe a phase jump of about  $\pi$  at the 31<sup>st</sup> harmonic, which is shifted with respect to the amplitude minimum at harmonic 29. We are currently working on an interpretation of this shift.

## **Future Plans**

*M. Gühr and P. H. Bucksbaum*

### **a) Attosecond pulse shaping**

The shaping of fs laser pulses in amplitude, phase and also polarization has given rise to powerful experiments in molecular reaction control [11]. The tools for pulse shaping are working on a reflective (deformable mirror) or transmission basis (LCDs, AOMs). Attosecond pulses are spectrally located in the VUV region. Unfortunately, transparent or reflective materials for attosecond pulse shaping are not readily available in this spectral range. Instead of shaping an attosecond pulse after its generation, we plan on shaping it during its generation. As stated above, molecules are shaping the HH emission according to the interference pattern that the recolliding electron function produces with the HOMO. Since a HH spectrum is represented by a train of attosecond pulses in the time domain, the pulses are amplitude and phase shaped and the generalization to single attosecond pulses can be accomplished by using the 6 fs CEP stabilized pulses available in our lab.

Apart from letting the molecular HOMO determine the spectral features of the as pulse, we plan to excite rotational, vibrational and electronic wave packets and thereby control the as pulse features by controlling the molecular state superposition. We will explore, to which extend we can change the amplitude, phase and polarization of the attosecond pulse by writing specially tailored wave functions on the molecule. The pulses will find applications for controlling electron motion in the valence and upper core levels of atoms, molecules and possibly also in steering the electron motion in solid state systems.

### **b) Chemical imaging of conical intersections**

A vast variety of chemical processes proceed via so called conical intersections (CI) [12]. The conical intersections are crucial for biological processes such as light harvesting, primary visual processes and UV stabilization of DNA and for chemical processes in the earth's atmosphere. A wave packet excited by an ultrafast laser pulse explores the potential landscape of the excited

state and reaches the conical intersection. At the intersection, part of the wave packet can stay on the initially excited surface, and another part can funnel through the intersection to a crossing state. In all ultrafast studies so far, a second, time delayed probe pulse excites (or stimulates down) parts of the wave packet to other electronic state and therefore detailed knowledge about those states is required to reconstruct the path of the wave packet from the pump-probe transients. We want to overcome this problem by establishing a HHG for probing. As stated above, the process of HHG is sensitive on the molecular orbital structure, from which the recolliding electron was initialized. It is therefore sensitive on the electronic state and the internuclear position, as the current literature and our own studies show. Since the change of the electronic state is the sign of the radiation less transition in the conical intersection, HHG probing will be an ideal tool for CIs. We plan to follow the nuclei and the occupied electronic orbitals as a function of pump probe delay time by observing the HH spectral amplitude and phase.

## References

- [1] P. B. Corkum, Phys. Rev. Lett. **71**, 1994 (1993)
- [2] J. L. Krause, K. J. Schafer, and K. C. Kulander, Phys. Rev. Lett., **68**, 3535 (1992)
- [3] M. Gühr, B. F. McFarland, J. P. Farrell, and P.H. Bucksbaum, submitted to J. Phys. B.
- [4] M. J. Frisch *et al.*, Gaussian 03, Revision C.02., Gaussian Inc, Wallingford, CT 2004
- [5] M. Lein *et al.*, Phys. Rev. A, **66**, 023805 (2002)
- [6] C. Vozzi *et al.*, Phys. Rev. Lett., **95**, 153902 , (2005)
- [7] J. Itatani *et al.*, Nature, **432**, 867, (2004)
- [8] J. Ortigoso *et al.*, J. Chem. Phys., **110**, 3870, (1999)
- [9] J. Itatani *et al.*, Phys. Rev. Lett., **94**, 123902, (2005)
- [10] T. Kanai *et al.*, Nature, **435**, 470, (2005)
- [11] A. M. Weiner, Rev. Sci. Instr., **71**, 1929, (2000)
- [12] D. R. Yakomy, J. Phys. Chem. A, **105**, 6277, (2001)

## Project Publications and Conference Contributions

- 1) M. Gühr, B. K. McFarland, J. P. Farrell and P. H. Bucksbaum, High harmonic generation on N<sub>2</sub> and CO<sub>2</sub> beyond the two point model, submitted to Journal of Physics B
- 2) M. Gühr, B. K. McFarland, J. P. Farrell and P. H. Bucksbaum, High Harmonic Imaging of Conical Intersections, German Physical Society Spring Meeting, Düsseldorf, 2007
- 3) M. Gühr, B. K. McFarland, J. P. Farrell and P. H. Bucksbaum, Probing Rotational Wave Packets by High Harmonic Generation, German Physical Society Spring Meeting, Düsseldorf, 2007
- 4) M. Gühr, B. K. McFarland, J.P. Farrell and P. H. Bucksbaum,High Harmonic Imaging of Conical Intersections, CLEO/QUELS 07, Baltimore 2007
- 5) B. K. McFarland, M. Gühr, J. P. Farrell and P. H. Bucksbaum,Probing Rotational Wave Packets by High Harmonic Generation DAMOP, Calgary 2007
- 6) J. P. Farrell, M. Gühr, B. K. McFarland, and P. H. Bucksbaum,High Harmonic Imaging of Conical Intersections, DAMOP Calgary 2007

## Laser Control of Molecular Alignment and Bond Strength

*Philip H. Bucksbaum and Ryan N. Coffee*

*Stanford PULSE Center, Stanford Linear Accelerator Center, Menlo Park, CA 94025*

### Scope

We are investigating various coherent processes in both atoms and molecules that may be of values for LCLS experiments and ultrafast x-ray diagnostics. The immediate goal is to obtain and study ro-vibrational quantum control in small molecules as a first step toward the laser control of larger more complicated molecules that will use the LCLS x-ray laser as a probe. One major focus of the program this year is the control of laser induced alignment of molecular gases at densities conducive to hard x-ray scattering. Another focus of the program is the use of selective resonant, or near resonant, excitations to produce aligned ensembles of vibrational wave packets. Wave packet dynamics can be imaged via differential optical absorption and birefringence, and later, nuclear imaging can be performed at LCLS. We have also initiated new collaborations with LBNL and CEA Saclay to investigate angle resolved soft x-ray absorption and photo-electron spectroscopy. These molecular gases can also be used as selective nonlinear absorbers for LCLS beam conditioning. For example, we are studying the use of an atomic or molecular gas as a possible pulse-cleaning system for the LCLS beam.

### Recent Progress

#### SLAC Laser Laboratory Commissioning

A major difficulty facing the PULSE center and LCLS is finding a safe and efficient procedure for working with high-power lasers of various and tunable wavelengths. Most of the molecular dynamics we intend to study near-resonantly uses visible wavelengths for the aligning mechanism. Simple small molecules tend to have electronic resonances in the ultraviolet. For larger diatomic molecules like I<sub>2</sub>, those resonances are more in the visible part of the spectrum. The drive to work with such heavy and large diatomic molecules is their simplicity (two atoms), their efficiency of x-ray scattering (many electrons), and their vibrational time scales are more conducive to 30fs to 50fs laser pulses (heavy nuclei and longer bonds). The PULSE Center has established detailed alignment procedures for each part of the respective laser systems, many hardware controls and enclosure systems to mediate the dynamically changing laser hazards.

#### Molecular Alignment

*Doug Broege, Ryan N. Coffee, and Phil H. Bucksbaum*

We are investigating impulsive laser alignment of molecular iodine a density of  $\sim 10^{18}$  molecules/cm<sup>3</sup> at a temperature of  $\sim 100$  C using a 1.5 mJ 40 fs 800 nm laser system in collaboration with Stanford postdoc David Cardoza. This experiment seeks an optimal pump and probe geometry for obtaining alignment. We split the 1.5mJ beam into two arms. One arm is sent through a 250mm BBO crystal and produces  $\sim 20\mu\text{J}$  of 400nm light. A polarizer ensures that this beam is horizontally polarized. The other arm serves as the alignment pulse. The alignment arm is polarization rotated to 45 degrees to the horizontal. This induces a transient birefringence in the gas cell. We observe this transient birefringence by measuring the amount of 400nm light exiting the cell with vertical polarization. In the bottom of figure 1 we show the fractional and full revivals

for an iodine in a gas cell at 385K. By comparing this to cold alignment signals, we see much more structure which we are currently investigating via both experiment and modeling.

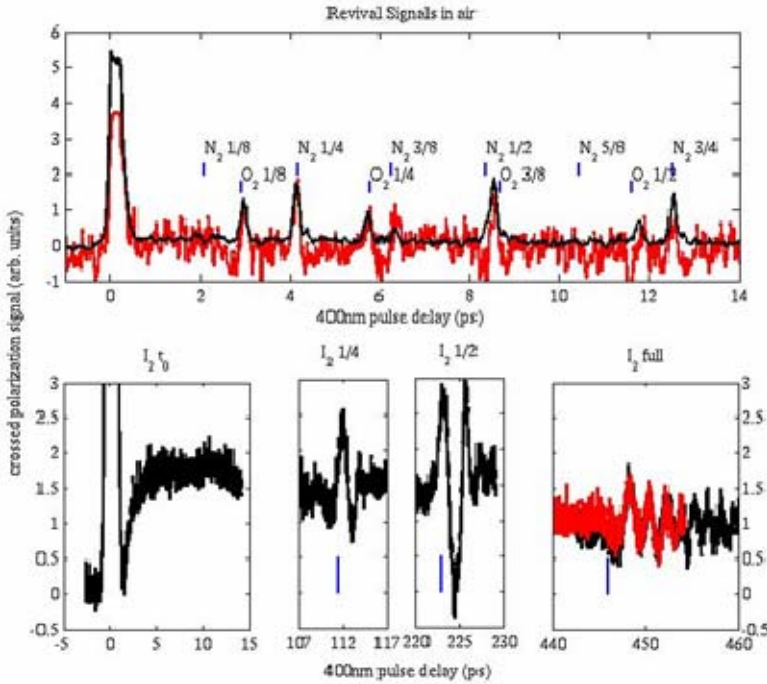


*Figure 1: Transient birefringence of air (top) and I<sub>2</sub> (bottom) following impulsive excitation with 800 nm 40 fs pulses. Note the onset of*

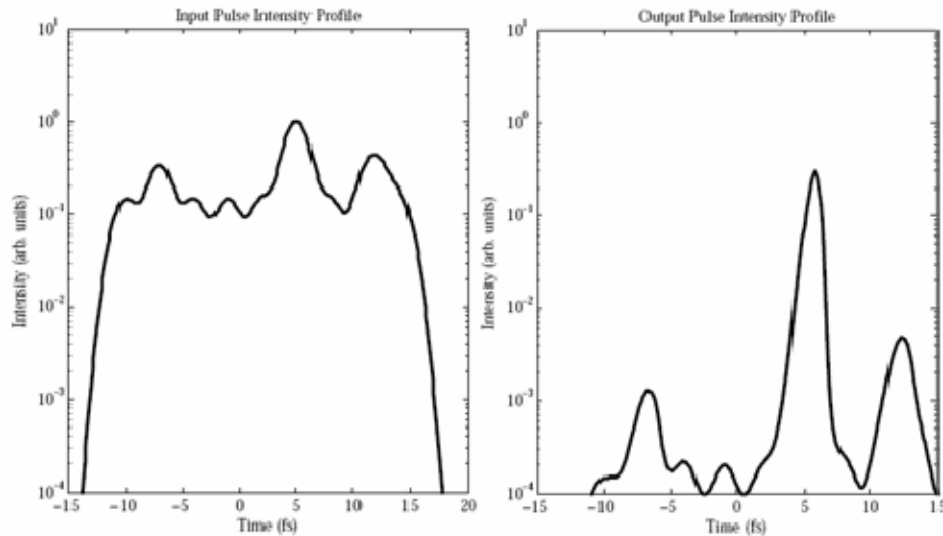
Toward the end of mastering single shot data acquisition and analysis we have the ability to record probe signals on every shot. The experiment is four meters from the laser system and as a result we suffer from laser fluctuations. Such instabilities will be much worse for experiments on the LCLS beam, and so our techniques in this preliminary experiment will acquaint us with the pitfalls of single shot acquisition and analysis. This experiment will also help us to investigate the decoherence mechanisms that might jeopardize the fractional revivals that will be used at the LCLS to produce transiently aligned molecular samples for x-ray studies.

### XFEL Cleaning

*Mike Gownia, Markus Guehr, Hamed Merdji, Ryan N. Coffee and Phil H. Bucksbaum*

We are also making some preliminary calculations that look into the use of either a molecular or atomic species as a saturable absorbing medium for x-ray pulses. Such an absorber could pave the way toward clean, single attosecond x-ray pulses from the rather chaotic "field of grass" micropulses of the xFEL. Figure 2 shows that, for certain parameters, a noisy intensity profile can be cleaned up with only moderate extinction of the primary pulse. Various schemes of balancing Auger-decay rates with edge shifts and absorption crosssections could be conceived to produce trains of regularly spaced

micropulses. By changing the atomic species, one could presumably adjust the delay between the train pulses, in steps fixed by nature of course.



*Pulse cleaning with a saturable absorber. Note the log scale.*

## Future Prospects

Angle Resolved photo-electron Spectroscopy of Aligned Molecules  
*Hamed Merdji, Ryan N. Coffee, and Phil H. Bucksbaum*

We are working in collaboration with the group of Hamed Merdji from Saclay and Ali Belkacem from (LBNL) to perform angle resolved photo-electron spectroscopy to image the electron orbitals of simple molecules. We would use the Berkeley soft xray/vuv pulses in conjunction with optical aligning pulses to make this measurement.

Wavepacket fringe spectroscopy  
*Ryan N. Coffee and Phil H. Bucksbaum*

We plan to investigate molecular wave packet interference using pulses separated in frequency rather than time. Co-polarized signal and idler from an OPA will produce a fringe pattern in a molecular rovibrational wave packet. This fringe will travel at the average velocity of the wave packet, and it will have a fringe spacing that is inversely proportional to  $\Delta\omega = \omega_{signal} - \omega_{idler}$ . The fringe pattern produces a "traveling ruler" that slides along the molecular potential energy surface, providing the added dimension of  $\Delta\omega$  to the techniques of wave packet interferometry. Eventually such novel systems could be extended to LCLS.

## ULTRA-FAST COHERENT IMAGING OF NON-PERIODIC STRUCTURE

PI: Janos Hajdu (1,2)

(1) PULSE Center, SLAC, MS 69, 2575 Sand Hill Road, Menlo Park, CA 94025, U.S.A.

(2) Laboratory of Molecular Biophysics, Department of Cell and Molecular Biology, Uppsala University, Husargatan 3 (Box 596), SE-751 24 Uppsala, Sweden.

Tel:+46-70-4250194, Fax: +46-18-511755

E-mail: janos@xray.bmc.uu.se

### PROGRAM SCOPE

Coherent diffraction imaging overcomes the restrictions of limited-resolution X-ray lenses, offering a means to produce images of general non-crystalline objects at a resolution only limited in principle by the X-ray wavelength and by radiation-induced changes of the sample during exposure. The use of this imaging technique with x-ray pulses from an FEL will allow structures of biological and other materials to be determined at atomic resolution, with ultrafast time resolution and represent a breakthrough for many areas of science. While we are primarily motivated to image biological macromolecules, the general imaging techniques, diagnostic and optics, sample manipulation, and understanding of materials in intense x-ray fields, are of fundamental importance to ultrafast x-ray science and cut across all areas of research of the PULSE Center. We propose to continue development of the high-resolution imaging techniques with emphasis on imaging single cells, and viruses in the first period. We also plan to undertake time-resolved imaging studies of the LCLS-matter interaction, x-ray optics for pulse compression and diagnostics, and LCLS imaging of synchronized laser-aligned particles.

Coherent diffraction imaging is elegant in its experimental simplicity: a coherent x-ray beam illuminates the sample and the far-field diffraction pattern of the object is recorded on an area detector. These measured diffraction intensities are proportional to the modulus squared of the Fourier transform of the wave exiting the object. An inversion of the diffraction pattern to an image in real space requires the retrieval of the phases of the diffraction pattern. This can be achieved by iterative transform algorithms if the object is isolated and the diffraction pattern intensities are adequately sampled (an approach known as oversampling). Our shrinkwrap algorithm is particularly robust and practical. The algorithm reconstructs images ab initio which overcomes the difficulty of requiring knowledge of the high-resolution shape of the diffracting object. This lensless imaging technique can be scaled all the way to atomic resolution, but in practice the resolution of the image of a single object is restricted by x-ray damage to the sample.

With a quasi-continuous synchrotron source it should be possible to image frozen biological cells to a resolution of about 10 nm, and perhaps 1 nm for radiation-tolerant inorganic materials. Ultrashort hard x-ray pulses from LCLS offer a means of vastly increasing the dose that can be applied to a specimen before damage effects the measurement. Simulations based on molecular dynamics and hydrodynamic models indicate that a few Ångström resolution could be achieved in single pulse X-ray diffraction experiments. The success of the technique requires the scattering measurement to be completed before the x-ray ionized protein undergoes a Coulomb explosion.

Achieving the goal of coherent diffractive imaging of a single particle requires extensive technical and theoretical advances. This will be achieved through a combination of simulation and experiments. The experiments will be carried out at synchrotron sources, the currently operational soft-X-ray FEL at DESY called FLASH, and the LCLS as it becomes operational in 2009. The results of the experimental efforts at FLASH will provide guidance for the development of instrumentation at the LCLS, not only for the coherent diffraction imaging experiment but also other experiments where high-resolution structural information is acquired. The theoretical models and simulations of the interaction of particles in intense XFEL beams will be compared and tested with short-pulse coherent imaging, holographic, and scattering experiments at FLASH and eventually the LCLS. This program will be expanded with an experimental investigation of X-ray optical components for XFEL-based

imaging. This will include the determination of optical specifications and the demonstration of prototypes for beam conditioning (focusing and pulse compression) as well as optics for diagnostics. A third component of the project is the development of laser alignment of molecules and particles using intense near-IR lasers which will be done in conjunction with other efforts in the Center.

## **RECENT PROGRESS**

Our major recent achievement is a proof of principle demonstration experiment of flash diffraction imaging with the FLASH soft x-ray free-electron laser at DESY in Hamburg. We continued working at FLASH, and succeeded in testing the single-particle injector system that is designed in Livermore to place single cells and various nanoparticles in the path of the FEL beam, and collected diffraction patterns from which the objects could be reconstructed.

Theoretical studies and simulations predict that with a very short and very intense coherent x-ray pulse a single diffraction pattern may be recorded from a large macromolecule, a virus, or a cell without the need for crystalline periodicity. A three-dimensional data set could be assembled from such patterns when copies of a reproducible sample are exposed to the beam one by one, and destroyed during the process. The over-sampled diffraction pattern permits phase retrieval and hence structure determination. The challenges in carrying out such an experiment are formidable, and engage an interdisciplinary approach drawing upon structural biology, atomic and plasma physics, mathematics, statistics, and x-ray laser physics.

These experiments at DESY represent the first experimental verification of the principle of flash diffraction imaging using the first soft X-ray laser in the world. The results indicate that an interpretable diffraction pattern can be obtained before the sample turns into a plasma as a consequence of an exposure to an intense and very short (10-30 fs) photon pulse. A second exposure shows scattering from a hole that was left behind where the sample used to be during the first exposure. These results provide evidence for the basic principle of flash imaging, showing that one can get an interpretable diffraction pattern before sample explosion. The results have implication for imaging non-periodic molecular structures in biology and in any other area of science and technology where structural information on the nano-scale is valuable.

Initial tests of single-shot imaging of injected nanoparticles have also been successful, using 200 nm sugar-DNA particles, test objects and living cells. In particular, experiments have started on picoplankton deposited on silicon nitride windows. These studies have produced interpretable diffraction patterns from which the image could be reconstructed. We are working on live picoplankton injected into the X-ray pulse at FLASH. This work will continue with the aim at achieving wavelength-limited resolution. Algorithm improvements will also continue.

## **FUTURE PLANS**

### **Expected Progress in FY2008**

We hope to begin incorporating our experience, and our instrument, into the LCLS single-molecule imaging instrument, while continuing our efforts at FLASH following its upgrade.

### **Expected Progress in FY2009**

Our efforts will concentrate on completing, commissioning and performing first experiments on single particles and biomolecules on LCLS.

**COLLABORATIONS:** This work is done with colleagues from Uppsala, LLNL, SLAC, Berlin, and DESY (Hamburg).

## **REFERENCES TO PUBLICATIONS OF DOE SPONSORED RESEARCH THAT HAVE APPEARED IN THE PAST 3 YEARS OR THAT HAVE BEEN ACCEPTED FOR**

## PUBLICATION.

Ziaja, B., London, R.A., Hajdu, J.: Unified model of secondary electron cascades in diamond. *J. Appl. Phys.* 97, 064905 (2005) (9 pages)

A. L. Cavalieri, D. M. Fritz, S. H. Lee, P. H. Bucksbaum, D. A. Reis, D. M. Mills, R. Pahl, J. Rudati, P. H. Fuoss, G. B. Stephenson, D. P. Lowney, A. G. MacPhee, D. Weinstein, R. W. Falcone, R. Pahl, J. Als-Nielsen, C. Blome, R. Ischebeck, H. Schlarb, Th. Tschentscher, J. Schneider, K. Sokolowski-Tinten, H. N. Chapman, R. W. Lee, T. N. Hansen, O. Synnergren, J. Larsson, S. Techert, J. Sheppard, J. S. Wark, M. Bergh, C. Caleman, G. Huldt, D. van der Spoel, N. Timneanu, J. Hajdu, E. Bong, P. Emma, P. Krejcik, J. Arthur, S. Brennan, K. J. Gaffney, A. M. Lindenberg, & J. B. Hastings: Clocking Femtosecond X-Rays. *Phys. Rev. Letts.* 94, Article No. 114801 (2005) (4 pages).

A.M. Lindenberg, J. Larsson, K. Sokolowski-Tinten, K. Gaffney, C. Blome, O. Synnergren, J. Sheppard, C. Caleman, A.G MacPhee, D. Weinstein, D.P. Lowney, T. Allison, T. Matthews, R.W. Falcone, A.L. Cavalieri, D.M. Fritz, S.H. Lee, P.H. Bucksbaum, D.A. Reis, J. Rudati, D.M. Mills, P.H. Fuoss, G.B. Stephenson, C.C. Kao, D.P. Siddons, R. Pahl, J. Als-Nielsen, S. Duesterer, R. Ischebeck, H. Schlarb, H. Shulte-Schrepping, Th. Tschentscher, J. Schneider, O. Hignette, F. Sette, H.N. Chapman, R.W. Lee, T.N. Hansen, S. Techert, J.S. Wark, M. Bergh, G. Huldt, D. van der Spoel, M. Timneanu, J. Hajdu, D. von der Linde, R.A. Akre, E. Bong, P. Emma, P. Krejcik, J. Arthur, S. Brennan, K. Luening & J.B. Hastings1: Atomic-scale visualization of inertial dynamics. *Science*, 308, 392-395 (2005).

K. J. Gaffney, A. M. Lindenberg, J. Larsson, K. Sokolowski-Tinten, C. Blome, O. Synnergren, J. Sheppard, C. Caleman, A. G. MacPhee, D. Weinstein, D. P. Lowney, T. Allison, T. Matthews, R. W. Falcone, A. L. Cavalieri, D. M. Fritz, S. H. Lee, P. H. Bucksbaum, D. A. Reis, J. Rudati, P. H. Fuoss, C. C. Kao, D. P. Siddons, R. Pahl, K. Moffat, J. Als-Nielsen, S. Duesterer, R. Ischebeck, H. Schlarb, H. Schulte-Schrepping, Th. Tschentscher, J. Schneider, D. von der Linde, O. Hignette, F. Sette, H. N. Chapman, R. W. Lee, T. N. Hansen, S. Techert, J. S. Wark, M. Bergh, G. Huldt, D. van der Spoel, N. Timneanu, J. Hajdu, R. A. Akre, E. Bong, P. Krejcik, J. Arthur, S. Brennan, K. Luening, J. B. Hastings: Observation of structural anisotropy and the onset of liquid-like motion during the nonthermal melting of InSb. *Phys. Rev. Letts.* 95, Article No. 125701 (2005).

Larsson, J., Synnergren, O., Hansen, T. N., Sokolowski-Tinten, K., Werin, S., Caleman, C., Hajdu, J., Shepherd, J., Wark, J. S., Lindenberg, A. M., Gaffney, K. J. and Hastings, J. B.: Opportunities and challenges using short-pulse X-ray sources. *Journal of Physics: Conference Series*, 21:87-94 (2005).

Ziaja, B., London, R.A., Hajdu, J.: Ionization by impact electrons in solids: Electron mean free path fitted over a wide energy range. *J. Appl. Phys.* 99, 033514 (2006).

Hajdu, J. Chapman, H.N. Ultrafast coherent diffraction imaging of single particles, clusters and biomolecules. *The European X-ray Free-electron Laser: Technical Design Report*. DESY 2006-097, ISBN 3-935702-17-5 pp. 352-386 (2006).

Chapman, H.N, Barty, A. Bogan, M.J., Boutet, S. Frank, M., Hau-Riege, S.P. Marchesini, S., Woods, B.W., Bajt, S., Benner, W.H., London, R.A., Plönjes, E., Kuhlmann, M., Treusch, R., Düsterer, S., Tschentscher, T., Schneider, J.R., Spiller, E., Möller, T., Bostedt, C., Hoener, M., Shapiro, D.A., Hodgson, K.O., van der Spoel, D., Burmeister, F., Bergh, M., Caleman, C., Huldt, G., Seibert, M.M., Maia, F.R.N.C., Lee, R.W., Szöke,, A. Timneanu, N., Hajdu, J.: Femtosecond diffractive imaging with a soft-X-ray free-electron laser. *Nature Physics* 2, 839-843 (2006).

D. M. Fritz, D. A. Reis, B. Adams, R. A. Akre, J. Arthur, C. Blome, P. H. Bucksbaum, A. L. Cavalieri, S. Engemann, S. Fahy, R. W. Falcone, P. H. Fuoss, K. J. Gaffney, M. J. George, J. Hajdu, M. P. Hertlein, P. B. Hillyard, M. Horn-von Hoegen, M. Kammler, J. Kaspar, R. Kienberger, P. Krejcik, S. H. Lee, A. M. Lindenberg, B. McFarland, D. Meyer, T. Montagne, É. D. Murray, A. J. Nelson, M. Nicoul, R. Pahl, J. Rudati, H. Schlarb, D. P. Siddons, K. Sokolowski-Tinten, Th.

Tschentscher, D. von der Linde, J. B. Hastings: Ultrafast Bond Softening in Bismuth: Mapping a Solid's Interatomic Potential with X-rays. *Science*, 315, 633 - 636 (2007)

Szoke, A., van der Spoel, D., Hajdu, J.: Energy Utilization, Catalysis and Evolution - Emergent Properties of Life. *Current Chemical Biology* 1, 53-57 (2007).

Chalupsky, J., Juha, L., Kuba, J., Cihelka, J., Hájková, V., Bergh, M., Bionta, R. M., Caleman, C., Chapman, H., Hajdu, J., Hau-Riege, S., Jurek, M., Koptyaev, S., Krásá, J., Krenz-Tronnier, A., Krzywinski, J., London, R., Meyer-ter-Vehn, J., Nietubyc, R., Pelka, J. B., Sobierajski, R., Sokolowski-Tinten, K., Stojanovic, N., Tiedtke, K., Toleikis, S., Tschentscher, T., Velyhan, A., Wabnitz, H. and Zastrau, U. Ablation of organic molecular solids by focused soft X-ray free-electron laser radiation. In Proceedings of the 10th International Conference on X-ray Lasers (Eds. Nickles, P.V.; Janulewicz, K.A.), Springer-Verlag, Berlin-Heidelberg-New York 2007, pp. 503-510.

148. J. Chalupsky, L. Juha, J. Cihelka, V. Hájková, S. Koptyaev, J. Krásá, A. Velyhan, J. Kuba, M. Bergh, C. Caleman, and J. Hajdu, R. M. Bionta, H. Chapman, S. Hau-Riege, R. A. London, M. Jurek, J. Krzywinski, R. Nietubyc, J. B. Pelka, R. Sobierajski, J. Meyer-ter-Vehn, A. Krenz-Tronnier, K. Sokolowski-Tinten, N. Stojanovic, K. Tiedtke, S. Toleikis, T. Tschentscher, H. Wabnitz, U. Zastrau: Characteristics of focused soft X-ray free-electron laser beam determined by ablation of organic molecular solids. *Optics Express* 15, 6036-6043 (2007).

P. B. Hillyard, K. J. Gaffney, A. M. Lindenberg, S. Engemann, R. A. Akre, J. Arthur, C. Blome, P. H. Bucksbaum, A. L. Cavalieri, A. Deb, R.W. Falcone, 8 D. M. Fritz, P. H. Fuoss, 9 J. Hajdu, 0 P. Krejcik, J. Larsson, S. H. Lee, D. A. Meyer, A. J. Nelson, R. Pahl, D. A. Reis, J. Rudati, D. P. Siddons, K. Sokolowski-Tinten, D. von der Linde, and J. B. Hastings. Carrier-Density-Dependent Lattice Stability in InSb. *Phys. Rev. Letts.*, Art. No. 125503 (2007).

H.N. Chapman, S.P. Hau-Riege, M. Bogan, S. Bajt, A. Barty, S. Boutet, S. Marchesini, M. Frank, B.W. Woods, W.H. Benner, R.A. London, U. Rohner, A. Szöke, E.A. Spiller, T. Möller, C. Bostedt, D.A. Shapiro, E. Plönjes, M. Kuhlmann, K.O. Hodgson, F. Burmeister, M. Bergh, C. Caleman, G. Huldt, M.M. Seibert, and J. Hajdu. Femtosecond Time-Delay X-ray Holography. *Nature*, in press. Scheduled to appear in the 9 August 2007 issue of *Nature*.

## **Structural Dynamics in Chemical Systems**

Stanford Synchrotron Radiation Laboratory  
Stanford Linear Accelerator Center

### **Principal Investigator**

**Kelly J. Gaffney**, PULSE Center, Photon Science, SLAC,  
Stanford University, Menlo Park, CA 94025  
Telephone: (650) 926-2382  
Fax: (650) 926-4100  
Email: kgaffney@slac.stanford.edu

### **Co-Principal Investigators**

**Michael D. Fayer**, Department of Chemistry, Stanford University, Stanford, CA 94305  
**Britt Hedman**, Stanford Synchrotron Radiation Laboratory, SLAC, Stanford University,  
Menlo Park, CA 94025

**Keith O. Hodgson**, Department of Chemistry and Stanford Synchrotron Radiation  
Laboratory, SLAC, Stanford University, Menlo Park, CA 94025

**I. Program Scope:** The research funded by this grant will focus on understanding the fundamental structural and dynamical properties that influence light harvesting efficiency and solar energy conversion in photo-catalysis. A natural connection exists between ultrafast experimental techniques with sub-picosecond resolution and photochemical reactivity because the initial events in molecular light harvesting invariably occur on the ultrafast time scale. Acquiring a better understanding of the fundamental events that shape photochemical reaction mechanisms will assist in the acquisition of affordable and renewable energy sources.

Developing and utilizing ultrafast x-ray pulses for the study of chemical dynamics represents a core objective of this research program. Our efforts have focused on the Sub-Picosecond Pulse Source (SPPS), a linear accelerator derived femtosecond hard x-ray source at SLAC. With the decommissioning of the SPPS, our efforts turn to preparing for the arrival of the Linac Coherent Light Source (LCLS), an x-ray free electron laser being built at SLAC. These ultrafast x-ray studies will be complemented by ultrafast vibrational and electronic spectroscopic studies of electron transfer dynamics, as well as ground state x-ray absorption and emission studies of electronic structure. These combined efforts will address fundamental questions regarding the interplay of electronic and molecular structure and dynamics in electron transfer complexes.

**II. Infrastructure development:** The past year has seen significant development of the infrastructure necessary for conducting experimental studies of chemical dynamics at the Stanford Synchrotron Radiation Laboratory (SSRL) and the Stanford Linear Accelerator Center (SLAC). SLAC has begun the building of laboratory space for the PULSE Center, a Center for Pulsed Ultrafast Laser Science and Engineering founded by the Department of Energy (DOE) in 2004. The ‘Structural Dynamics in Chemical Systems’ component of the PULSE Center received initial funds at the end of FY05. Completion of the laboratory space construction occurred in Fall 2006, the completion of the laser safety hardware occurred in February 2007, and the laser safety protocol received approval in March of 2007. We have installed the major components for generating independently tunable UV/visible and mid-IR femtosecond laser pulses, and are currently commissioning the system. We expect to be performing experiments this Fall.

**III. Scientific Progress:** The successful achievement of the scientific objectives of the ‘Structural Dynamics in Chemical Systems’ grant requires the development of experimental techniques and tools applicable to a wide range of ultrafast x-ray science. Our prior efforts in ultrafast x-ray science focused on x-ray scattering measurements using the SPPS facility. While these developments have direct significance for the study of chemical dynamics with ultrafast x-ray sources, they have been achieved with systems more relevant to materials science and solid state physics, than chemistry. A primary focus of our research will be the development of ultrafast x-ray spectroscopy for the study of photo-initiated electron transfer chemistry. We have focused on two areas: commissioning a femtosecond laser laboratory and preparing for time resolved x-ray spectroscopy studies.

The LCLS will produce intense femtosecond x-ray pulses with a first harmonic upper energy range of 8 keV, a narrow spectral width of ~20 eV FWHM, and limited frequency tuning capability in the beginning. All of these attributes make x-ray emission spectroscopy (XES), x-ray absorption near edge spectroscopy (XANES), and resonant inelastic x-ray scattering (RIXS) the preferred spectroscopic techniques for the LCLS. These techniques are ideally suited to studying electron transfer in organometallic compounds because they provide easily interpretable information about the oxidation state, spin multiplicity, and the local coordination of the metal centers in these complexes.

**Preparation for chemical dynamics experiments:** Given the completion of the SPPS collaboration, we have reassessed our experimental priorities and chosen to emphasize chemical systems best able to utilize the unique attributes of the femtosecond x-ray pulses emitted by the LCLS. We also will be investigating carrier dynamics in model photovoltaic systems, with an emphasis on laser based experiments. We have also chosen to utilize the time resolved beam lines present at the Advanced Light Source (ALS) and the Advanced Photon Source (APS) as a bridge between the SPPS and the LCLS.

We have decided to focus on mixed valence organometallic complexes for a variety of reasons. Our current understanding of electron transfer reactions has resulted in large part from investigations of mixed valence compounds. Mixed valence organometallic structures also catalyze a wide range of chemical reactions, most prominently in metalloenzymes. Given their prominence and diversity, as well as the compatibility of their x-ray absorption K-edges with the energy range of the LCLS, we have decided to emphasize iron and manganese mixed valence compounds.

We have also initiated studies of photo-induced electron transfer reactions in mixed valence systems. The goal of these studies is to use XES and XANES, and RIXS to investigate the electronic degrees of freedom during a photochemical reaction. Organometallic compounds have sufficiently complex excited state potential energy surfaces that the interpretation of time dependent valence electronic spectra rarely proves conclusive. The time evolution of the spin multiplicity represents one of the critical aspects of metal center photochemistry that can be difficult to extract from valence electronic spectroscopy. XES spectroscopy, provides a powerful and unambiguous probe of a metal atoms spin multiplicity.

This research program will investigate  $\text{RbMnFe}(\text{CN})_6$ , a model photoelectron transfer system for developing time resolved XES spectroscopy.  $\text{RbMnFe}(\text{CN})_6$  undergoes a thermal phase transition from the  $\text{Mn}^{2+}(\text{S}=5/2)\text{-NC-Fe}^{3+}(\text{S}=1/2)$  cubic high temperature (HT) phase to the  $\text{Mn}^{3+}(\text{S}=2)\text{-NC-Fe}^{2+}(\text{S}=0)$  tetragonal low temperature (LT) phase caused by the electron transfer between Mn to Fe and a Jahn-Teller distortion around the  $\text{Mn}^{3+}$  ion. The high temperature phase can also be transiently photo-excited to the high temperature phase well below the phase transition temperature. This photo-induced phase transition has been attributed to a metal-to-metal photoelectron transfer from  $\text{Fe}^{2+}$  to  $\text{Mn}^{3+}$ . We have chosen a solid state photoinduced phase

transition system, rather than a solution phase chemical system, to investigate initially because it will optimize the concentration of excited states and consequently the transient changes in the XES spectrum. At the LCLS, where the laser coincident x-ray flux greatly exceeded that achievable at current synchrotrons, solution phase studies will be possible and we will be able to observe the time evolution of the spin multiplicity of photon induced spin crossover complexes.

We have completed our steady state XES and RIXS measurements of the high and low temperature phases in  $\text{RbMnFe}(\text{CN})_6$ . This detailed characterization of the electronic structure in this compound paves the way for our studies of the photo-induced phase transition, to study the thermal phase transition, and will be initiating optical transient absorption measurements following the construction of our laser laboratory. The equilibrium and photoexcited phases have distinct spectra in the visible and the mid-IR, making these promising measurements that will effectively complement the time resolved x-ray studies. By combining a variety of time resolved techniques and methods, including time resolved powder diffraction, we have the potential to track structural and electronic degrees of freedom, making it possible to investigate their interdependence.

**Carrier dynamics in photovoltaic materials:** We have also initiated studies of carrier dynamics in photovoltaic systems. We have initiated collaborations with Professors Mike McGehee and Yi Cui at Stanford University to study carrier dynamics in organic and nano-structured inorganic semiconductors. While the focus of this research will be ultrafast laser based studies of transport dynamics, we will also be developing ultrafast soft x-ray spectroscopy for the study of excitation dynamics in photovoltaic materials. These studies will use the laser slicing source at the ALS. This ALS x-ray beamline uses the interaction of the electron bunch in the accelerator with an ultrafast laser pulse to slice a 200 fs duration x-ray pulses out of the nominally 70 ps x-ray pulses generated at the ALS. Our initial experiment involves the investigation of exciton dynamics in a  $\text{Cu}_2\text{O}$  semiconductor. We have established a collaboration with Pacific Northwest National Laboratories Environmental Molecular Sciences Institute to grow thin film samples, and we are participating in the beam line commissioning at the ALS. Following these commissioning experiments, we intend to extend our studies to organic photovoltaic, where we intend to characterize the chemical nature of the trap states in amorphous polymers with soft x-ray core hole spectroscopy.

## References:

1. Clocking Femtosecond X-rays: A.L. Cavalieri, *et al.* *Phys. Rev. Lett.* **94**, 114801(2005).
2. Atomic-scale Visualization of Inertial Dynamics: A.M. Lindenberg, *et al.* *Science* **5720**, 392 (2005).
3. Observation of Structural Anisotropy and the Onset of Liquid-like Motion During the Nonthermal melting of InSb: K.J. Gaffney, *et al.*, *Phys. Rev. Lett.* **95**, 125701 (2005).
4. Ultrafast X-ray Science at the Sub-Picosecond Pulse Source: K.J. Gaffney for the SPPS Collaboration, *Synchro. Rad. News* **18**, 32 (2005).
5. Opportunities and Challenges Using Short-Pulse X-ray Sources: J. Larsson, *et al.*, *J. Phys.* **21**, 87 (2005).
6. Ultrafast X-ray Studies of Structural Dynamics at SLAC: K.J. Gaffney, *et al.*, *Proc. SPIE* **5917**, 59170D1 (2005).
7. Ultrafast Dynamics of Laser-Excited Solids: D.A. Reis, K.J. Gaffney, G.H. Gilmer, D. Torralva, *Mat. Res. Soc. Bull.* **31**, 1 (2006).
8. Ultrafast Bond Softening in Bismuth: Mapping a Solid's Interatomic Potential with X-rays: D.M. Fritz, *et al.* *Science* **315**, 633 (2007).
9. Carrier Density Dependent Lattice Stability in InSb: P.B. Hillyard, *et al.* *Phys. Rev. Lett.* **98**, 125501 (2007).
10. Imaging Atomic Structure and Dynamics with Ultrafast X-ray Scattering: K.J. Gaffney, H.N. Chapman, *Science* **316**, 1444 (2007).

*University Research Summaries*  
*(by PI)*



## **PROBING COMPLEXITY USING THE ADVANCED LIGHT SOURCE**

Nora Berrah

Physics Department, Western Michigan University, Kalamazoo, MI 49008

e-mail:nora.berrah@wmich.edu

### **Program Scope**

The objective of our research program is to carry out experiments that will further our understanding of *fundamental interactions between photons and complex systems*. The unifying theme of this program is to probe the frontiers of *complexity* by investigating quantitatively how two classes of systems, anions as well as neutral atoms, molecules and clusters respond to vuv-x-ray radiation. Our studies include investigation of multi-electron interactions and of energy transfer processes within gas-phase systems which will advance our understanding of the general many-body problem. Furthermore, most of our work is carried out in a strong partnership with theorists.

We presently are using photons from the Advanced Light Source (ALS) but will also use in 2009 the linac coherent light source (LCLS), the first x-ray ultrafast free electron laser (FEL) facility. In addition, we have carried out this year preliminary cluster-based collaborative experiments at the ultrafast vuv FEL facility in Hamburg (FLASH), Germany.

We have added to our experimental detection systems a momentum imaging apparatus that is also used for coincidence experiments. In addition, a movable ion-photon beamline (MIPB) will be commissioned in December this year for photodetachment/photoionization of ions. It will be used in the collinear geometry in tandem with any photon beamlines at the Advanced Light Source or elsewhere. We present here results completed and in progress this past year and plans for the immediate future.

### **Recent Progress**

#### **1) Photo Double Detachment of CN<sup>-</sup>: Electronic Decay from an Inner-Valence Hole in Molecular Anions (Pub. [1])**

The first experimental and theoretical inner-valence photodetachment studies from a molecular negative ion, CN<sup>-</sup>, have been carried out around the 2-electron threshold (25–90 eV). The work is motivated by a phenomenon, similar to interatomic Coulombic decay (ICD), predicted by Santra et al. [a] to occur in molecular anions, but not generally in neutral or cationic targets. Specifically, theoretical work [a] predicted that the removal of one inner-valence electron from CN<sup>-</sup>, giving rise to inner valence excited CN, can result in the formation of vibrationally bound CN<sup>+</sup> through a relaxation mechanism that occurs via electron emission, effectively leading to double detachment. In the case of CN<sup>-</sup>, the majority of the singly detached 3σ states are located above the CN<sup>+</sup> continuum threshold, and can thus decay by electron emission. This mechanism is usually ruled out for small neutral molecules because insufficient internal energy is available for electron emission, but is predicted to be generally accessible for molecular anions. CN<sup>+</sup> is produced by the removal of two electrons either simultaneously or sequentially through an inner-valence mediated process, while the weaker C<sup>+</sup> and N<sup>+</sup> signals, which we also measure, are produced by dissociation of the excited molecule. The cross sections for all the products exhibit a similar shape [1]. In order to have detailed information about the onset of the photo-double-detachment process, we measured with improved statistics the molecular photodetachment and dissociation

channels near the  $\text{CN}^-$  double-detachment threshold. We observed a ‘knee’ in the cross section as a function of photon energy, consistent with the theoretical predictions [a,1]. This work demonstrates the inner-valence mediated production of  $\text{CN}^+$ , as predicted [a]. The present result is the first experimental demonstration of this effect in anions [1]. This electron emission relaxation mechanism is forbidden in isoelectronic neutral molecules ( $\text{CO}$  and  $\text{N}_2$ ) because their inner valence regions lie below the double ionization channels.

## 2) Size Effects in Angle-Resolved Photoelectron Spectroscopy of Free Rare-Gas Clusters (Pub. [2])

Cluster research continues to be an exciting area of science as most cluster properties remain much less known than those of their constituent atoms and molecules. Moreover, the scalability of clusters allows interpolation between the individual atom, the surface, and the bulk, bridging the gap between single atoms or molecules and condensed matter systems. Of particular interest are phenomena exhibiting cluster size dependence that underline the transition from individual atoms and molecules to large cluster systems with typical solid-state behavior, such as changes in cluster geometry and electronic structure. Cluster-size-dependent electronic properties can be probed directly using angle-resolved photoelectron spectroscopy although there is a paucity of angle-resolved measurements, mainly due to low target densities in the cluster beam and the resulting low signal intensities. To date, measurements of the photoelectron angular distribution parameter are only available for small metal clusters. For rare-gas clusters, recent qualitative studies by Öhrwall et al. [b] have shown differences in the angular dependence of the photoelectron intensity from Xe clusters compared to free Xe atoms, but their experiment did not provide absolute measurements of the angular distribution parameter as a function of photon energy.

We have carried out the first quantitative measurement of the photoelectron angular distribution parameter as a function of photon energy and cluster size for any rare-gas cluster system. Our experimental results are supported by multiple scattering calculations, which elucidate the effect of elastic electron scattering on the photoelectron. For the present experiment, xenon clusters with average sizes  $\langle N \rangle$  between 60 and 8000 atoms were produced. Photoelectrons were detected simultaneously in two electron TOF analyzers situated in the plane perpendicular to the light propagation direction at the “magic angle” ( $54.7^\circ$ ) and at  $0^\circ$  with respect to the light polarization [c]. Simultaneous measurement at both angles is crucial for a quantitative determination of the photoelectron angular distribution parameter as it is independent of temperature and density fluctuations of the cluster beam.

The cluster size dependence of the angular distribution parameter for Xe  $4d$  surface and bulk photoelectrons was measured at a photon energy  $h\nu=150$  eV, where the angular anisotropy  $\beta$  is highest. A significant decrease of the angular distribution parameter of the bulk component was observed for average cluster sizes larger than  $\langle N \rangle = 1000$ , while the angular distribution of the surface component is only slightly smaller than the atomic value and stays constant within the range of the experimental error. This effect is attributed to elastic scattering of the photoelectrons by neighboring atoms in the cluster, leading to more isotropic angular distributions for electrons from the interior of the cluster than for those from the surface or a free atom. In order to investigate the role of electron scattering in more detail, we have performed multiple scattering (MS) model calculations and compared them to our experimental data. Our model calculations reproduced the experimentally observed trends [2] and confirm that the increased isotropy of the

cluster photoelectrons can be attributed to elastic scattering of the ejected electrons by the neighboring atoms in the cluster.

### **3) Studies of Molecular Fragmentation with Velocity Map Ion Imaging and Coincidence Techniques (Pub. 3 & 4)**

We have recently developed a velocity map imaging (VMI) spectrometer [3,4] to be used also in coincidence studies of molecular and cluster fragmentation. The interaction region is defined by the crossing of the target of interest with the photons. An electric field of  $\approx 300$  V/cm is applied to the interaction region to extract fragment ions and electrons perpendicularly to the direction of the incident photon beam. The extraction field provides a full  $4\pi$  collection efficiency for slow electrons and ions ( $E_{kin} < 10$  eV). For  $4\pi$  detection of fragment ions with higher kinetic energies, the applied extraction potential has to be increased, which reduces the energy resolution. When using the VMI spectrometer in ion imaging mode, the detection of an electron by the opposite microchannel plate (MCP) detector provides a start pulse for a time-to-digital converter (TDC), thus allowing a timing operation of the spectrometer even in the typical multi-bunch mode of most storage rings. As the electron count rate is higher than the ion count rate, it is delayed and used as a stop rather than a start, thereby reducing the collection dead time. The four-lens system of our spectrometer is designed to improve the collection properties and to ensure space-focusing conditions for fragment ions emitted from different initial points within the interaction region. Ion trajectory simulations using the SIMION software show that ions of the same energy emitted within  $\pm 5$  mm from the center of the interaction region can be focused into a spot of  $< 3$  mm diameter on the anode. The anode is equipped with a multi-hit capable position-sensitive delay-line detector [d], thus providing the hit positions and times of flight of all ions originating from the same dissociation event. Experiments in CO<sub>2</sub>, OCS and N<sub>2</sub>O are presently being analyzed.

### **Future Plans.**

The principal areas of investigation planned for the coming year are to: 1) Continue the analysis of the spin and angle-resolved photoelectron and ion imaging fragmentation studies of van der Waals clusters. 2) Carry out photodetachment experiments in the carbon anions cluster chain using the MIPB. 3) Continue our collaborative efforts with the Technical University cluster group (Moeller et al.) at the FLASH facility.

### **References**

- [a] R. Santra, J. Zobeley, L.S. Cederbaum, Chem. Phys. Lett. **324**, 416 (2000).
- [b] G. Öhrwall *et al.*, J. Phys. B **36**, 3937 (2003).
- [c] N. Berrah, *et al.* J. Electr. Spectr. and relat. Phenom., **101**, 1, (1999).
- [d] O. Jagutzki, *et al.*, IEEE Trans. Nucl. Sci. **49**, 2477 (2002).

### **Publications from DOE Sponsored Research.**

1. R. C. Bilodeau, C. W. Walter, I. Dumitriu, N. D. Gibson, G. D. Ackerman, J. D. Bozek, B. S. Rude, R. Santra, L. S. Cederbaum, and N. Berrah "Photo Double Detachment of CN<sup>-</sup>: Electronic Decay of an Inner-Valence Hole in Molecular Anions, Chem. Phys. Lett. **426**, 237(2006)
2. D. Rolles, H. Zhang, A. Wills, R. Bilodeau, E. Kukk B. Rude, G. Ackerman, J. Bozek and N. Berrah "Size effects in Van der Waals clusters using angle resolved photoelectron spectroscopy, Phys. Rev. A, Rap Com. **75**, 032101(R) (2007).

3. D. Rolles , Z. D. Pešić, M. Perri, R. Bilodeau, G. Ackerman, B. Rude, D. Kilcoyne, J. D. Bozek, and N. Berrah "A velocity map imaging spectrometer for electron-ion and ion-ion coincidence experiments with synchrotron radiation, (in Press, Nuclear Instrument and Method)
4. Z. D. Pešić, D. Rolles, M. Perri, R. C. Bilodeau, G. D. Ackerman, B. S. Rude, A. L. D. Kilcoyne, J. D. Bozek, and N. Berrah, "Studies of Molecular Fragmentation using Velocity Map Imaging Spectrometer and Synchrotron Radiation", *J. Elect. Spec. and Rela. Phen.*, **155**, 155 (2007)
5. D. Cubaynes, H-L Zhou, N. Berrah, J-M. Bizau, J. D. Bozek, S. Canton, S. Diehl, X-Y Han, A. Hibbert, E. T. Kennedy, S. T. Manson, L. VoKy,F. Wuilleumier, "Dynamical and relativistics effects in experimental and theoretical studies of innershell photoionization of sodium", *J Phys B* **40**, F121, (2007).
6. R. C. Bilodeau, J. D. Bozek, A. Agular, G. D. Ackerman, and N. Berrah, "Photodetachment of He<sup>-</sup> near the 1s threshold: Absolute cross section measurements and post-collision interactions" *Phys. Rev. A* **73**, 034701 (2006).
7. X. Feng, A. A. Wills, E. Sokell, M. Wiedenhoeft, and N. Berrah, "Study of Auger decay in core-excited HBr by angle-resolved two-dimensional photoelectron spectroscopy" *Phys. Rev. A* **73**, 012716 (2006).
8. C. W. Walter, N.D. Gibson, R.C. Bilodeau, N. Berrah, J.D. Bozek, G.D. Ackerman, and A. Aguilar, "Shape Resonance in K-Shell Photodetachment from C", *Phys. Rev. A* **73**, 062702 (2006)
9. N. Berrah, R. C. Bilodeau, J.D. Bozek, C.W. Walter, N.D. Gibson, and G.D. Ackerman, "Double Auger decay, and shape resonances in negative ions" *Radiat. Phys. Chem.* **75**, 1447 (2006).
10. R. C. Bilodeau, J. D. Bozek, G. D. Ackerman, N. D. Gibson, C. W. Walter, A. Aguilar, G. Turri. I. Dumitriu and N. Berrah "Multi-Auger Decay in Negative Ion Photodetachment" (AIP, in press).
11. N. Berrah, "Women in Sciences and their Role to Advance the Societies from the South", "Advanced Scientific Workshops: "Méditerranée, le partage du savoir" Sciences; Revue de l'association française pour l'avancement des sciences, AFAS, **2006-2/3**, 26 (2006)
12. R. C. Bilodeau, J. D. Bozek, G. D. Ackerman, N. D. Gibson, C. W. Walter, A. Aguilar, G. Turri, I. Dumitriu and N. Berrah "High-charge-state formation following inner-shell photodetachment from S<sup>-</sup>" *Phys. Rev. A* **72**, 050701(R), (2005).
13. E. Sokell, A A Wills, M Wiedenhoeft, X Feng, S E Canton, D Rolles and N Berrah "An alternative explanation for the spectral hole attributed to continuum-continuum interference in HCl" *J. Phys. B* **38**, 1535 (2005).
14. B. Lohmann, B. Langer, G. Snell, U. Kleiman , S. Canton, A. Martins, , U. Becker and N. Berrah, "CI-Induced Spin Polarization of the Ar\* (2p<sup>-1</sup> 4s)<sub>j=1</sub> Resonant Auger decay ", *Phys. Rev. A* **71**, R020701 (2005).
15. B. Lohmann, B. Langer, G. Snell, U. Kleiman , S. Canton, A. Martins, , U. Becker and N. Berrah, "Configuration-interaction-induced dynamic spin polarization of the Ar\* (2p<sup>-1</sup><sub>1/2,3/2</sub> 4s<sub>1/2</sub>)<sub>j=1</sub> resonant Auger decay", *Phys. Rev. A* **71**, 039907 (2005).
16. J. Nikkinen, H. Aksela, S. Heinasmaki, E. Kukk, N. Berrah and S. Aksela, "Strong electron correlation in Ca 2p, Sr 3d and Ba 4d core hole states investigated by means of photoelectron spectroscopy and MCDF calculations", *Physica Scripta. Vol. T115*, 119–121, (2005).
17. J. Nikkinen, H. Aksela, S. Fritzsché, S. Heinasmaki, R. Sankari, E. Kukk, N. Berrah and S. Aksela, "Photoionization and Auger decay of the 3d vacancy state of atomic strontium: Electron-electron correlations" *Phys. Rev. A* **72**, 042706 (2005).
18. X. Feng, A. A. Wills, T. Goreczyc, M. Wiedenhoeft, E. Sokell, and N. Berrah " Photoelectron recapture investigation in Ar using two-dimensional photoelectron spectra" *Phys. Rev. A* **72**, 042712 (2005).
19. N. Berrah, R. C. Bilodeau, J. D. Bozek, G. Turri and G.D. Ackerman, "Double photodetachment in He<sup>-</sup>: Feshbach and triply excited resonances", *J. Elect. Spec. and Relat. Phen.* **144-147**,19 (2005).]
20. R. C. Bilodeau, J. D. Bozek, N. D. Gibson, C. W. Walter, G. D. Ackerman, I. Dumitriu, and N. Berrah, "Inner-shell Photodetachment Thresholds: Unexpected Long-range Validity of the Wigner Law", *Phys. Rev. Lett.* **95**, 083001 (2005).
21. S. E. Canton, E. Kukk, J. D. Bozek, D. Cubaynes, and N. Berrah "Imaging Wavepacket Interferences using Auger Resonant Raman Spectroscopy", *Chem. Phys. Lett.* **402**, 143, (2005).

## Bose and Fermi Gases with Strong Anisotropic Interactions

### Principal Investigator

John Bohn  
JILA, UCB 440  
University of Colorado  
Boulder, CO 80309  
Phone (303) 492-5426  
Email [bohn@murphy.colorado.edu](mailto:bohn@murphy.colorado.edu)

### Program Scope

This program pursues the theoretical study of ultracold, dilute, quantum degenerate matter, with a focus on the interplay of energy between different degrees of freedom. One aspect of this work centers on mixtures of bosonic and fermionic atoms, whose interspecies interaction can be tuned by a magnetic field. Here we are concerned with energy and population flow between atomic and molecular states of the many-body system. In a second area, we have considered the properties of Bose-Einstein condensates (BEC's) composed of dipolar particles. Here we study the balance of energy between translational and orientational degrees of freedom. Dipoles are also amenable to control by external fields. In the broad view, this work is a prerequisite for the precise control over atoms and molecules in an ultracold environment.

### Recent Progress

#### A. Bose-Fermi mixtures

The ability to tune interparticle interactions between atoms, via magnetic-field Feshbach resonances, has greatly enriched the phenomena available in ultracold quantum degenerate gases. For bosons, this has meant coherent atom-molecule oscillations and the rigged collapse of Bose-Einstein condensates. For fermions, it has allowed the study of the “crossover” regime between Cooper pairs of atoms on one side, and Bose-condensed molecules on the other. Now, experiments are also turning to mixtures of bosons and fermions, where the interaction can be tuned between the two.

The standard many-body theory of such systems posits a separate quantum field that keeps track of pairs of atoms. For dealing with pairs of bosons or pairs of fermions, this theory is reasonable, indeed often quantitative, at the mean-field level. We have found, however, that this is not the case for the boson-fermion mixture [P1]. We showed that the mean-field version of the theory is unable to reproduce the molecular binding energy in the limit where the density of the gas is low. We further traced this difficulty to the way in which the theory treats three-body correlation functions, showing that to correctly reproduce the two-body binding energy requires a careful treatment of the noncondensed bosons.

We have therefore also approached this problem from another direction. In the perturbative, low density limit, we can evaluate the scattering T-matrix. If there were only one fermion and one boson present, the poles of this T-matrix would accurately identify both the true molecular binding energy, and the positions and widths of

scattering resonances. The poles shift, however, in the many-body environment, in a way we can track perturbatively [P2]. A main result of this analysis is that the energetics and stability of the fermionic pairs in the gas depend strongly of the center-of-mass momentum of the pair.

### B. Dipolar Condensates

It was at first uncertain whether the mean-field, Gross-Pitaevski (GP) approach was a good approximation for gases in which the constituent molecules could exert significant forces on one another from across the gas. Consider that molecules with 1 Debye dipole moments contribute a 10 nK dipole-dipole interaction energy from a distance of 1  $\mu\text{m}$ . These length and energy scales are typical for atomic BEC's, and suggest that electric dipoles can supply a significant, perhaps dominant, contribution to the energy balance of the condensate. For this reason, we tested the GP equation against accurate diffusion quantum Monte Carlo simulations of our collaborator, Doerte Blume of Washington State University [P3]. The result showed, for the first time, that the GP treatment is indeed adequate to describe a dilute gas of condensed dipoles. In the cases studied, the energies, sizes, and aspect ratios of the gas were reproduced by the GP approximation. This work also illuminated the necessity to handle the two-body interaction correctly. Using the bare dipole-dipole interaction as the pseudopotential in the GP equation had already been discussed, as well as the variation of two-body scattering length with dipole moment. However, we completed the argument, by illustrating explicitly the pattern of alternating regions of stable and unstable gases as the dipole moment is varied [P4]. This is perhaps not immediately relevant to Cr BEC, where the dipole moment is small. However, it is of vital importance to recognize that a molecular BEC may be unstable for various values of its dipole moment, hence at various applied electric fields. This knowledge will be useful in future experiments that strive to make such condensates. Further refinement of this work, along with Doerte Blume, proved the utility of an anisotropic zero-range potential for reproducing energetics in systems containing dipoles [P5].

Armed with the knowledge that the GP equation works, we further studied properties of dipolar BEC. This led us again to assess and better understand a stability issue. For a gas with the dipoles aligned along the laboratory  $z$ -axis, it is energetically favorable for the gas to elongate in the  $z$ -direction. Ultimately, the increased interparticle attraction in this elongated gas leads to a mechanical instability, much like the macroscopic collapse of atomic condensates with attractive interactions. However, making the trap oblate – thereby pushing the gas back toward a pancake shape – might be expected to overcome this trend, and perhaps completely stabilize the gas.

This situation had been hinted at, but there was still much confusion in the literature. We therefore made a systematic study of gas stability versus particle number and trap aspect ratio, as shown in the figure below (left panel) [P6]. In brief, the more oblate the trap is, the more dipoles are required to lead it to instability. In the figure we have assumed that the two-body scattering length  $a=0$ . In unpublished work we have found that the same general considerations follow for nonzero  $a$ .

In calculating this result, we discovered an unusual and hitherto unexpected feature of dipolar gases. Namely, for certain regions of aspect ratio, the condensate does not have its peak density in the center. Rather, an iso-density plot (figure, right panel)

reveals a bi-concave shape, which we colloquially refer to as a “red blood cell”. This is not an artifact of numerics; it is seen identically in three-dimensional calculations on a Cartesian grid, as well as in cylindrical coordinates. It is also consistent with a variational trial wave function that allows for such a density minimum. It appears to be a new way in which the dipoles can distribute their energy, effectively by crowding to the “surface,” just as free charges in a conductor do. This shape is also tied to roton-like physics in the gas, as explained below.

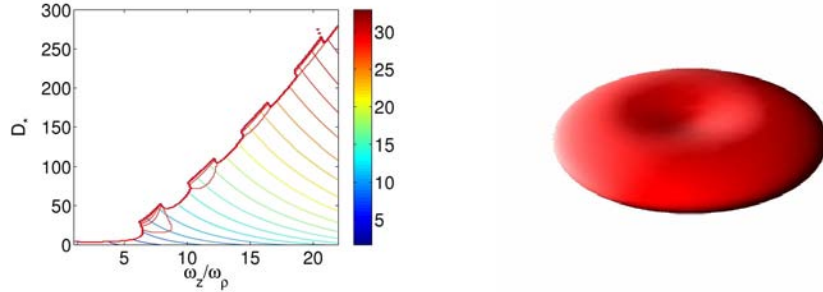


**Figure.** (Left) Stability diagram for dipolar condensates in an oblate trap with aspect ratio  $\omega_z/\omega_p$ . On the vertical axis is a normalized parameter proportional to the number of dipoles and to the square of the dipole moment. Below the red line the condensate is stable, above it is unstable. Iso-energy contours are also shown. (Right) A “red blood cell” (RBC) condensate, which occurs in small islands of parameter space in the left-hand figure. (From [P6]).

Collective excitations of the gas are also important. Prior to our work, these had been understood either by solving the time dependence of parameters in a variational trial wave function, or else by direct numerical solution of the perturbed time-dependent GP equation. Our group has, for the first time, successfully solved the Bogoliubov-deGennes equations for excited states of a dipolar condensate, yielding the entire low-lying spectrum for states of arbitrary symmetry. This is a difficult problem, due to the fact that the interaction potential is nonlocal and long-ranged. Nevertheless, we found a fast and stable algorithm, which exploits the Hankel transform in cylindrical coordinates; this method is detailed in [P7]. Using this algorithm, we explored breathing and quadrupole modes as a function of trap geometry, and made an assessment of the condensate depletion.

Further, we brought this new calculation to bear on the issue of condensates in oblate traps. Specifically, we tracked the excitation frequencies as a function of the number of dipoles. At the point where the GP equation no longer finds a stable ground state, one of the excitation frequencies drops abruptly to zero. This is interpreted as the gas becoming unstable against perturbations that have the symmetry of the excited state that is going soft. In the case of an “ordinary” condensate, i.e., one whose maximum density resides at the center, the soft mode has  $m=0$  rotational symmetry around the axis, and corresponds to instability via a radial mode. By contrast, for an RBC condensate, the soft mode has angular momentum  $m \neq 0$ , corresponding to an angular instability. An analogous soft mode has been ascribed to roton-like behavior of the gas in the two-dimensional limit where the molecules are untrapped and free to move in the plane

perpendicular to their polarization. Our results thus represent the discrete analogs of these rotons in a finite trap that confines the gas in all dimensions.

### Future Plans

The first funding cycle of this grant was a “building-up” period for the group. We learned how to calculate ground states of dipolar BEC’s, with confidence that we trust the GP equation and that we understand the role of the two-body interaction; we developed the in-house technology to compute excited states of these condensates; and we began to use these tools to uncover novel, nontrivial behavior of dipolar gases. And on the side, we were able to bring to bear our experience in two-body physics of dipolar interactions. We are now poised to take advantage of these tools to further pursue properties of these gases. We intend to pay close attention to both magnetic dipole interactions between atoms and electric dipole interactions between polar molecules. In general the former are “weak” and the latter are “strong,” hence would be expected to generate more impressive many-body physics. However, with the very recent achievement in Stuttgart of chromium BEC with *s*-wave interactions tunable by a Feshbach resonance, even this system is on the verge of becoming strongly interacting. Aspects of dipolar condensates to be studied in the future include vortices, finite temperature effects, and the influence of the internal structure of the dipoles.

### DOE-supported publications in the past three years

[P1] *Bose-Fermi Mixtures Near an Interspecies Feshbach Resonance: Testing a Nonequilibrium Approach* -- D. C. E. Bortolotti, A. V. Avdeenkov, C. Ticknor, and J. L. Bohn, *J. Phys. B* **39**, 189 (2006).

[P2] *Stability of Fermionic Feshbach Molecules in a Bose-Fermi Mixture* -- A. V. Avdeenkov, D. C. E. Bortolotti, and J. L. Bohn, *Phys. Rev. A* **74**, 012709 (2006).

[P3] *Scattering Length Instability in Dipolar Bose Gases* -- D. C. E. Bortolotti, S. Ronen, J. L. Bohn, and D. Blume, *Phys. Rev. Lett.* **97**, 160402 (2006).

[P4] *Dipolar Bose-Einstein Condensates with Dipole-Dependent Scattering Length* -- S. Ronen, D. C. E. Bortolotti, D. Blume, and J. L. Bohn, *Phys. Rev. A* **74**, 033611 (2006).

[P5] *Pseudo-potential Treatment of Two Aligned Dipoles Under External Harmonic Confinement* -- K. Kanjilal, J. L. Bohn, and D. Blume, *Phys. Rev. A* **75**, 052705 (2007).

[P6] *Radial and Angular Rotons in Trapped Dipolar Gases* -- S. Ronen, D. C. E. Bortolotti, and J. L. Bohn, *Phys. Rev. Lett.* **98**, 030406 (2007).

[P7] *Bogoliubov modes of a dipolar condensate in a cylindrical trap* -- S. Ronen, D. C. E. Bortolotti, and J. L. Bohn, *Phys. Rev. A* **74**, 013623 (2006).

# Exploiting Universality in Atoms with Large Scattering Lengths

Eric Braaten

## Contact info

Physics Department  
Ohio State University  
191 W Woodruff Ave  
Columbus OH 43210-1117  
(braaten@mps.ohio-state.edu)

## Program scope

Atoms whose scattering lengths are large compared to the range set by their interactions exhibit universal behavior at sufficiently low energies. Recent dramatic advances in cooling atoms and in manipulating their scattering lengths have made this phenomenon of practical importance for controlling ultracold atoms and molecules. This research project is aimed at developing a systematically improvable method for calculating few-body observables for atoms with large scattering lengths starting from the universal results as a first approximation. The ultimate goal is to be able to predict and control the behavior of ultracold atoms and molecules near a Feshbach resonance.

## Recent Progress

Hans-Werner Hammer and I completed a comprehensive review article (132 pages) entitled *Universality in Few-body Systems with Large Scattering Length* [1]. It provides an introduction to the concept of universality for non-relativistic particles with large scattering length, summarizes the universal results that had been obtained to date, and lays the groundwork for further progress in this direction. We also wrote an abbreviated version of this review (44 pages) entitled *Efimov Physics in Cold Atoms* [4]. It focuses on the applications to identical bosonic atoms and is intended to be more accessible to experimentalists.

I was the coorganizer of a workshop at the Institute for Nuclear Theory in Seattle in August 2005. At the workshop, I met Rudi Grimm and I communicated to him the results on Efimov states obtained by Hammer and me. Grimm's group at Innsbruck used these results in the analysis of their data on 3-body recombination in cold  $^{133}\text{Cs}$  atoms that led to their announcement in March 2006 of the first experimental evidence for Efimov states [T. Kraemer et al., *Nature* 440, 315-318 (2006)].

In collaboration with a graduate student Dongqing Zhang, I developed a new factorization approximation for the break-up and recombination rates for loosely-bound molecules composed of atoms with a large scattering length  $a$  in processes with large collision energy  $E \gg \hbar^2/ma^2$  [2]. The leading contributions to their rates can be separated into short-distance factors that are insensitive to  $a$  and long-distance factors that are insensitive to  $E$ . The short-distance factors are atom-atom cross sections at a lower collision energy. In simple cases, the long-distance factors simply count the number of atoms in the molecule. An example is an analytic formula for the 3-body recombination rate constant at a collision energy in the range  $\hbar^2/ma^2 \ll E \ll \hbar^2/mr_s^2$ , where  $r_s$  is the effective range:

$$K_3(E) = \frac{12288\sqrt{3}\pi^2\hbar^5}{3m^3E^2}.$$

Dongqing Zhang and I have developed a method for using few-body calculations to determine parameters that govern the phenomenon of atom-molecule coherence in Bose-Einstein condensates of atoms with large scattering length [6]. The method is based on the one-particle-irreducible effective action formalism for quantum field theory. Unlike previous approaches to this problem, this new approach does not require a microscopic model with an explicit molecular field. It can be applied equally easily to models in which the shallow dimer is generated dynamically. This method can be extended rather straightforwardly from dimers to Efimov trimers. It can therefore be used to determine parameters that govern the coherent flow of atoms between Bose-Einstein condensates consisting of atoms, dimers, and Efimov trimers.

In previous work that is summarized in Ref. [1], my collaborators and I have provided simple analytic expressions with numerical coefficients for all the most dramatic universal features associated with Efimov physics at zero temperature. In order to facilitate the comparison with experiment, we have launched a project to calculate the dependence of all these universal features

on the temperature  $T$ . This requires calculating 3-body rates as functions of kinematic variables such as the collision energy and averaging them over thermal distributions. We have already calculated the  $T$ -dependence of the atom-dimer relaxation rate [3]. We have also calculated the  $T$ -dependence of the 3-body recombination rate for  $^{133}\text{Cs}$  atoms approximately by applying Efimov scaling to previously published results for  $^4\text{He}$  atoms [5]. The  $^4\text{He}$  results were obtained by Suno, Esry, Greene, and Burke using accurate numerical solutions of the Schrödinger equation.

### Future Plans

Hammer and I plan to continue our project to calculate the dependence of Efimov features on the temperature  $T$ . The next step is to calculate the 3-body recombination rate for large positive  $a$  as a function of the collision energy  $E$ . This will give the extension to nonzero  $E$  of the universal result for the 3-body recombination rate at threshold derived by Petrov and by Gasaneo, Macek, and Ovchinnikov:

$$K_3(0) = \frac{768\pi^2(4\pi - 3\sqrt{3})\hbar a^4/m}{\sinh^2(\pi s_0) + \cosh^2(\pi s_0) \cot^2[s_0 \ln(a\kappa_*) + 1.16]},$$

where  $s_0 = 1.00624$  and  $\kappa_*$  is a 3-body parameter. After calculating the thermal average, the results will be compared with measurements by the Innsbruck group. They will soon have new measurements of the 3-body recombination rate in  $^{133}\text{Cs}$  atoms at a much lower temperature than their previous measurements. The final step in the project will be to calculate the 3-body elastic scattering rate for large negative  $a$  as a function of the collision energy. By using analytic continuation to introduce a 3-body inelasticity parameter  $\eta_*$ , the 3-atom inelastic collision rate will then be calculated as a function of  $T$ . The results will be compared with measurements by the Innsbruck group of the 3-body inelastic collision rate in  $^{133}\text{Cs}$  atoms. We will also compare our universal results to previous work by Jonsell and by Frederico et al., who used the adiabatic hyperspherical approximation and an ad hoc resonance approximation, respectively.

Our universal results for the Efimov features that are summarized in Ref. [1] were calculated at zero temperature and also in the zero-range limit. In addition to extending those results to nonzero temperature, we also want to calculate the leading corrections associated with the nonzero effective range in order to allow more accurate comparisons with experiment. Our

highest priority is to calculate the range corrections to the positions of the Efimov features at zero temperature. In the zero-range limit, the sequence of scattering lengths at which successive zeros or resonant peaks occur form a geometric sequence with a discrete scaling factor of approximately 22.7. Given a measurement of the scattering length for one Efimov feature, universality gives predictions for the positions of all the other Efimov features. The leading deviations from the geometric sequence are determined by the ratio  $r_s/a$  of the effective range to the scattering length. Once we have calculated the range corrections, experimentalists will be able to use our results to predict the positions of other Efimov features with much higher accuracy.

## Recent publications

1. *Universality in Few-body Systems with Large Scattering Length*, Eric Braaten and H.-W. Hammer, Physics Reports **428**, 259 (2006) [arXiv:cond-mat/0410417]
2. *Factorization in Break-up and Recombination Processes for Atoms with a Large Scattering Length*, E. Braaten and D. Zhang, Physical Review A **73**, 042707 (2006) [arXiv:cond-mat/0501510].
3. *Resonant dimer relaxation in cold atoms with a large scattering length*, E. Braaten and H.-W. Hammer, Phys. Rev. A **75**, 052710 (2007) [arXiv:cond-mat/0610116].
4. *Efimov Physics in Cold Atoms*, E. Braaten and H.-W. Hammer, Annals of Physics **322**, 120-163 (2007) [arXiv:cond-mat/0612123].
5. *Universality Constraints on Three-Body Recombination for Cold Atoms: from  ${}^4He$  to  ${}^{133}Cs$* , E. Braaten, D. Kang, L. Platter, Phys. Rev. A **75**, 052714 (2007) [arXiv:cond-mat/0612601].
6. *Condensates of Strongly-interacting Atoms and Dynamically Generated Dimers*, E. Braaten and D. Zhang, Phys. Rev. A **75**, 063624 (2007) [arXiv:cond-mat/0703308].
7. *Scattering Models for Cold Atoms*, E. Braaten, M. Kusunoki, and D. Zhang, to appear in Annals of Physics.

## Atomic and Molecular Physics in Strong Fields

Shih-I Chu

Department of Chemistry, University of Kansas

Lawrence, Kansas 66045

E-mail: [sichu@ku.edu](mailto:sichu@ku.edu)

### **Program Scope**

In this research program, we address the fundamental physics of the interaction of atoms and molecules with intense ultrashort laser fields. The main objectives are to develop new theoretical formalisms and accurate computational methods for *ab initio* nonperturbative investigations of multiphoton quantum dynamics and very high-order nonlinear optical processes of one-, two-, and many-electron quantum systems in intense laser fields, taking into account detailed electronic structure information and many-body electron-correlated effects. Particular attention will be paid to the exploration of the effects of electron correlation on high-harmonic generation (HHG) and multiphoton ionization (MPI) processes, time-frequency spectrum, and coherent control of HHG processes for the development of tabletop x-ray laser light sources, and attosecond laser pulses, etc.

### **Recent Progress**

#### 1. Effect of Electron Correlation on High-Order-Harmonic Generation of Helium Atoms in Intense Laser Fields [1]

We present a *time-dependent generalized pseudospectral* (TDGPS) approach in hyperspherical coordinates for fully *ab initio* and nonperturbative treatment of high-order harmonic generation (HHG) processes of atomic systems in intense laser fields. The procedure is applied to a detailed investigation of HHG processes of helium atoms in ultrashort laser pulses at a KrF wavelength of 248.6 nm. The six-dimensional coupled hyperspherical-adiabatic-channel equations are discretized and solved efficiently and accurately by means of the TDGPS method. The effects of electron correlation and doubly excited states on HHG are explored in detail. A HHG peak with Fano line profile is identified which can be attributed to a broad resonance of doubly excited states.

#### 2. Creation and Control of a Single Attosecond XUV Pulse by Few-Cycle Intense Laser Pulses

We perform *ab initio* quantum and classical investigations of the production and control of a single attosecond pulse by using intense few-cycle laser pulses as the driving field [2]. The HHG power spectrum is calculated by solving the time-dependent Schrödinger equation (TDSE) accurately and efficiently using the TDGPS method [3, 4]. The time-frequency characteristics of the attosecond xuv pulse are analyzed in detail by means of the wavelet transform of the time-dependent induced dipole. To better understand the physical processes, we also perform classical trajectory simulation of the strong-field electron dynamics and electron returning energy map. We found that the quantum and classical results provide complementary information regarding the underlying mechanisms responsible for the production of the coherent attosecond pulse. For few-cycle (5 fs) driving pulses, it is shown that the emission of the consecutive harmonics in the super continuum cutoff regime can be synchronized and locked in phase resulting in the production of a coherent attosecond pulse. Moreover, the time profile of the attosecond pulses can be controlled by tuning the carrier envelope phase.

#### 3. Extension of High-order Harmonic Generation Cutoff via Coherent Control of Intense Few-Cycle Chirped Laser Pulses

We present a fully *ab initio* quantum exploration of the HHG cutoff extension mechanisms controlled by a few cycle *chirped* laser pulse [5]. It is shown that significant cutoff extension can be achieved through the optimization of the chirping rate parameters. The HHG power spectrum is calculated by solving accurately and efficiently the TDSE by means of the TDGPS method and the time-frequency characteristics of the HHG power spectrum are analyzed in detail by means of the wavelet transform of the time-dependent induced dipole acceleration. It is found that the quantum and classical results provide consistent information regarding the underlying mechanisms responsible for the substantial extension of the cutoff region. Furthermore the time duration of the emitted attosecond bursts produced by the chirped laser pulse is significantly reduced from that of the chirp-free laser pulses.

#### 4. Time-Frequency Analysis of Molecular High-Harmonic Generation Spectrum by Means of Wavelet Transform and Wigner Distribution Techniques

Using an extended Lewenstein model, we perform a theoretical investigation of the HHG spectrum of diatomic molecular systems in intense short-pulse laser fields [6]. The wavelet transform and Wigner distribution, two complementary time-frequency analysis methods, are extended for the exploration of the underlying mechanisms responsible for the fine structure of HHG peaks in the plateau regime. We found that, under some conditions, the HHG fine structure is mainly due to the interference between the long and short trajectories. The extension of the cut-off in the molecular HHG spectrum is also observed when the internuclear separation is large. Detailed analysis shows that the one-centre and two-centre terms contribute, respectively, to the low- and high-energy parts of the molecular HHG spectrum.

#### 5. *Ab Initio* Nonperturbative Approach Beyond the Born Oppenheimer Approximation for the Exploration of the Coulomb Explosion Dynamics Through Excited Molecular Vibrational States

The study of ionization and molecular fragmentation is a subject of considerable interest in strong-field molecular physics. In particular, the response of the simplest prototype molecular systems  $H_2^+$  ( $D_2^+$ ) and  $H_2$  ( $D_2$ ) in intense laser fields have been experimentally studied in the recent past. In a recent work [7], we investigate the fragmentation dynamics of  $H_2^+$  molecular ions in intense laser fields by means of an *ab initio* method beyond the Born-Oppenheimer approximation. Special attention is paid to the exploration of the Coulomb explosion (CE) mechanisms and quantum dynamics through excited vibrational states of  $H_2^+$ . A novel kinetic-energy release (KER) spectrum and CE phenomenon are predicted, in which the kinetic-energy distribution of  $H^+$  ions exhibits a series of peaks separated by one photon energy. A proposed scheme for the experimental observation of the KER spectrum and CE dynamics is presented.

#### 6. Precision Study of MPI/HHG of $H_2^+$ in Intense Laser Fields: Time-Dependent Non-Hermitian Floquet Approach

The generalized Floquet approaches developed in the past involved the determination of the complex quasi-energies from a *time-independent* non-Hermitian Floquet matrix which has been widely used for the study of a number of atomic and molecular processes in intense laser fields in the last two decades [8]. For more complex many-electron quantum systems, the dimensionality of the Floquet matrix can become very large and the problem can become intractable. Recently we have introduced an alternative method, the *time-dependent* non-Hermitian Floquet approach [9, 10], for overcoming some of the ultra-large complex matrix eigenvalue problems. The procedure involves the complex-scaling generalized pseudospectral spatial discretization of the time-dependent Hamiltonian and non-Hermitian time propagation of the time-evolution operator in the *energy* representation. The new procedure is applied to a precision calculation of MPI and HHG rates of  $H_2^+$  [10] in linearly polarized laser fields with wavelength 532 nm and several laser intensities, as well as various internuclear distances  $R$  in the range between 2.0 and 17.5 a.u. We found that both the MPI and HHG rates are strongly dependent on  $R$ . Further, at some internuclear separations  $R$ , the HHG productions are strongly enhanced and this phenomenon can be

attributed to the resonantly enhanced MPI at these  $R$ . Finally, the enhancement of higher harmonics is found to take place mainly at <sup>larger</sup>  $R$ . Detailed study of the correlation between the behavior of MPI and HHG phenomena is presented. Extension of the work to the case of elliptical polarization is currently in progress [22].

## 7. Development of *Self-Interaction-Free* Time-Dependent Density Functional Theory (TDDFT) for Nonperturbative Treatment of Multiphoton Processes of Many-Electron Systems in Intense Pulsed Laser Fields

Recently we have continued the development of *self-interaction-free* time-dependent density functional theory (TDDFT) [11-15] for accurate and efficient treatment of strong-field AMO physics, taking into account electron correlations and detailed electronic structure. Given below is a brief summary of the progress in 2004-2007 [17-20].

### a) *Very-High-Order Harmonic Generation of Ar Atoms and Ar<sup>+</sup> Ions in Superintense Pulsed Laser Fields: An All-Electron Ab Initio Study*

Recently it has been demonstrated experimentally [16] that the generation of very high-order harmonics (HHG), up to 250 eV, can be obtained by using the Ar gas. To explore the underlying quantum dynamics responsible for the production of the very-high-order harmonics, we performed an *all-electron* treatment of the response of Ar and Ar<sup>+</sup> systems to superintense laser fields [17] using the self-interaction-free TDDFT [11-13]. In our study, all the valence electrons are treated explicitly & their partial contributions to the ionization are analyzed. Further, by introducing an effective charge concept, we can study at which laser intensity the contribution to the high-energy HHG from Ar<sup>+</sup> ions precede over the Ar atoms. Comparing the HHG power spectrum from Ar and Ar<sup>+</sup>, we conclude that the high-energy HHG observed in the recent experiment [16] originated from the ionized Ar atoms.

### b) *Role of the Electronic Structure and Multi-electron Response in Ionization Mechanisms of Diatomic Molecules in Intense Laser Fields*

Recently there has been much experimental and theoretical interest in the study of strong-field molecular ionization. Most theoretical studies in the recent past are based on approximate models such as the ADK (Ammosov-Delone-Krainov) model, etc. These models usually assume that ionization rates depend only upon laser wavelength and intensity, and the *field-free* ionization potential of the species of interest and consider only the response of the highest occupied molecular orbital (HOMO). The effects of detailed electronic structure and multi-electron responses are ignored. Although these models have some partial success in weaker field processes, they cannot provide an overall consistent picture of the ionization behavior of different molecules.

Recently we have extended the self-interaction-free TDDFT [14, 15] for nonperturbative investigation of the ionization mechanisms of homonuclear diatomic molecules (N<sub>2</sub>, O<sub>2</sub>, and F<sub>2</sub>) in intense short-pulsed lasers [18]. Our results indicated that the detailed electron structure and correlated multielectron responses are important factors for the determination of the strong-field ionization behavior. Further, we found that it is not adequate to use only the HOMO for the description of the ionization behavior since the inner valence electrons can also make significant or even dominant contributions. Finally, the ionization potential (IP) is laser-intensity and frequency dependent and it is also not the only major factor determining the molecular ionization rates. Further investigation will be continued along this direction.

### c) *Ab initio Nonperturbative Treatment of HHG Processes of Diatomic Molecules in Intense Ultrashort Laser Fields*

We introduce a self-interaction-free TDDFT, with proper asymptotic long-range potential, for nonperturbative treatment of HHG and MPI processes of homonuclear and heteronuclear diatomic molecules in intense ultrashort laser fields [19]. A time-dependent *two-center generalized pseudospectral method* is developed for accurate and efficient treatment of the TDDFT equations in space and time. The procedure allows *nonuniform* and optimal spatial grid discretization of the Hamiltonian in prolate spheroidal coordinates and a split-operator scheme in the *energy representation* is used for the time propagation of the individual molecular spin-orbital. The theory is applied to a detailed *all-electron* study of MPI and HHG processes of N<sub>2</sub> and CO molecules in intense laser pulses. The results reveal intriguing and substantially different nonlinear optical response behaviors for N<sub>2</sub> and CO, despite the fact that CO has only a very small permanent dipole moment. In particular, we found that the MPI rate for CO is higher than that of N<sub>2</sub>. Furthermore, while laser excitation of the homonuclear N<sub>2</sub> molecule can generate only odd harmonics, both even and odd harmonics can be produced from the heteronuclear CO molecule.

d) An invited review article for a special issue of the Journal of Chemical Physics, entitled “Recent development of self-interaction-free time-dependent TDDFT for nonperturbative treatment of atomic and molecular multiphoton processes in intense laser fields,” has been recently published [20].

### Future Research Plans

In addition to continuing the ongoing researches discussed above, we plan to initiate the following several new project directions: (a) Development and extension of the Floquet formulation of TDDFT to the more complex molecular systems. (b) Development and extension of self-interaction-free TDDFT to triatomic molecular systems for the study of the MPI mechanism and HHG phenomena in strong fields. (c) Development of spin-dependent *localized* Hartree-Fock (LHF)-DFT method for the study of singly, doubly, and triply excited states of Rydberg atoms and ions as well as inner shell excitations [21]. (d) Coherent control of rescattering and attosecond phenomena in strong fields.

### References Cited (\* Publications supported by the DOE program in the period of 2004-2007.)

- \* [1] X. X. Guan, X. M. Tong, and S. I. Chu, Phys. Rev. A **73**, 023406 (2006).
- \* [2] J. Carrera, X. M. Tong, and S. I. Chu, Phys. Rev. A **74**, 023404 (2006).
- [3] X. M. Tong and S. I. Chu, Chem. Phys. **217**, 119 (1997).
- [4] X. Chu and S. I. Chu, Phys. Rev. A **63**, 023411 (2001).
- \* [5] J. Carrera and S. I. Chu, Phys. Rev. A **75**, 033807 (2007).
- \* [6] J. Chen, S. I. Chu, and J. Liu, J. Phys. B **39**, 4747 (2006).
- \* [7] Z. Y. Zhou and S. I. Chu, Phys. Rev. A **71**, 011402 (R) (2005).
- \* [8] S. I. Chu and D. Telnov , Physics Reports **390**, 1-131 (2004).
- \* [9] D. Telnov and S. I. Chu, J. Phys. B **37**, 1489 (2004).
- \*[10] D. Telnov and S. I. Chu, Phys. Rev. A**71**, 013408 (2005).
- [11] X. M. Tong and S. I. Chu, Phys. Rev. A**57**, 452 (1998).
- [12] X. M. Tong and S. I. Chu, Int. J. Quantum Chem. **69**, 305 (1998).
- [13] X. M. Tong and S. I. Chu, Phys. Rev. A**64**, 013417 (2001).
- [14] X. Chu and S. I. Chu, Phys. Rev. A**63**, 023411 (2001).
- [15] X. Chu and S. I. Chu, Phys. Rev. A**64**, 063404 (2001).
- [16] E. A. Gibson, *et al.*, Phys. Rev. Lett. **92**, 033001 (2004).
- \*[17] J. Carrera, X. M. Tong, and S. I. Chu, Phys. Rev. A**71**, 063813 (2005).
- \*[18] X. Chu and S. I. Chu, Phys. Rev. A**70**, 061402 (R) (2004).
- \*[19] J. Heslar, J. Carrera, D. Telnov, and S. I. Chu, Int. J. Quantum Chem. (in press).
- \*[20] S. I. Chu, J. Chem. Phys. **123**, 062207 (2005).
- \*[21] Z.Y. Zhou and S. I. Chu, Phys. Rev. A**75**, 014501 (2007).
- \*[22] D. Telnov and S. I. Chu, Phys. Rev. A (submitted).

# Formation of Ultracold Molecules

Robin Côté

Department of Physics, U-3046  
University of Connecticut  
2152 Hillside Road  
Storrs, Connecticut 06269

Phone: (860) 486-4912  
Fax: (860) 486-3346  
e-mail: [rcote@phys.uconn.edu](mailto:rcote@phys.uconn.edu)  
URL: <http://www.physics.uconn.edu/~rcote>

## Program Scope

Current experimental efforts to obtain ultracold molecules (*e.g.*, photoassociation (PA), buffer gas cooling, or Stark deceleration) raise a number of important issues that require theoretical investigations and explicit calculations.

This Research Program covers interconnected topics related to the formation of ultracold molecules. We propose to investigate schemes to form ultracold molecules, such as homonuclear alkali metal dimers using stimulated and spontaneous processes. We will also study heteronuclear molecules, in particular alkali hydrides; these polar molecules have very large dipole moments. In addition, we will investigate the enhancement of the formation rate via Feshbach resonances, paying special attention to quantum degenerate atomic gases. Finally, we will explore the possible formation of a new and exotic type of molecules, namely ultralong-range Rydberg molecules.

## Recent Progress

Since the start of this Program (August 1<sup>st</sup> 2005), we have worked on the following projects:

### • Formation of alkali hydrides

We explored the formation of alkali hydrides from one- and two-photon photoassociative processes. We found that the one-photon formation rate for LiH and NaH in their  $X^1\Sigma^+$  ground electronic state is sizable in the upper ro-vibrational states  $|v'', J = 1\rangle$ ; assuming conservative values for the atom densities ( $10^{12} \text{ cm}^{-3}$ ), temperature (1 mK), laser intensity (1000 W/cm<sup>2</sup>), and the volume illuminated by it ( $10^{-6} \text{ cm}^3$ ), the rate coefficients are of the order  $3 \times 10^{-13} \text{ cm}^3/\text{s}$ , leading to about 30,000 molecules per second [1]. We also found that all of those molecules would populate a narrow distribution of  $J$ -states in the  $v'' = 0$  vibrational level by spontaneous emission cascading (see Fig.1); the momentum transfer due to the photon emission is not large enough for remove the molecules from traps deeper than 10  $\mu\text{K}$  or so. In the two-photon case, we calculated the formation rate of LiH into the singlet ground state via the  $B^1\Pi$  excited state. This excited electronic state has only three bound levels (in the  $J = 1$  manifold) and a fairly good overlap with the  $X^1\Sigma^+$  ground electronic state. We found rate coefficients about 1000 times larger [2]. However, the constraints brought by the possibility of back-stimulation from a bound state to the continuum limits these larger rates to values of the same order as the single photon process via an excited state [2].

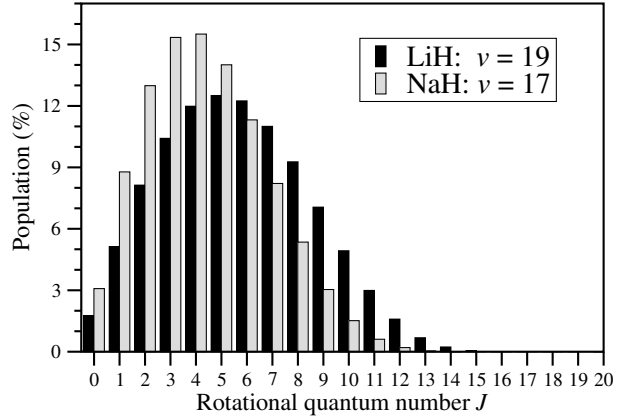


Figure 1: Distribution into the  $J$  states of the  $v = 0$  manifold starting from  $v = 19, J = 1$  for LiH and  $v = 17, J = 1$  for NaH. In both cases, we observe that the maximum population is achieved around  $J \sim 5$ .

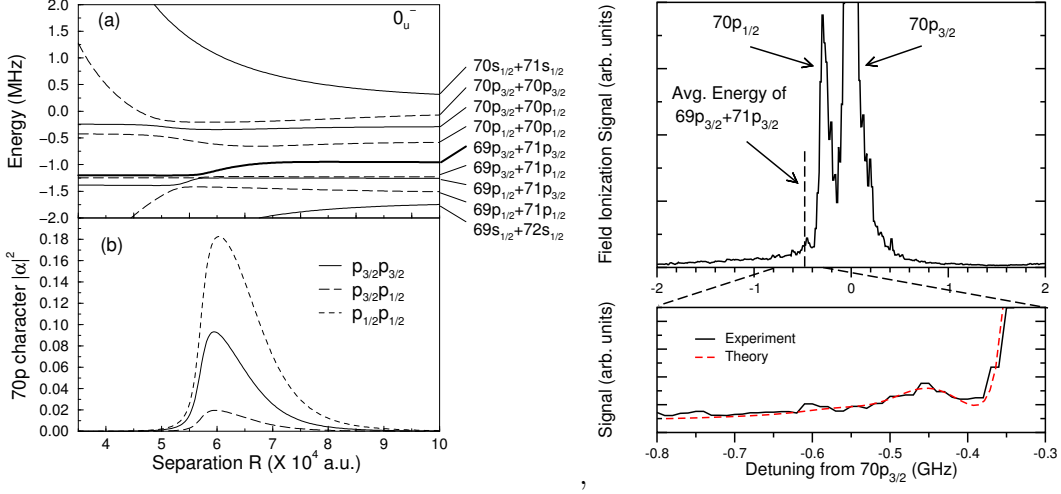


Figure 2: Left panel: (a) Potentials for the  $0_u^-$  symmetry for asymptotes between  $70s + 71s$  and  $69s + 72s$  (zero of energy set at the  $70p_{3/2} + 70p_{3/2}$  asymptote). (b) Fraction of  $70p$  character  $|\alpha|^2$  for  $p_{3/2}p_{3/2}$ ,  $p_{3/2}p_{1/2}$ , and  $p_{1/2}p_{1/2}$  mixtures of the  $69p_{3/2} + 71p_{3/2}$  curve. Right panel: Experimental spectrum near the  $70p$  atomic resonance. Zoom: comparison between experiment and theory (assuming a 120 MHz laser bandwidth, and contributions from the  $0_g^+$ ,  $0_u^-$ , and  $1_u$  symmetries).

More recently, we also explored the formation of LiH molecules in the  $a^2\Sigma^+$  electronic state [3]. It is predicted to support one ro-vibrational level, leading to a sample in a pure single ro-vibrational state. We found that very large rate coefficients can be obtained by using the  $b^3\Pi$  excited state, which supports only five or six bound levels. Because of the extreme spatial extension of their last “lobe”, the wave functions of the two uppermost bound levels have large overlap with the ( $v = 0, J = 0$ ) bound level of  $a^3\sigma^+$ , leading to branching ratios ranging from 1% to 90%. This property implies that large amounts of LiH molecules could be produced in a single quantum state, a prerequisite to study degenerate molecular gases [3].

### • Rydberg-Rydberg interactions

We began working on the Rydberg-Rydberg interactions to explain some spectral features observed in  $^{85}\text{Rb}$  experiments. We calculated the long-range molecular potentials between two atoms in  $70p$  in Hund’s case (c), by diagonalization of an interaction matrix. We included the effect of fine structure, and showed how the strong  $\ell$ -mixing due to long-range Rydberg-Rydberg interactions can lead to resonances in excitation spectra. Such resonances were first reported in S.M. Farooqi *et al.*, Phys. Rev. Lett. **91** 183002, where single UV photon excitations from the  $5s$  ground state occurred at energies corresponding to normally forbidden transitions or very far detuned from the atomic energies. We modeled a resonance correlated to the  $69p_{3/2} + 71p_{3/2}$  asymptote by including the contribution of various symmetries (see Fig. 2): the lineshape is reproduced within the experimental uncertainties [4]. More recently, we extended this work to the case of strong resonances observed near the  $69d + 70s$  asymptote [5]. We found that our theoretical results are in good agreement with the observations of our colleagues at UConn.

### • Evanescent-wave mirrors

In [6], we investigated the interaction of an ultracold diatomic polar molecule with an evanescent-wave mirror (EWM). Several features of this system were explored, such as the coupling between

internal rovibrational states of the molecule and the laser field. Using numerical simulations under attainable physical conditions, we found that the reflection/transmission coefficient depends on the internal (rovibrational) states of the molecules. Such molecular optics components could facilitate the manipulation and trapping of ultracold molecules, and might serve in future applications in several fields, e.g., as devices to filter and select state for ultracold chemistry, to measure extremely low temperatures of molecules, or to manipulate states for quantum information processing.

We extended this work from the static case, where the optical fields have constant intensities, to the time-varying case. We found that in addition to trapping molecules, one could use such devices to also cool them [7].

#### • Degenreate Fermi gas

In [8], we worked on the spectroscopic signature of Cooper pairs in a degenerate Fermi gas, namely  ${}^6\text{Li}$ . We calculated two-photon Raman spectra for fermionic atoms with interactions described by a single-mode mean-field BCS-BEC crossover theory. By comparing calculated spectra of interacting and non-interacting systems, we found that interactions lead to the appearance of correlated atomic pair signal - due to Cooper pairs; splitting of peaks in the spectroscopic signal - due to the gap in fermionic dispersion; and attenuation of signal - due to the partial conversion of fermions into the corresponding single-mode dimer. By exploring the behavior of these features, on can obtain quantitative estimates of the BCS parameters from the spectra, such as the value of the gap as well as the number of Cooper pairs.

#### • Feshbach Optimized Photoassociation (FOPA)

We have started to investigate the formation of polar molecules using photoassociation of atoms in mixtures in the vicinity of Feshbach resonances [9]. We calculated the rate coefficients to form singlet molecules of LiNa using this Feshbach Optimized Photoassociation (FOPA) mechanism, and found that they increase by  $10^{3-4}$  when compared to the off-resonance rate coefficients (see Fig. 3).

### Future Plans

In the coming year, we plan to continue the alkali hydride work. We also will extend this work to other polar molecules relevant to the experimental community, such as LiCs [10], LiRb, etc. We also plan to continue our work on FOPA.

We expect to carry more calculations on Rydberg-Rydberg interactions and explore the possibility of forming metastable long-range doubly-excited Rydberg molecules as well as the experimental signature to be expected [11]. Finally, we will investigate the possibility of trapping and cooling molecules using evanescent-wave mirrors with time-dependent laser fields.

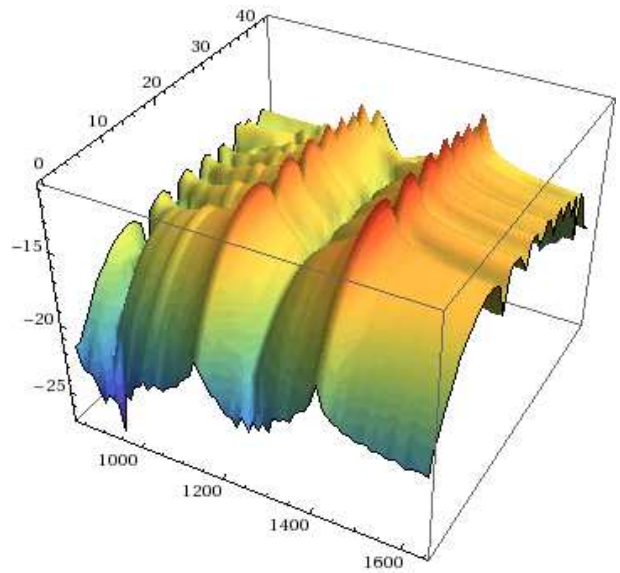


Figure 3: Rate coefficient (log-scale) in  $\text{cm}^3/\text{s}$  as a function of the  $B$ -field for various  $v = 0 - 42$  of the singlet state of LiNa. The rate coefficient increases drastically in the vicinity of the two Feshbach resonances shown here.

## Publications sponsored by DOE

1. E. Juarros, P. Pellegrini, K. Kirby, and R. Côté, *One-photon-assisted formation of ultracold polar molecules*. Phys. Rev. A **73**, 041403(R) (2006).
2. E. Juarros, K. Kirby, and R. Côté, *Laser-assisted Ultracold Lithium-hydride Molecule Formation: Stimulated vs. Spontaneous Emission*. J. Phys. B **39**, S965 (2006).
3. E. Juarros, K. Kirby, and R. Côté, *Formation of ultracold molecules in a single pure state: LiH in  $a^3\Sigma^+$* . In preparation.
4. J. Stanojevic, R. Côté, D. Tong, S.M. Farooqi, E.E. Eyler, and P.L. Gould, *Long-range Rydberg-Rydberg interactions and molecular resonances*. Eur. Phys. J. D **40**, 3 (2006).
5. J. Stanojevic, R. Côté, D. Tong, S.M. Farooqi, E.E. Eyler, and P.L. Gould, *Molecular resonances in ultracold Rydberg gases*. In preparation.
6. K. Shimshon, B. Segev, and R. Côté, *Evanescence-Wave Mirror for Ultracold Diatomic Polar Molecules*. Phys. Rev. Lett. **95**, 163005 (2005).
7. K. Shimshon and R. Côté, *Trapping and controlling molecules with Evanescence-Wave Mirrors*. Submitted to Phys. Rev. A.
8. M. Koštrun and R. Côté, *Two-color spectroscopy of fermions in mean-field BCS-BEC crossover theory*. Phys. Rev. A **73**, 041607(R) (2006).
9. P. Pellegrini, M. Gacesa, and R. Côté, *Formation of ultracold molecules using Feshbach-Optimized Photoassociation*. In preparation.
10. P. Pellegrini and R. Côté, *Formation of ultracold LiCs*. In preparation.
11. J. Stanojevic and R. Côté, *Rydberg-Rydberg Long-range Molecular states*. In preparation.

# Optical Two-Dimensional Fourier-Transform Spectroscopy of Semiconductors

Steven T. Cundiff

JILA, University of Colorado and National Institute of Standards and Technology  
Boulder, CO, 80309-0440  
[cundiffs@jila.colorado.edu](mailto:cundiffs@jila.colorado.edu)

**Program Scope:** The goal of this program is to implement optical 2-dimensional Fourier transform spectroscopy and apply it to semiconductors. Specifically of interest are quantum wells that exhibit disorder due to well width fluctuations and quantum dots. In both cases, 2-D spectroscopy will provide information regarding coupling among excitonic localization sites.

**Progress:** During the past year, the project has concentrated on understanding the polarization dependence of two-dimensional Fourier spectroscopy of the heavy- and light-hole exciton resonances in GaAs quantum wells. These results build on the successful demonstration of an optical 2D spectrometer with active locking of the pulse delays [1], measurement of amplitude spectrum for broad-band excitation of the exciton resonances and continua [2] and measurement of phase resolved spectra to reveal the microscopic origin of the many-body interactions [3]. Interpretation of the polarization dependence has been greatly aided by theoretical advances made by collaborators [4,5]. A detailed comparison between experiment and theory for different levels of approximation in the theory shows that only a full theory is capable of reproducing the experimental spectra [6].

Figure 1 shows experimental co-circularly polarized real 2D spectra for both the rephasing pulse sequence (conjugate pulse first, which would produce a photon echo in an inhomogeneously broadened system) and for the non-rephasing pulse sequence. Rephasing and non-rephasing spectra are shown for a waiting time between the second and third pulses of 100 fs and 2 ps. In the latter case, incoherent relaxation of exciton populations can change the relative strengths of the peaks. Note that we have adopted the convention that the emission frequency ( $\omega_t$ ) has a positive frequency. Thus for a rephasing spectrum, the absorption frequency ( $\omega_r$ ) has a negative frequency, whereas for a non-rephasing spectrum it is positive. These results show a number of striking features, including a strong cross peak between heavy- and light-hole excitons and “dispersive” like features

To understand why the cross peaks are surprising, the spins of the relevant bands need to be considered. As shown in

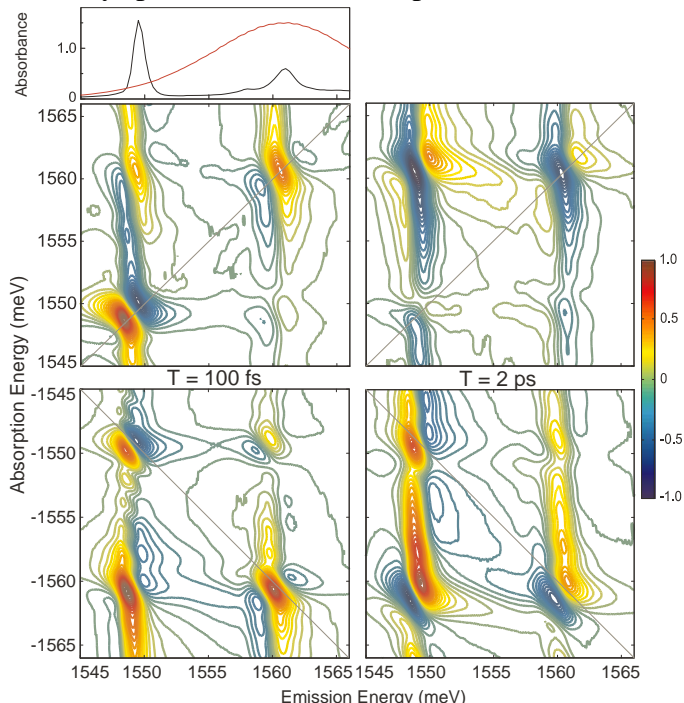


**Fig. 1.** Experimental rephasing (bottom) and non-rephasing (top) 2D spectra of heavy- and light-hole excitons for co-circularly polarized excitation at waiting times of 100 fs (left) and 2 ps (right). The topmost panel shows the absorption (black) and laser (red) spectra.

Fig. 2, the conduction band is  $\pm \frac{1}{2}$ , the heavy hole valence band is  $\pm \frac{3}{2}$  and the light hole valence band is  $\pm \frac{1}{2}$ . Thus for co-circularly polarized excitation, transitions from the heavy-hole valence band to the conduction band appear to be uncoupled from transitions from the light-hole valence band to the conduction band. These transitions are shown as arrows in Fig. 2. For uncoupled resonances, there should be no cross peaks. Whereas the measurements, not only show cross peaks, but the cross peaks are the strongest features on the spectra. A simple analysis based on a multi-level scheme concludes that the cross peaks should always between the diagonal peaks in strength, never the strongest.

Phenomenological calculations have been able to generate spectra with cross peaks that are stronger than the diagonal peaks [2] and dispersive lineshapes [3]. However these calculations cannot address polarization dependence and they allow for arbitrary adjustment of the strengths of different many-body phenomena.

To address the shortcomings of our phenomenological calculations, we have begun working with several theory groups. Figure 3 shows the results produced by the group in Marburg. The calculation is based on a coupled one-dimensional chain of sites. Each site has the

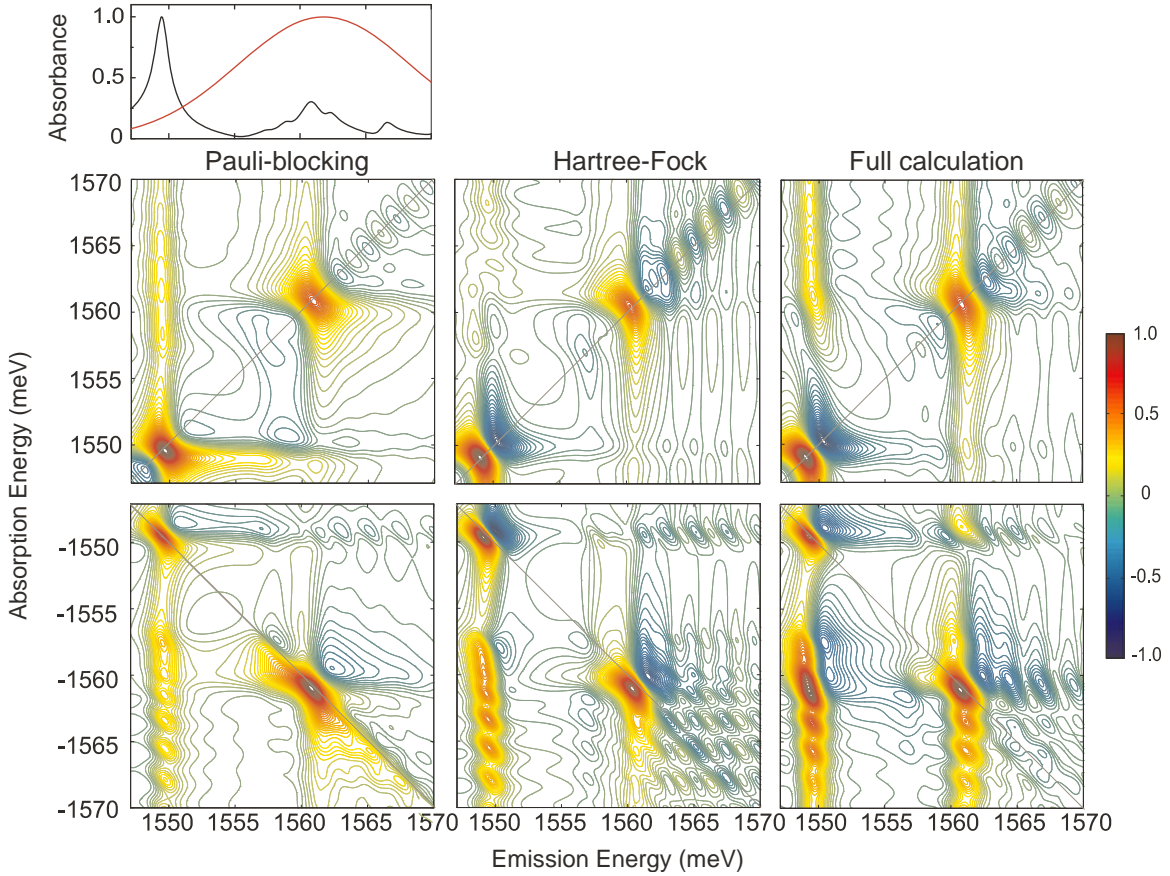


**Fig. 3.** Theoretical non-rephasing (upper) and rephasing (lower) spectra for co-circular polarized excitation. The calculations are for three different levels of theoretical approximation, shown from left to right. The calculated absorption and laser spectra are shown in the topmost pannel [Calculations performed by collaborators in Marburg.]

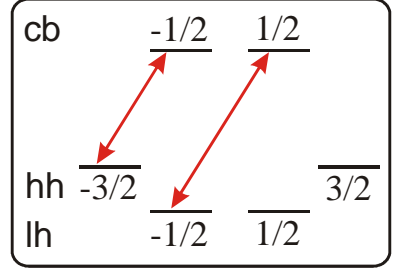


**Fig. 2.** Substates for the conduction band (cb), heavy hole (hh) and light hole (lh) valence bands in a GaAs quantum well. Arrows designate transitions for circularly polarized light.

level structure shown in Fig. 2. The coupling between sites is adjusted to give effective masses comparable to GaAs. The Coulomb interaction is then set to give the correct exciton binding energies, as determined from the absorption spectrum. The dipole moments are set to give the same exciton absorption coefficients. The dephasing rates are the only parameters adjusted based on the 2D spectra. In Fig. 3, theoretical results are shown for several levels of approximation. Including only Pauli blocking, where the Coulomb interaction is only included to the level of exciton formation, does not agree with the experiment at all. The cross peaks are missing and the lineshapes are absorptive, not dispersive. Including many-body terms to the Hartree-Fock level is an improvement, the lineshapes become dispersive, and weak cross peaks appear. However, the agreement is still poor. Only when a full calculation is performed, is good agreement obtained. In the full calculation, all terms that contribute to the third order optical response are retained, including terms beyond Hartree-Fock. The success of the theory sets the stage for more detailed comparisons in the future. There are limitations to the theory due to the use of a one-dimensional chain and the restricted number of sites due to limited computational resources. These mean that the excitation density cannot be directly related to the experiment and that the continuum will be weaker than in experiment. A further approximation is that the calculations are done in the coherent limit, i.e., phase relaxation and population relaxation are linked. This means that spectra for large 2<sup>nd</sup>—3<sup>rd</sup> pulse delay will not be properly reproduced.

Several other theory groups have also begun calculating 2D spectra [5,7], although without making detailed adjustment of the parameters to match the experiment. The work in reference 5 uses a model similar to that used to produce Fig. 3; whereas reference 7 uses a different approach.

**Future Plans:** At this point, a basic understanding of 2DFTS of excitons in semiconductors has been established. There are several more aspects that should provide important insight into the many prior results obtained with transient four-wave-mixing (TFWM). But the exciting direction is to begin working towards using it on systems that display strong localization, which ultimately leads to the spectroscopy of quantum dots.

The ability of TFWM to measure the decoherence rate (homogeneous linewidth), even in the presence of inhomogeneous broadening, was one of the primary motivations for using it. However, for broad band excitation, inconsistencies between different measurements (such as the spectrum versus the temporal decay) raised doubt that simple time-integrated TFWM truly gave the homogeneous dephasing rate. Coupling between states was eventually shown to result in rapid decay of the TFWM signal due to interference effects, rather than dephasing [8]. Preliminary theory results indicate that the dephasing rates can be uniquely and easily determined from 2D spectra, even in the presence of many-body coupling and inhomogeneous broadening. Experiments are underway for comparison to the theory.

To reveal the effects of inhomogeneous broadening due to disorder, specifically well width fluctuations, much lower excitation powers must be used than were used to acquire the data shown in Fig. 1. Higher excitation powers naturally give stronger signals and thus cleaner spectra. However, high excitation levels lead to strong exciton-exciton scattering that increases the homogeneous width. Recent data on a sample with 4 quantum wells (the data in Fig. 1 were obtained from a sample with 10 quantum wells) at lower excitation powers clearly show inhomogeneous broadening as elongation along the diagonal. The effects of disorder should be even more apparent for excitation with picosecond pulses, which will avoid generation free

carriers that strongly scatter the excitons. Currently, the laser is being switched to run in picosecond mode to study this regime.

Well width fluctuations localize excitons in the plane of the quantum well, producing three-dimensionally confined states similar to those in quantum dots. For properly chosen sample structures (narrow wells) and growth conditions (very flat interfaces) the similarity is strong enough for these states to be known as “natural quantum dots.” As a first step towards studying quantum dots, we have obtained such a sample. Natural quantum dots have two advantages over self-organized InGaAs quantum dots: they have a larger dipole moment and are in the range of standard Ti:sapphire lasers. Obtaining 2D Fourier transform spectra from natural quantum dots is a short term goal (next 6 months).

A more distant goal is to use 2DFTS to study self-organized InGaAs quantum dots. Coherent spectroscopy on these dots has proven challenging due to the weak signal from the dots and a strong non-resonant background signal from the surrounding matrix. 2DFTS should do a good job of eliminating the background signal, if sufficient signal from the dots can be obtained. An even more ambitious goal will be to study a small ensemble of dots, where each dot can be spectrally isolated. One challenge to working on InGaAs dots will be the longer wavelengths, with the highest quality dots falling beyond the tuning range of Ti:sapphire.

On a more technical note, we have been building a second generation 2DFTS apparatus. The new apparatus is built monolithically to provide a much greater level of passive stability. Moreover, it will generate 4 phase locked beams, allowing two-quantum transitions (e.g., biexcitons in semiconductors) to be studied. In addition, it should allow the optical phase to be determined optically, rather than through an auxiliary experiment, as is done currently.

- [1]\* T. Zhang, C.N. Borca, X. Li and S.T. Cundiff, “Optical two-dimensional Fourier transform spectroscopy with active interferometric stabilization,” *Opt. Expr.* **13**, 7432 (2005).
- [2]\* C.N. Borca, T. Zhang, X. Li and S.T. Cundiff, “Optical Two-dimensional Fourier Transform Spectroscopy of Semiconductors,” *Chem. Phys. Lett.* **416**, 311 (2005).
- [3]\* X. Li, T. Zhang, C.N. Borca and S.T. Cundiff, “Many-body Interactions in Semiconductors Probed by Optical Two-Dimensional Fourier Transform Spectroscopy,” *Phys. Rev. Lett.* **96**, 057406 (2006).
- [4]\* I. Kuznetsova, P. Thomas, T. Meier, T. Zhang, X. Li, R.P. Mirin, S.T. Cundiff, “Signatures of many-particle correlations in two-dimensional Fourier-transform spectra of semiconductor nanostructures,” *Sol. State Commun.* **142** 154–158 (2007).
- [5] L. Yang, I. V. Schweigert, S. T. Cundiff, and S. Mukamel, “Two-dimensional optical spectroscopy of excitons in semiconductor quantum wells: Liouville-space pathway analysis,” *Phys. Rev. B* **75**, 125302 (2007).
- [6]\* T. Zhang, I. Kuznetsova, T. Meier, X. Li, R. P. Mirin, P. Thomas, and S. T. Cundiff, “Polarization-dependent optical 2D Fourier transform spectroscopy of semiconductors,” *Proc. Nat. Acad. Sci.*, Early Edition doi/10.1073/pnas.0701273104 (July 2007).
- [7] M. Erementchouk, M. N. Leuenberger, and L. J. Sham, “Many-body interaction in semiconductors probed with 2D Fourier spectroscopy,” arXiv:cond-mat/0611196.
- [8] S. T. Cundiff, M. Koch, W. H. Knox, J. Shah and W. Stolz, “Optical Coherence in Semiconductors: Strong Emission Mediated by Nondegenerate Interactions,” *Phys. Rev. Lett.* **77**, 1107 (1996).

Stars indicate publications from this program. Other publications resulting from this program in the last 3 years:

- C. N. Borca, T. Zhang, and S. T. Cundiff, Two-dimensional fourier transform optical spectroscopy of GaAs quantum wells in *Ultrafast Phenomena in Semiconductors and Nanostructure Materials VII* ed., (SPIE - The International Society for Optical Engineering, Bellingham, WA, 2004), Vol. 5352, p. 257-265.
- A.G. VanEngen Spivey and S.T. Cundiff, “Inhomogeneous dephasing of heavy-hole and light-hole exciton coherences in GaAs quantum wells,” *J. Opt. Soc. of Am. B* **24**, 664 (2007).

July 2007

## Theoretical Investigations of Atomic Collision Physics

A. Dalgarno

Harvard-Smithsonian Center for Astrophysics  
Cambridge, MA 02138  
adalgarno@cfa.harvard.edu

The research develops and applies theoretical methods for the interpretation of atomic, molecular and optical phenomena and for the quantitative prediction of the parameters that characterize them. The program is responsive to experimental advances and influences them. A particular emphasis has been the study of collisions in ultracold atomic and molecular gases.

The major uncertainty in predicting accurately the effects of inelastic and elastic collisions is the determination of the potential energy curves characterizing the interactions between the colliding systems. Collisions of neutral atoms and ultracold temperatures are dominated by the long-range van der Waals forces arising from a mutual polarization of each atom by the other. The van der Waals interaction potential has a leading term  $C_6/R^6$  where R is the internuclear distance. Elastic scattering is sensitive to the isotropic component of  $C_6$  and inelastic scattering is sensitive to the anisotropic component. We extended time-dependent density functional theory to incorporate both components. We found by explicit calculations that for the rare earth atoms interacting with helium, the screening of the interaction by the outer 6s shell suppressed the anisotropy and we concluded that all the rare earth atoms are excellent candidates for trapping and cooling (Chu and Dalgarno 2005, Chu, Groenenboom and Dalgarno 2006).

Because of its exceptional interest in experiments, we have given particular attention to the case of Yb. We have explored it, applying several methods of quantum chemistry. The calculated static dipole polarizability of Yb clusters around 143 a.u. We have evaluated the corresponding  $C_6$  for the ground state of  $Yb_2$  using the Cauchy moment method and obtain  $C_6 = 2060$  (200) a.u. (Zhang and Dalgarno 2007). This is smaller than previous values, but is not very different from an empirical value of 1932 (30) derived from the measured vibrational energy level structure of  $Yb_2$  (Kitagawa et al. 2007). We are completing a quantum chemistry calculation of the entire potential energy curve which will yield an independent estimate of  $C_6$ .

There is increasing interest in the behavior of positive ions at ultracold temperatures. The interactions between a positive ion and neutral atom at large distances are modified by the polarization of the neutral atoms by the electric charge distribution of the ion and in addition to the van der Waals interaction there are multipole interactions. The dipole polarization gives rise to a term  $-\frac{1}{2}\alpha_d R^{-4}$  where  $\alpha_d$  is the static dipole polarizability of the atom and the quadrupole

polarization gives rise to a term  $-\frac{1}{2}\alpha_q R^{-4}$  where  $\alpha_q$  is the static quadrupole polarizability.

The quadrupole polarization term in  $R^{-6}$  will usually exceed the van der Waals  $R^{-6}$  term. (There

occurs also a small mass-dependent adiabatic contribution but it can be neglected (Dalgarno and Stewart 1956; Drake and Victor 1968).

We have calculated the coefficients for the alkali metal atoms (Marinescu and Dalgarno 1994). For ion-atom interactions, terms varying as  $R^{-7}$  occur. We intend to calculate a representative sample of the  $R^{-7}$  coefficients.

For interactions between one positive ion and another, there are additional interaction terms arising from the polarization of each ion by the other but the direct Coulomb repulsion due to the excess charges of the ions dominates all interactions at long range.

For atoms not in states of zero orbital angular momentum, the polarization forces have orientation-dependent components which drive inelastic collisions between fine-structure levels. They have been calculated by us as an integral part of the methods used to evaluate  $C_6$ . The scalar and tensor polarizabilities can also be derived by fitting the long-range potentials of the different symmetries of the quasi-molecular ion formed by the approach of the ion and the atom (Dalgarno and Rudge 1965; Wofsy et al. 1971).

In collaboration with Harvey Michaels and Robin Coté, Peng Zhang and I have carried out a direct calculation of the potential energies of the lowest  $^2\Sigma_u^+$  and  $^2\Sigma_g^+$  states of  $\text{Yb}_2^+$ , formed by the approach of  $\text{Yb}^+$  and Yb. We used sophisticated methods of quantum chemistry. They are demanding of computer resources and personal time and they become inaccurate at large distances because the method is such that a diminishingly small number is calculated as the difference between two large numbers. This difficulty may be overcome by the use of the Holstein- Herring formula expresses the differences between the energies  $E_g$  and  $E_u$  of the gerade and ungerade states for identical ion-atom pairs asymptotically as

$$\Delta E = E_g - E_u = -2 \int_M \Phi_a \nabla \Phi_a \cdot dS$$

where M is the midplane perpendicular to the internuclear axis and  $\Phi_a$  is a localized wave function centered on one of the nuclei, a, say. It is remarkable that apart from a normalization requirement,  $\Delta E$  depends only on the asymptotic form of a localized wave function and not on the region where a proper account of correlation is necessary. Its use leads to an expression for the exchange energy as an exponentially decreasing function multiplied by an expansion in  $1/R$ . We are engaged in extending the formula to the interactions between unlike systems and in applying the theory to some representative cases beginning with the alkali metals.

Given the potential energy curves, the determination of the elastic and charge transfer cross-sections is straightforward although there are issues concerning the formulation of the charge transfer process at ultralow energies that need to be addressed. We have preliminary results for  $\text{Y}_b^+$  in  $\text{Y}_b$ .

We have set up a general formulation of the scattering theory of heavy particle collisions in previous grants and we applied it to determine the rate coefficients for the quenching of metastable  $\text{O}({}^1\text{D})$  atoms by hydrogen atoms, an important process in atmospheric and astrophysical plasmas at moderate temperatures, and also to the fine-structure excitation of oxygen and carbon atoms by hydrogen atoms, important cooling processes.

Ionization and dissociation processes in weakly ionized plasmas produce energetic ions and atoms which then cool to the temperature of the plasma gas by elastic and inelastic collisions with the neutral particles of the plasma. The energetic species may, before they have cooled, participate in chemical reactions and modify the plasma chemistry. The cooling process is often characterized by a thermalization cross-section which is determined empirically from measurements of the time it takes the cooling to be completed. However there is no prescription for the calculation of the thermalization cross section except to regard it as some averaged diffusion or momentum transfer cross-section. We have solved the problem for specific cases of energetic nitrogen atoms moving in He and Ar for which experimental data exist (Nakayama et al. 2005). We calculated the interaction potentials for N-He and N-Ar and determined the angular and philosophy-dependent scattering cross-sections. We then used them in constructing and solving the corresponding integral Boltzmann equation for the velocity distribution function. We followed the evolution in detail and discovered that the thermalization process can be characterized by two timescales, one in which the distribution relaxes to a Maxwellian form and a longer second time in which the Maxwellian shape is preserved and its equivalent temperature decreases continuously to the bath gas temperature (Zhang et al. 2007). We propose to include the effects of inelastic collisions that occur if the target gas contains molecules.

## References

- Chu, X. , A. Dalgarno and G. C. Groenenboom, Phys. Rev. A. 75, 032723, 2007.  
 Chu, X. and A. Dalgarno, Adv. At. Mol. Opt. Phys. 51, 83, 2005.  
 Dalgarno, A. and A. L. Stewart, Proc. Roy. Soc. A. 238, 276, 1956.  
 Dalgarno, A. and M.R.H. Rudge, Proc. Roy. Soc A 286, 519, 1965.  
 Dalgarno, A. and R. McCarroll, Proc. Roy. Soc. A 237, 383, 1986.  
 Dalgarno, A., G.W.F. Drake and G.A.Victor, Phys. Rev. A. 176, 194, 1968.  
 Kitagala, M., K. Enomoto, K. Kasa, W. Takahashi, P. Churylo, P. Naidon, and P. Julienne, Phys. Rev. A 49, 982, 1994.  
 Marinescu, M., H. R. Sadeghpour and A. Dalgarno, Phys. Rev. A 49, 982, 1994.  
 Nakayama, T., K. Takahashi and Y. Matsumi, Geophys. Res. Lett. 32, L24803, 2005.  
 Wofsy, S., R.H.G. Reid and A. Dalgarno, ApJ 168, 161, 1971.  
 Zhang, P. and A. Dalgarno, J. Phys. Chem. A submitted 2007.  
 Zhang, P., V. Kharchenko, A. Dalgarno, Y. Matsumi, T. Nakayama and K. Takahashi, Phys. Rev. Lett. submitted 2007.

## Publications 2005-2007

- R. V. Krems, J. Klos, M.F.Rode, M.M.Szczesniak, G.Chalasinski and A. Dalgarno., Suppression of Angular Forces in Collisions of Non-S-State Transition Metal Atoms, Phys. Rev.Lett. 94, 013202, 2005.
- Teck-Ghee Lee, C. Rochow, R. Martin, T. K. Clark, R. C. Forrey, N. Balakrishnan, P. C. Stancil, D. R. Schultz, A. Dalgarno and Gary J. Ferland, Close-coupling calculations of low-energy inelastic and elastic processes in  $^4\text{He}$  collisions with  $\text{H}_2$ : A comparative study of two potential energy surfaces, J. Chem. Phys. 122, 024307, 2005.
- G. Barinovs, M.C. van Hemert, R. Krems and A. Dalgarno, Fine-structure Excitation of C+ And Si+ by Atomic Hydrogen, ApJ 620, 537, 2005.
- M. Bouledroua, A. Dalgarno and R. Côté, Viscosity and Thermal Conductivity of Li, Na, and K Gases, Physica Scripta, 71, 519, 2005 .
- H. Cybulski, R. V. Krems, H.R. Sadeghpour, A. Dalgarno, J. Klos, G.C. Groenenboom, A. van der Avoird, D. Zgid and G. Chalasinski, Interaction of  $\text{NH X}^3\Sigma^-$  with He: Potential Energy Surface, Bound States and Collisional Zeeman Relaxation, J. Chem. Phys. 122, 094307, 2005.
- X. Chu, A. Dalgarno, and G. C. Groenenboom, Polarizabilities of Sc and Ti Atoms and Dispersion Coefficients for their Interaction with Helium Atoms, Phys. Rev. A. 72, 032703, 2005.
- C. Zhu, J. F. Babb and A. Dalgarno, Theoretical Study of Pressure Broadening of Lithium Resonance Lines by Helium Atoms. Phys. Rev. A, 71, 052710, 2005.
- X. Chu and A. Dalgarno, Polarizabilities of  $^3\text{P}$  atoms and van der Waals coefficients for their interaction with helium atoms, Adv. Atom. Mol. Opt., 51, 032703, 2005.
- X. Chu, A. Dalgarno, and G. C. Groenenboom, Polarizabilities of Sc and Ti Atoms and Dispersion Coefficients for their Interaction with Helium Atoms, Phys. Rev. A 72, 032703, 2005.
- C.M. Dutta, C. Oubre, P. Nordlander, M. Kimura and A. Dalgarno, Charge Transfer Cross Sections in Collisions of Ground State Ca and  $\text{H}^+$ , Phys. Rev. A 73, 032714 , 2006.
- M P.J. van der Loo, G.C. Groenenboom, M. J. Jamieson and A. Dalgarno, Raman Association of  $\text{H}_2$  in The Early Universe, Disc. Farad Soc. 133, 43, 2006.
- Y. V. Vanne, A. Saenz, A. Dalgarno, R.C. Forrey, P. Froelich and S. Jonsell, Doubly Excited Autoionizing States of  $\text{H}_2$  Converging to the  $\text{H}(n=2)+\text{H}(n'=2)$  Limit, Phys. Rev. A 73, 2706, 2006.
- A. Dalgarno and M.P.J. van der Loo, Recombination of  $\text{H}_2$  by Raman Association in the Early Universe, ApJ Letters, 646 L91, 2006.
- E. Abrahamsson, R.V. Krems and A. Dalgarno, Fine Structure Excitation of OI and CI by Impact with Atomic Hydrogen, ApJ 654, 1171, 2007.
- Xi Chu, Alexander Dalgarno and Gerrit C. Groenenboom, Dynamic polarizabilities of rare-earth-metal atoms and dispersion coefficients for their interaction with helium atoms Phys. Rev. A. 75, 032723, 2007.
- P. Zhang, V. Kharchenko, A. Dalgarno, Y. Matsumi, T. Nakayama and K. Takahashi, Approach to Thermal Equilibrium in Atomic Collisions, Phys. Rev. Lett. submitted 2007.

# Coherent Control of Multiphoton Transitions in the Gas and Condensed Phases with Ultrashort Shaped pulses

DOE Grant No. DE-FG02-01ER15143

Marcos Dantus

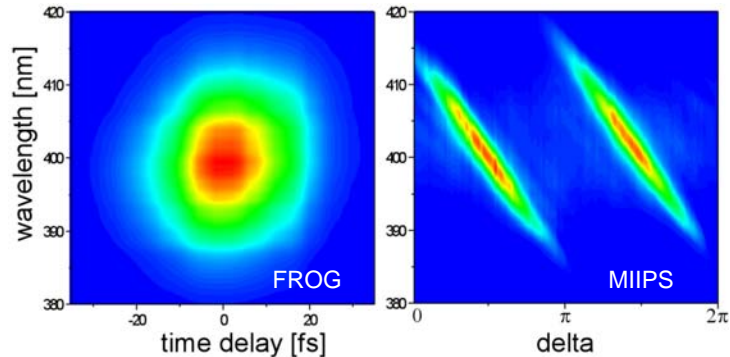
Department of Chemistry and Department of Physics, Michigan State University, East Lansing MI 48824  
[dantus@msu.edu](mailto:dantus@msu.edu)

## 1. Program Scope

Controlling laser-molecule interactions has become an integral part of developing future devices and applications in spectroscopy, microscopy, optical switching, micromachining and photochemistry. Coherent control of multiphoton transitions could bring a significant improvement of these methods. In microscopy, multi-photon transitions are used to activate different contrast agents and suppress background fluorescence; coherent control could bring selective probe excitation. In photochemistry, different dissociative states are accessed through two, three, or more photon transitions; coherent control could be used to select the reaction pathway and therefore the yield specific products. For micromachining and processing a wide variety of materials, femtosecond lasers are now used routinely. Understanding the interactions between the intense femtosecond pulse and the material could lead to technologically important advances. Pulse shaping could then be used to optimize the desired outcome. The scope of our research program is to develop robust and efficient strategies to control nonlinear laser-matter interactions using ultrashort shaped pulses in gas and condensed phases. Our systematic research has led to significant developments [1-21].

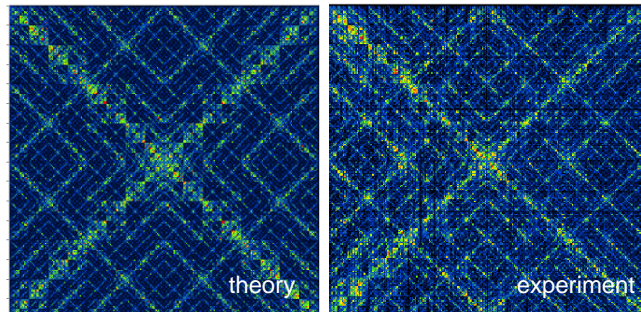
## 2. Recent Progress

Our research on accurate and reproducible pulse shaping led us to the development of multiphoton intrapulse interference phase scan (MIIPS) [2, 7, 10]. MIIPS has turned out to be an extremely accurate method for measuring arbitrary phase distortions in the spectral phase of femtosecond pulses with unprecedented  $0.5 \text{ fs}^2$  accuracy. Because MIIPS uses a pulse shaper, it can compensate spectral phase distortions to produce routinely transform limited pulses within 1% of the theoretical limit. We have compared MIIPS to other widely used methods for phase retrieval and MIIPS has been found to be more accurate than SPIDER, an order of magnitude more accurate than FROG, and even more accurate than white-light interferometry for measuring group velocity dispersion [10]. MIIPS is now integrated in our laser systems for automatically optimizing the output until it is transform limited, and then carrying out phase shaping projects. The figure on the right shows an SHG FROG trace on the left and a MIIPS scan for the same 18 fs, transform-limited pulses.



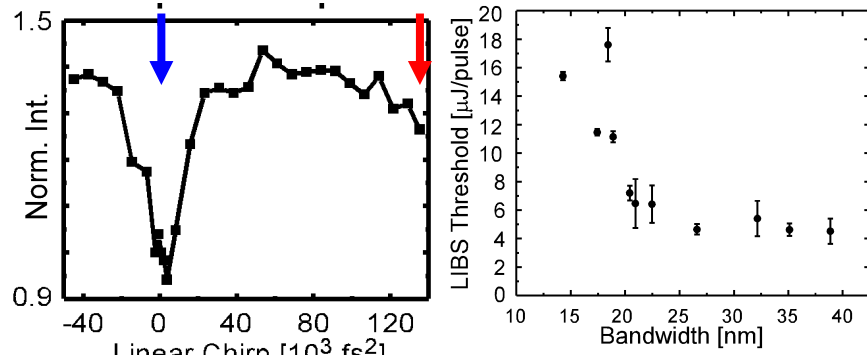
Projects using selective multiphoton excitation on large molecules led us to demonstrate selective two-photon microscopy. In these projects we demonstrated selective excitation of two different chromophores or a single chromophore but in different environments [1, 3, 5]. The latter experiment sparked the idea of using phase shaping for functional imaging. The goal was to use a two-photon active chromophore that was sensitive to a chemical gradient such as pH. We then use phase shaping to control the excitation of the chemically sensitive chromophore. Results from the initial measurements were very encouraging, especially when working with HPTS, a large organic molecule with a pH dependent two-photon cross section spectra that always emits at the same wavelength [1, 8, 9].

We embarked on a systematic study of the effects of phase shaping on multiphoton transitions [11]. This study primarily focused on selective two-photon excitation, the competition of two- versus three-photon transitions, and on selective CARS excitation. This study explores the most efficient methods for controlling multiphoton transitions.



Starting from first principles we review a number of different phase functions and conclude with very valuable lessons. The most valuable being that selective excitation requires the pixels of the pulse shaper to take only two phase values, and not a whole range of values as previously believed. Binary phase shaping, when the difference between the two phase values is  $\pi$ , represents a quantum leap in our progress towards controlling multiphoton processes and the design of robust applications using coherent control [6, 7, 11]. Theoretical work in our laboratory has progressed at the same rate as our experiments. We are presently able to calculate optimum phase functions using a computer operating at 3 GHz, and then implement those phase functions in the lab. We can alternatively make experimental measurements and also simulate them accurately using theory. To demonstrate our present capabilities we evaluated  $2^{16}$  different 16-bit binary phase functions for their ability to generate SHG intensity at 400 nm within a narrow 0.5 nm spectral width, while keeping the background SHG outside that spectral window to a minimum. The results from that research project are mapped on the left (theoretical prediction on the left and experimental result on the right). The measured figure of merit ranged from red (factor of 2.5 signal-to-background) to black (factor of 0.5 signal-to-background) in the figures on the left. The systematic evaluation of binary phase functions and mapping the results has now become a standard in our group that we have applied to a number of projects such as the identification of chemical warfare agents.

Our ability to control nonlinear optical excitation at low and intermediate intensities had to be tested at higher laser intensities ( $10^{14}$  to  $10^{18}$  W/cm<sup>2</sup>) where perturbation theory is no longer applicable. This research started by exploring the interaction of intense femtosecond pulses on metallic surfaces [12]. We focused the beam on a continuously refreshed surface (rotating the target) and measured the laser induced breakdown spectroscopy (LIBS) atomic emission. Because we used 30 fs pulses, we noticed that the threshold for LIBS was very low, far lower than the threshold reported by groups using longer pulses. Instead of requiring  $\sim$ 100 mJ of pulse energy we were able to obtain stable signals with  $\sim$ 5  $\mu$ J of energy per pulse. When we explored different pulse shaping strategies we found very small effects compared to those found earlier for multiphoton excitation. Although some degree of selectivity between copper and aluminum surfaces was found when using binary phase shaping, the extent of the effect was very modest (~30 %). The most intriguing finding, illustrated in the left panel in the figure below. As the 35 fs pulses (blue arrow) were stretched to a pulse duration of 10 ps (red arrow), the overall LIBS signal did not disappear; it actually was  $\sim$ 20% higher than for transform limited pulses. This was a surprising finding because the laser intensity was near threshold and we had assumed peak intensity was critical to observe LIBS near threshold. If the pulse duration of ultrashort pulses was not responsible for the very low LIBS threshold we observed, then it had to be their broad bandwidth. We tested this conclusion and found that the LIBS threshold depends on the inverse of the bandwidth of the pulses (see right panel of figure). We believe this observation will have important implications in the field of micromachining and surface processing by lasers and we plan to explore this further.

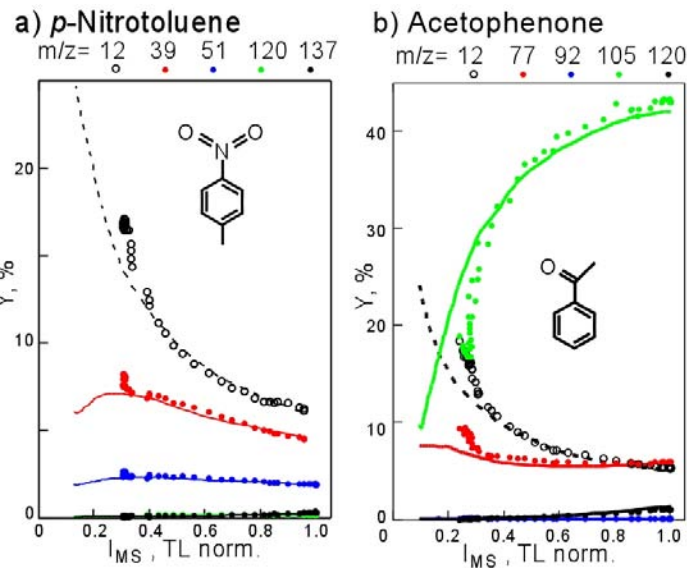
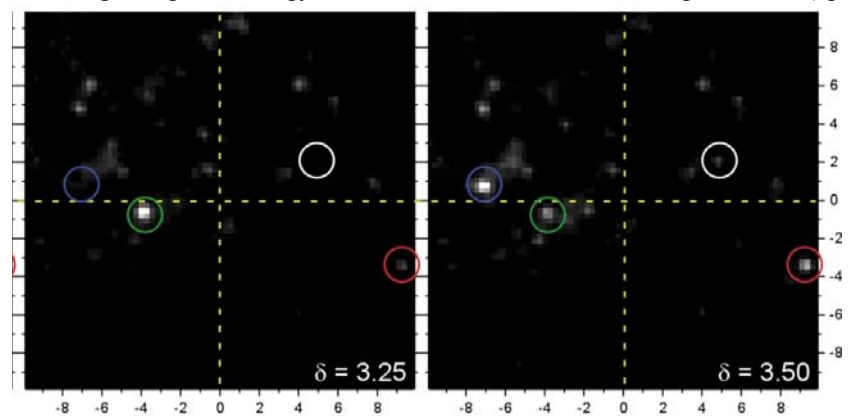


Having developed all the tools necessary for selective nonlinear optical microscopy, we turned our attention to the study of multiphoton excitation of silver nanoparticles [17]. Our first finding was that dendritic silver nanoparticles have a very large cross section for two-photon induced luminescence. When excited at 800 nm they exhibit strong two-photon induced luminescence near 550 nm. When imaging the dendritic silver nanoparticles in the microscope, we noticed that excitation at one location resulted in emission from multiple nanoparticles, some at distances up to 100  $\mu$ m, or approximately 100 focal-spot diameters away. The dendritic nanoparticles are interconnected during the deposition of a thin film during sample preparation. The remote emission results from surface plasmon waveguiding. What is most intriguing is that the remote emission spots can be controlled through the phase or polarization of the excitation beam. Control by phase shaping is shown in the figure below. To be able to obtain these images we had to use MIIPS to compensate all phase distortions introduced by the 60X 1.45 NA objective, and we also had to attenuate the beam to 0.1 pJ/pulse to avoid damaging the nanoparticles. The positions of the sample and laser were fixed, with the laser focused to a spot of about 0.5  $\mu$ m diameter at the center of the

crosshairs. A sinusoidal phase function was introduced to shape the ~12 fs pulses. We see that different phases preferentially cause two-photon luminescence at locations far from the focal spot (colored circles). This phenomenon, its implications to plasmon waveguiding, and energy transfer between molecules at long distances (up to 100  $\mu\text{m}$ ) will be studied in detail. By tracking the spectral phase dependence of the remote emitters, we are able to determine the dispersive properties of the nanowires that transmit the laser pulse energy. We have measured that in some instances, these nanowires have negative dispersion. The implication of these measurements is that these nanowires can compensate for positive dispersion and serve as pulse compressors [18-20].

Our most recent project on the interaction of intense near IR shaped femtosecond pulses with gas phase molecules has led to very significant findings.

Essentially, we found that under these circumstances the fragmentation pattern changes by one or more orders of magnitude upon pulse shaping. However, these changes depended only on pulse duration and not on precise phase-amplitude properties of the field. This finding goes against numerous publications where it was claimed that control over fragmentation required special computer algorithms that tested thousands of different shaped pulses. The figure on the right show changes in the relative yield of fragment ions as a function of the total yield of ions (a quantity proportional to pulse duration) for two very different types of shaped pulses. The lines correspond to positive chirp and the dots correspond to varying the period of a sinusoidal phase function. The resulting pulses for these two phase functions are completely different, yet the results are the same. These findings have been confirmed on 13 different molecules, so we can generalize. Our findings will be published in a feature article [21]. We also found a fragmentation pattern involving double ionization that is highly sensitive to pulse shaping. This pathway is presently under investigation in our group.



### 3. Future Plans

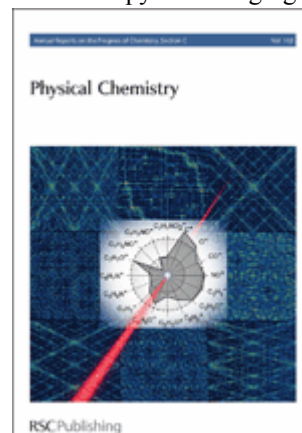
We are presently finishing a publication on the fragmentation pathways of isolate molecules that involve double ionization. These pathways show great sensitivity to phase unlike the majority of the dissociation pathways which do not. We hope to use state of the art in ion imaging to solve some of the prevalent questions in the observed changes in fragment ion yield resulting from laser-molecule interactions in the gas phase when using shaped pulses. These efforts will be complemented by critical analysis of the results using search space mapping and computer simulations.

### 4. Scientists Supported:

This grant has partially supported two postdocs, two undergraduate students, and five graduate students since 2004.

### Publications Resulting from this Grant 2004-2007:

1. J. M. Dela Cruz, I. Pastirk, V. V. Lozovoy, K. A. Walowicz and M. Dantus, "Multiphoton Intrapulse Interference 3: probing microscopic chemical environments," *J. Phys. Chem.* 108, 53 - 58, (2004) Our results were featured in the cover.
2. V. V. Lozovoy, I. Pastirk, M. Dantus, "Multiphoton intrapulse interference 4; Characterization and compensation of the spectral phase of ultrashort laser pulses", 29, 7, 775-777, *Optics Letters* (2004)
3. J. Dela Cruz, I. Pastirk, V.V. Lozovoy, K.A. Walowicz, and M. Dantus, "Control of nonlinear optical excitation with multiphoton intrapulse interference," *Ultrafast Molecular Events in Chemistry and Biology*, M. M. Martin and J.T. Hynes Eds. Elsevier, p. 95 (2004)
4. V.V. Lozovoy, M. Comstock, I. Pastirk, and M. Dantus, "Femtosecond Photon Echo Measurements of Electronic Coherence Relaxation of I<sub>2</sub> in the presence of He, Ar, N<sub>2</sub>, O<sub>2</sub>, C<sub>3</sub>H<sub>8</sub>," *Ultrafast Molecular Events in Chemistry and Biology*, M. M. Martin and J.T. Hynes Eds. Elsevier, p. 33 (2004)
5. M. Dantus and V.V. Lozovoy, "Experimental Coherent Laser Control of Physicochemical Processes", *Chem. Reviews*, Special Issue on Femtochemistry, A. H. Zewail and M. Dantus Eds. 104, 1813-1860, (2004)
6. M. Comstock, V. V. Lozovoy, I. Pastirk, and M. Dantus, "Multiphoton intrapulse interference 6; binary phase shaping", 12, 6, 1061-1066, *Optics Express* (2004)
7. V. V. Lozovoy and M. Dantus, "Systematic control of nonlinear optical processes using optimally shaped femtosecond pulses," *Chem. Phys. Chem. Invited Review*, 6, 1970 (2005)
8. J. M. Dela Cruz, I. Pastirk, M. Comstock, and M. Dantus, "Coherent control through scattering tissue, Multiphoton Intrapulse Interference 8," *Optics Express*, 12, 4144 (2004)
9. J. M. Dela Cruz, I. Pastirk, M. Comstock, V. V. Lozovoy, and M. Dantus, "Use of coherent control methods through scattering biological tissue to achieve functional imaging", *Proceedings of the National Academy of Sciences USA* 101, 16996-17001 (2004)
10. B. Xu, J. M. Gunn, J. M. Dela Cruz, V. V. Lozovoy, M. Dantus, "Quantitative investigation of the MIIPS method for phase measurement and compensation of femtosecond laser pulses," *J. Optical Society B* 23, 750-759 (2006).
11. V. V. Lozovoy, B. Xu, J. C. Shane and M. Dantus, "Selective nonlinear excitation with pseudorandom Galois fields," *A* 74, 041805(R) (2006).
12. T. Gunaratne, M. Kangas, S. Singh, A. Gross, and M. Dantus, "Influence of bandwidth and phase shaping on laser induced breakdown spectroscopy with ultrashort laser pulses." *Chem. Phys. Letters* 423, 197-201 (2006)
13. J. M.Gunn, B. Xu, J. M. Dela Cruz, V. V. Lozovoy, M. Dantus, " The MIIPS method for simultaneous phase measurement and compensation of femtosecond laser pulses and its role in two-photon microscopy and imaging." *Proc. SPIE Vol. 6108*, pgs. 61-68, Commercial and Biomedical Applications of Ultrafast Lasers VI; Joseph Neev, Stefan Nolte, Alexander Heisterkamp, Christopher B. Schaffer; Eds. (2006)
14. J. M.Gunn, B. Xu, J. M. Dela Cruz, V. V. Lozovoy, M. Dantus, "Quantitative phase characterization and compensation by multiphoton intrapulse interference phase scan (MIIPS)." *Femtochemistry VII*, W. Castelman Ed. Elsevier, 526-529 (2006).
15. M. Dantus V. V. Lozovoy, I. Pastirk, J.M. Dela Cruz, "Converting Concepts and Dreams of Coherent Control into Applications." *Femtochemistry VII*, W. Castelman Ed. Elsevier 434-440 (2006).
16. Vadim V. Lozovoy and Marcos Dantus, *Laser control of Physicochemical Processes; Experiments and Applications*, Annual Reports C, 102, 227-258, (2006). Our review was featured in the cover.
17. J. M. Gunn, M. Ewald and M. Dantus, "Properties of Two-Photon Induced Emission from Dendritic Silver Nanoclusters," *Ultrafast Phenomena XV*, P. Corkum, D. Jonas, D. Miller, A. M. Weiner Eds. Springer-Verlag, Berlin (2007).
18. J. M. Gunn, M. Ewald, and M. Dantus, "Polarization and phase control of remote surface-plasmon-mediated two-photon-induced emission and waveguiding," *Nano Letters* 6, 2804-2809 (2006).
19. J. M. Gunn, M. Ewald, M. Dantus, "Remote two-photon emission from dendritic silver nanoclusters," *Microscopy and Microanalysis* 12, 630-631 (2006).
20. M. Ewald, J. M. Gunn, M. Dantus, "Two-photon induced emission from silver nanoparticle aggregates on thin films and in solution," *Microscopy and Microanalysis*, 12 632-633, (2006).
21. V.V. Lozovoy, X. Zhu, T.C. Gunaratne, D. A. Harris, J.C. Shane and M. Dantus, "Control of molecular fragmentation using shaped femtosecond pulses," *J. Phys. Chem. A*, feature Article, in press (2007)



# Interactions of ultracold molecules: collisions, reactions, and dipolar effects

D. DeMille

*Physics Department, Yale University, P.O. Box 208120, New Haven, CT 06520*

e-mail: david.demille@yale.edu

**Program scope:** The primary goal of our project is to study the reactive, inelastic, and elastic collisions of polar molecules (specifically, RbCs) in the ultracold regime. A variety of physical effects associated with the low temperatures and/or the polar nature of the molecules should be observable for the first time. These include phenomena such as chemical reactions at vanishing temperature,<sup>1</sup> ultra-long range “field-linked” states of polar molecules in an external electric field,<sup>2</sup> extraordinarily large ( $\sim 10^8 \text{ \AA}^2$ ) elastic collision rates in the presence of a polarizing electric field,<sup>3,4</sup> etc. In addition, the study of inelastic (e.g., vibrationally or rotationally quenching) collisions will make it possible to produce optimized sources of ultracold polar molecules for a variety of applications. Finally, as a spin-off to this main effort, we have investigated the energy level structure of deeply-bound vibrational levels of the  $a^3\Sigma_u^+$  levels of Cs<sub>2</sub>, motivated by the possibility to use these levels in a sensitive search for possible variations in fundamental constants.

**Recent progress:** Two years ago, our group demonstrated the ability to produce and state-selectively detect ultracold heteronuclear molecules. These techniques yielded RbCs molecules at translational temperatures  $T < 100 \mu\text{K}$ , in any of several desired rovibronic states—including the absolute ground state, where RbCs has a substantial electric dipole moment. Our method for producing ultracold, ground state RbCs consisted of several steps. In the first step, laser-cooled and trapped Rb and Cs atoms were bound together into an electronically excited state, via photoassociation.<sup>5</sup> These initially created molecules decayed rapidly into a few, weakly bound vibrational levels in the ground electronic state manifold.<sup>6</sup> Specifically, by proper choice of the photoassociation resonance, we formed metastable molecules exclusively in the  $a^3\Sigma^+$  level. This sample had significant population in only a small number of rotational levels.

We state-selectively detected these long-lived molecules with a two-step, resonantly-enhanced multiphoton ionization process (1+1 REMPI) followed by time-of-flight mass spectroscopy.<sup>7</sup> This unique detection capability (for ultracold molecules) was enabled by our spectroscopic characterization of RbCs in a previously inaccessible range of energy levels. Our method made it possible to determine the distribution of population among vibrational levels; under typical conditions, the  $a(v=37)$  level (bound by  $\sim 5 \text{ cm}^{-1}$ ) was most highly populated, although this distribution could be changed considerably (towards higher or lower vibrational levels) by the choice of photoassociation resonance.

In the final stage of this work, we demonstrated the long-sought ability to transfer population from these high vibrational levels, into the lowest vibronic states  $X^1\Sigma^+(v=0,1)$  of RbCs.<sup>8</sup> The technique was based on a laser “pump-dump” scheme. Two sequential laser pulses (each  $\sim 5 \text{ ns}$  in duration,  $\sim 100 \mu\text{J}$  pulse energy) drove population first “upward” into an electronically excited level, then “downward” into the vibronic ground state. The vibronic ground-state molecules were spread over a small number (2-4) of the lowest rotational levels, determined by the finite spectral resolution of the pump/dump lasers. These ground-state molecules were also detected with 1+1 REMPI.

We have recently completed a major rebuilding of our experiment, which recently yielded our first observation of optically-trapped RbCs molecules. In the new apparatus, Rb and Cs atoms, initially captured and cooled in a magneto-optic trap, are loaded into a large-volume optical trap (a vertical 1-D lattice formed by a retroreflected 100W CO<sub>2</sub> laser beam). After switching off the MOT lasers, we form metastable, vibrationally excited RbCs molecules in the optical trap by photoassociation as in our previous work. However, unlike before, the resulting molecules remain trapped and accumulate in the 1-D lattice. We also state-selectively detect the molecules as before. In our first observations we have seen molecule trapping times as long as ~300 ms. With these samples, we have seen clear evidence for trap loss-inducing collisions of the molecules, likely with the remaining atoms in the trap. We are now poised to begin a detailed investigation of collisional properties of RbCs molecules.

During the rebuilding effort, we also used our existing apparatus to perform precision spectroscopy of deeply-bound levels of the Cs<sub>2</sub>  $a^3\Sigma_u^+$  electronic state. These experiments were motivated by a new idea to amplify the effect of a possible variation in the electron-to-proton mass ratio,  $\mu$ . This amplification arises when a highly-excited vibrational level of one electronic state (e.g., the  $X^1\Sigma_g^+$  state of Cs<sub>2</sub>) is nearly degenerate with a deeply bound vibrational level of another electronic state (e.g. the Cs<sub>2</sub>  $a^3\Sigma_u^+$  state). Using the technique of two-color photoassociation spectroscopy,<sup>9</sup> we probed Cs<sub>2</sub>  $a^3\Sigma_u^+$  state vibrational levels with binding energies as large as 1500 GHz (~30x more strongly bound than levels accessed in previous work of this type<sup>10</sup>). We have identified a clear case of the desired near-degeneracy, which appears as a hyperfine-induced perturbation of the  $a^3\Sigma_u^+$  state substructure. We have received crucial theoretical guidance from E. Tiesenga (NIST) on state assignments in our spectra, and from T. Bergeman (Stony Brook) on a global fit to all Cs<sub>2</sub> data. Based on this analysis, we infer that this system of nearly-degenerate levels in Cs<sub>2</sub> could be used to search for variations in  $\mu$  at the level of  $\delta\mu/\mu \sim 10^{-18}/\text{year}$ , a factor of ~1000 more sensitive than any existing laboratory or cosmological test of such variations.

**Future plans:** Our initial goal for the optically-trapped sample of RbCs molecules is to quantitatively study the collisional loss processes we have observed. We have implemented a system to push each atomic species from the optical trap. Hence, we will separately measure both Rb-RbCs and Cs-RbCs trap-loss cross sections, and study their dependence on the binding energy of the molecular state (which varies by over a factor of 30 in our system). We also expect to observe molecule-molecule collisions—which our initial observations appear to indicate are already occurring—and measure their cross-sections. Finally, we will search for evidence of reactive collisions in this sample.

The next phase of our work will move towards transferring population to the rovibronic ground state  $X^1\Sigma^+(v=0, J=0)$  in the trapped RbCs sample, and then “distilling” the sample so that only these ground-state molecules remain. With a simple system using two CW diode lasers and a Stimulated Raman Adiabatic Passage excitation scheme, we expect to have high efficiency and excellent state selectivity for the transfer process. The first step of this work will entail precise spectroscopy of the first step of the Raman transition, using one of the CW diode lasers. Finally, we have worked out a plausible protocol for the distillation, which takes advantage of the large DC electric polarizability characteristic of the rovibronic ground state (and of no other states or species present in the trap). The pure sample of dense, ultracold, strongly polar molecules we anticipate producing will represent a near-ideal starting point for studying the new phenomena mentioned above.

- 
- <sup>1</sup>E. Bodo, F. A. Gianturco, N. Balakrishnan, and A. Dalgarno, J. Phys. B: At. Mol. Opt. Phys. **37**, 3641 (2004), and references therein.; R.V. Krems, in Recent Research Developments in Chemical Physics, vol. 3 pt. II, p. 485 (2002).
- <sup>2</sup>A.V. Avdeenkov and J. L. Bohn, Phys. Rev. Lett. **90**, 043006 (2003); A.V. Avdeenkov, D.C.E. Bortolotti and J.L. Bohn, Phys. Rev. A **69**, 012710 (2004).
- <sup>3</sup>D. DeMille, D.R. Glenn, and J. Petricka, Eur. Phys. J. D **31**, 275 (2004).
- <sup>4</sup>M. Kajita, Eur. Phys. J. D **20**, 55 (2002).
- <sup>5</sup>A.J. Kerman *et al.*, Phys. Rev. Lett. **92**, 033004 (2004).
- <sup>6</sup>T. Bergeman *et al.*, Eur. Phys. J. D **31**, 179 (2004).
- <sup>7</sup>A.J. Kerman *et al.*, Phys. Rev. Lett. **92**, 153001 (2004).
- <sup>8</sup>J.M. Sage, S. Sainis, T. Bergeman, and D. DeMille, Phys. Rev. Lett. **94**, 203001 (2005).
- <sup>9</sup>E. R. I. Abraham, W. I. McAlexander, C. A. Sackett, and R. G. Hulet, Phys. Rev. Lett. **74**, 1315 (1995).
- <sup>10</sup>N. Vanhaecke, Ch. Lisdat, B. T'Jampens, D. Comparat, A. Crubellier, and P. Pillet, Eur. Phys. J. D **28**, 351 (2004).

## ATTOSECOND SCIENCE: GENERATION, METROLOGY AND APPLICATION

Louis F. DiMauro

Department of Physics

The Ohio State University

Columbus, OH 43210

[dimauro@mps.ohio-state.edu](mailto:dimauro@mps.ohio-state.edu)

DOE grant #: DE-FG02-05ER15757

### 1. PROJECT SCOPE

This document describes the BES funded project entitled “Attosecond Science: Generation, Metrology & Application” at The Ohio State University (OSU), DOE grant number DE-FG02-05ER15757. The objective is to study high harmonic generation in gases and attosecond synthesis using long wavelength laser sources. The objective is to explore the scaling of the intense laser-atom interaction and provide a potential path towards the production of *light pulses with both the time-scale and the length-scale each approaching atomic dimension*. In other words, the formation of kilovolt x-rays bursts with attosecond ( $10^{-18}$  s) duration.

### 2. PROGRESS IN FY07

#### 2.1 LABORATORY OPERATIONS

The following is a list of the laser sources developed for this project and demonstrated performance.

1. **0.8  $\mu\text{m}$  source:** A CPA based titanium sapphire system that produces 0.8 mJ, 23 fs pulses at 3 kHz repetition rate with carrier-envelope phase (CEP) stabilization.
2. **2  $\mu\text{m}$  source:** An optical parametric amplifier (OPA) that produces 0.7 mJ, 50 fs (7-cycles), 2  $\mu\text{m}$  CEP stabilized pulses. Helium ionization experiments establish a focused intensity of 1 PW/cm<sup>2</sup>.
3. **4  $\mu\text{m}$  source:** A parametric arrangement that produces 0.17 mJ, 80 fs (7-cycles), 3.6  $\mu\text{m}$  pulses. The 3.6  $\mu\text{m}$  light has a measured focused intensity of 0.1-0.2 PW/cm<sup>2</sup>.

#### 2.2 TWO-CYCLE CARRIER-ENVELOPE PHASE STABILIZED 2 $\mu\text{M}$ PULSES

The output of the 50 fs, 2  $\mu\text{m}$  OPA has been temporally compressed, producing a pulse duration of 12 fs (2-cycles). The pulse reduction is achieved by forming a plasma filament in a high pressure xenon cell using a loose focusing geometry. The plasma filament provides two crucial elements: (1) self-phase modulation generates new frequencies (bandwidth) around the 2  $\mu\text{m}$  central wavelength and (2) wave guiding of the 2  $\mu\text{m}$  light due to the interplay of self-focusing and free electron dispersion. The output of the filament produces 2-octaves of bandwidth. Pulse compression is achieved by passing the chirped 2  $\mu\text{m}$  light through a prescribed thickness of GaAs (negative GVD at 2  $\mu\text{m}$ ). Figure 1(a) shows the 12 fs interferometric autocorrelation at the output. The 6.7 fs optical period of the 2  $\mu\text{m}$  light corresponds to a 2-cycle pulse. We also measure that the 2  $\mu\text{m}$  CEP is preserved and has long-term stability. The CEP measurement was performed by observing the fringe stability of an  $f$ - $2f$  spectrogram (beating of the filament's octave emission against the frequency-doubled 2  $\mu\text{m}$  light). Figure 1(b) shows that the spectral fringes are ultra-stable over a 10 second period. This is the first demonstration of filament compression for the production of 2-cycle CEP mid-infrared pulses and has been reported in Optic Letters. The 2-cycle, 2  $\mu\text{m}$  CEP light has been used for argon HHG production but the majority of the work reported here uses the uncompressed 50 fs light. However we now have the technology for producing 200 eV isolated attosecond pulses.

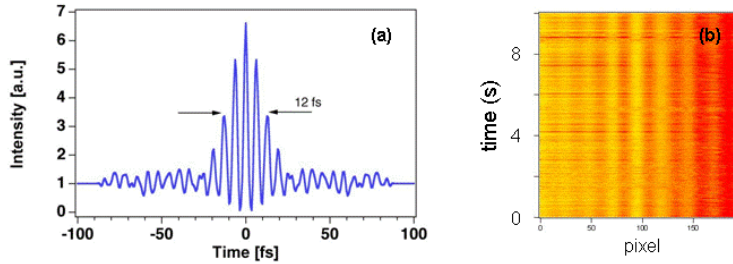


Figure 1: (a) The measured interferometric autocorrelation of a 12 fs, 2  $\mu\text{m}$  pulse produced in an optical filament. (b) The spectral  $f$ - $2f$  fringes recorded over a 10 s period demonstrating the CEP stability of the 2  $\mu\text{m}$  source.

### 2.3 THEORETICAL MODELING OF SCALING IN ATTOSECOND GENERATION

The experiments at long wavelengths are entering unexplored territory in strong-field physics consequently the program will benefit from theoretical guidance. We have developed a “realistic” 3-D quantum mechanical code capable of exploring the strong-field scaling. Currently, we are capable of calculating the response of an “isolated” inert gas atom in an intense long wavelength ( $\lambda \leq 2 \mu\text{m}$ ) field. The calculations are based on numerical solutions of the time-dependent Schrödinger equation (TDSE) using a single active electron (SAE) approximation. We calculate both the photoelectron energy and the high harmonic spectral and phase distributions. This work has given us a theoretical tool that will provide a roadmap for the experimental program. The first results from these calculations have been published in Physical Review Letters.

### 2.4 EXPERIMENTAL REALIZATION OF HHG FROM LONG WAVELENGTH DRIVERS

The critical milestone achieved over the current grant cycle is the observation of strong-field ionization and HHG from inert gas atoms using mid-infrared sources (2  $\mu\text{m}$  and 4  $\mu\text{m}$ ). This result is a major step forward for utilizing the scaling strategy of intense field physics for generating shorter bursts, higher-frequency attosecond pulses. Note that the results presented in this section have been submitted to Nature Physics.

**2.4.1 PRODUCTION OF HIGH-ENERGY PHOTONS FROM RARE GASES AT LONG WAVELENGTHS.** The following presents experimental verification of the crucial element of this proposal, the production of high harmonic light at long wavelengths. We believe that this is a major advance for the production of attosecond pulses with brighter, shorter duration and higher photon energies.

The discussion presented here is confined to HHG generated from an argon target. The data is preliminary and not optimized for the most efficient production of photon number but our initial evidence strongly suggests that the brightness of a 2  $\mu\text{m}$  HHG source can be competitive with a 0.8  $\mu\text{m}$  driven source below 50 eV and superior at higher energies up to 200 eV while the “single” atom TDSE calculations shows the efficacy for producing shorter attosecond pulses over the entire spectral region.

Figure 2 shows a series of argon HHG spectra recorded with a 3-grating, 1.5 meter Hettrick monochromator equipped with an x-ray CCD. The spectrometer has a short wavelength limit of 450 eV. The target is a 2.5 mm long *cw*-gas cell with a permissible maximum pressure of 250 torr (pump limited). The fundamental laser enters and exits the cell through  $\sim 50 \mu\text{m}$  diameter holes. For these spectra the standard 0.8  $\mu\text{m}$  prescription of focusing before the cell is used for optimal “short” trajectory phase-matching. Work is in progress for incorporating macroscopic effects into our calculations but preliminary results indicate that this geometry may not be optimal for the longer wavelengths. Either aluminum or

zirconium metal transmission filters are used downstream of the harmonic source for spectral filtering and removal of the fundamental light.

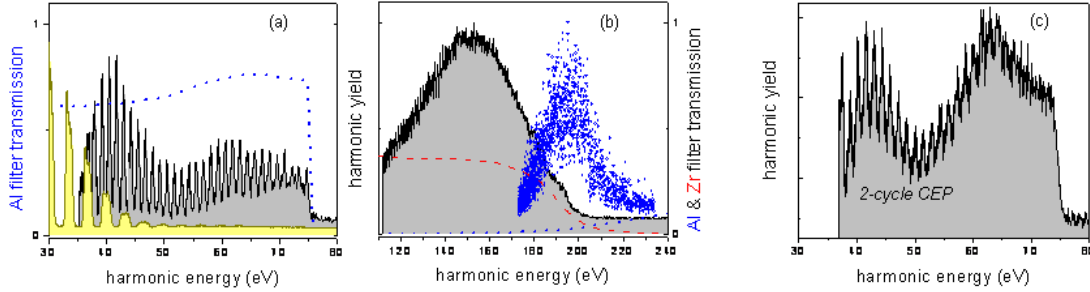


Figure 2: HHG spectrum of argon and the corresponding Al (blue dotted) and Zr (red dashed) filter transmission curves. (a) HHG spectrum for 0.8  $\mu\text{m}$  (yellow shaded) and 2  $\mu\text{m}$  (light gray shaded) excitation at constant intensity. (b) The high-energy portion of the 2  $\mu\text{m}$  HHG (see text). (c) HHG produced by a 2-cycle CEP 2  $\mu\text{m}$  pulse.

Figure 2(a) shows the argon HHG distribution driven by a 0.8  $\mu\text{m}$  (yellow shade) and 2  $\mu\text{m}$  (light gray) fundamental field viewed through an aluminum filter. The focusing optics is chosen to produce the same Rayleigh range at the two different wavelengths and same saturated intensity ( $\geq 0.2 \text{ PW/cm}^2$ ). The 0.8  $\mu\text{m}$  distribution has a clear 50 eV harmonic cutoff, in agreement with previous measurements, our TDSE calculations and the empirical cutoff  $3U_p + I_p$  law. However as seen in Fig. 2(a) excitation with 2  $\mu\text{m}$  pulses produces harmonics to  $\sim 70$  eV energy and with an harmonic spacing smaller by the ratio of  $(0.8 \mu\text{m}/2 \mu\text{m}) = 0.4$ . The cutoff observed in Fig. 2(a) is produced by the decrease in the aluminum filter transmission (blue dotted line). In Fig. 2(b) the harmonics are observed using a zirconium filter that has a transmission window (red dashed line) of 70 eV to 200 eV. HHG from 2  $\mu\text{m}$  excitation is observed over the entire window. In fact the fast structure on the lower energy edge is the  $2\hbar\omega$  spacing but the overall shape is a convoluted instrument response. Needless to say, no harmonics are observed in this region using 0.8  $\mu\text{m}$  excitation. The blue dotted spectrum (transmission through the second Al-filter edge) in Fig. 2(b) establishes that the 2  $\mu\text{m}$  harmonic cutoff is 220 eV which is consistent with our TDSE results. *Incredibly, the nonlinear order of the process changed from a maximum of 31 at 0.8  $\mu\text{m}$  to 351 at 2  $\mu\text{m}$  with a 2.5 change in the fundamental frequency.* This clearly demonstrates the  $\lambda^2$ -increase in the ponderomotive energy or harmonic cutoff and the effectiveness of our approach.

Figure 2(c) shows the argon harmonic spectrum observed through an Al-filter using our 2-cycle compressed CEP stabilized 2  $\mu\text{m}$  pulses. Again the sharp high-energy cutoff is caused by the filter. Note that the 2  $\mu\text{m}$  harmonics are less resolved in comparison to Fig. 2(a) due to the increased fundamental bandwidth. This demonstrates that our 2-cycle driver is effective for harmonics generation and provides the tool for producing “isolated” attosecond pulses at 2  $\mu\text{m}$ .

**2.4.2 HHG YIELD COMPARISON FOR 0.8  $\mu\text{M}$  AND 2  $\mu\text{M}$  FUNDAMENTAL WAVELENGTHS.** The results presented here are very preliminary but are extremely encouraging for the future direction of this proposal. The obvious question in the context of a “useable” attosecond source is the wavelength-dependence of the absolute photon yield. The “single” atom scaling of the power spectrum derived from the TDSE calculations shows a  $\lambda^{(5-6)}$  scaling for constant intensity and this dependence is not yet understood from the classical model. Although we believe that these and other questions are of fundamental importance, the “user” of attosecond light may place a higher priority on the number of photons needed for conducting an experiment.

Our first comparison was performed for argon at 0.8  $\mu\text{m}$  and 2  $\mu\text{m}$ . All other conditions were kept constant, e.g. intensity, argon density, focusing & collection system. In this situation, as discussed above,

the harmonic cutoff is 50 eV and 220 eV for 0.8  $\mu\text{m}$  and 2  $\mu\text{m}$  excitation, respectively. Limiting comparison to the spectral bandwidth (35-50 eV) common to both fundamental wavelengths, we find that the 2  $\mu\text{m}$  harmonics are 1000-times weaker than 0.8  $\mu\text{m}$ . However, varying only the argon density for optimizing photon number at both wavelengths, one finds that the 2  $\mu\text{m}$  harmonics are only 85-times weaker. Comparing the entire bandwidth (2  $\mu\text{m}$  harmonic comb is spectrally 4-times broader) in both cases yields a difference less than a factor of 20.

Suppose the interest is constructing an attosecond pulse with 200 eV photon energy. Obviously, the above comparison is inappropriate since argon excited by a 0.8  $\mu\text{m}$  pulse has zero emission. However, neon excited by 0.8  $\mu\text{m}$  pulses does emit harmonics at 200 eV, although the intensity needed is much higher (1 PW/cm<sup>2</sup>). Comparing argon at 2  $\mu\text{m}$  with neon at 0.8  $\mu\text{m}$  in a bandwidth from (165-208 eV), we find that the number of photons are equal. The caveat for this comparison is that the conditions were optimized for the 0.8  $\mu\text{m}$  neon source not the 2  $\mu\text{m}$  argon source. We believe that this initial result is strong evidence that the 2  $\mu\text{m}$  source will be brighter due to differences in phase-matching and cross-section between argon and neon. In fact, the above comparison of the 35-50 eV harmonics from argon at both fundamental wavelengths will look different using xenon at 2  $\mu\text{m}$  which will easily emit over this bandwidth.

### 3. PROPOSED STUDIES IN FY08

The following is a brief description of experimental plans in FY08:

1. Measure the phases as a function of harmonic order for 0.8  $\mu\text{m}$  and 2  $\mu\text{m}$  excitation.
2. Perform source optimization studies at 2  $\mu\text{m}$  for high-Z targets.
3. Perform FROG measurements on scaled atomic systems using 4  $\mu\text{m}$  excitation.
4. Construct attosecond beamline at OSU.

### 4. PUBLICATIONS RESULTING FROM DOE CONTRACT DE-FG02-05ER15757

1. "Complete Characterization of Attosecond Pulses", E. M. Kosik, L. Corner, A. S. Wyatt, E. Cormier, I. A. Walmsley and L. F. DiMauro, J. Mod. Optics **52**, 361-378 (2005).
2. "Self-Referencing, Spectrally or Spatially Encoded Spectral Interferometry for the Characterization of Attosecond Electromagnetic Pulses", E. Cormier, I. A. Walmsley, E. M. Kosik, L. Corner and L. F. DiMauro, Phys. Rev. Lett. **94**, 033905-1-4 (2005).
3. "The Scaling of Wave Packet Dynamics in an Intense Mid-Infrared Field", J. Tate, T. Auguste, H. G. Muller, P. Salieres, P. Agostini and L. F. DiMauro, Phys. Rev. Lett. **98**, 013901 (2007).
4. "Intense self-compressed, self-phase-stabilized few-cycle pulses at 2  $\mu\text{m}$  from an optical filament", C. Hauri *et al.*, Optics Lett. **32**, 868-870 (2007).
5. "Strong-Field Physics with Mid-Infrared Lasers", K. D. Schultz, C. I. Blaga, R. Chirla, P. Colosimo, J. Cryan, A. M. March, C. Roedig, E. Sistrunk, J. Tate, J. Wheeler, P. Agostini and L. F. DiMauro, J. Mod Optics **54**, 101-108 (2007).

## IMAGING OF ELECTRONIC WAVE FUNCTIONS DURING CHEMICAL REACTIONS

Louis F. DiMauro

Department of Physics

The Ohio State University

Columbus, OH 43210

[dimauro@mps.ohio-state.edu](mailto:dimauro@mps.ohio-state.edu)

co-PIs: Pierre Agostini (OSU Physics) & Terry A. Miller (OSU Chemistry)

DOE grant #: DE-FG02-06ER15833

### 1. PROJECT SCOPE

This document describes the BES funded project (grant #: DE-FG02-06ER15833) entitled “Imaging of Electronic Wave Functions during Chemical Reactions” at The Ohio State University (OSU). The proposal outlines an experimental program designed to meet the challenge of “watching” and “clocking” the electron motion during chemical bond breaking. The program is built on two seminal technical advances made over the past few years. The first is the realization of attosecond ( $10^{-18}$  s) burst of XUV light (the electronic “clock”) and the second is the method of tomographic imaging of the molecular wave function (the detector to “watch”). A novel approach was proposed in our grant for combining these techniques while exploiting the fundamental scaling principles of strong-field physics.

### 2. PROGRESS IN FY07

Over the past year progress has been made in developing the metrology needed for the imaging method and the construction of kilohertz repetition rate pulsed valve for pre-cooling molecules prior to impulsive alignment. Also in this period, a post-doctoral research associate and an OSU graduate student were hired for this project.

#### 2.1 LABORATORY OPERATIONS

The following is a list of the laser sources developed for this project and demonstrated performance.

1. **0.8  $\mu$ m source:** A CPA based titanium sapphire system that produces 0.8 mJ, 23 fs pulses at 3 kHz repetition rate with carrier-envelope phase (CEP) stabilization.
2. **2  $\mu$ m source:** An optical parametric amplifier (OPA) that produces 0.7 mJ, 50 fs (7-cycles), 2  $\mu$ m CEP stabilized pulses. Helium ionization experiments establish a focused intensity of 1 PW/cm<sup>2</sup>.
3. **4  $\mu$ m source:** A parametric arrangement that produces 0.17 mJ, 80 fs (7-cycles), 3.6  $\mu$ m pulses. The 3.6  $\mu$ m light has a measured focused intensity of 0.1-0.2 PW/cm<sup>2</sup>.

#### 2.2 SPECTRALLY RESOLVED HIGH HARMONIC RADIATION GENERATED BY DRIVING WAVELENGTHS OF 0.8 $\mu$ M AND 2 $\mu$ M.

The high harmonics studies were mainly confined to argon atoms although other inert gases were explored. The 2  $\mu$ m observations were particularly important since the unique scaling strategy discussed in the proposal exploits the behavior of a molecule in long wavelength ( $\lambda > 1 \mu$ m) fields. In our 2  $\mu$ m observations we could establish that high harmonic generation in argon extends to a photon energy of 220 eV. This should be contrasted with a 0.8  $\mu$ m driver that will only produce maximum photon energy of 50 eV at the same intensity. The increasing high harmonic photon energy with decreasing driver wavelength is consistent with our expectations based on quasi-classical scaling (maximum harmonic energy  $\propto \lambda^2$ ). This scaling is a key principle upon which this proposal is based and is now confirmed by our measurement. Furthermore, the consistency of this scaling with our observation also supports the quasi-classical physics expected at longer wavelength and central to the idea of molecular imaging. See project summary for DoE grant # DE-FG02-04ER15614 for more details.

### 2.3 MEASUREMENT OF THE RELATIVE HARMONIC SPECTRAL PHASE USING AN ALL-OPTICAL TECHNIQUE.

Central to the tomographic reconstruction of a molecular orbital image is the measurement of the spectral phase and the high harmonic spectrum as a function of the molecular alignment. We originally proposed to perform these measurements using the RABBITT technique demonstrated by Pierre Agostini. The construction of this apparatus is on-going and part of our DoE program (grant # DE-FG02-04ER15614) in attoseconds. It is anticipated that this apparatus will be operational by end of calendar year 2007 and available for this project.

In order to gain some initial insight into the relative phase of the high harmonic spectrum we have begun measurements using an all-optical method introduced by Dudovich *et al.*<sup>1</sup>. This technique was not yet published at the time of submission of the original imaging proposal. In this measurement, harmonics are generated using a two-color field composed of an intense fundamental field ( $\omega$ ) and a weak  $2\omega$  field. The  $2\omega$  field is derived using 2<sup>nd</sup> harmonic generation in a standard nonlinear crystal and sufficiently weak not to cause HHG alone. The two colors have a defined phase relationship that is controlled by introducing a differential optical path length. Figure 1(a) is a contour plot of a portion of the argon harmonic spectrum as a function of delay between the two colors (0.8  $\mu\text{m}$  and 0.4  $\mu\text{m}$ ). The spectrum is composed of intense odd-order (H17-H21) harmonics (saturated scale) and weaker even-orders (H16-H22). The phase information is extracted in the amplitude oscillation of the even harmonics with a period of  $[4*v_f]^{-1}$  (0.67 fs), where  $v_f$  is the fundamental frequency.

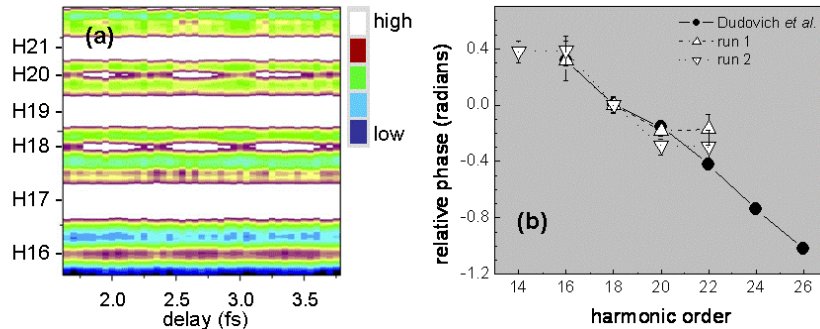


Figure 1: (a) Argon HHG as a function of delay between an intense 0.8  $\mu\text{m}$  and weak 0.4  $\mu\text{m}$  fields. (b) The relative phase extracted from (a) and compared with the results of Dudovich *et al.*<sup>1</sup>.

Physically, the weak 2<sup>nd</sup> harmonic light introduces an asymmetry between the electron trajectories corresponding to consecutive half cycles which have different propagation times for a given initial phase  $\Phi*\text{mod}(\pi)$ . The maximum asymmetry, which is a function of the phase between  $\omega$  and  $2\omega$  fields and  $\Phi$ , can be calculated either quantum mechanically using the saddle-point method or approximated classically. From the knowledge of the experimentally determined even-order harmonic phase (oscillation in Fig. 1[a]) and the calculated phase one can retrieve the recombination time  $T(2q)$  for the even order harmonics. The corresponding phases for the odd orders are obtained by simple interpolation. Once this relative phase is known, the attosecond pulse can be reconstructed.

Figure 1(b) shows the HHG phase extracted from our 0.8  $\mu\text{m}$ /0.4  $\mu\text{m}$  argon measurements (two separate runs) and those of Dudovich *et al.*<sup>1</sup>. The agreement is reasonable and demonstrates our ability to conduct these measurements. We are in the process of modeling these two-color results using our TDSE calculations. We will next perform the argon harmonics measurement using the 2  $\mu\text{m}$ /1  $\mu\text{m}$  two-color field. In principle, the method should work better at the longer wavelength since argon should adhere more to the quasi-classical result. We believe that a weakness of this technique is that the retrieved phase

is model dependent. However it does provide an initial means for examining the predicted phase for our longer wavelength harmonics. Ultimately the more direct RABBITT measurement will be applied.

**Construction of a kilohertz repetition rate pulsed gas valve for pre-cooling of molecules.** Critical to the imaging of a molecular orbital using high harmonic generation is alignment of the target molecule. We will use impulsive excitation for alignment. The quality of the image will depend upon the degree of molecular alignment during the harmonic generation. One way to achieve this is to wait for the first rotational revival following impulsive excitation by an ultra-short pulse. However the degree of alignment will depend upon the initial thermal population<sup>2</sup> of the target molecule. So it is advantageous to cool the rotational distribution and the technique of free jet supersonic expansion is typically used.

During the past year we have designed, constructed and tested a pulsed valve that operates at the 1 kilohertz repetition rate of our drive lasers. No commercial valve is available at these repetition rates. The valve is constructed using a piezoelectric actuator. The valve produces 100  $\mu\text{s}$  gas bursts and operates at a maximum backing pressure of 2.5 atm. We have tested the valve using argon atoms at both 0.8  $\mu\text{m}$  and 2  $\mu\text{m}$ . In both cases we found that high harmonics are generated and are more abundant than with the static cell design that we, and others, normally use. The enhancement in harmonic yield varies from 10-20 depending upon the harmonic order. The enhancement in yield will also benefit the dynamic range over which our experiments can be conducted.

### 3. PROPOSED STUDIES IN FY08

The following is a brief description of experimental plans in FY08:

1. Test and compare the degree of molecular alignment using both the static cell and pulsed valve.
2. Evaluate the efficacy of the all optical technique for measuring the phase of high harmonic generation produced by the 2  $\mu\text{m}$  fundamental field.
3. Generate high harmonics and measure relative phase from the nitrogen molecule using both 0.8  $\mu\text{m}$  and 2  $\mu\text{m}$ .
4. Begin experiments on the NO molecule.

### 4. PUBLICATIONS RESULTING FROM DOE CONTRACT DE-FG02-06ER15833

None

### 5. REFERENCES

- <sup>1</sup> N. Dudovich, O. Smirnova, J. Levesque, et al., *Nature Phys.* **2**, 781 (2006).
- <sup>2</sup> H. Stapelfeldt and T. Seideman, *Rev. Mod. Phys.* **75**, 2787 (2003).

# High Intensity Femtosecond XUV Pulse Interactions with Atomic Clusters

Project DE-FG02-03ER15406  
**Abstract (Summer 2007)**

Principal Investigator:  
Todd Ditmire

*The Texas Center for High Intensity Laser Science*  
*Department of Physics*  
*University of Texas at Austin, MS C1600, Austin, TX 78712*  
*Phone: 512-471-3296*  
*e-mail: [tditmire@physics.utexas.edu](mailto:tditmire@physics.utexas.edu)*

*Collaborators: J. W. Keto, B. Murphy and K. Hoffman*

## Program Scope:

The nature of the interactions between high intensity, ultrafast, near infrared laser pulses and atomic clusters of a few hundred to a few thousand atoms has come under study by a number of groups world wide. Such studies have found some rather unexpected results, including the striking finding that these interactions appear to be more energetic than interactions with either single atoms or solid density plasmas and that clusters explode with substantial energy when irradiated by an intense laser. Under this phase of BES funding we have extended investigation in this interesting avenue of high field interactions by beginning a study of the interactions of intense extreme ultraviolet (XUV) pulses with atomic clusters. These experiments have been designed to look toward high intensity cluster interaction experiments on the Linac Coherent Light Source (LCLS) under development at SLAC. The goal of our program is to extend experiments on the explosion of clusters irradiated at 800 nm to the short wavelength regime (10 to 100 nm). The clusters studied range from a few hundred to a few hundred thousand atoms per cluster (ie diameters of 1-30 nm). Our studies with XUV light are designed to illuminate the mechanisms for intense pulse interactions in the regime of high intensity but low ponderomotive energy by measurement of electron and ion spectra. This regime of interaction is significantly different from interactions of intense IR pulses with clusters where the laser ponderomotive potential is significantly greater than the binding potential of electrons in the cluster. With our XUV studies we are trying to mimic closely the low ponderomotive potential, high intensity short wavelength conditions expected in the focus of the LCLS beam.

We are conducting these studies by converting a high-energy (1 J) femtosecond laser to the short wavelength region through high order harmonic generation. These harmonics are focused into a cluster jet and the ion and electrons ejected are analyzed by time-of-flight methods. We plan to study both van der Waals clusters and solid-state clusters, including metallic clusters. The latter targets will be studied with an eye toward understanding the consequences of irradiating metal clusters chosen such that the intense XUV pulse rests at a wavelength that coincides with the giant plasma resonance of the cluster.

## Progress During the Past Year

During the past year, we performed two campaigns of experiments using a femtosecond laser driven high harmonic source beamline constructed in the first year of this present funding period. We have initially concentrated in noble gas clusters, particularly Xe clusters as these are easy to produce and have been well studied by our group and others when irradiated by intense IR pulses. An illustration of our beam line is illustrated in figure 1. Production of harmonic radiation is accomplished by loosely focusing (f/40) the compressed output of the 20 TW, 40 fs THOR Ti:sapphire laser into a jet of argon at 200 psi. We separated the harmonics from the IR by imaging an annular beam mask in the infrared beam before the focusing lens

onto an aperture after the focus, taking advantage of the fact that the XUV harmonics have substantially less divergence than the infrared beam. This allows the removal of most of the infrared radiation. To reject scattered infrared light and to pass high harmonics with the energies between 15 eV and 73 eV an additional a 200 nm thin Al filter (Luxel Corp.) is used. To select a single XUV harmonic we then employed a specially designed Sc/Si short focal length multilayer mirror optimized for the 21<sup>st</sup> harmonic at 32.5 eV (38.1 nm) at close to normal incidence. (This mirror was fabricated at the Lebedev Physical Institute in Moscow). The harmonic focus was characterized by a scanning knife edge measurement and an AXUV-10 diode (IRD Inc.). We measured a focal intensity of  $\sim 10^{11}$  W/cm<sup>2</sup> at the focus of the 21<sup>st</sup> harmonic assuming an XUV pulse duration of 30 fs.

The cluster interaction experiment was conducted in a separated vacuum chamber by putting a supersonic xenon cluster beam in the XUV focus. A Wiley McLaren time-of -flight (TOF) spectrometer was used to extract positive ions after photo ionization. A typical TOF example is shown in figure 2 when xenon clusters with rough average size of 3,000 atoms are irradiated by the focused 21<sup>st</sup> harmonic. Though the photon energy is sufficient only to ionize electrons by direct photo ionization up to Xe<sup>3+</sup>, in fact we observe charge states up to Xe<sup>6+</sup>. (The argon ions present in the spectrum derive from single photon ionization of an Ar atomic background coming from the higher harmonic generation gas jet up stream). Similar charge states were reported earlier from measurements performed at the DESY FEL at longer wavelength [1]. The authors of this paper interpreted the high charge states accompanied by high kinetic ion energies in the keV range as a result of cluster disintegration by Coulomb explosion. We, however, believe that these high Xe charge states result from electron collisional ionization in a warm nanoplasma created by XUV irradiation of the Xe cluster.

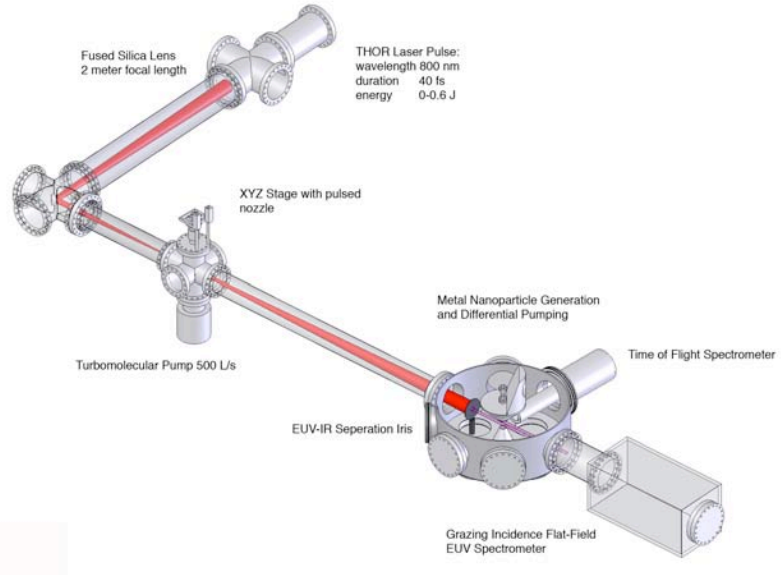


Figure 1: Schematic and specs of the new HHG cluster beamlne on the THOR 20 TW laser

Evidence for this comes from measurements that we have made of the Xe cluster ion spectrum. By removing the TOF extraction and acceleration grids, kinetic energy measurements were made of the released ions by field-free time-of-flight. The ion spectrum derived in this way is illustrated in figure 3. This broad energy spectrum is characteristic of a plasma explosion and exhibits ion temperature much colder than would be expected from Coulomb explosion. We have also conducted a preliminary study of the electron spectra from such interactions. These data are preliminary and require additional study but

<sup>1</sup> H.Wabnitz et al., "Multiple ionization of atom clusters by intense soft X-rays from a free electron laser", *Nature (London)* **420**, 482 (2002).

nonetheless show interesting features. Electrons ejected from Xe clusters irradiated by the 21<sup>st</sup> harmonic are illustrated in figure 4. This spectrum is qualitatively similar to that observed at DESY during Xe cluster irradiation at 95 nm [2], though we observe a number of additional distinct lines. Some of these lines such as the strong feature at 36 eV, appear to be the consequence of multi-photon absorption in atomic species. This particular line probably arises from two photon ionization of the background neutral Ar atoms.

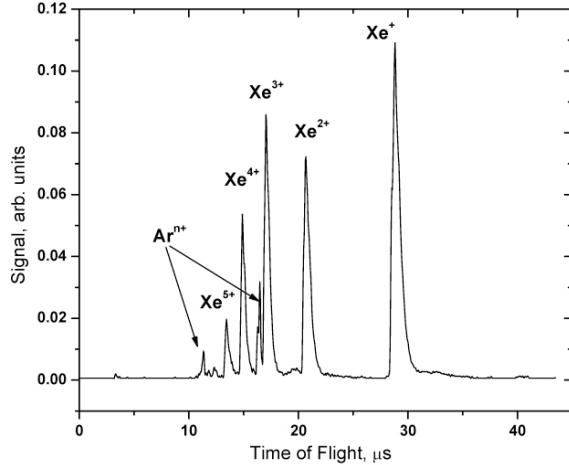


Figure 2: Time of flight spectrum of Xe cluster irradiated at  $\lambda = 38$  nm with intensity  $\sim 10^{11} \text{ W/cm}^2$ . Argon ions arise from Ar gas leaking up stream from the harmonic producing jet.

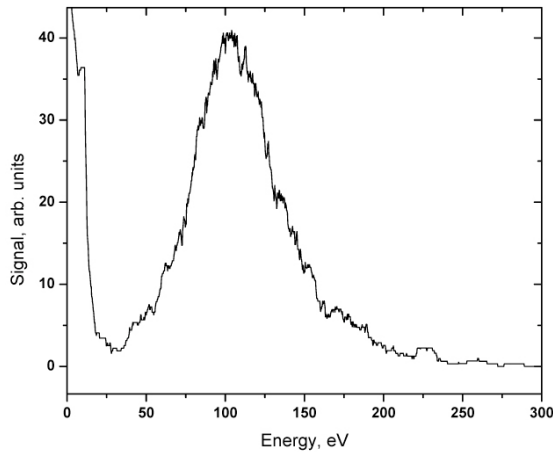


Figure 3: Ion spectrum from exploding Xe clusters irradiated at 38 nm, derived from field free time of flight measurement and the integration of 1000 laser shots.

## Future Research Plans

Our future plans are aimed at continued study of both Xe and Ar rare gas clusters at 38 nm. We will also likely study methane clusters as the presence of low Z ions (like H<sup>+</sup>) leads to qualitatively different dynamics in near IR irradiation. We are also in the process of fabricating an add-on chamber that will allow us to create metal clusters via the laser ablation of micro-particles technique [3]. We will start by investigating Ag clusters, which exhibit interesting absorption resonances at around 20–30 eV attributed to giant collective plasma resonance of both s and d electrons.

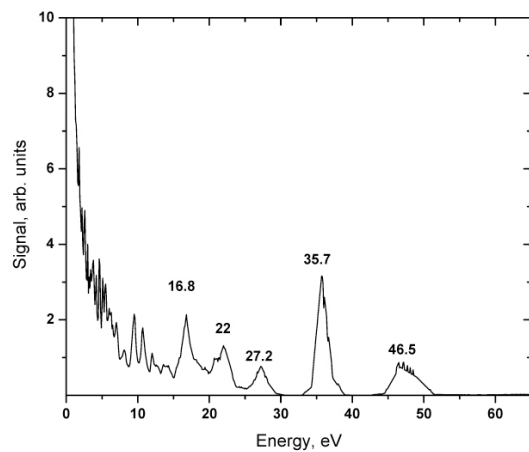


Figure 4: Electron spectrum from Xe clusters irradiated with 32 eV photons (38 nm light).

<sup>2</sup> T. Laarmann et al. "Emission of thermally activated electrons from rare gas clusters irradiated with intense VUV light pulses from a free electron laser" *Phys. Rev. Lett.* **95**, 063402 (2005)

<sup>3</sup> W.T. Nichols, D.E. Henneke, G. Malyavanatham, M.F. Becker<sup>†</sup>, J.R. Brock, and J.W. Keto, and H. D. Glicksman, "Large scale production of nanocrystals by laser ablation of aerosols of microparticles," *Appl. Phys. Lett.* **78**, 1128 (2001).

**Papers published on work supported by this grant during the past three years:**

- 1) D. R. Symes, M. Hohenberger, A. Henig, and T. Ditmire, "Anisotropic Explosions of Hydrogen Clusters under Intense Femtosecond Laser Irradiation" *Phys. Rev. Lett.* **98**, 123401 (2007).
- 2) B. Shim, G. Hays, R. Zgadzaj, T. Ditmire, and M. C. Downer, "Enhanced harmonic generation from expanding clusters" *Phys. Rev. Lett.* **98**, 123902 (2007).
- 3) H. A. Sumeruk, S. Kneip, D. R. Symes, I. V. Churina, A. V. Belolipetski, T. D. Donnelly, and T. Ditmire, "Control of Strong-Laser-Field Coupling to Electrons in Solid Targets with Wavelength-Scale Spheres" *Phys. Rev. Lett.* **98**, 045001 (2007).
- 4) H. A. Sumeruk, S. Kneip, D. R. Symes, I. V. Churina, A. V. Belolipetski, G. Dyer, J. Landry, G. Bansal, A. Bernstein, T. D. Donnelly, A. Karmakar, A. Pukhov and T. Ditmire "Hot Electron and X-ray Production from Intense Laser Irradiation of Wavelength-scale Polystyrene Spheres" *Phys. Plas.* **14**, 062704 (2007).
- 5) M. Hohenberger, D. R. Symes, K. W. Madison, A. Sumeruk, and T. Ditmire, "Dynamic Acceleration Effects in Explosions of Laser Irradiated Heteronuclear Clusters", *Phys. Rev. Lett.* **95**, 195003 (2005).
- 6) F. Buersgens, K. W. Madison, D. R. Symes, R. Hartke, J. Osterhoff, W. Grigsby, G. Dyer and T. Ditmire , "Angular distribution of neutrons from deuterated cluster explosions driven by fs-laser pulses", *Phys. Rev. E* **74**, 016403 (2006)
- 7) R. Hartke, D. R. Symes, F. Buersgens, L. Ruggles, J. L. Porter, T. Ditmire, "Neutron Detector Calibration using a table-top laser heated plasma neutron source" *Nuc. Inst. And Methods A* **540**, 464 (2005).
- 8) T.D. Donnelly, J. Hogan, A. Mugler, M. Schubmehl, N. Schommer, Andrew J. Bernoff, S. Dasnurkar and T. Ditmire, "Using ultrasonic atomization to produce an aerosol of micron-scale particles", *Rev. Sci. Instr.* **76**, 113301 (2005).
- 9) K. W. Madison, R. Fitzpatrick, P. K. Patel, D. Price, T. Ditmire, "The role of laser pulse duration in Coulomb explosions of deuterium cluster targets" *Phys. Rev. A* **70**, 053201 (2004).
- 10) K. W. Madison, P. K. Patel, D. Price, A. Edens, M. Allen, T. E. Cowan, J. Zweiback, and T. Ditmire, "Fusion neutron and ion emission from laser induced explosions of deuterium and deuterated methane clusters" *Phys. Plas.* **11**, 270 (2004).
- 11) T. Ditmire, S. Bless, G. Dyer, A. Edens, W. Grigsby, G. Hays, K. Madison, A. Maltsev, J. Colvin, M. J. Edwards, R. W. Lee, P. Patel, D. Price, B. A. Remington, R. Sheppherd, A. Wootton, J. Zweiback, E. Liang and K. A. Kiely, " Overview of future directions in high energy-density and high-field science using ultra-intense lasers" *Rad. Phys. And Chem.* **70**, 535 (2004).
- 12) K. W. Madison, P. K. Patel, M. Allen, D. Price, T. Ditmire, "An investigation of fusion yield from exploding deuterium cluster plasmas produced by 100 TW laser pulses" *J. Opt. Soc. Am. B* **20**, 113 (2003).
- 13) J. W. G. Tisch, N. Hay, K. J. Mendham, E. Springate, D. R. Symes, A. J. Comley, M. B. Mason, E. T. Gumbrell, T. Ditmire, R. A. Smith, J. P. Marangos, M. H. R. Hutchinson, "Interaction of intense laser pulses with atomic clusters: Measurements of ion emission, simulations and applications" *Nuc. Inst. Meth. B – Beam Interactins with Materials and Atoms* **205**, 310 (2003).

# Ultracold Molecules: Physics in the Quantum Regime

John Doyle

Harvard University

17 Oxford Street

Cambridge MA 02138

[doyle@physics.harvard.edu](mailto:doyle@physics.harvard.edu)

## 1. Program Scope

Our research encompasses a unified approach to the trapping of both atoms and molecules. Our goal is to extend our work with CaH to NH and approach the ultracold regime. Our plan is to trap and cool NH molecules loaded directly from a molecular beam, and measure elastic and inelastic collisional cross sections. Cooling to the ultracold regime will be attempted. We note that as part of this work, we are continuing to develop an important trapping technique, buffer-gas loading. This method was invented in our lab and is able to cool large numbers of atoms and molecules.

## 2. Recent Progress

Milestones for this project include (x indicates complete):

- x-spectroscopic detection of ground-state NH molecules via LIF
- x-production of NH in a pulsed beam
- x-spectroscopic detection of ground-state NH molecules via absorption
- x-injection of NH beam into cryogenic buffer gas (including LIF and absorption detection)
- x-realization of 4 T deep trap run in vacuum
- x-injection of NH molecules into cryogenic trapping region
- x-loading of NH molecules into cryogenic buffer gas with 4 T deep trap
- x-trapping of NH
- x-measurement of spin-relaxation rate of NH with He
- o-removal of buffer gas after trapping of NH
- o-measurement of elastic and inelastic cross sections
- o-attempt evaporative cooling

NH, like many of the diatomic hydrides, has several advantages for molecular trapping including large rotational constant and relatively simple energy level structure. Some of the several key questions before us when this project began were: Could we produce enough NH using a pulsed beam? Is it possible to introduce a large number of NH molecules into a buffer gas? Would the light collection efficiency be enough for us to adequately detect fluorescence from NH? Could we get absorption spectroscopy to work so that absolute number measurements could be performed? Could we achieve initial loading of NH into the magnetic trap? Will the spin relaxation rates with helium be low enough for us to remove the buffer gas? We have now answered these questions, all to the positive.

There are important questions left. For example, will the NH-NH collision rates be adequate for evaporative cooling or will another method (like sympathetic or laser cooling) be necessary to cool NH into the ultracold regime. What will be the nature of an ultracold dense sample of heteronuclear molecules. Specifically, what about the hydrides, with their large rotational constants? These questions are still open and answering them are some of the stated long-term goals of this work.

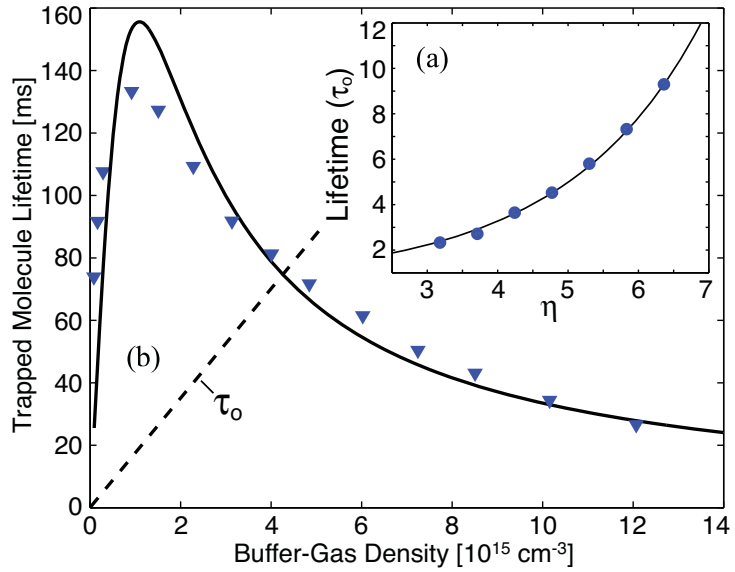


Figure 1: Lifetimes for magnetically trapped NH radicals vs. (a) trap depth and (b) buffer gas density. The decreasing lifetime with increasing buffer gas density is due to spin relaxation. This (and similar) data can be used to extract the He-NH spin relaxation cross section.

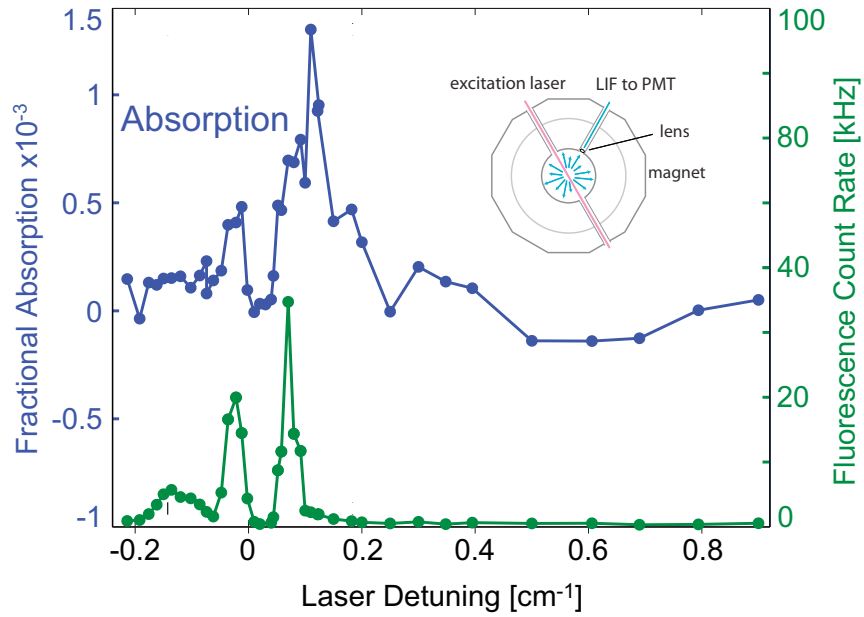


Figure 2: Spectra of trapped NH molecules in both absorption and fluorescence. The extension of the absorption spectra shows that absorption is not limited by the spatial filtering in collecting fluorescence photons. In the low field region of the trap the correspondence is excellent.

## Summary of Status of Project

The heart of the apparatus is a beam machine that we use to produce pulsed NH in a supersonic beam (see figure 2). (We are in the supersonic regime only to maximize NH flux; 3 dimensional translational cooling and rotational cooling are provided by the buffer gas.) The design of the pulsed source is based on the production of OH via DC discharge as executed by Nesbitt. In short, we have a pulsed valve and a slit plate with a layer of BN in between. A voltage between the plates and the nozzle of the pulsed valve produces a discharge whenever we allow gas into the nozzle. This is done by opening the pulsed valve, with a solenoid, for times about 1 ms.

This beam is directed toward our trapping magnet, inside of which is a cryogenic buffer-gas cell. This cell can be cooled to as low as 500 mK by a He<sup>3</sup> refrigerator. A small entrance orifice of a few mm in diameter to allow the beam of NH to enter the cell. Thus, buffer-gas cooling of the NH takes place. Several windows exist for the introduction and collection of light.

The basic experimental procedure is as follows. The pulse valve of our NH source is opened for times from about 10-100 ms. During this time a jet of ammonia exits the valve, entering the discharge region near the jaws, creating a beam of ammonia, NH and other species. This long pulse beam travels about 10 cm to the face of the cell where some portion enter through the orifice and into the cell. The NH are then cooled by the buffer gas to their rotational ground state. In our latest experiments we have been using fluorescence and absorption spectroscopy to detect the NH in the trapping region. We have been able to observe trapped NH molecules for longer than a second (1/e lifetimes as long as 900 ms). With such long trap lifetimes we are able to make measurements of key spin relaxation cross sections and compare with theory.

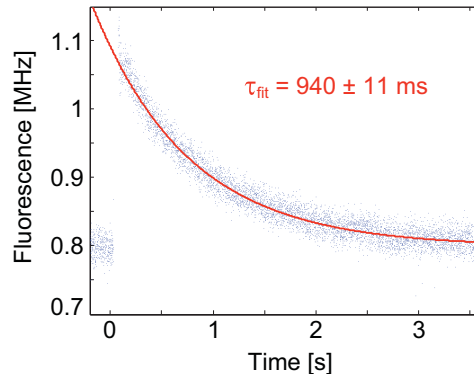
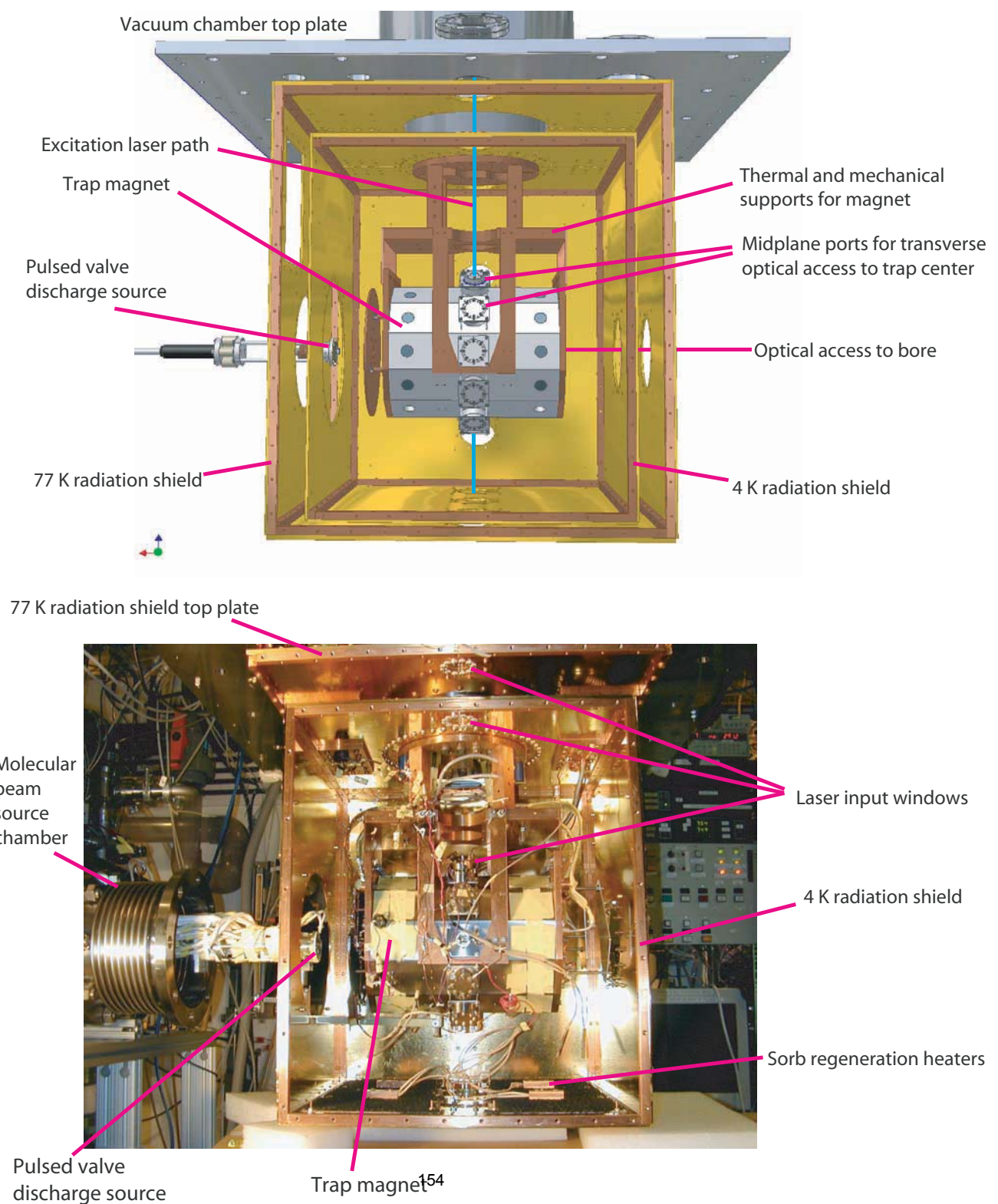


Figure 3: At fixed detection laser frequency the fluorescence signal is proportional to the number of trapped NH molecules. In this plot, the lifetime of the trapped molecules is evident, close to 1 second 1/e lifetime. The temperature is around 600 mK and the peak number of trapped NH is above  $10^8$ .

## 3. Future Plans

We continue on our program of trapping of NH. The next step is to lower the background He gas pressure by cryogenic pump out of the helium. We expect to first see a dramatic lengthening of the trap molecule lifetime to greater than 100 seconds. This should allow us to start seeing NH-NH collisional processes and determine the NH-NH spin relaxation rates. This will naturally lead to attempting evaporative cooling. It is our hope to increase the number of trapped NH molecules to make this regime even more accessible.

Figure 4:



# Atomic Electrons in Strong Radiation Fields

J. H. Eberly

Department of Physics and Astronomy  
University of Rochester, Rochester, NY 14627  
eberly@pas.rochester.edu

July 31, 2007

## Scope: Electron Correlation under Strong Laser Fields

We are interested to understand how very intense laser light couples to multi-electron atoms and molecules. Substantial challenges to theoretical study arise from the fully phase-coherent character, and the rapid time-dependence, of femtosecond-scale laser pulses bringing electric field forces on par with the coulomb forces of the nucleus and the pairwise electron-electron repulsion, as well as from the need to account accurately for two or more dynamically active electrons.

During 2006-2007 we have begun to obtain results from a large-scale extension of our fully classical ensemble method (summarized previously). Our conjecture about the reliability of a classical approach was originally based on close correspondences between our two-electron solutions of Schrödinger's 1d equation and the 1d statistical results we obtained with classical ensembles for two active electrons [1, 2]. Our current extensions follow a track outlined and published in several intervening reports [3, 4, 5, 6, 7]. We are now carrying out what we believe to be the first systematic calculations for three and four active atomic electrons in strong time-dependent and phase-coherent fields. We are also making the first direct full-dimensioned comparisons of the classical ensemble approach with both experimental data and with existing so-called S-matrix calculations.

## Recent Progress #1: Classical-Quantum Comparison

In confirmation of increasingly solid preliminary indications, our 3d classical results [8] are proving superior in matching experimental two-electron end-of-pulse momentum data (e.g. from neon [9]) to existing “S-matrix” predictions [10], as shown in Fig. 1 below. This superiority is not as surprising at it may seem, because the classical theory is a seamless unit, whereas in this regime the quantum calculations almost have to be *ad hoc* in nature. That is, the near-equality of the three active forces mentioned above precludes the rigorous step-by-step perturbative procedure of true S-matrix scattering theory. Instead, existing “S-matrix” calculations patch together classical and quantum and semi-classical elements as realistically as possible. They are typically characterized by a multi-stage sequence in which one electron is first identified as having tunneled out according to quantum barrier penetration theory. It is then classically thrown back to the nucleus (via Volkov theory, in wave function language), but is not permitted its own interaction with the nucleus. Finally,

an inner electron, which is not permitted to react to the laser force at all, is scattered out, along with the recolliding electron.

Both the classical calculations and the experimental neon data show that a majority of the ionized electrons have pairwise-similar momenta along the laser polarization axis (highest density of data points localized inside the 1st and 3rd quadrants in Fig. 1). The figure also shows that this is not what is achieved by the *S*-matrix calculations, which tend to predict one fast and one slow electron (densest data points near to one or the other of the axes).

We can adapt our classical method to make direct further comparisons with the *S*-matrix calculations by applying classically various approximations adopted in the *S*-matrix calculations, except for tunneling, of course. This comparison study [8] then allows us to determine the role of quantum tunneling. However, there is apparently no effect in this short-pulse and strong-field regime that is specifically due to tunneling, i.e., not also found in the completely classical simulation. The recollision dynamics initiated by a quantum tunneling process are not in any appreciable way distinct from the dynamics initiated by a fully classically correlated pathway. Our earlier conjecture appears to be supported, that a laser field strong enough to bend down the coulomb well far enough to make tunneling likely is also sufficiently strong to enforce energy exchanges among the bound electrons and give one of them enough energy to escape without tunneling.

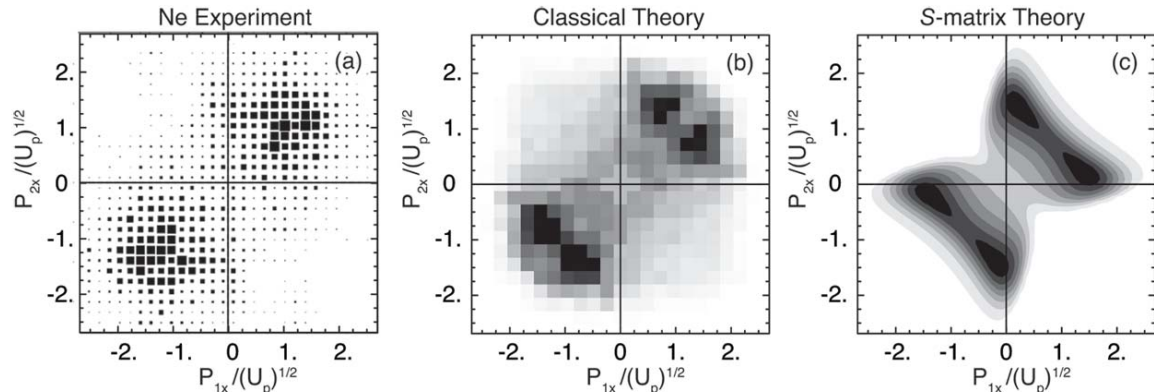


Figure 1: End-of-pulse two-electron momentum distributions along the laser polarization axis obtained from (a) COLTRIMS experiments with neon [9], (b) 3d classical ensemble calculations [8] and (c) *S*-matrix calculations [10]. Both (b) and (c) are based on a Coulomb-tail potential. Momentum is scaled to  $(U_p)^{1/2}$ , where  $U_p = I/4\omega^2$  is the ponderomotive energy of an electron. Both classical calculation and experimental neon data show a majority of ionized electrons with pairwise-similar momenta (densest data points well inside the 1st and 3rd quadrants of the figure). The *S*-matrix calculation produces mainly one fast and one slow electron (densest data points near to one or the other of the axes).

## Recent Progress #2: Multi-electron and Attosecond Dynamics

The other major element of our program to expand a completely classical approach to strong laser-field ionization is now also coming on line, in allowing more than two electrons to be dynamically active. There is generally conceded to be no realistic hope of similarly extending full-dimensional pulsed-laser quantum solutions at optical wavelengths, which were pioneered in the work on hydrogen by the Kulander team [11] and extended to the two-active-electron regime with solutions for helium by the Taylor group [12]. Fully quantum aspects of the three-active-electron regime are well beyond computational feasibility at the present time, requiring at least terabyte memory capacity.

However, pulsed-laser multi-electron ionization experiments with attention to electron correlation have been underway for a number of years [13]. Fortunately classical calculations can be more or less easily carried beyond two electrons. Within this reporting period our first results were published on three-electron ionization [6] for an in-plane scenario. Full-dimensioned work is underway, but the in-plane calculations already show some surprising consequences, e.g., one-to-three energy sharing (possibly even “thermalization”) among electrons in a recollision event. The time scale for sharing was very short, only 20-30 attoseconds.

In fully three-dimensional work some first-run multi-electron results have also been reported, particularly argon-like three-electron trajectories in intense-field double and triple ionization [14]. We continue to value our cooperation on multi-electron strong-field effects with the group of S.L. Haan at Calvin College [15, 16].

## Future Plans

Strong electron correlation of a classical nature is evident in laser-driven extreme conditions arising in ionization, and this makes continued classical modelling attractive for deeper examination of very complex high-field atomic phenomena on very short time scales. However, classical dominance of electron correlation is almost certainly not inevitable in extreme environments. The distinction between classical and quantum correlation is ultimately a matter of the degree of state entanglement between electrons. This raises important questions about issues of specifically quantum complexity under extreme conditions, and the dynamics of entanglement. We are planning that a fraction of our effort going forward will be devoted to an examination of questions related to this, to cooperative mechanisms for quantum correlation, and whether they exist or can be controlled.

## Acknowledgement

We are very pleased to note the recent announcement that Phay J. Ho, key student in this project for 3 years, has been awarded an Argonne National Lab Director’s Postdoctoral Fellowship beginning in the fall, working in the Chemistry Division in the group of Santra and Young. / Valuable extended discussions with S.L. Haan are acknowledged. / Publications marked with \*\*\* in the listing below have been supported by DOE Grant DE-FG02-05ER15713.

## References

- [1] R. Panfili, S. L. Haan, and J. H. Eberly, *Phys. Rev. Lett.* **89**, 113001 (2002). See also R. Panfili, J. H. Eberly and S. L. Haan, *Opt. Express* **8**, 431 (2001).
- [2] S. L. Haan, P. S. Wheeler, R. Panfili and J. H. Eberly, *Phys. Rev. A* **66**, 061402(R) (2002).
- [3] Phay J. Ho, R. Panfili, S. L. Haan and J. H. Eberly, *Phys. Rev. Lett.* **94**, 093002 (2005).
- [4] Phay J. Ho, *Phys. Rev. A* **74**, 045401 (2005).
- [5] \*\*\*Phay J. Ho and J.H. Eberly, *Phys. Rev. Lett.* **95**, 193002 (2005).
- [6] \*\*\*Phay J. Ho and J.H. Eberly, *Phys. Rev. Lett.* **97**, 083001 (2006).

- [7] \*\*\*S.L. Haan, L. Breen, A. Karim, and J. H. Eberly, *Phys. Rev. Lett.* **97**, 103008 (2006) [also selected for Virtual Journal of Ultrafast Science].
- [8] \*\*\*Phay J. Ho, X. Liu and W. Becker, arXiv:physics/0703219.
- [9] R. Moshammer, J. Ullrich, B. Feuerstein, D. Fischer, A. Dorn, C. D. Schröter, J. R. Crespo López-Urrutia, C. Höhr, H. Rottke, C. Trump, M. Wittmann, G. Korn, K. Hoffmann, and W. Sandner, *J. Phys. B* **36**, L113 (2003).
- [10] C. Figueira de Morisson Faria, X. Liu, H. Schomerus, and W. Becker, *Phys. Rev. A* **69**, 021402(R) (2004).
- [11] See, for example, K.J. Schafer and K. C. Kulander, *Phys. Rev. Lett.* **69**, 2642 (1992).
- [12] See, for example, the report on helium in J. S. Parker *et al.*, *J. Phys. B* **36**, L393 (2003).
- [13] Early examples are S. Laroche, A. Talebpour and S. L. Chin, *J. Phys. B* **31**, 1201 (1998), and E.A. Chowdhury and B. Walker, *J. Opt. Soc. Am. B* **20**, 109 (2003).
- [14] \*\*\*Phay J. Ho and J. H. Eberly, *Optics Expr.* **15**, 1845-1850 (2007).
- [15] \*\*\*S.L. Haan, L. Breen, A. Karim and J.H. Eberly, “Recollision Dynamics and Time Delay in Strong-Field Double Ionization,” *Optics Expr.* **15**, 767 (2007).
- [16] S.L. Haan and Z.S. Smith, “Classical explanation for electrons above the  $2U_p$  cutoff in strong-field double ionization at 390 nm” (submitted).

# Few-Body Fragmentation Interferometry

*Department of Energy 2007-2008*

James M Feagin

*Department of Physics*

*California State University–Fullerton  
Fullerton CA 92834*

jfeagin@fullerton.edu

We continue two parallel efforts with (i) emphasis on *detection interferometry* while (ii) pursuing longtime work on *collective Coulomb excitations*. We thus continue our ongoing DOE work to extract basic understanding and quantum control of few-body microscopic systems based on our practiced experience with more conventional studies of correlated electrons and ions. We have transitioned our efforts from few-body Coulomb dynamics and reaction detection—a longstanding theme of the BES program—to a somewhat broader perspective of reaction imaging interferometry. Although the work is theoretical, our interest in these topics has been strongly motivated by colleagues in this country and in Europe involved with charged-particle fragmentation experiments and seeking control over the resulting quantum correlations, which has become fairly routine in photon physics.

## Einstein's Recoiling-Slit Experiment

Some time ago, Wootters and Zurek<sup>1</sup> revisited the Einstein recoiling-slit gedanken experiment to analyze Young's double-slit interferometry to include in detail the photon which-path information stored in the recoiling entrance slit. They assumed an entrance slit cut into a spring-mounted plate that could be treated as a quantum oscillator under the action of a passing photon. They then considered alternative position and momentum measurements of the plate and the effect of the measurements on the photon interference. Wootters and Zurek thus exploited the underlying photon-plate entanglement to formulate quantitative statements about wave-particle duality, and their work became one of the first major publications on the subject.

We have analyzed photon scattering by a trapped ion as a modern realization of Wootters and Zurek's quantum analysis of the recoiling-slit experiment.<sup>2</sup> While a harmonically trapped ion provides a perfect quantum realization of a spring-mounted plate and entrance slit, we find that a coherent-state measurement of the recoiling ion, besides likely having experimental advantages, can mimic both position and momentum measurements of the ion in full analogy with Wootters and Zurek. One readily identifies the resulting photon fringe visibility as the overlap of recoil-ion marker states describing a photon scattered towards one or the other slit. When the overlap vanishes, the direction of the scattered photon can in principle be determined via the photon-ion entanglement by a measurement of the recoil ion, blocking an interference effect. On the other hand, when the overlap is perfect the interference is as well, and neither the direction of the recoiling ion nor of the scattered photon is discernible. The intermediate stage of duality characterized by moderate overlap continues to warrant further study.

Trapped-ion interferometry has advanced extraordinarily in recent years. Young's fringes formed by photons scattered by a pair of harmonically trapped  $^{198}\text{Hg}^+$  ions have been observed and analyzed in detail by Wineland, Itano, and co-workers at NIST-Boulder.<sup>3</sup> Coherent and

---

<sup>1</sup> W. K. Wootters and W. H. Zurek, Phys. Rev. D**19**, 473 (1979).

<sup>2</sup> R. S. Utter and J. M. Feagin, Phys. Rev. A **75**, 062105 (2007). (**Utter** was a CSUF masters degree student. This work was highlighted in the June 2007 issue of the Virtual Journal of Quantum Information, [vjquantuminfo.org/](http://vjquantuminfo.org/).)

<sup>3</sup> U. Eichmann et al., Phys. Rev. Lett. **70**, 2359 (1993); W. Itano et al., Phys. Rev. A **57**, 4176 (1998).

squeezed states<sup>4</sup> as well as double-humped *Schrödinger-cat* superpositions of displaced coherent states<sup>5</sup> of (external) motion of a harmonically trapped  ${}^9\text{Be}^+$  ion have been engineered by Monroe, Meekhof, Wineland, and coworkers. Entanglement analogous to the photon-ion-CM entanglement we have considered has been observed between the *internal* states of a trapped ion and a polarization-analyzed fluorescence photon by Blinov, Monroe, and co-workers at Michigan.<sup>6</sup> And in a recent tour de force, quantum teleportation between three trapped ions has been achieved by Wineland, Itano, and coworkers at NIST<sup>7</sup> and independently by Blatt and coworkers at the Universität Innsbuck.<sup>8</sup>

In order for the photon phase relations characterizing the system entanglement to remain accessible for local observation and interference, the ion-CM-recoil marker states must overlap. Otherwise, the ion recoil could be cleanly measured and the photon path (which port entered) determined unambiguously. If the overlap is perfect the fringes will be perfect, and if the overlap vanishes the fringes will as well. The ion recoil thus stores information on the port and path taken by the scattered photon. As articulated originally by Wootters and Zurek, the question becomes what goes on between these two extremes. For a given fringe visibility, how reliably can the photon path be predicted?

Although there is no definitive answer to this question, a straightforward estimate is simply to evaluate the difference between the joint probabilities for scattering the photon into one or the other port while detecting the recoiling ion summed over all possible recoil-ion measurement outcomes, the so called classical *trace distance*, or what Englert has referred to as the *which-path knowledge*.<sup>9</sup> One is thus led to consider the quantum trace distance, or distinguishability of the ways, as an upper bound on the classical trace distance, and one thereby recovers Englert's duality relation between the distinguishability and the fringe visibility.

We have also begun to examine various information-transfer strategies in the context of trapped-ion interferometry. The ion-recoil state (density operator) difference for photon scattering between the two ports defines an optimum observable of sorts whose eigenstates determine optimum ion measurements to maximize the which-path knowledge for a given fringe visibility if only which-port probabilities are accessible experimentally. One can also quantify the photon-path information transfer to the ion's external motion by evaluating the decrease in the ion's Shannon entropy due to the photon scattering for a given fringe visibility. Alternatively, we have found that one might wish to avoid the which-port probabilities altogether and introduce instead a POVM to distinguish for a given fringe visibility the state of the ion some of the time with certainty, but with the tradeoff that some of the tests will yield no information.

## Hardy Nonlocality

In parallel work, we have analyzed<sup>10</sup> the detection of a pair of recoiling reaction fragments, each by its own interferometer, to demonstrate Hardy's contradiction between quantum mechanics and local hidden variables.<sup>11</sup> Hardy's theorem sidesteps Bell's inequality by establishing the contradiction with just four measurement outcomes on two system fragments. Whereas Bell's theorem involves fully statistical violations of the quantum description, the Hardy result is simpler and hinges on essentially perfect correlations to establish nonlocality. Our interferometry is

<sup>4</sup> D. M. Meekhof, C. Monroe, W. Itano and D. J. Wineland, Phys. Rev. Lett. **76**, 1796 (1996).

<sup>5</sup> C. Monroe, D. M. Meekhof, B. E. King and D. J. Wineland, Science **272**, 1131 (1996).

<sup>6</sup> B. B. Blinov, D. L. Moehring, L.-M. Duan, and C. Monroe, Nature **428**, 153 (2004) and also E. Polzik, Nature **428**, 129 (2004).

<sup>7</sup> M. D. Barrett et al., Nature **429**, 737 (2004).

<sup>8</sup> M. Riebe, H. Häffner, C. F. Roos, W. Hnsel, J. Benhelm, G. P. T. Lancaster, T. W. Körber, C. Becher, F. Schmidt-Kaler, D. F. V. James and R. Blatt, Nature 429, 734 (2004).

<sup>9</sup> B.-G. Englert, Phys. Rev. Lett. **77**, 2154 (1996); Zeit. f. Naturforschung, **54a**, 11 (1999).

<sup>10</sup> J. M. Feagin, Phys. Rev. A **69**, 062103 (2004). (*This work was highlighted in the June 2004 issue of the Virtual Journal of Quantum Information, vjquantuminfo.org.*)

<sup>11</sup> L. Hardy, Phys. Rev. Lett. **71**, 1665 (1993)

based on the projectile-target momentum entanglement and is independent of the identity and internal state of the fragments. Although no doubt a very difficult experiment, our approach is thus relatively straightforward, at least conceptually.

We have recently revisited the Hardy theorem as a possible application of trapped-ion interferometry. Hardy nonlocality has thus far only been verified with down-converted and polarization-entangled photon pairs. Our current efforts have been to extend Hardy's analysis to the nonorthogonal coherent CM states of the trapped ion we used to analyze Einstein's recoiling-slit experiment, as described above.<sup>12</sup>

### Dichroism and Nondipolar Effects

Two-slit detection would also provide new probes of photoionization angular distributions. Even with the photo *single* ionization of an unoriented atom, we have demonstrated<sup>13</sup> that one could generate a circular dichroism analogous to the well established effect seen in photo *double* ionization<sup>14</sup> and thereby extract phase information on nondipolar amplitudes.

A related dichroism and nondipolar probe is expected in ordinary fluorescence in which a photon takes the role of the photoionized electron and is analyzed by two-port interferometry. Such an experiment is currently in progress at the University of Nebraska and interference fringes have been observed with rubidium fluorescence photons.<sup>15</sup> Our analysis indicates the technique may provide a useful method for extracting electric and magnetic *quadrupole* contributions to dipole allowed transitions.

### Two-Center Interferometry

It is natural to regard the position of a macroscopic object to be quasi-sharply defined: if a cat is sleeping in the chair, we don't consider for a moment that she may in fact be out on a bench in the garden. Yet, quantum mechanics encourages us to superpose displaced and narrow wavepackets to describe states of a single 'sleeping cat' that could be either in the chair or on a bench. This quantum reality and the wider notion of entanglement (something bumps the cat and adds bench and chair markers) are profound and continue to generate debate over what the wavefunction actually describes. Nevertheless, it is now widely recognized that interactions with the environment and their inevitable entanglements can dephase the quantum superpositions. The resulting decoherence eliminates macroscopic interferences and thereby restores a natural sense of reality. Our interest in this problem is an outgrowth of our general considerations of scattering interferometry and two-center interference effects from extended targets.<sup>16</sup>

Advances in atom interferometry and ion trapping now afford systematic study of quantum interferences in mesoscopic systems with parameters that can be tracked from quantum towards macroscopic limits. Along with the double-humped Schrödinger-cat CM states of a trapped ion engineered by Monroe and coworkers in Boulder,<sup>5</sup> Pritchard and coworkers at MIT<sup>17</sup> observed the interference fringes of a sodium atom passing through the two arms of a Mach-Zehnder interferometer and scattering a photon. Besides their novelty in traditional AMO collision physics, such target systems allow one to study quantum correlations in well controlled environments with relatively few quantum parameters. Within the impulse approximation, we have

<sup>12</sup> R. S. Utter and J. M. Feagin, Phys. Rev. A, *in preparation* (2007).

<sup>13</sup> J. M. Feagin, Phys. Rev. Lett. **88**, 043001 (2002).

<sup>14</sup> V. Mergel et al., Phys. Rev. Lett. **80**, 5301 (1998) and references therein; A. Knapp et al, J. Phys. B: At. Mol. Opt. Phys. **35**, L521 (2002). (*Feagin is a coauthor on these papers.*)

<sup>15</sup> T. Gay and H. Batelaan, *private communication*.

<sup>16</sup> J. M. Feagin and S. Han, Phys. Rev. Lett. **86**, 5039 (2001); Phys. Rev. Lett. **89**, 109302 (2002). (*Han was a CSUF masters degree student.*)

<sup>17</sup> M. S. Chapman et al., Phys. Rev. Lett. **75**, 3783 (1995); D. A. Kokorowski et al., Phys. Rev. Lett. **86**, 2191 (2001).

developed a framework<sup>18</sup> to connect these and related experiments including the observation of Young's fringes with photons scattered by a *pair* of trapped ions.<sup>19</sup>

## Collective Coulomb Excitations

These projects continue to link to our more conventional and longtime work in the AMO field of collective Coulomb excitations. For example, *multihit* detection of continuum electron pairs<sup>20</sup> has been extended to the photo double ionization of molecular hydrogen in the isotopic form D<sub>2</sub> including coincident detection of the deuterons.<sup>21</sup> In good analogy with the two-center interference discussed above, electron interference fringes have been recently observed by Weber and coworkers in both the electron and the recoil-ion angular distributions following H<sub>2</sub> full photo fragmentation.<sup>22</sup> Moreover, two-center interference effects have been observed in the double ionization of aligned hydrogen molecules by fast heavy ion impact.<sup>23</sup>

Parallel to these interests, we developed a model of molecular photo double ionization based closely on an analogous double-ionization model we established for helium.<sup>24</sup> These lowest-order approximations in the electron-pair angular momentum relative to a molecular axis have the advantage of providing approximate dynamical quantum numbers and propensity rules for excitation of certain molecular fragmentation configurations.<sup>25</sup> Our predictions have recently been studied in detail experimentally by T. Reddish and A. Huettz and coworkers in Paris.<sup>26</sup>

Dörner and coworkers have also recently extracted evidence that the photoionized electron pairs originate from one or the other center of the H<sub>2</sub>, namely, from the ionic (H<sup>-</sup>) contribution to the molecular ground state.<sup>22</sup> Thus, we are working to generalize our molecular model of double ionization to include these two-center ionic contributions along with the orientation of the molecular axis. We also intend to compare our predictions with the state-of-the-art *ab initio* computations which have been achieved by T. Rescigno and W. McCurdy and coworkers at LBNL.<sup>27</sup>

## Publications

*Trapped-Ion Realization of Einstein's Recoiling-Slit Experiment*, R. S. Utter and J. M. Feagin, Phys. Rev. A **75**, 062105 (2007). (**Utter** was a CSUF masters degree student. This work was highlighted in the June 2007 issue of the Virtual Journal of Quantum Information, [vjquantuminfo.org](http://vjquantuminfo.org).)

*Two-Center Interferometry and Decoherence Effects*, J. M. Feagin, Phys. Rev. A **73**, 022108 (2006).

*Hardy Nonlocality via Few-Body Fragmentation Imaging*, J. M. Feagin, Phys. Rev. A **69**, 062103 (2004). (This work was highlighted in the June 2004 issue of the Virtual Journal of Quantum Information, [vjquantuminfo.org](http://vjquantuminfo.org).)

*Fully Differential Cross Sections for Photo Double Ionization of Fixed-in-Space D<sub>2</sub>*, Th. Weber et al, Phys. Rev. Lett. **92**, 163001 (2004). (Feagin is a coauthor.)

---

<sup>18</sup> J. M. Feagin, Phys. Rev. A **73**, 022108 (2006).

<sup>19</sup> W. Itano et al., Phys. Rev. A **57**, 4176 (1998).

<sup>20</sup> A. Knapp et al, J. Phys. B: At. Mol. Opt. Phys. **35**, L521 (2002). (Feagin is a coauthor.)

<sup>21</sup> Th. Weber et al., Phys. Rev. Lett. **92**, 163001 (2004) and references therein. (Feagin is a coauthor.)

<sup>22</sup> R. Dörner (Frankfurt) and L. Cocke (Kansas State), private communication.

<sup>23</sup> A. L. Landers, E. Wells, T. Osipov, K. D. Carnes, A. S. Alnaser, J. A. Tanis, J. H. McGuire, I. Ben-Itzhak, and C. L. Cocke, Phys. Rev. A **70**, 042702 (2004).

<sup>24</sup> J. M. Feagin, J. Phys. B: At. Mol. Opt. Phys. **31**, L729 (1998); T. J. Reddish and J. M. Feagin, J. Phys. B: At. Mol. Opt. Phys. **32**, 2473 (1999).

<sup>25</sup> M. Walter, J. S. Briggs and J. M. Feagin, J. Phys. B: At. Mol. Opt. Phys. **33**, 2907 (2000).

<sup>26</sup> M. Gisselbrecht et al., Phys. Rev. Lett. **96**, 153002 (2006).

<sup>27</sup> W. Vanroose, F. Martin, T. N. Rescigno and C. W. McCurdy, Phys. Rev. A **70**, 050703 (R) (2004); Science **310**, 1787 (2005); C. W. McCurdy, private communication.

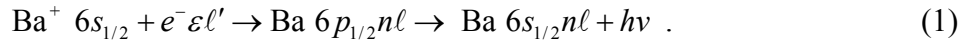
# Studies of Autoionizing States Relevant to Dielectronic Recombination

**T.F. Gallagher**  
**Department of Physics**  
**University of Virginia**  
**P.O. Box 400714**  
**Charlottesville, VA 22904-4714**  
tfg@virginia.edu

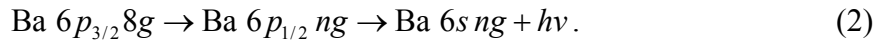
This program is focused on the doubly excited autoionizing states of alkaline earth atoms. The practical motivation of direct interest to the Department of Energy is that a systematic study of autoionization allows us to understand the reverse process, dielectronic recombination (DR), i.e., recombination of ions and electrons via intermediate autoionizing states. DR provides an efficient recombination mechanism for both laboratory and astrophysical plasmas.<sup>1-3</sup> The most important pathway for DR in high temperature plasmas, such as fusion plasmas, is through the autoionizing Rydberg states converging to the lowest lying excited states of the parent ion. As a result, DR rates are profoundly influenced by small electric and magnetic fields, which can originate in the charged particles of the plasma or be externally applied.

During the past year we have examined the effects of small electric, magnetic, and microwave fields on DR and developed microwave resonance techniques for bound states. These techniques should enable us to populate high angular momentum states without recourse to kV/cm electric fields.

In Ba, the atom we have studied, DR is the recombination of a free electron with a Ba<sup>+</sup> ion via an intermediate autoionizing state. This process can be written explicitly as



The incoming  $\varepsilon \ell'$  electron excites Ba<sup>+</sup> from the  $6s_{1/2}$  to  $6p_{1/2}$  state and is itself captured in the  $n\ell$  orbit. If radiative decay to the bound  $6s_{1/2} n\ell$  state occurs, recombination has taken place. In our experiments we do not really study DR but a process which we term DR from a continuum of finite bandwidth. In DR from a continuum of finite bandwidth we replace the true continuum with a continuum of finite bandwidth, the broad  $6p_{3/2}8g$  ionizing state straddling the Ba<sup>+</sup>  $6p_{1/2}$  limit.<sup>4</sup> Specifically, we have examined the process



An atom in the  $6p_{3/2}8g$  state makes the interchannel transition to the degenerate  $6p_{1/2}ng$  state ( $20 < n < \infty$ ). If it decays radiatively to the bound  $6s_{1/2}ng$  state, DR has occurred. The primary attractions of this technique are the energy resolution of  $\sim 0.5 \text{ cm}^{-1}$  ( $< 0.1 \text{ meV}$ ), the fact that the experiments can be done in zero electric and magnetic field, and that the partial wave of the entrance channel has a well defined  $\ell$ . In true DR all incoming  $\ell$  channels are allowed, but the capture rate from high  $\ell$  states is low. As a result, DR from a continuum of finite bandwidth is very similar to true DR. Nonetheless, the control of the incoming channel gives us more detailed

insight into the process. In the continuum of finite bandwidth experiments the  $8g$  electron makes about twenty orbits and collides with the  $\text{Ba}^+$  core twenty times before it autoionizes. Our experiments are similar to DR experiments done in storage rings,<sup>5</sup> in which the electrons have many opportunities to collide and recombine with the ions.

Enhancement of the process of Eq. (2) occurs at very low electric fields, those exceeding

$$E = \frac{3\delta_g}{2n^5}, \quad (3)$$

where  $\delta_g$  is the quantum defect of the  $6s_{1/2}ng$  state. The enhancement occurs because for fields in excess of this field the  $n\ell$  states of  $\ell \geq 4$  are converted to  $nk$  Stark states, all of which can contribute to DR.<sup>6</sup> In general we see an enhancement of DR by a factor of twenty. The enhancement is entirely expected,<sup>7</sup> but at several energies we observe narrow,  $3 \text{ cm}^{-1}$ , holes in the DR signals. We attribute these holes to the coupling of the  $6s_{1/2}nk$  states to the  $6p_{3/2}8h$  and  $6p_{3/2}8i$  states, which provide rapid autoionization pathways, which are a loss for DR. Similar spectral holes have recently been observed in fluorescence yield spectra of doubly excited He,<sup>8</sup> for essentially the same reason, and they ought to be visible in storage ring DR measurements as well.

Our original motivation for concentrating on DR from a continuum of finite bandwidth via the  $ng$  states, the process of Eq. (2), is that the requisite electric fields for enhancing the DR rate are small, and the hydrogenic energy spacing between the Stark states,  $3nE$ , is small. Thus the magnetic field required to produce comparable shifts is small, and it should be possible to observe a decrease in the DR signal when the magnetic field shift overwhelms the E field splitting and turns off the E field mixing.<sup>9,10</sup> in fact, working in a very low electric field has another very interesting benefit. Specifically, the E field splitting,  $3nE$ , is small enough that it does not in all cases determine the magnetic field required for enhancement of the DR rate. Our measurements show that the magnetic field coupling must also exceed the autoionization and radiative decay rates of the  $6p_{1/2}nk$  states, and we have observed the crossover from the requirement of the B field mixing's exceeding the autoionization rate to exceeding the Stark splitting of adjacent levels.

We have previously shown that a microwave field resonant with the  $n$  to  $n+1$  transition resonantly enhances the DR rate.<sup>11</sup> The mechanism is the resonant mixing of the higher angular momentum states, thereby converting them to Stark states. Our first measurements were done using the  $6p_{3/2}11d$  state as the continuum of finite bandwidth. In this case the entrance channel into the  $6p_{1/2}nl$  Rydberg states is a  $6p_{1/2}nd$  state, which has a quantum defect of magnitude 0.25. The transition from the  $6p_{1/2}nd$  state to the  $6p_{1/2}nf$  state is 25% higher than the hydrogenic frequency, while the  $6p_{1/2}ng$  to  $6p_{1/2}nh$  frequency is only 2% from the hydrogenic frequency. Due to the smaller detuning from the hydrogenic, or high  $\ell$ , frequency we expected a smaller field to be required to enhance DR from the  $6p_{3/2}8g$  continuum of finite bandwidth than from the  $6p_{3/2}11d$  continuum of finite bandwidth. Using a 21 GHz frequency microwave field we have observed that a factor of ten smaller field is required for the former than for the latter. Specifically, at the  $\Delta n=1$  resonance, occurring at  $n=68$ , we observe enhancement at 0.47 V/cm for DR via the  $ng$  states, but at 4.4 V/cm for DR via the  $nd$  states.

One of the motivations for applying the microwave field was to mimic electron collisions, which do not produce fields with well defined frequencies. Accordingly, we have examined the enhancement of DR by microwave noise, specifically, a 3 GHz wide noise source centered at 21 GHz. The result is very similar to that observed with a narrow band 21 GHz source of the same power. Apparently using the microwave field to mimic electron collisions is reasonable.

We have recently discovered that we are able to transfer all the atoms from the Ba  $6s(n+2)d$  states to the  $6sng$  states by resonant two photon microwave transitions. The surprising aspect of the process is its high resolution, 100kHz, in spite of the fact that the transitions are occurring in the earth's magnetic field. The narrow linewidth results from the fact that the g factor for singlet states is always one, so all  $\Delta m = 0$  transitions are coincident in frequency. We have measured these intervals from  $n=31$  to  $n=44$ , using microwave frequencies from 13 to 40 GHz. By carefully controlling the stray electric fields we are able to make accurate measurements of the  $6sng$  to  $6s(n+2)d$  intervals. These intervals link previous optical measurements of the  $6sng$  and  $6snd$  energies,<sup>12,13</sup> and enable us to transfer the higher accuracy of the  $6sng$  energies to the  $6snd$  states. The result is an improvement of an order of magnitude in the accuracy of the  $6snd$  quantum defects. What is more interesting is that by applying fields of 1 V/cm we are able to observe the Stark states originating from the  $6sn\ell$  states of  $\ell > 4$ , and it should be possible to produce high  $\ell$  states by Stark switching with 1 V/cm fields instead of 1 kV/cm fields.<sup>14</sup> This capability should enable us to probe autoionization of high angular momentum states in manageably small electric fields.

In the coming year we plan to finish the ongoing work on the enhancement of DR from  $ng$  states in combined E and B fields. Specifically, we plan to explore the effects of magnetic and electric fields applied at angles other than 0 and 90° and attempt to apply magnetic fields strong enough to undo the mixing produced by the electric field. To do the latter experiment we plan to use a circularly polarized microwave field, which has the same effect as a magnetic field, except that there is no diamagnetism. In addition, we plan to begin exploring autoionization of higher  $\ell$  states converging to the Ba<sup>+</sup>  $6p_{3/2}$  limit in low electric fields.

## References

1. A. Burgess, *Astrophys. J.* **139**, 776 (1964).
2. A.L. Merts, R.D. Cowan, and N.H. Magee, Jr., Los Alamos Report No. LA-62200-MS (1976).
3. S. B. Kraemer, G. J. Ferland, and J. R. Gabel, *ApJ.* **604** 556 (2004).
4. J.P. Connerade, *Proc. R. Soc. London, Ser. A*, **362**, 361 (1978).
5. G. Kilgus, J. Berger, P. Blatt, M. Grieser, D. Habs, B. Hochadel, E. Jaeschke, D. Kramer, R. Neumann, G. Neureither, W. Ott, D. Schwalm, M. Steck, R. Stokstad, E. Smolza, A. Wolf, R. Schuch, A. Muller, and M. Wagner, *Phys. Rev. Lett.* **64**, 737 (1990).
6. V. L. Jacobs, J. L. Davis, and P. C. Kepple, *Phys. Rev. Lett.* **37**, 1390 (1976).
7. L. Ko, V. Klimenko and T.F. Gallagher, *Phys. Rev. A*, **59**, 2126 (1999).
8. C. Sathe, M. Strom, M. Agaker, J. Soderstrom, J. E. Rubenson, R. Richter, M. Alagia, S. Stranges, T. W. Gorczyca, and F. Robicheaux, *Phys. Rev. Lett.* **96**, 043002 (2006).
9. F. Robicheaux and M. S. Pindzola, *Phys. Rev. Lett.* **79**, 2237 (1997).
10. V. Klimenko and T.F. Gallagher, *Phys. Rev. A* **66**, 023401 (2002).
11. V. Klimenko and T.F. Gallagher, *Phys. Rev. Lett.* **85**, 3357 (2000).
12. W. Vassen, E. Bente, and W. Hogervorst, *J. Phys. B* **20**, 2383 (1987).
13. J. Neukammer, G. Jonsson, A. Konig, K. Vietzke, H. Hieronymus, and H. Rinneberg, *Phys. Rev. A* **38**, 2804 (2002).
14. R. R. Jones and T. F. Gallagher, *Phys. Rev. A* **38**, 2846 (1988).

## Publications 2004-2006

1. E.S. Shuman and T.F. Gallagher, "Resonant Enhancement of dielectronic recombination by a high frequency microwave field," *Phys. Rev. A* **71**, 033415 (2005).
2. E. S. Shuman and T. F. Gallagher, "Microwave Spectroscopy of autoionizing Ba  $5d_{3/2}n\ell$  states" *Phys. Rev. A* **73**, 032511 (2006).
3. E. S. Shuman and T. F. Gallagher, "Ionic dipole and quadrupole matrix elements from nonadiabatic core polarization" *Phys. Rev. A* **74**, 022502 (2006).
4. W. Yang, E. S. Shuman, and T. F. Gallagher, "Spectral hole burning in the dielectronic recombination from a continuum of finite bandwidth," *Phys. Rev. A* **75**, 023411 (2007).
5. E. S. Shuman, J. Nunkaew, and T. F. Gallagher, "Two-photon spectroscopy of Ba  $6sn\ell$  states," *Phys. Rev. A* **75**, 044501 (2007).

## **Experiments in Ultracold Collisions and Ultracold Molecules**

Phillip L. Gould  
Department of Physics U-3046  
University of Connecticut  
2152 Hillside Road  
Storrs, CT 06269-3046  
[<phillip.gould@uconn.edu>](mailto:<phillip.gould@uconn.edu>)

### **Program Scope:**

Ultracold atoms and molecules have come to play a central role in modern atomic, molecular and optical (AMO) physics. Various cooling techniques, including laser cooling, buffer gas cooling, electrostatic slowing, and evaporative cooling, have been coupled with numerous confinement devices, such as magneto-optical traps, laser dipole traps, electrostatic traps, and magnetic traps, thereby enabling the preparation of extremely cold and dense samples. A variety of applications have emerged including: quantum degenerate gases (bosons, fermions, and mixtures); precision measurements and atomic clocks; quantum optics and cavity QED; atom optics and interferometry; targets for ionization studies; optical lattices and quantum computation; ultracold plasmas; ultracold chemistry; and ultracold collisions. At the high densities and low temperatures typically encountered in these studies, interactions between the particles are important. Inelastic collisions can cause undesirable heating and/or loss in high-density samples. On the other hand, processes such photoassociation and magnetoassociation (using a Feshbach resonance) are useful in forming ultracold molecules from the constituent atoms. The main goal of our experimental program is to exploit our ability to control the collision dynamics with frequency-chirped laser light. An especially exciting prospect is to bring the elements of coherent control to the photoassociative formation of ultracold molecules.

Our ultracold collision experiments use a diode-laser-based Rb magneto-optical trap (MOT). Rb is a convenient atom for several reasons: 1) its resonance lines are well-matched to readily available diodes lasers; 2) there are two stable and abundant isotopes ( $^{85}\text{Rb}$  and  $^{87}\text{Rb}$ ); 3) because of its favorable collisional properties,  $^{87}\text{Rb}$  has emerged as the most popular atom for BEC studies; and 4) formation of ultracold  $\text{Rb}_2$  molecules by photoassociation has been extensively studied. In our experiments, a phase-stable MOT is loaded from a slow atomic beam. To date, our studies have focused on inelastic collisions, measured via the density-dependent atomic loss rate from the trap.

### **Recent Progress:**

Recently, we have explored two aspects of ultracold collisions induced by pulses of frequency-chirped laser light: the dependence on chirp direction; and the effects of multiple pulses. The dominant long-range interaction between two colliding atoms, separated by  $R$ , is the  $1/R^3$  dipole-dipole potential. The detuning of the light relative to the atomic resonance determines the Condon radius  $R_c$ , the separation at which the atom pair is excited to this potential. If the excited pair subsequently gains sufficient kinetic

energy (e.g., >1 K) in rolling down the attractive potential, the atoms will escape from the trap. By “chirping” the light, i.e., changing its frequency as a function of time, atom pairs spanning a wide range of  $R$  can be excited and caused to undergo inelastic trap-loss collisions. One advantage of using chirped light is that for sufficiently high intensities, the population transfer to the excited state can be adiabatic, and therefore efficient and robust. Also, if the time scale of the chirp is comparable to that of the atomic motion, the collision can be controlled by the details of the chirp.

We have examined the dependence of the collision rate on chirp direction and found interesting differences for certain center detunings of the chirp. For the positive (red-to-blue) chirp, the collision rate is small at large negative detunings, and increases smoothly as the detuning approaches zero (i.e., as the center frequency of the chirp approaches the atomic resonance). The increase is due to excitation at longer range where more pairs are available. The smooth behavior is expected because the chirp causes  $R_c$  to move *outward*, while the resulting excited atom pairs accelerate *inward* on the attractive potential. Only the initial excitation is important since an atom pair, once excited, does not further interact with the positively chirped field. The negative (blue-to-red) chirp exhibits a rather different behavior. In this case, the Condon radius and the trajectory of the excited atom pair both proceed inward and further interactions between the two are therefore possible. The data show that for center detunings around -700 MHz, fewer collisions occur with the negative chirp than with the positive chirp. Based on comparisons with classical Monte-Carlo simulations of the collisional trajectories, we attribute this reduction to “collision blocking”: an atom pair is initially excited to the attractive potential by the negative chirp, then a short time later is de-excited by the same chirp. This stimulated de-excitation occurs before the atom pair has gained sufficient kinetic energy to escape from the trap, and thereby prevents an observable collision. By contrast, for smaller negative detunings (e.g., -300 MHz), we find that the negative chirp yields more collisions than the positive chirp. We attribute this to “flux enhancement”. In this process, an atom pair is excited at long range early in the chirp, but gains minimal kinetic energy before spontaneously decaying back to the ground state. This same pair of atoms, now moving towards each other, can be re-excited later in the chirp, this time at short range, where an observable inelastic collision is much more likely to occur. The first excitation enhances the collisional flux available for the second excitation. These two effects, collision blocking and flux enhancement, do not occur with the positive chirp. In this case, only one interaction between the light and the atom pair is possible.

We have also investigated multiple-chirp effects. By varying the delay between successive chirped pulses, we measure how the collisions induced by a given pulse are influenced by the preceding pulse. In the limit of long delay (e.g., 1  $\mu$ s), the chirped pulses act independently. For shorter delays, we observe both enhancement and depletion effects. At a center detuning for the chirp of -300 MHz, an earlier chirp enhances the rate of collisions induced by a later chirp. This is similar to the flux enhancement discussed above for a single chirp, but now involving two chirps. At a -600 MHz center detuning, we observe depletion at the shortest delay (200 ns). The first chirp efficiently excites (and causes to collide) all available atom pairs within the chirp range, leaving none to be excited by the second chirp. This depleted pair distribution is eventually replenished by the thermal motion of the ultracold atoms.

To date, our experiments have used frequency-chirped light (e.g., 1 GHz in 100 ns) generated by a current-ramped external-cavity diode laser and amplified by a separate “slave” laser. We have developed a new technique based on a fiber-based electro-optic phase modulator driven by an arbitrary waveform generator. In this scheme, a pulse of light from a diode laser is sent through the modulator multiple times, acquiring the prescribed phase shift during each pass. Each time it emerges from the fiber loop, the light is re-injected into the initial laser to boost the power. We realize much higher chirp rates (e.g., 1 GHz in 10 ns) and have the ability to produce chirps of arbitrary shape. A similar fiber-based device allows us to control the intensity on the nanosecond time scale.

#### Future Plans:

We will use our new chirping method to vary the chirp shape and optimize the trap-loss collision rate. This will be similar to short-pulse coherent control experiments, but on a much slower time scale. Instead of dispersing the pulse, manipulating the various frequency components, and then reassembling the pulse, we will directly control the phase and amplitude in the time domain. Since we are ultimately interested in applying our techniques to coherently control the formation of ultracold molecules, we will modify our apparatus to allow the direct detection (by pulsed laser ionization) of ground-state molecules. We will then use chirped photoassociation, as well as photoassociation enhanced by chirped long-range excitation, to optimize the production of ground-state molecules. In general, we anticipate that our ability to control the temporal variation of both the laser frequency (by chirping) and amplitude (by pulsing) will open up new opportunities in the manipulation of ultracold collisions and molecule formation.

#### Recent Publications:

“Landau-Zener Problem for Trilinear Systems”, A. Ishkhanyan, M. Mackie, A. Carmichael, P.L. Gould, and J. Javanainen, Phys. Rev. A **69**, 043612 (2004).

“Frequency-Chirped Light from an Injection-Locked Diode Laser”, M.J. Wright, P.L. Gould, and S.D. Gensemer, Rev. Sci. Instrum. **75**, 4718 (2004).

“Control of Ultracold Collisions with Frequency-Chirped Light”, M.J. Wright, S.D. Gensemer, J. Vala, R. Kosloff, and P.L. Gould, Phys. Rev. Lett. **95**, 063001 (2005).

“Probing Ultracold Collisional Dynamics with Frequency-Chirped Pulses”, M.J. Wright, J.A. Pechkis, J.L. Carini, and P.L. Gould, Phys. Rev. A **74**, 063402 (2006).

“Coherent Control of Ultracold Collisions with Chirped Light: Direction Matters”, M.J. Wright, J.A. Pechkis, J.L. Carini, S. Kallush, R. Kosloff, and P.L. Gould, Phys. Rev. A **75**, 051401(R), (2007).

“Generation of Arbitrary Frequency Chirps with a Fiber-Based Phase Modulator and Self-Injection-Locked Diode Laser”, C.E. Rogers III, M.J. Wright, J.L. Carini, J.A. Pechkis, and P.L. Gould, J. Opt. Soc. Am. B **24**, 1249 (2007).

Physics of Correlated Systems

Chris H. Greene

Department of Physics and JILA

University of Colorado, Boulder, CO 80309-0440

[chris.greene@colorado.edu](mailto:chris.greene@colorado.edu)

**Program Scope**

This project concentrates on the quantum theory of atomic and molecular systems that interact, in some cases with incident photons, electrons, or ions. Such interactions mediate the transformation of energy from one form into another in a numerous diverse contexts. Frequently in systems studied in atomic, molecular, and optical physics, the starting point for theoretical descriptions of the interacting bodies is achieved through an independent particle approximation, where one degree of freedom has little effect on other degrees of freedom. But in energy control or generation processes, these approximations are invariably inadequate and must be treated more realistically.

Our group concentrates on building theoretical methodologies that describe complicated phenomena associated with energy exchange between different degrees of freedom in an atomic or molecular system. Most of the systems studied possess multiple interacting channels or pathways through which energy can flow. The fundamental underlying equations of quantum mechanics are believed to be known, dating all the way back to the work of Erwin Schrödinger. However, the exact solution of the quantum mechanical equations is highly challenging, or even impossible, with present day computational capabilities, especially for systems where energy exchange occurs readily. In such systems, strong resonance phenomena often dominate and weak-coupling methods fail to capture the key physics. Our group formulates nonperturbative techniques and approximations that encapsulate the essential aspects, and applies these techniques to systems of experimental interest through numerical computations. Over the period of time this project has received support, this strategy has been applied to many different atomic and molecular systems. One recent area of study has been a theoretical calculation of resonant electron scattering by the bases, phosphate, and sugar components of DNA and RNA, which is relevant to studying mechanisms by which secondary electrons produced by radiation cause strand breaks. [1-4] This connects with studies we have been carrying out on the dissociative recombination of triatomic molecules such as  $\text{NO}_2^+$ .[5-7] We have also studied in depth the explosion of a rare gas cluster after it has been subjected to a pulse of vacuum-ultraviolet radiation from a free-electron laser.[8] In another project related to dynamics triggered by a short-pulse laser, we have identified the quantum mechanical pathways relevant to vibrational excitations that accompany the high-harmonic generation process in polyatomic molecules.[9]

**Recent Progress**

We have continued a project initiated within the past two years, in which a theoretical treatment is developed that can describe resonant excitation of the DNA and RNA bases subjected to collisions with low energy electrons. The crucial role of such resonances has been particularly stressed in the work of Leon Sanche and his collaborators. Previous theoretical progress in electron collisions with polyatomic molecules, at least in our

group, has primarily been restricted to species smaller than biologically interesting molecules.

A recent PhD student funded by this project, Stefano Tonzani, developed a three-dimensional finite-element R-matrix scattering program[1,4] capable of treating molecules as large as the DNA and RNA bases, the two purines adenine( $C_5H_5N_5$ ), guanine( $C_5H_5N_5O$ ), and the pyrimidines thymine( $C_5H_6N_2O_2$ ), cytosine( $C_4H_5N_3O$ ), and uracil( $C_4H_4N_2O_2$ ).[2,3] The shape resonances in these bases are of importance for understanding single and double strand breaks that are caused by collisions with low energy secondary electrons; this has become realized through the important work of the Sanche group. Our most recent publication along these lines was an application [2] of these techniques to the other major parts of DNA other than the bases, namely to predict electron scattering resonances in tetrahydrofuran (THF,  $C_4H_8O$ ), which is similar to deoxyribose, and in phosphoric acid ( $H_3PO_4$ ). The work to date has concentrated on solving the clamped-nucleus part of the problem, and it remains a future goal to describe the transformation of this electronic resonance energy into bond breakage in these complicated species. Eventually we plan to build on the progress we have made in recent years on the description of dissociative recombination in polyatomic molecules, including the role of the Jahn-Teller and Renner-Teller effects.[5-7] For such studies, we anticipate that our improved understanding of Siegert pseudostates, achieved in the course of paper [10] below, should prove to be very useful.

Last year, graduate student Zachary Walters completed a first set of calculations aimed at interpreting a recent experiment by the Kapteyn-Murnane group on high-harmonic generation in the  $SF_6$  molecule.[9] He also finished calculations that introduced a number of improvements to the initial model calculations we initially presented in our 2003 Physical Review Letter on the behavior of a xenon cluster in an intense short-pulse of radiation from a VUV free-electron laser. The new study has provided a more complete and quantitative description of this new regime of laser-cluster interaction dynamics, including specifically a successful model for understanding the distribution of ejected electron energies.[8]

### Immediate Plans

Among the projects that will continue during the coming year, we have already made significant headway in a collaborative effort with former student Tonzani and with the Sanche group that is developing a multiple scattering treatment of resonant electron scattering by a segment of DNA. In particular, we are combining the individual scattering matrices for an incident electron, from the various major DNA components, and then using this to treat scattering from a full twist of the DNA double helix. Hopefully this will demonstrate whether there are further resonance-enhancing or – diminishing effects associated with the global structure of DNA, which can modify the resonant scattering by individual component subunits. In a continuation and nontrivial extension of our studies of dissociative recombination of triatomic molecules, a major thrust during the coming year will attempt to predict for the first time the low-energy

dissociative recombination rate coefficient for electrons that collide with the  $\text{NO}_2^+$  molecule. Somewhat surprisingly, there has been no theoretical or experimental rate yet determined for this atmospherically-relevant species, but postdoc Dan Haxton has already made good headway. The study of high-harmonic generation by current graduate student Zachary Walters is also continuing, refining and hopefully extending the treatment of vibrational effects in high harmonic generation that follows molecular excitation by a weaker Raman pulse. Some supporting calculations have also been initiated in collaboration with Dan Elliott's group to explore a class of single-photon and multiphoton ionization processes in atomic barium.

### **Papers published since 2005 that were supported at least in part by this grant**

- [1] *FERM3D: A finite element R-matrix general electron molecule scattering code*, S. Tonzani, Comp. Phys. Commun. **176**, 146-156 (2007).
- [2] *Radiation damage to DNA: electron scattering from the backbone subunits*. S. Tonzani and C. H. Greene, J. Chem. Phys. **125**, 094504-1 to -7 (2006).
- [3] *Low energy electron scattering from DNA and RNA bases: shape resonances and radiation damage*, S. Tonzani and C. H. Greene, J. Chem. Phys. **124**, 054312-1 to -11 (2006).
- [4] *Electron-molecule scattering calculations in a 3D finite element R-matrix approach*, S. Tonzani and C. H. Greene, J. Chem. Phys **122**, 014111-1 to -8 (2005).
- [5] *Theoretical progress and challenges in  $H_3^+$  dissociative recombination*, C. H. Greene and V. Kokououline, Phil. Trans. R. Soc. A **364**, 2965-2980 (2007). (This study and the next one below were both supported partially by DOE and partially by NSF).
- [6] *Theoretical study of the  $H_3^+$  ion dissociative recombination process*, V. Kokououline and C. H. Greene, J. Phys. Conf. Series **4**, 74-82 (2005).
- [7] *Dissociative recombination of  $\text{HCO}^+$* , A. Larson, S. Tonzani, R. Santra, and C. H. Greene, J. Phys. Conf. Series **4**, 148-154 (2005).
- [8] *Interaction of intense VUV radiation with large xenon clusters*, Z. B. Walters, R. Santra, and C. H. Greene, Phys. Rev. A **74**, 043204-1 to -14 (2006).
- [9] *High harmonic generation in  $\text{SF}_6$ : Raman-excited vibrational quantum beats*, Z. B. Walters, S. Tonzani, and C. H. Greene, arXiv:physics/0701113.
- [10] *Siegert pseudostates: Completeness and time evolution*, R. Santra, J. M. Shainline, and C. H. Greene, Phys. Rev. A **71**, 032703-1 to -12 (2005).

## Strongly-Interacting Quantum Gases

**Principal Investigator:** Murray Holland

[murray.holland@colorado.edu](mailto:murray.holland@colorado.edu)

*440 UCB, JILA, University of Colorado, Boulder, CO 80309-0440*

### Program Scope

The dilute quantum gas is a controllable system in which to study strongly-interacting many-body phenomena in both equilibrium and dynamic regimes. There can be many avenues of interest, ranging from fundamental to applied, in which the aim is to explore and study the effect of strong interactions on the macroscopic properties and observables. Our program of research is based on the theoretical description of these quantum systems, and in making connections with a diverse set of fields of physics for which these problems are relevant. In essence, strongly-interacting phenomena occur when either individual interactions between particles are resonantly enhanced, or in which a macroscopic degeneracy exists in the spectrum of single-particle energy states, so that the interactions between particles then completely determine the form of the stationary and non-stationary properties.

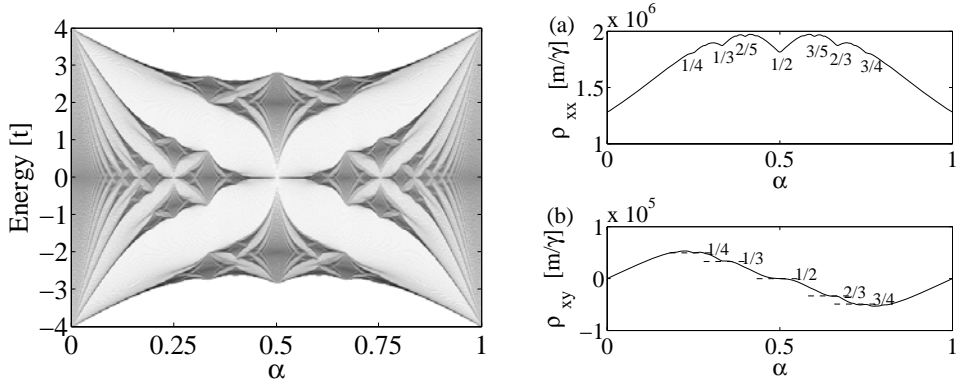
Over this past year, we have continued our studies in a few specific emerging areas. We have analyzed atoms in a rotating optical lattice and demonstrated direct links to the fractional quantum Hall effect from condensed matter physics. We have constructed a systematic approach to the hierarchy of many-body correlations in the BEC/BCS crossover through the unitary limit. We have also explored a new and promising topic called *atomtronics*—an atom analogue of semiconductor devices such as diodes and transistors. An interesting aspect of this strongly-interacting system is that it operates in the steady-state rather than stationary regime and can be far from equilibrium in this sense. A major new development has been a new branch of research in the study of spin squeezing in optical lattice clocks via lattice-based QND measurements.

### Hall effects in Bose-Einstein condensates in a rotating optical lattice

The fractional quantum Hall effect has been predicted theoretically for a two-dimensional condensate rotating at a frequency matching that of the confining harmonic trap. However, the strongly-correlated regime has eluded experimentalists in cold quantum gases due to two problems: it is difficult to confine condensates at rotation speeds matching the trapping frequency and vortex shears destroy condensates at high rotation. We have shown a potential solution to be the use of a two dimensional lattice. Introducing a co-rotating optical lattice in the tight-binding regime, in which particles on a lattice site can only tunnel to adjacent sites, provides strong confinement and enhances interactions to enable entry into the strongly-correlated regime. Similar rotating lattice systems have recently been experimentally demonstrated in the group of Cornell at JILA. As the rotation is increased, such a system undergoes a series of transitions of quasi-angular-momentum, analogous to the

introduction of vortices into the lattice (Peden *et al.*, condmat preprint 2007).

The Hamiltonian for this system is similar to that for Bloch electrons in a magnetic field. Density redistribution in strongly-correlated many-particle systems shows the equivalent of the classical effect and the mapping between the Coriolis and Lorentz forces. In order to predict observables of relevance to experiments, we developed over this past year a linear response theory and Kubo formalism (Bhat *et al.*, condmat preprint 2007), demonstrating fractional quantum Hall features in a rotating Bose-Einstein condensate in a two-dimensional optical lattice. The co-rotating lattice and trap potential allow for an effective magnetic field and compensation of the centrifugal potential. Fractional quantum Hall features are seen for the single-particle system and for few strongly interacting many-particle systems.



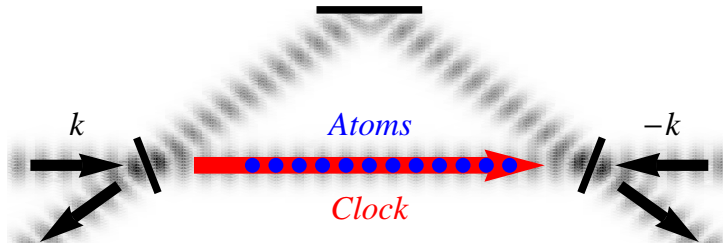
(Left) Single particle energy spectra (analogous to the well-known Hofstadter butterfly) as a function of the rescaled angular velocity  $\alpha$  for a  $40 \times 40$  lattice. Darker shading indicates greater density of states. The origin of the  $y$ -axis has been shifted to coincide with the onsite energy. (Right) (a) Diagonal and (b) transverse resistivity as a function of angular velocity for a single particle in a  $40 \times 40$  lattice subject to a linear-ramp perturbation. Fractional statistics are evident.

### Spin squeezing in optical lattice clocks via lattice-based QND measurements

In recent years atomic clocks in the optical frequency domain with neutral atoms in optical lattices have reached a level of precision of one part in  $10^{15}$  and have become competitive with the most accurate clocks in the microwave regime and with clocks using trapped ions. The rapid improvement of the precision of optical clocks over the past decade is largely due to two breakthroughs: First, novel trapping and cooling techniques have made ultra-cold neutral atoms available and second extremely broadband coherent light sources have been developed that can be used for optical frequency combs. In the latest generation of lattice clocks technical and external noise sources have been eliminated to the point where the precision of the clock is limited by the intrinsic projection noise. Projection noise which scales as  $1/\sqrt{N}$  for  $N$  uncorrelated atoms arises from the intrinsic quantum uncertainty in the populations of the atoms after lasers are used to drive transitions between clock levels.

Our basic idea, worked out in collaboration with Jun Ye, is to improve the clock as illustrated below. The optical lattice is generated inside a ring resonator supporting two counterpropagating modes with wave vectors  $k$  and  $-k$ , respectively. The cavity serves to enhance the signal. The atoms are trapped in the red detuned standing wave and are driven by the clock laser. After a  $\pi/2$ -pulse the atoms have absorbed some recoil momentum

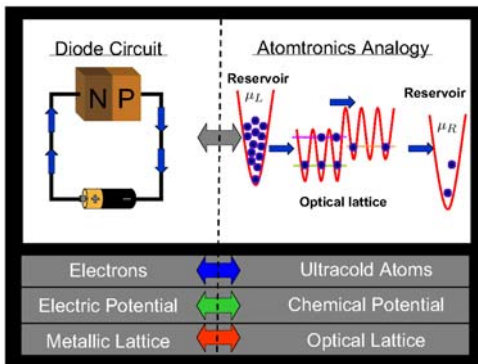
and oscillate in the optical lattice. This oscillation modulates the amplitudes of the two counterpropagating lattice beams. The modulation can be detected at the cavity output by heterodyne measurement. Preliminary calculations show this to lead to potential gains in signal to noise a hundredfold above the projection noise limit (Meiser *et al.* quant-ph preprint 2007).



Schematic of the quantum non-demolition measurement scheme. The optical lattice is generated inside a ring resonator to enhance the signal. Atoms are trapped at the magic wavelength and driven by the clock laser from ground to excited state. The modulation of the lattice beams due to the atomic motion is detected at the cavity output.

### Atomtronics: ultracold atom analogs of electronic devices

The field coming to be known as ‘Atomtronics’ (Seaman *et al* and Pepino *et al* condmat preprint 2007) focuses on establishing ultracold atom analogs of electronic circuits and devices. We have developed diode and transistor device models and showed that these devices form complete atomtronic circuits, demonstrating essential diodic and transistor-like logic.



The atomtronic analogy of a diode formed from the joining of p-type and n-type semiconductor materials. Electrons are replaced by ultracold atoms, the battery is replaced by high and low chemical potential reservoirs, and the metallic crystal lattice (the microscopic medium that the electrons traverse) is replaced by an optical lattice. The atomtronic diode is achieved by energetically shifting one half of the optical lattice with respect to the other.

A major component of this research program was that in order to enable the study of atomtronic circuits, rather than atomtronic devices, we had to develop a theoretical method for solving the dynamics of strongly interacting many-body, *open* quantum systems. Atomtronic devices are intrinsically interesting and a completely different physical system in which to pursue device physics: unlike electrons, they have a complex internal structure, the atoms

can be bosons or fermions, they are massive and affected by gravitational fields, the lattice can be dynamically varied, and many undesirable effects present in solid-state systems such as crystalline impurities, dislocations, and phonon scattering are absent.

## Future work

In future work, we will extend our atomtronic devices to consider more sophisticated logic gates constructed from the basic elements already developed. Our optical lattice clock calculations, although preliminary, show remarkable potential for entering the spin-squeezing regime and we plan to continue a more detailed analysis of this problem. Finally, our aim is to make specific connection on the rotating optical lattice idea with experimental proposals, looking at realizable parameter regimes and observable effects.

## Publications in peer-reviewed journals on DOE supported research

- [1] B. T. Seaman, L. D. Carr, and M. J. Holland, *Reply to comment on ‘Nonlinear band structure in Bose-Einstein condensates: Nonlinear Schrödinger equation with a Kronig-Penney potential’*, Phys. Rev. A **76**, 017602 (2007).
- [2] B. T. Seaman, M. Krmer, D. Z. Anderson, and M. J. Holland, *Atomtronics: Ultracold-atom analogs of electronic devices*, Phys. Rev. A **75**, 023615 (2007).
- [3] Rajiv Bhat, B. M. Peden, B. T. Seaman, M. Krmer, L. D. Carr, and M. J. Holland, *Quantized vortex states of strongly interacting bosons in a rotating optical lattice*, Phys. Rev. A **74**, 063606 (2006).
- [4] M.L. Chiofalo, S. Giorgini, and M. Holland *Released momentum distribution of a Fermi gas in the BCS-BEC crossover*, Phys. Rev. Lett. **97**, 070404 (2006).
- [5] Rajiv Bhat, M. J. Holland, and L. D. Carr, *Bose-Einstein Condensates in Rotating Lattices*, Phys. Rev. Lett. **96**, 060405 (2006).
- [6] L. D. Carr, M. J. Holland, B. A. Malomed, *Macroscopic quantum tunneling of Bose-Einstein condensates in a finite potential well*, J. Phys. B: At. Mol. Opt. Phys. in press (2005).
- [7] C. A. Regal, M. Greiner, S. Giorgini, M. Holland, and D. S. Jin *Momentum distribution of a Fermi gas of atoms in the BCS-BEC crossover*, Phys. Rev. Lett. **95**, 250404 (2005).
- [8] B. T. Seaman, L. D. Carr, and M. J. Holland *Period doubling, two-color lattices, and the growth of swallowtails in Bose-Einstein condensates*, Phys. Rev. A **72**, 033602 (2005).
- [9] L. D. Carr and M. J. Holland *Quantum phase transitions in the Fermi-Bose Hubbard model*, Phys. Rev. A **72**, 033602 (2005).
- [10] B. T. Seaman, L. D. Carr, M. J. Holland *Nonlinear Band Structure in Bose Einstein Condensates: The Nonlinear Schrödinger Equation with a Kronig-Penney Potential*, Phys. Rev. A **71**, 033622 (2005).
- [11] B. T. Seaman, L. D. Carr, M. J. Holland *Effect of a potential step or impurity on the Bose-Einstein condensate mean field*, Phys. Rev. A **71**, 033609 (2005).
- [12] M. Holland *Atomic Beads on Strings of Light*, News and Views, Nature **429**, 251 (2004).
- [13] L. D. Carr, R. Chiaramonte, and M. J. Holland *End-point thermodynamics of an atomic Fermi gas subject to a Feshbach resonance*, Phys. Rev. A **70**, 043609 (2004).
- [14] Jelena Stajic, J. N. Milstein, Qijin Chen, M. L. Chiofalo, M. J. Holland, and K. Levin *Nature of superfluidity in ultracold Fermi gases near Feshbach resonances*, Phys. Rev. A **69**, 063610 (2004).

## Using Intense Short Laser Pulses to Manipulate and View Molecular Dynamics

Robert R. Jones, Physics Department, University of Virginia

382 McCormick Road, P.O. Box 400714, Charlottesville, VA 22904-4714

[rrj3c@virginia.edu](mailto:rrj3c@virginia.edu)

### I. Program Scope

This project focuses on the exploration and control of non-perturbative dynamics in small molecules driven by strong laser fields. Intense non-resonant laser pulses can radically affect molecules, both in internal and external degrees of freedom. The energy and angular distributions of electrons, ions, and/or photons that are emitted from irradiated molecules contain a wealth of information regarding molecular structure and field-driven dynamics. Not surprisingly, a molecule's alignment with respect to the laser polarization is a critical parameter in determining the effect of the field, and information encoded in photo-fragment distributions may only be interpretable if the molecular axis has a well-defined direction in the laboratory frame. Moreover, even molecules which possess a symmetry axis that can be aligned at a well-defined angle relative to the laser polarization are typically not symmetric with respect to inversion along that axis. These asymmetric molecules can respond very differently to the alternating positive and negative half-cycles of the electric field in an intense laser pulse. The ability to optically manipulate the head vs. tail orientation of molecules is, therefore, critical for observing and characterizing this asymmetric response in standard, symmetric laser fields.

Alternatively, by using 2-color ( $1\omega+2\omega$ ) fields with well-defined relative phases, or few-cycle laser pulses with well-defined carrier-envelope (CE) phase, molecules can be exposed to intense oscillating fields in which there is a pronounced difference in the peak amplitude in one direction over another. Such fields break the up/down symmetry of the problem. For symmetric targets (including ensembles of non-oriented molecules), asymmetric fields make it possible to control the directionality of laser driven processes [1], e.g. whether dissociation results in the ejection of an ion from the top or bottom of the molecule. Such fields also destroy/reduce constructive or destructive interferences resulting from equal amplitude, coherent wavepacket emission in multiple directions, enabling, for example, the generation of even-order harmonics in bichromatic fields [2]. For oriented molecules, the handedness of the molecule combined with that of the field affords substantial control over total as well as differential process yields.

Our recent efforts have focused on field-free laser alignment and orientation of molecular targets, and on the characterization of molecular ionization, fragmentation, and high-harmonic generation (HHG) from aligned targets in symmetric and asymmetric fields.

### II. Recent Progress

During the past year, we have used 2-color ( $1\omega+2\omega$ ) laser fields to control strong-field electron localization [1,3] and the direction of ion emission following charge symmetric dissociation (CSD) of heteronuclear diatomic molecules as well as charge asymmetric dissociation (CAD) of homonuclear species [4,5]. We have also continued to explore methods for improving transient field-free alignment and orientation of diatomic molecules for use in intense laser ionization, fragmentation, and HHG experiments. All of the experiments utilize one or more relatively weak ( $I < 10^{14} \text{ W/cm}^2$ ) "pump" laser pulses as well as a more intense ( $I < 10^{15} \text{ W/cm}^2$ ) probe. In all cases the intense probe laser pulses are produced by a 30 fsec amplified Ti:Sapphire laser. The pump pulses are derived either from the same 30 fsec amplifier, or from a second 100 fsec amplified laser system. For the 2-color experiments, two pump pulses (800 nm and 400 nm) with

similar intensities are overlapped in time. The relative optical phase,  $\phi$ , between the two pump pulses is controlled using a pair of rotating glass plates in the collinear beams.

#### *A. Controlled Directional Dissociation in an Asymmetric 2-Color Laser Field*

In the asymmetric field experiments, we use a time-of-flight spectrometer to measure molecular ion fragment kinetic energy spectra as a function of  $\phi$  for different polarizations of the two pump pulses and at different pump/probe delays. Our primary interest is the control of the emission direction for ions with  $Z > 1$ . The pump lasers alone produce negligible quantities of these species. The pump and probe lasers cross at a small angle in the interaction region such that the relative phases between the pump beams and the probe vary by several full cycles across the interaction region. Thus, there is no well-defined phase between the pumps and probe, and the pump-phase  $\phi$  serves as the only relevant control knob.

For CO, we consider 4 distinct polarization combinations for the pump/probe beams: linear/linear, linear/circular, circular/linear, and circular/circular. Linear polarizations are parallel to the spectrometer axis ( $z$ ) and circular polarizations are in the  $xz$ -plane. A pronounced,  $\phi$ -dependent asymmetry in the total pump field is produced when the two pump beams have parallel linear or circular polarizations. We measure forward/backward asymmetry parameters,  $\beta_C = (C_+^{m+} - C_-^{m+}) / (C_+^{m+} + C_-^{m+})$  and  $\beta_O = (O_+^{n+} - O_-^{n+}) / (O_+^{n+} + O_-^{n+})$ , where  $C_{+(-)}^{m+}$  is the carbon ion yield along the  $(-)$   $z$ -axis and  $O_{+(-)}^{n+}$  is the oxygen yield in the opposite direction. When the pump and probe beams are overlapped in time, we find substantial variations in these  $\beta$ 's for several species  $m$  and  $n$  and all polarization combinations except circular/circular. In particular, for  $m=n=2$ ,  $\beta_O$  varies from 0.2 to -0.2 as the relative delay between the two pump beams changes by  $\frac{1}{2}$  of the 400 nm period (670 asec). The accompanying variations in  $\beta_C$  are  $180^\circ$  out of phase with those in  $\beta_O$  as required. This is a substantial level of control given the imperfect overlap between the crossing pump and probe beams and the small asymmetry in the total field due to the large intensity difference between the pumps and probe.

The primary advantage of using distinct pump and probe fields is that we can distinguish the effects of selective directional ionization along the spectrometer axis from transient orientation of the molecules driven by the asymmetric probe field (see section C below). Indeed, when the probe laser is delayed by the fundamental CO rotational period, no asymmetry is observed. Thus, the control we observe is not due to transient (periodic) orientation of the molecule.

Very similar asymmetries are observed in  $N_2$  when comparing the forward/backward asymmetry for dissociation to  $N^{m+}$  and  $N^{n+}$  with  $m \neq n$ . In particular, for CAD in  $N_2$  with  $m=2$  and  $n=0$  [4,5], the variations in  $\beta$  are essentially identical to those in CO for  $m=n=2$ . Maxima in the  $N_+^{2+}$  and  $O_+^{2+}$  yields (the species that require the highest intensities to produce) are observed at the same control phase. In CO, we suspect that the control is due to differences in the enhanced ionization (EI) rate for electrons that have been non-adiabatically localized near the O nucleus in the upper well of the dication-potential as the C and O nuclei approach the critical separation,  $R_c$ , for EI [3]. Depending on  $\phi$ , the tunneling ionization rate will be greater for O ions in the upper well nearest to, or furthest from, the ion detector. A similar mechanism might be responsible for the  $m=2$ ,  $n=0$  control in  $N_2$ . However, the lack of a strong asymmetry in the  $m=2$ ,  $n=1$  dissociation channel in  $N_2$  is puzzling. In this case, the variations in  $\beta$  are in phase with those for  $m=2$ ,  $n=0$  in  $N_2$ , but are an order of magnitude smaller in amplitude. Of course, our naïve picture only considers the effect of the asymmetric field at  $R_c$ , but  $\phi$  might also influence the dynamics associated with the expansion of the molecule toward  $R_c$  [4]. Our analysis is continuing.

### *B. HHG from Transiently Aligned Molecules in a Hollow-core Waveguide*

Transient laser alignment of linear rigid molecules is a well established technique for producing ensembles of molecules which preferentially align along a laboratory fixed axis at well-defined times [6]. In essence, a short laser pulse gives the molecules an angular impulse, creating a rotational wavepacket which exhibits periodic angular localization along the kick axis and in the plane perpendicular to the kick direction. In practice, the initial rotational temperature of the molecular sample, and the restriction on the maximum alignment laser intensity set by the molecular ionization threshold, limits the achievable degree of alignment. We use aligned molecules to study anisotropies in the efficiencies for intense laser ionization and HHG. Once well understood, these anisotropies might be exploited to probe molecular dynamics [7].

In our initial HHG experiments we measured substantial differences (factors of 1.5-2.5x) in the harmonic yields for molecules preferentially aligned parallel vs. perpendicular to the drive laser polarization in a hollow-core fiber. However, the degree of achievable alignment was significantly limited due to the high (room) temperature of the gas in the fiber. Rather than abandon the waveguide geometry [8] for the HHG measurements, we recently developed a liquid-nitrogen-cooled, fiber source. We also constructed a liquid-nitrogen-cooled, effusive low-pressure source for the ionization/fragmentation experimental chamber. Using Coulomb explosion imaging we confirmed a ~20% improvement in the degree of achievable alignment of N<sub>2</sub> and CO at 75K rather than 300 K. Accordingly we observed a ~20% improvement in the alignment-dependent variation in our HHG yields. We now intend to explore the use of a counter-propagating alignment/signal beam geometry to produce a periodic variation in the HHG efficiency along the fiber, thereby modifying (and hopefully in some cases improving) the phase-matching conditions within the waveguide. We have already designed a source that allows us to send counter-propagating beams through the waveguide, and are currently using argon to characterize the effects of the counter propagating beam on phase-matching conditions [9] in the absence of alignment. We will next explore alignment effects using N<sub>2</sub>.

### *C) Towards Field-Free Transient Orientation of Heteronuclear Molecules*

As noted previously, oriented molecules would be valuable targets for strong-field physics applications. For example, using oriented targets in combination with an asymmetric field, one could explore and exploit anisotropies in tunneling ionization rates from different sites within a molecule. Because of this ionization rate anisotropy, both even and odd order harmonics could be generated from an oriented sample, allowing one to better characterize the recollision electrons responsible for HHG and providing greater flexibility for the synthesis of attosecond waveforms.

While single-frequency laser pulses create periodically aligning, rotational wavepackets by driving Raman transitions between rotational states of the same parity ( $\Delta J = \pm 2$ ), transient orientation of non-symmetric molecules requires the creation of rotational wavepackets in which states of both even and odd parity are coherently superimposed. We are investigating two different approaches for producing such oriented wavepackets. First, we are attempting to use subpicosecond unipolar half-cycle pulses (HCPs) to directly drive  $\Delta J = \pm 1$  transitions between rotational levels of opposite parity in polar molecules [10]. Second, we are utilizing phase-coherent excitation with 400 nm and 800 nm laser pulses to induce asymmetric  $\Delta J = \pm 1, \pm 3$  Raman transitions (e.g. absorption of one ~400 nm photon and emission of two ~800 nm photons) within molecules.

According to our numerical simulations, we have sufficient rotational cooling and sufficient HCP field strength to preferentially orient HBr molecules in the supersonic expansion in our apparatus. We are continuing to search for experimental signatures of orientation via Coulomb explosion using a time-delayed 30 fsec laser pulse. We also plan to investigate other schemes that utilize HCP and optical fields in combination that we and others [11] predict will be more effective for aligning polar molecules .

We have also attempted to observe 2-color laser orientation of room temperature CO using linearly polarized, phase-controlled 400 nm and 800 nm pulses. Unfortunately, we now believe that the large initial rotational kinetic energy of the CO molecules combined with the second-order alignment torques produced by the 800 nm and 400 nm beams individually overpowers the relatively weak, third-order orienting torque that is produced by the 2-color linearly polarized field. Therefore, we are now utilizing circularly polarized 800 nm and 400 nm fields in an attempt to induce orientation. Our numerical simulations indicate that in this case, both component fields act to align the molecules to the common polarization plane, but neither can preferentially align the molecules within the polarization plane. However, the net field has a pronounced asymmetry which can orient the molecules within the plane.

### **III. Future Plans**

In addition to the continuing work noted in the previous section, we have acquired a CE-phase stabilized Ti:Sapphire oscillator and are now working to integrate it as the seed for one of our Ti:Sapphire amplifiers. We plan to install a fiber compressor to generate few-cycle carrier-phase controlled pulses for exploring asymmetric strong field effects in molecules.

### **IV. Publications from Last 3 Years of DOE Sponsored Research (July 2004- July 2007)**

- i) D. Pinkham, K. E. Mooney, and R.R. Jones, "Optimizing Dynamic Alignment in Room Temperature CO," *Physical Review A* **75**, 013422 (2007).
- ii) D. Pinkham and R.R. Jones, "Intense Laser Ionization of Transiently Aligned CO," *Physical Review A* **72**, 023418 (2005).
- iii) E. Wells, K.J. Betsch, C.W.S. Conover, M.J. DeWitt, D. Pinkham, and R.R. Jones, "Closed-Loop Control of Intense-Laser Fragmentation of S<sub>8</sub>," *Physical Review A* **72**, 063406 (2005).
- iv) E. Wells, I. Ben-Itzhak, and R.R. Jones, "Ionization of Atoms by the Spatial Gradient of the Ponderomotive Potential in a Focused Laser Beam," *Physical Review Letters* **93**, 23001 (2004).

### **References**

1. M.F. Kling *et al.*, *Science* **312**, 246 (2006).
2. N. Dudovich, *Nature Phys.* **2**, 781 (2006).
3. T. Seideman, M.Yu. Ivanov, and P.B. Corkum, *Phys. Rev. Lett.* **75**, 2819 (1995).
4. C. Guo, M. Li, and G.N. Gibson, *Phys. Rev. Lett.* **82**, 2492 (1999).
5. R.N. Coffee, L. Fang, and G. N. Gibson, *Phys. Rev. A* **73**, 043417 (2006).
6. H. Stapelfeldt and T. Seideman, *Rev. Mod. Phys.* **75**, 543 (2003) and references therein.
7. Itatani *et al.*, *Nature* **432**, 867 (2004); S. Baker *et al.*, *Science* **312**, 424 (2006).
8. A. Rundquist *et al.*, *Science* **280**, 1412 (1998).
9. A. Lytle *et al.*, *Phys. Rev. Lett.* **98**, 123904 (2007).
10. M. Machholm and N.E. Henriksen, *Phys. Rev. Lett.* **87**, 193001 (2001).
11. E. Gershkabel, I. Sh. Averbukh and R.J. Gordon, *Phys. Rev. A* **73**, 061401 (2006).

## Ultrafast Atomic and Molecular Optics at Short Wavelengths

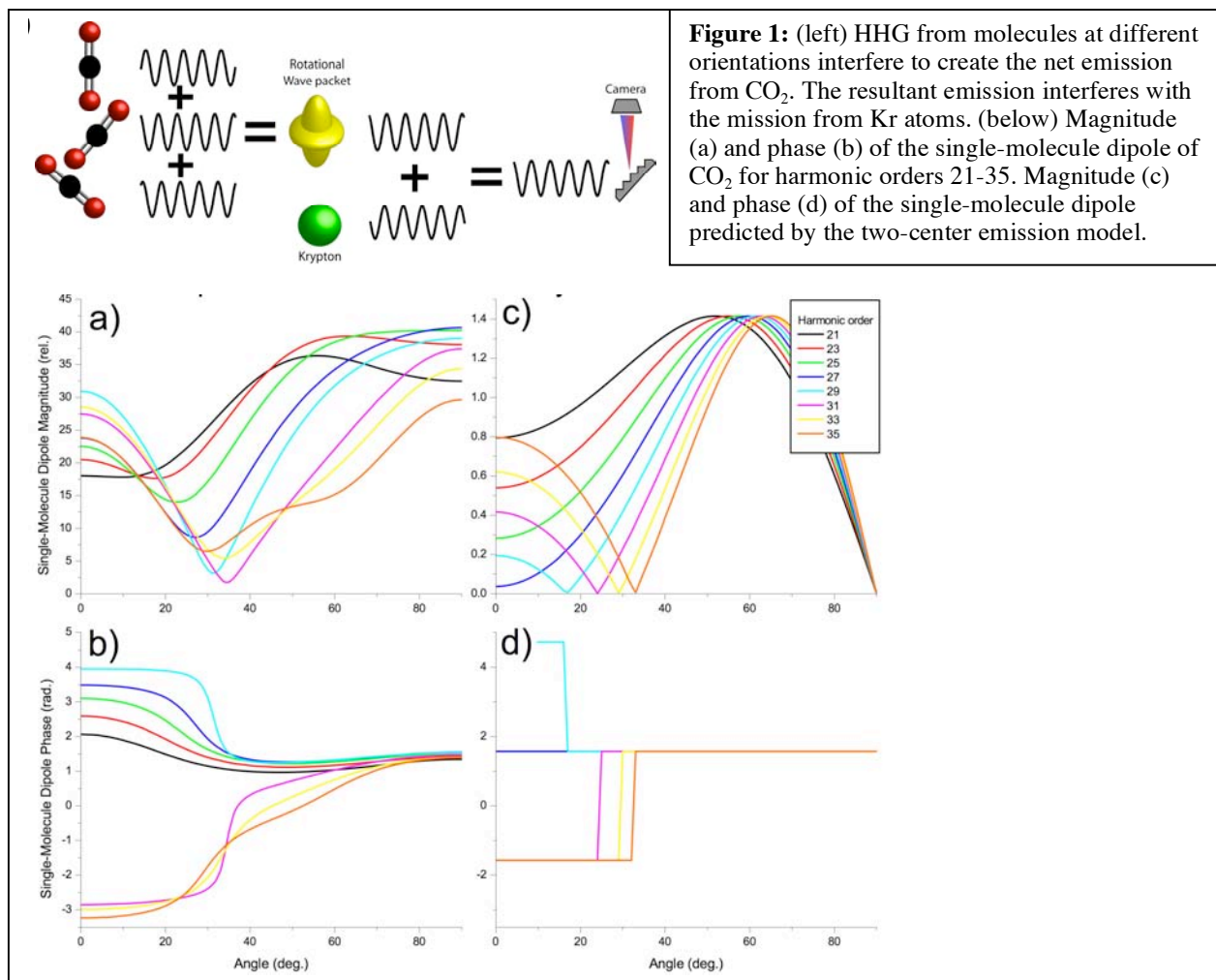
P.I.s: Henry C. Kapteyn and Margaret M. Murnane  
University of Colorado at Boulder, Boulder, CO 80309-0440  
Phone: (303) 492-8198; FAX: (303) 492-5235; E-mail: kapteyn@jila.colorado.edu

The goal of this work is to study of the interaction of atoms and molecules with intense and very short (<20 femtosecond) laser pulses, with the purpose of developing new short-wavelength light sources. Novel short wavelength probes of materials and molecules are also being developed.

### Recent Progress

We have made exciting advances in several experiments in recent months, to probe molecular and materials dynamics using soft-x-ray sources and to advance x-ray generation from ions.

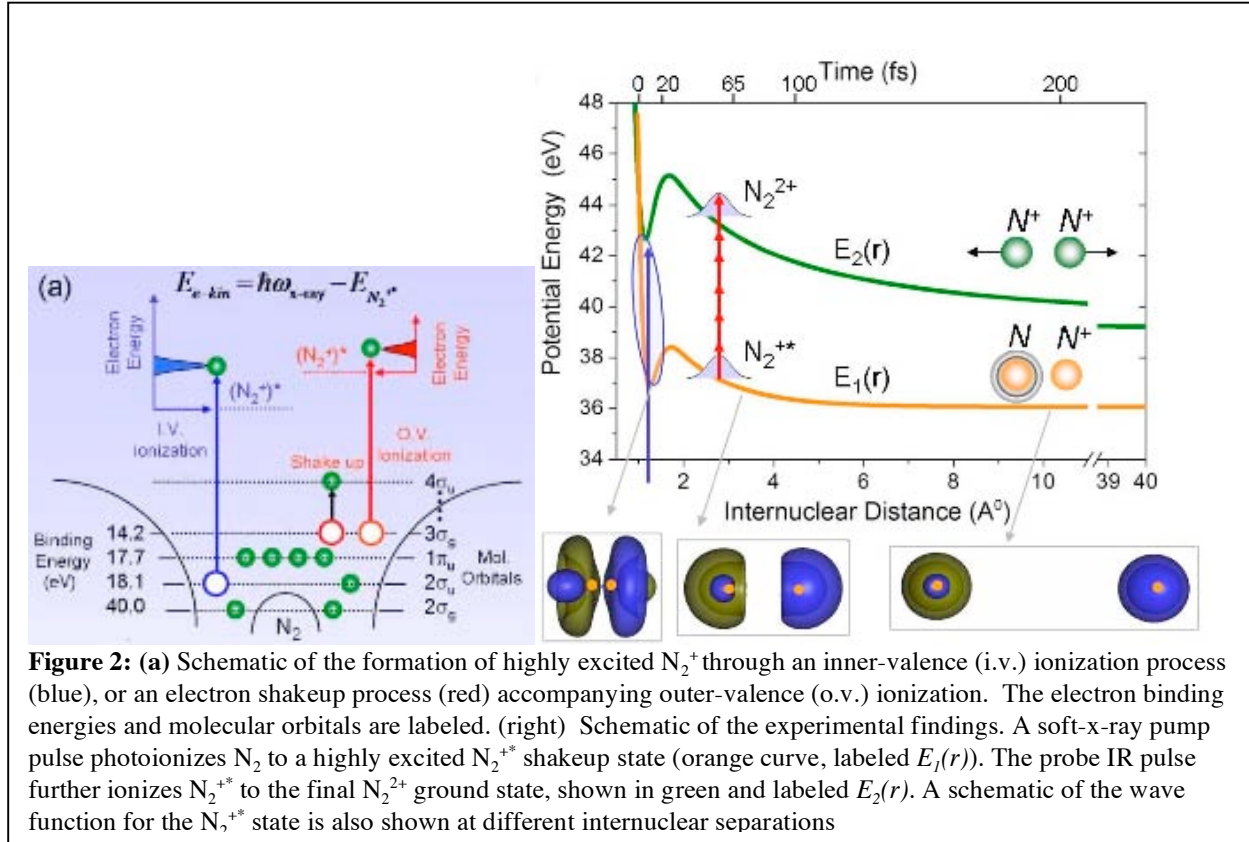
1. Probing molecular dynamics using coherent electron rescattering: In work just submitted for publication, we measured both the phase and intensity of high harmonic emission from a *single* molecule for the first time, using a mixture of a molecular and an atomic gas. The molecules were transiently aligned using an ultrashort pulse, and a subsequent stronger pulse was used to generate high harmonics from a mixed Kr/CO<sub>2</sub> sample. The high harmonic emission from the molecules interferes with the reference emission from the atoms. By monitoring the change in harmonic emission as a function of gas mixture and molecular alignment, we deconvolved the phase of the EUV light emission for a single molecule as a function of orientation.



We also directly visualized the phase shift in harmonic emission due to molecular structure. Our results are consistent with a two-center emission model for high harmonic generation from molecules. This work is significant because it separates the contributions to the total high harmonic signal due to an isolated molecule from the signal due to an averaged rotational wavepacket that contains the signals from many molecules in a rotational distribution. This work is important for determining molecular structure from a measurement of the high harmonic signal as a function of molecular orientation.

In related work, we are extending past work in observing vibrational dynamics in SF<sub>6</sub> by monitoring the modulations in the high harmonic signal in several other molecules that undergo large dynamic structural changes. We also simultaneously observe rotational and vibrational dynamics. This work is being done in collaboration with Chris Greene at JILA.

**2. Observation of x-ray driven femtosecond molecular dynamics:** In recent work, we demonstrated the first soft x-ray driven femtosecond molecular dynamics. The direct observation of molecular dynamics initiated by x-rays has been hindered to date by the lack of bright femtosecond sources of short wavelength light. We used soft-x-ray beams generated by high harmonic upconversion of a femtosecond laser to photoionize an N<sub>2</sub> molecule, creating highly-excited N<sub>2</sub><sup>+</sup> ions. A strong infrared pulse was then used to probe the ultrafast electronic and nuclear dynamics as the molecule explodes. We found that significant fragmentation occurs through an electron shakeup process, in which a second electron is simultaneously excited during the soft-x-ray photoionization process. During fragmentation, the molecular potential seen by the electron changes rapidly from nearly spherically symmetric, to a two-center molecular potential. Our approach can capture in real time and with Å resolution the influence of ionizing radiation on a range of molecular systems, probing dynamics that are inaccessible using other techniques. This work was done in collaboration with Lew Cocke at Kansas State. Ongoing work is investigating highly-excited electron dynamics in other molecules with higher time resolution.



**3. Observation of very high order harmonics from ions:** In work done in collaboration with Jorge Rocca at Colorado State University, we significantly extended the energy range of high harmonic generation from Ar, Kr and Xe ions to 450eV, 170eV and 160eV respectively. We also developed new phase matching approaches that apply in the hard-x-ray regime.

**4. Femtosecond x-ray holography:** In work done in collaboration with Keith Nelson at MIT, we demonstrated femtosecond time-resolved dynamic Gabor holography using ultrafast EUV beams for the first time. We also probed thin film thermoacoustic responses and nano-thermal heat transport using spatially coherent EUV beams.

### Publications as a result of DOE support since 2006

1. D.. Gaudiosi et al., "High harmonic generation from ions in a capillary discharge", Phys. Rev. Lett. **96**, 203001 (2006).
2. A. Paul, E.A. Gibson, X. Zhang, A. Lytle, T. Popmintchev, X. Zhou, M.M. Murnane, I.P. Christov, and H.C. Kapteyn, "Phase matching techniques for coherent soft-x-ray generation", invited paper, IEEE Journal of Quantum Electronics **42**, 14 - 26 (2006).
3. N. Wagner, A. Wüest, I. Christov, T. Popmintchev, X. Zhou, M. Murnane, H. Kapteyn, "Monitoring Molecular Dynamics using Coherent Electrons from High-Harmonic Generation", Proceedings of the National Academy of Sciences **103**, 13279 (2006).
4. R.I. Tobey, M.E. Siemens, M. M. Murnane, H. C. Kapteyn, K.A. Nelson, "Ultrasensitive Transient Grating Measurement of Surface Acoustic Waves in Thin Metal Films with Extreme Ultraviolet Radiation ", Applied Physics Letters **89**, 091108 (2006).
5. J. Rocca, H. Kapteyn, D. Attwood, M. Murnane, C. Menoni, E. Anderson, "Table-top lasers in the Extreme Ultraviolet bring new light to science and nanotechnology", Optics and Photonics News, pp 24 (Nov. 2006).
6. N. Wagner, A. Wüest, I. Christov, T. Popmintchev, X. Zhou, M. Murnane, H. Kapteyn, "High-Order X-Ray Raman Scattering using Coherent Electrons from High Harmonic Generation", "Optics in 2006", Optics and Photonics News pp 43 (Dec. 2006). Also featured on cover.
7. D. Gaudiosi, B. Reagan, T. Popmintchev, M. Grisham, M. Berril, O. Cohen, B. Walker, M. Murnane, H. Kapteyn, J. Rocca, "High harmonic generation from ions in a capillary discharge", "Optics in 2006", Optics and Photonics News, pp 44 (Dec. 2006).
8. R.I. Tobey, M.E. Siemens, O. Cohen, M.M. Murnane, H.C. Kapteyn "Ultrafast Extreme Ultraviolet Holography: Dynamic Monitoring of Surface Deformation", Optics Letters **32**, 286 (2007).
9. B.A. Reagan, T. Popmintchev, M.E. Grisham, D.M. Gaudiosi, M. Berrill, O. Cohen, B. C. Walker, M.M. Murnane, J.J. Rocca, H.C. Kapteyn, "Enhanced High Harmonic Generation from Xe, Kr, and Ar in a Capillary Discharge", Physical Review A **76**, 013816 (2007).
10. O. Cohen, X. Zhang, A.L. Lytle, T. Popmintchev, M.M. Murnane, H.C. Kapteyn, "Optically-induced grating-assisted phase matching in high-harmonic generation", to be published in Phys. Rev. Lett. **99** (August 3, 2007).
11. E. Gagnon, P. Ranitovic, A. Paul, C. L Cocke, M.M. Murnane, H.C. Kapteyn, A.S. Sandhu, "Soft X-ray driven femtosecond molecular dynamics," to be published in *Science* (2007).
12. H.C. Kapteyn, O. Cohen, I. Christov, M.M. Murnane, "Harnessing Attosecond Science in the Quest for Coherent X-Rays," to be published in *Science* (August 11, 2007).
13. N. Wagner, X. Zhou, R. Hooper, W. Li, A. Wüest, M. Murnane, H. Kapteyn, "Extracting the Phase of High Harmonic Emission from a Molecule using Mixed Samples," Phys. Rev. Lett. *submitted* (2007).

## **Detailed Investigations of Interactions between Ionizing Radiation and Neutral Gases**

**Allen Landers**

[landers@physics.auburn.edu](mailto:landers@physics.auburn.edu)

Department of Physics  
Auburn University  
Auburn, AL 36849

### **Program Scope**

We are investigating phenomena that stem from the many body dynamics associated with ionization of an atom or molecule by photon or charged particle. Our program is funded through a new Department of Energy EPSCoR Laboratory Partnership Award in collaboration with Lawrence Berkeley National Laboratory. We are using variations on the well established COLTRIMS technique to measure ions and electrons ejected during these interactions. Photoionization measurements take place at the Advanced Light Source at LBNL. Additional experiments on charged particle impact are conducted locally at Auburn University with a 2MV tandem NEC Pelletron accelerator. Finally, a new experiment is being developed that will allow the investigation of ion production following ionization of atoms and molecules by electron impact. Presented here are a report of recent work at the ALS-LBNL and an update on the construction of the low-energy electron impact apparatus.

### **Recent Results: Continuum Correlation in the Photoionization of Neon**

For a single multi-level atom such as neon, the photoionization process is yet to be understood in full detail. In particular, just above the core photoionization threshold two interesting phenomena can occur: (1) the three body post-collision interaction (PCI) between the photoelectron, residual ion and subsequent Auger electron [1]; and (2) the possible recapture of the photoelectron [2]. Both processes are associated with the change in potential caused by the fast Auger decay of the core-excited  $\text{Ne}^{*+}$  that occurs after photoionization. Shortly after emerging from the atom, the outgoing photoelectron is subject to a change in potential associated with the change of parent ion from  $\text{Ne}^{*+}$  to  $\text{Ne}^{2+}$ . Within the sudden approximation, the loss in energy (in atomic units) of the photoelectron is simply the change in potential energy given by  $1/r$ , where  $r$  is the distance traveled from the ion before Auger decay occurs. If this energy loss is less than the original continuum energy, then the electron simply remains in the continuum with reduced kinetic energy (process 1). In this case, all three bodies can exchange momentum and energy. If, however, the energy loss is greater than the photoelectron's initial energy, the electron can be recaptured into Rydberg state orbiting the  $\text{Ne}^{2+}$  core (process 2).

At the LBNL-ALS in Berkeley, California, we have used the COLTRIMS technique to investigate in detail both processes (1) and (2) above along with the associated fundamental physics. We have measured the full momentum vectors of both

the slow photoelectron and the recoiling neon ion in coincidence. For case (1), the momentum of the faster Auger electron has been determined by conservation laws. Furthermore, the measurement of the final photoelectron energy determines the radial coordinate at the time of Auger decay, which in turns yields the actual decay time, giving us an attosecond stopwatch on the decay process.

An illustrative example of the detail in these measurements is the plot of the photoelectron momentum distribution in the frame of the Auger electron in order to directly observe the continuum correlation between the two particles (Fig 1). Faint underlying discrete isotropic bands correspond to the recapture/re-emission channel. The “C” shaped feature corresponds to escaping photoelectrons that are repelled as they are overtaken by the faster subsequent Auger electrons, providing a direct and revealing look at the post-collision interaction.

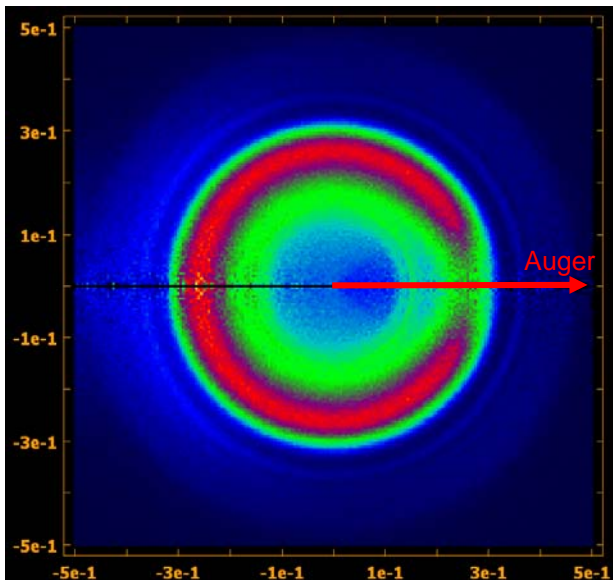


Fig. 1 Core photoionization of neon. Shown is the correlated photoelectron momentum in the plane defined by the photo- and Auger electron momentum vectors.

In addition to the continuum correlation and recapture process described above, we observe additional details through the simultaneous measurement of other ionization decay pathways. These include single ionization of the outer shell, core ionization followed by radiative decay and core ionization followed by Auger cascades up to  $\text{Ne}^{4+}$ . Model calculations by Francis Robicheaux have been used to help interpret our results.

### **Future Plans: Modified COLTRIMS Technique to Measure Electron Interactions with Atoms and Molecules**

One of the main challenges associated with applying imaging techniques to measurements of low-energy electron processes is that the typical fields involved strongly influence the incident electron's trajectory. To approach this problem, we have built a modified COLTRIMS apparatus to measure electron collisions with atoms and molecules that uses both pulsed incident electrons and pulsed electric fields. A beam from a pulsed electron gun passes through a diffuse target, followed by a synchronized

electric field pulse which extracts the ions to a multi-channel plate detector with delay-line anode (see Fig 2). By measuring positions and times of the extracted ions, information similar to that of more traditional RIMS methods can be obtained (see Fig 3). For example, knowledge of charge state distributions, ion energy/momenta and molecule orientation become accessible. Initial experiments will focus on differential measurements of fragment production in the dissociative ionization of molecules by low energy electrons.

### Electron and Field Pulse Scheme

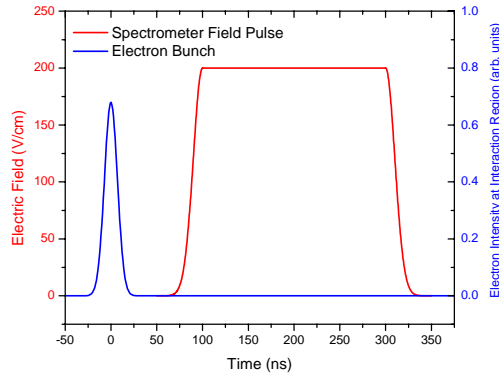


Fig. 2 After a short burst of electrons passes through the target gas, a field pulse of up to 800V/cm of controllable length is produced in a 1 cm plate gap around the interaction region. The impulse given to measured ions is directly proportional to the area under the red curve. The pulsed electric field is synchronized to the same clock as the electron bunch, with a controllable delay.

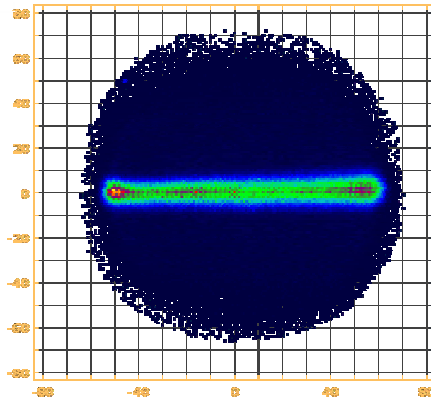
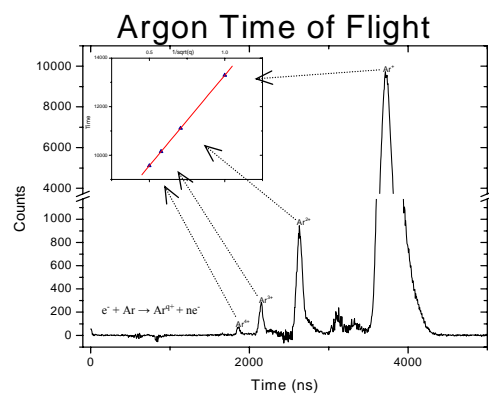


Fig. 3 Time of flight and position spectra with background gas subtracted. Charge state distribution includes ions up to at least 4+. The inlaid graph at left shows the  $1/\sqrt{q}$  charge state dependence. In this case, an energetic bunched electron beam was used along with a small DC field to extract argon ions. Development of measurements using pulsed field extraction is moving forward.

### References

- [1] A. Russek and W. Mehlhorn, *J. Phys. B* **19** 911 (1986), and references therein.
- [2] T. W. Gorczyca, O. Zatsarinny, H.-L. Zhou, S. T. Manson, Z. Fel and A. Z. Msezane, *Phys Rev A* **68**, 050703(R) (2003).

**Co-authored Publications over past 2 years (Present funding began Feb 2007)**

10. **A two-electron double slit experiment: interference and entanglement in photo double ionization of H<sub>2</sub>** D. Akoury, K. Kreidi, T. Jahnke, Th. Weber, A. Staudte, M. Schöffler, N. Neumann, J. Titze, L. Ph. H. Schmidt, A. Czasch, O. Jagutzki, R.A. Costa Fraga, R. Grisenti, R. Diez Muino, N. Cherepkov, S. Semenov, P. Ranitovic, C.L. Cocke, T. Osipov, H. Adaniya, M.H. Prior, A. Belkacem, A. Landers, H. Schmidt-Böcking, and R. Dörner (submitted Science, under review for publication)
9. **Auger electron molecular frame angular distributions as a probe for molecular structure** T. Jahnke, J. Titze, L. Foucar, R. Wallauer, T. Osipov, E.P. Benis, A. Alnaser, O. Jagutzki, W. Arnold, L. Ph. H. Schmidt, A. Czasch, M. S. Schöffler, Th. Weber, A. L. Landers, A. Belkacem, C. L. Cocke, M. H. Prior, H. Schmidt-Böcking, and R. Dörner (Phys. Rev. Lett., submitted)
8. **Single Photon-Induced Symmetry Breaking of H<sub>2</sub> Dissociation** F. Martín, J. Fernández, T. Havermeier, L. Foucar, Th. Weber, K. Kreidi, M. Schöffler, L. Schmidt, T. Jahnke, O. Jagutzki, A. Czasch, E. P. Benis, T. Osipov, A. L. Landers, A. Belkacem, M. H. Prior, H. Schmidt-Böcking, C. L. Cocke, R. Dörner, *Science* **315**, 629 (2007).
7. **Nondipole effects in the angular distribution of photoelectrons from the C K shell of the CO molecule** K. Hosaka, J. Adachi, A. V. Golovin, M. Takahashi, T. Teramoto, N. Watanabe, T. Jahnke, Th. Weber, M. Schöffler, L. Schmidt, T. Osipov, O. Jagutzki, A. L. Landers, M. H. Prior, H. Schmidt-Böcking, R. Dörner, A. Yagishita, S. K. Semenov, and N. A. Cherepkov, *Phys. Rev. A* **73**, 022716 (2006).
6. **Interference phenomena associated with electron-emission from H<sub>2</sub> by (1–5) MeV H<sup>+</sup> impact** S. Hossain, A. L. Landers, N. Stolterfoht, and J. A. Tanis, *Phys. Rev. A* **72**, 010701 (2005).
5. **Photon-Ion Collisions and Molecular Clocks** T. Osipov, A.S. Alnaser, S. Voss, M.H. Prior, T. Weber, O. Jagutzki, L. Schmidt, H. Schmidt-Böcking, R. Dörner, A. L. Landers, E. Wells, B. Shan, C. Maharjan, B. Ullrich, P. Ranitovic, X.M. Tong, C.D. Lin and C.L. Cocke, *J. Modern Optics*, **52**, 439 (2005).
4. **Photo double ionization of helium 100 eV and 450 eV above threshold: A. linearly polarized light** A. Knapp, A. Kheifets, I. Bray, Th. Weber, A.L. Landers, S. Schossler, T. Jahnke, J. Nickles, S. Kammer, O. Jagutzki, L. Schmidt, M. Schöffler, T. Osipov, M.H. Prior, H. Schmidt-Böcking, C.L. Cocke, and R. Dörner, *J. Phys. B: At. Mol. Opt. Phys.* **38** 615-633 (2005).
3. **Photo double ionization of helium 100 eV and 450 eV above threshold: B. Circularly polarized light** A. Knapp, A. Kheifets, I. Bray, Th. Weber, A.L. Landers, S. Schossler, T. Jahnke, J. Nickles, S. Kammer, O. Jagutzki, L. Schmidt, M. Schöffler, T. Osipov, M.H. Prior, H. Schmidt-Böcking, C.L. Cocke, and R. Dörner, *J. Phys. B: At. Mol. Opt. Phys.* **38** 635-643 (2005).
2. **Photo double ionization of helium 100 eV and 450 eV above threshold: C. Gerade and ungerade amplitudes and their relative phase** A. Knapp, A. Kheifets, I. Bray, Th. Weber, A.L. Landers, S. Schossler, T. Jahnke, J. Nickles, S. Kammer, O. Jagutzki, L. Schmidt, M. Schöffler, T. Osipov, M.H. Prior, H. Schmidt-Böcking, C.L. Cocke, and R. Dörner, *J. Phys. B: At. Mol. Opt. Phys.* **38** 645-657 (2005).
1. **Electron Correlation in the Formation of Hollow States along the Li-like Isoelectronic Sequence** A. S. Alnaser, A. L. Landers, and J. A. Tanis, *Phys. Rev. Lett.* **94**, 023201 (2005).

**Program Title:**

"Properties of actinide ions from measurements of Rydberg ion fine structure"

**Principal Investigator:**

Stephen R. Lundeen,  
Dept. of Physics  
Colorado State University  
Ft. Collins, CO 80523  
Lundeen@Lamar.colostate.edu

**Program Scope:**

Measurements of the fine structure of non-penetrating, high-L Rydberg states of atoms or ions can be used to deduce polarizabilities and permanent moments of the positive ions that form the cores of these Rydberg systems. Special experimental techniques developed under previous DOE support now make it possible to carry out such studies in a wide range of elements and charge states. The current focus of this project is the application of these techniques to measure some properties of chemically interesting actinide ions, such as  $U^{6+}$ ,  $Th^{4+}$ , and other open shell U and Th ions. Since *a priori* prediction of the properties of such highly relativistic ions is very challenging but still much simpler than predicting their behavior in chemical compounds, it is hoped that such measurements will contribute to improved understanding of actinide chemistry.

**Recent Progress:**

Work on this project takes place at two locations. At Colorado State University (CSU), we carry out studies of neutral Rydberg systems, with the aim of testing and improving the theoretical framework used to relate the measured fine structure patterns to positive ion properties. At Kansas State University (KSU), we share the use of an ECR source which produces beams of multiply-charged ions needed to study Rydberg ion fine structure. Over the past year, the progress achieved at both locations has resulted in approval for purchase of a new permanent magnet ECR source to be installed at KSU for the production of the multiply-charged U and Th ion beams necessary for this project.

At KSU our major effort this year has been a study of fine structure of  $Kr^{5+}$  Rydberg ions, intended as a test of the methods to be used to study Rydberg ions built on  $U^{6+}$  ions. This study has now been reported [1], and has resulted in a measurement of the dipole polarizability of the  $Kr^{6+}$  ion,  $\alpha_d = 2.69(4) a_0^3$ . In the process, a number of experimental factors that will be critical to the actinide ion studies have been explored. The two most important issues are the background rate, which limits the signal to noise, and the excitation linewidth, which limits the resolution. Continued efforts to improve system performance in both of these areas will be important to the long-term success of the proposed actinide ion measurements.

At CSU, part of our effort was directed at understanding the contradiction between the quadrupole polarizability of  $Si^{3+}$  that was apparently implied by our recent study of Rydberg states of  $Si^{2+}$ [2] and recent high quality theoretical calculations. This troubling discrepancy suggested a weakness in the link between fine structure measurements and core ion properties that could reduce the usefulness of our proposed measurements. After considering many possible explanations, we resolved the discrepancy by calculating the next two higher-order terms in the long-range potential between Rydberg electron and ion core and estimating their coefficients. A report of this

conclusion has now been published [3]. The same effect turned out to resolve the apparent discrepancy between calculated quadrupole polarizabilities of  $\text{Ba}^+$  and the values implied by our measurements of fine structure in Ba Rydberg states [4].

Also completed at CSU this year was an improved study of Ba Rydberg fine structure using the RESIS/microwave technique. Measurements were made of  $n=17$  and  $n=20$  fine structure intervals in the range  $7 \leq L \leq 11$ , resulting in improved values of both the dipole and quadrupole polarizabilities of  $\text{Ba}^+$  and in greatly improved measurements of the spin-splittings in high-L Ba Rydberg levels. A report of this work is in the final stages of preparation [5]

### **Immediate Plans:**

At KSU, we are working towards the installation of the new ECR source, and the related modifications of laboratory floor plan. It is expected that the new floor plan will allow at least one additional beam port where other experiments using the multiply-charged U and Th beams could be initiated. Our RESIS apparatus will transfer with only minor modifications to the new configuration. Our first studies will be of Rydberg ions built on the Ra-like ions,  $\text{U}^{6+}$  and  $\text{Th}^{4+}$ . Because of the lead time in production of the source, the installation is not expected to be completed before early 2008. We hope to have our first actinide data before summer 2008.

At CSU, we are working on a RESIS/microwave study of Rydberg states of argon. Since  $\text{Ar}^+$  is a  ${}^2\text{P}_{3/2}$  ion with a non-zero quadrupole moment, the fine structure of argon Rydberg states is much more complex than those of Ba, though still not as complex as the structure expected for Rydberg levels bound to open shell actinide ions like  $\text{Th}^{3+}$ . The argon study will be only the second extensive study of a high-L Rydberg system with anisotropic ion core [6], and it should help to stimulate the development of the theoretical tools needed to understand these systems in detail.

An additional project involves the prediction of the behavior of  $\text{Th}^{3+}$  in the electric field and electric field gradient of a nearby point charge. As input to this study, we use recent relativistic many-body calculations of the energy levels and electric dipole and quadrupole matrix elements in this Fr-like ion [7]. Our goal is to develop a better understanding of the connection between free actinide ion properties and the chemistry of actinide compounds. In this case, we hope to make contact with recent ZEKE studies of the low-lying levels of  $\text{ThO}^+$  [8] and with recent quantum chemistry calculations of the levels of this molecular ion [9].

### **References**

- [1] "Polarizability of  $\text{Kr}^{6+}$  from High-L  $\text{Kr}^{5+}$  Fine Structure Measurements", S.R. Lundeen and C.W. Fehrenbach, Phys. Rev. A 75, 032523 (2007)
- [2] "Determination of the polarizability of Na-like Silicon by study of the fine structure of high-L Rydberg states of  $\text{Si}^{2+}$ ", R.A. Komara, M.A. Gearba, S.R. Lundeen, and C.W. Fehrenbach, Phys. Rev A 67, 062502 (2003)
- [3] "Higher-order contributions to fine structure in high-L Rydberg states of  $\text{Si}^{3+}$ ", E.L. Snow and S.R. Lundeen, Phys. Rev. A 75, 062512 (2007)

- [4] "Determination of dipole and quadrupole polarizabilities of  $\text{Ba}^+$  by measurement of the fine structure of high-L, n=9 and 10 Rydberg states of Barium" E.L. Snow, M.A. Gearba, W.G. Sturrus, and S.R. Lundeen, Phys. Rev A 71, 022510 (2005)
- [5] "Fine Structure Measurements in high-L, n=17 and n=20 Rydberg states of Barium", E.L. Snow and S.R. Lundeen (In preparation)
- [6] "Adventures of a Rydberg electron in an anisotropic world", William Clark and Chris H. Greene, Rev. Mod. Phys. 71, 821 (1999)
- [7] "Excitation energies, polarizabilities, multipole transition rates, and lifetimes in Th IV", U.I. Safronova, W.R. Johnson, and M.S. Safronova, Phys. Rev. A 74, 042511 (2006)
- [8] "Spectroscopy of the ground and low-lying excited states of  $\text{ThO}^{+}$ ", Vasilii Goncharov and Michael C. Heaven, J. Chem Phys. 124, 064312 (2006)
- [9] "Ab initio studies of systems containing actinides using relativistic effective core potentials", R.Tyagi, PhD Thesis, Ohio State University, 2005

### **Recent Publications:**

"Ion Properties from High-L Rydberg Fine Structure: Dipole Polarizability of  $\text{Si}^{2+}$ " R.A. Komara, M.A. Gearba, C.W. Fehrenbach, and S.R. Lundeen, J. Phys. B. At. Mol. Opt. Phys. 38, S87 (2005)

"Stark-induced X-ray emission from H-like and He-like Rydberg ions", M.A. Gearba, R.A. Komara, S.R. Lundeen, C.W. Fehrenbach, and B.D. DePaola, Phys. Rev A 71, 013424 (2005)

"Determination of dipole and quadrupole polarizabilities of  $\text{Ba}^+$  by measurement of the fine structure of high-L, n=9 and 10 Rydberg states of Barium" E.L. Snow, M.A. Gearba, W.G. Sturrus, and S.R. Lundeen, Phys. Rev A 71, 022510 (2005)

"Fine Structure in High-L Rydberg states: A Path to Properties of Positive Ions" in *Advances in Atomic, Molecular, and Optical Physics*, Vol. 52 edited by Chun C. Lin and Paul Berman (Academic Press, 2005)

"Relative charge transfer cross section from Rb(4d)", M.H. Shah, H.A. Camp, M.L. Trachy, X. Flechard, M.A. Gearba, H. Nguyen, R. Bredy, S.R. Lundeen, and B.D. DePaola, Phys. Rev. A 72, 024701 (2005)

"Optical spectroscopy of high-L Rydberg states of Argon" L.E. Wright, E.L. Snow, S.R. Lundeen, and W.G. Sturrus, Phys. Rev. A 75, 022503 (2007)

"Higher-order contributions to fine structure in high-L Rydberg states of  $\text{Si}^{3+}$ ", E.L. Snow and S.R. Lundeen, Phys. Rev. A 75, 062512 (2007)

"Polarizability of  $\text{Kr}^{6+}$  from High-L  $\text{Kr}^{5+}$  Fine Structure Measurements", S.R. Lundeen and C.W. Fehrenbach, Phys. Rev. A 75, 032523 (2007)

"Fine Structure Measurements in high-L, n=17 and n=20 Rydberg states of Barium", E.L. Snow and S.R. Lundeen (In preparation)

# **Photoabsorption by Free and Confined Atoms and Ions**

Steven T. Manson, Principal Investigator

*Department of Physics and Astronomy, Georgia State University, Atlanta, Georgia 30303*  
[\(smanson@gsu.edu\)](mailto:smanson@gsu.edu)

## ***Program Scope***

The goals of this research program are: to provide a theoretical adjunct to, and collaboration with, the various atomic and molecular experimental programs that employ third generation light sources, particularly ALS and APS; to generally enhance our understanding of the photoabsorption process; and to study the properties (especially photoabsorption) of confined atoms and ions. To these ends, calculations are performed employing and enhancing cutting-edge methodologies to provide deeper insight into the physics of the experimental results; to provide guidance for future experimental investigations; and seek out new phenomenology, especially in the realm of confined systems. The general areas of programmatic focus are: manifestations of nondipole effects in photoionization; photodetachment of inner and outer shells of atoms and atomic ions (positive and negative); exploratory studies of atoms endohedrally confined in buckyballs, C<sub>60</sub>. Flexibility is maintained to respond to opportunities that present themselves as well.

## ***Recent Progress***

### **1. Nondipole Effects in Atoms**

Up until relatively recently, the conventional wisdom was that nondipole effects in photoionization were of importance only at photon energies of tens of keV or higher, despite indications to the contrary more than 35 years ago [1]. The last decade has seen an upsurge in experimental and theoretical results [2] showing that nondipole effects in photoelectron angular distributions could be important down to hundreds [3] and even tens [4] of eV. Our recent work included a combined calculational and laboratory investigation that has provided the first experimental evidence for a quadrupole Cooper minimum, a phenomenon that had been predicted to exist much earlier [5], revealed in studies of nondipole effects in Xe 5s and 5p [5]. While the evidence is much “cleaner” for the 5s case, the 5p case shows how much can be learned by a careful analysis of a combined theoretical and experimental investigation.

In addition, a study of the photoionization of Hg, an atom heavy enough so that relativistic effects are important, has been initiated [6]. To begin with, the investigation concentrated on the valence 6s subshell, and revealed the importance of relativistic interactions that split single Cooper minima into several minima. And, since Cooper minima were found in the *quadrupole* photoionization channels, these relativistic splitting had significant effects upon the nondipole photoelectron angular distribution parameter  $\gamma_{6s}$  which exhibits strong oscillations, as a function of photon energy, down to threshold. These oscillations were found to be the result of interchannel coupling of the 6s photoionization channels with the various inner-shell channels. These results provide an excellent case for experimental scrutiny.

## 2. Atomic Photoionization

The study of photoionization of atoms, particularly open-shell atoms, leads to results of great complexity. Our effort is to perform state-of-the-art calculations, in concert with high-resolution synchrotron experiments, to understand this complexity. This philosophy has been applied to inner-shell photoionization of atomic Na, one of the simplest open-shell atoms. Nevertheless,  $2p$  ionization, leaving the  $\text{Na}^+$  ion in  $2p^63s$ ,  $2p^63p$ ,  $2p^63d$  and  $2p^64s$  states, leads to a total of 32 thresholds and more than 110 resonance series. The cross sections are further complicated by the fact that the  $3d$  and  $4s$  thresholds are nearly degenerate so that the small spin-orbit force mixes many of the  $\text{Na}^+$  states. This results in thresholds that are of mixed  $2p^63d$  and  $2p^64s$  character and, the autoionizing resonances below each of these thresholds are of very complex character. We have performed extensive photoionization calculations of  $2p$  photoionization in Na [7] in conjunction with an ALS experiment, and agreement was quite good overall. Using the theoretical and experimental results in combination, we have begun to characterize the resonances and make sense of the complex situation. In addition, we have learned how relativistic interactions can be important at such low Z.

We have also looked at the dipole photoelectron angular distribution parameter,  $\beta$ , of the near-valence ns subshell in the vicinity of the  $nd \rightarrow \epsilon p$  transitions in Kr and Xe [8]. Absent relativistic effects, the value of  $\beta$  for an ns subshell must be 2 for a closed-shell atom [9]. The calculations were stimulated by an experimental study which found deviations from the value of 2. Using an explicitly relativistic methodology, we were able to explain the experimental data both qualitatively and quantitatively.

## 3. Confined Atoms

The study of confined atoms is in its infancy. There are a handful of theoretical investigations of various atoms endohedrally confined in  $C_{60}$  [10], but no experiment as of yet. Thus, we are involved in a program of exploratory calculations aimed at providing a compendium of the properties of such systems, especially photoionization, to tempt the experimental community. One of our recent studies has considered the combined role of correlation, relativity and confinement upon an extremely sensitive facet of the photoionization cross section of the alkali earth atoms, Mg, Ca, Rb and Ba, the Cooper minima in valence ns photoionization [11]. This work showed that the confining potential of the encapsulating  $C_{60}$  could alter the ground state charge density of these atoms very considerably, thereby engendering dramatic changes in the location of these Cooper minima. Furthermore, this potential also causes a sizable change in the threshold cross section, in many cases.

### ***Future Plans***

Fundamentally our future plans are to continue on the paths set out above. In the area of nondipole effects the inner subshells of Hg will be investigated to try to unravel the combined effects of many-body correlation effects and relativistic interactions. In addition, the search for cases where nondipole effects are likely to be significant, as a guide for experiment, will continue. The study of the photodetachment of  $C^-$  shall move on to the photoabsorption in the vicinity of the K-shell edge of both the ground  $^4S$  and excited  $^2D$  states in order to understand how the slight excitation of the outer shell affects the inner-shell photoabsorption and to pave the way for experiment, in addition to further

study of Na<sup>-</sup>. Additionally, a study of the photoionization of confined Hg atoms will be pursued in order to learn how the much larger relativistic effects in heavy systems affect the photoabsorption properties of caged atoms.

#### ***Publications Citing DOE Support Since September, 2003***

- "Nondipole Effects in the Photoionization of Xe 4d<sub>5/2</sub> and 4d<sub>3/2</sub>: Evidence for Quadrupole Satellites," O. Hemmers, R. Guillemin, D. Rolles, A. Wolska, D. W. Lindle, K. T. Cheng, W. R. Johnson, H. L. Zhou and S. T. Manson, Phys. Rev. Letters **93**, 113001-1-4 (2004).
- "Photodetachment of the Outer Shell of C<sup>-</sup> in the Ground State," H.-L. Zhou, S. T. Manson, A. Hibbert, L Vo Ky, N. Feautrier and J. C. Chang, Phys. Rev. A **70**, 022713-1-7 (2004).
- "Experimental Investigation of Nondipole Effects in Photoemission at the Advanced Light Source," R. Guillemin, O. Hemmers, D. W. Lindle and S. T. Manson, Radiation Phys. Chem. **73** 311-327 (2005).
- "Nondipole Effects in the Photoabsorption of Electrons in Two-Center Zero-Range Potentials," A. S. Baltenkov, V. K. Dolmatov, S. T. Manson and A. Z. Msezane, J. Phys. B **37**, 3837-3846 (2004).
- "Photoionization of the Ground-State Be-Like B<sup>+</sup> Ion Leading to the n=2 and n=3 States of B<sup>2+</sup>," D.-S. Kim and S. T. Manson, J. Phys. B **37**, 4013-4024 (2004).
- "Nondipole Effects in Xe 4d Photoemission," O. Hemmers, R. Guillemin, D. Rolles, A. Wolska, D. W. Lindle, K. T. Cheng, W. R. Johnson, H. L. Zhou and S. T. Manson, J. Electron Spectrosc. **144-147**, 51-52 (2005).
- "Photoionization of the Excited 1s<sup>2</sup>2s2p <sup>1,3</sup>P States of Be-like B<sup>+</sup>," D.-S. Kim and S. T. Manson, Phys Rev. A **71**, 032701-1-12 (2005).
- "Photoabsorption By Atoms and Ions," S. T. Manson, in *The Physics of Ionized Gases*, Eds. L. Hadzievski, T. Grozdanov and N. Bibic (AIP, Melville, New York, 2004), pp. 49-58.
- "Photoionization of the Ground-State Be-Like C<sup>+2</sup> Ion Leading to the n=2 and n=3 States of C<sup>3+</sup>," D.-S. Kim and S. T. Manson, J. Phys. B **37**, 4707-4718 (2004).
- "Gigantic Enhancement of Atomic Nondipole Effects: the 3s→3d Resonance in Ca," V. K. Dolmatov, D. Bailey and S. T. Manson, Phys. Rev A **72**, 022718-1-6 (2005).
- "Photodetachment of the Outer Shell of C<sup>-</sup> in the Excited <sup>2</sup>D State", H.-L. Zhou, S. T. Manson, A. Hibbert, L. Vo Ky and N. Feautrier, Phys. Rev. A **72**, 032723-1-12 (2005).
- "Photoelectron Spectra of N@C<sub>60</sub> Molecule on Crystalline Si Surface," A. S. Baltenkov, U. Becker, S. T. Manson and A. Z. Msezane, Phys Rev. B **73**, 075404-1-8 (2006).
- "Elastic Electron Scattering From Multicenter Potentials," A. S. Baltenkov, S. T. Manson and A. Z. Msezane, J. Phys. B **40**, 769-777 (2007).
- "Strong Final-State Term-Dependence of Nondipole Photoelectron Angular Distributions from Half-Filled Shell Atoms," V.K. Dolmatov and S. T. Manson, Phys. Rev A **74**, 032705-1-7 (2006).
- "Resonance Induced Deviations of β from 2.0 for Rare Gas s-Subshell Photoionization," S. B. Whitfield, R. Wehlitz, H. R. Varma, T. Banerjee, P. C. Deshmukh and S. T. Manson, J. Phys. B **39**, L335-L343 (2006).

- “Spin-Polarized Photoelectrons from Half-Filled Shell Atoms,” V. K. Dolmatov and S. T. Manson, Phys. Rev. A **75**, 022701-1-4 (2007).
- “Dipole and Quadrupole Cooper Minima and their Effects on Dipole and Nondipole Photoelectron Angular Distributions in Hg 6s,” T. Banerjee, P. C. Deshmukh and S. T. Manson, Phys. Rev. A **75**, 042701-1-8 (2007).
- “Dynamical and Relativistic Effects in Experimental and Theoretical Studies of Inner-Shell Photoionization of Sodium,” D. Cubaynes, H. L. Zhou, N. Berrah, J.-M. Bizau, J. D. Bozek, S. Canton, S. Diehl, X.-Y. Han, A. Hibbert, E. T. Kennedy, S. T. Manson, L. VoKy and F. J. Wuilleumier, Phys. Rev. A **40**, F121-F129 (2007).
- “Theoretical and Experimental Demonstration of the Existence of Quadrupole Cooper Minima,” P. C. Deshmukh, T. Banerjee, H. R. Varma, O. Hemmers, R. Guillemin, D. Rolles, A. Wolska, S. W. Yu, D. W. Lindle, W. R. Johnson, and S. T. Manson, J. Phys. B (submitted).
- “Confinement, Correlation and Relativistic Effects on the Photoionization of the 6s Subshell of Hg,” H. R. Varma, T. Banerjee, S Sunil Kumar, P. C. Deshmukh, V. K. Dolmatov and S. T. Manson, J. Phys. B (submitted).
- “Krypton E2 Photoionization Cross-sections and Angular Distribution of Photoelectrons,” T. Banerjee, P. C. Deshmukh and S. T. Manson, J. Phys. B (submitted).
- “Correlation and Relativistic Effects in the Photoionization of Confined Atoms,” H. R. Varma, P. C. Deshmukh, V. K. Dolmatov and S. T. Manson, Phys. Rev. A (in press).
- “Photoionization of Hydrogen-like Ions Surrounded by a Charged Spherical Shell,” A. S. Baltenkov, S. T. Manson and A. Z Msezane, Phys. Rev. A (submitted).

### **References**

- [1] M. O. Krause, Phys. Rev. **177**, 151 (1969).
- [2] O. Hemmers, R. Guillemin and D. W. Lindle, Radiation Phys. and Chem. **70**, 123 (2004) and references therein.
- [3] O. Hemmers, R. Guillemin, E. P. Kanter, B. Kraessig, D. W. Lindle, S. H. Southworth, R. Wehlitz, J. Baker, A. Hudson, M. Lotrakul, D. Rolles, W. C. Stolte, I. C. Tran, A. Wolska, S. W. Yu, M. Ya. Amusia, K. T. Cheng, L. V. Chernysheva, W. R. Johnson and S. T. Manson, Phys. Rev. Letters **91**, 053002 (2003).
- [4] V. K. Dolmatov and S. T. Manson, Phys. Rev. Letters **83**, 939 (1999).
- [5] L. A. LaJohn and R. H. Pratt, Radiation Phys. and Chem. **61**, 365 (2001); **71**, 665 (2004); and references therein.
- [6] T. Banerjee, P. C. Deshmukh and S. T. Manson, Phys. Rev A **75**, 042701 (2007).
- [7] P. C. Deshmukh, T. Banerjee, H. R. Varma, O. Hemmers, R. Guillemin, D. Rolles, A. Wolska, S. W. Yu, D. W. Lindle, W. R. Johnson, and S. T. Manson, J. Phys. B (submitted).
- [8] S. B. Whitfield, R. Wehlitz, H. R. Varma, T. Banerjee, P. C. Deshmukh and S. T. Manson, J. Phys. B **39**, L335 (2006).
- [9] S. T. Manson and A. F. Starace, Rev. Mod. Phys. **54**, 389 (1982).
- [10] V. K. Dolmatov, A. S. Baltenkov, J.-P. Connerade and S. T. Manson, Radiation Phys. Chem. **70**, 417 (2004).
- [11] H. R. Varma, P. C. Deshmukh, V. K. Dolmatov and S. T. Manson, Phys. Rev. A (in press).

## PROGRESS REPORT

### ELECTRON-DRIVEN PROCESSES IN POLYATOMIC MOLECULES

Investigator: Vincent McKoy

A. A. Noyes Laboratory of Chemical Physics  
California Institute of Technology  
Pasadena, California 91125  
*email:* mckoy@caltech.edu

### PROJECT DESCRIPTION

The focus of this project is the continued development, extension, and application of accurate, scalable methods for computational studies of low-energy electron–molecule collisions, with emphasis on larger polyatomics relevant to materials-processing and biological systems. Because the required calculations are highly numerically intensive, efficient use of large-scale parallel computers is essential, and the computer codes developed for the project are designed to run both on tightly-coupled parallel supercomputers and on workstation clusters.

### HIGHLIGHTS

In the past year, we have made significant progress in our understanding of the low-energy electron–molecule scattering resonances of the DNA nucleobases. Principal developments include:

- A comparative study of elastic electron scattering by the pyrimidine bases and nucleosides of DNA (thymine, cytosine, deoxythymidine, and deoxycytidine)
- A detailed study of elastic scattering by the model system pyrazine, which revealed strong resonant channel-coupling effects that are relevant to the RNA and DNA nucleobases
- Initiation of a collaborative experimental-theoretical effort to explore electron scattering by alcohols, which are of interest both as biomolecules and as alternative fuels

### ACCOMPLISHMENTS

During 2007, we completed our initial survey of DNA and RNA constituents with a study of the pyrimidine nucleobases and nucleosides thymine, cytosine, 2'-deoxythymidine, and 2'-deoxycytidine [1]. This study complements our earlier work on the RNA base uracil [2], on the purine nucleobases, nucleosides, and nucleotides [3], and on the DNA backbone subunits [4]. In general we observe good agreement between the  $\pi^*$  resonance energies that we calculate for the nucleobases and the energies of features in the electron transmission spectrum that Burrow and coworkers [5,6] previously assigned as the  $\pi^*$  resonances. Therefore, a principal conclusion from our survey of the nucleobases is that the assignments by Burrow and coworkers are likely correct, although previous calculations had yielded significantly higher resonance energies [7,8]. A correct assignment of the  $\pi^*$  resonances is essential to the understanding of electron–DNA dynamics, in particular the resonant dissociation processes that appear to drive DNA damage by slow electrons.

One surprising result from our work on the DNA/RNA bases was that our energies for the two lowest-energy  $\pi^*$  resonances were always much closer to the experimental positions than our results for the third  $\pi^*$  resonance. Similar behavior had been seen in earlier calculations on benzene [9,10], suggesting a systematic problem. We explored the issue in a series of calculations on the

model system pyrazine (1,4-diazabenzene) and determined that the third  $\pi^*$  resonance is strongly mixed with core-excited resonances built on low-lying triplet states [11,12]. Accounting for this channel coupling or continuum configuration interaction effect turns out to be essential to obtaining an accurate energy for the third  $\pi^*$  resonance. Moreover, the decay of such a mixed resonance into triplet electronic states provides a possible doorway mechanism for initiating damage to DNA.

In the past year, we also broadened the scope of our biomolecular studies as participants in a U.S.–Brazil, experimental–theoretical collaboration that is just getting under way and that will explore electron collisions with alcohols and related molecules. Initial efforts have been concentrated on elastic scattering by the simplest alcohols, methanol and ethanol. Later work will consider more complex alcohols, inelastic processes, and dissociative attachment. The alcohols are of interest both as models of larger biomolecules that contain hydroxyl groups and as biofuels, and studies of their interactions with electrons may assist in the modeling of spark ignition in alcohol-fueled engines.

## PLANS FOR COMING YEAR

In the coming year, we intend to revisit scattering by the nucleobases in order to explore the consequences of resonant channel coupling of the type that we found in pyrazine. We will start with the simplest base, uracil, and examine how channel coupling affects both the energy of the third  $\pi^*$  resonance and the magnitude of the near-threshold cross sections for electron-impact excitation to low-lying triplet states. We will also continue studies of other DNA constituents and subassemblies, and we will continue our work on the alcohols with studies of 1-propanol, 1-butanol, and, as time permits, other systems. As part of the code development in support of ongoing calculations, we plan to parallelize the remaining sequential section of our main scattering code in order to remove the present limitation ( $\sim$ 16,000 configuration state functions) on the size of our variational basis sets. We have already rewritten much of the relevant code in a form that is more amenable to parallelization and less disk-intensive, and the remaining steps should be straightforward.

## REFERENCES

- [1] C. Winstead, V. McKoy, and S. d’A. Sanchez, *J. Chem. Phys.* (in press).
- [2] C. Winstead and V. McKoy, *J. Chem. Phys.* **125**, 174304 (2006).
- [3] C. Winstead and V. McKoy, *J. Chem. Phys.* **125**, 244302 (2006).
- [4] C. Winstead and V. McKoy, *J. Chem. Phys.* **125**, 074302 (2006).
- [5] K. Aflatooni, G. A. Gallup, and P. D. Burrow, *J. Phys. Chem. A* **102**, 6205 (1998).
- [6] A. M. Scheer, K. Aflatooni, G. A. Gallup, and P. D. Burrow, *Phys. Rev. Lett.* **92**, 068102 (2004).
- [7] S. Tonzani and C. H. Greene, *J. Chem. Phys.* **124**, 054312 (2006).
- [8] F. A. Gianturco and R. R. Lucchese, *J. Chem. Phys.* **120**, 7446 (2004).
- [9] F. A. Gianturco and R. R. Lucchese, *J. Chem. Phys.* **108**, 6144 (1998).
- [10] M. H. F. Bettega, C. Winstead, and V. McKoy, *J. Chem. Phys.* **112**, 8806 (2000).
- [11] C. Winstead and V. McKoy, *Phys. Rev. Lett.* **98**, 113201 (2007).
- [12] C. Winstead and V. McKoy, *Phys. Rev. A* **76**, 012712 (2007).

## PROJECT PUBLICATIONS AND PRESENTATIONS, 2004–2007

1. “Low-Energy Electron Collisions with Sulfur Hexafluoride, SF<sub>6</sub>,” C. Winstead and V. McKoy, J. Chem. Phys. **121**, 5828 (2004).
2. “Elastic Electron Scattering by C<sub>2</sub>F<sub>4</sub>,” C. Winstead and V. McKoy, J. Chem. Phys. **122**, 234304 (2005).
3. “Low Energy Electron Scattering by DNA Bases,” S. d’A. Sanchez, C. Winstead, and V. McKoy, XXIV International Conference on Photonic, Electronic, and Atomic Collisions, Rosario, Argentina, 20–26 July, 2005.
4. “Recent Progress with the Schwinger Multichannel Method,” C. Winstead, V. McKoy, and S. d’A. Sanchez, Fourteenth International Symposium on Electron–Molecule Collisions and Swarms, Campinas, Brazil, 27–30 July, 2005 (*invited talk*).
5. “Low-Energy Electron Scattering by N<sub>2</sub>O and C<sub>2</sub>H<sub>4</sub>,” M. H. F. Bettega, C. Winstead, and V. McKoy, Fourteenth International Symposium on Electron–Molecule Collisions and Swarms, Campinas, Brazil, 27–30 July, 2005.
6. “Elastic Electron Scattering by Ethylene, C<sub>2</sub>H<sub>4</sub>,” C. Winstead, V. McKoy, and M. H. F. Bettega, Phys. Rev. A **72**, 042721 (2005).
7. “Low-Energy Electron Collisions with Fullerene, C<sub>60</sub>,” C. Winstead and V. McKoy, Phys. Rev. A **73**, 012711 (2006).
8. “Total Dissociation Electron Impact Cross Sections for C<sub>2</sub>F<sub>6</sub>,” D. W. Flaherty, M. A. Kasper, J. E. Baio, D. B. Graves, H. F. Winters, C. Winstead, and V. McKoy, J. Phys. D **39**, 4393 (2006).
9. “Electron Collisions with Large Molecules: Computational Advances,” V. McKoy, American Chemical Society National Meeting, Atlanta, March 28, 2006 (*invited talk, Symposium on Theoretical and Experimental Advances in the Study of Low-Energy Electron-Induced Processes in Complex Systems*).
10. “Low-Energy Electron Scattering by N<sub>2</sub>O,” M. H. F. Bettega, C. Winstead, and V. McKoy, Phys. Rev. A **74**, 022711 (2006).
11. “Low-Energy Electron Collisions with Gas-Phase Uracil,” C. Winstead and V. McKoy, submitted to J. Chem. Phys. **125**, 174304 (2006).
12. “Low-Energy Electron Scattering by Deoxyribose and Related Molecules,” C. Winstead and V. McKoy, J. Chem. Phys. **125**, 074302 (2006).
13. “Electron Collisions with Large Molecules,” C. Winstead, Colloquium, Department of Physics, Federal University of Paraná, Curitiba, Brazil, July 27, 2006.
14. “Interaction of Low-Energy Electrons with the Purine Bases, Nucleosides, and Nucleotides of DNA,” C. Winstead and V. McKoy, J. Chem. Phys. **125**, 244302 (2006).
15. “Electron-Driven Processes in Polyatomic Molecules,” V. McKoy, XVI National Conference on Atomic and Molecular Physics, Tata Institute of Fundamental Research, Mumbai, India, 8–11 January, 2007 (*invited talk*).

16. "Resonant Channel Coupling in Electron Scattering by Pyrazine," C. Winstead and V. McKoy, Phys. Rev. Lett. **98**, 113201 (2007).
17. "Interactions of Slow Electrons with Biomolecules," V. McKoy, Molecular Theory for Real Systems Program, University of Tokyo, Japan, 18–19 March, 2007 (*invited talk*).
18. "Recent Computations of Electron Collisions with Large Molecules," V. McKoy, EIPAM 07 (Electron Induced Processes at the Molecular Level), Hveragerði, Iceland, 25–29 May, 2007 (*invited talk*).
19. "Interactions of Slow Electrons with Biomolecules," V. McKoy, XXV International Conference on Photonic, Electronic, and Atomic Collisions, Freiburg, Germany, 25–30 July, 2007 (*invited talk*).
20. "Electron Collisions with Biomolecules," V. McKoy, Fifteenth International Symposium on Electron–Molecule Collisions and Swarms, Reading, United Kingdom, 1–4 August, 2007 (*invited talk*).
21. "Low-Energy Electron Scattering by Pyrazine," C. Winstead and V. McKoy, Phys. Rev. A **76**, 012712 (2007).
22. "Interaction of Low-Energy Electrons with the Pyrimidine Bases and Nucleosides of DNA," C. Winstead, V. McKoy, and S. d'A. Sanchez, J. Chem. Phys. (in press).
23. "Resonant Interactions of Slow Electrons with DNA Constituents," C. Winstead, ASR 2007 (International Symposium on Charged Particle and Photon Interactions with Matter), JAEA Advanced Science Research Center, Tokaimura, Japan, 6–9 November, 2007 (*invited talk*).

## ELECTRON/PHOTON INTERACTIONS WITH ATOMS/IONS

Alfred Z. Msezane (email: [amsezane@cau.edu](mailto:amsezane@cau.edu))

Clark Atlanta University, Department of Physics and CTSPS, Atlanta, Georgia 30314

### Program Scope

We develop methodologies for calculating Regge pole trajectories and residues for both singular and nonsingular potentials, important in heavy particle collisions, chemical reactions and atom-diatom systems. Methods are developed for calculating the generalized oscillator strength (GOS), useful in probing the intricate nature of the valence- and open-shell as well as inner-shell electron transitions. Standard codes are used to generate sophisticated wave functions for investigating CI mixing and relativistic effects in atomic ions. The wave functions are utilized in exploring correlation effects in dipole and non-dipole photoionization studies. Regge trajectories probe the near-threshold formation of negative ions as Regge resonances in electron scattering, revealing new and interesting manifestations and yielding a better understanding of the underlying physics in this energy region.

### Recent Progress

#### A. Complex Angular Momentum Methods and Applications to Collisions

##### A.1 QUB Collaboration, UTK TEAM, CAU TEAM

Macek *et al.* [1] reported the novel and elegant Mulholland method, implemented within the complex angular momentum (CAM) representation of scattering, to calculate integral elastic scattering cross sections and demonstrated the approach by explaining the observed oscillations in proton-H scattering. Subsequently, the above important collaboration was formed.

Regge pole analysis has been applied to ion-atom [1], electron-atom [2] and reactive atom-diatom [3] scattering as well as to the resonance reactive scattering in the exchange reaction  $I + HI \rightarrow HI + I$  [4] through the Mulholland formula [5] to understand the low-energy oscillations in the total elastic cross section (TCS). Recently, it has been used for a fundamental understanding of the near-threshold electron attachment mechanism in  $e^-$  - Fr and  $e^-$  - Cs [6], capturing easily and unambiguously the main results of the Dirac R-matrix [7] and predicting new manifestations. Very recently, sinusoidal Regge oscillations have been demonstrated in the TCS in the F + H<sub>2</sub> reaction [8]. In general, the strength of the method lies in replacing the partial wave sum for the quantity of interest by a sum over the Regge singularities of the S-matrix element.

The robustness of the Thomas-Fermi (T-F) potential, used in [2, 4, 6], with respect to the variation of the parameters  $a$  and  $b$  of the polarization potential has been investigated for low-energy  $e^-$ -Ar,  $e^-$ -Kr and  $e^-$ -Rb elastic scattering. The optimized values of  $b$  with respect to the Ramsauer-Townsend (R-T) minima were then used in the  $e^-$ -Ar,  $e^-$ -Kr and  $e^-$ -Rb scattering. The calculated positions of the R-T minima and the corresponding TCS's minima compared very well with the values obtained by Savukov [9] and attendant measurements. It was concluded that the T-F potential captures the essential physics (Ramsauer-Townsend minima, the Wigner threshold law and Regge resonances) when used with the appropriate parameters. In  $e^-$ -Rb scattering we found, using the optimized  $b$  value, that the predicted resonance corresponding to  $\text{Re}(L) = 4$  remained and was enhanced in the DCS at  $\theta = 180^\circ$ , making its observation strongly possible. These results give great credence to our methodology and the T-F potential.

## A.2 Near-Threshold Electron Attachment as Regge Resonances: Cross Sections for K, Rb and Cs Atoms

This paper [10] explores in the near-threshold energy region the Wigner threshold law, the R-T minima, Regge resonances and the dominant orbital to which the electron preferentially attaches itself to form the temporary negative ions ( $K^-$ ,  $Rb^-$  or  $Cs^-$ ) as Regge resonances in  $e^-$ -K,  $e^-$ -Rb and  $e^-$ -Cs scattering. The DCS's critical minima, defined as the values where the differential cross sections have their smallest values as functions of the impact energy,  $E$  and scattering angle,  $\theta$ , are also investigated. We note that attachment of a very weakly bound electron by the polarization potential of the neutral state [11] produces inter-shell-type resonances. In particular K has an enormous dipole polarizability, causing the appearance of an extra characteristic minimum in its generalized oscillator strength [12]; consequently other peculiarities could be anticipated. Recently, it has been demonstrated through the low-energy electron scattering by  $N_2O$ , that sufficient representation of polarization effects can yield the measured shape resonance and a Ramsauer-Townsend minimum [13]. The Wigner threshold law is essential in high precision measurements of binding energies of valence electrons using photo-detachment threshold spectroscopy [14] and, recently, the s-wave Wigner law has been observed, accompanied by a d-wave component [15].

We found that the near-threshold electron collisions in these systems are characterized by the Wigner threshold law, Ramsauer-Townsend minima and Regge resonances, all discernible through Regge partial cross sections scrutiny. Additionally, the interesting results have been discovered for the  $e^-$ -Rb scattering: a d-wave Wigner threshold law, a d-wave R-T minimum and a d-wave resonance centered around 0.435 eV, all identifiable through even the TCS and that near-threshold electron attachment is preferentially to a d-orbital to form the temporary  $Rb^-$  ion. The sharp resonance at 1.727 eV is also identifiable through the DCS and is prominent at  $\theta = 180^\circ$ , thus permitting experimental verification.

In  $e^-$ -Cs scattering the near-threshold electron attachment is predominantly to a d-orbital and the combined s- and d-waves define the R-T minimum. In the  $e^-$ -K scattering the near-threshold dynamic interplay among the s-, p-, and d- wave Regge partial cross sections modifies the position, magnitude and shape of the R-T minimum. Also hidden within the innocent-looking TCS is the well-defined substructure extractable only through Regge partial cross sections scrutiny.

We conclude by noting that a short-lived resonance whose angular life is of the order of one full rotation may produce an oscillatory behavior in the energy dependence of the integral elastic cross sections and this has recently been demonstrated using the  $F + H_2$  reaction [8]. Finally, the present near-threshold data are expected to alleviate the lack of threshold scattering parameters such as elastic cross sections and the attendant understanding of the collision dynamics, which has severely curtailed the utilization of particularly K in Bose-Einstein condensation.

## B. Random Phase Approximation with Exchange (RPAE) for Open-Shell Atoms

The generalization of the RPAE to atoms (ions) with unfilled shells, a difficult problem, has recently been achieved by our group [16, 17] and used to study the inner-shell electron transition of an open-shell atom, such as the  $4d - \varepsilon f$  photoionization, the so-called giant resonance, of the atom I and the ions  $Xe^+$  and  $I^+$ , thereby greatly extending the scope and utility of the RPAE method. Recently, the theory has been extended to open outer-shells [17] and inner open-shells [18] and applied to  $Xe$  4d, 5s and 5d photoionization. Most recently, the method has been used to investigate the angular distribution of the open-shell Sc 4s photoionization [19] and the results compare very well with the measured data [20].

### C. Octupole Contribution to Dipole GOS's in Noble Gas Atoms

The optical oscillator strength, which determines the interactions with photons, is a special case of the GOS. Recently, we have investigated the contribution of discrete octupole to the dipole GOS's in the noble gas atoms [21], i.e.  $np \rightarrow (n+1)d$  and  $np \rightarrow (n+1)s$  ( $n \geq 2$ ) transitions for both dipole ( $L=1$ ) and octupole ( $L=3$ ) transitions,  $L$  being the total angular momentum. We found that the GOS's corresponding to  $L=3$  are characterized by an extra maximum near  $q^2=0$ ,  $q$  being the momentum transfer, and dominate over those of the  $L=1$  beyond about  $q^2=1.5$  a.u. Importantly, we also found that those levels with the same configurations  $np \rightarrow nd$  but different  $L$ 's,  $L=1$  and  $L=3$  are closely located and hardly separable in existing experiments. This implies they will be excited by electron (or other charged particles) impact simultaneously, but decay via photon emission separately; the decay of the octupole excitation being about eight orders of magnitude slower than the dipole one. Hence, the importance of the GOS investigations.

### D. Fine-Structure Energies, Oscillator Strengths and Lifetimes for Mn XIII

We have performed [22] large scale CIV3 calculations of excitation energies from ground state for 98 fine-structure levels as well as of oscillator strengths and radiative decay rates for all electric-dipole-allowed and intercombination transitions among the fine-structure levels of the terms belonging to the  $(1s22s22p6)3s23p$ ,  $3s3p2$ ,  $3s23d$ ,  $3p3$ ,  $3s3p3d$ ,  $3p23d$ ,  $3s3d2$ ,  $3s24s$ ,  $3s24p$ ,  $3s24d$ ,  $3s24f$ , and  $3s3p4s$  configurations of Al-like Manganese. Very extensive CI wave functions were employed and important relativistic effects in intermediate coupling were incorporated by means of the Breit-Pauli Hamiltonian. Our calculated excitation energies, including their ordering, are in excellent agreement with the available experimental results. A very significant difference between our calculated lifetimes and the corresponding values of Froese Fischer *et al* [23] for several fine-structure levels is discussed and new data for several fine-structure levels are also presented.

### Future Plans

The development and application of the CAM theory continue, particularly in chemical reactions and electron-atom/ion collisions. Other research activities, such as GOS and inner-shell of open-shell atoms (ions) investigations are pursued, including the probing of correlations. Extension of the Regge approach to the interesting and challenging multichannel case is advancing.

### References

1. J. H. Macek, P.S. Krstic' and S. Yu. Ovchinnikov, Phys. Rev. Lett. **93**, 183202 (2004)
2. D. Sokolovski, Z. Felfli, S. Yu. Ovchinnikov, J. H. Macek and A. Z. Msezane, Phys. Rev. A **76**, 012705 (2007)
3. D. Sokolovski, V. Aquilanti, S. Cavalli and D. de Fazio, J. Chem. Phys. **126**, 12101 (2007)
4. D. Sokolovski, A.Z. Msezane, Z. Felfli, S.Yu. Ovchinnikov and J.H. Macek, Nucl. Instr. and Meth. B, At Press (2007)
5. H.P. Mulholland, Proc. Camb. Phil. Soc. (London) **24**, 280 (1928)
6. Z. Felfli, A.Z. Msezane and D. Sokolovski, J. Phys. B **39**, L353 (2006)
7. C. Bahrim, U. Thumm and I.I. Fabrikant, Phys. Rev. A **63**, 042710 (2001)
8. D. Sokolovski, Z. Felfli, and A.Z. Msezane, Bull. Am. Phys. Soc. **52**, 96 (2007)
9. I.M. Savukov, Phys. Rev. Lett. **96**, 073202 (2006)
10. A.Z. Msezane, Z. Felfli and D. Sokolovski, J. Phys. Chem. (2007) [To appear in Lester Symposium, UC Berkeley, March 28-31, 2007]
11. V.I. Lengyel, V.T. Navrotsky, and E.P. Sabad, *Resonance Phenomena in Electron-Atom Collisions* (Springer-Verlag, Berlin, 1992), Chapt. 7
12. Z. Chen and A.Z. Msezane., J. Phys. B **33**, 5397 (2000)

13. M.H.F. Bettega, C. Winstead and V. McKoy, Phys. Rev. A **74**, 022711 (2006)
14. T. Andersen, H.K. Haugen and H. Hotop, J. Phys. Chem. Ref. Data **28**, 1511 (1999)
15. R.C. Bilodeau, J.D. Bozek, N.D. Gibson, C.W. Walter, G.D. Ackerman, I. Dumitriu and N. Berrah, Phys. Rev. Lett. **95**, 083001 (2005)
16. Zhifan Chen and A.Z. Msezane, Phys. Rev. A**72**, 050702 (R) (2005)
17. Zhifan Chen and A.Z. Msezane, J. Phys. B**39**, 4355 (2006)
18. Zhifan Chen and A.Z. Msezane, Phys. Rev. A, submitted (2007)
19. Zhifan Chen and A.Z. Msezane, Proc. XXV ICPEAC (Freiburg, Germany, 2007) to be presented July 2007
20. S. B. Whitfield *et. al.*, Phys. Rev. A **66**, 060701 (2002)
21. M. Ya. Amusia, L.V. Chernysheva, Z. Felfli and A.Z. Msezane, Phys. Rev. A **75**, 062703 (2007)
22. G.P. Gupta and A.Z. Msezane, Physica Scripta, At Press (2007)
23. C. Froese Fischer, G. Tachiev and A. Irimia, *At. Data Nucl. Data Tables* **92**, 607 (2006)

### Some Other Publications 2005 – 2007

1. “Superluminal Tunnelling as a Quantum Measurement Effect”, D. Sokolovski, A.Z. Msezane and V.R. Shaginyan Phys. Rev. A**71**, 064103 (2005)
2. “Non-dipole Effects in Spin Polarization of Photoelectrons from 3d Electrons of Xe, Cs and Ba”, M.Ya. Amusia, N.A. Cherepkov, L.V. Chernysheva, Z. Felfli and A.Z. Msezane, J. Phys. B**38**, 1133 (2005)
3. “Large Scale CIV3 Calculations of Fine-Structure Energy Levels, Oscillation Strengths and Lifetimes in Fe XIV and Ni XVI”, G.P. Gupta and A.Z. Msezane, Atomic Data Nuclear Data Tables **89**, 1 (2005)
4. “Dramatic Distortion of Xe 4d Giant Resonance by the C<sub>60</sub> Fullerene Shell”, M. Ya. Amusia, A.S. Baltenkov, L.V. Chernysheva, Z. Felfli and A.Z. Msezane, J. Phys. B **38**, L169 (2005)
5. “Modification of the Xe 4d Giant Resonance by the C<sub>60</sub> Shell in Molecular Xe@C<sub>60</sub>”, M. Ya. Amusia, A.S. Baltenkov, L.V. Chernysheva, Z. Felfli and A.Z. Msezane, Journal of Experimental and Theoretical Physics **102**, 53 (2006)
6. “Random Phase Approximation with Exchange for Inner-Shell Electron Transitions”, Zhifan Chen and A.Z. Msezane, Phys. Rev. A **72**, 050702 (R) (2005)
7. “Minima in Generalized Oscillator Strengths and the Approach to High Energy Limit”, N.B. Avdonina, D. Fursa, A.Z. Msezane and R.H. Pratt, Phys. Rev. A**71**, 062711 (2005)
8. “Soft X-ray Emission Lines of Fe XV in Solar Flare Observations and the Chandra Spectrum of Capella”, F.P. Keenan, J.J. Drake, S. Chung, N.S. Brickhouse, K.M. Aggarwal, A.Z. Msezane, R.S.I. Ryans and D.S. Bloomfield, ApJ **449**, 1203 (2006)
9. “Oscillator Strengths and Lifetimes in Kr XXV”, G.P. Gupta and A.Z. Msezane, Physica Scripta **73**, 556 (2006)
10. “Photoelectron Spectra of N@C<sub>60</sub> Molecule on Crystalline Si Surface”, A.S. Baltenkov, U. Becker, S.T. Manson and A.Z. Msezane, Phys. Rev. B**73**, 075404 (2006)
11. “Universal Cause of High-Tc Superconductivity and Anomalous Behavior of Heavy Fermion Metals”, V.R. Shaginyan, M.Ya. Amusia, A.Z. Msezane and K.G. Popov, in *New Topics in Superconductivity Research* (NOVA, Publishers, 2006) Ed. B.P. Martins pp.
12. “Near Threshold Behavior of Angular Anisotropy Parameters in Negative Ions Photo-Detachment”, M.Ya. Amusia, A.S. Baltenkov, L.V. Chernysheva, Z. Felfli and A.Z. Msezane, Phys. Rev. A**72**, 032727 (2005)
13. “Generalized Oscillator Strengths for the 3d Electrons of Cs, Ba, and Xe: Effects of Spin-Orbit-Activated Interchannel Coupling”, M. Ya. Amusia, L.V. Chernysheva, Z. Felfli, A.Z. Msezane, Phys. Rev. A**73**, 062716 (2006)
14. “Elastic Electron Scattering From Multicenter Potentials”, A. S. Baltenkov, S. T. Manson and A. Z. Msezane, J. Phys. B **40**, 769 (2007)

# Theory and Simulations of Nonlinear X-ray Spectroscopy of Molecules

Shaul Mukamel

*Department of Chemistry, University of California,  
Irvine Irvine, CA 92697-2025, Email: smukamel@uci.edu*

## Program Scope

Fourth generation x-ray light sources and pulses produced by high harmonic generation are expected to make coherent nonlinear spectroscopic measurements possible. Concepts used in multidimensional NMR and recently adapted to femtosecond optical and infrared spectroscopy are extended to design, predict, and simulate two-dimensional correlation x-ray spectroscopy(2DCXS) signals. 2DXCS depends on pulse coherence in an essential way, and should become feasible once intense, attosecond, transform-limited pulses become available. It will provide a unique probe for interactions between the core-transitions and electronic states that mediate these interactions, disentangle congested spectral features by projecting the signal on multiple axes, and monitor electron dynamics in real time.

A systematic theoretical framework for the description and computation of nonlinear ultrafast x-ray spectroscopies is developed based on the nonlinear response formalism. The response function is given by a sum of multitime correlation functions of the dipole operator that couples the molecule to the field. Different time orderings appearing in the time-dependent perturbative expansion of the density matrix are described as Liouville space-pathways and represented by double-side Feynman diagrams. Resonant experiments capable of testing electronic structure theory directly are designed by using core hole excitations as local switches to perturb valence electronic states and probes for the changes induced by these perturbations.

## Recent Progress

### Ab initio electronic structure methods for simulating nonlinear x-ray signals

The calculation of valence excitations in molecules is a routine task for modern quantum chemical methods. A variety of many-body methods are available. In contrast, first-principles techniques for core-excitations are mostly limited to independent-particle approaches. X-ray signals involve states with different numbers of core-holes and thus require methods capable of describing the valence and core excited states on an equal footing. This can be done using the equivalent-core approximation (ECA) whereby the core transitions are described by the valence transitions of the equivalent-core molecule, which has an additional valence electron and modified nuclei configuration. Within the ECA, states with multiple core electrons excited correspond to valence transitions of multielectron character. The existing implementations of time dependent density functional theory TDDFT rely on the adiabatic approximation and are not capable of describing such states. We thus adopted a simplified algorithm whereby the valence states are described using determinants made of the original and equivalent-core KS orbitals. Within this ECA/determinants approximation, the valence transitions of two electron character are described as determinants where two occupied KS orbitals are substituted by two unoccupied orbitals. This approximation captures the ordering and relative intensities of the core transitions, and is thus adequate for predicting the x-ray correlation techniques as described below.

### Studying valence electronic states with all-x-ray stimulated Raman spectroscopy

An all x-ray pump-probe experiment was simulated, whereby the interaction with an attosecond x-ray pump tuned resonantly to a specific core hole transition creates an electronic wavepacket, which is then detected by a delayed x-ray probe. The dependence of the probe absorption on the delay provides information on the time evolution of the electronic states constituting the wavepacket. The valence wavepacket is initially centered on the atom whose core shell is resonant with the pump frequency. Similarly, the probe absorption reflects the unoccupied states in the vicinity of the core-shell resonant with the probe frequency. By tuning the pump and the probe frequencies, one can control where the wavepacket is created and where it is probed. Tuning the pump and probe

frequencies to different core transitions makes it possible to study the delocalization of the electronic states.

We have used the doorway-window representation of the nonlinear response, whereby the signal is written as the Liouville-space overlap between the doorway operator representing the electronic wavepacket created by the pump and the window operator representing the interaction with the probe. This representation provides an intuitive picture of the pump-probe measurement by dividing it into wavepacket creation, propagation, and detection stages.

The stimulated Raman signal of 5-quinolinol, a two-ring system in which the O and N atoms are located on the different rings was simulated and analyzed using this algorithm.

### Two-dimensional x-ray coherent correlation spectroscopy of molecules

The 2DXCS signal represents a time-resolved coherent all-x-ray four-wave mixing process carried out by subjecting the molecule to a sequence of three pulses (Figure 1a) and use a fourth pulse for heterodyne detection. The coherent signal generated in the  $\mathbf{k}_I = -\mathbf{k}_1 + \mathbf{k}_2 + \mathbf{k}_3$  direction is recorded as a function of the delays  $t_1$ ,  $t_2$ , and  $t_3$  between consecutive pulses. The spectrum is then Fourier-transformed with respect to the  $t_1$  and  $t_3$  delays, and displayed as a two-dimensional frequency correlation plot.

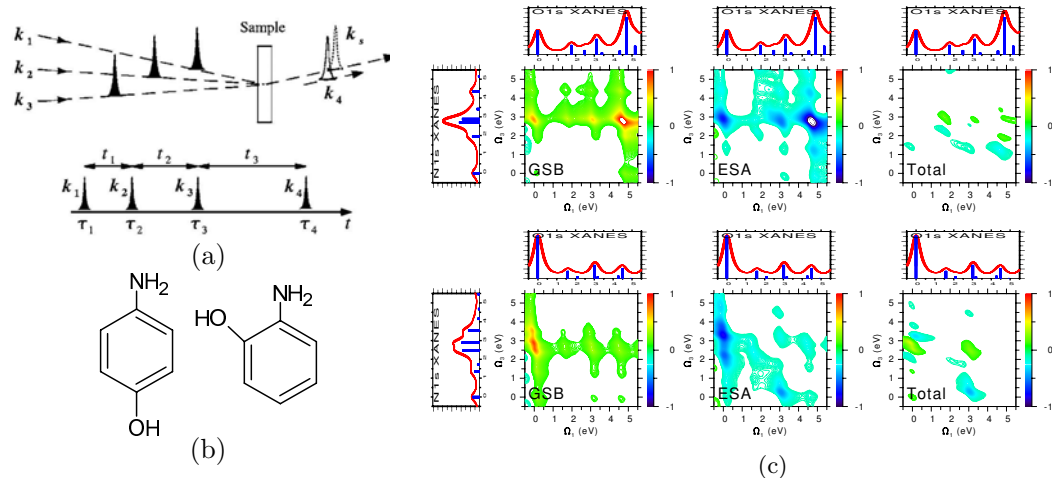


FIG. 1: (a) Pulse sequence and time intervals in a four-wave mixing experiment. Three pulses  $\mathbf{k}_1$ ,  $\mathbf{k}_2$ , and  $\mathbf{k}_3$  induce a polarization in the molecule, which is probed by the heterodyne field  $\mathbf{k}_4$ . (b) Para and ortho isomers of aminophenol. (c) Simulated O1s/N1s 2DXCS cross peak ( $t_2 = 0$ ) and its GSB and ESA components for para- (upper panel) and ortho-aminophenol (lower panel). Insets show the simulated O1s and N1s XAS.

Multiple core-excited states are resonantly excited with the pulses' bandwidths (10 eV for a 125 attosecond pulse). These are much smaller than the splitting between the N1s and O1s transitions ( $\sim 120$  eV). The carrier frequencies thus select the desired type of core transitions, while the envelopes control which valence excitations of the selected type contribute to the response. Transitions of the same type contribute to the diagonal part of the correlation spectrum, while features arising from interactions among spectrally separated transitions appear as off-diagonal cross peaks. By spreading the signal over multiple frequency axes, the weak signatures of interactions between different transitions can be separated from strong same-transition signals.

The capabilities of this technique were demonstrated in the simulations of the 2DXCS spectrum for aminophenols isomers (Figure 1b). In both isomers, the calculated ground-state bleaching (GSB) component is identical to a two-dimensional product of the O1s and N1s XANES spectra. In the para isomer, the O and N atoms are spatially separated, and promoting the O1s electron only weakly affects the N1s transitions. Consequently, the excited-state absorption (ESA) and GSB components are similar and interfere destructively. The total 2DXCS cross peak is weak. In the ortho isomer, the O and N atoms are close, and exciting the O1s electron strongly affects the N1s transitions. The ESA peaks are shifted, resulting in a stronger 2DXCS cross peak. Thus, the 2DXCS cross peak is highly sensitive to the relative position of the N and O atoms in the two isomers.

## Future plans

X-ray spectroscopy of molecules with multiple identical cores such as the nitrogen K-edge of the DNA nucleobases and basepairs will be calculated. Sequence-specific response properties will be identified. DNA is a logical choice of system to apply 2DXCS techniques. Other possible techniques which use different phase-matching directions will be systematically classified and their information content will be explored using Liouville-space pathway analysis. Higher level electronic structure calculations for core excitations will be developed. Our simulation studies demonstrated how coherent control combined with adaptive polarization pulse shaping and a genetic algorithm may be used to simplify femtosecond coherent nonlinear optical signals of excitons. Cross-peaks are amplified and resolved, and diagonal peaks are suppressed by shaping the second pulse in a two-pulse echo experiment on the Soret band of a porphyrin dimer. Various optimization strategies of the pulse spectral, temporal and polarization profiles were compared. These strategies will be extended to the x-ray regime. We had demonstrated how dynamic correlations of heavy-hole and light-hole excitons in semiconductor quantum wells may be investigated by two-dimensional correlation spectroscopy. The coherent response to three femtosecond optical pulses was predicted to yield cross peaks that contain direct signatures of many-body two-exciton correlations. A theory for two-dimensional optical spectroscopy of excitons in semiconductor nanostructures will be developed.

## Publications Resulting from the Project

- [P1] "The Role of Water on Electron-Initiated Processes and Radical Chemistry: Issues and Scientific Advances", B.C. Garrett, et.al, Chem. Rev. 105, 355-389 (2005)
- [P2] "Multipoint Fluorescence Quenching Time Statistics for Single Molecules with Anomalous Diffusion", V. Barsegov and S. Mukamel, J. Phys. Chem, 108, 15-24 (2004)
- [P3] "Simulation of Optical and X-ray Sum Frequency Generation Spectroscopy of 1-dimensional Molecular Chain," S. Tanaka and S. Mukamel, J. Electron Spectrosc. Relat. Phenom. 136, 185-190 (2004)
- [P4] "Simulation of x-ray absorption near edge spectra of electronically excited ruthenium tris-2,2'-bipyridine," S. Mukamel and L. Campbell, J. Chem. Phys. 121(24), (2004)
- [P5] "Generalized TDDFT Response Functions for Spontaneous Density Fluctuations and Nonlinear Response: Resolving the Causality Paradox in Real Time," S. Mukamel, Phys. Rev. A 71, 024503 (2005)
- [P7] "Superoperator Many-body Theory of Molecular Currents:Non-equilibrium Green Functions in Real Time", U. Harbola and S. Mukamel in Theory and Applications of Computational Chemistry: The First 40 Years. C. E. Dykstra, G. Frenking, K. S. Kim and G. E. Scuseria, 373-396, Elsevier, Amsterdam (2005)
- [P8] "Coherent-Control of Pump-Probe Signals of Helical Structures by Adaptive Pulse Polarizations," D. Voronine, D. Abramavicius, S. Mukamel, J. Chem. Phys. 124, 034104 (2006)
- [P9] "Anomalous continuous-time-random-walk spectral diffusion in coherent third order optical response," F. Sanda, S. Mukamel, Phys. Rev. E 73, 011103 (2006)
- [P10] "Multiple Core-Hole Coherence in X-Ray Four-Wave-Mixing-Spectroscopies," S. Mukamel, Phys. Rev. B 72, 235110 (2005)
- [P11] "Simulation of XANES and X-ray Fluorescence Spectra of Optically Excited Molecules," R.K. Pandey and S. Mukamel, J. Chem. Phys 124, 094106 (2006)
- [P13] "Quantum Master Equation for Electron Transport Through Quantum Dots and Single Molecules", U. Harbola, M. Esposito and S.Mukamel. Phys. Rev. B. 74,235309 (2007)
- [P14] "Manipulating Multidimensional Electronic Spectra of Excitons by Polarization Pulse-Shaping," D. Voronine, D. Abramavicius, S. Mukamel, J.Chem. Phys. 126,044508(2007)

- [P15] "Manipulating Multidimensional Nonlinear Spectra of Excitons by Coherent Control with Polarization Pulse Shaping," D. Voronine, D. Abramavicius and S. Mukamel. In *Ultrafast Phenomena XV*, R.J.D. Miller, A.M. Weiner, P. Cornum and D.M. Jonas (editors) Springer Verlag (2006)
- [P16] "Multipoint Correlation Functions for Photon Statistics in Single Molecule Spectroscopy; Stochastic Dynamics in Liouville Space," F. Sanda and S. Mukamel. In "Theory, Modeling and Evaluation of Single-Molecule Measurements", Editors E. Barkai, F. Brown, M. Orrit and H. Yang, World Scientific, (2007).
- [P17] "Simulation of X-ray Absorption Near Edge of Organ Metallic Compounds in the Ground and Optically Excited States," R. Pandey and S. Mukamel., *J.Phys.Chem.A.* 111,805-816 (2007).
- [P18] "Two-Dimensional Optical Spectroscopy of Excitons in Semiconductor Quantum Wells: Liouville-Space Pathways Analysis," L. Yang, I.V. Schweigert, S. Cundiff and S. Mukamel, *Phys.Rev.B.*, 75,125302(2007).
- [P19] Comment on "Failure of the Jarzynski Identify for a Simple Quantum System," S.Mukamel. *Cond-mat/0701003vl*, Dec. 30, 2006.
- [P20] "Two-Dimensional Infrared Surface Spectroscopy for CO on Cu(100):Detection of Intermolecular Coupling of Adsorbates," Y. Nagata, Y. Tanimura and S. Mukamel *J.Chem.Phys.* 126, 204703 (2007).
- [P21] "Probing Valence Electronic Wavepacket Dynamics by all X-ray Stimulated Raman Spectroscopy; A Simulation Study," I.V. Schweigert and S. Mukamel *Phys. Rev. A.* 76, 0125041 (2007).
- [P22] "Coherent Ultrafast Core-hole Correlation Spectroscopy: X-ray Analogues of Multidimensional NMR," I. Schweigert and S. Mukamel, *Phys. Rev. Lett* (Submitted, 2006)
- [P23] "Partially-Time-Ordered Keldysh-Loop expansion of Coherent Nonlinear Susceptibilities," S. Mukamel, *Phys. Rev.A.* (Submitted, 2007)
- [P24] "Two-Dimensional Correlation Spectroscopy of Two-Exciton Resonances in Semiconductor Quantum Wells," L. Yang and S. Mukamel, *Phys. Rev. Lett* (Submitted, 2007)
- [P26] "Ultrafast Optical Spectroscopy of Spectral Flucuations in a Dense Atomic Vapour," V.O. Lorenz, S. Mukamel, W. Zhuang and S.T. Cundiff, *Phys. Rev. Lett.* (Submitted, 2007)

## **Nonlinear Photoacoustic Spectroscopies Probed by Ultrafast EUV Light**

Keith A. Nelson  
Department of Chemistry  
Massachusetts Institute of Technology  
Cambridge, MA 02139  
Email: [kanelson@mit.edu](mailto:kanelson@mit.edu)

Henry C. Kapteyn  
JILA  
University of Colorado and National Institutes of Technology  
Boulder, CO 80309  
E-mail: [kapteyn@jila.colorado.edu](mailto:kapteyn@jila.colorado.edu)

Margaret M. Murnane  
JILA  
University of Colorado and National Institutes of Technology  
Boulder, CO 80309  
E-mail: [murnane@jila.colorado.edu](mailto:murnane@jila.colorado.edu)

### **Program Scope**

This project is aimed at direct spectroscopic access to mesoscopic (nanometer) length scales and ultrafast time scales in condensed matter, with the objective of revealing the length and time scales associated with dynamical collective behavior. The primary effort in the project is directed toward nonlinear time-resolved spectroscopy with coherent soft x-ray, or extreme ultraviolet (EUV), wavelengths. Time-resolved four-wave mixing, or transient grating, measurements are conducted in order to directly define an experimental length scale as the interference fringe spacing formed by two crossed excitation pulses. [1] Dynamics are recorded through measurement of time-resolved coherent scattering, or diffraction, of probe pulses from the induced grating pattern. Measurements of the dynamical responses at various transient grating fringe spacings (i.e. grating wavevectors) can provide both correlation length and time scales for the processes under study. For most complex materials, especially those in which dynamical responses span a wide range of time scales (e.g. polymer relaxation dynamics, dipole or spin glass polarization or magnetization dynamics, etc.), we know little about the correlation length scales involved or whether they are associated with the dynamical time scales. For example, it is far from clear whether the faster and slower components of polymer relaxation dynamics should be associated with motions on shorter and longer lengths scales (e.g. molecular end groups and segments or whole polymer backbones) respectively. Transport properties also pose difficult problems involving wide-ranging time and length scales and their interrelation. Thermal transport in insulators and semiconductors may be largely ballistic on nanometer length scales (which might extend entirely across fabricated nanostructural elements) and diffusive across longer distances depending on the attenuation rates (i.e. mean free paths) of high-wavevector acoustic phonons that carry much of the energy. In these and many other complex condensed matter systems, direct experimental measurements on the relevant length as well as time scales are needed for elucidation of the underlying mechanisms of dynamical processes.

Continued progress in high harmonic generation [2] has yielded femtosecond soft x-ray pulses with nanojoule energies and excellent spatial coherence and focusability. The possibility of intensity levels comparable to those used in much of condensed matter nonlinear spectroscopy encourages the effort to extend the spectroscopic methods to EUV wavelengths. EUV transient grating (TG) measurements will provide fringe spacings in the range of a few tens of nanometers, permitting direct assessment of condensed matter correlation lengths that are almost all in the mesoscopic range. These correlation lengths have eluded study with optical wavelengths, since the shortest transient grating fringe spacing is on the order of the wavelength.

The key experiments are aimed at generation and time-resolved detection of acoustic waves with wavelengths and frequencies covering much of the Brillouin zone. In TG measurements, optical absorption of the crossed excitation pulses gives rise to spatially periodic heating and thermal expansion which launches the acoustic response. Time-resolved diffraction of probe light yields the wavevector-dependent acoustic frequency and decay (i.e. mean free path). [1] Acoustic wave characterization permits direct determination of structural relaxation time scales  $\tau$  that are a significant fraction of the acoustic oscillation period, i.e. acoustic absorption is maximized when  $\omega\tau = 1$  where  $\omega$  is the acoustic frequency. It also permits assessment of correlation length scales  $d$ , i.e. acoustic scattering increases dramatically as  $qd \rightarrow 1$  where  $q = 2\pi/\Lambda$  is the acoustic wavevector magnitude and  $\Lambda$  the acoustic wavelength. TG measurements with optical wavelengths have permitted study of acoustic waves with wavelengths in the micron range and frequencies in the MHz range. With soft x-ray wavelengths, acoustic waves with wavelengths of a few tens of nanometers and frequencies in the 100-GHz range will be reached. This will provide access to picosecond structural relaxation dynamics and nanometer structural correlation lengths in a wide range of complex materials. In polymers and other glass formers, the full range of relaxation dynamics obtained through EUV and optical experiments will permit direct determination of multiscale relaxation dynamics across a very wide range, and connections between these and nanometer correlation lengths will be tested.

EUV probing of acoustic responses also offers important advantages relative to optical probing because the shorter wavelengths mean correspondingly greater acoustically induced phase shifts and therefore correspondingly greater sensitivity to the acoustic displacements. Demonstration of facile EUV detection of dynamical acoustic responses is a central element of the experimental program and a prerequisite to high-wavevector photoacoustic measurements.

Strong absorption of EUV wavelengths at bulk material surfaces will lead to generation of surface acoustic waves whose characterization will yield dynamic shear and longitudinal modulus properties at ultrahigh frequencies. A parallel set of experiments has been undertaken to extract a subset of this information, the longitudinal component, for some materials including those that can be deposited as thin films. In these measurements, a thin metal film is irradiated by a sequence of femtosecond optical pulses, and temporally periodic thermal expansion of the film launches an acoustic wave into and through an underlying material layer and a second metal film. The acoustic frequency is given by the repetition rate of the optical pulse sequence. The acoustic wave is detected optically upon reaching the back of the sample. This approach resembles traditional ultrasonics, with photoacoustic rather than piezoelectric transducers. It is not as generally applicable as the EUV transient grating method since it must be possible to fabricate the multilayer metal-sample-metal structure with suitable sample thicknesses, often submicron since ultrahigh-frequency acoustic waves are strongly absorbed and/or scattered by many complex materials. However, for those materials that are amenable, this approach provides a useful segue to the EUV measurements.

## Recent Progress

The short wavelength, femtosecond duration, and high spatial coherence of EUV pulses generated through HHG source make them ideal for probing coherent surface acoustic waves, making it possible to probe higher acoustic frequencies and shorter acoustic wavelengths and providing far higher sensitivity than in similar experiments using visible-wavelength probe light. In work published in Applied Physics Letters in 2006 [3], we used coherent EUV high harmonic pulses at a wavelength of 30 nm to probe thin film thermoacoustic responses that were generated by crossed 800-nm or 400-nm excitation pulses. This is an important step toward all-EUV TG measurements. Surface acoustic wave dispersion in thin nickel films was characterized by measuring the acoustic frequency at several excitation periods (acoustic wavelengths), and film thickness values in the 10-100 nm range were determined. Our measurements and models demonstrate that probing surface deformations with 30 nm EUV pulses leads to a greater than *700-fold increase in diffracted efficiency* over visible 800 nm probing, since the diffracted efficiency is related to the square of the ratio of the surface displacement to the probe wavelength. Moreover, the EUV light is not sensitive to fast electronic dynamics that would dominate the signal at  $t = 0$  with a visible probe. This inherent property of EUV probing permits unambiguous determination of the initiation of thermoacoustic dynamics.

In work published this year in Optics Letters [4], we demonstrated femtosecond time-resolved dynamic Gabor holography using ultrafast EUV beams for the first time. We used a novel excitation geometry in which 800-nm pump laser light was focused to a narrow line on a Ni film sample, which was probed by a much larger EUV beam. The unperturbed sample reflected the EUV (reference) beam, while the pumped region diffracted the object beam to form a dynamic hologram. This is a simple, robust, single-reflection geometry for studying transient dynamics with femtosecond time resolution. We demonstrated sub-picometer sensitivity to surface displacements arising from initial thermal expansion (as above, largely free of ambiguity associated with electronic dynamics) and subsequent periodic return to the surface of a longitudinal acoustic wavepacket that propagated back and forth through the film. *Phase sensitivities of better than  $\lambda/43000$  at 30 nm were obtained in these measurements.*

In our experiments using multiple optical excitation pulses to generate a multiple-cycle GHz longitudinal acoustic wave that propagates through a sample to be detected at the other side [5,6], results from amorphous silica have revealed far longer propagation lengths than previously believed. The results require a reanalysis of the roles of thermally assisted structural rearrangements and static heterogeneity in the temperature-dependent phonon properties and thermal conductivity of amorphous solids. New results from glass-forming liquids are for the first time revealing structural relaxation dynamics probed through acoustic phonons with frequencies up to 100 GHz, permitting analysis in terms of empirical and first-principles models of viscoelastic behavior.

In a novel development, optical excitation of DC-sputtered gold films has revealed generation of shear acoustic responses as well as longitudinal acoustic waves. Detailed x-ray analysis of the films suggests that shear wave generation occurs because the films consist of nanocrystallites with random orientations. Light absorption and heating results in through-plane thermal expansion, and the through-plane stress that is exerted produces quasilongitudinal and quasitranverse acoustic waves in nanocrystallites whose crystallographic axes are tilted such that the through-plane direction is not a high-symmetry direction. The results were recently submitted for publication. [7] This does not generate a shear plane wave since the shear

displacements in different nanocrystallites are oriented in random directions. However it provides a novel assessment of thin film mesoscale structure and elastic heterogeneity.

## Future Plans

During the present year, we plan to conduct EUV-probed TG measurements with still shorter grating fringe spacings by using deep-UV (200 nm) excitation with a water cell, as in immersion lithography. Acoustic wavelengths in the 100-nm range should be reached in this manner. This will provide access to important structural relaxation dynamics that will be monitored at EUV wavelengths.

The EUV dynamic Gabor holography method is being used to examine quasi-ballistic thermal transport in nanostructures. The approach is ideal for this problem since the EUV probe should be larger than the photoexcited region (the nanostructure) and because the crucial short-time dynamics can be examined unambiguously.

Detailed theoretical modeling of amorphous solids and supercooled liquids is being applied to the results of multiple-pulse photoacoustic measurements on these material classes and experiments on additional materials in both classes are under way. The range of acoustic wavelengths and frequencies is being extended even farther through the use of GaN quantum wells as the photoacoustic transducers. Femtosecond optical excitation can generate acoustic waves with frequencies exceeding 1 THz and wavelengths of only  $\sim$ 5 nm. This should enable us to examine correlation lengths as short as 1 nm. In some disordered materials we may observe the end of acoustic wave propagation as inherent structural heterogeneity gives rise to acoustic localization.

## References

1. "Impulsive stimulated light scattering from glass-forming liquids: I. Generalized hydrodynamics approach; II. Salol relaxation dynamics, nonergodicity parameter, and testing of mode coupling theory," Y. Yang and K.A. Nelson, *J. Chem. Phys.* **103**, 7722-7731; 7732-7739 (1995).
2. "Phase-matched generation of coherent soft-x-rays," A. Rundquist, C. Durfee, Z. Chang, S. Backus, C. Herne, M. M. Murnane and H. C. Kapteyn, *Science* **280**, 1412 – 1415 (1998).
3. "Transient grating measurement of surface acoustic waves in thin metal films with extreme ultraviolet radiation," R.I. Tobey, M.E. Siemens, M.M. Murnane, H.C. Kapteyn, D.H. Torchinsky and K.A. Nelson, *Appl. Phys. Lett.* **89**, 091108 1-3 (2006).
4. "Ultrafast extreme ultraviolet holography: Dynamic monitoring of surface deformation", M.E. Siemens, R.I. Tobey, O. Cohen, M. M. Murnane, H. C. Kapteyn, and K.A. Nelson, *Optics Letters* 32, 286-288 (2007).
5. "Generation of ultrahigh frequency tunable acoustic waves," J. D. Choi, T. Feurer, M. Yamaguchi, B. Paxton, and K. A. Nelson, *Appl. Phys. Lett.*, **87**, 081907 (2005).
6. "Ultrahigh frequency acoustic phonon generation and spectroscopy with Deathstar pulse shaping," J.D. Beers, M. Yamaguchi, T. Feurer, B. Paxton, and K.A. Nelson, *Ultrafast Phenomena XIV*, S. DeSilvestri, T. Kobayashi, T. Kobayashi, K.A. Nelson, and T. Okada, eds. (Springer-Verlag, Berlin 2005), pp. 236-238.
7. "Picosecond ultrasonics in locally asymmetrical inhomogeneous gold media," T. Pezeril, F. Leon, D. Chateigner, and K.A. Nelson, *Phys. Rev. Lett.*, submitted.

# Nonlinear Frequency Mixing with Coupled Gold Nanoparticles

Lukas Novotny ([novotny@optics.rochester.edu](mailto:novotny@optics.rochester.edu))

University of Rochester, Institute of Optics, Rochester, NY, 14627.

## 1 Program Scope

This project is aimed at controlling a single quantum emitter by use of an optical antenna. More specifically, we use the plasmon resonance of a metal nanostructure to locally influence the emission rate and the excited state lifetime of an electronic multilevel system (atom, ion, molecule, defect center) [1]. The goal is the development of an understanding of how a quantum mechanical system (molecule) interacts with a mesoscopic structure (antenna) at very close separations. In this regime, nonlocal effects become important and it is not a priori clear what theoretical framework has to be adopted to understand the details of the interaction mechanism. We use nonlinear frequency mixing to assess the separation between individual metal nanoparticles and to measure the onset of the nonlocal regime. It can be expected that optical antennas will be employed to artificially enhance the absorption cross-section or quantum yield of optoelectronic devices (e.g. solar cells). Likewise, optical antennas will find application for efficiently releasing energy from nanoscale devices (e.g. LED lighting) and to boost the efficiency of biochemical detectors relying on a distinct spectroscopic response (Raman scattering, fluorescence, etc.).

## 2 Recent Progress

In the past project period we concentrated on the development of optical half-wave antennas based on metal nanorods for establishing optical field localization below 10 nm. These nanorods are irradiated with laser light and are used as excitation sources for single molecule fluorescence. To improve light localization even further we are making use of the nonlinear response of metal nanoparticles [2, 3]. Of particular interest is the nonlinear frequency mixing efficiency at close distances between metal surfaces because macroscopic dielectric theory breaks down at sub-nanometer separations and nonlocal effects become important. Therefore, during the past project period we have invested much effort in understanding nonlinear signal generation in nanoparticle junctions and this report will be focused on this topic. Antenna-based single molecule fluorescence was already described in last year's report.

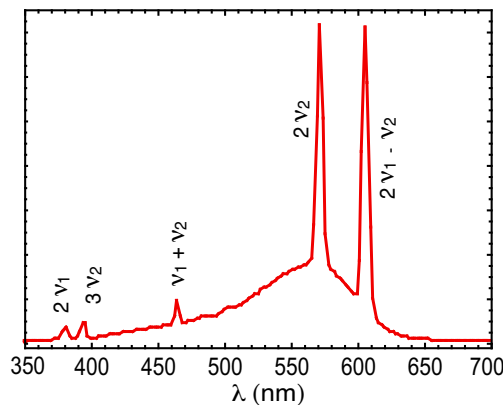


Figure 1: Spectrum of photons emitted from a gold nanostructure when irradiated with laser pulses of wavelength  $\lambda_1 = 780$  nm and  $\lambda_2 = 1160$  nm.

For our studies we used pairs of metal nanoparticles near touching contact [3]. This geometry is favorable because of its simplicity. It allows measurements to be easily reproduced and makes accompanying theoretical studies feasible. Fig. 1a shows a typical spectrum of light emitted from a metal nanostructure when irradiated with 150fs laser pulses of wavelength  $\lambda_1 = 810$  nm and  $\lambda_2 = 1210$  nm. Each peak is associated with a particular nonlinear process. In our previous work we have studied the origin of the second-harmonic peak [2], the broad underlying continuum [4], and the four-wave mixing peak [3]. We have found that the 4WM yield increases by 4 orders of magnitude as the distance between a pair of nanoparticles is decreased (c.f. Fig. 2). The reason for this dramatic enhancement lies in the shift of the localized plasmon resonance to infrared wavelengths as the dimer is formed, making one of the input wavelengths doubly resonant. At the touching point, the 4WM signal changes discontinuously because of a sudden charge redistribution imposed by the formation of a conductive bridge. Therefore, the 4WM signal provides an ultrasensitive measure for the contact point between a pair of particles and it can be employed as a spatially and temporally controllable photon source. In our future work we are interested to investigating the contact point in more detail. In particular, we propose to perform simultaneous electrical (conduction) and optical measurements in order to correlate the onset of field emission with the abrupt change of slope in the optical response. We will continue to collaborate with theorists using TDDFT to model the contact region.

Interestingly, we find that the 4WM yield of a dimer can be even more enhanced by coupling to a third particle placed in close proximity to it. To demonstrate this effect we have attached two 60nm particles to a glass tip (c.f. Fig. 3a) and recorded the emitted 4WM intensity while raster-scanning a sample with 60nm gold particles underneath the dimer tip. An image of a cluster of three gold particles is shown in Fig. 3b,c. While the topography clearly shows the lateral agglomeration of three nanoparticles, the 4WM image reveals that the signal is strongest when the dimer probe is placed between individual particles. In these configurations the dimer probe interacts simultaneously with two or three neighboring particles and the local fields become particularly strong.

To summarize we find that third-order nonlinear optical frequency mixing at coupled gold nanoparticles is very efficient. The 4WM yield increases by  $\times 10^4$  as the inter-particle distance is decreased to the contact point. At the contact point a conductive bridge is formed which gives rise to an abrupt jump of the plasmon resonance frequency into the near-infrared and which makes the 4WM distance-dependence discontinuous. By controlling the interparticle distance we can generate bursts of narrowband photons. Alternatively, a stable photon source is obtained by permanently joining two particles rigidly together. We have demonstrated

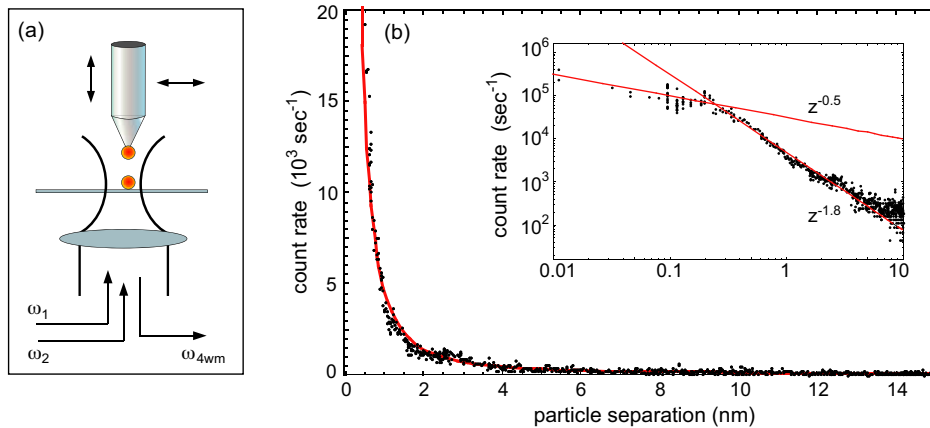


Figure 2: (a) Sketch of the experiment. The nonlinear signal at frequency  $2\omega_1 - \omega_2$  is measured as a function of the relative position between individual gold nanoparticles (diameter 60nm). The two laser wavelengths used are  $\lambda_1 = 830$  nm and  $\lambda_2 = 1185$  nm. (b) Four-wave mixing photon count rate ( $\lambda = 639$  nm) as a function of the separation of two 60nm gold nanoparticles. The inset shows a detailed view on a log-log scale.

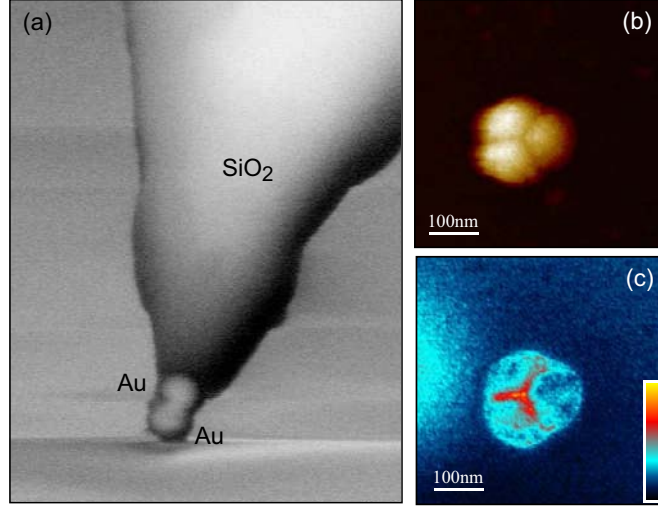


Figure 3: *Four-wave mixing with a gold dimer tip.* (a) Near-field probe consisting of an 80nm gold dimer attached to a pointed fiber. (b) Topography of a particle trimer imaged with the probe shown in (a). (c) Four-wave mixing image revealing the hot contact region. The image reflects the intensity recorded at  $\omega_{4WM} = 2\omega_1 - \omega_2$ .

that this source can be employed for high-resolution nonlinear near-field imaging. Further applications of these nonlinear photon sources are under investigation, including extinction spectroscopy and imaging.

### 3 Future Plans

In our previous work [3] we have assigned the change of slope in Fig. 2 to a sudden charge redistribution when a conductive bridge between the two particles is established. This explanation is based on theoretical predictions [5] but it is not a definitive proof. Typical laser-intensities in our nonlinear experiments are on the order of  $I_o \sim 1 \text{ GW/cm}^2$  which corresponds to electric fields of  $E_o \sim 10^8 \text{ V/m}$ . However, the fields in the gap region reach values that are a factor of  $f = [100..1000]$  stronger than the incident field. Therefore, the true local field strength is  $E = fE_o \sim 10 - 100 \text{ GV/m}$ . Assuming a gap of  $\Delta z = 1 \text{ nm}$  the associated potential is  $V_o \sim 1 - 10 \text{ eV}$ , which is comparable to typical work functions of metals. Hence, it is likely that field emission comes into play for sub-nanometer gaps between particles.

Once field emission sets in and electrons are being ejected from one particle to the other, further field enhancement becomes suppressed. This 'shortening' of the gap fields should have a clear signature in the nonlinear response between the particles as the distance  $\Delta z$  between the particles is decreased. Hence, it is also plausible that the change of slope in Fig. 2 is due to the onset of field emission. In order to understand the interplay between optical and conductive properties we intend to pursue simultaneous nonlinear optical and electrical measurements.

### References

- [1] P. Anger, P. Bharadwaj, and L. Novotny, "Enhancement and quenching of single molecule fluorescence," *Phys. Rev. Lett.* **96**, 113002 (2006).
- [2] A. Bouhelier, M. Beversluis, A. Hartschuh, and L. Novotny, "Near-field second-harmonic generation induced by local field enhancement," *Phys. Rev. Lett.* **90**, 13903 (2003).

- [3] M. Danckwerts and L. Novotny, "Optical frequency mixing at coupled gold nanoparticles," *Phys. Rev. Lett.* **98**, 026104 (2007).
- [4] M. R. Beversluis, A. Bouhelier, and L. Novotny, "Continuum generation from single gold nanostructures through near-field mediated intraband transitions," *Phys. Rev. B* **68**, 115433 (2003).
- [5] I. Romero, J. Aizpurua, G. W. Bryant, and F. J. Garcia de Abajo, *Opt. Express* **14**, 9988 (2006).
- [6] J. R. Zurita-Sanchez, J.-J. Greffet, and L. Novotny, "Near-field friction due to fluctuating fields," *Phys. Rev. A*, vol. 69, 02290, 2004.
- [7] A. Hartschuh, M. R. Beversluis, A. Bouhelier, and L. Novotny, "Tip-enhanced optical spectroscopy," *Phil. Trans. R. Soc. Lond. A*, vol. 362, pp. 807–819, 2004.
- [8] A. Hartschuh, H. N. Pedrosa, J. Peterson, L. Huang, P. Anger, H. Qian, A. J. Meixner, M. Steiner, L. Novotny, and T. D. Krauss, "Single carbon nanotube optical spectroscopy," *ChemPhysChem*, vol. 6, pp. 1–6, 2005.
- [9] A. Hartschuh, H. Qian, A. J. Meixner, N. Anderson, and L. Novotny, "Nanoscale optical imaging of excitons in single-walled carbon nanotubes," *Nano Lett.* vol. 5, pp. 2310–2313, 2005.
- [10] N. Anderson, A. Bouhelier and L. Novotny, "Near-field photonics: tip-enhanced microscopy and spectroscopy on the nanoscale," *J. Opt. A: Pure Appl. Opt.*, vol. 8, pp. S227-S233, 2006.
- [11] M. R. Beversluis, L. Novotny, and S. J. Stranick, "Programmable vector point-spread function engineering," *Opt. Express*, vol. 14, 2650, 2006.
- [12] L. Novotny and S. J. Stranick, "Near-field optical microscopy and spectroscopy with pointed probes," *Ann. Rev. Phys. Chem.* vol. 57, pp. 303-331, 2006.
- [13] A. Hartschuh, H. Qian, A. J. Meixner, N. Anderson, and L. Novotny "Tip-enhanced optical spectroscopy for surface analysis in biosciences," *Surface and Interface Analysis*, vol. 38, pp. 1472-1480, 2006.
- [14] H. Qian, T. Gokus, N. Anderson, L. Novotny, A. J. Meixner, and A. Hartschuh, "Near-field imaging and spectroscopy of electronic states in single-walled carbon nanotubes," *Phys. Stat. Sol. (b)*, vol. 243, pp. 1–5, 2006.
- [15] P. Anger, P. Bharadwaj, and L. Novotny, "Nanoplasmonic enhancement of single molecule fluorescence," *Nanotechnology*, vol. 18, 044017, 2006.
- [16] L. Novotny and A. Bouhelier, "Near-field optical excitation and detection of surface plasmons," in *Surface Plasmon Nanophotonics*, M. Brongersma (ed.), Kluwer Academic Press, 2007.
- [17] L. Novotny, "The history of near-field optics," *Progress in Optics*, E. Wolf (ed.), in print, 2007.
- [18] P. Bharadwaj and L. Novotny, "Spectral dependence of single molecule fluorescence enhancement," *J. Microsc.*, in print, 2007.

## 4 DOE sponsored publications (2004-2007):

Refs. [1, 3, 6, 7, 8, 9, 10, 11, 12, 13, 14, 15, 16, 17, 18]

# Electron-Driven Excitation and Dissociation of Molecules

A. E. Orel

Department of Applied Science  
University of California, Davis  
Davis, CA 95616  
[aeorel@ucdavis.edu](mailto:aeorel@ucdavis.edu)

## Program Scope

This program will study how energy is interchanged in electron-polyatomic collisions leading to excitation and dissociation of the molecule. Modern *ab initio* techniques, both for the electron scattering and the subsequent nuclear dynamics studies, are used to accurately treat these problems. This work addresses vibrational excitation, dissociative attachment, and dissociative recombination problems in which a full multi-dimensional treatment of the nuclear dynamics is essential and where non-adiabatic effects are expected to be important.

## Recent Progress

We have carried out a number of calculations studying low-energy electron scattering from polyatomic systems leading to vibrational excitation and dissociative attachment. Much of this work has been done in collaboration with the AMO theory group at Lawrence Berkeley Laboratory headed by T. N. Rescigno and C. W. McCurdy. AMO experimental group headed by A. Belcamen. He is currently carrying out experiments on dissociative attachment of systems where we have carried out calculations, both on NO and C<sub>2</sub>H<sub>2</sub>.

## Low-Energy Electron Scattering from Formic Acid

There has been recent experimental work showing that low-energy electrons (<2 eV) can fragment gas phase formic acid (HCOOH) molecules through resonant dissociative attachment processes. Two experiments have been published that have concentrated on differential and vibrational excitation cross sections. Vizcaino *et al.* [1] studied elastic electron scattering from formic acid using a crossed-beam electron spectrometer and derived momentum transfer cross sections. Allan [2] carried out high-resolution electron energy-loss experiments and reported absolute differential elastic and vibrational excitation cross sections at 135° from threshold to 5 eV. This experiment showed that the  $\pi^*$  resonance causes strong vibrational excitation as well as serves as the precursor to dissociate attachment. In previous work (publication #5) we explained the mechanism for low-energy electron attachment to formic acid. Recently (publication #8) we presented *ab initio* elastic differential and momentum transfer cross sections of low-energy electron scattering from formic acid obtained by employing the Complex Kohn variational method. We also presented evidence, obtained from the low-energy behavior of the cross section and its dependence on target geometry, to support our earlier claim that there must necessarily exist a virtual state in this system.

The results of the calculation are described in a paper published in Physical Review A (Publication 8).

### Dissociative attachment of ClCN and BrCN

We have completed our studies of the dissociative attachment of ClCN and BrCN. Electron scattering calculations using the Complex Kohn variational method were used to determine the position and autoionization widths of the contributing resonance states. The Multiconfiguration Time-Dependent Hartree method (MCTDH) of the Heidelberg group [3] was used to compute the dynamics in three dimensions. Significant changes going from one (X-CN) to two dimensions (X-CN and C-N stretch) were found, but the addition of the bend caused only minor changes in the dissociative attachment cross section.

The results of the calculation are described in a paper published in Journal of Chemical Physics (Publication 7).

### Electron interactions with the CF<sub>2</sub> radical

In collaboration with T.N. Rescigno, LBL, we have carried out preliminary calculations on electron interactions with CF<sub>2</sub> radicals. Currently, the gases used in the plasma production of microelectronic devices have been shown to have a strong greenhouse effect. CF<sub>3</sub> and C<sub>2</sub>F<sub>4</sub> have been proposed as alternate feedstock gases. When these compounds are bombarded with electrons CF<sub>x</sub> radicals (x=1,2,3) are produced. These radicals significantly affect the behavior of these fluorocarbon plasmas. Little is known about the interaction of electrons with these radicals.

Previously we have carried out extensive calculations on dissociative attachment and vibrational excitation following electron collisions with the radical CF (Publication #4). These calculations showed that there was little F<sup>-</sup> produced from low-energy electron collisions with the molecules in the ground vibrational state. As in NO, the addition of vibrational energy caused a dramatic increase in the dissociative attachment cross section. We have now begun calculations on electron scattering from CF<sub>2</sub>. We have performed fixed-nuclei scattering calculations using the Complex Kohn variational method and extracted the resonance parameters, for each geometry of interest, by analyzing the energy dependence of the eigenphase sums. These preliminary calculations have showed a single resonance at low energy that at the static exchange level is unbound at the equilibrium geometry of the ground state. However, at the relaxed SCF level of calculation, which correctly balances the anion and target correlation and has been used previously with great success to study similar resonances, the anion is bound at the equilibrium geometry. This is in contrast to the R-matrix calculations [4] that show the anion to be unbound at the equilibrium geometry.

### Dissociative Attachment of Acetylene

There has been recent experimental work showing that low-energy electrons (<2 eV) can fragment acetylene (C<sub>2</sub>H<sub>2</sub>) molecules through resonant dissociative attachment processes. The principal reaction products of such collisions were found to be C<sub>2</sub>H<sup>-</sup> and hydrogen atoms [5]. We have carried out *ab initio* calculations for elastic electron scattering from acetylene using the complex Kohn variational method. We identified the responsible negative ion state as a transient π\* anion with the electron temporarily trapped in the CC antibonding π orbital. The products have A' symmetry and the resonance is A'', so symmetry considerations dictate that the associated dissociation

dynamics are intrinsically polyatomic. We found that the molecule must first bend, followed by stretching of the CH bond leading to dissociation.

The results of the calculation are being prepared for submission to Physical Review A (Publication 9).

## FUTURE PLANS

### Electron interactions with $\text{CF}_x$ radicals

We plan to complete our studies of electron scattering from  $\text{CF}_2$  and then study the dynamics of dissociation in this system. We will then extend these calculations to  $\text{CF}_3$ .

### Dissociative Attachment of Acetylene

Recent experimental work shows that at a higher energy ( $>7$  eV) the channel, which fragments into  $\text{C}_2^-$  and  $\text{H}_2$ , becomes open. This reaction proceeds through a higher-lying Feshbach resonance, and involves a dramatic change in geometry to proceed to products. We have begun a series of *ab initio* calculations, with a number of open electronic channels for electron scattering from acetylene using the Complex Kohn variational method. We will identify the responsible negative ion and calculate the multi-dimensional dynamics leading to dissociation.

### Dissociative Attachment in Halogenated Molecules

There have been no theoretical systematic studies of dissociative attachment in organic molecules. There have been some such experimental studies, but these have been limited [6,7,8]. We have begun a series of calculations on mono-substituted organic compounds to look for general trends and to better understand what controls the energy flow leading to dissociation in these systems. We have chosen the systems,  $\text{HCCl}$ ,  $\text{H}_3\text{CCCl}$ ,  $\text{H}_5\text{CCCl}$ , showing a series from triple, double to single bond respectively.

We started calculations on  $\text{ClCCH}$ , chloroacetylene. In our first calculations, the molecule was studied as a pseudo-diatom, varying the Cl–C internuclear separation and keeping all other bond distances fixed. We can then investigate an intriguing possibility with this system. There has been some experimental evidence of dramatic effects in the DA cross section due to coupling between channels arising from  $\sigma^*$  and  $\pi^*$  antibonding orbitals [10]. Of course, for  $\text{ClCCH}$  in its linear configuration, these channels cannot mix. However, mixing can occur if the molecule is bent. We are investigating this effect by carrying out the scattering for the bent structure. We are also looking at variations as other bonds are modified. In our studies of  $\text{ClCN}$  and  $\text{BrCN}$ , there was no significant mixing between the  $\sigma^*$  and  $\pi^*$  channels. However, in acetylene, it was that coupling that allowed dissociation to occur.

We plan to combine these structure and electron scattering into a multi-dimensional study of the dissociation dynamics. If the dynamics are only studied in one-dimension, that is, as a function of the C–Cl bond distance, the physics of the energy transfer process is lost. The effect of the double vs. the triple C–C bond is combined with the effect of the increased symmetry in the linear  $\text{HCCl}$  system which does not allow

the  $\Sigma/\Pi$  mixing to occur. However, if the system is studied in multiple dimensions, such that this mixing can occur, a more direct comparison is possible. This is a case where it is critical to go beyond the usual one-dimensional picture to truly understand the dissociation dynamics and energy flow within the modes of the system. We then plan to consider  $\text{H}_3\text{CCCl}$ , the double-bond case and  $\text{H}_5\text{CCCl}$ , the single bond case.

## REFERENCES

1. V. Vizcaino, M. Jelisavcic, J. Sullivan, and S. J. Buckman, Bull. Am Phys. Soc. **50**, 37 (2005).
2. M. Allan, J. Phys. B. **39**, 2939 (2006).
3. M. H. Beck, A. Jackle, G. A. Worth and H. -D. Meyer, Phys. Rep., **324** (2000).
4. I. Rozum, N. J. Mason and Jonathan Tennyson, *J. Phys. B*, **35**, 1583 (2002).
5. R. Dressler and M. Allan, *J. Chem. Phys.*, **87**, 4510 (1987).
6. D. M. Pearl and P. D. Burrow, *J. Chem. Phys.*, **101**, 2940 (1994).
7. K. Aflatooni and P. D. Burrow, *J. Chem. Phys.*, **113**, 1455 (2000).
8. G. A. Gallup, K. Aflatooni and P. D. Burrow, *J. Chem. Phys.*, **118**, 2562 (2003).
9. M. Allan and L. Andric, *J. Chem. Phys.*, **105**, 3559 (1996).

## PUBLICATIONS

1. Low-energy electron scattering of NO : *Ab initio* analysis of the  $^3\Sigma^-$ ,  $^1\Delta$  and  $^1\Sigma^+$  shape resonances in the local complex potential model, Z. Zhang, W. Vanroose, C. W. McCurdy, A. E. Orel, and T. N. Rescigno Phys. Rev. A, **69**, 062711 (2004).
2. *Ab initio* study of low-energy electron collisions with tetrafluoroethene  $\text{C}_2\text{F}_4$ , C. S. Trevisan, A. E. Orel, and T. N. Rescigno, Phys. Rev. A, **70**, 012704 (2004).
3. A nonlocal *ab initio* model of dissociative electron attachment and vibrational excitation of NO, C. S. Trevisan, Karel Houfek, Zhiyong Zhang, A. E. Orel, C. W. McCurdy, and T. N. Rescigno, Phys. Rev. A, **71**, 052714 (2005).
4. Resonant electron-CF collision processes, C. S. Trevisan, A. E. Orel, and T. N. Rescigno, Phys. Rev. A, **72**, 627720 (2005).
5. Dynamics of Low-Energy Electron Attachment to Formic Acid, T. N. Rescigno, C. S. Trevisan and A. E. Orel, Phys. Rev. Lett. **96** 213201 (2006).
6. Elastic Scattering of Low-energy Electrons by Tetrahydrofuran, C. S. Trevisan, A. E. Orel and T. N. Rescigno, J. of Phys. B **39** L255 (2006).
7. Dissociative Attachment of ClCN and BrCN, J. Royal and A. E. Orel, J. Chem. Phys, **125** 214307 (2006).
8. Low-Energy Electron Scattering by Formic Acid, C. S. Trevisan, A. E. Orel and T. N. Rescigno, Phys. Rev. A **74** 042716 (2006).
9. Dissociative Electron Attachment of Acetylene, S. Chourou and A. E. Orel, in preparation for publication

**2007 Progress Report /Renewal Request for Program: DOE-FG02-02ER15337**  
**“Low-Energy Electron Interactions with Interfaces and Biological Targets”**

Thomas M. Orlando

*School of Chemistry and Biochemistry and School of Physics,  
Georgia Institute of Technology, Atlanta, GA 30332-0400*

[Thomas.Orlando@chemistry.gatech.edu](mailto:Thomas.Orlando@chemistry.gatech.edu), Phone: (404) 894-4012, FAX: (404) 894-7452

**1. Program Scope:** The primary objectives of this program are to investigate the fundamental physics and chemistry involved in low-energy (1-100 eV) electron scattering with interfaces and biological targets. Specifically, we have examined electron excitations of i) water co-adsorbed with rare gas solids, ii) molecular solids such as thin-films of water, iii) complicated biologically relevant molecules such as DNA and metabolites. The program is primarily experimental and concentrates on electron initiated damage and energy exchange in the deep valence and shallow core regions of the collision partners.

**2. Recent Progress:**

***Project 1: Low-energy (5 –250 eV) electron stimulated desorption of cluster ions from water adsorbed on rare-gas overlayers.***

We have examined the roles of hole transfer, Auger decay and Intermolecular Coulomb Decay (ICD) in the electron stimulated production and desorption of water cluster ions from water adsorbed on graphite and rare gas spacer layers. Over the course of this project, we have developed and refined a model of ionization and Coulomb explosion that leads to the production of protonated water clusters.<sup>1-3</sup> The source term for cluster ejection derives from shallow core level ionization induced by low energy electrons. Cluster growth, according to our model, derives from nucleated condensation of water around the newly formed point charge during the process of lattice distortion. Substrate interactions, specifically comparing an insulator (Xe overlayers) to a conductor, graphite, (Figure 1) show that long range electronic coupling can quench cluster growth by allowing fast hole transfer to delocalize and reduce the desorption probability.

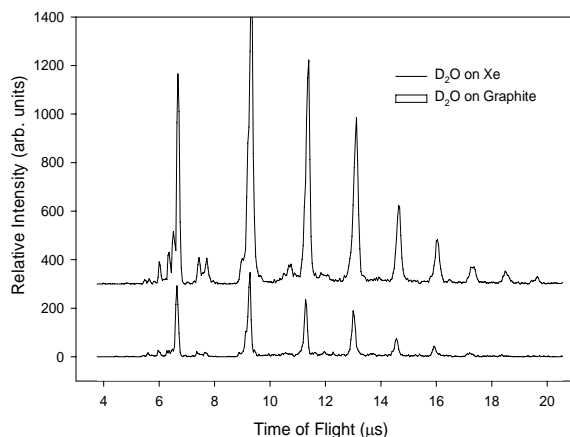


Figure 1. Comparison of protonated water cluster production from a conducting substrate (graphite, lower) to an insulator (Xe spacer layer, upper).

Core levels can undergo Auger decay to produce a two-hole localized final state if and only if an Auger cascade will result in enough energy to liberate an Auger electron.

The minimum energy threshold (within the manifold of discrete molecular electronic states) is significantly lowered when molecules are coupled via hydrogen bonding. This mechanism, known as ICD<sup>4-6</sup>, allows deep valence/shallow core levels to undergo Auger decay that are forbidden in the isolated molecule. As a test of this model, we have used submonolayer ice layers above rare gas underlayers to study hole transfer from atomic core levels to identify the position of this threshold.<sup>6</sup> The primary threshold for cluster production from pure ice<sup>2</sup> is 70 eV. When an argon spacer layer is added, the threshold drops to 30 eV. This value corresponds to the 3s atomic core level in argon at 29.3 eV. When xenon is used the threshold is shifted further to 20 eV, but with a primary threshold at 65 eV. These correspond very closely with the core levels of xenon (5s 23.3 eV, 4d 67.5 eV). Ionization out of these levels allows ICD to take place, secondarily ionizing a nearby water molecule, resulting in Coulomb explosion into water clusters. As a further test, the cluster intensity distribution (not shown) follows a Poisson distribution, reflecting the nascent abundance of water forming islands on the rare gas surface, rather than the hole localization model we developed for pure ice.

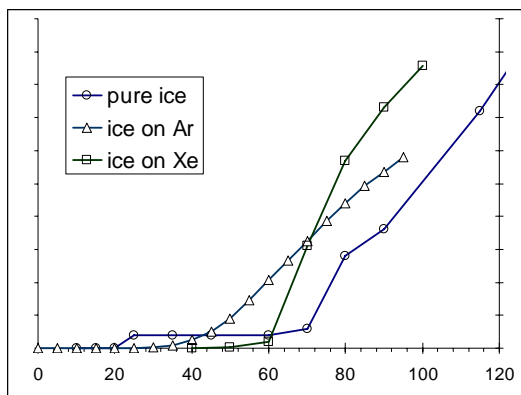


Figure 2. Protonated cluster threshold measurements on various spacer layers. Cluster production from thick ice has a primary threshold at 70 eV. Addition of an argon spacer layer lowers this to 30 eV. Xenon lowers the threshold to 20 eV, with a primary threshold at 65 eV.

### ***Project 2: The Role of Diffraction, Feshbach Resonances and Interfacial Water in Electron-Induced Damage of DNA***

We have calculated the elastic scattering of 5-30 eV electrons within DNA using the separable representation of a free-space electron propagator and a curved wave multiple scattering formalism. Constructive interference is revealed at 5-11, 14-18 and 22-28 eV when examining major groove structural waters. We correlate these calculated features with observed strand breaks vs. incident electron energy. Specifically, the feature centered at 6 eV, can occur as a result of enhanced excitation and decay of the  $^2\text{B}_1$  resonance which produces H<sup>+</sup> and OH at the interface. The second feature between 10-17 eV must involve excitation of a compound resonance likely correlated with the phosphates. This excitation can decay to produce O<sup>-</sup> or O atoms in the major groove and produce both SSBs and DSBs. Electron autodetachment is also an important decay channel which can lead to secondary scattering and excitation of lower low-lying  $\sigma^*$  or  $\pi^*$  orbitals of the phosphate. These excitations can be localized on the initial site or on a site on the opposite strand and this may be required for DSBs. Finally, though diffraction is important in locally enhancing DEA resonances, the spatial specificity inherent in diffraction is not necessarily conserved in the DNA damage process.

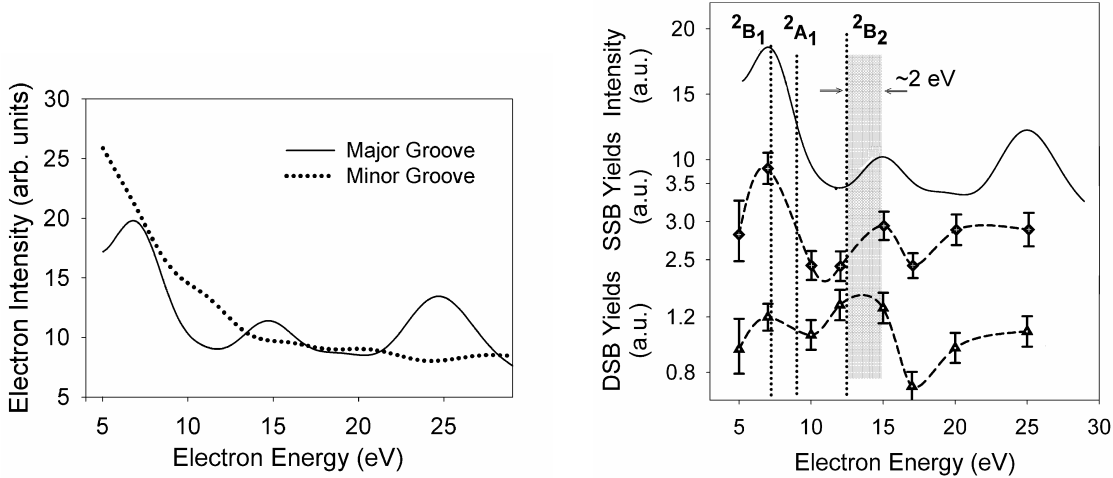


Figure 3 (left) shows a comparison of the calculated electron intensities associated with the structural waters located at the major (solid line) or minor (dotted line) groove of DNA as a function of incident electron beam energy. The calculation included 8 waters at the minor groove and 14 at the major groove. Figure 3 (right) compares the calculated electron intensity associated with the major groove structural water (solid line) with the measured SSB and DSB yields as a function of electron beam energy. The known dissociative electron attachment resonances of water are shown at the top of the Figure. A 2 eV shift to higher energy relative to the known DEA resonances of water and phosphates is also indicated.

**Project 3: Detecting metabolites using electronic excitation/laser ionization.** We have developed a system to allow sensitive detection of metabolites using VUV photoionization of neutrals which desorb from a surface via non-thermal channels. We have utilized this approach to detect metabolites and biomarkers in complex mixtures with femtomolar sensitivities.

### 3. Future Plans:

This program is a multifaceted approach to the study of low-energy electrons with water films and biological targets containing intrinsic waters of hydration. We will continue to investigate the role of water and negative ion resonances in low-energy electron-induced damage of phosphate linked sugars, DNA and RNA. We will utilize VUV photoionization to detect the neutral fragments produced and desorbed as a function of incident electron energy. The role of the underlying substrate and intrinsic solvated cations on the electronic states of water and DNA damage will also be investigated using new liquid sample and beam deposition techniques. Aligned targets will be used and spatially resolved data will be obtained using ion-imaging techniques.

**Publications supported by this DOE program (2005-2007):**

1. J. Herring-Captain, G. A. Grieves, M. T. Sieger, A. Alexandrov, H. Chen and T. M. Orlando, "Electron-stimulated desorption of  $H^+$ ,  $H_2^+$ , and  $H^+(H_2O)_n$  from nanoscale water thin-films" *Phys. Rev. B.* 72, 035431 (2005).
2. D. Oh, M. T. Sieger and T. M. Orlando, "Zone specificity in the low-energy electron stimulated desorption of  $Cl^+$  from reconstructed Si(111)-7×7 surfaces" *Surf. Sci.* 600, L245-249 (2006).
3. Y. Chen, C. Sullards, T. Huang, S. May and T. M. Orlando, "Analysis of Organoselenium and Organic Acid Metabolites by Laser Desorption Single Photon Ionization Mass Spectrometry", *Anal. Chem.* 78(24), 8386-8394 (2006).
4. T. M. Orlando, G. Grieves, J. Herring-Captain, and A. Alexandrov, "Probing the interaction of hydrogen chloride on low-temperature water ice surfaces using electron stimulated desorption", *J. Chem. Phys.* (submitted).
5. T. M. Orlando, D. Oh, Y. Chen, and A. Alexandrov, "The Role of Diffraction and Compound Feshbach Resonances in Low-energy Electron Induced Damage of Hydrated DNA", *Phys. Rev. Lett.* (submitted).

**References:**

- (1) Herring, J.; Aleksandrov, A.; Orlando, T. M. *Phys. Rev. Lett.* **2004**, 92, 187602/1.
- (2) Herring-Captain, J.; Grieves, G. A.; Alexandrov, A.; Sieger, M. T.; Chen, H.; Orlando, T. M. *Phys. Rev. B: Condens. Matter Mater. Phys.* **2005**, 72.
- (3) Grieves, G. A.; Olanrewaju, B.; Herring-Captain, J.; Petrick, N.; Aleksandrov, A.; Tonkyn, R.; Kimmel, G.; Orlando, T. *J. Chem. Phys.* **submitted**.
- (4) Cederbaum, L. S.; Zobeley, J.; Tarantelli, F. *Physical Review Letters* **1997**, 79, 4778.
- (5) Santra, R.; Zobeley, J.; Cederbaum, L. S.; Tarantelli, F. *Journal of Electron Spectroscopy and Related Phenomena* **2001**, 114-116, 41.
- (6) Zobeley, J.; Santra, R.; Cederbaum, L. S. *Journal of Chemical Physics* **2001**, 115, 5076.

# Energetic Photon and Electron Interactions with Positive Ions

Ronald A. Phaneuf,  
Department of Physics /220  
University of Nevada  
Reno NV 89557-0058  
phaneuf@physics.unr.edu

## Program Scope

This experimental program investigates processes leading to ionization of positive ions by photons and electrons. The objective is a deeper understanding of both ionization mechanisms and electron-electron interactions in ions of atoms, molecules and nano-scale molecular clusters. Monoenergetic beams of photons and electrons are merged or crossed with mass/charge analyzed ion beams to probe their internal electronic structure as well as the dynamics of their interaction. Of particular interest are highly-correlated processes such as collective electron excitations that are manifested as giant dipole resonances in the ionization of atomic ions and also of fullerene ions, whose unique cage structure bridges the gap between molecules and solids. In addition to precision spectroscopic data for understanding ionic structure and interactions, high-resolution measurements of absolute cross sections for photoionization and electron-impact ionization provide critical benchmarks for testing theoretical approximations such as those used to generate opacity databases. Improving their accuracy is critical to modeling and diagnostics of astrophysical, fusion-energy and laboratory plasmas. Of particular relevance to DOE are those produced by the Z pulsed-power facility at Sandia National Laboratories, the world's brightest and most efficient x-ray source, and the National Ignition Facility at Lawrence Livermore National Laboratory, the world's most powerful laser. Both are dedicated to high-energy-density science and fusion-energy research.

## Recent Progress

The major thrust has been the application of an ion-photon-beam (IPB) research endstation to experimental studies of photoionization of singly and multiply charged positive ions using monochromatized synchrotron radiation. The high photon beam intensity and energy resolution available at ALS undulator beamline 10.0.1 make photoion spectroscopy a powerful probe of the internal electronic structure of atomic and molecular ions, permitting tests of sophisticated structure and dynamics computer codes at unprecedented levels of detail and precision. Measurements using the IPB endstation at ALS define the current state of the art worldwide in energy resolution available to studies of photon-ion interactions. This program developed and continues to have primary responsibility for maintenance and upgrade of this permanently installed multi-user research endstation.

- Due to their size and hollow cage structure, fullerene ions are of particular interest as intermediates between molecules and solids. As is the case for conducting solids, their large number of valence electrons may be collectively excited in plasmon modes, whereas the excitation of core electrons is localized and of molecular character. Absolute cross sections for photoionization of  $C_{60}^+$ ,  $C_{70}^+$ ,  $C_{80}^+$ ,  $C_{82}^+$  and  $C_{84}^+$  were measured over the energy range 17-70 eV as part of a systematic

investigation of collective electron excitations. The measurements for  $C_{80}^+$  and  $C_{82}^+$  serve as a reference for exploratory measurements with endohedral fullerene ions noted below. Photoionization measurements were made for  $C_{60}^+$  and  $C_{70}^+$  in the energy range 270-320 eV where carbon K-shell excitation occurs. This research was conducted in collaboration with the University of Giessen. At photon energies below 100 eV, the cross sections for these fullerene ions are dominated by giant resonances associated with collective surface and volume plasmon excitations of the valence electrons [2, 3, 19]. Above 280 eV, localized K-shell excitations of carbon atoms dominate the cross sections, which become distinctly molecular in character. A comprehensive report on this work is being prepared for publication.

- Complementary measurements of photoionization and electron-impact ionization of ions of the krypton isonuclear sequence were completed. Measurements on  $Kr^{3+}$ ,  $Kr^{4+}$  and  $Kr^{5+}$  constituted the Ph.D. dissertation of Miao Lu [9]. The  $Kr^{3+}$  measurements indicate that the ionization potential tabulated in the NIST database is in error by nearly 2 eV [10], whereas the cross section for direct photoionization of  $Kr^{5+}$  is too small to reliably determine the ionization potential [11].
- An investigation of photoionization of the xenon isonuclear sequence was completed in collaboration with the NIST EBIT group, with a focus  $Xe^{4+}$ ,  $Xe^{5+}$  and  $Xe^{6+}$  for applications in the development of 13.5 nm light sources for EUV lithography [12].
- A detailed comparison was made of benchmark high-resolution measurements of photoionization of He-like  $Li^+$  at ALS with predictions of state-of-the-art R-matrix calculations [14]. This was the product of a multi-institutional collaboration.
- Complementary measurements of photoionization and electron-impact ionization of  $Ar^{5+}$  were compared to Hartree-Fock calculations of energies and oscillator strengths for core excitations. This project constituted the M.S. thesis of Jing Cheng Wang [15], from which the major results were recently published [16].
- Measurements of photoionization of chlorine-like  $K^{2+}$  and  $Ca^{3+}$  were compared to predictions of the energies and oscillator strengths of core excitations made using the Cowan Hartree-Fock atomic structure code. This research constituted the Ph.D. dissertation of Ghassan Alna’Washi [18] and is being prepared for publication.

### Future Plans

In addition to the completion of work already in progress on photoionization and electron-impact ionization of atomic ions, research is planned in two new directions.

- A growing number of theoretical and experimental studies have demonstrated that single atoms and even molecules or radicals may be stably trapped inside the hollow cage of a fullerene molecule. The technology to produce so-called endohedral fullerenes in macroscopic quantities has now advanced to a stage where it is feasible to produce endohedral fullerene ions in a low-power discharge and to accelerate and mass-analyze them. Exploratory experiments were carried out at the ALS in collaboration with A. Müller and S. Schippers of the University of Giessen, and L. Dunsch and S. Yang of the Institute for Solid State and Materials Research in Dresden, where the endohedral molecules were synthesized. In addition to probing

the influence of the fullerene cage on atomic resonances, an objective of such experiments is to investigate the possible influence of a caged atom on the properties of collective plasmon oscillations of the valence-shell electrons of fullerene molecular ion. Proof-of-principle measurements with picoampere beams of mass-analyzed  $\text{Sc}_3\text{N}@\text{C}_{80}^+$  and  $\text{Ce}@\text{C}_{82}^+$  ions were successful, indicating that strong resonances of the caged species may be photo-excited and contribute distinct structures to the photoionization cross section. A report on the  $\text{Sc}_3\text{N}@\text{C}_{80}^+$  measurements has been submitted to Physical Review Letters. The Ph.D. dissertation research of Mustapha Habibi will include photoionization of  $\text{Ce}@\text{C}_{82}^+$  as well as reference measurements on 4d-4f giant resonances in isolated  $\text{Ce}^{q+}$  ions in different charge states, in order to determine their valency within the  $\text{C}_{82}^+$  cage. Photoionization of other endohedral fullerene ion species will be investigated as the materials become available.

- Photoionization of the fullerene fragment ions  $\text{C}_{58}^+$ ,  $\text{C}_{56}^+$ ,  $\text{C}_{54}^+$ ... is of interest to explore the effects of the size and symmetry of the molecular cage structure on the collective plasmon resonances, as well as the chemical stability of the fragment ions. Such measurements will be compared with existing data for  $\text{C}_{60}^+$ ,  $\text{C}_{70}^+$ ,  $\text{C}_{80}^+$ ,  $\text{C}_{82}^+$  and  $\text{C}_{84}^+$  in order to systematically explore the cross-section scaling with the number of carbon atoms, as well as effects of the cage symmetry on the plasmon resonances. This systematic investigation will constitute part of the Ph.D. dissertation research of David Esteves.

### References to Publications of DOE-Sponsored Research (2005-2007)

1. *K-shell photoionization of Be-like carbon ions: experiment and theory for  $\text{C}^{2+}$* , S.W.J. Scully, A. Aguilar, E.D. Emmons, R.A. Phaneuf, M. Halka, D. Leitner, J.C. Levin, M.S. Lubbell, R. Püttner, A.S. Schlachter, A.M. Covington, S. Schippers, A. Müller and B.M. McLaughlin, *J. Phys. B* 38, 1967 (2005).
2. *Photoexcitation of a volume plasmon in  $\text{C}_{60}$  ions*, S.W.J. Scully, E.D. Emmons, M.F. Gharaibeh, R. A. Phaneuf, A.L.D. Kilcoyne, A.S. Schlachter S. Schippers, A. Müller, H.S. Chakraborty, M.E. Madjet and J.-M. Rost, *Phys. Rev. Lett.* 94, 065503 (2005).
3. *240 Electrons Set in Motion*, Physics News Update 722 #1 American Institute of Physics, (March 17, 2005).
4. *Photoionization of ions of the nitrogen isoelectronic sequence: experiment and theory for  $\text{F}^{2+}$  and  $\text{Ne}^{3+}$* , A. Aguilar, E.D. Emmons, M.F. Gharaibeh, A.M. Covington, J.D. Bozek, G. Ackerman, S. Canton, B. Rude, A.S. Schlachter, G. Hinojosa, I. Alvarez, C. Cisneros, B.M. McLaughlin and R.A. Phaneuf, *J. Phys. B At. Mol. Opt. Phys.* 38, 343 (2005).
5. *Photoionization and electron-impact ionization of  $\text{Xe}^{3+}$* , E.D. Emmons, A. Aguilar, M.F. Gharaibeh, S.W. J. Scully, R.A. Phaneuf, A.L.D. Kilcoyne, A.S. Schlachter, I. Alvarez, C. Cisneros and G. Hinojosa, *Phys. Rev. A* 71, 042704 (2005).
6. *Photofragmentation of ionic carbon monoxide*, G. Hinojosa, M.M. Sant'Anna, A.M. Covington, R.A. Phaneuf, I.R. Covington, I. Domínguez, A.S. Schlachter, I. Alvarez and C. Cisneros, *J. Phys B* 38, 2701 (2005).

7. *Systematic photoionization study along the iron isonuclear sequence*, M. F. Gharaibeh, Ph.D. Dissertation, University of Nevada, Reno (2005).
8. *A theoretical and experimental study of the photoionization of Al II*, C.E. Hudson, J.B. West, K.L. Bell, A. Aguilar, R.A. Phaneuf, F. Folkmann, H. Kjeldsen, J. Bozek, A.S. Schlachter and C. Cisneros, *J. Phys. B: At. Mol. Opt. Phys.* 38, 2911 (2005).
9. *Photoionization and electron-impact ionization of multiply charged krypton ions*, Miao Lu, Ph.D. Dissertation, University of Nevada, Reno (2006).
10. *Photoionization and electron-impact ionization of Kr<sup>5+</sup>*, M. Lu, M.F. Gharaibeh, G. Alna'Washi, R.A. Phaneuf, A.L.D. Kilcoyne, E. Levenson, A.S. Schlachter, A. Müller, S. Schippers, J. Jacobi and C. Cisneros, *Phys. Rev. A* 74, 012703 (2006).
11. *Photoionization and electron-impact ionization of Kr<sup>3+</sup>*, M. Lu, G. Alna'Washi, M. Habibi, M.F. Gharaibeh, R.A. Phaneuf, A.L.D. Kilcoyne, E. Levenson, A.S. Schlachter, C. Cisneros and G. Hinojosa, *Phys. Rev. A* 74, 062701 (2006).
12. *Absolute photoionization cross sections for Xe<sup>4+</sup>, Xe<sup>5+</sup> and Xe<sup>6+</sup> near 13.5 nm: Experiment and theory*, A. Aguilar, J.D. Gillaspy, G.F. Gribakin, R.A. Phaneuf, M.F. Gharaibeh, M.G. Kozlov, J.D. Bozek and A.L.D. Kilcoyne, *Phys. Rev. A* 74, 032717 (2006).
13. *Interaction of photons with ionized matter*, Ronald A. Phaneuf, p.p. 171-175 in McGraw-Hill Yearbook of Science and Technology 2006, McGraw-Hill, New York (2006).
14. *Doubly excited resonances in the photoionization spectrum of Li<sup>+</sup>: experiment and theory*, S.W.J. Scully, I. Álvarez, C. Cisneros, E.D. Emmons, M.F. Gharaibeh, D. Leitner, M.S. Lubbell, A. Müller, R.A. Phaneuf, R. Püttner, A.S. Schlachter, S. Schippers, W. Shi, C.P. Balance and B.M. McLaughlin, *J. Phys. B: At. Mol. Opt. Phys.* 39, 3957 (2006).
15. *Photoionization and Electron-impact Ionization of Ar<sup>5+</sup>*, Jing Cheng Wang, M.S. Thesis, University of Nevada, Reno (2006).
16. *Photoionization and electron-impact ionization of Ar<sup>5+</sup>*, Jing Cheng Wang, M. Lu, D. Esteves, M. Habibi, G. Alna'Washi, R.A. Phaneuf and A.L.D. Kilcoyne, *Phys. Rev. A* 75, 062712 (2007).
17. *Colliding-beams Experiments for Studying Fundamental Atomic Processes*, 13<sup>th</sup> International Conference on the Physics of Highly Charged Ions, Belfast, Northern Ireland, August 28, 2006; *J. Phys. Conf. Ser.* 58, 1 (2007).
18. *Photoionization of Cl-like K<sup>2+</sup> and Ca<sup>3+</sup>*, Ghassan Alna'Washi, Ph.D. Dissertation, University of Nevada, Reno (2007).
19. *Reply to Comment on photoexcitation of a volume plasmon in C<sub>60</sub> ions*, S.W.J. Scully, E.D. Emmons, M.F. Gharaibeh, R.A. Phaneuf, A.L.D. Kilcoyne, A.S. Schlachter, S. Schippers, A. Müller, H.S. Chakraborty, M.E. Madjet and J.M. Rost, *Phys. Rev. Lett.* 98, 179602 (2007).

# Resonant and nonresonant photoelectron-vibrational coupling

Erwin Poliakoff, Department of Chemistry, Louisiana State University, Baton Rouge, LA 70803, [epoliak@lsu.edu](mailto:epoliak@lsu.edu)  
Robert Lucchese, Department of Chemistry, Texas A&M University, College Station, TX, 77843  
[lucchese@mail.chem.tamu.edu](mailto:lucchese@mail.chem.tamu.edu)

## Scope of program

Molecular photoionization provides an ideal means of studying correlations between electronic and molecular degrees of freedom. In our research, resonant and nonresonant photoionization are studied for systems ranging from diatomics to large polyatomic systems. High resolution photoelectron spectroscopy measurements at the Advanced Light Source provide the experimental data, and we employ adiabatic static model-exchange (ASME) and Schwinger variational calculations to provide a theoretical foundation for the analysis. The goal is to develop an understanding of how photoelectrons traverse anisotropic molecular frameworks and exchange energy with vibrations. This research benefits the goals of the Department of Energy because the results elucidate structure/spectra correlations that will be indispensable for probing complex and disordered systems of DOE interest such as clusters, catalysts, reactive intermediates, transient species, and related species that are difficult to study with traditional methods.

## Recent progress

We describe recent studies from both the previous and current grant periods. The previous grant focused on resonant processes in relatively symmetric polyatomic systems, including linear triatomics ( $\text{CO}_2$ ,  $\text{CS}_2$ ,  $\text{N}_2\text{O}$ ), tetrahedral molecules ( $\text{SiF}_4$ ,  $\text{CF}_4$ ), simple planar systems ( $\text{BF}_3$ ,  $\text{C}_2\text{F}_4$ ,  $\text{C}_2\text{Cl}_4$ ,  $\text{C}_2\text{F}_3\text{Cl}$ ), and aromatic hydrocarbons ( $\text{C}_6\text{F}_6$ , 1,4- $\text{C}_6\text{H}_4\text{F}_2$ , 1,3,5- $\text{C}_6\text{H}_3\text{F}_3$ ). The newest studies have shifted to nonresonant phenomena. For an example of a resonant process, we describe recent work on  $\text{C}_6\text{F}_6$ ,<sup>1</sup> while recent studies of two simple asymmetric systems (CO and ICN) are discussed to illustrate the surprising nonresonant phenomena that arise over very wide ranges of energy.

### 1. $\text{C}_6\text{F}_6 \text{ } b_{2u} \rightarrow \text{k}e_{2g}$ shape resonance: launching a particle-on-a-ring

Hexafluorobenzene ( $\text{C}_6\text{F}_6$ ) was investigated in detail.<sup>1</sup> It has many more vibrational degrees of freedom than any previously studied system, which makes it possible to deduce a qualitative picture of the continuum photoelectron localization. In particular, we find that an electron launched into the continuum can become trapped in an unprecedented quasibound state, namely, one that extends through the backbone of the 6-member carbon ring of  $\text{C}_6\text{F}_6$ . The vibrationally mode specific response to the electron trapping provides an experimental signature, while adiabatic static model-exchange scattering calculations are used to map the wave function, which corroborate the interpretation. Photoelectron spectra were taken at many energies, and vibrational branching ratios were extracted from these spectra, i.e., the ratio of an excited vibrational level relative to that of the vibrational ground state. Vibrational branching ratio curves have been generated for many vibrational modes, and a few selected ones are plotted in Fig. 1.

The branching ratio curves in Fig. 1 are striking, particularly the dramatic differences between the  $v_1$  curve (top frame) and the  $v_2$  curve (middle frame). We see that the  $v_1$  curve is essentially flat (i.e., Franck-Condon behavior) whereas the  $v_2$  branching ratio curve exhibits a strong, relatively broad peak that is typical of a shape resonance. The question naturally arises why one vibration is lighting up following resonant excitation while the other is completely unresponsive. Both are totally symmetric vibrations, but the  $v_1$  vibration primarily affects the motion of the fluorine atoms whereas the  $v_2$  vibration distorts the carbon ring of the molecule. Thus, the results suggest that the resonance is localized along the carbon backbone of the molecule. This interpretation is supported by the results for the  $v_{17}$  branching ratio curve. The  $v_{17}$  vibration distorts the ring via asymmetrically, and like the  $v_2$  mode, results in a strongly non-Franck-Condon energy dependence, similar though not identical to the branching ratio curve for the  $v_2$  mode.

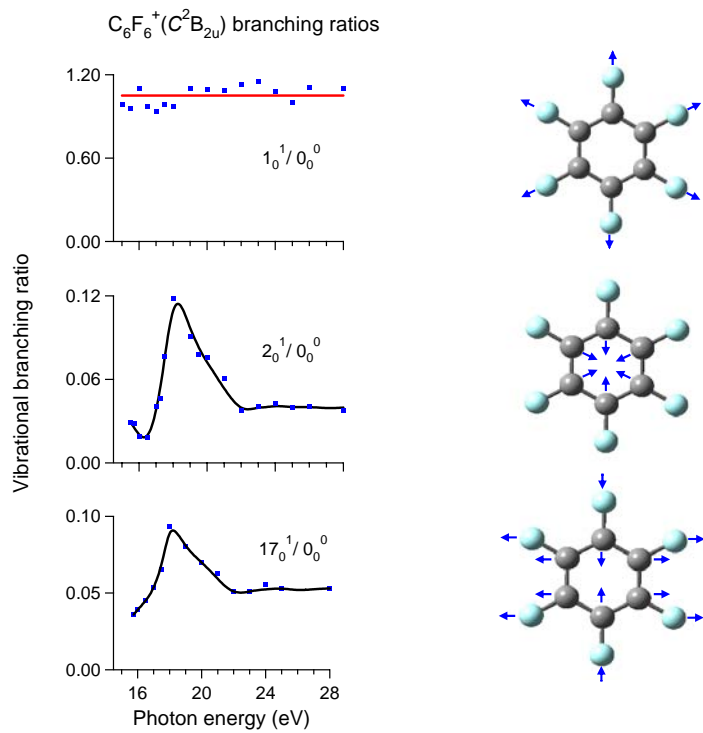


**Figure 1.** Vibrational branching ratio curves for selected single quantum vibrational excitations. These results show that distortions of the ring strongly affect the resonance. Note that the branching ratio curve for  $v_1$  (top frame), corresponding to the C-F stretch, is flat, while the curve for  $v_2$  (middle frame) – the ring breathing motion – displays pronounced deviations from Franck-Condon predictions. The  $v_{17}$  curve (bottom frame), corresponding to a vibration which results in an asymmetric skewing of the aromatic ring, also displays a clear deviation from the Franck-Condon prediction. The curves are hand-drawn to guide the eye, not theoretical results.

The theoretical results corroborate the interpretation that the quasibound continuum electron is trapped along the carbon ring. ASME calculations directly yield resonant the wave function for a model potential using a local exchange approximation. The result for the resonant wavefunction is shown in Fig. 2.

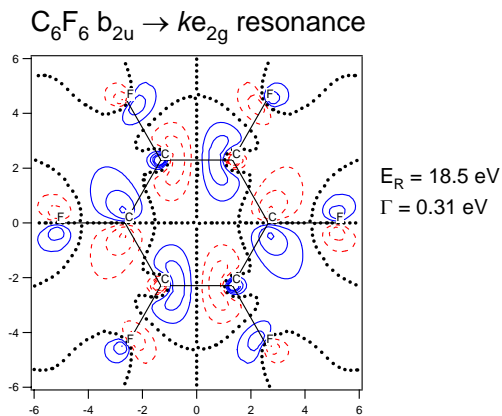


**Figure 2.** Contour map for the relevant  $b_{2u} \rightarrow k e_{2g}$  continuum shape resonant wave function. Note the enhancement of electron density lying along the C<sub>6</sub> backbone of the molecule, leading to the strong sensitivity to the ring breathing motion.

The theoretical wavefunction contour map for C<sub>6</sub>F<sub>6</sub> shows that a  $b_{2u} \rightarrow k e_{2g}$  shape resonance centered at ~18 eV is responsible for the observed non-Franck-Condon behavior. This is consistent with the observed vibrational mode-specificity, as there is considerable electron density along the C-C bonds of the benzene backbone, as suggested by the experiment.

## 2. Nonresonant studies

While much of our previous work has focused on resonant ionization, nonresonant processes can also strongly influence the ionization dynamics and lead to vibrational excitation.<sup>2</sup> However, such effects have not been investigated in detail, even though it is an area ripe for study. The principal reason for this neglect has been that the technical requirements for such studies are daunting, particularly experimentally. In particular, highly resolved measurements are required over a energy ranges that easily exceed hundreds of eV.

One nonresonant phenomenon that has been shown to result in coupling between photoelectron and vibrational motion is the Cooper minimum, which results from a transition matrix element going through zero as a consequence of the target radial wavefunction going through a change of sign. While Cooper minima have been studied for many decades,<sup>3</sup> it was not anticipated that their characteristics would be influenced by vibrational motion. As a result, it was something of a surprise when it was learned that vibration could couple strongly to photoelectron motion, and with a spectral extent that was astonishingly broad.<sup>2</sup> In order to see if photoelectron spectroscopy was suitable for studying such nonresonant effects, we performed some initial  $\text{CO}^+(X^2\Sigma^+)$  photoelectron measurements at the ALS, and those data are also shown in Fig. 3.

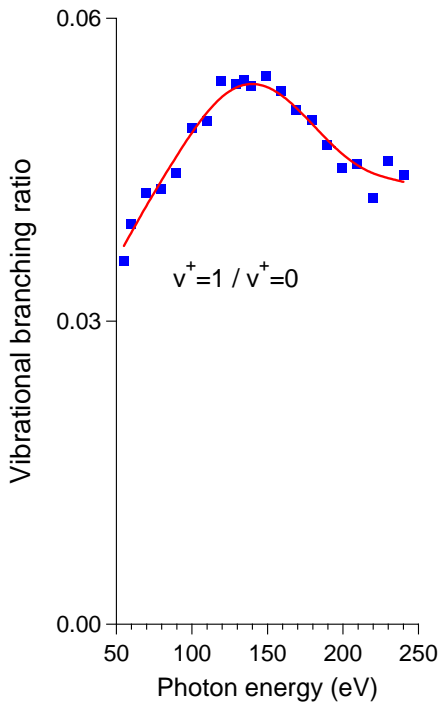


**Figure 3.** Vibrational branching ratio for  $\text{CO}^+(X^2\Sigma^+)$  over a very large energy range acquired via photoelectron spectroscopy at the ALS. The vibrational branching ratio is varying over a range of more than 150 eV. The line is hand-drawn line to guide the eye .

A theoretical effort is underway to analyze the results shown in Fig. 3. It is clear that the photoelectron-vibrational coupling occurs over much too wide a range of energy to be attributed to a resonance. We suspect that it is due to a Cooper minimum, or possibly a series of Cooper minima. Another point is that not all electronic states exhibit such behavior. For example, the  $\text{CO}^+(B^2\Sigma^+)$  state vibrational branching ratio curve (not shown) was determined to be constant, in contrast to the data in Fig. 3.

We are also studying nonresonant ionization for more complex systems. Interesting data have been obtained for ICN photoionization, where nonresonant coupling between the photoelectron and vibrational motion is observed. Several results are currently being analyzed. First, Schwinger variational calculations have demonstrated that the mechanism responsible for the Franck-Condon breakdown is not one which has been previously identified, i.e., it does not result from either a resonance or geometry-dependent behavior of Cooper minima. Second, the results are vibrationally mode-specific, with the vibration that principally affects the I-C stretch being more strongly influenced than the vibrational mode that is dominated by the C-N stretch. Third, the different spin orbit components show differing behavior. These initial results are guiding new directions that we are currently pursuing.

## **Future plans**

The ICN results are extremely interesting, and we will pursue different directions that are suggested by these data. Other molecules containing iodine and bromine will be studied, and the systematics of the behavior will be probed. Secondly, we will continue studies of resonant processes, but the focus will be on asymmetric systems, particularly those of biological interest.

## **Publications resulting from this research:**

Ten papers have appeared during the grant period based on the work described here. Those papers are listed below. Several more are in preparation.

G.J. Rathbone, E.D. Poliakoff, J.D. Bozek, R.R. Lucchese, P. Lin, *Mode-specific photoelectron scattering effects on CO<sub>2</sub><sup>+</sup>(C<sup>2</sup>Σ<sub>g</sub><sup>+</sup>) vibrations*, J. Chem. Phys. **120**, 612 (2004)

G.J. Rathbone, R.M. Rao, E. D. Poliakoff, K. Wang, V. McKoy, Vibrational branching ratios in photoionization of CO and N<sub>2</sub>, J. Chem. Phys. **120**, 778 (2004)

G.J. Rathbone, E.D. Poliakoff, John D. Bozek, R.R. Lucchese, *Observation of the symmetry-forbidden 5σ<sub>u</sub>→kσ<sub>u</sub> CS<sub>2</sub> transition: A vibrationally driven photoionization resonance*, Phys. Rev. Lett. **92**, 1430021 (2004)

G.J. Rathbone and E.D. Poliakoff, J.D. Bozek, R.R. Lucchese, *Intrachannel vibronic coupling in molecular photoionization*, Can. J. Chem. **82**, 1043 (2004)

G.J. Rathbone, E.D. Poliakoff, J.D. Bozek, R.R. Lucchese, *Electronically forbidden (5σ<sub>u</sub>→kσ<sub>u</sub>) photoionization of CS<sub>2</sub>: Mode-specific electronic-vibrational coupling*, J. Chem. Phys. **122**, 064308 (2005).

G.J. Rathbone, E.D. Poliakoff, J.D. Bozek, D. Toffoli, R.R. Lucchese, *Photoelectron trapping in N<sub>2</sub>O 7σ→kσ resonant ionization*, J. Chem. Phys. **123**, 014307 (2005).

E.D. Poliakoff and R.R. Lucchese, *Evolution of photoelectron–vibrational coupling with molecular complexity*, Physica Scripta **74**, C71 (2006).

A. Das, E.D. Poliakoff, R.R. Lucchese, and J.D. Bozek, *Launching a particle on a ring: b<sub>2u</sub>→ke<sub>2g</sub> ionization of C<sub>6</sub>F<sub>6</sub>*, J. Chem. Phys. **125**, 164316 (2006).

R. Montuoro, R.R. Lucchese, J.D. Bozek, A. Das, and E.D. Poliakoff, *Quasibound continuum states in SiF<sub>4</sub> D<sup>2</sup>A<sub>1</sub> photoionization: Photoelectron-vibrational coupling*, J. Chem. Phys. **126**, 244309 (2007).

A. Das, J.S. Miller, E.D. Poliakoff, R.R. Lucchese, and J.D. Bozek, *Vibrationally resolved photoionization dynamics of CF<sub>4</sub> in the D<sup>2</sup>A<sub>1</sub> state*, J. Chem. Phys. (in press).

## **References:**

<sup>1</sup> A. Das, E. D. Poliakoff, R. R. Lucchese, and J. D. Bozek, J. Chem.. Phys. **125**, 164316 (2006).

<sup>2</sup> R. M. Rao, E. D. Poliakoff, K. Wang, and V. McKoy, Phys. Rev. Lett. **76**, 2666 (1996).

<sup>3</sup> S. T. Manson, Phys. Rev. A **31**, 3698 (1985).

# Control of Molecular Dynamics: Algorithms for Design and Implementation

Herschel Rabitz and Tak-San Ho, Princeton University  
Frick Laboratory, Princeton, NJ 08540, hrabitz@princeton.edu, tsho@princeton.edu

## A. Program Scope

This research is concerned with developing concepts for the systematic study of controlled quantum phenomena. Theoretical studies and simulations play central roles guiding the achievement of control over quantum dynamics, especially in conjunction with the use of optimal control theory and its realization in closed-loop learning experiments. The research in this program involves several interrelated components aiming at developing a deeper understanding of the principles of quantum control and providing new algorithms to extend the laboratory control capabilities.

## B. Recent Progress

In the past year several projects were pursued whose results are summarized below.

1. **The Landscape of Unitary Transformations in Controlled Quantum Dynamics<sup>1</sup>** We have extended a previous analysis of optimal control landscapes for unitary transformations from a kinematic perspective to a dynamical one in the infinite-dimension function space of the time-dependent control field. The dynamical control landscape is analyzed via the minimization of the Frobenius matrix distance in conjunction with an arbitrary non-singular landscape adaptation matrix. The landscape adaptation matrix enables additional manipulations of the control landscapes. The dynamical analysis reveals many essential geometric features of the unitary transformation optimal control landscapes, including the bounds on the magnitude of landscape slopes and curvatures and the non-trapping nature of the local critical points at which the slopes vanish. The properties of Hessians at the critical points are analyzed in detail. Moreover, the geometric properties of the control landscape around the critical points are qualitatively depicted via a gradient flow analysis. The gradient flow expresses the important nature of the landscape global maximum, global minimum and local saddles in terms of vector fields, and this information can be significant for effecting efficiency, accuracy, and stability in the construction of unitary transformations.
2. **Optimal control over an ensemble of quantum systems in an inhomogeneous environment<sup>2</sup>** We have explored the ability of a single optimal control pulse to simultaneously steer all members of such an ensemble of systems to the same target despite the inhomogeneous effects and with constraints

also present on the controls. The simulations were carried out in two stages of (i) random shifts in the system energy levels and dipole elements along with (ii) random decoherence coupling to the environment. The concepts were illustrated for an ensemble of four level model systems, and the results indicate that effective controls can overcome the effects of the inhomogeneities to a good degree.

3. **Controlling quantum dynamics regardless of laser beam spatial profile and molecular orientation<sup>3</sup>** In a typical experiment aiming to control quantum dynamics phenomena, each molecule experiences the same temporal laser field, but with an amplitude that depends on the spatial location and orientation of the molecule in the laser beam. We proved under commonly arising conditions that at least one optimal laser field exists which will control all molecules in the sample, regardless of their orientation or spatial location. The optimal laser field may consist of a multipolarization control containing up to three orthogonal, independently shaped components. The analysis also includes the prospect of multipartite control where the field couples distinct groupings of states e.g., multiple vibronic states , but without direct coupling within a group of states. This conclusion shows that achieving quantum control is not a matter of striking a compromise over the sample diversity, but rather a task subject to optimization to reach the highest possible level of control for all molecules in the sample.
4. **Controllability of open quantum systems with Kraus-map dynamics<sup>4</sup>** We have found a constructive proof of complete kinematic state controllability of finite-dimensional open quantum systems whose dynamics are represented by Kraus maps. For any pair of states (pure or mixed) on the Hilbert space of the system, we explicitly showed how to construct a Kraus map that transforms one state into another. Moreover, we proved by construction the existence of a Kraus map that transforms all initial states into a predefined target state. Thus, in sharp contrast to unitary control, Kraus-map dynamics allows for the design of controls which are robust to variations in the initial state of the system. The capabilities of non-unitary control for population transfer between pure states is illustrated for an example of a two-level system by constructing a family of non-unitary Kraus maps to transform one pure state into another. The problem of dynamic state controllability of open quantum systems (i.e., controllability of state-to-state transformations, given a set of available dynamical resources such as coherent controls, incoherent interactions with the environment, and measurements) was also addressed.
5. **Optimal control of quantum gates and suppression of decoherence in a system of interacting two-level particles<sup>5</sup>** We have applied methods of optimal control to a model system of interacting two- level particles (e.g., spin-half atomic nuclei, electrons, or two-level atoms) to produce high-fidelity quantum gates while simultaneously negating the detrimental effect of decoherence. One set of particles functions as the quantum information processor, whose evo-

lution is controlled by a time-dependent external field. The other particles are not directly controlled and serve as an effective environment, coupling to which is the source of decoherence. The control objective is to generate target one- and two-qubit unitary gates in the presence of strong environmentally-induced decoherence and under physically motivated restrictions on the control field. The quantum-gate fidelity, expressed in terms of a novel state-independent distance measure, is maximized with respect to the control field using combined genetic and gradient algorithms. The resulting high-fidelity gates demonstrated the feasibility of precisely guiding the quantum evolution via optimal control, even when the system complexity is exacerbated by environmental coupling. It was found that the gate duration has an important effect on the control mechanism and resulting fidelity. By performing an analysis of the sensitivity of the gate performance to random variations in the system parameters, we found a significant degree of robustness attained by the optimal control solutions.

6. **Foundations for cooperating with control noise in the manipulation of quantum dynamics<sup>6</sup>** We have developed the theoretical foundations for the ability of a control field to cooperate with noise in the manipulation of quantum dynamics. The noise enters as run-to-run variations in the control amplitudes, phases, and frequencies with the observation being an ensemble average over many runs as is commonly done in the laboratory. Weak field perturbation theory was formulated to show that noise in the amplitude and frequency components of the control field can enhance the process of population transfer in a multilevel ladder system. Our analytical results support the assessment that under suitable conditions an optimal field can cooperate with noise to improve the control outcome.

## C. Future Plans

The research in the coming year will mainly focus on the mechanism and the landscape of quantum control for both closed and open quantum systems and its future prospects in the laboratory. Via judicious control-mechanism analysis, we aim to explore the detailed dynamics of the decoherence and environmental management processes in various optimally controlled quantum problems, including unitary transformations. With the aid of detailed control landscape analysis, especially from the dynamics around the landscape critical points, we aim to describe how and why the control landscape can influence the optimal control. Moreover, we plan to apply the methods of landscape analysis to study (1) the controls of multi-observables, including multi-times observations, and (2) the effects of control noises and environment inhomogeneities.

## D. References

1. The Landscape of Unitary Transformations in Controlled Quantum Dynamics, T.-S. Ho, J. Dominy, and H. Rabitz, preprint (2007).

2. Optimal control over an ensemble of quantum systems in an inhomogeneous environment, R. Wu and H. Rabitz, preprint (2007).
3. Controlling quantum dynamics regardless of laser beam spatial profile and molecular orientation, H. Rabitz and G. Turinici, Phys. Rev. A. **75**, 043409 (2007).
4. Optimal control of quantum gates and suppression of decoherence in a system of interacting two-level particles, M. Grace, C. Brif, H. Rabitz, et al. J. Phys. B-Atom. Mole. Opti. Phys. **40** S103-S125 (2007).
5. Controllability of open quantum systems with Kraus-map dynamics, R. Wu, A. Pechen, C. Brif, H. Rabitz, J. Phys. A-Math. Theo. Phys., **40**, 5681-5693 (2007).
6. Foundations for cooperating with control noise in the manipulation of quantum dynamics, F. Shuang, H. Rabitz, M. Dykman, Phys. Rev. E, **75**, 021103 (2007).
7. Global analytical potential energy surfaces for  $H_2(\tilde{X}^2A'')$  based on high-level ab initio calculations, D. Q. Xie, C. X. Xu, T.-S. Ho, H. Rabitz, et al., J. Chem. Phys., **126**, 074315 (2007).
8. The topology of optimally controlled quantum mechanical transition probability landscape, H. Rabitz, T.-S. Ho, M. Hsieh, B. Kosut, and M. Demiralp, Phys. Rev. A, **74**, 012721 (2006).
9. Optimal control landscapes for quantum observables, H. Rabitz, M. Hsieh, and C. Rosenthal, J. Chem. Phys. **124**, 204107 (2006)
10. Revealing the key variables and states in optimal control of quantum dynamics, M. Artamonov, T.-S. Ho, and H. Rabitz, Chem. Phys. Lett. **421**, 81 (2006).
11. Quantum optimal control of molecular isomerization in the presence of a competing dissociation channel, M. Artamonov, T.-S. Ho, and H. Rabitz, J. Chem. Phys. **124**, 064306 (2006)
12. Quantum observable homotopy tracking control, A. Rothman, T.-S. Ho, and H. Rabitz, J. Chem. Phys. **123**, 134104 (2005)
13. The single-molecule dye laser, Z. S. Wang, H. A. Rabitz, and M. O. Scully, Laser Physics, **15**, 118 (2005).
14. Observable-preserving control of quantum dynamics over a family of related systems, A. Rothman, T.-S. Ho, and H. Rabitz, Phys. Rev. A **72**, 023416 (2005)
15. Quantum control of molecular motion including electronic polarization effects with two stage toolkit, G. Balint-Kurti, F. Manby, Q. Ren, M. Artamonov, T.-S. Ho, and H. Rabitz, J. Chem. Phys., **122**, 084110 (2005).

# Interactions of Cold Rydberg Atoms in a High-Magnetic-Field Atom Trap

G. Raithel, FOCUS Center, Physics Department, University of Michigan  
450 Church St., Ann Arbor, MI 48109-1120, [graithel@umich.edu](mailto:graithel@umich.edu)  
<http://cold-atoms.physics.lsa.umich.edu>

## 1 Program scope

Highly magnetized, cold Rydberg-atom gases and magnetized plasmas are investigated. In our experiments, we use a particle trap that operates at magnetic fields up to 6 Tesla and that can simultaneously function as a ground-state atom trap, Rydberg-atom trap and nested Penning ion and electron trap. Ground-state atom clouds collected in the trap are laser-excited into clouds of magnetized Rydberg atoms or cold plasmas. The combination of low temperatures, strong magnetic fields, and substantial collision rates leads to a rich variety of atomic and plasma processes; these are the focus of this project. Our studies relate to the physics of atoms and plasmas in astrophysical environments, in magnetized man-made plasmas, in anti-hydrogen research, and in quantum information processing.

In studies of low-angular-momentum Rydberg atoms directly excited by high-resolution narrow-band lasers, we are interested in coherent single-atom dynamics and in coherent interactions in many-body Rydberg-atom systems. Coherent effects of the internal motion include spin oscillations of the Rydberg electron induced by spin-orbit coupling. Investigations of coherent interactions and correlations in cold, magnetized many-body Rydberg systems rely on spatially resolved Rydberg-atom detection, which can be implemented in fairly straightforward ways in high-magnetic-field atom traps such as ours. In the future, coherent Rydberg-atom interactions may become useful in the implementation of quantum information processing schemes.

At higher Rydberg-atom or plasma densities, collisions and / or recombination lead to the formation of atoms in gyration-center states (=drift states), which exhibit distinct cyclotron, bounce and magnetron motions of the Rydberg electron. These drift-state atoms have large  $z$ -components of the angular momentum, high densities of states, long lifetimes, and are suitable for magnetic trapping. Using our recently demonstrated capability to magnetically trap such atoms, we intend to measure their polarizabilities, cyclotron quantum numbers, and decay rates. We further prepare cold plasmas in nested Penning traps by photo-ionization of trapped ground-state atoms, and study the coupled dynamics of the ion and electron components of these plasmas. Employing the capability of our apparatus to combine Rydberg-atom and Penning traps, we study Rydberg-atom-electron collisions and recombination in strong-magnetic-field environments.

## 2 Recent results

### 2.1 Cold-plasma expansion dynamics in strong magnetic fields

We generate magnetized plasmas by photo-ionization of laser-cooled and magnetically trapped atoms in a bias magnetic field of 2.9 T at densities  $\approx 10^7 \text{ cm}^{-3}$ . The plasmas are created in a nested Penning trap. A pair of inner electrodes ( $E2$  and  $E3$ ) in Fig. 1(a) are held at  $V_{in} = -1 \text{ V}$  while outer electrodes ( $E1$  and  $E4$ ) are grounded. The calculated electric potential in the axial direction exhibits a local maximum at  $z = 0$ ; this maximum is created by the quadrupole electric field that arises mostly due to vertical, optical-access apertures in the electrodes. The combined magnetic and electric fields produce a trapping potential for both ions and electrons [Fig. 1(b)]. The depth of the trapping potential is tuned by varying  $V_{in}$  between -0.5 V and -4 V. On time scales of about 1 ms, the  $\mathbf{E} \times \mathbf{B}$  drift motion associated with the transverse components of the trapping electric field causes a slow alignment of the plasma with a diagonal plane, and a slow escape

of the plasma along that plane. The plasma lifetime increases with decreasing depth of the plasma trapping potential. This plasma escape dynamics is well understood.

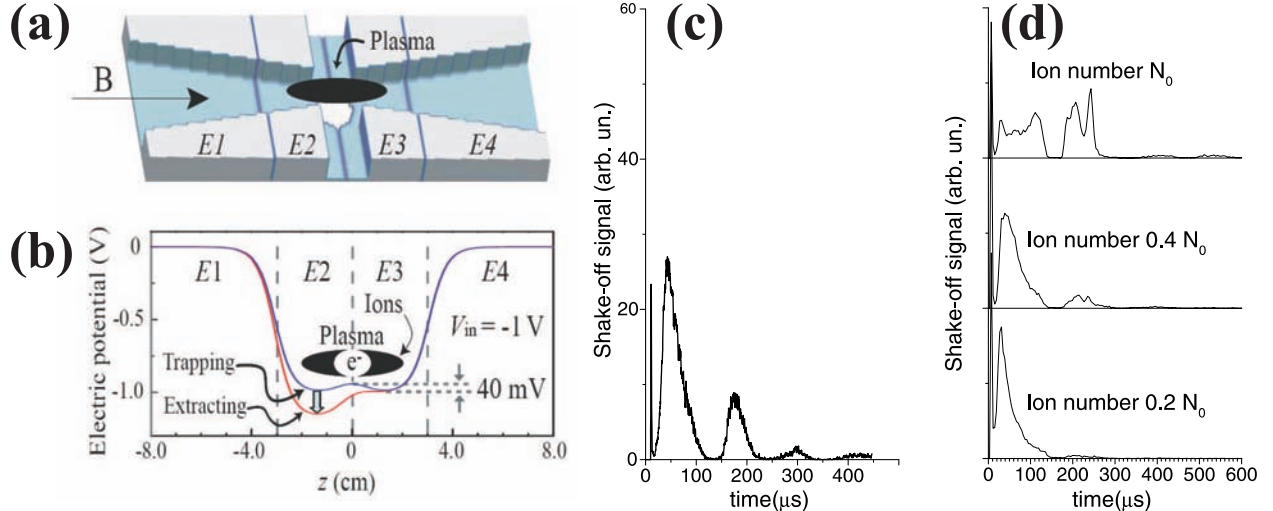


Figure 1: (a) Electrodes that generate Penning-trap, DC bias, and plasma extraction electric fields. Only the bottom half is shown. The holes in the structure provide 6-way optical access. (b) Axial electric-potential profile in the two-component plasma trap. To extract electrons from the trap, the voltage on the electrode  $E_2$  changes in time. (c) Periodic electron shake-off signal caused by oscillations of the ion component of the plasma. (d) Effect of the initial ion number on the shake-off signal ( $N_0 \lesssim 10^6$ ). Irregularities observed at high numbers are interpreted as ion pressure-wave effects.

Immediately after photo-excitation, the ions undergo a breathing-type oscillation in the outer, double-well potential within the range  $|z| \lesssim 2$  cm. This oscillation is equivalent to a space-charge oscillation, which in turn leads to a modulation of the net trapping potential for the electron component of the plasma. The modulation in electron-trap depth causes a periodic electron “shake-off” signal, which can be observed over a few hundred microseconds [see Fig. 1(c)]. The shake-off signal exhibits reproducible structures that develop with increasing density [see Fig. 1(d)]. We believe that these structures are a manifestation of ionic waves. We are able to explain most of the dynamics shown in Figs. 1(c) and (d).

## 2.2 Energy distribution of trapped electrons

The electron component of the strongly magnetized plasma is contained in the central well of the potential shown in Fig. 1(b). The well is largely due to the external electrodes; it is modulated by the space-charge potential produced by the ions. The energy distribution of the electrons is analyzed by application of a stepped electric-field electron extraction ramp. At each step of the extraction ramp, a fraction of the electrons is released [see Fig. 2(a)]. The electron energy spectra reveal the overall potential depth and the electron temperature. From the distributions in Fig. 2(a), an initial electron temperature  $T \approx 250$  K is calculated. To identify the source of initial thermal energy, we first note that the wavelength of the photo-ionization laser is 478.8 nm, which generates photo-electrons with an initial energy that is insufficient to explain the observed temperature. However, since the trapped-atom cloud has a diameter of a few millimeters, the photo-electrons created within the potential depicted in Fig. 1(b) have a substantial average initial potential energy; of order half of that energy is converted into thermal kinetic energy after photo-ionization. In our estimates we find that this amount is consistent with the observed electron temperature.

The correlation between the ionic oscillations in the outer, double-well potential in Fig. 1(b) and the electron motion has already become evident in the periodic electron shake-off signal in Fig. 1(c). The ionic oscillations

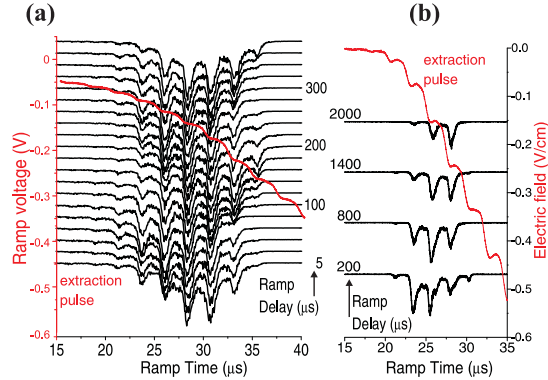


Figure 2: (a) Spectra of the electron-component of a strongly, magnetized plasma obtained with a stepped electron extraction ramp (overlaid curve, left axis) for the indicated values of the delay time between photo-excitation and application of the extraction ramp (ramp delay indicated on the right). (b) Long-term evolution of the electron energy spectra. The longer the delay time, indicated on the left, the more electric field is needed to extract the electrons from the plasma. Hence, the electron gas cools as a function of time. The overlaid curve shows the stepped electron extraction ramp (right axis).

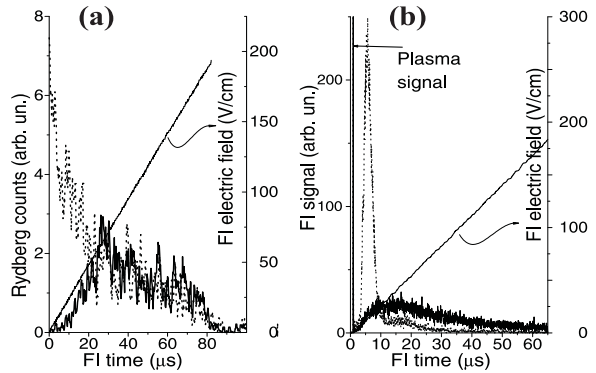


Figure 3: (a) State-selective field ionization spectra of Rydberg atoms forming in an unconfined plasma (dotted line) and in a nested electron/ion trap (solid). In the trap case, atoms in high-lying Rydberg states are missing; this absence is attributed to ionizing Rydberg-atom-electron collisions. (b) Effect of electron collisions on Rydberg atoms prepared with a well-defined initial energy. Initially, most Rydberg atoms ionize at a well-defined electric field (dotted curve). After an interaction time of 1 ms with trapped electrons, about a quarter of the Rydberg-atom population has ionized (“plasma signal”), while the remaining Rydberg atoms have been shifted to lower-energy states that have higher ionization electric fields (solid curve). The linear curves show the electric-field ionization ramps [right axes in (a) and (b)].

also manifest themselves in a periodic variation of the average arrival time of the electron signal relative to the onset of the forced extraction ramp in Fig. 2(a). In addition, over a time scale of a few milliseconds we observe significant electron cooling. In calculations based on Fig. 2(b), the electron temperature is found to drop from about 280 K to 120 K over a time ranging from 0 to 2 ms. At times  $> 3$  ms, the temperature levels out at about 50 K (data not shown in this abstract). There appear to be several possible mechanisms for the electron cooling (evaporative cooling and / or energy transfer from longitudinal into transverse degrees of freedom); the investigation of electron cooling mechanisms is ongoing.

### 2.3 Recombination and Rydberg-atom collisions

It is of interest how many drift-state Rydberg atoms are formed in a cold, strongly magnetized plasma, and how quickly these atoms percolate from high-lying Rydberg states down into the ground state. Here, we obtain state-selective field ionization spectra of recombined Rydberg atoms for different values of the initial ion number, the electron temperature, the electron trapping conditions, and the plasma evolution time after photo-excitation. We find that Rydberg atoms initially form in a broad energy distribution that peaks at very high-lying levels. Due to the interaction of the Rydberg atoms with the electron component of the plasma, the total number of detected Rydberg atoms declines with increasing delay time after photo-excitation, and the state-distribution shifts to lower states. A typical data set is shown in Fig. 3(a). We believe that the Rydberg atoms form due to three-body recombination, and that Rydberg-atom-electron collisions cause the gradual decay of atoms into lower-lying states. Using photo-excitation below the photo-ionization threshold,

we can also prepare clouds of strongly magnetized Rydberg atoms at a well-defined energy. If the Rydberg gas is created in a nested Penning trap, electrons originating in Rydberg-Rydberg collisions remain trapped and collide frequently with the remaining Rydberg atoms. Under the conditions of Fig. 3(b) we find that the energy distribution of the Rydberg-atom gas is significantly shifted towards lower-lying states, and that about a quarter of the atoms ionize. The observed atomic processes may be relevant to experiments on cold anti-hydrogen elsewhere.

### 3 Plans

Low-angular-momentum Rydberg atoms in strong magnetic fields at energies very close to the continuum have significantly stronger spin-orbit coupling than Rydberg atoms in zero or weak fields. We have observed indications of spin-orbit oscillations caused by the coupling. Using narrow-linewidth excitation, we intend to study coherent spin oscillations in real-time. Further, we have seen evidence for the effects of classical resonances of radial and  $z$ -motion on radiative decay. This will be explored further. The work on trapping of high-angular-momentum Rydberg atoms will evolve towards using the Rydberg atom trap as an analytic tool to measure single-atom properties (electric polarizabilities, magnetic moments, etc.).

We plan to continue our studies of cold, strongly magnetized plasmas. Interesting topics include the (already observed) electron cooling, which still needs to be explained in full. The fate of Rydberg atoms that form via recombination in such plasmas will be further explored. Exploiting our capability to trap both atoms and electrons at the same spatial location, we intend to study collisions between cold-electron clouds and Rydberg atoms implanted into these clouds. Two separate lasers will be used in order to independently control the electron temperature and the initial Rydberg-atom energy.

Using narrow-bandwidth laser excitation and spatially resolved Rydberg-atom detection, it is planned to investigate the effects of coherent electric-quadrupole interactions between strongly magnetized Rydberg atoms.

### 4 Publications 2005 - 2007

“Trapping and evolution dynamics of ultracold two-component plasmas,” J.-H. Choi, X. Zhang, A. P. Povilus, and G. Raithel, submitted (2007).

“Cold Rydberg atoms”, J.-H. Choi, B. Knuffman, T. Cubel Liebisch, A. Reinhard, G. Raithel, in Advances in Atomic, Molecular and Optical Physics vol. 54, eds. E. Arimondo and P. Berman, (Elsevier, 2006).

“Time dependence and Landau quantization in the ionization of cold, magnetized Ryberg atoms,” J.-H. Choi, J. R. Guest, E. Hansis, A. P. Povilus, and G. Raithel, Phys. Rev. Lett. **95**, 253005 (2005).

“Magnetic trapping of long-lived cold Rydberg atoms,” J.-H. Choi, J. R. Guest, A. P. Povilus, E. Hansis, and G. Raithel, Phys. Rev. Lett. **95**, 243001 (2005).

“Laser cooling and magnetic trapping at several Tesla,” J. R. Guest, J.-H. Choi, E. Hansis, A. P. Povilus and G. Raithel, Phys. Rev. Lett. **94**, 073003 (2005).

“A simple pressure-tuned Fabry-Perot interferometer,” E. Hansis, T. Cubel, J.-H. Choi, J. R. Guest, and G. Raithel Rev. Sci. Instrum. **76**, 033105 (2005).

“Coherent population transfer of ground-state atoms into Rydberg states”, T. Cubel, B. K. Teo, V. S. Malinovsky, J. R. Guest, A. Reinhard, B. Knuffman, P. R. Berman, and G. Raithel Phys. Rev. **A 72**, 023405 (2005). (J. R. Guest supported by DoE).

## **Dual Quantum Gases of Bosons: From Atomic Mixtures to Heteronuclear Molecules**

### **Principal Investigator:**

Dr. Chandra Raman  
Associate Professor  
School of Physics  
Georgia Institute of Technology Atlanta, GA 30332-0430  
[craman@gatech.edu](mailto:craman@gatech.edu)

### **Program Scope:**

This program centers on creating a dual species atomic Bose-Einstein condensate of  $^{23}\text{Na}$  and  $^{87}\text{Rb}$ . The eventual goal is to synthesize heteronuclear molecules of the two species. Our approach involves trapping and cooling of large ( $\sim 10^{10}$ ) Na atom numbers to sympathetically cool Rb to quantum degeneracy. Once the mixture is trapped, we will create molecules by magneto-association using a number of recently predicted Feshbach resonances (these have been supported by new experimental data from Tiemann's group PRA 72, 062505 (2005)). The eventual goal of the molecular effort is to create a dipolar superfluid, a novel strongly correlated quantum system.

Since the interactions in each mixture is unique, our measurement of the inter-species scattering length will provide essential data on the Na-Rb interatomic potentials and is a key ingredient in the theory of cold collisions. The Na-Rb system is versatile, as the second Rb isotope,  $^{85}\text{Rb}$ , offers additional opportunities to observe resonant interactions with Na.

### **Recent Progress:**

**System Upgrades.** In this first year of our renewed research program we have focused on significant upgrades to the existing Na apparatus to accommodate the second atomic species, Rb. In the process we have made the following improvements: 1) installation of a quartz vacuum cell for improved optical access to the two species, 2) new magnetic trap design which increases the atomic confinement (magnetic field gradient) by a factor of 3 while allowing us to search for Feshbach resonances up to 1 kiloGauss magnetic bias field.

**Dual Species Zeeman Slowing.** Dual atom trapping requires a source of slow atoms of both species. Rather than using two separate atom sources, we previously demonstrated a novel approach that creates a single atomic beam containing both species Na and Rb. This approach has the advantage of requiring one fewer vacuum port in an already crowded apparatus accommodating a magnetic trap, imaging and magneto-optical trap (MOT) optics. Very recently we have also demonstrated that the Zeeman slower which was designed to slow the Na beam will *also* slow Rb down to velocities of a few m/s that

will allow capture into a MOT. That is, we can now produce *slow atoms* of both species from a single Zeeman slower (see Figure 1). The Rb flux achieved was comparable (within an order of magnitude) to the Na flux. This important first step demonstrates that our approach toward trapping mixtures of the two species is feasible. Future plans are to set up the dual atom MOT and begin magnetic trapping of the two species.

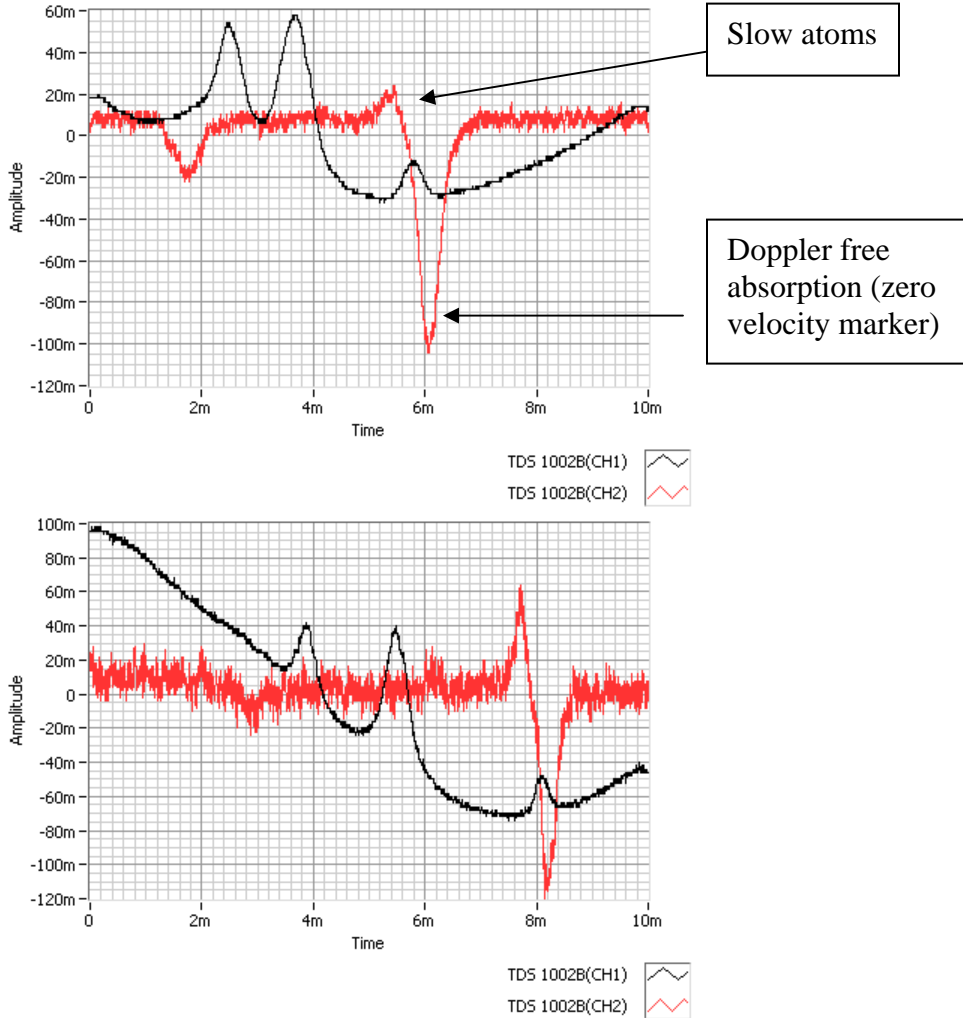


**Figure 1:** Zeeman slowing of  $^{85}\text{Rb}$  (top) and  $^{87}\text{Rb}$  (bottom). The red curves are probe laser absorption by the atomic beam versus the atoms' velocity, which decreases from left to right. The velocity is determined by scanning the laser frequency in time and calibrating the Doppler shifted resonant absorption by simultaneous measurement of saturation spectroscopy of the 3P hyperfine levels in a Rb vapor cell (black curves). Zero velocity corresponds to the large negative (downward) peak on the right, which is Doppler free absorption by the beam. Slow atoms appear as a *positive* peak at low velocities near the Doppler free peak. Additional negative peaks are Doppler free absorption on other hyperfine transitions.

**Detecting Curve Crossings.** We have discovered a powerful algebraic method of finding level crossings in physical systems by mapping it to the problem of locating the roots of a polynomial [M. Bhattacharya and C. Raman: *Detecting Level Crossings without Looking at the Spectrum*, Phys. Rev. Lett. **97**, 140405 (2006)]. This has implications in performing searches for Feshbach resonances. Recently we have published two additional papers detailing the mathematical basis of this technique and elaborating on its application to atoms and molecules:

1. M. Bhattacharya and C. Raman: *Detecting level crossings without solving the Hamiltonian I. Mathematical background*. Phys. Rev. A **75**, 033405 (2007).
2. M. Bhattacharya and C. Raman: *Detecting level crossings without solving the Hamiltonian II. Applications to Atoms and Molecules*. Phys. Rev. A **75**, 033406 (2007).

## **“Coherent and Incoherent Evolution of Rydberg Atoms”**

**F. Robicheaux**

*Auburn University, Department of Physics, 206 Allison Lab, Auburn AL 36849  
(robicfj@auburn.edu)*

### **Program Scope**

This theory project focuses on the time evolution of Rydberg states. This study is divided into three categories: (1) coherent evolution of highly excited quantum states, (2) incoherent evolution of highly excited quantum states, and (3) the interplay between ultra-cold plasmas and Rydberg atoms. Some of the techniques we developed have been used to study collision processes in ions, atoms and molecules.

### **Recent Progress 2006-2007**

*Three body recombination in strong magnetic fields:* There has been a resurgence of theoretical interest in electron scattering and recombination in strong magnetic fields motivated by recent experiments that have demonstrated the formation of anti-hydrogen when anti-protons traverse a positron plasma. In Ref. [15], we investigated how three body recombination is affected if there are two light species present with opposite charges (for example, an antiproton in the presence of positrons and electrons). The most important parameter was the fraction of the light species of the wrong sign for recombination because it can destroy newly made atoms by charge transfer. We found that a surprisingly small fraction would substantially reduce the recombination rate. We identified the main mechanisms controlling the recombination process.

*Photon-atom processes in strong magnetic fields:* We studied how the radiative cascade in highly excited states can affect the center of mass motion of the atom.[13] If an atom is in a spatially varying magnetic field, it can be trapped using its magnetic dipole moment. For highly excited states, the dipole moment can substantially decrease as the atom emits successive photons. This makes the center of mass potential appear to be opening up. Thus the center of mass motion of the atom cools as the cascade proceeds. In future attempts at trapping antihydrogen, this effect might become quite important because it could reduce the center of mass energy to the point it can be captured.

*Rydberg atoms in strong fields:* We computed[18] the time dependent ionization of a H atom excited to a highly excited wave packet in strong, parallel Electric and Magnetic fields. This calculation was purely quantum mechanical and was undertaken due to interesting classical calculations by Mitchell and Delos that found a chaotic pattern to the ionization of the electron. Classically, the system scales so that the same behavior is apparent as long as simple relations between energy, electric field and magnetic field are held fixed. We solved for the time dependent wave function for quantum numbers up to  $n \sim 120$ . We found a similar pattern to the ionization as was seen in the classical calculation for the total electron current, but the angular dependence showed non-trivial interference patterns. We were able to manipulate the ionization current by manipulating the angular

distribution of the initial outgoing wave packet. This was the first quantum calculation of the time dependent ionization of a classically chaotic system.

*Electron-Rydberg collisions:* The ionization balance in a dense plasma is largely controlled by multistep ionization where the atom/ion is first excited and then is ionized from the weakly bound state. There have been almost no calculations of the electron impact ionization of atoms/ions from highly excited states because it is beyond current computational resources. Currently, extensive use is made of classical calculations without knowing the accuracy of that approximation. We examined[14] a model problem that is computationally tractable and investigated how the ionization depended on charge state and principal quantum number. We found that the classical results converged to the quantum results with increasing  $n$ , but much more slowly than might be expected.

*Molecules:* Some of the techniques we developed for highly excited atoms can be used to investigate processes in molecules. In Ref. [17], we investigated the double ionization of  $H_2$  molecules by a single photon. In particular, we were interested in the triple differential cross sections which characterize the energy and direction dependence of the outgoing electron pair. This is a difficult problem due to the long range for the electron-electron interaction and the non-spherical potential resulting from the separated charges. We found excellent agreement with a completely independent calculation, thus confirming the size and shape of the differential cross section.

*Two electron continua:* Over the past decade we have performed many calculations of processes involving two electron escape from an atom/ion. The computational tool has been the direct solution of the time dependent Schrodinger equation. There are many aspects of this method that are not obvious and have slowly been grafted to the basic method over the years. We recently gathered some of the high points of these calculations in a review paper.[16]

Finally, this program has several projects that are strongly numerical but only require knowledge of classical mechanics. This combination is ideal for starting undergraduates on publication quality research. Since 2004, 7 undergraduates have participated in this program. Daniel Phalen completed the quantum scattering calculation of Ref. [5] during the summer of 2004. Chris Norton and Michael Wall completed the double charge exchange calculation[7] during spring of 2005; MW later completed a time dependent quantum calculation for a different grant. Michael Wall was one of 5 undergraduates invited to give a talk on their research at the undergraduate session of the DAMOP 2006 meeting. Michelle Zhang and Christine Taylor completed a project to simulate the motion of an anti-hydrogen atom interacting with the complicated magnetic fields in the proposed anti-hydrogen traps in order to test ideas about measuring whether or not the anti-hydrogen atoms are trapped[13]. Jennifer Hurt and Patrick Carpenter are performing calculations of the scattering of positrons from antiprotons. In addition to these undergraduates, this grant supports the investigations of Turker Topcu who is a graduate student; he has completed the investigation of radiative cascade in strong B[10], the component of Ref. [8] related to model double photoionization near threshold, model quantum calculations of electron impact ionization of Rydberg atoms ( $n \sim 25$ )[14], the calculation of the time dependent escape of Rydberg electrons in parallel electric

and magnetic fields[18], and is currently studying the effect of near resonant microwaves on highly excited states.

### Future Plans

*Ultra-cold plasmas* Recent experiments by S. Bergeson's group at BYU and G. Raithel's group at U.Michigan have uncovered interesting behavior of ultra-cold plasmas at short time (BYU) or with cylindrical symmetry(UM). The BYU experiments have  $B \sim 0$  while the UM experiments are in high  $B$ . We have developed programs to study these systems but have applied them to specific problems. We plan to: (1) simulate the expansion of ultracold plasma in cylindrical symmetry with and without high  $B$  and compare to experiment and our previous results for spherical symmetry and (2) simulate TBR in an expanding ultracold plasma in strong  $B$  and the properties of the atoms.

*Anti-hydrogen motivated calculations* The next generation of anti-hydrogen experiments are aimed at trapping the anti-hydrogen. To address possible issues, we will investigate processes that arise from this goal. In particular, we plan to: (1) develop a program to compute the radiative recombination rate in strong magnetic field and also use it for ion charges other than 1 in order to determine the effect on electron cooling of ions in storage rings and (2) study the three body recombination rate when all of the particles have the same mass.

*Coherent evolution* A recent experiment by T. Gallagher's group showed that it is possible to drive a 10 photon transition in Rydberg states without any of the intermediate photons being resonant. We will perform classical and quantum calculations of this system to understand how it works.

### DOE Supported Publications (2004-2007)

- [1] F. Robicheaux and J.D. Hanson, Phys. Rev. A **69**, 010701 (2004).
- [2] F. Robicheaux, Phys. Rev. A **70**, 022510 (2004).
- [3] M.S. Pindzola, F. Robicheaux, J.A. Ludlow, J. Colgan, and D.C. Griffin, Phys. Rev. A **72**, 012716 (2005).
- [4] D.C. Griffin, C.P. Balance, M.S. Pindzola, F. Robicheaux, S.D. Loch, J.A. Ludlow, M.C. Witthoeft, J. Colgan, C.J. Fontes, and D.R. Schultz, J. Phys. B **38**, L199 (2005).
- [5] D.J. Phalen, M.S. Pindzola, and F. Robicheaux, Phys. Rev. A **72**, 022720 (2005).
- [6] M.S. Pindzola, F. Robicheaux, and J. Colgan, J. Phys. B **38**, L285 (2005).
- [7] M.L. Wall, C.S. Norton, and F. Robicheaux, Phys. Rev. A **72**, 052702 (2005).
- [8] U. Kleiman, T. Topcu, M.S. Pindzola, and F. Robicheaux, J. Phys. B **39**, L61 (2006).
- [9] F. Robicheaux, Phys. Rev. A **73**, 033401 (2006).
- [10] T. Topcu and F. Robicheaux, Phys. Rev. A **73**, 043405 (2006).
- [11] M.S. Pindzola, F. Robicheaux, S.D. Loch, and J.P. Colgan, Phys. Rev. A **73**, 052706 (2006).
- [12] A. Wetzels, A. Gurtler, L.D. Noordam, and F. Robicheaux, Phys. Rev. A **73**, 062507 (2006).
- [13] C.L. Taylor, Jingjing Zhang, and F. Robicheaux, J. Phys. B **39**, 4945 (2006).

- [14] T. Topcu, M.S. Pindzola, C.P. Balance, D.C. Griffin, and F. Robicheaux, Phys. Rev. A **74**, 062708 (2006).
- [15] F. Robicheaux, J. Phys. B **40**, 271 (2007).
- [16] M.S. Pindzola, F. Robicheaux, S.D. Loch, J.C. Berengut, T. Topcu, J. Colgan, M. Foster, D.C. Griffin, C.P. Balance, D.R. Schultz, T. Minami, N.R. Badnell, M.C. Witthoeft, D.R. Plante, D. M. Mitnik, J.A. Ludlow, and U. Kleiman, J. Phys. B **40**, R39 (2007).
- [17] J. Colgan, M.S. Pindzola, and F. Robicheaux, Phys. Rev. Lett. **98**, 153001 (2007).
- [18] T. Topcu and F. Robicheaux, J. Phys. B **40**, 1925 (2007).

## High Harmonic Generation in Discharge-Ionized Plasma Channels

Jorge J. Rocca,

*Electrical and Computer Eng Department, Colorado State University, Fort Collins, CO 80523-1373*

*rocca@engr.colostate.edu*

Henry C. Kapteyn

*JILA/Physics Department, University of Colorado, Boulder, CO 80309-0440*

*kapteyn@jila.colorado.edu*

### Program description

We have successfully used a pre-ionized medium created by a compact capillary discharge to extend the cutoff photon energy in high-order harmonic generation. The observed enhancements result from a combination of reduced ionization energy loss and reduced ionization-induced defocusing of the driving laser. We observed harmonic emission from Xe up to an unprecedented photon energy of 160 eV, and we extend this technique to other noble gases for the first time, observing photons with energies up to 170 eV from Kr, and 275 eV from Ar. We show the discharge plasma also provides a means to spectrally tune the harmonics by tailoring the initial level of ionization of the medium. Our results were interpreted using a hydrodynamic / atomic physics model of the discharge plasma. This work demonstrates that capillary discharges are a versatile and general method for generating harmonics, in particular from ions. Finally, this approach should be scaleable to efficiently generate coherent light at much shorter wavelengths ( $> 1$  KeV photon energy), in combination with novel phase-matching techniques.

### High harmonic generation from ions in a capillary discharge

High-order harmonic generation (HHG) has proven to be a useful source of coherent extreme ultraviolet (EUV) and soft x-ray radiation for applications. When a medium is illuminated by an intense laser field, odd-order harmonics of the fundamental laser are generated. The highest photon energy that can be produced through this process is predicted by the cutoff rule to be  $h\nu_{\max} = I_p + 3.17U_p$ , where  $I_p$  is the ionization potential of the target atom and  $U_p$  is the ponderomotive energy of the liberated electron in the laser field. ( $U_p = E^2/4\omega^2$  in atomic units where  $E$  is the peak of the laser electric field with frequency  $\omega$ ). In principle with long wavelength or high field lasers,  $h\nu_{\max}$  may be as high as 6 keV before relativistic effects suppress rescattering and HHG. To date however, for many experiments the highest harmonic photon energies observed have not been limited by the available laser intensity, but rather by the ionization of the nonlinear medium by the driving laser. The depletion of neutrals does not terminate the harmonic emission since high harmonics may also be generated from ions. Rather, the electron density from photoionization refractively defocuses the driving laser, reducing the peak laser intensity and consequently the highest harmonic photon energy observed. Moreover, the resulting plasma imparts different phase velocities to the driving laser and the HHG light, which results in poor phase-matching and conversion efficiency. Finally, the loss of the laser energy due to photoionization limits the length in the medium over which a high peak intensity can be maintained.

The intensity at which an atom (or ion) ionizes depends directly on the ionization potential of the atom. Because ions have much higher ionization potentials than neutrals, significantly higher energy photons can be generated from ions than from neutrals. The use of a

capillary discharge to create a preformed plasma with a tailored level of ionization allows HHG from ions while avoiding ionization losses of the driving laser and ionization-induced defocusing. This leads to the generation of higher photon energies from ions with higher ionization potentials and an increase in efficiency of the entire generation process. Additionally, the radial electron density profile of the capillary discharge plasma is concave, producing an index waveguide. This plasma waveguide combats additional ionization-induced defocusing of the laser and allows for a decreased laser intensity near the walls of the capillary, making it possible to guide the higher intensities required for shorter wavelength generation without damaging the walls.

## Results

In recent work, we demonstrated that the “cut-off,” i.e. the highest observable photon energy generated through the high-order harmonic generation process, can be extended significantly using a capillary discharge plasma. The observed enhancements result from a combination of reduced ionization energy loss and reduced ionization-induced defocusing of the driving laser. A schematic of the capillary discharge and set up used to generate the harmonics is shown in Fig. 1. Using this technique, we observed photon energies generated in Xe up to  $\sim$ 160 eV (Fig. 2a), well above the highest previously observed value of  $\sim$ 70 eV. In addition to extending the cutoff photon energy, the harmonic flux near the cutoff was enhanced by nearly two orders of magnitude. Also, the reduced self-phase modulation that results from pre-ionization made it possible to observe clearly resolved harmonic peaks up to 85 eV photon energy. The cases of Kr and Ar are shown in Figs. 2b and 2c. Using a capillary waveguide without the discharge running, the HHG signal extends to 125 eV for Kr and 225 eV for Ar. When the discharge was used, the observed maximum photon energies were extended further, to 170 eV and 275 eV, respectively. Prior to these experiments, the highest photon energies generated from these two gases using an 800 nm driving laser were 70 eV and 250 eV, respectively. In both cases, the emission was attributed to ions. Thus, the cutoff in Kr was extended by 100 eV while the cutoff in Ar was extended by 25 eV, compared with all past measurements. The presence of the discharge also enhances the harmonic flux in Kr and Ar at high photon energies, where this emission necessarily originates from ionization of ions. The plasma defocusing and ionization loss are smaller in the case of Kr and Ar when compared to Xe; as a result, the enhancement of the HHG flux is less than in the case of Xe. The data of Fig. 3 further demonstrate that these effects originate from a reduced ionization-induced defocusing of the laser. In this data, the laser pulse energy was varied in the capillary, with and without discharge preionization. Without the discharge running, the HHG spectrum does not change significantly as the laser pulse energy is increased from 9 mJ to 11 mJ, indicating that the peak

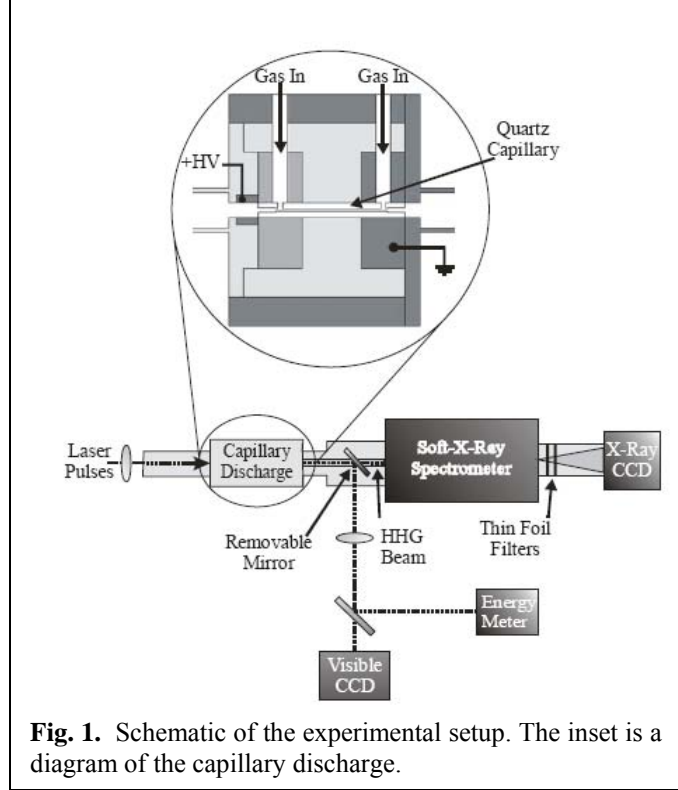


**Fig. 1.** Schematic of the experimental setup. The inset is a diagram of the capillary discharge.

intensity is clamped by ionization induced defocusing. However, when the discharge is present, there is a large enhancement in HHG flux because of the higher laser intensity. The observed cutoff is due to poor phasematching as measurements of the laser energy transmitted through the discharge indicate that the cutoff photon energy should extend to  $> 400$  eV for the estimated laser intensity of  $2.3 \times 10^{15}$  W/cm<sup>2</sup> used in these experiments.

In summary, these experiments demonstrate that the use of a discharge plasma as a nonlinear medium for high-order harmonic generation is a general method for generating high harmonics from ions, and for extending the cutoff to higher photon energies. Moreover, the ionized medium created by the discharge also provides a method to spectrally tune the harmonics by tailoring the initial level of ionization of the medium. These effects are a consequence of the fact that, by creating a preformed, ionized medium, the discharge reduces ionization-induced refraction losses of the laser, making it possible to maintain a high laser intensity over a long interaction length. We also verified these results through a hydrodynamic model of the discharge plasma, coupled with a simulation of beam propagation. These data also imply that any further extension of the cutoff in Ar is primarily limited by the large plasma-induced phase mismatch between the fundamental and harmonic waves. In the proposed future work, we plan to develop new phase-matching techniques to further extend the range of photon energies that can be efficiently generated, into the keV spectral region.

### Future plans

Having solved the problem of generation of high harmonics from ions in a plasma waveguide, the remaining barrier to overcome for efficient high harmonic generation at much higher photon energies than are currently accessible (100 eV – keV) is that of phase matching. During the stage of the project we plan to investigate new optical phase matching schemes in capillary discharge plasmas, where we can control the phase matching conditions and can also guide an intense laser beam. This will allow us to generate sufficient harmonic flux for a variety of new application experiments.

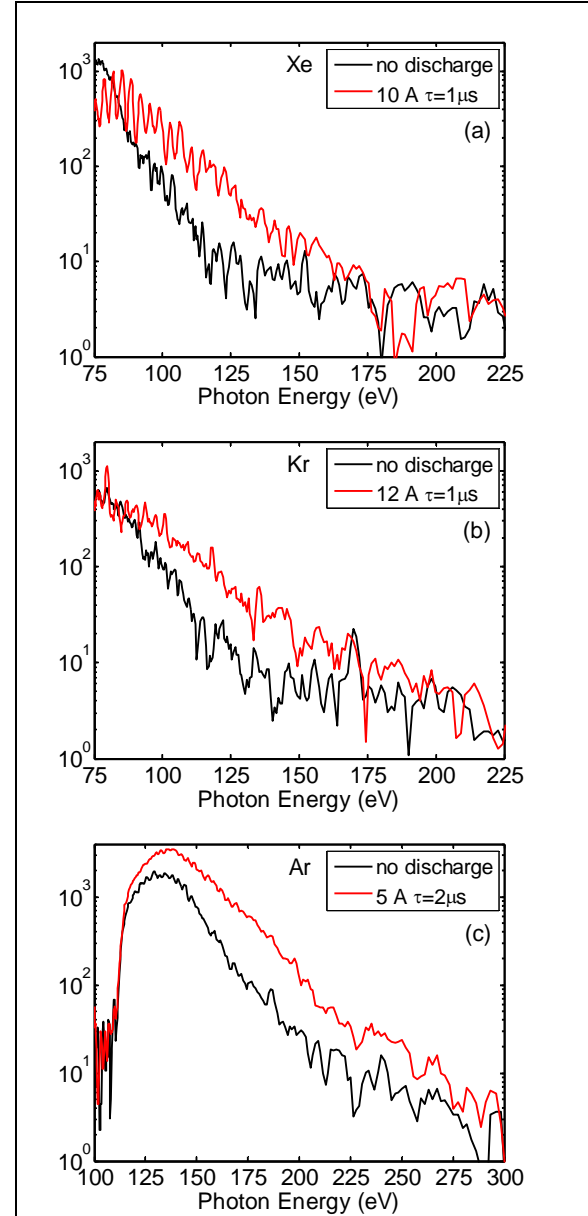


**Fig. 2.** High harmonic spectra from (a) Xe, (b) Kr, and (c) Ar plasmas showing the increased flux and higher photon energies made possible using the capillary discharge.

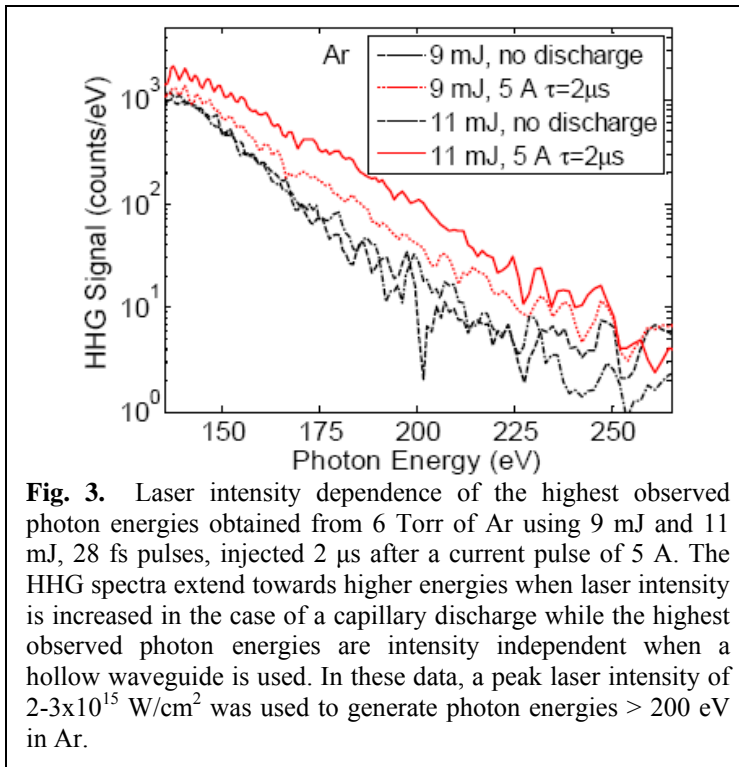


**Fig. 3.** Laser intensity dependence of the highest observed photon energies obtained from 6 Torr of Ar using 9 mJ and 11 mJ, 28 fs pulses, injected 2  $\mu$ s after a current pulse of 5 A. The HHG spectra extend towards higher energies when laser intensity is increased in the case of a capillary discharge while the highest observed photon energies are intensity independent when a hollow waveguide is used. In these data, a peak laser intensity of  $2-3 \times 10^{15}$  W/cm<sup>2</sup> was used to generate photon energies > 200 eV in Ar.

### Journal publications from DOE sponsored research 2005-2007

1. B.A. Reagan, T. Popmintchev, M.E. Grisham, D.M. Gaudiosi, M. Berrill, O. Cohen, B.C. Walker, M.M. Murnane, J.J. Rocca, and H.C. Kapteyn, "Enhanced High Harmonic Generation from Xe, Kr, and Ar in a Capillary Discharge", Physical Review A, , 013816, (2007)
2. D.M. Gaudiosi, B. Reagan, T. Popmintchev, M. Grisham, M. Berrill, O. Cohen, B.C. Walker, M.M. Murnane, H.C. Kapteyn, J.J. Rocca, "High-Order Harmonic Generation from Ions in a Capillary Discharge", Physical Review Letters, **96**, 203001 (2006).
3. J.J. Rocca, H.C Kapteyn, D.T. Attwood, M.M. Murnane, C.S. Menoni, and E. Anderson, "Tabletop Lasers in the Extreme Ultraviolet", (Invited) Optics & Photonics News, **17**, No. 11, pg. 30, (2006).
4. D. Gaudiosi, B. Reagan, T. Popmintchev, M. Grisham, M. Berrill, O. Cohen, B.C. Walker, M.M. Murnane, H.C. Kapteyn, and J.J. Rocca, "High Harmonic Generation from Ions in a Capillary Discharge Plasma Waveguide", Optics & Photonics News , **17**, No. 12, p. 44, (2006).
5. X. Zhang, A. L. Lytle, H. C. Kapteyn, M. M. Murnane, and O. Cohen, "Quasi Phase Matching and Quantum Path Control of High Harmonic Generation using Counterpropagating Light", Nature Physics **3**, 270 (2007).
6. M.A. Larotonda, Y. Wang, M. Berrill, B.M. Luther, J.J. Rocca, Mahendra Man Shakya, S. Gilbertson, and Zenghu Chang , "Pulse duration measurements of grazing incidence pumped high repetition rate Ni-like Ag and Cd transient soft x-ray lasers". Optics Letters, **31**, 3043, (2006).
7. Y. Wang, B.M. Luther, M. Berrill, M. Marconi, J.J. Rocca, "Capillary discharge-driven metal vapor plasma waveguides", Physical Review E, **72**, 026413, (2005)
8. S. Heinbuch, M. Grisham, D. Martz, and J.J. Rocca, "Demonstration of a desk-top size high repetition rate soft x-ray laser", Optics Express, **13**, 4050, (2005).

# Development and Characterization of Replicable Tabletop Ultrashort Pulse X-ray Sources

Christoph G. Rose-Petrucci

\* Department of Chemistry, Box H, Brown University, Providence, RI 02912  
phone: (401) 863-1533, fax: (401) 863-2594, [Christoph\\_Rose-Petrucci@brown.edu](mailto:Christoph_Rose-Petrucci@brown.edu)

## 1 Program Scope

The work focused on the engineering and characterization of laser-driven tabletop, ultrashort pulse, hard-x-ray sources with high brightness. Initially, ultrafast x-ray absorption spectroscopic measurements of a chemical process were done. Based on the experiences gained with these measurements, a new laser plasma source with integrated x-ray goniometer and camera holding arm was constructed with the specific goal to improve x-ray flux, lower the maintenance work, and improve the stability of the experiments. The new x-ray source has been designed for time-resolved x-ray absorption spectroscopy as well as imaging applications. This marks the first laser-driven plasma x-ray source that continuously recycles the target material, facilitating maintenance-free operation. As a consequence, this work lays the foundation for ultrafast x-ray sources that can operate as maintenance-free as conventional x-ray tubes.

The mercury target enables the generation of x-ray pulses with a full width at half maximum of a few tens of femtoseconds. The Hg source was subsequently used for in-line holographic imaging applications.

## 2 Recent Progress

The highlights of this project are listed below.

1. Ultrafast XAFS measurements of a chemical reaction using a laser plasma source
2. High x-ray flux ultrafast source with Hg-target and 5-kHz kilohertz repetition rate
3. PIC-MC simulations of 50-fs x-ray pulse emission from Hg targets
4. Propagation-based Differential Phase Contrast Imaging (PDPCI) of murine tissue and computer tomography with the Hg x-ray source
5. PDPCI formation in cylindrical symmetry systems

### 2.1 Ultrafast XAFS measurements of a chemical reaction using a laser plasma source

At the beginning of the funding period, ultrafast x-ray absorption fine structure (UXAFS) spectra were measured of a ligand substitution reaction of  $[\text{Fe}(\text{CN})_6]^{4-}$  in aqueous solutions. 400-nm laser pulse excitation this complex yields  $[\text{Fe}(\text{CN})_5\text{H}_2\text{O}]^{3-}$  through the reaction  $[\text{Fe}(\text{CN})_6]^{4-} + \text{hv}_{400\text{nm}} \rightarrow [\text{Fe}(\text{CN})_6]^{4-} + \text{H}_2\text{O} \rightarrow [\text{Fe}(\text{CN})_5\text{H}_2\text{O}]^{3-} + \text{CN}^-$ . This chemical process is accompanied by structural changes that are observable by UXAFS measurements. The spectra of solvated  $[\text{Fe}(\text{CN})_6]^{4-}$  at pump-probe delay times tens of picoseconds before and after photoexcitation have been measured. These data are, to my knowledge, the first ultrafast XAFS measurements of a chemical reaction have been performed using a laser plasma source. The results are in qualitative agreement with thermal iron-ligand elongations by several picometers.

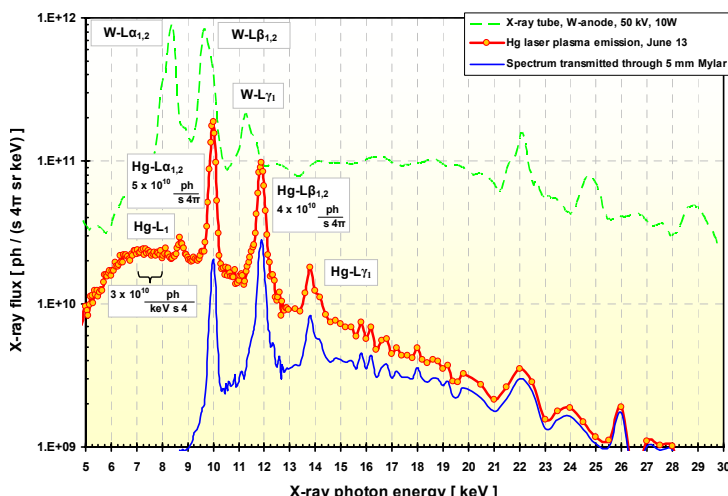


**Figure 1:** Absolutely calibrated x-ray emission spectrum from laser plasma source. For comparison the emission spectrum of a 10W x-ray tube with W-anode is shown. The lower line represents the approximate x-ray spectrum transmitted through the objects shown in Figure 2 and Figure 3.

### 2.2 High x-ray flux ultrafast source with Hg-target and 5-kHz kilohertz repetition rate

The constructed x-ray source is based on a liquid mercury target and operates over long periods at 5-kHz repetition rates with x-ray wavelengths in the range of

single Å and x-ray pulse durations that have been simulated to be 70 fs. The driving laser produces 40-fs laser pulse with an average power of 16-W on target. The liquid mercury is continuously recycled.

The x-ray emission spectrum of the source has been measured and is shown in Figure 1. The flux has been increased by one order of magnitude compared to the performance reported last year. The shown radiation has been generated with a 4%-prepulse 50ps before the main pulse. The current flux is the largest continuum-flux ever measured from a liquid target. The x-radiation was detected by direct exposure of the CCD-chip of a liquid-nitrogen cooled x-ray camera. The spectrum consists of continuum radiation and mercury L fluorescence lines. The emitted x-ray flux in the spectral range from 6.5 to 7.5 keV photon energy is  $3 \times 10^{10} \text{ ph} / (\text{s } 4\pi \text{ 1keV})$ . For comparison, a measured x-ray spectrum emitted from an x-ray tube with tungsten anode operated at 50 kV and 10 W electrical power is shown. The laser plasma source emission is equal to that of a tube operated at 30 kV acceleration voltage and 2.5 W power.

The horizontal and vertical diameters of the source were knife-edge measured as 38 μm x 13 μm (hor. x vert.). In summary, the x-ray flux was improved by a factor 20 compared to the average x-ray flux used for the measurements of the UXAFS spectra introduced above. The x-ray spot size, in particular in the vertical direction, is small. As a consequence, the source has significant spatial coherence, a feature that has been used for in-line holographic imaging shown below.

### 2.3 PIC-MC simulations of 50-fs x-ray pulse emission from Hg targets

The second major design consideration is the selection of the target material to enable the production of the shortest possible x-ray pulse for the chosen source geometry. We addressed this effect theoretically by carrying out particle-in-cell (PIC) simulations of the laser plasma interaction at a laser intensity on target of  $10^{17} \text{ W/cm}^2$ , 55-fs laser pulse length, and an incidence angle of 45 degrees in p-polarization. These are the approximate conditions during the measurements of the spectrum shown in Figure 1. The generated plasma electrons were propagated along the surface normal into the target using a Monte-Carlo (MC) code. The generated x-rays were propagated out of the target taking into consideration the x-ray absorption of the target material. The results of a calculation comparing the x-ray pulse properties using mercury and Copper targets are listed in Table 1. The fwhm of the calculated x-ray pulses is listed along with the pulse lengths at 90% of the pulse energy. The calculation predicts a substantially shorter x-ray pulse using a mercury target compared to a copper target under identical illumination and x-ray detection conditions. The fwhm of the pulses are on the order of the driving laser pulse lengths but have an emission “tail” that can be up to an order of magnitude longer, as illustrated by the 90% pulse length numbers. The remaining 10% of the pulse energy is emitted up to several picoseconds. The emission beyond the fwhm contains more than half of the x-ray flux yielding negative consequences for time resolution in ultrafast experiments. At the 90% level mercury produces pulse lengths with approximately half the temporal duration as copper.

### 2.4 Propagation-based Differential Phase Contrast Imaging (PDPCI) of murine tissue and computer tomography with the Hg x-ray source

Our laser-driven x-ray source produces significant x-ray flux with high brightness. The source's imaging performance is illustrated in Figure 2. An image of a mouse leg is shown in false color. While in this image absorption contributes to the image contrast, PDPCI features are visible at the interfaces of soft tissues as slight contrast enhancements. The sequence of images below shows the image of an excised mouse liver fixed in formaldehyde. The vascular tree is clearly visible. Contrast agent injections into the portal vein verified that the veins are imaged and not the arteries or bile ducts. To my knowledge, these images exhibit the highest resolution and contrast of the vasculature of any organ taken with any laboratory x-ray source to date. The smallest vessels have a diameter of about 10 μm, just a little larger than the diameter of red blood cells (6.6 - 7.5 μm). For illustration, properly scaled pictures of erythrocytes are pasted into the rightmost image. The vessels are phase-contrast highlighted which

Target material	X-ray energy keV	X-ray pulse		target dispersion	
		fwhm fs	90% length fs	fwhm fs	90% length fs
Hg	3 - 3.5	60	105	15	45
	7 - 7.5	70	230	20	200
	8 - 8.5	75	275	20	245
Cu	7 - 7.5	85	480	30	500
	8.05 (K <sub>a</sub> )	100	545	37	490

**Table 1:** Theoretical pulse lengths for continuum and K<sub>a</sub> x-radiation radiation emission; The calculations were carried out for orthogonal laser, target, and x-ray beam directions.

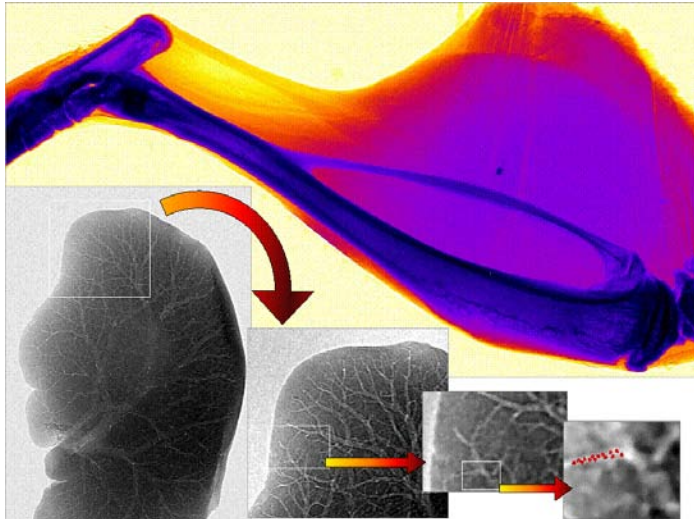


**Figure 2:** X-ray images measured with the laser plasma source. The upper section shows a mouse leg. The sequence of images on the bottom, are in-line holographic images of a mouse liver. The vascular tree in the liver is visible. The veins are “outlined” by dark PDPCI lines. The image on the very right shows veins with a diameter of approx. 20  $\mu\text{m}$  diameter. For scale comparison, pictures of blood cells are pasted into the image. Exposure time: 3 min / image

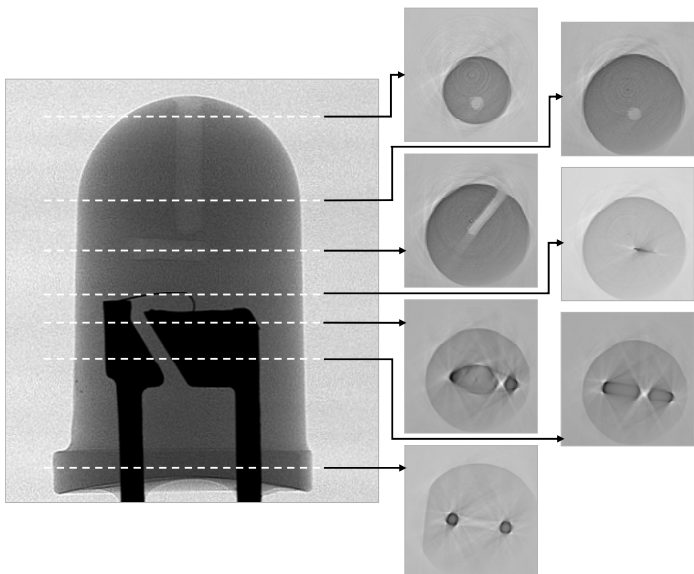


**Figure 3:** In-line holographic computer tomogram of a light emitting diode with drilled holes measured with the laser plasma source. Left: One of 360 images taken at 1° rotation angle intervals. The PDPCI features are visible at the surfaces of the plastic body.

Right: Computer reconstructions at various levels. PDPCI features are preserved in the reconstruction of the cross sections.

measurements of shockwaves induced with a laser beam that is co-propagating with the x-ray beam. The expressions for the image intensity were evaluated for cases where the magnification is greater than one. Figure 4 shows calculations for a sphere with perfect transparency assuming a point (top) and non-vanishing x-ray source (bottom). The fast oscillations of the interference fringes, even if they average out for a non-vanishing source, require that the numerical solution of the F-K integral is done with 100 significant figures. The calculation for a non-vanishing source are not a simple convolution of the results

enhances their visibility. The images were measured with a magnification of 3, a source-CCD camera (Princeton Instruments, PI-SCX, 4k x 4k, 1:1 fiber-coupled) distance of 1.5 m and an exposure time of 3 min, and a detected x-ray flux similar to the blue curve in Figure 1. The samples absorb all radiation below 10 keV resulting in a transmission of 20 - 30% of the radiation an effect called beam hardening. Thus, the image-forming x-rays are in the spectral range between 10 and 30 keV.

Figure 3 shows the, to my knowledge, first ever measured computer tomographic (CT) set of an object using a laser plasma x-ray source. 360 images at 1 degree steps were measured. The exposure time was 1 min. per image. The cross sections were subsequently reconstructed with a filtered back projection algorithm. PDPCI features are visible at the surfaces. These features are preserved in the tomographic reconstruction. Streak artifacts, in particular between the metal parts, are a consequence of beam hardening.

## 2.5 PDPCI formation in cylindrical symmetry systems

The intensity pattern produced by x-ray waves propagating from the plasma source through the object to the detector can be described by the Fresnel-Kirchhoff (F-K) integral. It can be used to calculate x-ray PDPCI images when the transmission function of the object is known. In two mostly theoretical papers we derived expressions for the image intensity for objects with axial symmetry and for an x-ray source with non-vanishing dimensions and a Gaussian intensity profile. This profile substantially simplifies the solution of the F-K integral and is simultaneously a good approximation for the laser plasma source. The solution for the F-K integral in cylindrical symmetry is, for instance, applicable, for laser pump - x-ray imaging

for a point source with a source function. For the size of our laser plasma source, the PDPCI modulation is 10%.

## 2.6 Future plans

The developed x-ray source is one of the brightest ultrafast laboratory x-ray sources in existence to date. Despite the fact that laser plasma sources (LPSs) are generally considered incoherent emitters, the source's brightness is high and permits time-resolved x-ray holographic measurements of condensed matter dynamics.

The focus of our planned work is to develop ultrafast, holographic x-ray imaging methods suitable for use with the liquid metal source and generally laser plasma x-ray sources. The methods will image structural dynamics and motions in materials using phase shifts imparted on the x-ray waves as they propagate through the material. The planned work seeks to directly observe, for instance, picosecond phonon wave packets, shock waves, or phonon solitons propagating in the bulk of materials.

Imaging of bulk materials relies on PDPCI (measuring the Laplacian of the real part of the index of refraction,  $n_r$ ) and Talbot Effect (TE) imaging (measuring the 1<sup>st</sup> spatial derivative of  $n_r$ ). No x-ray interferometers will be used. The sensitivity to of the measurements of, for instance, density variations is up to 1000 times larger than that of conventional x-ray absorption based imaging methods. Initial experiments will achieve spatial resolutions of several  $\mu\text{m}$ . However, the resolution in the range of several hundred nanometers should be possible at later stages of the research program.

## 3 References

1. "X-ray Phase Contrast Imaging: Transmission Functions Separable in Cylindrical Coordinates," G. Cao, T. Hamilton, C. M. Laperle, C. Rose-Petrucci and G. J. Diebold, *J. Am. Optical Soc. A*, subm. (2007).
2. "High-resolution angiography of murine livers and computed tomography with a laser-driven plasma x-ray source" B. Ahr, X. Li, C. M. Laperle, P. Wintermeyer, D. Shi, M. Anastasio, G. Diebold, J. R. Wands and C. Rose-Petrucci, *Appl. Phys. Lett.*, subm. (2007).
3. "Ultrafast x-ray generation from a liquid mercury target," C. Reich, C. M. Laperle, X. Li, B. Ahr, F. Benesch-Lee and C. G. Rose-Petrucci, *Optics Letters* 32 (4), 427 (2007).
4. "Ultrafast XAFS of transition metal complexes," T. Lee, C. Reich, C. M. Laperle, X. Li, M. Grant and C. G. Rose-Petrucci, in *Ultrafast Phenomena*, Vol. XV, edited by R.J.D. Miller, A.M. Weiner, P. Corkum, and D.M. Jonas (Springer Verlag, Berlin, 2006).
5. Ultrafast laser-pump x-ray probe measurements of solvated transition metal complexes; T. Lee, F. Benesch, C. Reich and C. G. Rose-Petrucci, Eds.; Elsevier: Washington, DC, 2005, pp 23
6. "Ultrafast table-top laser pump - x-ray probe measurement of solvated Fe(CN)<sub>6</sub><sup>4-</sup>," T. Lee, Y. Jiang, C. Rose-Petrucci and F. Benesch, *J. Chem. Phys.* 122 (8), 084506/1 (2005).
7. "Acoustically Modulated X-ray Phase Contrast and Vibration Potential Imaging," A. C. Beveridge, C. J. Bailat, T. J. Hamilton, S. Wang, C. Rose-Petrucci, V. E. Gusev and G. J. Diebold, in *Photons Plus Ultrasound: Imaging and Sensing 2005*, edited by A.A. Oraevsky and L.V. Wang (SPIE Publishing, Bellingham, WA, 2005), Vol. 5697, p. 90
8. "Acoustically Modulated X-ray Phase Contrast Imaging," T. Hamilton, C. J. Bailat, C. Rose-Petrucci and G. J. Diebold, *Physics in Medicine and Biology* 49, 4985 (2004).
9. "Acoustic radiation pressure: a "phase contrast" agent for x-ray phase contrast imaging," C. J. Bailat, T. Hamilton, C. Rose-Petrucci and G. J. Diebold, *Applied Physics Letters* 85 (19), 4517 (2004).

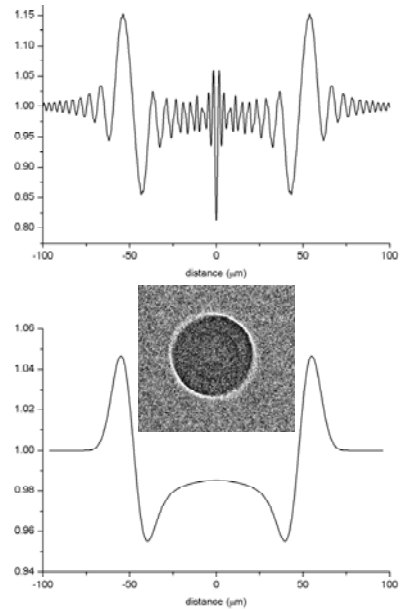


**Figure 4:** Top: Intensity versus radial coordinate calculated for a 100- $\mu\text{m}$  diameter polystyrene sphere, with  $\delta = 10^{-6}$ , no absorption, irradiated by a point source of x-radiation. The source-to-object and object-to-image planes used in all of the calculations were 0.2 m 2.4 m, respectively. For numerical reasons the x-ray photon energy is 1.7 k eV. Bottom: Same calculation but with a Gaussian x-ray source ( $\sigma = 6.75 \mu\text{m}$ ). Inserted image 100- $\mu\text{m}$  diameter polystyrene sphere imaged with an x-ray spectrum centered at 45 keV.

# New Directions in Intense-Laser Alignment

Tamar Seideman

Department of Chemistry, Northwestern University

2145 Sheridan Road, Evanston, IL 60208-3113, t-seideman@northwestern.edu

## 1. Program Scope

Nonadiabatic molecular alignment by short, moderately-intense pulses has been the topic of rapidly growing activity during the past few years. This activity owes both to the fascinating fundamental physics associated with rotational wavepacket dynamics and to a variety of already demonstrated and projected applications in fields ranging from molecular spectroscopy and laser optics through reaction dynamics and stereochemistry, to quantum storage and information processing.<sup>5</sup> In this approach, a moderately intense laser pulse of duration short with respect to the rotational periods aligns a given molecular axis (axes) to the field polarization vector(s). Nonadiabaticity (rapid turn-off as compared to the system time scales) guarantees that the alignment will survive subsequent to the pulse turn-off, under field-free conditions.

The main goal of our DOE-sponsored research has been to extend the concept of nonadiabatic alignment from the domain of isolated diatomic molecules to complex systems, including large polyatomic molecules, solvated molecules, and molecular assembly. Work toward this goal during the past year includes the extension of alignment to control the torsions of molecules,<sup>1</sup> the application of torsional control to manipulate and to better understand charge transfer events in solutions, the development of an approach to 3D alignment and controlled spinning of molecules, and the extension of alignment to guide the assembly of molecules, hence producing molecular devices with long range orientational order.

In related research within the nonadiabatic alignment theme, inspired by experimental research of AMOS colleagues, we developed a theoretical framework for the calculation of HHG spectra from nonadiabatically aligned molecules<sup>2</sup> that goes beyond several approximations of the previous model. In particular, by accounting exactly for rotations, our theory illustrates the origin of the time-dependencies of the harmonic spectra found in all experiments. It also points to the information content of harmonic spectra regarding the rotational wavepacket dynamics.

## 2. Recent Progress

We begin (Secs. 2.1–2.2) with recent progress on the nonadiabatic dynamics of diatomic molecules in complex environments, proceed with alignment of isolated large polyatomic systems (Secs. 2.3–2.4) and conclude (Secs. 2.5–2.6) with the challenges offered by complex systems in condensed phases.

### 2.1 *Optimal control theory of alignment in dissipative media*

In Ref. 4 and in related ongoing research, we apply a density matrix variation of optimal control theory to the problem of molecular alignment in dense environments. One goal of this research is to use rotational coherences as a model, to explore more general questions in coherent control in dissipative environments. A second goal is to apply optimal control as a coherence spectroscopy, to gain new insights into the dissipative properties of the medium. A third is to time the post-pulse (field-free) alignment to a specific instance while controlling also its duration. Last, we attempt to construct superposition states that would live long in a gas cell environment, as required, for instance, for quantum information applications.

## ***2.2 On the information content of high harmonics generated from aligned molecules***

In Ref. 2 we derive an expression for the harmonic signal from nonadiabatically-aligned molecules, accounting for both electronic and rotational motions, and identify a single approximation, which converts the expression into a physically transparent and computationally convenient form. Our analytical result gives explicitly the time dependence of the harmonic spectra, thus explaining the observations of the complete set of published experiments. Moreover, it points to new opportunities for generating insights into the structure and dynamics of molecular systems through harmonic generation experiments from aligned molecules. This includes information regarding the rotational and electronic dynamics of isolated systems, as well as regarding the decoherence and relaxation in molecules subject to a dissipative environment.

## ***2.3 The revival structure of asymmetric tops***

Our effort in the area of nonadiabatic alignment of large isolated polyatomics has focused on two objectives: (1) the development of theory and numerical approaches to address the problem of alignment and 3D alignment of complex structures subject to an arbitrary combination of differently polarized fields, and (2) the application of the theory in collaborative research with an experimental group (H. Stapelfeldt and coworkers, University of Aarhus, Denmark) to explore new phenomena in the alignment dynamics of complex molecules. The second item is related to the first, as it requires a theory and a numerical implementation that can handle the massive molecules that experiments can efficiently align and probe in a nonperturbative, fully quantum mechanical fashion. A review of our theory and numerical methods is given in Ref. 5.

In Ref. 3 we were able for the first time to make quantitative comparison of numerical and experimental results for a nonlinear molecule. This work illustrates an interesting intensity effect that was previously seen in our numerical work but was not observed before. In the low temperature limit, the revival spectra exhibit a detailed quantum mechanical structure, which is qualitatively different for asymmetric tops compared to symmetric or linear tops, and is rapidly washed out by rotational temperature. With increasing fluence, the structure gradually simplifies, illustrating a transformation of the complex “wobbling” of asymmetric top molecules into a simple, nearly separable, rotation about the molecular axis.

The problem of optimizing the alignment is addressed through collaborative experimental-theoretical research in Ref. 7, where we study the alignment dynamics of polyatomic molecules subject to two temporally overlapping nonresonant laser pulses. We illustrate the advantage of combining a long (compared to the molecular rotational periods) with a short pulse, theoretically, numerically and experimentally. In particular, significant enhancement of the alignment attainable under nondestructive conditions is predicted and found.

## ***2.4 Toward controlled rotations in polyatomics. Holding and spinning molecules in space***

In a recent extension of nonadiabatic alignment, we collaborate with an experimental group to develop an approach to 3D nonadiabatic alignment and controlled rotations in polyatomic molecules. Our approach applies two linearly and orthogonally polarized laser pulses, one long and one short with respect to the molecular rotational periods. The long pulse tightly aligns the most polarizable molecular axis along its polarization vector. The subsequent short pulse sets the molecule into coherent revolution about the arrested molecular axis. Our results show that the long pulse constructs a tightly aligned eigenstate of the complete Hamiltonian in the presence of the long pulse field. The short pulse excites this state into a coherent wavepacket of helicity states that

subsequently exhibits a revival pattern at a period characterizing the field-free rotational motion. By populating a very broad rotational wavepacket with the long pulse, we are able to near the classical limit of a rigid body held fixed in space and controllably spined about its axis.

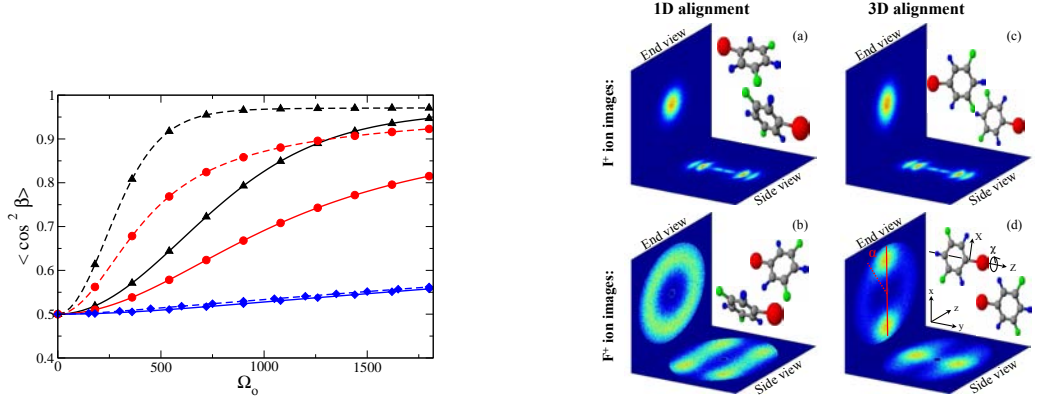


FIG. 1: Beyond nonadiabatic alignment. Left: Torsional alignment vs the interaction parameter  $\Omega_0 = 0.16 (\Delta\alpha/B) I_0$  at a temperature of  $T = 30$  K (dashed curves) and  $T = 77$  K (solid curves). The field-free torsional potential is  $V_{\text{tor}}(\beta) = V_0(1 - \cos(4\beta - \pi))$  (diamonds);  $V_{\text{tor}}(\beta) = 0$  (circles); and  $V_{\text{tor}}(\beta) = V_0(1 - \cos(4\beta))$  (triangles) with a barrier  $2V_0 = 62$  meV<sup>1</sup> (Sec. 2.5). Right: Holding and spinning molecules in free space. Application to 3,5 difluoriodobenzene (Sec. 2.4).

## 2.5 Torsional alignment. Application to molecular switches

In recent and ongoing research we extend the concepts of alignment and 3D alignment from a means of controlling solely the overall rotations of molecules with respect to the space-fixed axes, to a means of simultaneously controlling also their torsional motions.<sup>1</sup> In particular, we illustrate numerically the application of circularly or elliptically polarized pulses to eliminate the torsional motions of polyatomic systems while hindering their overall rotations in space. The approach is applied to control of charge transfer reactions in solution with a view to making a new form of molecular switches. As a simple example, we consider torsional control and manipulation of a charge transfer event in donor-acceptor biphenyls.

## 2.6 Guided molecular assembly. Making constructs with long range orientational order

The orientational order of molecular mono- or multi-layers at a solid or liquid surface determines not only the mechanical and structural properties of the thin film, but also its electric, magnetic and optical properties. Consequently, the combination of translational and orientational order forms an important challenge to different areas of science and technology, including controlled crystallography, structural determination of biological molecules, understanding of organic interfaces, development of advanced materials, and fabrication of molecular electronics with desired properties.

The extension of laser alignment to guided molecular assembly has been a major goal of this research program for several years, but is a nontrivial task, both numerically and experimentally. A first step toward this goal is made in a submitted publication, where we use moderately intense laser pulses to induce alignment of poly-benzyl-L-glutamate (PBLG) molecules during their self-assembly process on a water surface. Our work is carried out in collaboration with an experimental group at the Weizmann Institute of Science (Israel). We find alignment extending to a sub-millimeter scale, limited in size by the alignment laser dimension.

## 3. Future Plans

**3.1** Our research on the problem of HHG from nonadiabatically-aligned molecules (Sec. 2.2) will be extended in several ways. We will apply the theory developed in Ref. 2 in collaborative

research with the group of Kapteyn and Murnane to explore questions raised by recent and ongoing experiments. We will extend the theory from the case of linear molecules subject to co-linearly polarized fields to the case of a general polyatomic subject to a combination of alignment and ionizing pulses of arbitrary polarizations. We will implement a fully quantum mechanical approach for description of the electronic motions, that will go beyond the strong field approximation employed in our previous work.<sup>2</sup> Using HHG spectra from aligned polyatomics, we expect to gain new insights into rotational coherences, rotational dissipation and the dynamics of classically chaotic motions.

**3.2** Our work on torsional control in general, and its application to charge transfer reactions in particular<sup>1</sup> (Sec. 2.4) will be continued, as current experimental interest in realizing this scheme offers new questions for theoretical research. The concept will be extended from the static (long-pulse-induced, adiabatic alignment) domain to the case of short pulses, where the alignment dynamically entangles with the charge transfer and new opportunities arise, both for analyzing and for controlling charge transfer events.

**3.3** Our work on guided molecular assembly (Sec. 2.6) will continue along two routes. First, we will improve our numerical approach to make reliable predictions of the intramolecular forces involved for different molecules of experimental interest. Second, we will continue collaborative research with our experimental coworkers to design improved set-ups for study of different assembly problems. The experimental research will be carried out in Stapelfeldt's laboratory in Aarhus.

**3.4** Nonadiabatic orientation will be used as the first step in two coherent control studies. One study considers ignition of electronic toroidal ring current around an oriented linear molecule. The second uses orientation for selective bond-breaking in polyatomic molecules. Both projects have been recently initiated.

#### 4. Published and accepted articles from DOE sponsored research, 07/04–07/07

1. S. Ramakrishna and T. Seideman, *On the Information Content of High Harmonics Generated from Aligned Molecules*, Phys. Rev. Lett. in press.
2. S. Ramakrishna and T. Seideman, *Torsional Alignment by Intense Pulses*, Phys. Rev. Lett. in press.
3. L. Holmegaard, V. Kumarappan, S. S. Viftrup, C. Z. Bisgaard, H. Stapelfeldt, E. Hamilton and T. Seideman, *Control of Rotational Wavepacket Dynamics in Asymmetric Top Molecules*, Phys. Rev. A in press.
4. A. Pelzer, S. Ramakrishna and T. Seideman, *Optimal Control of Molecular Alignment in Dissipative Media*, J. Chem. Phys. **126**, 034503 (2007).
5. T. Seideman and E. Hamilton, *Nonadiabatic Alignment by Intense Pulses. Concepts, Theory, and Directions*, Ad. At. Mol. Opt. Phys. **52**, **52**, 289 (2006) (**invited**).
6. N. Moiseyev and T. Seideman, *Alignment of Molecules by Lasers: Derivation of the Hamiltonian within the (t,t') Formalism*, J. Phys. B: At. Mol. Opt. Phys. **39** L211 (2006).
7. M.D. Poulsen, T. Ejdrup, H. Stapelfeldt, E. Hamilton and T. Seideman, *Alignment Enhancement by the Combination of a Short and a Long Laser Pulse*, Phys. Rev. A **73**, 033405 (2006).
8. S. Ramakrishna and T. Seideman, *Dissipative Dynamics of Laser Induced Nonadiabatic Molecular Alignment*, J. Chem. Phys. **124**, 034101 (2006).
9. E. Hamilton, T. Seideman, T. Ejdrup, M.D. Poulsen, C.Z. Bisgaard, S. S. Viftrup and H. Stapelfeldt, *Alignment of Symmetric Top Molecules by Short Laser Pulses*, Phys. Rev. A, **72**, 043402 (2005).
10. S. Ramakrishna and T. Seideman, *Intense Laser Alignment in Dissipative Media as a Route to Solvent Properties*, Phys. Rev. Lett. **95**, 113001 (2005).
11. E. Péronne, M.D. Poulsen, H. Stapelfeldt, C.Z. Bisgaard, E. Hamilton, and T. Seideman, *Nonadiabatic Laser Induced Alignment of Iodobenzene Molecules*, Phys. Rev. A **70**, 063410 (2004).
12. M.D. Poulsen, E. Peronne, C.Z. Bisgaard, H. Stapelfeldt E. Hamilton and T. Seideman, *Revivals of Nonadiabatic Alignment of Asymmetric Top Molecules*, J. Chem. Phys. **121**, 783 (2004).

# Ro-vibrational Relaxation Dynamics of PbF Molecules

Neil Shafer-Ray, Greg Hall, and Trevor Sears  
shafer@physics.ou.edu, gehall@bnl.gov, sears@bnl.gov

## Program Scope

In 1950 Purcell and Ramsey suggested that the electron might have a CP-violating electric dipole moment (EDM) proportional to its spin angular momentum[1]. This possibility initiated an ongoing hunt for the e-EDM. This hunt has been spurred on by the recognition of the importance of CP-violation to the formation of a matter-dominated universe[2] as well as by the marked difference in the prediction of the magnitude of the e-EDM by Supersymmetry[3] and the Standard Model[4].

The current limit on the e-EDM is  $1.6 \times 10^{-27}$ e·cm as determined in a Ramsey beam resonance study of the Tl atom[5]. The PbF molecule provides a unique opportunity to search for an even smaller moment. The molecule's odd electron, heavy mass, and large internal field combine to give it an intrinsic sensitivity to an e-EDM that is over three orders of magnitude bigger than that of the Tl atom[6]. In addition to this increased intrinsic sensitivity, the ground state of the PbF molecule allows for a "magic" electric field at which the magnetic moment vanishes[7]. All of these advantages create an opportunity to significantly lower the current limit on the e-EDM. These advantages can only be realized if an intense source of ground-state PbF molecules can be created. The scope of this project is to (1) create a rotationally cold molecular beam source of PbF, (2) achieve a continuous ionization scheme for sensitive state selective detection of the PbF molecule.

## Recent Progress

Previous workers have created the PbF molecule by cracking PbF<sub>2</sub>[8–12], by reaction of fluorine with lead[13–16], and by the reaction of NF<sub>3</sub> with lead in a continuous discharge[17]. We have discovered that the reaction of molten lead with MgF<sub>2</sub> leads to the efficient production of PbF. Our reactor source is shown in Fig 1. It consists of a nozzle constructed from MgF<sub>2</sub>. Inside this nozzle is a small removable vessel in which lead pellet is placed. When the nozzle is heated to temperatures above 900°C, the reaction of this lead with the MgF<sub>2</sub> vessel creates PbF. An inert buffer gas is used to carry this PbF product into the vacuum chamber. The yield of PbF created in this way is comparable to the production we achieved using a Pb+F<sub>2</sub> flow reactor. The MgF<sub>2</sub> reactor has the advantage of both simplicity and stability.

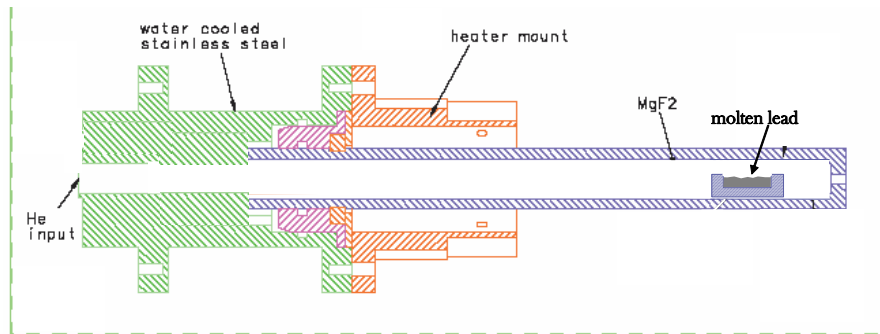


Figure 1: Pb+MgF<sub>2</sub> reactor.

Because of the weak intensity of our PbF source as compared to an atomic beam source, it is desirable to choose an extremely sensitive detection scheme. Our first attempt at such a scheme was 1+1 ionization of the molecule via the B-state of PbF[18]. Unfortunately, the short lifetime of the B-state made rotational-state-resolution impossible. Despite the failure of this strategy for state-selective detection, we were able to use this 1+1 ionization scheme to determine the ionization potential of the molecule.

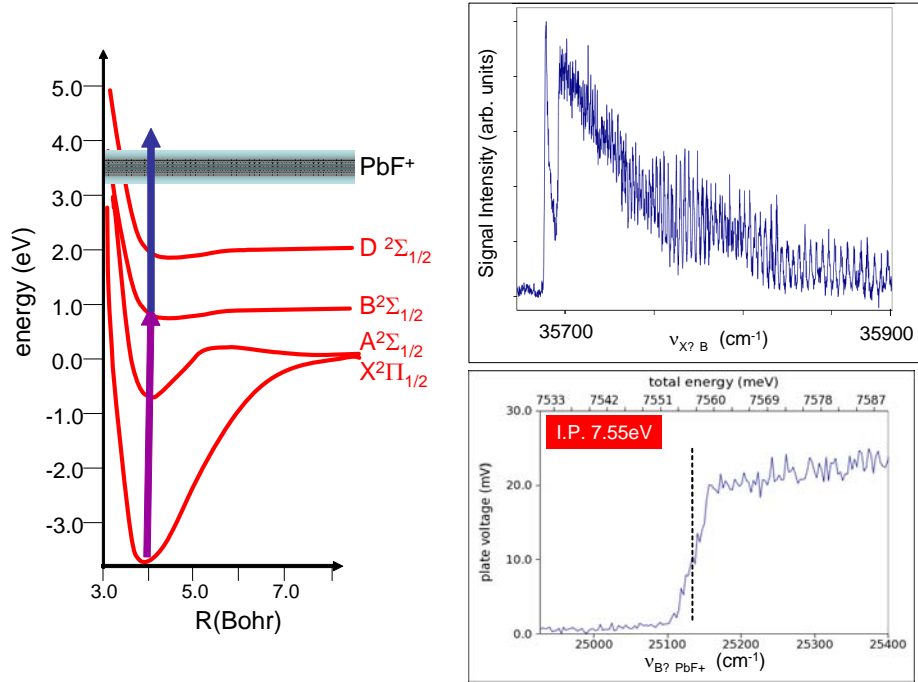


Figure 2: 1+1 REMPI of PbF via the X-B transition

After B-state ionization proved an ineffective tool for state selective detection, we developed the ionization scheme shown in Figure 3. The scheme is doubly resonant, requiring three sources of laser radiation. The first laser is used to drive the  $X \rightarrow A$  transition at 436.7 nm. The second laser, at 476.7 nm, is used to drive the  $A \rightarrow D$  transition that we have begun to characterize. The third source of laser radiation is a frequency doubled Nd:YAG laser that drives the D state to ionization. To attempt to characterize the vibrational structure of the D state, we fixed the frequency of laser radiation driving the  $X \rightarrow A$  transition to the Q-branch pile up at  $22897\text{cm}^{-1}$  and scanned the laser driving the  $A \rightarrow D$  transition. The resulting vibrational structure is irregularly spaced and difficult to interpret. A second vibrational level, centered at 442.2 nm, shows similar rotational structure as does the transition at 476.7 nm whereas vibrational bands at 455 nm and 463 nm show no rotational

structure indicating a very short D-state lifetime.

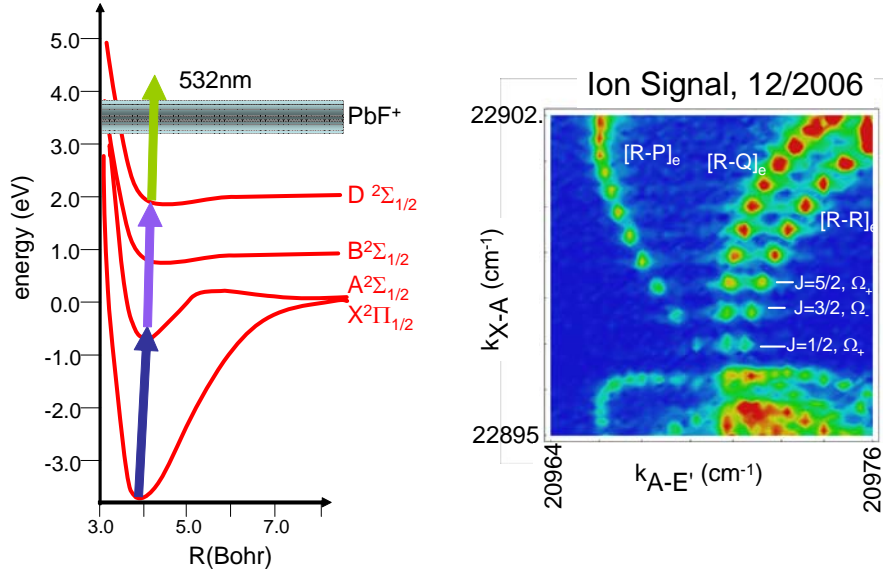


Figure 3: 1+1+1 REMPI of PbF via the  $X \rightarrow A$  and  $A \rightarrow D$  transitions.

### Future Plans

In our present set up, the rotational state distribution of the PbF molecules entering our vacuum system is hot, with only 1 molecule in  $10^4$  in the ground state. Because only the ground state of the molecule is useful to an e-EDM measurement, it is important to gain back this loss in population. We have already observed that when Neon is used as a carrier gas, the population of ground-state PbF is enhanced by a factor of two, whereas the backing pressure of He has little affect on the rotational state distribution. When the heavier noble gasses (namely Ar, Kr, and Xe) are used, the ground state of PbF is diminished, presumably because of the loss due clustering of the radical with the inert gas. We have begun construction of a new pumping system that will allow us to create a true supersonic molecular beam. When this machine is completed, we will be able to determine if Neon can be used to rotational cool the PbF molecule.

We are also working to improve our detection scheme. Our current laser system operates at just 10 Hz, creating a detection duty cycle of  $10^{-5}$ . This five-order-of-magnitude loss in sensitivity is not acceptable for an e-EDM experiment. To remedy this problem, we plan to implement a continuous or pseudo-continuous source of laser radiation in order to drive the  $X \rightarrow A$ ,  $A \rightarrow D$ , and  $D \rightarrow PbF^+$  transitions. We have carried out saturation curves on each of the three transitions and the lifetime of the D state has been measured. We are now in the process of engineering an optical bench in order to state-selectively ionize a large fraction of the PbF molecules entering the focussed waist of cw and pseudo-cw laser radiation.

---

[1] E. Purcell and N. Ramsey, Phys Rev **78**, 807 (1950).

[2] Sakharov, JETP Lett **5**, 24 (1967).

- [3] R. Arnowitt, B. Dutta, and Y. Santoso, Phys. Rev. D **64**, 113010 (2001).
- [4] F. Hoogeveen, Nuclear Physics **B341**, 322 (1990).
- [5] B. Regan, E. D. Commins, C. J. Schmidt, and D. DeMille, Physical Review Letters **88**, 71805 (2002).
- [6] M. Kozlov, V. Fomichev, Y. Y. Dmitriev, L. Labzovsky, and A. Titov, J. Phys. B: At. Mol. Opt. Phys. **20**, 4939 (1987).
- [7] N. Shafer-Ray, Physical Review A **73**, 34102 (2006).
- [8] Rochester, Proc. R. Soc. London A **153**, 407 (1936).
- [9] F. Morgan, **49**, 47 (1936).
- [10] R. Barrow, D. Butler, J. Johns, and J. Powell, Proceedings of the Physical Society of London **73**, 317 (1958).
- [11] S. Singh, Indian J. of Pure Appl. Phys. **5**, 292 (1967).
- [12] D. Lumley and R. Barrow, Journal of Physics B **10**, 1537 (1977).
- [13] C. Dickson and R. Zare, Optica Pura y Aplicada **10**, 157 (1977).
- [14] R. Green, L. Hanko, and S. Davis, Chemical Physics Letters **64**, 461 (1977).
- [15] F. Melen and I. Dubois, Journal of Molecular Spectroscopy **124**, 476 (1987).
- [16] J. Chen and P. Dagdigian, J Chem Phys **96**, 1030 (1992).
- [17] K. Ziebarth, K. Setzer, O. Shestakov, and E. Fink, Journal of Molecular Spectroscopy **191**, 108 (1998).
- [18] C. McRaven, S. Poopalsingham, and N. Shafer-Ray, Physical Review A **75**, 024502 (2007).

## Recent Publications

1. N.E. Shafer-Ray, *Possibility of zero-g-factor paramagnetic molecules for the measurement of the electron's electric dipole moment*, Phys. Rev. A, **73**, 034102 (2006.)
2. C. McRaven, P. Sivakumar, N.E. Shafer-Ray, *Multi-photon ionization of lead monofluoride resonantly enhanced by the  $X_1^2\Pi_{1/2} \rightarrow B^2\Sigma_{1/2}$  transition*, Phys. Rev. A. **75** 023502 (2007.)

(The publications here are relevant publications in the last two years, but are not the result of DOE funded research.)

# DYNAMICS OF FEW-BODY ATOMIC PROCESSES

**Anthony F. Starace**

*The University of Nebraska  
Department of Physics and Astronomy  
116 Brace Laboratory  
Lincoln, NE 68588-0111*

*Email: astarace1@unl.edu*

## PROGRAM SCOPE

The goals of this project are to understand and describe processes involving energy transfers from electromagnetic radiation to matter as well as the dynamics of interacting few-body, quantum systems. Investigations of current interest are in the areas of high energy density physics, attosecond physics, strong field physics, and double photoionization processes. In some cases our studies are supportive of and/or have been stimulated by experimental work carried out by other investigators funded by the DOE AMO physics program.

## RECENT PROGRESS

### A. GeV Electrons from Ultra Intense Laser Interactions with Highly Charged Ions

We have investigated in great detail recently [9] the interaction of intense laser radiation with highly charged hydrogenic ions using a three-dimensional relativistic Monte Carlo simulation. This work extended an earlier investigation [S.X. Hu and A.F. Starace, *Phys. Rev. Lett.* **88**, 245003 (2002)] in which it was demonstrated that free electrons cannot be accelerated to GeV energies by the highest intensity lasers because they are quickly expelled from the laser pulse before it reaches peak intensity. We showed that highly charged ions exist that (1) have deep enough potential wells that tunneling ionization is insignificant over the duration of an intense, short laser pulse, and (2) have potentials that are not too deep, so that the laser pulse is still able to ionize the bound electron when the laser field reaches its peak intensity. We showed that when the ionized electron experiences the peak intensity of the laser field, then it is accelerated to relativistic velocity along the laser propagation direction (by the Lorentz force) within a tiny fraction of a laser cycle. Within its rest frame it then “rides” on the peak laser amplitude and is accelerated to GeV energies before being expelled from the laser pulse. Our recent work [9] includes an extensive set of calculations to demonstrate the dependence of the ionized electron energy spectrum on the experimentally controllable parameters. These include the target ion species and the laser intensity, frequency, duration, and, especially, the laser focal properties.

## **B. Photodetachment of H<sup>-</sup> by a Short Laser Pulse in Crossed Static Electric and Magnetic Fields**

We have carried out a detailed quantum mechanical treatment of the photodetachment of H<sup>-</sup> by a short laser pulse in the presence of crossed static electric and magnetic fields [10]. An exact analytic formula is presented for the final state electron wave function (describing an electron in both static electric and magnetic fields and a short laser pulse of arbitrary intensity). In the limit of a weak laser pulse, final state electron wave packet motion is examined and related to the closed classical electron orbits in crossed static fields predicted by Peters and Delos [*Phys. Rev. A* **47**, 3020 (1993)]. Owing to these closed orbit trajectories, we show that the detachment probability can be modulated, depending on the time delay between two laser pulses and their relative phase, thereby providing a means to partially control the photodetachment process. In the limit of a long, weak pulse (i.e., a monochromatic radiation field) our results reduce to those of others; however, for this case we analyze the photodetachment cross section numerically over a much larger range of electron kinetic energy (i.e., up to 500 cm<sup>-1</sup>) than in previous studies and relate the detailed structures both analytically and numerically to the above-mentioned, closed classical periodic orbits.

## **C. Elliptic and Circular Dichroism in Two-Photon Double Ionization of Atoms**

Recent advances in generating XUV light of higher intensity than provided by synchrotrons make possible studies of multi-electron ejection due to multiphoton interactions of atomic electrons with XUV radiation. Two-photon double ionization (TPDI) of He has recently attracted much attention, as its study provides new insights into two-electron ejection dynamics. However, so far all studies of TPDI have been limited to the case of linearly polarized light. Over the past two years, we have investigated how the shape of the photoelectron angular distribution in TPDI [i.e., of the triply-differential cross section (TDCS)] depends upon the handedness of elliptically-polarized XUV radiation. We have derived [11] an *ab initio* parametrization of the two-photon double ionization amplitude from an s<sup>2</sup> subshell of an atom in a <sup>1</sup>S-state and used it to predict two light polarization effects on photoelectron angular distributions that do not exist in single-photon double ionization: (i) elliptic dichroism and (ii) circular dichroism at equal energy sharing. Our estimates for He show significant magnitudes for these effects, which provide a means for polarization control of double ionization by XUV light.

## **D. CWDVR Method for Atomic Systems in Short Laser Pulse Fields**

We have developed an efficient and accurate grid method for solving the time-dependent Schrödinger equation for an atomic system interacting with an intense laser pulse [12]. Instead of the usual finite difference (FD) method, the radial coordinate is discretized using the discrete variable representation (DVR) constructed from Coulomb wave functions. For an accurate description of the ionization dynamics of atomic systems, we have found that the Coulomb wave function discrete variable representation (CWDVR) method needs 3-10 times fewer grid points than the FD method owing to the fact that the CWDVR grid points are distributed unevenly but more effectively. The other important advantage of the CWDVR method is that it treats the Coulomb singularity accurately and gives a good representation of continuum wave functions. The time propagation of the wave function is implemented using the well-known Arnoldi

method. We have tested the method for treating multiphoton ionization of both the  $H$  atom and the  $H^-$  ion in intense laser fields. The short-time excitation and ionization dynamics of  $H$  interacting with an abruptly introduced static electric field has also been investigated. For a wide range of field parameters, ionization rates calculated using the CWDVR method are found to be in excellent agreement with those of other accurate theoretical calculations.

### **E. Attosecond Pulse Carrier-Envelope-Phase Effects on Ionized Electron Momentum and Energy Distributions**

Recently, we have analyzed carrier-envelope-phase (CEP) effects on electron wave packet momentum and energy spectra produced by one or two few-cycle attosecond XUV pulses. The few-cycle attosecond pulses are assumed to have arbitrary phases. We predict CEP effects on ionized electron wave packet momentum distributions produced by attosecond pulses having durations comparable to those obtained by G. Sansone et al. [Science **314**, 443 (2006)]. The onset of significant CEP effects is predicted to occur for attosecond pulse field strengths close to those possible with current experimental capabilities. Our results are based on single-active-electron solutions of the three-dimensional, time-dependent Schrödinger equation including atomic potentials appropriate for the H and He atoms. A manuscript on these results has been submitted to *Physical Review A*.

### **F. Resonant and Threshold-Related Enhancements of Plateaus in Laser-Assisted Electron-Atom Scattering**

We have recently developed a time-dependent effective range theory (TDER) that combines the well-known effective range theory (for electrons interacting with a short-range potential) and the equally well-known Floquet theory (for atomic systems interacting with a monochromatic laser field) to give an essentially exact account of laser-assisted, electron-atom scattering (LAES) processes. Our initial focus has been the study of threshold-related and resonant enhancements in LAES spectra. The former correspond to known threshold phenomena that occur at the closing of a multiphoton ionization channel, while the latter correspond to virtual attachment of the incident electron to the target atom. We find that resonant and threshold-related enhancements in LAES cross sections corresponding to absorption of  $n$  laser photons can modify strong field LAES plateau features by orders of magnitude. Numerical results for e - H and e - F scattering have been investigated thus far. Our initial results have been presented at the 2007 Freiburg ICPEAC meeting.

## **FUTURE PLANS**

Our group is currently carrying out research on the following additional projects: (1) Analysis of few-cycle XUV attosecond pulse carrier-envelope-phase effects on ionized electron momentum and energy distributions in the presence of a few-femtosecond IR laser pulse; (2) Modelling of XUV attosecond pulse ionization plus excitation processes in He.

## PUBLICATIONS STEMMING FROM DOE-SPONSORED RESEARCH (2004 – 2007)

- [1] A.Y. Istomin, N.L. Manakov, and A.F. Starace, “Perturbative Analysis of the Triply Differential Cross Section and Circular Dichroism in Photo Double Ionization of He,” Phys. Rev. A **69**, 032713 (2004).
- [2] A.Y. Istomin, N.L. Manakov, A.V. Meremianin, and A.F. Starace, “Non-Dipole Effects in Photo Double Ionization of He by a VUV Photon,” Phys. Rev. Lett. **92**, 063002 (2004).
- [3] A.Y. Istomin, N.L. Manakov, A.V. Meremianin, and A.F. Starace, “Circular Dichroism at Equal Energy Sharing in Photo Double Ionization of He,” Phys. Rev. A **70**, 010702(R) (2004).
- [4] A.V. Flegel, M.V. Frolov, N.L. Manakov, and A.F. Starace, “Circularly Polarized Laser Field-Induced Rescattering Plateaus in Electron-Atom Scattering,” Phys. Lett. A **334**, 197 (2005).
- [5] A.Y. Istomin, N.L. Manakov, A.V. Meremianin, and A.F. Starace, “Nondipole Effects in the Triply-Differential Cross Section for Double Photoionization of He,” Phys. Rev. A **71**, 052702 (2005).
- [6] A.Y. Istomin, A.F. Starace, N.L. Manakov, A.V. Meremianin, A.S. Kheifets, and I. Gray, “Parametrizations and Dynamical Analysis of Angle-Integrated Cross Sections for Double Photoionization Including Nondipole Effects,” Phys. Rev. A **72**, 052708 (2005).
- [7] A.Y. Istomin, N.L. Manakov, A.V. Meremianin, and A.F. Starace, “ Non-Dipole Effects in Double Photoionization of He,” in *Ionization, Correlation, and Polarization in Atomic Collisions*, ed. A. Lahmam-Bennani and B. Lohmann (A.I.P., Melville, NY, 2006), pp. 18-23.
- [8] A.Y. Istomin, A.F. Starace, N.L. Manakov, A.V. Meremianin, A.S. Kheifets, and I. Bray, “Nondipole Effects in Double Photoionization of He at 450 eV Excess Energy,” J. Phys. B **39**, L35 (2006).
- [9] S.X. Hu and A.F. Starace, “Laser Acceleration of Electrons to GeV Energies Using Highly Charged Ions,” Phys. Rev. E **73**, 066502 (2006).
- [10] L.Y. Peng, Q. Wang, and A.F. Starace, “Photodetachment of H<sup>-</sup> by a Short Laser Pulse in Crossed Static Electric and Magnetic Fields,” Phys. Rev. A **74**, 023402 (2006).
- [11] A.Y. Istomin, E.A. Pronin, N.L. Manakov, S.I. Marmo, and A.F. Starace, “Elliptic and Circular Dichroism Effects in Two-Photon Double Ionization of Atoms,” Phys. Rev. Lett. **97**, 123002 (2006).
- [12] L.Y. Peng and A.F. Starace, “Application of Coulomb Wave Function Discrete Variable Representation to Atomic Systems in Strong Laser Fields,” J. Chem. Phys. **125**, 154311 (2006).
- [13] G. Lagmago Kamta, A.Y. Istomin, and A.F. Starace, “Thermal Entanglement of Two Interacting Qubits in a Static Magnetic Field,” Eur. Phys. J. D **44**, 389 (2007).

# **FEMTOSECOND AND ATTOSECOND LASER-PULSE ENERGY TRANSFORMATION AND CONCENTRATION IN NANOSTRUCTURED SYSTEMS**

**DOE Grant No. DE-FG02-01ER15213**

**Mark I. Stockman, Pi**

**Department of Physics and Astronomy, Georgia State University, Atlanta, GA 30303**  
**E-mail: [mstockman@gsu.edu](mailto:mstockman@gsu.edu), URL: <http://www.phy-astr.gsu.edu/stockman>**

## **Report for the Grant Period of 2005-2007 (Publications 2005-2007)**

### **1 Program Scope**

The program is aimed at theoretical investigations of a wide range of phenomena induced by ultrafast laser-light excitation of nanostructured or nanosize systems, in particular, metal/semiconductor/dielectric nanocomposites and nanoclusters. Among the primary phenomena are processes of energy transformation, generation, transfer, and localization on the nanoscale and coherent control of such phenomena.

### **2 Recent Progress**

#### **2.1 Attosecond Nanoplasmonics [1, 2]**

In collaboration with M. Kling, U. Kleineberg, and F. Krausz from Max Plank Institute for Quantum Optics (Garching, Germany), we have theoretically developed a novel concept called Attosecond Nanoplasmonic Field Microscope [1]. It is based on the use of attosecond laser pulses synchronized with an intense, waveform-stabilized optical field driving a nanosystem. The attosecond pulses cause photoemission of electrons in a given phase of the optical excitation, which are accelerated in the local nanoplasmonic fields. These electrons are detected by an energy-resolving photoemission electron microscope (PEEM). The energy of these electrons yields the potential of the local optical fields at the surface of the nanosystem with nanometer spatial resolution and  $\sim 100$  attosecond temporal resolution. This work sets the foundation of a novel direction in nanoplasmonics that is attosecond nanoplasmonics that studies that fastest phenomena existing at the nanoscale.

In a related development, we have shown that the carrier-envelope phase (CEP) of an excitation pulse significantly defines ultrafast responses of metal nanostructures in the regime of the above-threshold ionization (optical field emission) [2]. This suggests a way to build ultrasensitive detectors of the CEP, which is an important problem of the quantum optics.

#### **2.2 Criterion of Negative Refraction with Low Optical Losses [3]**

We have derived a novel criterion that defines a possibility of a negative-index material that would have a negligible loss at a given, working frequency [3]. This criterion is rigorous and general, based on the fundamental principle of causality. It shows that to achieve a negative refraction, a significant loss must be present in the vicinity of the working frequency. This criterion will guide the further quest for the low-loss negative index materials worldwide.

#### **2.3 Anomalous Dispersion and Reflection of Surface Plasmon Polaritons at Metal-Dielectric Interfaces [4]**

We have predicted a new effect, the total external reflection of surface plasmon polaritons (SPP) for nanometric dielectric films on plasmonic metal [4]. This effect can be used to create efficient SPP mirrors and resonators.

#### **2.4 Octupolar Metal Nanoparticles as Optically Driven, Coherently Controlled Nanorotors [5]**

We have proposed that metal nanoparticles with an octupolar symmetry, in particular regular metal nanotriangles and nanotetrahedra, will rotate by a predetermined angle when subjected to the simultaneous action of the fundamental and second harmonic radiations that are circularly polarized in the opposite directions [5]. This angle is coherently controlled by the phase difference between the fundamental and second harmonic. This project is carried out in collaboration with Prof. Joseph Zyss (ENS Cachan, France).

## **2.5 SPASER: Effect, and Prospective Devices [6]**

Recently, we have shown theoretically that the efficient nanolens, which is a self-similar aggregate of a few metal nanosphere, in an active medium of semiconductor quantum dots is an efficient spaser [6]. This spaser possesses a sharp hot spot of local fields in its nanofocus between the minimum-radius nanospheres. A related recent development has been an experiment by a group of L. Eng of Technical University of Dresden (Germany) where the principles of spaser have been confirmed [7].

## **2.6 Coherent Control of Ultrafast Energy Localization on Nanoscale [8]**

Our research has significantly focused on problem of controlling localization of the energy of ultrafast (femtosecond) optical excitation on the nanoscale. We have proposed and theoretically developed a distinct approach to solving this fundamental problem [9-14]. This approach, based on the using the relative phase of the light pulse as a functional degree of freedom, allows one to control the spatial-temporal distribution of the excitation energy on the nanometer-femtosecond scale.

Recently, we have shown [8] that using two-pulse (interferometric) coherent control in a complex random nanosystem it is possible to localize the ultrafast optical fields in with spatial resolution of down to 2 nm. In specially designed V-shape nanoantennas, it is possible to move the “hot spot” of plasmonic excitation to a given nanometric hot spot along a 30 nm extension of this nanoantenna [8].

Following our pioneering work, there has recently been an explosion of activity on both theoretical [15-18] and experimental [19-23] investigations of the ultrafast coherent control on the nanoscale. This field will rapidly grow into one of the most important in the nanoscience with application to the nanoscale computations, sensing, spectroscopy, etc. It will require our increased attention to stay at the forefront.

## **2.7 Efficient Nanolens [6, 24, 25].**

As an efficient nanolens, we have proposed a self-similar linear chain of several metal nanospheres with progressively decreasing sizes and separations [26]. The proposed system can be used for nanooptical detection, Raman characterization, nonlinear spectroscopy, nano-manipulation of single molecules or nanoparticles, and other applications. Recently, we have shown [6] that this nanolens surrounded by an active medium of nanocrystal quantum dots can be an efficient spaser. Another development has been a theory of the second-harmonic generation in an efficient nanolens (a linear self-similar aggregate of a few metal nanospheres) [24]. The second harmonic local fields form a very sharp nanofocus between the smallest spheres where these fields are enhanced by more than two orders of magnitude. This effect can be used for diagnostics and nanosensors. We have also obtained the first results on the Surface Enhanced Raman Scattering (SERS) in the nanosphere nanolens [25] where we show the SERS enhancement factor differ significantly from the commonly used fourth power of the local field enhancement.

## **2.8 Second Harmonic Generation on Nanostructured Surfaces [27]**

This research resulted from an international collaboration with the group of Prof. Joseph Zyss (ENS Cachan, France). [27-29]. Based on the spectral-expansion Green’s function theory, we theoretically describe the topography, polarization, and spatial-coherence properties of the second-harmonic (SH) local fields at rough metal surfaces. We have recently investigated this class of phenomena to predict and describe giant fluctuations of local SH fields in random nanostructures [27].

## **2.9 Strong Field Effects in Nanostructures: Forest Fire Mechanism of Dielectric Breakdown [30]**

This research is a result of an extensive international collaboration (UK, Germany, Canada, and the USA) [30-32]. We have described the interaction of ultrashort infrared laser pulses with clusters and dielectrics. Rapid ionization occurs on a sub-laser wavelength scale below the conventional breakdown threshold. It starts with the formation of nanodroplets of plasma that grow like forest fires, without any need for heating of the electrons promoted to the conduction band. This effect is very important for the physics of laser damage of semiconductors and dielectrics by a moderate-intensity radiation. This research has recently been extended to include some effects of the nanostructured plasmas generated in the process of the photoinduced damage (modification) of the solids [30].

## **2.10 Nanoplasmonics at Metal Surface: Enhanced Relaxation and Superlensing [33]**

We have considered a nanoscale dipolar emitter (quantum dot, atom, fluorescent molecule, or rare earth ion) in a nanometer proximity to a flat metal surface [33, 34]. There is strong interaction of this emitter with unscreened metal electrons in the surface nanolayer that causes enhanced relaxation due to surface plasmon excitation and Landau damping. For the system considered, conventional theory based on metal as continuous dielectric fails both qualitatively and quantitatively.

In a recent development [33], we have considered a principal limitations on the spatial resolution on the nanoscale of the “Perfect Lens” introduced by Pendry, also known as the superlens. In the conventional, local electrodynamics, the superlens builds a 3d image in the near zone without principal limitations on the spatial resolution.

We have shown that there is a principal limitation on this resolution, ~5 nm in practical terms, which originates from the spatial dispersion and Landau damping of dielectric responses of the interacting electron fluid in metals.

## 2.11 Theory of SERS [35]

We have revisited theory of one of the most important phenomena in nanoplasmonics, Surface Enhanced Raman Scattering. This theory shows that the predicted levels of enhancement in the red spectral region are still several orders of magnitude less than the enhancement factors  $\sim 10^{13} - 10^{14}$  observed experimentally. The difference may be due to the effects not taken into account by the theory: self-similar enhancement [26] or chemical enhancement [36].

## 2.12 Excitation of Surface Plasmon Polaritons (SPPs) by Free Electron Impact [37]

We have provided theoretical support and interpretation for the experimental investigation of the SPP generation by free-electron impact. This effect can be used as a basis of a novel method to visualize eigenmodes of plasmonic nanosystem by exciting them with an electron microscope beam.

## 3 Future Plans

We will develop both the theory in the directions specified above and the collaborations with the experimental and theoretical groups that we have developed. Among the future projects, we will develop attosecond nanoplasmonics. We will also consider the coherent control by time reversal in the nanosystems.. Another direction will be theory of full spatio-temporal control on the nanoscale. We plan also to consider ultrafast phenomena in a novel area of studies: left-handed materials also called negative-index media.

## 4 Publications Resulting from the Grant

The major articles published by our group during this Report (2005-2007) period are indicated by bold typeface at the corresponding headings above. These are Refs.[1-6, 8, 24, 25, 27, 30, 33, 35, 37]. Most supported by this grant are publications of Refs.[1-6, 8, 25, 27, 30, 37].

## References

1. M. I. Stockman, M. F. Kling, U. Kleineberg, and F. Krausz, *Attosecond Nanoplasmonic Field Microscope*, Nature Photonics **1**, (In Print; Scheduled for September 2007 Issue) (2007).
2. M. I. Stockman and P. Hewageegana, *Absolute Phase Effect in Ultrafast Optical Responses of Metal Nanostructures*, Appl. Phys. A (In Print; Published on Line: DOI: 10.1007/s00339-007-4105-7) (2007).
3. M. I. Stockman, *Criterion for Negative Refraction with Low Optical Losses from a Fundamental Principle of Causality*, Phys. Rev. Lett. **98**, 177404-1-4 (2007).
4. M. I. Stockman, *Slow Propagation, Anomalous Absorption, and Total External Reflection of Surface Plasmon Polaritons in Nanolayer Systems*, Nano Lett. **6**, 2604-2608 (2006).
5. M. I. Stockman, K. Li, S. Brasselet, and J. Zysy, *Octupolar Metal Nanoparticles as Optically Driven, Coherently Controlled Nanorotors*, Chem. Phys. Lett. **433**, 130–135 (2006).
6. K. Li, X. Li, M. I. Stockman, and D. J. Bergman, *Surface Plasmon Amplification by Stimulated Emission in Nanolenses*, Phys. Rev. B **71**, 115409-1-4 (2005).
7. J. Seidel, S. Grafstroem, and L. Eng, *Stimulated Emission of Surface Plasmons at the Interface between a Silver Film and an Optically Pumped Dye Solution*, Phys. Rev. Lett. **94**, 177401-1-4 (2005).
8. M. I. Stockman and P. Hewageegana, *Nanolocalized Nonlinear Electron Photoemission under Coherent Control*, Nano Lett. **5**, 2325-2329 (2005).
9. M. I. Stockman, S. V. Faleev, and D. J. Bergman, *Coherent Control of Femtosecond Energy Localization in Nanosystems*, Phys. Rev. Lett. **88**, 67402-1-4 (2002).
10. M. I. Stockman, S. V. Faleev, and D. J. Bergman, *Coherently Controlled Femtosecond Energy Localization on Nanoscale*, Appl. Phys. B **74**, S63-S67 (2002).
11. M. I. Stockman, S. V. Faleev, and D. J. Bergman, *Coherently-Controlled Femtosecond Energy Localization on Nanoscale*, Appl. Phys. B **74**, 63-67 (2002).
12. M. I. Stockman, D. J. Bergman, and T. Kobayashi, in Proceedings of SPIE: Plasmonics: Metallic Nanostructures and Their Optical Properties, edited by N. J. Halas, *Coherent Control of Ultrafast Nanoscale Localization of Optical Excitation Energy* (SPIE, San Diego, California, 2003), Vol. 5221, p. 182-196.
13. M. I. Stockman, S. V. Faleev, and D. J. Bergman, in Ultrafast Phenomena XIII, *Coherently-Controlled Femtosecond Energy Localization on Nanoscale* (Springer, Berlin, Heidelberg, New York, 2003).
14. M. I. Stockman, D. J. Bergman, and T. Kobayashi, *Coherent Control of Nanoscale Localization of Ultrafast Optical Excitation in Nanosystems*, Phys. Rev. B **69**, 054202-10 (2004).
15. M. Sukharev and T. Seideman, *Phase and Polarization Control as a Route to Plasmonic Nanodevices*, Nano Lett. **6**, 715-719 (2006).

16. M. Sukharev and T. Seideman, *Coherent Control Approaches to Light Guidance in the Nanoscale*, J. Chem. Phys. **124**, 144707-1-8 (2006).
17. T. Brixner, F. J. G. d. Abajo, J. Schneider, C. Spindler, and W. Pfeiffer, *Ultrafast Adaptive Optical near-Field Control*, Physical Review B **73**, 125437 (2006).
18. T. Brixner, F. J. G. d. Abajo, J. Schneider, and W. Pfeiffer, *Nanoscopic Ultrafast Space-Time-Resolved Spectroscopy*, Phys. Rev. Lett. **95**, 093901-1-4 (2005).
19. A. Kubo, K. Onda, H. Petek, Z. Sun, Y. S. Jung, and H. K. Kim, *Femtosecond Imaging of Surface Plasmon Dynamics in a Nanostructured Silver Film*, Nano Lett. **5**, 1123-1127 (2005).
20. A. Kubo, K. Onda, H. Petek, Z. Sun, Y. S. Jung, and H. K. Kim, in *Ultrafast Phenomena XIV*, edited by T. Kobayashi, T. Okada, T. Kobayashi, K. A. Nelson and S. D. Silvestri, *Imaging of Localized Silver Plasmon Dynamics with Sub-Fs Time and Nano-Meter Spatial Resolution* (Springer, Niigata, Japan, 2004), Vol. 79, p. 645-649.
21. P. v. d. Walle, L. Kuipers, and J. L. Herek, in *Ultrafast Phenomena XV, Coherent Control of Light in Metal Nanostructures* (Pacific Grove, California, 2006), p. Paper TuD3.
22. M. Bauer, D. Bayer, T. Brixner, F. J. G. d. Abajo, W. Pfeiffer, M. Rohmer, C. Spindler, and F. Steeb, in *Ultrafast Phenomena XV, Adaptive Control of Nanoscopic Photoelectron Emission* (Pacific Grove, California, 2006), p. Paper ThB3.
23. M. Aeschlimann, M. Bauer, D. Bayer, T. Brixner, F. J. G. d. Abajo, W. Pfeiffer, M. Rohmer, C. Spindler, and F. Steeb, *Adaptive Subwavelength Control of Nano-Optical Fields*, Nature **446**, 301-304 (2007).
24. K. Li, M. I. Stockman, and D. J. Bergman, *Enhanced Second Harmonic Generation in a Self-Similar Chain of Metal Nanospheres*, Phys. Rev. B **72**, 153401-1-4 (2005).
25. K. Li, M. I. Stockman, and D. J. Bergman, *Li, Stockman, and Bergman Reply to Comment On "Self-Similar Chain of Metal Nanospheres as an Efficient Nanolens"*, Phys. Rev. Lett. **97**, 079702 (2006).
26. K. Li, M. I. Stockman, and D. J. Bergman, *Self-Similar Chain of Metal Nanospheres as an Efficient Nanolens*, Phys. Rev. Lett. **91**, 227402-1-4 (2003).
27. M. I. Stockman, *Giant Fluctuations of Second Harmonic Generation on Nanostructured Surfaces*, Chem. Phys. **318**, 156-162 (2005).
28. M. I. Stockman, D. J. Bergman, C. Anceau, S. Brasselet, and J. Zyss, *Enhanced Second-Harmonic Generation by Metal Surfaces with Nanoscale Roughness: Nanoscale Dephasing, Depolarization, and Correlations*, Phys. Rev. Lett. **92**, 057402-1-4 (2004).
29. M. I. Stockman, D. J. Bergman, C. Anceau, S. Brasselet, and J. Zyss, in *Complex Mediums V: Light and Complexity*, edited by M. W. McCall and G. Dewar, *Enhanced Second Harmonic Generation by Nanorough Surfaces: Nanoscale Depolarization, Dephasing, Correlations, and Giant Fluctuations* (SPIE, 2004), Vol. 5508.
30. L. N. Gaier, M. Lein, M. I. Stockman, G. L. Yudin, P. B. Corkum, M. Y. Ivanov, and P. L. Knight, *Hole-Assisted Energy Deposition in Dielectrics and Clusters in the Multiphoton Regime*, J. Mod. Optics **52**, 1019-1030 (2005).
31. L. N. Gaier, M. Lein, M. I. Stockman, P. L. Knight, P. B. Corkum, M. Y. Ivanov, and G. L. Yudin, *Ultrafast Multiphoton Forest Fires and Fractals in Clusters and Dielectrics*, J. Phys. B: At. Mol. Opt. Phys. **37**, L57-L67 (2004).
32. G. L. Yudin, L. N. Gaier, M. Lein, P. L. Knight, P. B. Corkum, and M. Y. Ivanov, *Hole-Assisted Energy Deposition in Clusters and Dielectrics in Multiphoton Regime*, Laser Phys **14**, 51-56 (2004).
33. I. A. Larkin and M. I. Stockman, *Imperfect Perfect Lens*, Nano Lett. **5**, 339-343 (2005).
34. I. A. Larkin, M. I. Stockman, M. Achermann, and V. I. Klimov, *Dipolar Emitters at Nanoscale Proximity of Metal Surfaces: Giant Enhancement of Relaxation in Microscopic Theory*, Phys. Rev. B **69**, 121403(R)-1-4 (2004).
35. M. I. Stockman, in *Springer Series Topics in Applied Physics*, edited by K. Kneipp, M. Moskovits and H. Kneipp, *Surface Enhanced Raman Scattering – Physics and Applications* (Springer-Verlag, Heidelberg New York Tokyo, 2006), p. 47-66.
36. J. Jiang, K. Bosnick, M. Maillard, and L. Brus, *Single Molecule Raman Spectroscopy at the Junctions of Large Ag Nanocrystals*, J. Phys. Chem. B **107**, 9964-9972 (2003).
37. M. V. Bashevoy, F. Jonsson, A. V. Krasavin, N. I. Zheludev, Y. Chen, and M. I. Stockman, *Generation of Traveling Surface Plasmon Waves by Free-Electron Impact*, Nano Lett. **6**, 1113-1115 (2006).

# Molecular Structure and Electron-Driven Dissociation and Ionization

Vladimir Tarnovsky<sup>1</sup> and Kurt H. Becker<sup>2</sup>

<sup>1</sup> Department of Physics, Stevens Institute of Technology, Hoboken, NJ 07030

<sup>2</sup> Polytechnic University, Brooklyn, NY 11201

(vtarnovs@stevens.edu; kbecker@poly.edu)

## Program Scope:

This program is aimed at investigating the molecular structure and the collisional dissociation and ionization of selected molecules and free radicals. The focus areas are (1) ionization studies of selected molecules and free radicals and (2) the study of electron-impact induced neutral molecular dissociation processes – this part of the work is being phased out. Targets of choice for ionization studies include  $\text{SiCl}_4$  and  $\text{BCl}_3$  and their radicals, the molecular halogens  $\text{Br}_2$  and  $\text{F}_2$  and the compounds  $\text{SF}$ ,  $\text{SF}_2$ , and  $\text{SF}_4$ . The choice of target species is motivated on one hand by the relevance of these species in specific technological applications involving low-temperature processing plasmas and, on the other hand, by basic collision physics aspects. The scientific objectives of the research program can be summarized as follows:

- (1) provide the atomic and molecular data that are required in efforts to understand the properties of low-temperature processing plasmas on a microscopic scale
- (2) identify the key species that determine the dominant plasma chemical reactions
- (3) measure cross sections and reaction rates for the formation of these key species and to attempt to deduce predictive scaling laws
- (4) establish a broad collisional and spectroscopic data base which serves as input to modeling codes and CAD tools for the description and modeling of existing processes and reactors and for the development and design of novel processes and reactors
- (5) provide data that are necessary to develop novel plasma diagnostics tools and to analyze more quantitatively the data provided by existing diagnostics techniques

## **Recent Progress and Ongoing Work:**

***Ionization of  $\text{SiCl}_x$  ( $x=1-3$ )*** Following the work on the ionization of the  $\text{SCl}_4$  molecule, we subsequently measured absolute partial and total cross sections for the electron-impact ionization of  $\text{SiCl}_x$  ( $x=1-3$ ).

The measured cross sections are summarized in figures 1-3. In the case of  $\text{SiCl}_3$  (fig. 1), the largest partial cross sections are those for the formation of  $\text{Cl}^+$  and  $\text{SiCl}^+$  followed by the partial  $\text{SiCl}_2^+$  and  $\text{SiCl}_3^+$  cross sections. The Si cross section is the smallest partial cross section for  $\text{SiCl}_3$ .

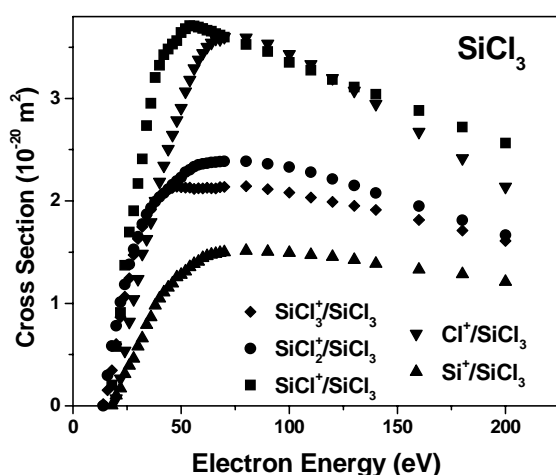


**Fig. 1.** Electron impact ionization of  $\text{SiCl}_3$ . The partial cross sections for the formation of the  $\text{SiCl}_3^+$  parent ion and all other singly charged fragments are shown as a function of electron energy from threshold to 200 eV.

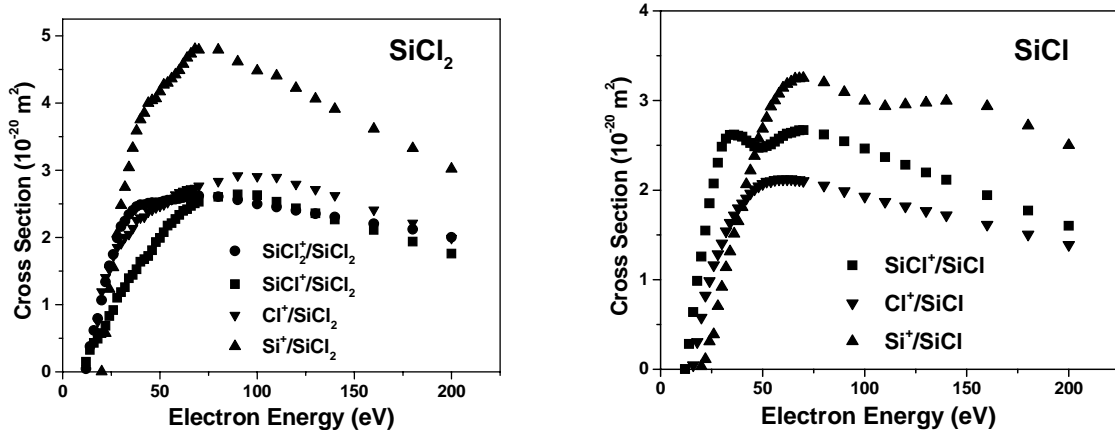


**Fig. 2 (left).** Electron impact ionization of  $\text{SiCl}_2$ . The partial cross sections for the formation of the  $\text{SiCl}_3^+$  parent ion and all other singly charged fragments are shown as a function of electron energy from threshold to 200 eV.

**Fig. 3 (right).** Electron impact ionization of  $\text{SiCl}$ . The partial cross sections for the formation of the  $\text{SiCl}_3^+$  parent ion and all other singly charged fragments are shown as a function of electron energy from threshold to 200 eV.

This is quite in contrast to  $\text{SiCl}_2$  (fig. 2) and  $\text{SiCl}$  (fig. 3), where the partial  $\text{Si}^+$  cross section dominates. For  $\text{SiCl}_2$ , the other partial cross sections ( $\text{SiCl}_2^+$ ,  $\text{SiCl}^+$ , and  $\text{Cl}^+$ ) are essentially of equal value. For  $\text{SiCl}$ , the partial  $\text{SiCl}^+$  and  $\text{Cl}^+$  partial cross sections are only slight smaller than the  $\text{Si}^+$  section. Note that some of the cross section curves show a pronounced structure around 30 eV. This is highlighted in fig. 4, which shows the parent ionization cross section for all four  $\text{SiCl}_x$  ( $x = 1 - 4$ ) compounds. Similar structures near the same energy were also observed earlier for other partial cross sections from  $\text{SiCl}_4$  as well as for some partial cross sections of  $\text{TiCl}_4$  and  $\text{Cl}_2$ . Figure 4 shows the parent ionization cross sections of all four  $\text{SiCl}_4$  ( $x = 1 - 4$ ) compounds.

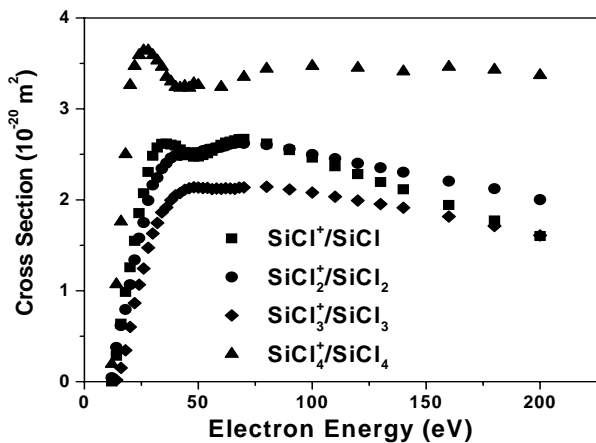


**Fig. 4.** Parent ionization cross sections for the  $\text{SiCl}_x$  ( $x = 1 - 4$ ) compounds as a function of electron energy from threshold to 200 eV. The pronounced structure in the cross section shape around 30 eV is apparent more or less prominently, in all four cross section curves.

**Ionization Cross Section Calculations.** All experimental ionization studies were also supported by our continuing effort to extend and refine our semi-classical approach to the calculation of the

total single ionization cross sections for atoms, molecules, free radicals, and ions. Recent calculations were carried out for atomic with atomic numbers in the range 20 – 56, which includes many atoms of technical relevance (for which no experimental data are available), the lanthanides (which are characterized by an unfilled (5d) sub-shell and a partially filled (4f) sub shell), and the molecular ions  $CD_x^+$  ( $x = 1 - 4$ ). Figure 5 shows a comparison of the calculated  $CD^+$  ionization cross section using the DM formalism and the BEB approach with the experimental data of Defrance and co-workers. It is evident that the two calculated cross section

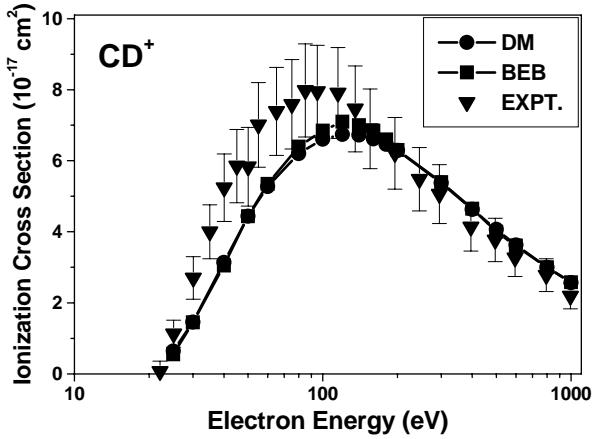


**Fig. 5.** Calculated cross sections for the electron impact ionization of the  $CD^+$  ion using the DM formalism (circles) and the BEB approach (squares) in comparison with the measured data of Defrance and co-workers from threshold to 1000 eV.

calculated cross section curves. This could be indicative of the presence of an additional ionization channel not described by the calculations, which include contributions from direct ionization of ground-state  $CD^+$  only. In the case of  $CD_2^+$  and  $CD_3^+$  there is excellent agreement between the DM calculation and the measured cross section data. However, in the case of  $CD_4^+$  (figure 6), both the BEB approach and the DM formalism yield calculated cross sections that are significantly higher than the measured data. The reason for this discrepancy is not clear.

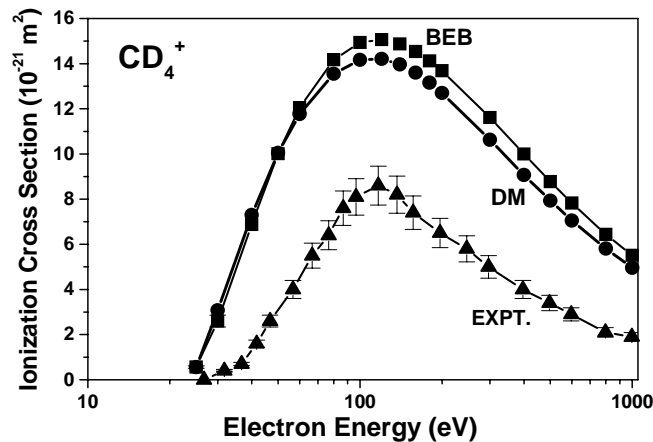


**Fig. 6.** Calculated cross sections for the electron impact ionization of the  $CD_4^+$  ion using the DM formalism (circles) and the BEB approach (squares) in comparison with the measured data of Defrance and co-workers from threshold to 1000 eV.

### Planned Work in the Next Year

The research plan for the coming year will closely follow the work plan outlined in our original proposal.

### **Publications Acknowledging DOE Support (since 2005)**

1. S. Matt-Leubner, S. Feil, K. Gluch, J. Fedor, A. Stamatovic, O. Echt, P. Scheier, K. Becker, and T.D. Märk “Energetics, Kinetics, and Dynamics of Decaying Metastable Ions Studied with a High Resolution Three-Sector-Field Mass Spectrometer”, *Plasma Sources Sci. Techn.* 14, 26-30 (2005)
2. H. Deutsch, P. Scheier, S. Matt-Leubner, K. Becker, and T.D. Märk “A Detailed Comparison of Calculated and Measured Electron-Impact Ionization Cross Sections of Atoms Using the Deutsch-Märk (DM) Formalism”, *Int. J. Mass Spectrom.* 243, 215-21 (2005)
3. H. Deutsch, K. Becker, A.N. Grum-Grzhimailo, M. Probst, S. Matt-Leubner, and T.D. Märk, “Calculated Electron Impact Ionization Cross Sections of Excited Ne Atoms Using the DM Formalism”, *Contr. Plasma Phys.* 7, 494-499 (2005)
4. R. Basner, M. Gutkin, J. Mahoney, V. Tarnovsky, H. Deutsch, and K. Becker, “Electron Impact Ionization of Silicon Tetrachloride”, *J. Chem. Phys.* 123, 05313 (2005)
5. H. Deutsch, K.B. MacAdam, K. Becker, H. Zhang, and T.D. Märk, “Calculated Cross Sections for the Electron Impact Ionization of Na(ns) and Na(nd) Rydberg Atoms”, *J. Phys. B* 39, 343-353 (2005)
6. S. Denifl, B. Sonnweber, J. Mack, L. T. Scott, P. Scheier, K. Becker, and T.D. Märk, “Appearance Energies of Singly, Doubly, and Triply Charged Coronene and Corannulene Ions Produced by Electron Impact”, *Int. J. Mass Spectrom.* 249/250, 353-358 (2006)
7. H. Deutsch, K. Becker, P. Defrance, M. Probst, J. Limtrakul, and T.D. Märk, “Newly Calculated Absolute Cross Sections for the Electron Impact Ionization of  $C_2H_2^+$ ”, *Europ. Phys. J. D* 38, 489-493 (2006)
8. K. Becker, J. Mahoney, M. Gutkin, V. Tarnovsky, and R. Basner, “Electron Impact Ionization of  $SiCl_x$  and  $TiCl_x$  ( $x = 1-4$ ): Contributions from Indirect Ionization Channels”, *Jap. J. Appl. Phys.* 45, 8818-8891 (2006)
9. J. Lecontre, D.S. Belic, J. Jureta, K. Becker, H. Deutsch, J. Limtrakul, T.D. Märk, M. Probst and P. Defrance, “Absolute cross sections and kinetic energy release for doubly and triply charged fragments produced by electron impact on  $CO^+$ ”, *J. Phys. B* 39, 85-100 (2006)
10. J. Lecontre, S. Cherkani-Hassani, D.S. Belic, J.J. Jureta, K. Becker, H. Deutsch, T.D. Märk, M. Probst, R.K. Janev, and P. Defrance, “Absolute Cross Sections and Kinetic Energy Release distributions for Electron Impact Ionization of  $CD^+$ ”, *J. Phys. B* 40, 2201-2221 (2007)
11. Deutsch, K. Becker, and T.D. Märk, “Calculated Absolute Cross Sections for the Electron-Impact Ionization of Atoms with Atomic Numbers between 20 and 56 Using the DM Formalism”, *Int. J. Mass Spectrom.* (2007), submitted
12. H. Deutsch, K. Becker, H. Zhang, M. Probst, and T.D. Märk, “Calculated Absolute Cross Sections for the Electron-Impact Ionization of the Lanthanide Atoms Using the DM Formalism”, *Int. J. Mass Spectrom.* (2007), submitted

# **Inner-shell electron spectroscopy and chemical properties of atoms and small molecules**

T. Darrah Thomas, Principal Investigator  
[T.Darrah.Thomas@oregonstate.edu](mailto:T.Darrah.Thomas@oregonstate.edu)

Department of Chemistry  
153 Gilbert Hall  
Oregon State University  
Corvallis, OR 97331-4003

## **Program scope**

Many chemical phenomena depend on the ability of a molecule to accept charge at a particular site in the molecule. Examples are acidity, basicity, proton affinity, rates and regiospecificity of electrophilic reactions, hydrogen bonding, and ionization. Among these, inner-shell ionization spectroscopy (ESCA or x-ray photoelectron spectroscopy) has proven to be a useful tool for investigating how a molecule responds to added or diminished charge at a particular site. The technique is element specific and is applicable to all elements except hydrogen. It is, in many cases site specific. As a result, x-ray photoelectron spectroscopy (XPS) can probe all of the sites in a molecule and identify the features that cause one site to have different chemical properties from another. In addition, inner-shell ionization energies, as measured by XPS, provide insight into the charge distribution in the molecule – a property of fundamental chemical importance.

For nearly 40 years inner-shell electron spectroscopy has been a source of much useful chemical information. Until recently, however, the investigation of the carbon 1s photoelectron spectra of hydrocarbons (or the hydrocarbon portion of molecules containing a heteroatom) has been hampered by lack of resolution. Carbon atoms with quite distinct chemical properties may have carbon 1s ionization energies that differ by less than 1 eV, whereas historically the available resolution has been only slightly better than this. In addition, the vibrational excitation accompanying core ionization adds complexity to the spectra that has made analysis difficult.

The availability of third-generation synchrotrons coupled with high-resolution electron spectrometers has made a striking difference in this situation. It is now possible to measure carbon 1s photoelectron spectra with a resolution of about half the natural line width (~100 meV), with the result that recently measured carbon 1s spectra in hydrocarbons show a richness of chemical effects and vibronic structure.

During the last ten years this program has endeavored to exploit this capability in order to investigate systems where new features can be revealed by high-resolution carbon 1s photoelectron spectroscopy. The primary goal has been to determine carbon 1s ionization energies not previously accessible in order to use the relationships between these energies and other chemical properties to elucidate the chemistry of a variety of systems. Early work focused on understanding the features of the spectra: line shape, line width, vibrational structure, and vibronic coupling, since understanding these features is essential to unraveling the complex spectra that are found for molecules having several carbon atoms. Now that these features are (more or less) understood, emphasis has shifted to investigation of chemically significant systems and to gaining further insights into the relationships between core-ionization energies and chemical properties. New areas of research include the effects of molecular conformation and recoil on inner-shell photoelectron spectra.

## **Recent progress (2006-2007)**

During the last 12 months, we have had 33 shifts of synchrotron time – 15 at the SPring8 in April 2007 and 18 at MAX II in May 2007. At SPring8, the time was devoted to investigating recoil effects on the inner-shell photoelectron spectra of  $\text{CF}_4$ ,  $\text{BF}_3$ , and CO. At MAX II we acquired carbon 1s photoelectron spectra for a number of compounds of interest. Particular emphasis was on substituted molecules in which the substituent affects the acidity of the molecule or in which there is an effect of the molecular conformation on the carbon 1s photoelectron spectra, especially where the spectra can serve as models for the photoelectron spectra of polymers.

The year has seen publication of work on the effects of methyl substituents on the carbon 1s photoelectron spectra of substituted benzenes<sup>1</sup> and the first report of the effects of molecular conformation on core-ionization energies.<sup>2</sup>

### **Core-ionization energies, proton affinities, and reactivities in substituted benzenes.**

Benzene plays a special role in chemistry as the building block for many important compounds. Its properties, reactivity, and spectroscopy are all strongly influenced by any substituents that are attached to the ring. As a consequence the study of substituent effects in the chemistry of benzene has a very long history, as does the study of substituent effects on the carbon 1s ionization energies in benzene. However, because of limitations of resolution, obtaining unequivocal experimental results on such effects on the carbon 1s ionization energies has been difficult. Now, with third-generation synchrotrons and advanced electronic structure theory, it is possible to assign carbon 1s ionization energies to all of the carbon atoms in a substituted benzene ring.

We have recently published results of our measurements and analysis of the fluoro-<sup>3</sup> and methyl<sup>1</sup>-substituted benzenes. In the work on fluorobenzenes we have shown, first, that the effect of multiple substituents is additive, and, second, that there are linear correlations between carbon 1s ionization energies and proton affinities for these molecules. From these correlations we have obtained insight into the role of fluorine as a  $\pi$ -electron donor. Specifically, the results show that a fluorine substituent that is ortho or para to the site of ionization or protonation is a better  $\pi$ -electron donor to an added proton than it is to a core hole. This difference can be understood in terms of the specific structure of the protonated molecule, which has a more extensive system of  $\pi$  molecular orbitals than does the core-ionized species.

The work on the methyl-substituted benzenes shows that the additivity model holds for methyl substituents and that there are linear correlations with proton affinities for these substituents. However, the  $\pi$ -donor effect is smaller for the methyl group than it is for fluorine. In addition, this research has investigated the correlations between chemical reactivities, proton affinities, and core ionization energies.<sup>1</sup>

Measurements on molecules that have both fluoro and methyl substituents have been made to provide further insight into the additivity model. Preliminary results indicate that this model will work well for these mixed compounds. Analysis of these results is complicated by the large number of inequivalent carbon atoms in some of these molecules. We expect to have the analysis complete by the end of summer 2007.

**Conformational effects on carbon 1s photoelectron spectra and ionization energies.** In general, there has been little reason to expect that different conformers of a molecule would give different photoelectron spectra, and, until recently, where this possibility has been investigated no conformational effects on the spectra have been observed. We have, however, found a number of examples in which conformational effects are very apparent in carbon 1s photoelectron spectra. Two different effects are seen. In one, the existence of more than one form is reflected in the degree of vibrational excitation that accompanies core-ionization. In the other the existence of more than one

form leads to there being more than one carbon 1s ionization energy for a given carbon atom.

An example of the first effect is found in ethanol, which exists in two conformers in about equal abundance. In the *anti* form the hydroxyl group is pointed away from the methyl group, with an HOCC dihedral angle of 180°. By contrast, in the *gauche* form this angle is about 60°, with the result that the hydroxyl group can interact strongly with the methyl group. Carbon 1s ionization at the methyl group leaves a localized positive charge at the methyl group, and this positive charge interacts repulsively with the positive charge on the hydroxyl group. In the *anti* form, these charges are far apart, and the interaction is weak. By contrast, in the *gauche* form, the interaction is strong and the *gauche* form is strongly destabilized. As a consequence, core ionization of the methyl group in *gauche* ethanol leads to considerable excitation of torsional motion, but ionization of the *anti* form leads to no excitation of this motion.<sup>4</sup>

The second effect is illustrated by molecules of the type  $\text{CH}_3\text{CH}_2\text{CH}_2\text{X}$ , where X is an electronegative group such as F, C≡N, C≡CR, or O. These molecules typically exist in two conformations, one with X pointed more or less away from the terminal methyl group (that is, with the XCCC dihedral angle greater than 90°) and one with it pointed more or less towards the methyl group (XCCC < 90°). The distance between of the negatively charged electronegative group and the methyl carbon affects the carbon 1s ionization energy and hence the photoelectron spectrum. We have found that this hitherto unobserved effect has a noticeable influence on the spectra of a number of molecules of this type – butyronitrile, 1-fluoropropane, and propanal, for instance, as well as other related compounds. A paper reporting some of these results was published in 2007,<sup>2</sup> and additional investigations of this effect are in progress.

**Recoil effects in inner-shell ionization.** An inner-shell photoelectron spectrum often shows vibrational structure. Typically this reflects differences in the equilibrium geometries of the ionized and unionized molecules, and studies of this vibrational structure have been a fruitful source of information on these differences. There is, however, another mechanism for vibrational excitation, as was pointed out by Domcke and Cederbaum,<sup>5</sup> and that is recoil excitation. When a photoelectron is ejected the remaining ion has a momentum that is equal to and opposite to that of the photoelectron. For an atom the kinetic energy associated with this recoil appears as kinetic energy of the ion. For core-ionization of a molecule, however, the recoil energy is imparted to the core-ionized atom and is then shared between kinetic energy of the recoiling molecular ion and vibrational and possibly rotational excitation of the molecule.

This recoil effect has been observed in methane,<sup>6</sup> but here the effect is small. More promising candidates are tetrafluoromethane, boron trifluoride, and, for observing possible rotational effects, carbon monoxide. We investigated these molecules at SPring8 during April 2007 and found quite clear evidence for the recoil-induced excitation of the asymmetric CF stretching mode in tetrafluoromethane. For the other two molecules the evidence is not clear, and further analysis of these results is underway.

These measurements also produced excellent high-resolution inner-shell photoelectron spectra of tetrafluoromethane and boron trifluoride. These results are providing insight into the changes in bond length that accompany core ionization. In addition the measurements on boron trifluoride give the first measurement of the boron 1s hole lifetime in a molecule, and those for tetrafluoromethane provide a better measurement of the carbon 1s hole lifetime in this molecule.

## Future plans

For the immediate future, work related to core-ionization and chemical properties will focus on the analysis and interpretation of data that we have already collected. Other areas of interest will

be continued studies of recoil effects in inner-shell photoelectron spectra, investigation of molecules whose spectra provide prototypical spectra for understanding the photoelectron spectra of polymers, additional research into the effects of molecular conformation on photoelectron spectra, and studies of fluorine 2s photoelectron spectroscopy.

1. V. Myrseth, L. J. Sæthre, K. J. Børve, and T. D. Thomas, *J. Org. Chem.* **72**, 5715 (2007).
2. T. D. Thomas, L. J. Sæthre, and K. J. Børve, *Phys. Chem. Chem. Phys.* **9**, 719 (2007).
3. T. X. Carroll, T. D. Thomas, H. Bergersen, K. J. Børve, and L. J. Sæthre, *J. Org. Chem.* **71**, 1961 (2006).
4. M. Abu Samha, K. J. Børve, L. J. Sæthre, and T. D. Thomas, *Phys. Rev. Lett.*, **95**, 103002 (2005).
5. W. Domcke and L. S. Cederbaum, *J. Electr. Spectrosc. and Relat. Phenom.* **13**, 161 (1978).
6. E. Kukk, K. Ueda, U. Hergenhahn, X.-J. Liu, G. Pruemper, H. Yoshida, Y. Tamenori, C. Makachekanwa, T. Tanaka, M. Kitajima, and H. Tanaka, *Phys. Rev. Lett.* **95**, 13301 (2005).

### Publications involving DOE support, 2004-2007

Carbon 1s photoelectron spectroscopy of six-membered cyclic hydrocarbons, V. M. Oltedal, K. J. Børve, L. J. Sæthre, T. D. Thomas, J. D. Bozek, and E. Kukk, *Phys. Chem. Chem. Phys.*, **6**, 4254 (2004). <http://dx.doi.org/10.1039/b405109b>

Reactivity and core-ionization energies in conjugated dienes. Carbon 1s photoelectron spectroscopy of 1,3-pentadiene, T. D. Thomas, L. J. Sæthre, K. J. Børve, M. Gundersen, and E. Kukk, *J. Phys. Chem. A*, **109**, 5085 (2005). <http://dx.doi.org/10.1021/jp051196y>

Conformational effects in inner-shell photoelectron spectroscopy of ethanol, M. Abu Samha, K. J. Børve, L. J. Sæthre, and T. D. Thomas, *Phys. Rev. Lett.*, **95**, 103002 (2005). <http://dx.doi.org/10.1103/PhysRevLett.95.103002>

Fluorine as a  $\pi$  donor. Carbon 1s photoelectron spectroscopy and proton affinities of fluorobenzenes, T. X. Carroll, T. D. Thomas, H. Bergersen, K. J. Børve, and L. J. Sæthre, *J. Org. Chem.* **71**, 1961 (2006). <http://dx.doi.org/10.1021/jo0523417>

Effect of molecular conformation on inner-shell ionization energies. T. D. Thomas, L. J. Sæthre, and K. J. Børve, *Phys. Chem. Chem. Phys.* **9**, 719 (2007). <http://dx.doi.org/10.1039/b616824h>

The substituent effect of the methyl group. Carbon 1s Ionization energies, proton affinities, and reactivities of the methylbenzenes, V. Myrseth, L. J. Sæthre, K. J. Børve, and T. D. Thomas *J. Org. Chem.* **72**, 5715 (2007). <http://dx.doi.org/10.1021/jo0708902>

# Quantum Dynamics of Optically-Trapped Fermi Gases

Grant #DE-FG02-01ER15205  
Report for the Period: 11/1/06-10/31/07

John E. Thomas  
Physics Department, Duke University  
Durham, NC 27708-0305  
e-mail: jet@phy.duke.edu

## 1. Scope

The purpose of this program is to study the many-body quantum dynamics of a very general fermionic system: Optically trapped, strongly-interacting mixtures of spin-up and spin-down  $^6\text{Li}$  fermions, in the regime of quantum degeneracy. Strongly-interacting, highly degenerate samples are directly produced in an ultrastable CO<sub>2</sub> laser trap by forced evaporation at a magnetic field tuned near a Feshbach resonance. The resonance permits wide tunability of the s-wave scattering length which determines the interaction strength.

Strongly-interacting mixtures of spin-up and spin-down atomic Fermi gases provide unique systems for stringent tests of competing quantum theories of superfluidity and high temperature superconductivity. In the controlled environment of an optical trap, such mixtures permit wide variation of temperature, density, spin composition and interaction strength. Indeed, strongly-interacting Fermi gases provide scale models of a variety of exotic systems in nature, not only high temperature superconductors, but neutron stars, strongly-interacting matter in general, the expansion dynamics of a quark-gluon plasma, and most recently, low viscosity strongly interacting fields in string theory. The scale is set by the Fermi temperature, which is a few  $\mu\text{K}$  in a quantum gas and about an electron volt in a metal or  $10^4$  K. Near a Feshbach resonance, spin-up and spin-down mixtures of atomic Fermi gases exhibit super-strong pairing interactions. In our experiments, observed changes in the thermodynamics signal a superfluid transition at 30% of the Fermi temperature. Such high transition temperatures correspond to achieving superconductivity in a metal at thousands of degrees, far above room temperature.

## 2. Recent Progress

During the past year, we achieved two important breakthroughs. We made the first model-independent study of the thermodynamics of a strongly-interacting Fermi

gas by measuring the entropy as a function of energy [11]. Using this method, we were able to make model-independent measurements of the critical energy, critical entropy and critical temperature for the superfluid transition in this unique quantum gas. We also made the first measurements of the velocity of sound [12] in the gas as a function of magnetic field, enabling studies of the quantum hydrodynamics of sound propagation and of the equation of state. These experiments test the best recent nonperturbative microscopic many-body calculational methods. Our results are in very good agreement with quantum Monte Carlo predictions of the finite temperature thermodynamics at resonance and with the predicted zero temperature equation of state as function of interaction strength. In addition, we have brought a new second-generation apparatus online [10] and now have two working fermion laboratories. The primary results are described briefly below.

### *Measuring Entropy versus Energy in a Strongly-Interacting Fermi Gas [11]*

Strongly-interacting Fermi gases provide a paradigm for strong interactions in nature. For this reason, measurements of the thermodynamic properties of this unique system are of paramount importance.

We developed previously a method for model-independent measurement of the energy [6]. In the strongly interacting regime near a Feshbach resonance, the gas obeys the virial theorem, so that the total energy  $E_{strong}$  is precisely twice the potential energy in a harmonic trap,

$$E_{strong} = 3m\omega_z^2 \langle z^2 \rangle_{strong}. \quad (1)$$

This is a remarkable result, since the gas generally contains superfluid pairs, noncondensed pairs, and unpaired Fermi atoms, all strongly interacting in a highly nonperturbative regime. We simply measure the mean square axial cloud size of the trapped gas to determine the energy.

Last year, we combined this method with model-independent entropy measurement. Entropy measurement is accomplished with an adiabatic sweep of the magnetic field from the strongly interacting regime near the Feshbach resonance at 834 G to a weakly interacting regime well above the resonance at 1200 G.

At 1200 G, where the cloud is weakly interacting, the entropy is essentially equal to that of an ideal Fermi gas (the perturbative corrections are known). The cloud size at 1200 G then determines all of the thermodynamic properties of the weakly interacting gas, in particular its entropy,  $S_{weak}$ . Since the sweep is adiabatic, as verified by a round trip, we have

$$S_{strong} = S_{weak}. \quad (2)$$

Based on this method, we completed experiments to measure  $S(E)$  for a strongly-interacting Fermi gas [11].

These measurements have already enabled the first precision experimental tests for predictions of the thermodynamics. The data are in very good agreement with recent quantum Monte Carlo calculations by the theory group of Aurel Bulgac. They are also in excellent agreement with recent NSR results by Peter Drummond's group.

Our data yield an estimate of the critical temperature,  $T_c \simeq 0.29 T_F$ , which is in very good agreement with current predictions based on the many-body microscopic dynamics.

### *Sound Velocity Measurement*

We completed the first measurements on the propagation of first sound throughout the entire BEC-BCS crossover regime [12]. As is well known, by tuning the magnetic field in the vicinity of a Feshbach resonance, it is possible to access a variety of superfluids, including a BEC of molecules well below resonance, a strongly-interacting Fermi gas on resonance, and a weakly interacting Fermi gas above resonance. By measuring the sound velocity over a wide range of magnetic fields, we are able to test predictions for the zero temperature equation of state over a wide range of interaction strengths.

In the experiments, we use a 532 nm beam to excite a ripple in a cigar-shaped cloud. The center of the ripple propagates along the axial direction as a function of time and determines the sound velocity. The ripple covers the  $200 \mu$  cloud in about 10 ms. The statistical error in the measurements is quite small. Our measurements are in very good agreement with quantum Monte Carlo calculations and rule out the Leggett ground state.

## **3. Future Plans**

Currently, we are undertaking a comprehensive measurement of the entropy as a function of energy for imbalanced spin mixtures. Further, we hope to measure the dependence of the sound velocity on the energy at resonance and on BEC fraction in the BEC-BCS crossover regime. These measurements will test the best finite-temperature many-body predictions of the thermodynamics in the crossover regime.

## **4. References to Publications of DOE Sponsored Research (Past 3 Years)**

- 1) J. Kinast, S. L. Hemmer, M. E. Gehm, A. Turlapov, and J. E. Thomas, "Evidence for superfluidity in a resonantly interacting Fermi gas," Phys. Rev. Lett. **92**, 150402 (2004).
- 2) J. E. Thomas and M. E. Gehm, "Optically trapped Fermi gases," Amer. Sci. **92**, 238-245 (2004).
- 3) J. Kinast, A. Turlapov, and J. E. Thomas, "Breakdown of hydrodynamics in the radial breathing mode of a strongly interacting Fermi gas," Phys. Rev. A **70**, 051401(R) (2004).

- 4) J. Kinast, A. Turlapov, and J. E. Thomas, "Heat capacity of a strongly-interacting Fermi gas," *Science* **307**, 1296 (2005).
- 5) J. Kinast, A. Turlapov, and J. E. Thomas, "Damping of a unitary Fermi Gas," *Phys. Rev. Lett.* **94**, 170404 (2005).
- 6) J. E. Thomas, J. Kinast and A. Turlapov, "Virial theorem and universality in a unitary Fermi gas," *Phys. Rev. Lett.* **95**, 120402 (2005).
- 7) J. Kinast, A. Turlapov, and J. E. Thomas, "Optically trapped Fermi gases model strong interactions in nature," *Opt. Phot. News*, **16**, 21 (December, 2005).
- 8) J. E. Thomas, J. Kinast, and A. Turlapov, "Thermodynamics and mechanical properties of a strongly-interacting Fermi gas," Proceedings of the 17th International Conference on Laser Spectroscopy, Aviemore, Scotland (June 19-24, 2005), E. A. Hinds, A. Ferguson and E. Riis editors, p.223-238 (World Scientific London 2005).
- 9) J. E. Thomas, J. Kinast, and A. Turlapov, "Universal thermodynamics of a strongly-interacting Fermi gas," Proceedings of the 24th International Conference on Low Temperature Physics, Orlando, Florida (August 10-17, 2005).
- 10) L. Luo, B. Clancy, J. Joseph, J. Kinast, A. Turlapov, and J. E. Thomas, "Evaporative cooling of unitary Fermi mixtures in optical traps," *New J. Phys.* **8**, 213 (2006).
- 11) L. Luo, B. Clancy, J. Joseph, J. Kinast, and J. E. Thomas, "Measurement of the entropy and critical temperature of a strongly interacting Fermi gas," *Phys. Rev. Lett.* **98**, 080402 (2007).
- 12) J. Joseph, B. Clancy, L. Luo, J. Kinast, A. Turlapov, and J. E. Thomas, "Measurement of sound velocity in a Fermi gas near a Feshbach resonance," *Phys. Rev. Lett.* **98**, 170401 (2007).

## Laser-Produced Coherent X-Ray Sources

Donald Umstadter, Physics and Astronomy Department, 212 Ferguson Hall, University of Nebraska, Lincoln, NE 68588-0111, dpu@unlserve.unl.edu

### Program Scope

In this project, we experimentally and theoretically explore the physics of novel x-ray sources, based on the interactions of ultra-high-intensity laser light with matter. The x-ray source design parameters are angstrom-wavelength, femtosecond-duration, and a footprint small enough to fit in a university laboratory. A promising approach involves nonlinear or relativistic Thomson scattering of intense laser light from a relativistic electron beam. In this process, eV-energy laser light can be Doppler-shifted into up to 100-keV-energy x-rays. Moreover, because the electron beam is accelerated by the ultra-high gradient of a laser wakefield – driven by a pulse from the same laser system – the combined length of both the accelerator and wiggler regions is only a few millimeters. We have recently completed the development of the required laser system, which delivers  $> 100$  terawatts ( $10^{14}$  W) at a repetition rate of 10 Hz. The durations of the laser and the x-ray pulses are less than 30 femtoseconds ( $3 \times 10^{-14}$  s). When focused, this laser can reach an intensity of  $6 \times 10^{22}$  W/cm<sup>2</sup>, which produces a relativistic mass shift, due to the electron's quiver motion, of 100 times the electron rest mass. The development of these sources involves the physics of relativistic plasma physics and nonlinear optics. The sources have applications in the ultrafast chemical, biological and physical processes, such as inner-shell electronic or phase transitions. They also have industrial applications to non-destructive testing, imaging of cracks, remote sensing and the detection of shielded nuclear materials.

### Recent Results

During the most recent year of the grant, a novel model for the fields of focused laser light was developed, which was applied to the vacuum acceleration of electrons. A novel relativistic nonlinear optical effect was published: relativistic cross phase modulation. The 100-TW laser system, the experimental apparatus, and auxiliary diagnostics were all installed and characterized in our newly renovated laboratory. Our first experiments with the new laser, on the acceleration of electrons to high-energy (75-MeV), was also completed.

### Relativistic cross phase modulation

It was demonstrated experimentally (Ref. 1), that the index of refraction of the plasma is modified by a high intensity laser pulse, increasing the bandwidth of another separate laser pulse; thereby significantly reducing the latter's pulse duration. Calculations indicate that high-power pulses with as little as 5-femtosecond duration can be generated in this manner. Relativistic cross phase modulation provides a path for the generation of attosecond pulses of light with orders-of-magnitude higher photon numbers than have been generated previously. Pulses with such characteristics will provide a route to advances in ultrafast science.

### Acceleration of electrons in vacuum

The electron beams that are generated by conventional means have relatively long pulse durations, due to the effects of space charge. However, in a follow-up to our experimental study (Ref. 8), we have now shown – in a numerical simulation (Ref. 2) – that a quasi-monoenergetic and ultra-short duration electron

bunch can be produced by deflecting a laser-accelerated electron beam by a synchronized high-intensity laser pulse. In the simulation, a laser of intensity  $10^{19}$  W/cm<sup>2</sup> produces a 2.8-MeV energy electron beam with  $10^8$  electrons and energy spread of only 0.3 MeV. Most importantly, the electron bunch has a pulse duration of only 30 fs, which is significantly shorter than any produced by any other means. These parameters can be realized experimentally with our current laser (discussed below), and an electron beam with these characteristics would enable time-resolved studies, such as ultrafast structural dynamics.

### Electromagnetic field model

In a separate theoretical study, we found an exact solution for the fields of a focused laser for arbitrary spot size and pulse duration. In comparison with monochrome fields, the inclusion of longer wavelengths reduces the fraction of laser energy in the focus from 86.5% to 72.7% in a single-cycle Ti:Sapphire laser pulse. Thus, unlike light with long pulse duration (many optical cycles), the transverse distribution of the field is found to depend on the longitudinal field profile (Refs. 3, 6 and 7).

### Laser system commissioning

All specifications of the recently installed UNL laser parameters, shown in Table 1, have either been met or have exceeded their design targets. A schematic diagram of the system is shown in Fig. 1.

Laser Parameter	Measurement
Peak power	140 TW (1 PW, 2008)
Repetition rate	10 Hz (0.1 Hz)
Central wavelength	805 nm
Pulse duration	< 30 fs
Pulse energy	3.5 J (compressed)
Energy stability (8 hours)	0.8% rms, 4.9%
Strehl ratio	0.95
Pointing stability	(1 min): 3.5 mrad

*Table 1: Laser parameter measured during full-power operation by means of beam sampling.*

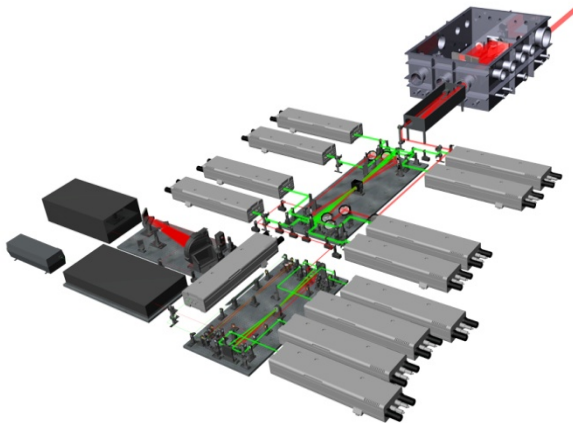


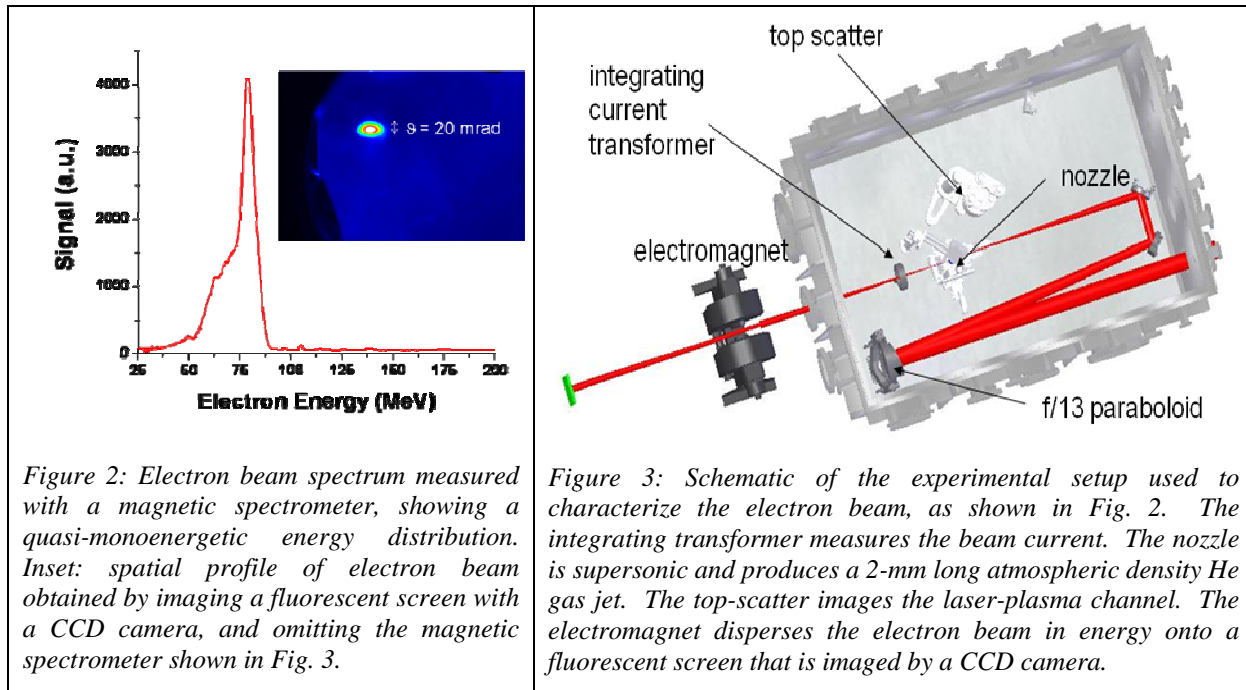
*Figure 1: Schematic diagram of the laser system.*

### First experiments with the UNL laser system

It has been demonstrated previously – with laser systems having parameters similar to the one at UNL – that ~75-MeV energy, quasi-monoenergetic, well-collimated, and self-injected electron beams can be accelerated in the resonant regime by means of a laser wakefield in a He plasma over a distance of only 2 mm.<sup>i</sup> Calculations,<sup>ii</sup> and extrapolations from experiments conducted at lower laser power,<sup>iii</sup> indicate that a highly collimated, ultrashort (~30 fs), ~100-keV photon energy x-ray beam is achievable when this electron beam Thomson scatters from a laser pulse of 1-eV energy photons, which can be derived from the same laser system that accelerates the electron beam. In our first experiments, the electron beam was optimized, while simultaneously the instrumentation required for the Thomson scattering and characterization of the x-ray beam is being tested (see following list).

- (i) Optimization and monitoring of laser characteristics on target, specifically focal spot and pulse duration, in-situ during experiments.

- (ii) Multiple paraboloids have been used to determine the best focusing condition for electron acceleration. A deformable mirror is now incorporated, which can generate specially modulated focal spots tailored for improved electron acceleration.
- (iii) Optimization of high-density gas targets. Nozzles and gas jets of various lengths have been characterized by means of optical interferometry.
- (iv) Optimization of plasma formation – specifically a detailed study of the gas density and laser power needed to induce efficient self-channeling in the plasma.
- (v) Stable 75-MeV energy electron beams, having 20-mrad divergence, have been experimentally observed (see Figs 2 and 3). Optimization of the electron beam parameters is ongoing. The total beam charge has been measured to be 12 nC with an integrating current transformer, and the high energy component ( $>10$  MeV) is  $\sim 1$  nC.
- (vi) Two laser beams, one that is used for electron acceleration, and one that will be used for Thomson scattering, have been synchronized and spatially overlapped by means of an optical beam splitter, delay line, and parabolic reflectors.



## Future Plans

The x-ray beam produced by Thomson scattering will be characterized, including its spatial profile, spectrum, brightness and pulse duration. It will then be used for preliminary pump-probe Laue diffractive imaging studies of the ultrafast (femtosecond) structural dynamics of laser-heated or photo-excited matter. A parametric study will be conducted to optimize the reproducibility of, and minimize the systematic errors in, the experimental results.

An upgrade of the peak power of the laser by a factor of ten, to the petawatt level, is scheduled for completion in 2008. This will allow us to either increase the x-ray photon number per shot, or access the highly relativistic regime of Thomson scattering, in which high-order harmonics are produced.<sup>iv</sup>

## Acknowledgements

The P.I. gratefully acknowledges the significant contributions of Sudeep Banerjee, Nate Chandler-Smith, Shouyuan Chen, Nathan Powers, and Scott Sepke. Additional support (besides DOE) for some of the facilities used in this project was provided by AFOSR, DARPA, DHS and NSF.

## DOE-Sponsored Publications

1. S. Chen, M. Rever, P. Zhang, W. Theobald, and D. Umstadter, "Observation of relativistic cross-phase modulation in high-intensity laser-plasma interactions," *Phys. Rev. E* **74**, 046406 (2006).
2. Scott M. Sepke, Donald P. Umstadter, "Exact analytical solution for the vector electromagnetic field of Gaussian, flattened Gaussian, and annular Gaussian laser modes," *Optics Letters* **31**, 1447-1449 (2006).
3. Scott M. Sepke and Donald P. Umstadter, "Analytical solutions for the electromagnetic fields of tightly focused laser beams of arbitrary pulse length," *Optics Letters* **31**, 2589-2591 (2006).
4. Scott M. Sepke, Donald P. Umstadter, "Analytical solutions for the electromagnetic fields of flattened and annular Gaussian laser modes. I. Small F-number laser focusing," *JOSA B* **23**, 2157-2165 (2006).
5. D. Umstadter, S. Banerjee, S. Chen, S. Sepke, A. Maksimchuk, A., Valenzuela, A. Rousse, R. Shah, and K. Ta Phuoc, "Generation of ultrashort pulses of electrons, X-rays and optical pulses by relativistically strong light," AIP Conference Proceedings, Third International Conference on Superstrong Fields in Plasmas, p. 86, vol. 827, (2006).
6. Scott M. Sepke, Donald P. Umstadter, "Analytical solutions for the electromagnetic fields of flattened and annular Gaussian laser modes. II. Large F-number laser focusing," *JOSA B* **23**, 2166-2173 (2006).
7. Scott M. Sepke, Donald P. Umstadter, "Analytical solutions for the electromagnetic fields of flattened and annular Gaussian laser modes. III. Arbitrary length pulses and spot sizes," *JOSA B* **23**, 2295-2302 (2006).
8. Sudeep Banerjee, Scott Sepke, Rahul Shah, Anthony Valenzuela, Anatoly Maksimchuk, and Donald Umstadter, "Optical Deflection and Temporal Characterization of an Ultrafast Laser-Produced Electron Beam," *Phys. Rev. Lett.* **95**, 035004 (2005).
9. Donald Umstadter, "Einstein's impact on optics at the frontier," *Phys. Letts. A* **347**, 121 (2005) [Einstein Special Issue - Edited by P. Holland].
10. Scott Sepke, Y. Y. Lau, James Paul Holloway, and Donald Umstadter, "Thomson scattering and ponderomotive intermodulation within standing laser beat waves in plasma," *Phys. Rev. E* **72**, 026501 (2005).
11. Kim Ta Phuoc, Frédéric BurgýJean-Philippe Rousseau, Victor Malka, Antoine Rousse, Rahul Shah, Donald Umstadter, Alexander Pukhov, Sergei Kiselev, "Laser based synchrotron radiation," *Phys. Plasmas* **12**, 023101 (2005).

---

<sup>i</sup> Mangels et al., *Nature* **431**, 535 (2004); Geddes et al., *Nature* **431**, 538 (2004); Faure et al., *Nature* **431**, 541 (2004) ; Hidding et al., *Phys. Rev. Lett.* **96**, 105004 (2006) ; Hsieh et al., *Phys. Rev. Lett.* **96**, 095001 (2006).

<sup>ii</sup> F. He et al., *Phys. Rev. Lett.* **90**, 055002 (2003).

<sup>iii</sup> S. Banerjee et al., *J. Opt. Soc. Am. B* **20**, 182 (2003); K. Ta Phuoc et al., *Phys. Plasmas* **12**, 023101 (2005); H. Schwoerer et al. *Phys. Rev. Lett.* **96**, 014802 (2006).

<sup>iv</sup> S. Y. Chen, A. Maksimchuk and D. Umstadter, *Nature* **396**, 653 (1998); Y.Y. Lau, F. He and D. Umstadter, *Phys. Plasmas* **10**, 2155 (2003).



## Author Index

Acremann, Y.	.....	87
Agostini, P.	.....	144
Aliabadi, H.	.....	66,69,72,75
Alnaser, A.	.....	39,40,43
Anis, F.	.....	14
Arms, D.A.	.....	1
Bahati, E.	.....	66,72
Bannister, M.E.	.....	66,72,75
Becker, K.H.	.....	270
Belkacem, A.	.....	3,53,54,62
Ben-Itzhak, I.	.....	14,15,43
Berrah, N.	.....	105
Bocharova, I.	.....	22,23,38
Bohn, J.	.....	109
Braaten, E.	.....	113
Broege, D.	.....	95
Bucksbaum, P.	.....	87,91,93,95,96,97
Buth, C.	.....	1,3,5
Carnes, K. D.	.....	14,15
Chang, Z.	.....	14,18,19,20,43
Chu, S.I.	.....	117
Cocke, C. L.	.....	22,23,24,38,43
Coffee, R.N.	.....	95,96,97
Comtois, D.	.....	39,40
Côté, R.	.....	121
Cundiff, S.T.	.....	125
Dalgarno, A.	.....	129
Dantus, M.	.....	133
DeMille, D.	.....	137
DePaola, B.D.	.....	26
DiMauro, L.	.....	140,144
Ditmire, T.	.....	147
Dörner, R.	.....	24
Doyle, J.	.....	151
Dunford, R.W.	.....	1,3,5,8,9
Ederer, D.L.	.....	3,8
Eberly, J.H.	.....	155
Esry, B.D.	.....	14,15,30
Falcone, R.	.....	62
Farrell, J.P.	.....	91
Fayer, M.	.....	87,102
Feagin, J.M.	.....	159
Fogle,Jr., M.R.	.....	66,72
Fritz, D.	.....	87
Gaffney, K.	.....	87,102
Gaire, B.	.....	14,15

## Author Index

- Gallagher, T.F. ....163  
Gessner, O.....62  
Gilbertson, S. ....18  
Glover, T.E. ....3,62  
Glownia, M .....96  
Gould, P. ....167  
Gramkow, B. ....22,23  
Greene, C.H. ....170  
Gühr, M.....91,93,96  
Hajdu, J. ....87,98  
Hale, J.W. ....66  
Hall, G.....258  
Hasan, A.....39,40  
Havener, C.C. ....66,69,71,75  
Head-Gordon, M. ....62  
Hedman, B. ....87,102  
Heimann, P.....3  
Hertlein, M. ....53,54  
Ho, T.S. ....231  
Hodgson, K. ....87,102  
Höhr, C.M. ....1,8  
Holland, M. ....173  
Johnson, N.G.....14,15  
Jones, R.R. ....177  
Khan, S.....18  
Kanter, E.P. ....1,3,5,8,9  
Kapteyn, H.C. ....181,207,246  
Klimov, V. ....49  
Krässig, B. ....1,3,5,8,9  
Krause, H.F. ....66,67,74,75  
Kristic, P.S. ....77  
Landahl, E. C. ....1,8  
Landers, A. ....24,184  
Lee, T.G .....79  
Leone, S. ....62  
Li, C. ....18,19,20  
Lin, C. D. ....23,34  
Lindenberg, A. ....87  
Litvinyuk, I.V. ....22,23,38,39,40  
Lucchese, R. ....227  
Lundeen, S.R. ....188  
Macek, J.H. ....66,79,80  
Magrakevildze, M.....22,23,38  
Manson, S.T. ....191  
Maharjan, C.M. ....22,23,24,38  
Mashiko, H.....14,18,19,20

## Author Index

- McCurdy, C.W. ....53,58,62  
McFarland, B.K. ....91  
McKenna, J. ....14  
McKoy, V. ....195  
Merdji, H. ....96,97  
Meyer, F.W. ....66,67,71,74  
Miller, T.A. ....144  
Minami, T. ....79  
Moon, E. ....14,18,19,20  
Msezane, A.Z. ....199  
Mukamel, S. ....203  
Murnane, M.M. ....181,207  
Nakamura, C.M. ....14,18,19,20  
Nelson, K.A. ....207  
Neumark, D. ....62  
Novotny, L. ....211  
Orel, A.E. ....215  
Orlando, T.M. ....219  
Osipov, T. ....24,38,53,54  
Ovchinnikov, S.Y. ....79,80  
Parke, E. ....14,15  
Paulus, G. ....23  
Peterson, E.R. ....1,8  
Phaneuf, R.A. ....223  
Pindzola, M.S. ....79  
Poliakoff, E. ....227  
Pratt, S.T. ....1  
Prior, M.H. ....24  
Rabitz, H. ....231  
Raithel, G. ....235  
Raman, C. ....239  
Ranitovic, P. ....22,23,24,38  
Ray, D. ....22,23,38  
Reinhold, C.O. ....66,77,78  
Rescigno, T.N. ....53,58  
Richard, P. ....42,43  
Robicheaux, F. ....242  
Rocca, J.J. ....246  
Rohringer, N. ....7  
Rose-Petruck, C.G. ....250  
Rudati, J. ....8  
Santra, R. ....1,3,5,7,8,10  
Sayler, A.M. ....14,15  
Schmidt, L. ....24  
Schmidt-Böcking, H. ....24  
Schoenlein, R.W. ....3,62

## Author Index

- Schultz, D.R. .... 66,79  
Sears, T ..... 258  
Seely, D.G..... 69,71  
Seideman, T. .... 254  
Shafer-Ray, N ..... 258  
Shakya, M ..... 18  
Siegmann, H. .... 87  
Singh, M.J ..... 43  
Smolarski, M. .... 38  
Southworth, S.H. .... 1,3,5,8,9  
Starace, A.F. .... 262  
Staudte, A. .... 24  
Stockman, M.I. .... 266  
Stohr, J. .... 87  
Tackett, J. .... 18,19,20  
Tarnovsky, V. .... 270  
Tawara, H. .... 43  
Thomas, J.E. .... 278  
Thomas, T.D. .... 274  
Thumm, U. .... 45  
Ulrich, B ..... 22,23,24  
Umstadter, D. .... 282  
Ünal, R ..... 43  
Vane, C.R. .... 66,69,72,74,75  
Vergara, L.I. .... 66  
Villenueve, D.M. .... 39,40  
Wang, H. .... 18,19,20  
Wang, P.Q. .... 15  
Weber, T ..... 24,53,54,62  
Woody, N. .... 43  
Young, L. .... 1,3,5,8,9  
Zamkov, M. .... 43  
Zhang, H. .... 66,67

## Participants

Ali Belkacem  
Lawrence Berkeley National Laboratory  
MS: 2R0100  
Berkeley, CA 94720  
Phone: (510)486-7778  
E-Mail: abelkacem@lbl.gov

Nora Berrah  
Western Michigan University  
Physics Department  
Kalamazoo, MI 49008  
Phone: (269)387-4055  
E-Mail: nora.berrah@wmich.edu

Eric Braaten  
Ohio State University  
191 West Woodruff Avenue  
Columbus, OH 43210  
Phone: (614)688-4228  
E-Mail: braaten@mps.ohio-state.edu

Michael Casassa  
DOE/BES  
SC22.1 DOE, 19901 Germantown Rd.  
Germantown, MD 20874  
Phone: (301)903-0448  
E-Mail: michael.casassa@science.doe.gov

C.L. Cocke  
Kansas State University  
Physics Department, Cardwell Hall  
Manhattan, KS 66503  
Phone: (785)532-1609  
E-Mail: cocke@phys.ksu.edu

Michael Crisp  
U. S. Department of Energy, Office of Fusion  
Energy Sciences  
1000 Independence Ave, SW,  
Washington, DC 20585  
Phone: (301)903-4883  
E-Mail: michael.crisp@science.doe.gov

Alexander Dalgarno  
Harvard University  
CFA,60 Garden Street  
Cambridge, Ma 02138  
Phone: (617)495-4403  
E-Mail: adalgarno@cfa.harvard.edu

Itzik Ben-Itzhak  
J.R. Macdonald Laboratory, Kansas State  
University  
Department of Physics, Cardwell Hall, KSU  
Manhattan, KS 66506  
Phone: (785)539-2155  
E-Mail: ibi@phys.ksu.edu

John Bohn  
JILA, University of Colorado  
UCB 440  
Boulder, CO 80305  
Phone: (303)492-5426  
E-Mail: bohn@murphy.colorado.edu

Philip Bucksbaum  
Stanford/SLAC  
2575 Sand Hill Road  
Menlo Park, CA 94025  
Phone: (650)926-5337  
E-Mail: phb@slac.stanford.edu

Shih-I Chu  
University of Kansas  
Department of Chemistry  
Lawrence, KS 66045  
Phone: (785)864-4094  
E-Mail: sichu@ku.edu

Robin Cote  
University of Connecticut  
2152 Hillside Road, U-3046  
Storrs, CT 06269  
Phone: (860)486-4912  
E-Mail: rcote@phys.uconn.edu

Steven Cundiff  
JILA/NIST  
440 UCB  
Boulder, CO 80309  
Phone: (303)492-7858  
E-Mail: kalethl@jila.colorado.edu

Marcos Dantus  
Michigan State University  
58 Chemistry Building  
East Lansing, MI 48824  
Phone: (517)355-9715  
E-Mail: dantus@msu.edu

## Participants

David DeMille  
Yale University  
P.O. Box 208120  
New Haven, CT 06520  
Phone: (203)432-3833  
E-Mail: david.demille@yale.edu

Louis DiMauro  
The Ohio State University  
191 W. Woodruff Avenue  
Columbus, OH 43210  
Phone: (614)688-5726  
E-Mail: dimauro@mps.ohio-state.edu

John Doyle  
Harvard University  
17 Oxford Street  
Cambridge, MA 02138  
Phone: (617)230-7880  
E-Mail: doyle@physics.harvard.edu

Brett Esry  
J.R. Macdonald Laboratory, Kansas State University  
116 Cardwell Hall, Dept. of Physics  
Manhattan, KS 66506  
Phone: (785)532-1620  
E-Mail: esry@phys.ksu.edu

Jim Feagin  
Cal State University Fullerton  
800 N State College Ave  
Fullerton, CA 92834  
Phone: (714)278-3366  
E-Mail: jfeagin@fullerton.edu

Thomas Gallagher  
University of Virginia  
Department of Physics  
Charlottesville, VA 22904  
Phone: (434)924-6817  
E-Mail: tfg@virginia.edu

Phillip Gould  
University of Connecticut  
Physics Department U-3046, 2152 Hillside Rd.  
Storrs, CT 06269  
Phone: (860)486-2950  
E-Mail: phillip.gould@uconn.edu

Brett DePaola  
Kansas State University  
Department of Physics  
Manhattan, KS 66506  
Phone: (785)532-6777  
E-Mail: depaola@phys.ksu.edu

Todd Ditmire  
University of Texas at Austin  
2511 Speedway RLM 12.204  
Austin, TX 78712  
Phone: (512)471-3296  
E-Mail: tditmire@physics.utexas.edu

Robert Dunford  
Argonne National Laboratory  
9700 S. Cass Ave.  
Argonne, IL 60439  
Phone: (630)252-4052  
E-Mail: dunford@anl.gov

Roger Falcone  
Lawrence Berkeley National Laboratory  
One Cyclotron Road, MS 80R0114  
Berkeley, CA 94720  
Phone: (510)486-6692  
E-Mail: r wf@berkeley.edu

Kelly Gaffney  
SLAC  
2575 Sand Hill Rd.  
Menlo Park, CA 94025  
Phone: (650)926-2382  
E-Mail: kgaffney@slac.stanford.edu

Oliver Gessner  
Lawrence Berkeley National Laboratory  
1 Cyclotron Rd  
Berkeley, CA 94706  
Phone: (510)486-6929  
E-Mail: ogessner@lbl.gov

Chris Greene  
JILA, University of Colorado  
440 UCB  
Boulder, CO 80309  
Phone: (303)492-4770  
E-Mail: chris.greene@colorado.edu

## Participants

Charles Havener  
Oak Ridge National Laboratory  
Physics Division, Bldg. 6010,  
P.O. Box 2008  
Oak Ridge, TN 37831  
Phone: (865)574-4704  
E-Mail: havenercc@ornl.gov

Murray Holland  
JILA, University of Colorado  
440 UCB  
Boulder, CO 80309  
Phone: (303)492-4172  
E-Mail: murray.holland@colorado.edu

Elliot Kanter  
Argonne National Laboratory  
9700 S. Cass Ave.  
Argonne, IL 60439  
Phone: (630)252-4050  
E-Mail: kanter@anl.gov

Victor Klimov  
Los Alamos National Laboratory  
MS-J567  
Los Alamos, NM 87545  
Phone: (505)665-8284  
E-Mail: klimov@lanl.gov

Jeffrey Krause  
National Science Foundation  
901 N. Pollard St., Apt. 709  
Arlington, VA 22203  
Phone: (513)293-0439  
E-Mail: krause@qtp.ufl.edu

Chii-Dong Lin  
Kansas State University  
Department of Physics  
Manhattan, KS 66506  
Phone: (785)532-1617  
E-Mail: cdlin@phys.ksu.edu

Robert Lucchese  
Texas A&M University  
Department of Chemistry  
College Station, TX 77843  
Phone: (979)845-0187  
E-Mail: lucchese@mail.chem.tamu.edu

Richard Hilderbrandt  
DOE/BES  
SC22.1 DOE, 19901 Germantown Rd.  
Germantown, MD 20874  
Phone: (301)903-0035  
E-Mail:  
richard.hilderbrandt@science.doe.gov

Robert Jones  
University of Virginia  
Physics Department, 382 McCormick Road,  
P.O. Box 400714  
Charlottesville, VA 22904  
Phone: (434)924-3088  
E-Mail: rrj3c@virginia.edu

Henry Kapteyn  
JILA, University of Colorado  
440 UCB  
Boulder, CO 80303  
Phone: (303)492-6763  
E-Mail: kapteyn@jila.colorado.edu

Bertold Kraessig  
Chemistry Division,  
Argonne National Laboratory  
9700 S Cass Ave  
Argonne, IL 60439  
Phone: 630-252-9230  
E-Mail: kraessig@anl.gov

Allen Landers  
Auburn University  
206 Allison Laboratory  
Auburn, AL 36849  
Phone: (334)844-4048  
E-Mail: landers@physics.auburn.edu

Igor Litvinyuk  
Kansas State University  
116 Cardwell Hall  
Manhattan, KS 66506  
Phone: (785)532-1615  
E-Mail: ivl@phys.ksu.edu

Stephen Lundeen  
Colorado State University  
Dept. of Physics  
Fort Collins, CO 80523  
Phone: (970)491-6647  
E-Mail: lundeen@lamar.colostate.edu

## **Participants**

<p>Joseph Macek University of Tennessee and Oak Ridge National Laboratory 401 Nielsen Physics Bldg 1408 Circle Dr Knoxville, TN 37996 Phone: (865)974-0770 E-Mail: jmacek@utk.edu</p>	<p>Steven Manson Georgia State University Dept of Physics &amp; Astronomy Atlanta, GA 30303 Phone: (404)413-6046 E-Mail: smanson@gsu.edu</p>
<p>Diane Marceau Office of Basic Energy Sciences, Department of Energy 19901 Germantown Road Germantown, MD 20874 Phone: (301)903-0235 E-Mail: diane.marceau@science.doe.gov</p>	<p>William McCurdy U. C. Davis and LBNL One Cyclotron Road, MS 50B-2245 Berkeley, CA 94720 Phone: (510)486-4283 E-Mail: cwmccurdy@ucdavis.edu</p>
<p>Vincent McKoy California Institute of Technology 1200 E. California Blvd. Pasadena, CA 91125 Phone: (626)395-6545 E-Mail: mckoy@caltech.edu</p>	<p>Terry Miller Ohio State University 120 W. 18th Columbus, OH 43210 Phone: (614)292-2569 E-Mail: tamiller@chemistry.ohio-stte.edu</p>
<p>Alfred Z. Msezane Clark Atlanta University 223 James P. Brawley Drive SW Atlanta, GA 30314 Phone: (404)880-8663 E-Mail: amsezane@cau.edu</p>	<p>Shaul Mukamel University of California, Irvine 1102 Natural Sciences II Irvine, CA 92697 Phone: (949)824-7600 E-Mail: smukamel@uci.edu</p>
<p>Margaret Murnane JILA, University of Colorado 440 UCB Boulder, CO 80303 Phone: (303)492-6763 E-Mail: murnane@jila.colorado.edu</p>	<p>Keith Nelson MIT 77 Massachusetts Avenue, Rm. 6-235 Cambridge, MA 02139 Phone: (617)253-1423 E-Mail: kanelson@mit.edu</p>
<p>Lukas Novotny University of Rochester The Institute of Optics Rochester, NY 14627 Phone: (585)275-5767 E-Mail: novotny@optics.rochester.edu</p>	<p>Ann Orel University of California, Davis Dept. of Applied Science, One Shields Ave. , UC Davis Davis, CA 95616 Phone: (530)752-6025 E-Mail: aeorel@ucdavis.edu</p>
<p>Thomas Orlando Department of Chemistry &amp; Biochemistry; Georgia Institute of Technology 901 State Street, MS&amp;E Bldg., Atlanta, GA 30332 Phone: (404)894-8222 E-Mail: thomas.orlando@chemistry.gatech.edu</p>	<p>Ronald Phaneuf University of Nevada, Reno Department of Physics, MS-220 Reno, NV 89557 Phone: (775)784-6818 E-Mail: phaneuf@physics.unr.edu</p>

## Participants

Erwin Poliakoff  
Louisiana State University  
Chemistry Department  
Baton Rouge, LA 70803  
Phone: (225)578-2933  
E-Mail: epoliak@lsu.edu

Georg Raithel  
University of Michigan  
450 Church Street  
Ann Arbor, MI 48105  
Phone: (734)647-9031  
E-Mail: graithel@umich.edu

David Reis  
University of Michigan  
Department of Physics, 450 Church Street  
Ann Arbor, MI 48109  
Phone: (734)763-9649  
E-Mail: dreis@umich.edu

Francis Robicheaux  
Auburn University  
206 Allison Lab  
Auburn, AL 36849  
Phone: (334)844-4366  
E-Mail: robicfj@auburn.edu

Christoph Rose-Petrucci  
Brown University  
Dept. of Chemistry  
Providence, RI 02912  
Phone: (401)863-1533  
E-Mail: Christoph\_Rose-Petrucci@brown.edu

Robert Schoenlein  
Lawrence Berkeley National Laboratory  
1 Cyclotron Rd. MS: 2-300  
Berkeley, CA 94720  
Phone: (510)486-6557  
E-Mail: rwschoenlein@lbl.gov

Tamar Seideman  
Northwestern University  
2145 Sheridan Road  
Evanston, IL 60208  
Phone: (847)467-4979  
E-Mail: t-seideman@northwestern.edu

Herschel Rabitz  
Princeton University  
Frick Laboratory  
Princeton, NJ 08544  
Phone: (609)258-3917  
E-Mail: hrabitz@princeton.edu

Chandra Raman  
Georgia Tech  
School of Physics, 837 State St.  
Atlanta, GA 30332  
Phone: (404)894-9062  
E-Mail: craman@gatech.edu

Thomas Rescigno  
LBNL  
1 Cyclotron Rd. MS-2-100  
Berkeley, CA 94720  
Phone: (510)486-8652  
E-Mail: tnrescigno@lbl.gov

Jorge Rocca  
Colorado State University  
1320 Campus Delivery ERC B329  
Fort Collins, CO 80523  
Phone: (970)491-8371  
E-Mail: rocca@engr.colostate.edu

Robin Santra  
Argonne National Laboratory  
9700 S. Cass Avenue  
Argonne, IL 60439  
Phone: (630)252-4994  
E-Mail: rsantra@anl.gov

David Schultz  
Oak Ridge National Laboratory  
Physics Div., Bldg. 6010, P.O. Box 2008  
Oak Ridge, TN 37831  
Phone: (865)576-9461  
E-Mail: schultzd@ornl.gov

Neil Shafer-Ray  
University of Oklahoma  
440 West Brooks Street  
Norman, OK 73019  
Phone: (405)325-2890x36123  
E-Mail: shaferry@physics.ou.edu

## Participants

Steve Southworth  
Argonne National Laboratory  
Bldg. 203, 9700 S. Cass Ave.  
Argonne, IL 60439  
Phone: (630)252-3894  
E-Mail: southworth@anl.gov

Mark Stockman  
Georgia State University  
University Plaza  
Atlanta, GA 30303  
Phone: (678)457-4739  
E-Mail: mstockman@gsu.edu

John Thomas  
Duke University  
Physics Department Box 90305  
Durham, NC 27708  
Phone: (919)660-2508  
E-Mail: jet@phy.duke.edu

Donald Umstadter  
University of Nebraska, Lincoln  
212 Ferguson Hall  
Lincoln, NE 68588  
Phone: (402)472-8115  
E-Mail: dpu@unlserve.unl.edu

Thorsten Weber  
Lawrence Berkeley National Lab  
One Cyclotron Road  
Berkeley, CA 94720  
Phone: (510)486-5588  
E-Mail: TWeber@lbl.gov

Linda Young  
Argonne National Laboratory  
9700 S. Cass Ave.  
Argonne, IL 60439  
Phone: (630)252-8878  
E-Mail: young@anl.gov

Anthony F. Starace  
University of Nebraska  
Dept. of Physics & Astronomy, 116 Brace  
Lab  
Lincoln, NE 68588  
Phone: (402)472-2795  
E-Mail: astarace1@unl.edu

Vladimir Tarnovsky  
Stevens Institute of Technology  
Castle Point on Hudson  
Hoboken, NJ 07410  
Phone: (201)216-5099  
E-Mail: vtarnovs@stevens-tech.edu

T. Darrah Thomas  
Oregon State University  
153 Gilbert Hall  
Corvallis, OR 97331  
Phone: (541)737-6711  
E-Mail: T.Darrah.Thomas@oregonstate.edu

Albert Wagner  
Argonne National Laboratory - Chemistry  
Division  
9700 S. Cass Avenue, Bldg. 200  
Argonne, IL 60439  
Phone: (630)252-3570  
E-Mail: wagner@tcg.anl.gov

Jun Ye  
JILA, University of Colorado  
UCB 440  
Boulder, CO 80309  
Phone: (303)735-3171  
E-Mail: ye@jila.colorado.edu